1976-3

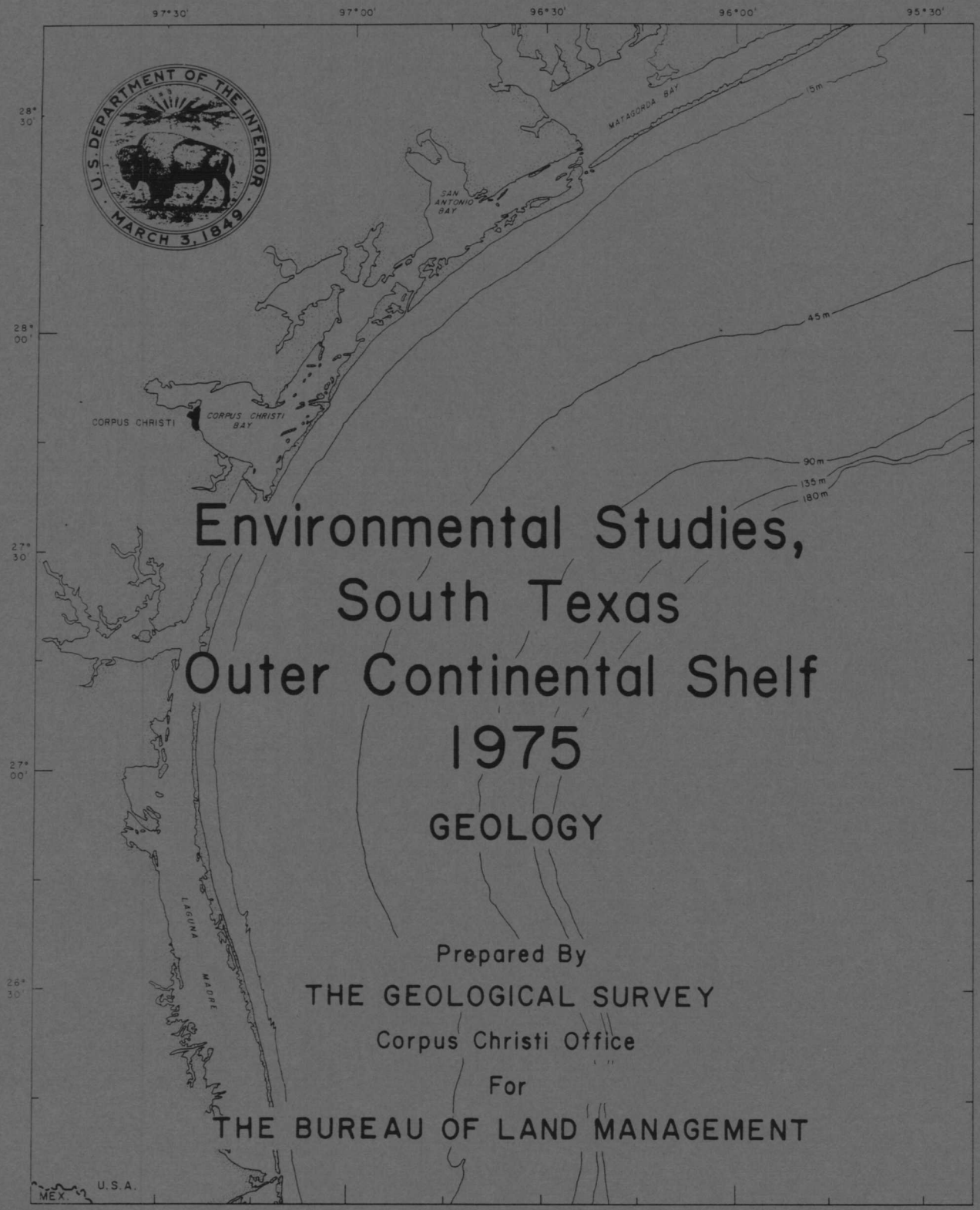

Environmental Studies, South Texas Outer Continental Shelf 1975

GEOLOGY

Prepared By

THE GEOLOGICAL SURVEY

Corpus Christi Office

For

THE BUREAU OF LAND MANAGEMENT

ENVIRONMENTAL STUDIES, SOUTH TEXAS OUTER CONTINENTAL SHELF

GEOLOGY

Part I--Geologic Description and Interpretation

Part II--Inventory of Data Archived and Analyzed

A report to the Bureau of Land Management
in fulfillment of Contract 08550-MU5-20
for the period October 25, 1974 to December 1, 1975

Editor and Element Leader
Henry L. Berryhill, Jr.

Contributors:
Gerald L. Shideler
Charles W. Holmes
Gary W. Hill
Steven S. Barnes
Henry L. Berryhill, Jr.
Ray G. Martin, Jr.

U.S. Geological Survey

ENVIRONMENTAL STUDIES, SOUTH TEXAS OUTER CONTINENTAL SHELF

GEOLOGY

Part I--Geologic Description and Interpretation

TABLE OF CONTENTS

LIST OF ILLUSTRATIONS

Text Figures and Plates*

*For management utility, copies of key maps have been prepared at the compilation scale of 1:480,000. These are separate and larger scale copies of the smaller scale figures that appear in the text. The plate number that corresponds to a text figure is indicated both in the listing that follows and in the text.

LIST OF TEXT TABLES

LIST OF CHARTS

EXECUTIVE SUMMARY

The South Texas Outer Continental Shelf covers 19,250 sq km (7,400 sq mi) and extends northwards from the International Boundary to the northern end of Matagorda Island, Texas and seaward from the Federal-State territorial boundary 16.6 km (10.3 mi) offshore to the outer edge of the continental shelf.

The depth of water over the South Texas OCS ranges seaward from an average of about 26 m (85 ft) along the Federal-State boundary to an average of about 180 m (600 ft) at the edge of the continental shelf.

The surface of the sea floor across the South Texas OCS is relatively smooth and has an average seaward gradient of about 3.5 m (12 ft) per mile. Topographic features are minor in extent and consist of a series of small mound-shaped structures that protrude from 8 to 20 m (24 to 61 ft) above the sea floor. The mounds are carbonate reefs that formed along the shoreline near the outer edge of the continental shelf during the last glacial epoch when sea level was some 137 m (450 ft) lower than now.

Purpose and Scope of Study

The geologic investigations are one element of a coordinated interdisciplinary environmental assessment which also includes the chemistry, both trace metals and hydrocarbon, the biology and the physical oceanography. The overall environmental assessment is a part of a national program to provide the Bureau of Land Management with the scientific information necessary to make sound management decisions regarding the development of mineral resources on the OCS and to provide the basis for predicting the impact of oil and gas exploration and development on the marine environment.

The two broad objectives of the geologic studies are to establish a descriptive baseline for the geologic aspects of the area and to relate these to the regional environmental processes. The specific objectives include study of: 1) the subsurface geologic framework of the continental terrace; 2) the nature and physical sedimentology of surficial and shallow subsurface sea floor sediments; 3) the biogeologic or animal-sediment relationships in surficial and shallow subsurface sediments; 4) the geochemistry of surficial sea floor sediments, including the trace metals and organic carbon content; 5) the amount and mineralogy of sediments suspended in the water column; 6) the trace metals content of sediments suspended in the water column; and 7) sea floor stability, which includes the identification and location of features such as faults which indicate vertical movement and displacement of subseafloor strata, areas of slumping where unstable surficial sediments are sliding along the sea floor, and the chronology of displacement of strata by faulting through time.

Geologic Framework

The basic data for the interpretation of the geologic framework are approximately 8,860 km of high resolution acoustic reflection profiles arranged in a traverse grid spacing of approximately 5 x 10 km. Some 35,000 navigation fix points established along traverses during the acoustic profiling served as points for plotting and mapping the geologic data from the geophysical records.

The primary structural features within the continental terrace are a series of anticlinal folds or upbuckles whose regional trend is N 30° to N 45° east. The average depth from the sea floor to the crests of the

anticlines is -200 ms (milliseconds) or approximately -146 m (480 ft). The anticlinal crests at the relatively shallow depth recorded tend to be discontinuous; however, several extend for distances of 29 km or more. Two domal structures, probably formed by upward movement of salt, are located at the outer edge of the shelf and are associated with branching anticlinal crests that lie along the juncture of the continental shelf and the continental slope.

Associated with the anticlinal folds are faults that indicate vertical displacement and movement of strata within the continental terrace during upward movement along the anticlines. Faulting of late Pleistocene and Holocene sediments is extensive over the outer two-thirds of the South Texas OCS. Along many of the faults, throw increases with depth, indicating progressive movement through time. Sound analog patterns recorded in the water column above a sizeable area of intense faulting near the outer edge of the continental shelf, and locally elsewhere, suggest strongly that natural gas is seeping upward to the sea floor along fault planes. Whether the gas is emanating from shallow sources within the sediments or from deep-lying reservoirs is not known.

Structure contour and sediment thickness maps were prepared for two strong sound reflecting surfaces lying at average subseafloor depths of 30 and 70 ms (22 and 51 m) respectively to determine the extent, magnitude, and influence of tectonic or structural movements in molding the continental terrace and the sea floor surface during and since late Pleistocene time. The uneven configuration of the two surfaces demonstrates that during late Pleistocene time tectonic movements influenced the sea floor surface as follows: localized crustal subsidence in the southern part of the South Texas OCS created a topographic depression and tilted the sea floor surface slightly

southward; low magnitude progressive upward movement along the anticlinal folds created coincident topographic ridges of low relief. In response to the imposed topographic pattern, sediments carried to the continental shelf tended to move along and parallel to the trend of the shelf and accumulated to greater thickness in the topographic depression and in the shallow broad swales between the low fold ridges. This pattern is most evident in the configuration of the lower of the two horizons contoured and to a less extent by the configuration of the shallower horizon. Progressive sedimentation during most recent geologic time has filled in the topographic irregularities formed by the late Pleistocene tectonic movements.

Sea Floor Sediments

Sea floor sediments for the purposes of the study includes both the surficial sediments at the water interface and underlying sediments to the depth penetrated by the pipe and box cores. The sediments were analyzed for texture or grain size, color and heavy minerals content. Sample material was obtained for analysis at 263 bottom stations.

Texturally, the surficial seafloor sediments are made up principally of silt and clay-sized particles (<0.063 mm). Quantitatively, the highly dominant fraction is silt, which appears to be effectively trapped hydraulically within the OCS environment. In contrast, the subordinate clay fraction reflects a more open dispersal system, with substantial clay-sized detritus escaping into deeper Gulf waters. The coarser sand-sized detritus is quantitatively dominant only along the near shore sector and within portions of the ancestral Brazos-Colorado and Rio Grande deltas of the northern and southern sectors. Textural variability is most pronounced in the ancestral delta regions of the

northern and southern sectors and transitions from sand to finer detritus is most pronounced in the southern sector. The central sector of the South Texas OCS is a fine-sediment depocenter of relatively uniform particle size. Two primary directions of sediment movement over the South Texas OCS are indicated by the distribution pattern for silt, the predominant textural component; seaward onto the OCS; and southward along the OCS as a net regional trend.

For the shallow subsurface sediments, the ratio of sand to silt and clay and the number of discrete sand layers per each 30 cm of core were determined as a means of establishing the stratigraphy of the youngest sediments deposited over the area studied and to gain some understanding of two sedimentological factors: 1) the temporal variability of sediment dispersal patterns; and 2) the relative significance of storm versus fair-weather sedimentation.

The regional pattern outlined by the sand/silt-clay ratios in the cored sediments indicates a fine-grained central sector of the shelf and increasing sand contents shoreward as well as both northward and southward away from the central sector. Comparison of the pattern with the sand/silt-clay ratio pattern of surficial sediments shows a high degree of similarity of regional trends, indicating that the regional pattern of sediment dispersal was established several thousand years ago. Discrete sand layers in the cored sediments range from a maximum of 5.17 per 30 cm standard core length to zero along the outer shelf edge. Although the sand layers are more numerous along the inner part of the OCS, several extend as much as 30 miles offshore. The most obvious mechanism for spreading sand so far across the shelf is the strong current regime that accompanies passage of hurricanes. The pattern of sand dispersal over the South Texas OCS suggests that hurricanes cause significant dispersal of OCS sediments over wide areas.

Rates of sediment deposition were not a specific study topic. However, impirical evidence indicates an average rate of sediment accumulation over the South Texas OCS of about one meter per thousand years during Holocene time. Even assuming a deposition rate of somewhat less, the shelf off south Texas can be classified as an area of relatively high sediment accumulation.

Animal-sediment Relations

Sediment modification by infaunal organisms includes the physical destruction of depositional structures, the creation of biogenic structures and alteration of grain size relationships. Consequently, biogenic processes are directly involved in geochemical processes and the redistribution of chemical elements in the sediments.

The South Texas OCS is not homogeneous relative to distribution patterns of biological components. Generally, number of species and individuals, biomass, and diversity decrease with increasing water depth. Equitability increases across the shelf as water depth increases. The central sector has less dense and diverse infaunal populations than the general areas of the ancestral Rio Grande and Brazos-Colorado deltas to the south and north. Consequently, biogenic processes or modification of sediment by bioturbation are most intense along the inner part of the South Texas OCS. For the shelf as a whole, bioturbation is high over the inner third and progressively lower over the outer part. Bioturbation is very low near the shelf edge. In terms of pollution impact, pollutants introduced to the surface of the sea floor will be worked downward into the sediments by organisms relatively rapidly over the inner part of the OCS and will remain on the surface for longer periods of time farther offshore.

Geochemistry: Trace Metals Content of Surficial Sediments

Subsamples from the 263 bottom grab samples were analyzed for content of ten trace metals: barium, cadmium, copper, chromium, iron, manganese, nickel, lead, vanadium, and zinc.

As a regional pattern, the trace metals content of sediments in bays and estuarines adjacent to the continental shelf are relatively higher than in the sediments of the South Texas OCS. Compared to the average trace metals content for the South Texas OCS as a whole, only cadmium and manganese are significantly high. For several trace metals, including cadmium, the highest concentrations are in the area of suspected gas seeps along the outer edge of the continental shelf. The suspected gas seeps appear to be emanating upward along fault planes and may be depositing trace metals in the sea floor sediments, thus explaining the higher concentrations there. In the South Texas OCS, the average levels for all trace metals analyzed are lower than the average levels for the adjacent segment of the continental shelf to the north. For the overall northern Gulf of Mexico continental shelf, the average levels within the South Texas are comparable. Knowledge of trace metals concentrations in sediments of other continental shelves of the United States is too scant to permit comparison with the shelf off south Texas.

Suspended Sediments: Grain Size, Amount, and Mineralogy

Water column samples for suspended analysis were obtained at three levels in the water column at 23 stations spaced along four traverses across the shelf. As the samples were taken over a two month period, the sampling was not synoptic and only the relative values at a specific station have scientific significance.

The overall range of mean grain size for all stations was from a minimum of 9.37 ϕ (clay) to a maximum of 5.30 ϕ (medium silt). Generally, the size of grains showed a wide range and, in most samples, the size of grains has a complex polymodal distribution. The individual modes probably reflect a mixture of organic particulate subpopulations (nanoplankton, microplankton) as well as inorganic subpopulations (silt and clay minerals).

Sediment concentrations for all water sample stations ranged from a minimum of 5,746 particle counts to a maximum of 237,297. Variable sediment concentration-depth relationships prevailed over the OCS during the sampling period. Concentration gradient reversals occur at the majority of stations; the reversals are most frequently, but not exclusively, associated with thermoclines. The majority of stations show a net increase in sediment concentration with depth. However, a net increase was not uncommon, especially at the shallower stations. Based on bottom photography, a significant layer of suspended sediment near the bottom of the water column was indicated for most of the South Texas OCS during the two-months sampling period.

X-ray analysis showed that the detrital suspended material was made up primarily of clay minerals; quartz and other material were present in only trace amounts. The mineralogical data, although not synoptic, does define two water masses: A montmorillonite-rich water mass over the northwesternmost part of the OCS and an illitic-rich water mass over the remainder of the shelf off south Texas. A feature of the mineralogy is the low content of montmorillonitic material in the bottom water, indicating that the clay minerals in suspension are not being derived from the surficial bottom sediments which are high in montmorillonitic clay but are being introduced from elsewhere.

Suspended Sediments: Trace Metals Content

Sample material for analyzing trace metals content of suspended sediments was taken at the same stations as for grain size and concentration, and amounts of the same ten elements analyzed in surficial bottom sediments were determined. The analyses indicate that the trace metals concentrations in near bottom suspended sediments were more invariant than those of surface waters. The surface waters showed an apparent higher ridge of metal concentrations offshore. In summary, trace metals concentrations showed decidedly different patterns when the surface and bottom waters were compared. The near-bottom samples appeared to be predominantly inorganic; the surface samples showed a greater variability probably because of the influence of biogenic material on the trace metals concentrations.

Sea Floor Stability

Surficial and shallow subsurface sediments of the South Texas OCS are typically fine grained and characteristically are soft rather than firm and compact. Bearing strength of the sediments can be assumed to be greatest in areas where the ratio of sand to silt/clay is higher than 1.00 and least in areas where the ratio is less than 0.12. The more unstable areas in terms of bearing strength are those where the textural gradients are steepest, as over the ancestral Rio Grande delta. Possible firmer foundation surfaces at depth are those represented by the two prominent acoustic reflecting horizons that were contoured to show structural or deformation patterns. Whether or not the two surfaces are at suitable depths to serve as foundations would depend on the type and size of the engineering structures planned.

Displacement of sediments by gravity sliding or slumping along the sea floor is restricted to the outer edge of the ancestral Rio Grande delta. Within the area outlined, slumps of relatively large scale displacement are at the outer edge of the shelf coincident with the upper continental slope. Landward and adjacent to the area of active slumping is a belt of older slumped sediments now covered by undeformed sediments.

Fault movement has progressed upward and outward across the continental terrace with time. The youngest faults are along the outer one-third of the OCS with some exceptions. Approximately the inner third of the South Texas OCS, except beneath the ancestral Rio Grande delta, has been faulted during late Pleistocene time. The mid-OCS was extensively faulted during latest Pleistocene time and the outer OCS to a lesser extent. The outer one-quarter of the South Texas OCS has been extensively faulted during Holocene time. The few faults that extend to the surface of the sea floor and represent very recent movement, excluding those associated with slumping, are at mid-shelf and near the outer edge of the shelf. The history of faulting during late Pleistocene and Holocene times suggests that movements of a similar nature and pattern might occur in the future. The part of the shelf probably most susceptible to future movements is the outer third; however, the most recent faulting, though not intense, has been scattered rather widely, indicating that structural adjustments within the continental terrace, probably related to diapiric movements at depth, are not confined to the outer edge of the continental terrace. The South Texas OCS, though not a highly seismic area, nevertheless, is a region of continuing mobility.

Salient Environmental Implications

1. The predominantly fine grained sediments typical of much of the South Texas OCS might have a greater tendency for retention of industrial pollutants, as compared to a more permeable and aerated sandy province.
2. Areas of pronounced textural variability, such as the northern and southern sectors of the OCS, would be more prone to differential compaction and subsidence. This could produce instability hazards associated with platform and pipeline construction. The probability of this hazard would tend to be greatest in areas of high textural gradients, such as within the ancestral Rio Grande delta.
3. Because the most dense and diverse infaunal communities occur in the shallower waters of the OCS and over the ancestral deltas, the impact of man's activities on infaunal populations would be greatest in those areas.
4. In the same sectors of the OCS as noted above, where infaunal activity is greatest, the mixing of the sediment vertically occurs relatively rapidly. Any pollutants introduced into these areas will be more rapidly worked downward into the sediments. Consequently, the probability of long-term retention and progressive build-up of pollutant levels increases.
5. The outer one-quarter of the South Texas OCS must be classed as a potentially mobile area; it is subject to possible future movement. The outer shelf edge off the ancestral Rio Grande delta is an area of active slumping. Consequently, plans for platform and pipeline construction along the outer part of the OCS should be based on detailed site-specific studies before construction is undertaken and design should take into consideration the possibility of the future of the sea floor. The suitability of the active slump areas for any type of construction is highly questionable.

INTRODUCTION

LOCATION OF AREA AND BATHYMETRY

The South Texas Outer Continental Shelf (OCS) as described herein corresponds to the area formally outlined by the Department of the Interior for oil and gas leasing. The area covers approximately 19,250 sq km (7,400 sq mi) and extends northward from the International Boundry to the northern end of Matagorda Island, Texas and seaward from the Federal-State territorial boundary 16.6 km (10.3 mi) to the approximate position of the 200 m isobath, or outer edge of the continental shelf. The location of the area is shown by figure 1 and the lease block grid for the area is shown both by figure 2 and by the larger scale index base map for the geologic framework (plate A). The subdivisions of the South Texas OCS lease area are shown by figure 2a.

The bathymetry of the South Texas OCS is shown by figure 3. The primary topographic features outlined by the bathymetric contours on the map are the deltaic bulge seaward of the Rio Grande, the comparable outline of an ancestral delta near the shelf edge seaward of Matagorda Bay and the very broad ramp-like identation on the outer shelf between the two deltaic bulges. Second order topographic features are the north-to-northeastward trending low ridges, terraces and small scarps over the ancestral Rio Grande delta, the series of small closures associated with a band of irregular topography along the ramp area between water depths of 35 to 50 fm (64 to 91 m) and the terrace-like area along the outer shelf beginning at the 50 fm (91 m) isobath. The secondary features seem to be relicts of late Pleistocene and early Holocene deposition and erosion associated with migration of the shoreline. Several of the small topographic closures on the outer shelf were identified as carbonate reefs by Parker and Curray (1956). However, later work has located more reefs than were known to Parker and Curray.

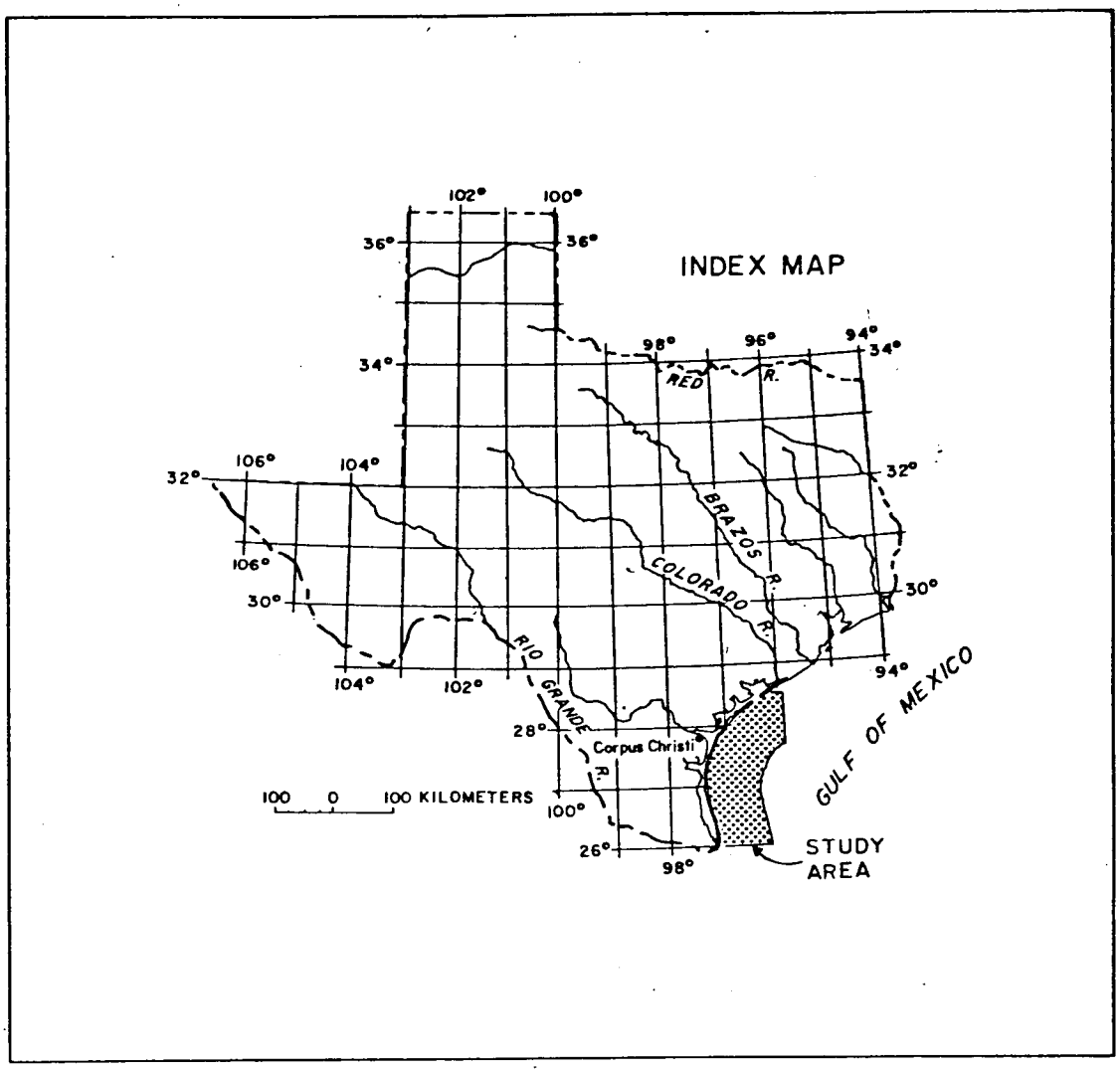

Figure 1. Location of the study area

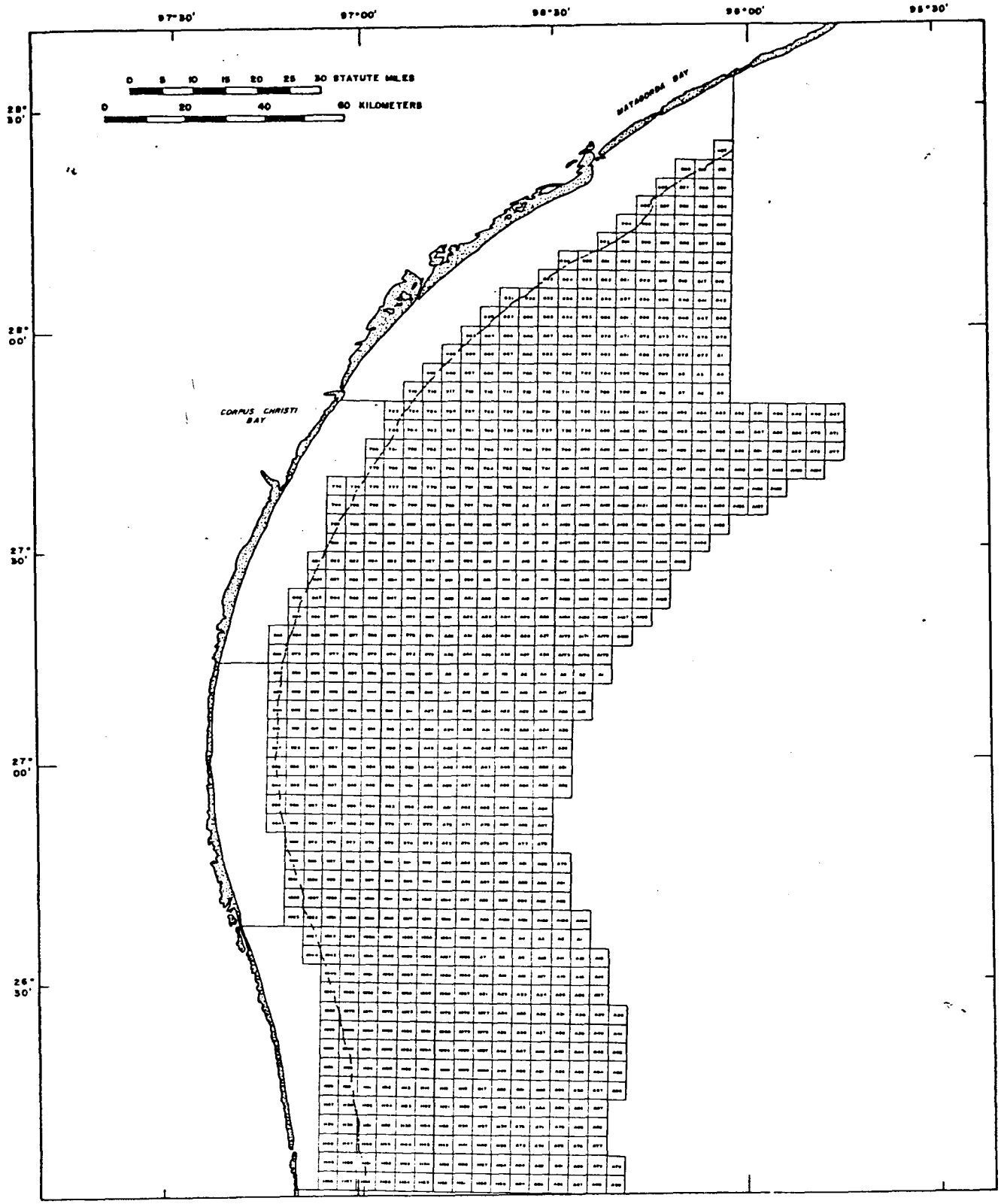

Figure 2. Petroleum lease block grids for south Texas Outer Continental Shelf

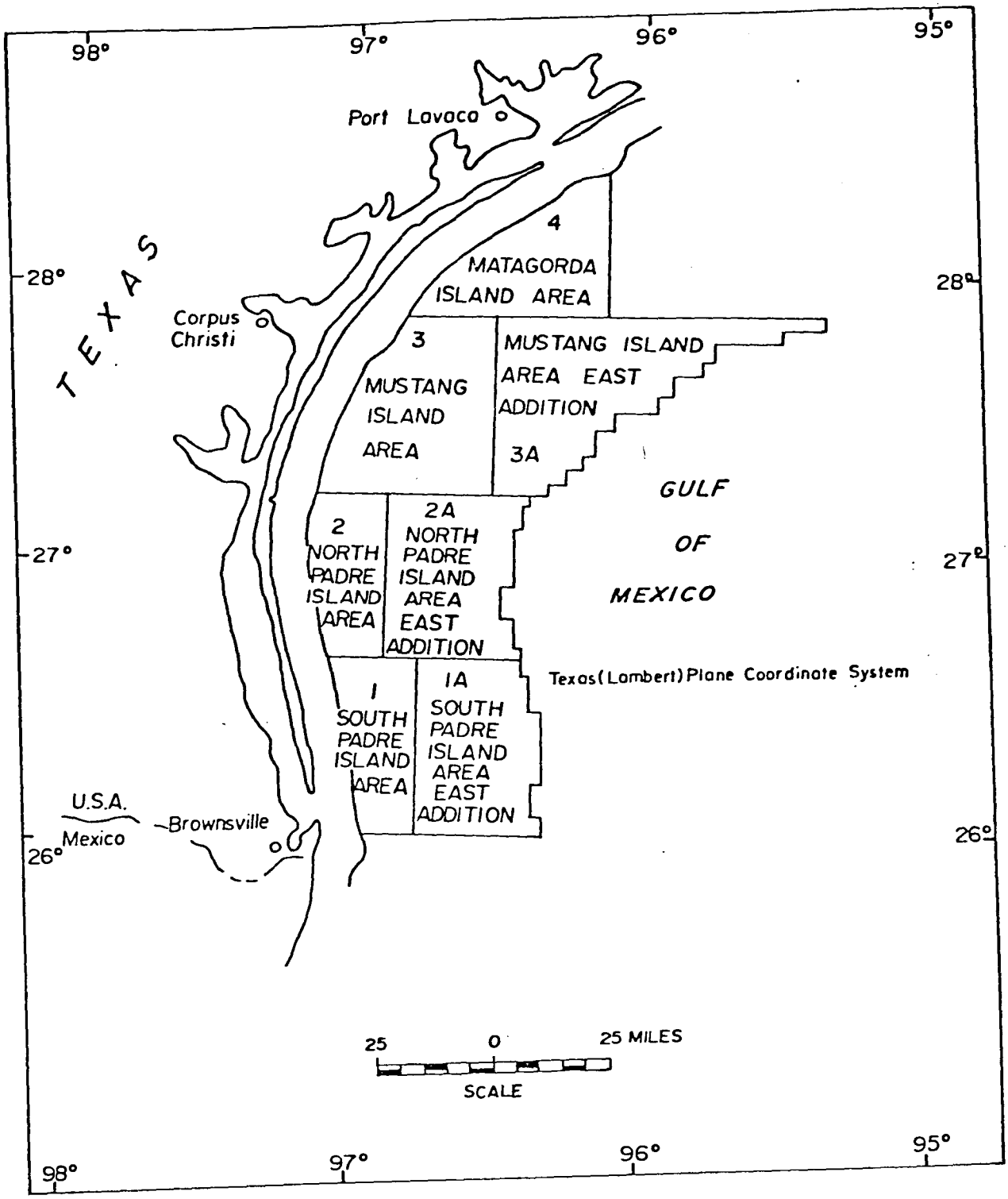

Figure 2a. Subdivisions of the South Texas Outer Continental Shelf lease area.

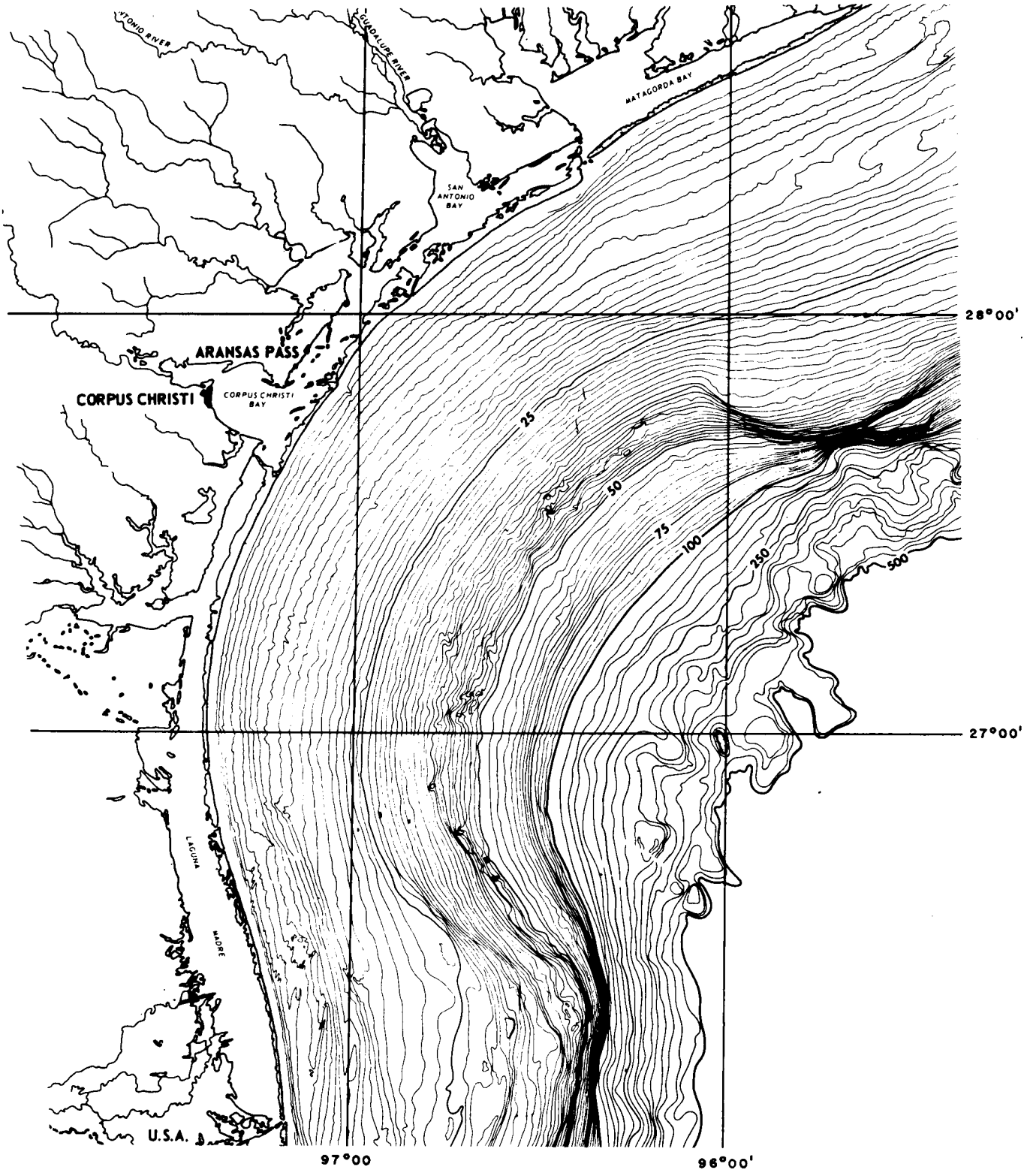

Figure 3. Bathymetry of the South Texas Outer Continental shelf, depth in fathoms. Taken from Bathymetric Maps, Eastern Continental Margin, U.S.A.; sheet three, Northern Gulf of Mexico: American Association of Petroleum Geologists, 1970.

For clarity in presenting data and interpretive results the base map was modified to remove all but a few key isobaths and depths in fathoms were converted to meters. The modified base map used for reporting results is shown by figure 4. Furthermore, the three primary topographic features outline three physiographic subprovinces of the shelf: north, central and southern, that are used for convenience in the numerous geographic references in the text to the several parts of the shelf. The three subprovinces also are shown by figure 4.

PURPOSE AND SCOPE OF STUDY

General Statement

In 1974, the Bureau of Land Management was authorized to initiate a National Outer-Continental Shelf Environmental Studies Program. The objectives of the program as stated by the BLM are:

- provide information about the OCS environment that will enable the Department and the Bureau to make sound management decisions regarding the development of mineral resources;
- provide basis for predicting the impact of oil and gas exploration and development on the marine environment;
- establish a basis for predication of impact of OCS oil and gas activities in frontier areas;
- provide impact data that would result in modification of leasing regulations, operating regulation, or operating orders.

The initial study approach to the program, as outlined by the BLM, is to establish environmental base lines (bench marks) in selective OCS regions prior to oil and gas exploration.

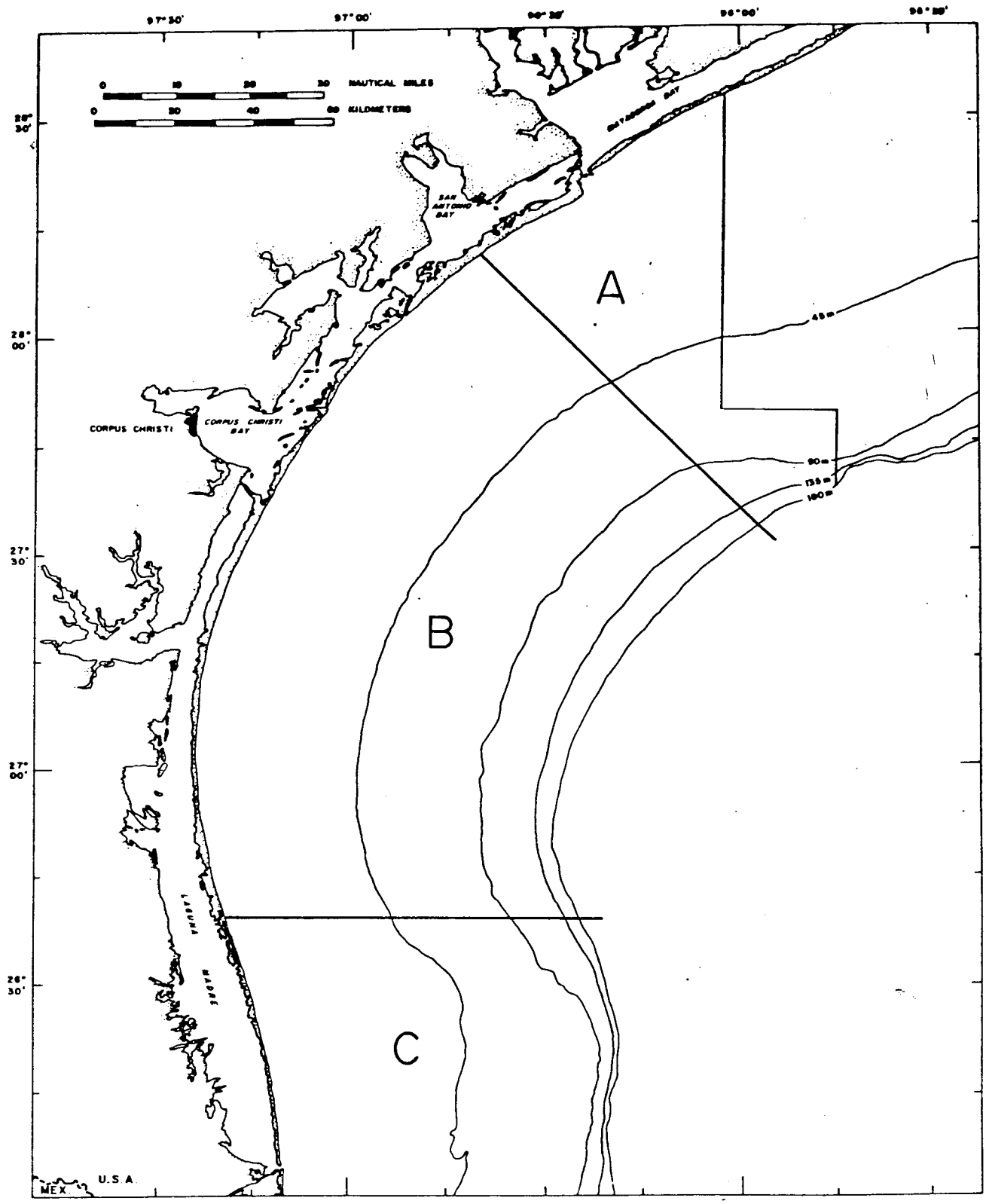

Figure 4. Physiographic subprovinces of the south Texas Continental shelf: A - northern sector; B - central sector; C - southern sector. Depth in meters

Work Plan

Time Frame for Study

The South Texas OCS region was selected for initial study by the BLM in the summer of 1974 with the intent of having the initial base line or benchmark sampling over the area completed prior to late January 1975. By contractual arrangement, the U.S. Geological Survey, through the office at Corpus Christi, Texas, implemented the work plan for the marine geologic investigations on October 25, 1974 with a reporting deadline of December 1, 1975. The field sampling was completed in the period October 25 to December 22, 1974.

The geologic investigations are a part of a coordinated interdisciplinary study which also includes chemistry, both trace metals and hydrocarbons, biology and physical oceanography, all to be incorporated into an integrated final report for the project by May 1976.

Objectives

The general focus for the studies has been to describe definitively the various aspects that make up the geologic environment and to relate these to the regional marine environmental processes.

The geologic aspects include: 1) the nature and amount of sediments suspended in the water column; 2) the Holocene sediments of the shelf; 3) trace metal content of the suspended sediments and the surficial Holocene sediments; 4) the contact relation of the Holocene sequence to the underlying Pleistocene deposits; 5) the nature of Pleistocene sediments where exposed; 6) the geologic framework of the continental terrace; and 7) the identification and location of features such as faults and slumps that can be more properly defined as an evaluation of the stability of the sea floor.

As the late Pleistocene and Holocene sediments reflect the response of the sea floor in latest geologic time to the processes acting on the OCS, more specific objectives related to Pleistocene and Holocene deposits include for Holocene sediments:

- distribution of surficial and near surface sediments by texture;
- description of internal depositional and biogenic structures in the near surface sediments;
- depositional/erosional patterns of latest Holocene sediments;
- thickness of the Holocene sequence;

and for Pleistocene sediments:

- paleotopography of the upper Pleistocene/Holocene contact;
- delineate the various types of late Pleistocene deposits to the extent possible.

Survey Vessel

The vessel used for the investigations was the R/V KANA KEOKI, leased by the USGS from the University of Hawaii. The R/V KANA KEOKI, originally built as an offshore supply boat in 1967 and converted and outfitted for marine geologic and geophysical research by the University of Hawaii in 1970, has an overall length of 156 feet and beam of 36 feet. The vessel carries an operating crew of 15 and has accommodations for a scientific crew of 15.

The work at sea was divided into three cruise legs: two of 15 days duration and a third lasting 21 days. A total of 31 scientists and technicians participated in the three cruises. Chief scientists for the cruise legs were: Alpha, Charles Holmes; Bravo, Gerald Shideler; and Charlie, Henry Berryhill, Jr.

Navigation and Positioning

Field station positioning for the sampling and vessel navigation for the geophysical surveying for most of the work was provided by Decca Survey Systems, Inc. on a subcontract to USGS. The precision system was Hi Fix^{R} operating in a hyperbolic mode with a lane transmitting separation of 50 feet. The system consisted of a master transmitting station, two slave stations and a shipboard receiving system consisting of two receivers and an antenna. For the South Texas OCS two Hi Fix^{R} service chains were utilized during the geological cruise: Palacios and Brownsville. Lane counts were acquired at specified petroleum production platforms and temporary buoys, and were tracked on an analog recorder. During the seismic reflection profiling, shot point fixes were taken every 2000 feet. All station locations and geophysical tracks were preplotted by Decca from material and specifications provided by USGS.

Use of alternate navigation systems in lieu of Hi Fix^{R} during parts of Leg Charlie were necessary because of sky wave problems during the night hours when it was necessary to run continuously during seismic reflection profiling. A combination of Satellite, Loran A and Hi Fix^{R} within two to three lane counts was used during the night hours. When Hi Fix^{R} positioning within two to three lane counts was used, the lane count was tied to a petroleum platform position during daylight hours so that the lane counts could be post-plotted as accurately as possible.

Station Sampling

A sampling net of 274 bottom stations spaced along 27 transects was established. The location of the bottom stations is shown on figure 5 (plate B). The unmodified base has been used to show all sample locations so that station locations can be related to the more detailed bathymetry shown. The following

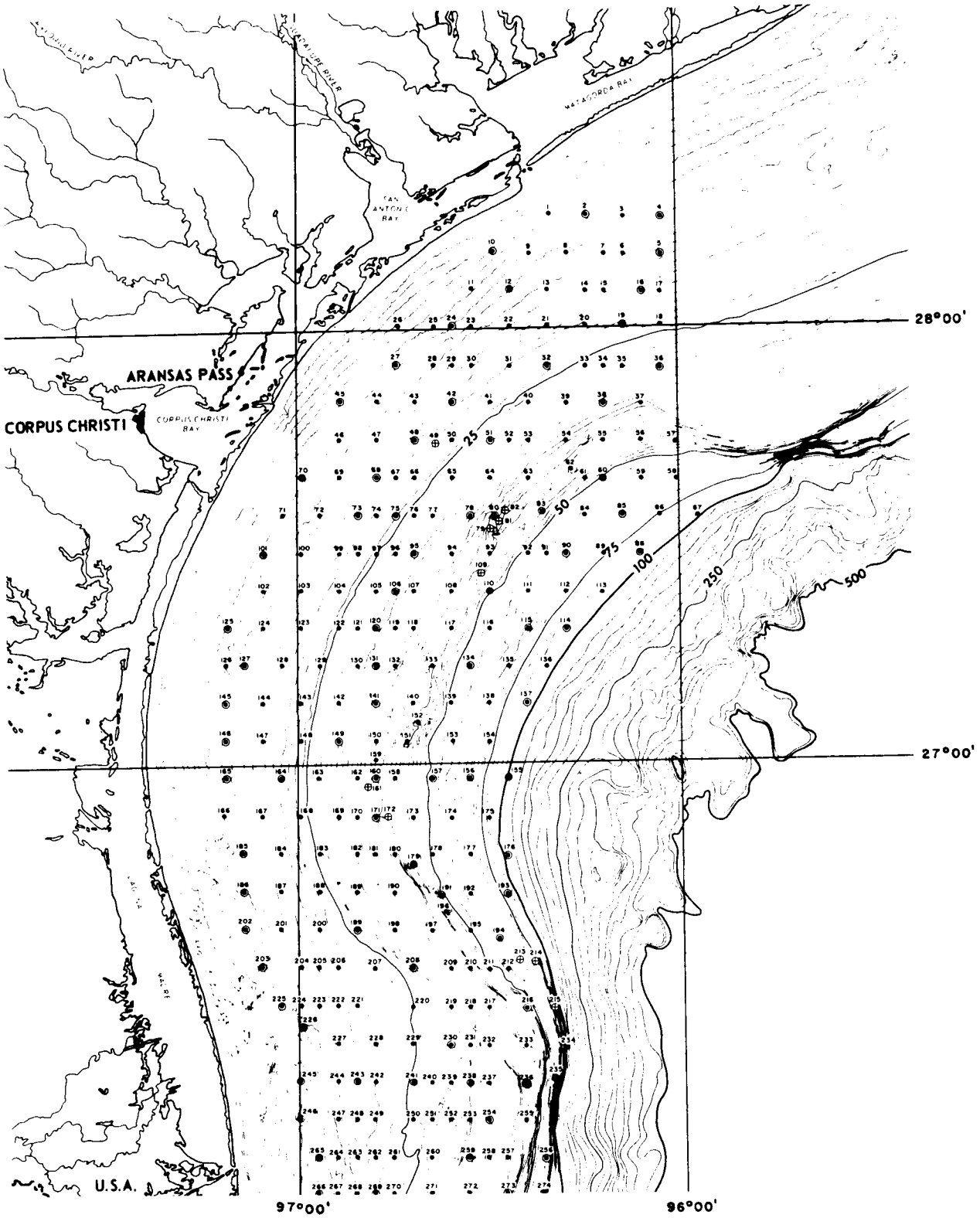

Figure 5. Location of benthic sample stations for geologic studies. • indicates bottom grab; ● indicates both pipe core and box core in addition to bottom grab; ⊕ indicates pipe core only.

rationale was used in establishing the bottom station network: adequate regional coverage; spacing to provide a sample for each of the blocks nominated for lease bid; and the geology of the area to the extent known prior to the study, including the physiography of the sea floor and general sedimentological and tectonic patterns.

At 264 stations, a bottom grab was taken using a Smith-MacIntyre sampler having 0.1 m^3 capacity. From each grab sample, seven subsamples were taken for the various analyses to be made and for the archives. The subsamples were taken by inserting plastic tubes 15 cm long and 3.8 cm in diameter into the sediment. The tubes were capped and sealed. Subsamples for organic carbon, carbonate and archive samples were frozen aboardship and transferred to the laboratory frozen. At 90 selected stations, a pipe core was obtained: 80 cores were taken at the grab sample stations; 10 cores were taken at stations other than at bottom grab stations. The gravity-fall pipe corer was constructed of stainless steel and the core was retained in a plastic liner having an inside diameter of 7 cm (2.75 in). At 74 of the 90 pipe core stations, a box core was taken using a sampler of 1 ft^3 capacity. The location of the pipe core stations is shown by figure 6 and the box core stations by figure 7. Although they are included on figure 5, the locations of the pipe core and box core stations are repeated for clarity and utility.

At 24 of the 264 bottom grab stations, samples were taken at three levels in the water column for suspended sediment: surface, mid-water depth, and near-bottom. The locations for the suspended sediment samples are shown by figure 8.

As augmentation to the physical oceanographic studies, XBT (expendable bathythermograph) casts were made at 128 of the 264 bottom grab stations and surface drifter bottle casts at 80 stations. The locations of the XBT and surface drifter stations are shown by figures 9 and 10.

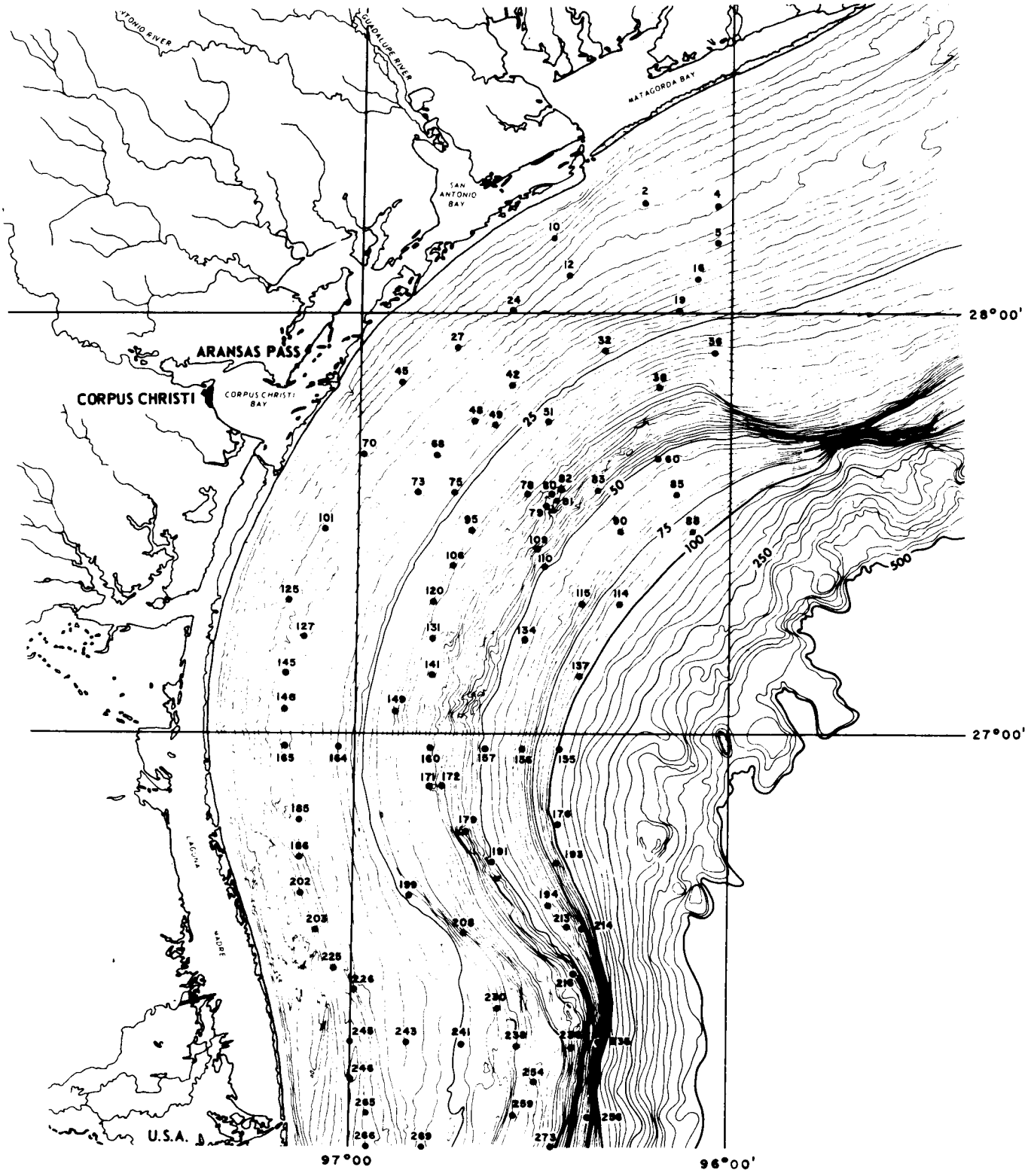

Figure 6. Location of pipe core stations.

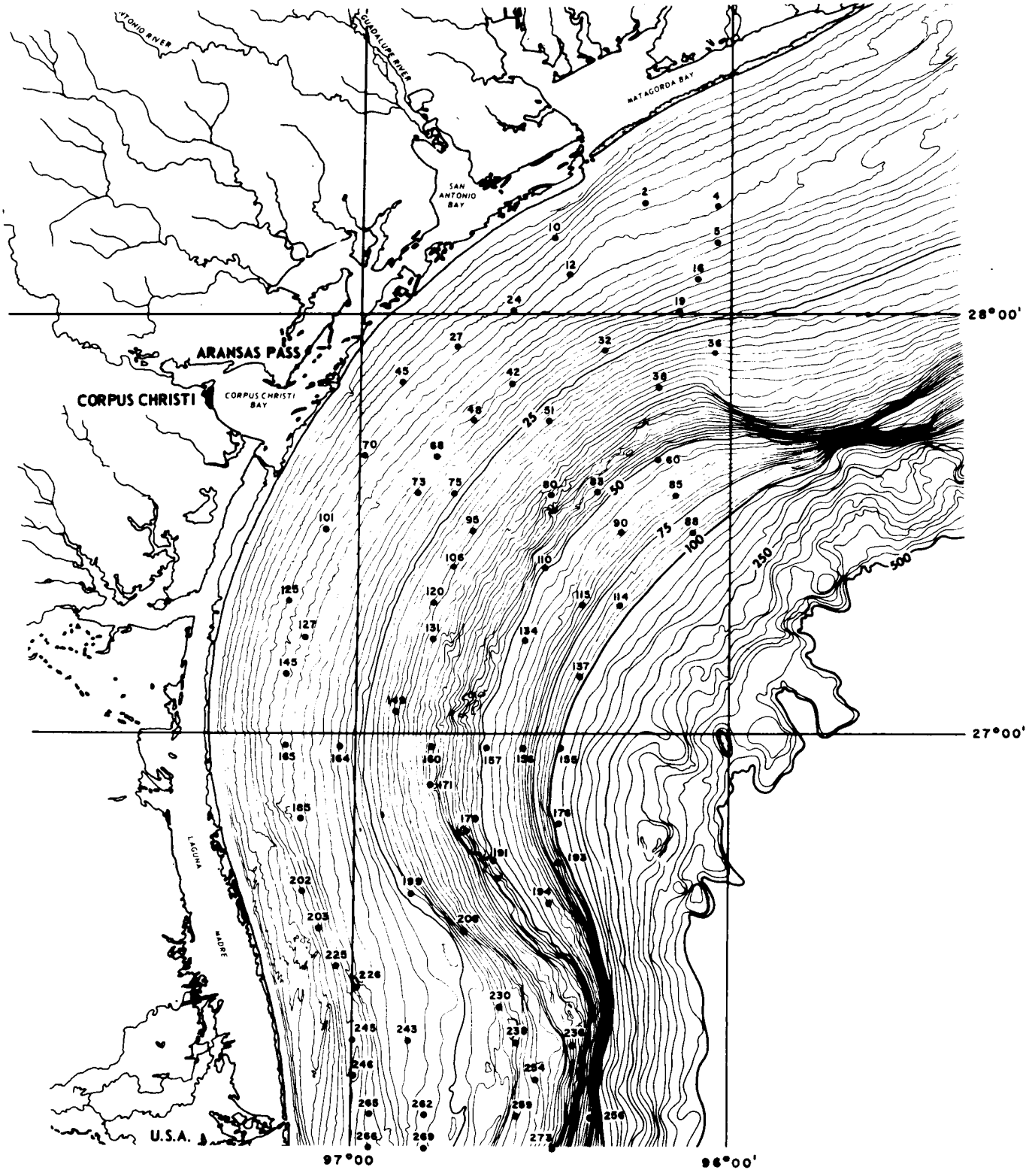

Figure 7. Location of box core stations.

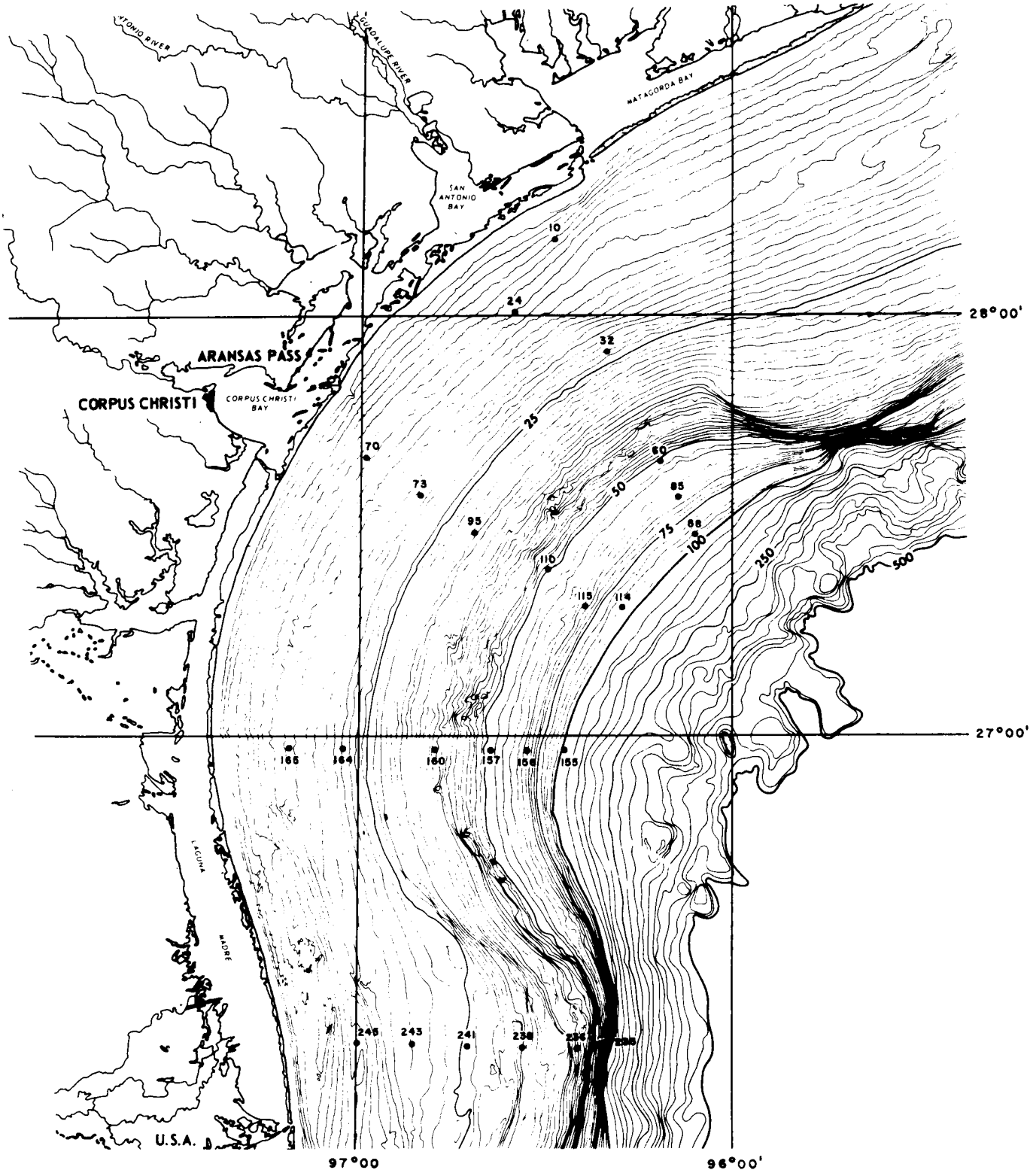

Figure 8. Location of sample stations for suspended sediments.

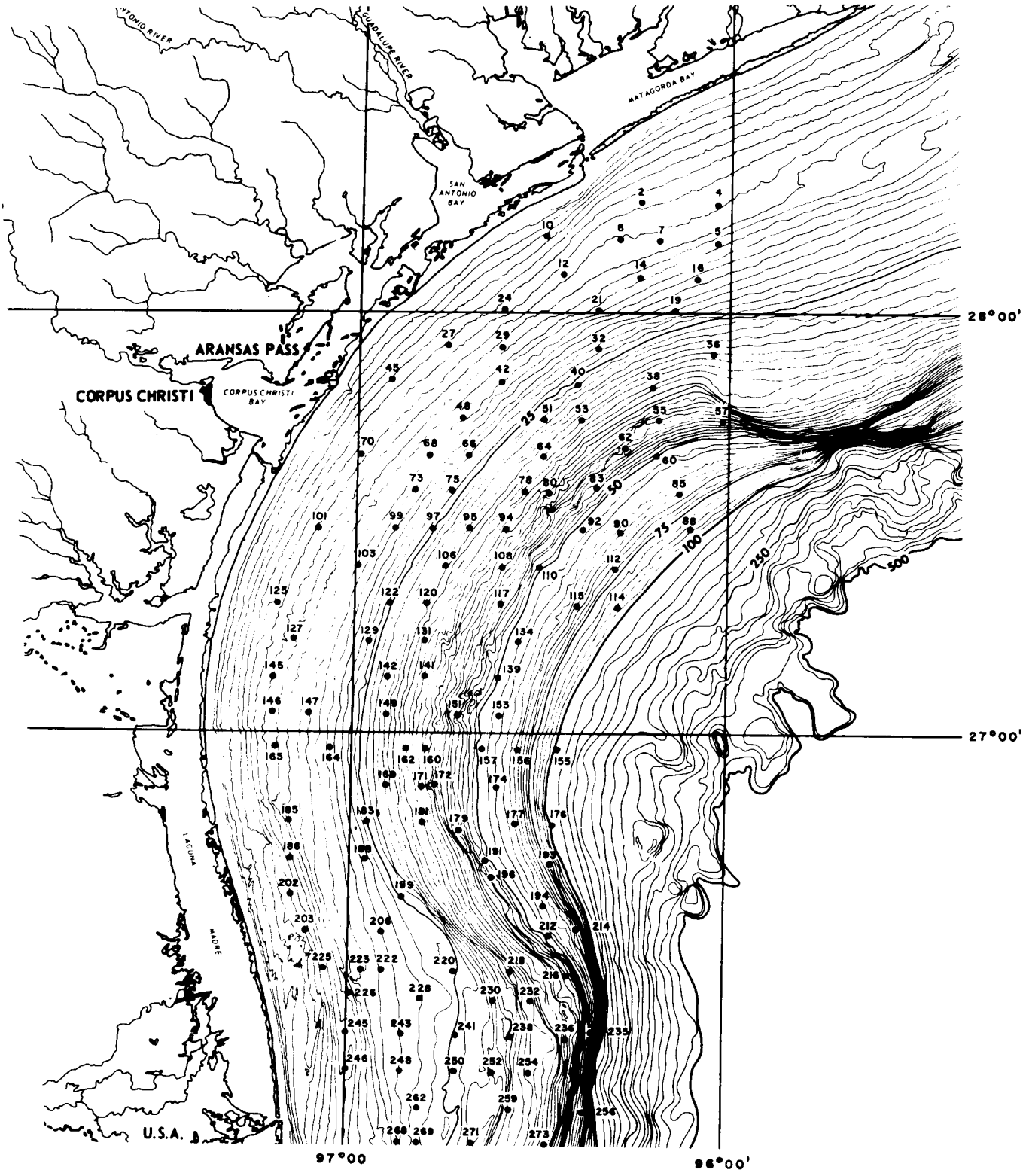

Figure 9. Location of XBT stations.

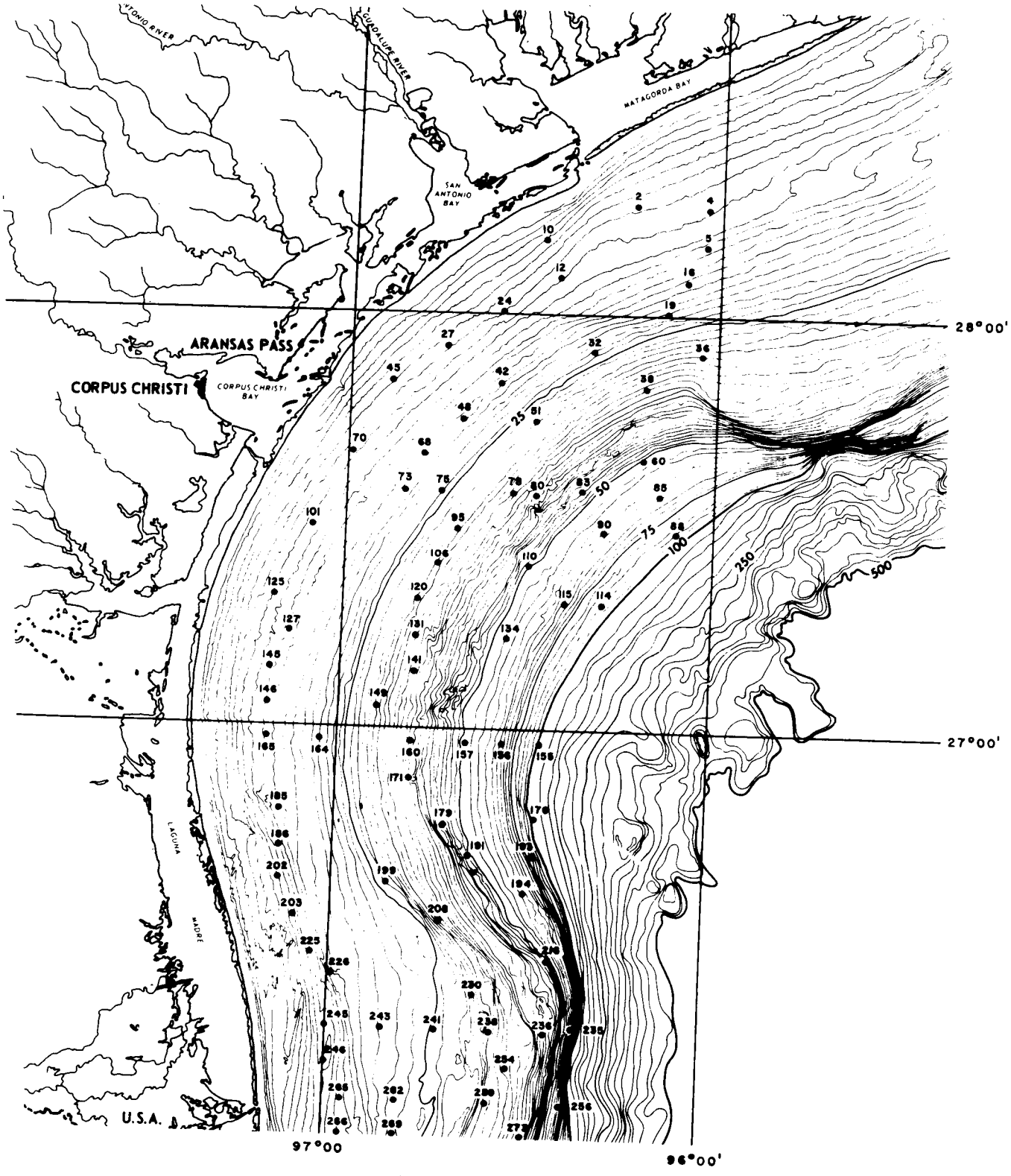

Figure 10. Location of surface drifter cast stations.

A summary of samples collected by type and number is shown by the listing.

Summary: samples collected by type and number

Temperature and depth (XBT)	128
Suspended sediments for trace metal analysis	72
Sediment samples for benthic infauna analysis (box core stations)	74
Sediment stations for hydrocarbon analysis (box core stations)	74
Sediment samples for trace metals analysis	264
Sediment samples for textural analysis	264
Sediment samples for clay mineralogy	74
Sediment samples for percent heavy minerals	74
Sediment samples for carbonate analysis	264
Sediment samples for organic C analysis	264
Cores for lithologic stratification and biogenic structures	90
Box cores for near surface depositional structures	74
Bottom photographs	60
Sediment samples for biogeologic studies (washings of all grab samples)	264
Drop of surface drifters (bottles), three at each of 80 stations	80
Total	2,120

Geophysics

Geophysical data used for compiling the geologic framework were 11,260 km of high resolution seismic reflection analog profiles, including 8,860 km made available by the Conservation Division of USGS and some 1,600 km collected on cruise leg Charlie. In addition several hundred miles of side scan profiles

were obtained on leg Charlie, principally to serve as augmentation to the reef studies being conducted on the South Texas OCS by Texas A & M University under a separate contract with the BLM.

No commitment for a specific amount of acoustic profiling was stated in the USGS contract with the BLM. As originally planned, cruise leg Charlie was to have been devoted entirely to geophysical surveying. However, continuing severe problems with the Hi Fix^{R} navigation system plus loss of the box corer halfway through leg Bravo pushed some 10 days of station work into leg Charlie, thus decreasing the amount of geophysical data ultimately obtained.

The side scan sonar system used was a Klein Model 400 leased from Ocean Systems, Inc. Scale ranges of 75 and 150 m were used depending on the detail desired and some 483 km of side scan imagery was obtained. In the early part of the geophysical surveying the side scan sonar was used across the shelf to determine the general nature of small scale topographic features on the continental shelf. However, the bottom proved to be so smooth and featureless that it was not worth the loss of time necessitated by the slow ship speed required to routinely use the side scan sonar on regular shelf traverses. Consequently, the side scan sonar surveying was concentrated over the topographic highs (reefs) on the outer shelf. The side scan sonar imagery for the reef traverses was turned over to personnel of Texas A & M University for use in their study.

Several different acoustic profiling systems were used to acquire the reflection data. The systems used are described in detail in the introduction to the geologic framework.

Principal Investigators

Element leader for the geologic investigations is Henry Berryhill, Jr. who also serves as Manager/Coordinator for the overall South Texas OCS project.

Principal investigators delegated responsibility for carrying out laboratory analysis, interpretation, compilation and reporting of data for the various aspects of the geologic investigations are:

Sediment texture, mineralogy and general sedimentation	Gerald Shideler
Sediment stratification and depositional structures, pipe and box cores	Henry Berryhill, Jr.
Trace metal, carbonate, organic C, and clay mineralogy of sediments	Charles Holmes
Trace metals, suspended sediments	Stephen Barnes
Clay mineralogy of suspended sediments	Charles Holmes
Geologic framework	Henry Berryhill, Jr.
Sea floor stability	Henry Berryhill, Jr.
Biogeology and biogenic structures	Gary Hill

Support investigators on the contract were John Dillon and Ann Martin. In addition, Ray Martin, though not paid under terms of the contract, gave assistance in the interpretation of the geologic framework. Charles Holmes, in addition to his responsibilities for the trace metals work, also gave assistance in interpreting the acoustic profiles.

Reporting

The report covering the geologic investigations has been divided into two parts. Part I is the text which describes and interprets the data: Part II includes the listing of the sample material and hard copy raw data archived and the basic analytical data in a series of tables. For ease in transferring the basic analytical data in Part II to NODC, the tables are computer print-outs using a modification of the USGS RASS-STATPAC system in which all analytical data are keyed to the descriptive data for individual sample stations. Table I

in Part II is the basic inventory listing for each bottom station giving the location of the station in both geographic and Lambert X-Y coordinates, water depth, and types of samples collected at the station. The basic analytical data in the tables that follow in Part II are keyed to the station numbers and type of sample listed in Table I.

Analytical results, descriptions and interpretations have been compiled and are presented in map form wherever possible so that the regional geologic characteristics of the area will be readily apparent and the interrelationships of the various environmental aspects more easily understood. First order descriptive and interpretive maps have been compiled for all data; in addition second order derivative maps have been compiled for some aspects to increase utility and to relate the data to regional processes. Most of the maps are presented at two scales: larger scale of 1:480,000 to facilitate management use; and reduced scale in the text for ease of reference. The Hi Fix^{R} plots for the station locations are at a scale of 1:96,000 on a lease block grid.

Mapping, except for the geologic framework, has been done on a modified bathymetric base; the geologic framework has been compiled on the lease block grid because the location of all shot points or precision navigation fixes along acoustic profile traverses were plotted at sea and compiled on a lease block grid map. The bathymetric base was modified by removal of all but several key isobaths so that the compilations, which by necessity must be presented in black and white, would not be rendered illegible by the numerous closely spaced isobath lines. Unfortunately this problem could not be resolved in the case of the lease block grid base, as removal of the lease block numbers would make the data less usable.

The two base maps are not exactly conformable because two different map projections were used when the base maps were compiled originally.

All analytical techniques and processing steps used in the laboratory analysis and treatment of the raw sample material and data are described in detail in the pertinent sections of the text.

The order in which the topical subject material is presented has been arranged for the maximum integration of subject matter relative to the cause and effect relationship of the geologic processes and the relative spans of time involved. The tectonic movements within the continental terrace establish the geologic framework to which surficial sedimentation processes respond. Thus the geologic framework, which represents the cumulative effect of forces acting over relative long periods of time, are discussed first, followed by sedimentation and related aspects of study which represent the most recent response to the structure of the sea floor as well as response to the physical oceanographic characteristics of the region.

ACKNOWLEDGMENT

The 8,860 km of acoustic profiles that served as the main source of data for interpreting and compiling the geologic framework were acquired by the Conservation Division on USGS funding and made available to the Corpus Christi office for use in the South Texas OCS environmental assessment. Special thanks are extended to the personnel of the USGS Conservation Division office at Metairie, Louisiana for their cooperation and help. Without the sizable amount of geophysical data contributed by the Conservation Division, the geologic framework could not have been compiled.

STRUCTURAL FRAMEWORK, LATE PLEISTOCENE AND HOLOCENE SEQUENCE

INTRODUCTION

Geologic processes of the continental shelf are not restricted to sedimentation and the geochemical transformations that take place at and directly beneath the surface of the sea floor. The structural development of the continental terrace through geologic time is an evolutionary process and a response to both regional tectonic movements and depositional processes along the submerged continental margin. Tectonic movements may influence patterns of sediment transport and deposition by changing the configuration and gradient of the sea floor; sediment accumulation may trigger tectonic movement. To assess properly the modern sedimentary regime of any segment of the continental terrace, patterns of modern sediment movement and deposition must be related to subsurface deformational structures formed by crustal movement. Furthermore, effective safety guidelines for offshore engineering must be based on a firm knowledge of the deformational history of the continental terrace. Proper definition of the structural framework must include precise location and characterization of the salient geologic structures, particularly faults, and determination of the magnitude, frequency and chronology of their movement. Obviously, those tectonic events that have taken place in the relatively recent past are the most critical in assessing the modern environment in terms both of the impact on the pattern of sedimentation and the susceptibility of the sea floor to movement in the future.

The structural framework has been determined by mapping all folds and faults that have affected late Pleistocene and Holocene sediments. The chronology of movement of the folds and faults has been established by the

preparation of isopach maps for two prominent horizons of regional extent within the late Pleistocene/Holocene sequence and by relating fault movement through time to the two key horizons and to the sea floor.

METHODS OF STUDY

The basic data for interpretation of the geologic framework are approximately 8,860 km of high resolution acoustic reflection profiles arranged in a track grid spacing of approximately 5 by 10 km. The systems used for collecting the geophysical data were: Acoustipulse^{R} with a transmitting power of 1000 joules and recorded at a sweep rate of 250 ms (1/4 sec); Analog Reflection^{R} sparker transmitting 900 joules and recorded at a sweep rate of 1000 ms (1 sec); Sparker transmitting 10,000 joules and recorded at a sweep rate of 1000 ms (1 sec); and Sub-bottom Profiler^{R} transmitting 10 kw (3.5 kHz frequency) and recorded at a sweep rate of 500 ms (1/2 sec). The location of the acoustic profiles coded as to the several types of acoustic reflection data obtained are shown by figure 11 and plate 1. The navigation fixes taken at intervals of 305 m along most of the traverses and at 610 m along others established the data points for plotting.

Geologic and structural features recorded on the geophysical profiles were identified, marked and coded. Depths of the marked features and key reflecting horizons beneath the sea floor were then plotted on the navigation charts at each of the 35,000 fix points or navigation stations. Interpretive and derivative maps were compiled from the fix-point data plots. The following basic interpretive maps were prepared: geologic position of all folds and diapirs recorded on the 10,000 joule sparker profiles; an isopach map for the sediments above reflecting horizon A, including the geographic position of all faults that

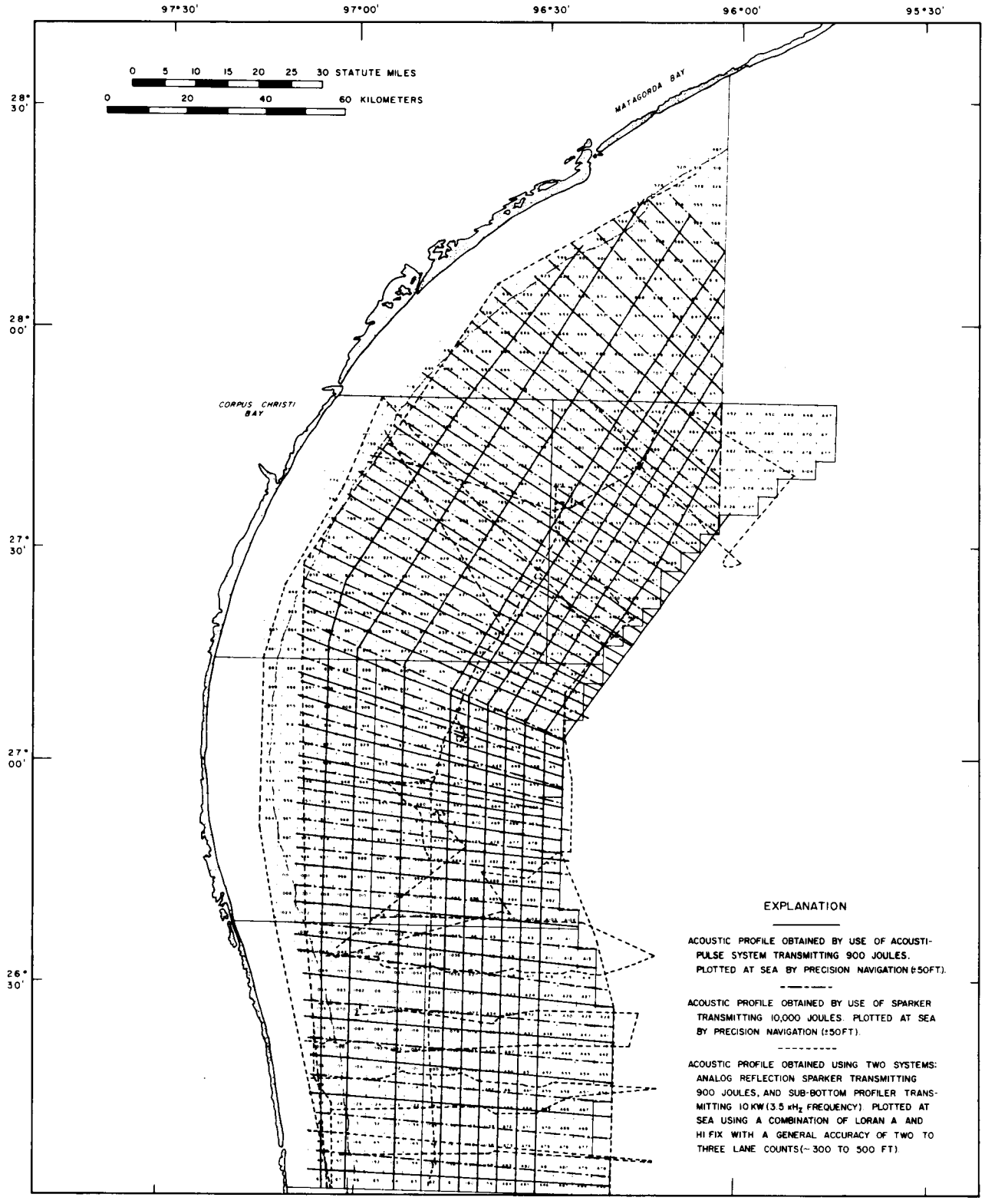

Figure 11. Location of geophysical track lines.

offset reflector A as well as those that extend to the sea floor; an isopach map for the sediments above a deeper lying reflecting horizon designated as reflector B, including the geographic position of all faults that offset reflector B; and a fault movement chronology map that relates both general fault movement and growth fault movement to the two mapped reflecting horizons and to the sea floor.

The depths and thicknesses of subsurface features on all maps are given as two-way travel time of sound in milliseconds (ms). No data were available for determining the actual velocity of sound travel through the sediments mapped. Consequently thicknesses referred to in the discussions that follow are approximations based on use of the average travel time of sound through sea water which is 0.78 m (2.4 ft) per millisecond.

FOLDS

A number of anticlinal crests were recorded on the 10,000 joule sparker analog profiles. The average depth from the sea floor to the crests is -200 ms or approximately -146 m (480 ft). The location of the anticlinal crests and the magnitude of their closure at a subsurface depth of 800 ms are shown on figure 12 and plate 2. The anticlinal crests at the relatively shallow depth recorded tend to be discontinuous; however, several extend for distances of 29 km or more. Some of the anticlines which seem to die out over a short distance along strike may connect at greater depth.

The regional trend of most of the anticlines is N 30° to N 45° east but there are exceptions. Over the northern half of the South Texas OCS the northeastward regional trend of the anticlines generally is parallel to the present trend of the shoreline; over the southern half the trend is oblique to the shoreline which bends to the south-southeast except on the outer shelf where the orientation is north-south.

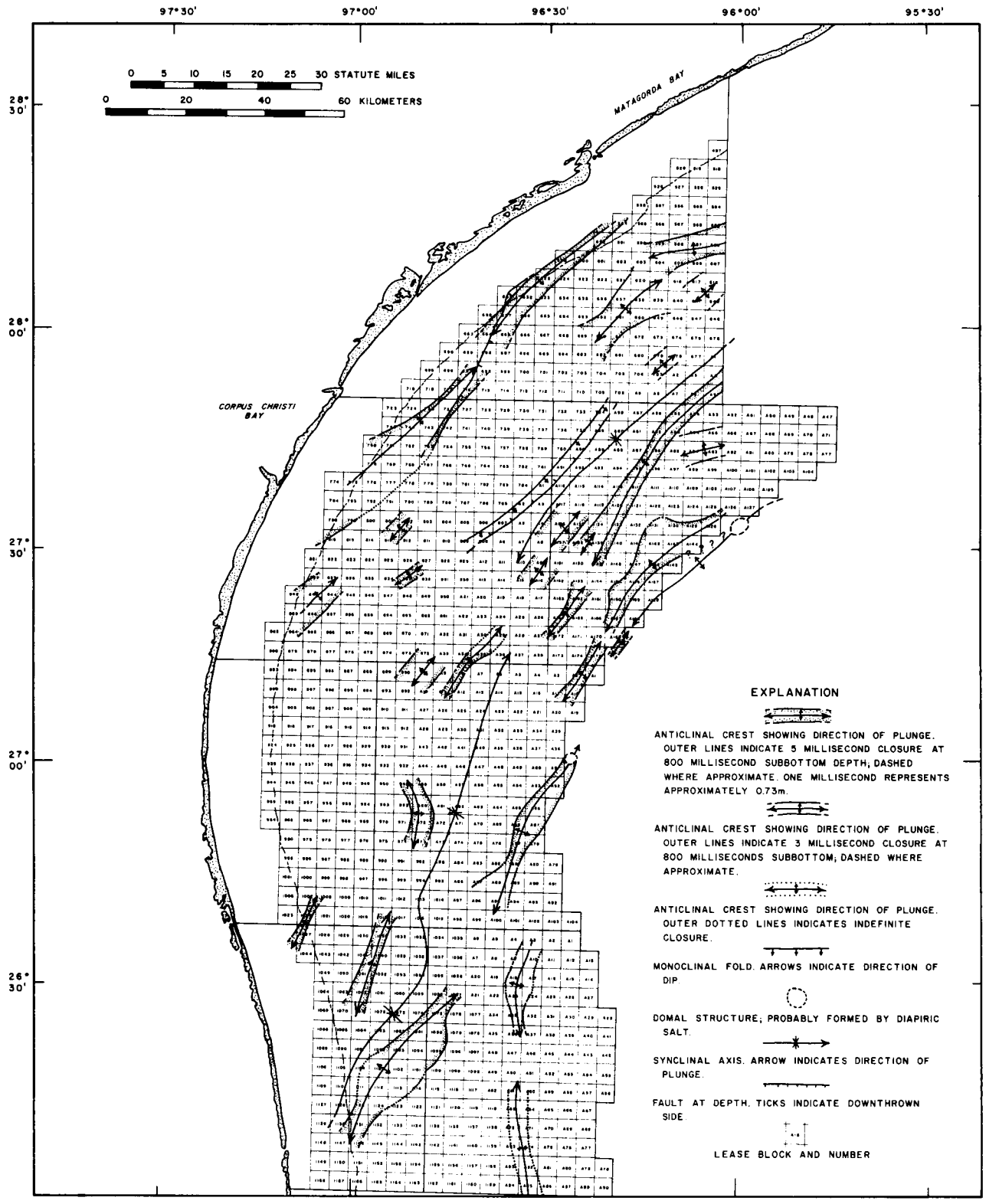

Figure 12. Location of geologic structures within the continental terrace.

The synclinal troughs between the anticlines are not well defined within the limits of the acoustic profiler, and the axis of the synclinal troughs could not be mapped. Consequently, the symmetry of the folds could not be determined. Two broad synclinal troughs of very shallow amplitude trend northeast along the mid-shelf in an en echelon pattern.

Two domal structures probably formed by diapiric movement of salt are located at the outer shelf edge, just beyond the South Texas OCS lease block grid (see figure 12 and plate 2). The domal structures are associated with branching anticlinal crests that lie along the juncture of the continental shelf and the continental slope.

FAULTS

Every anticlinal crest shown on figure 12 (plate 2) is faulted. The faults are on both sides of the anticlinal crests and they tend to converge downward toward depth points that commonly lie beneath the limits of the sparker records. Along many of these faults, throw increases with depth, indicating progressive movement through time. A typical example of the pattern of faulting associated with the anticlines is shown by figure 13. The segment of geophysical profile shown in the figure lies normal to the trend of the anticline where the anticlinal crest crosses lease block A-86 from northeast to southwest.

The faults were not mapped on plate 2 but instead are shown on the isopach maps for reflectors A and B so that fault movement and chronology of faulting can be related to progressive stages of tectonic movement and sediment accumulation during late Pleistocene and Holocene times. On the isopach maps, only those faults that have displaced strata above reflectors A and B are shown.

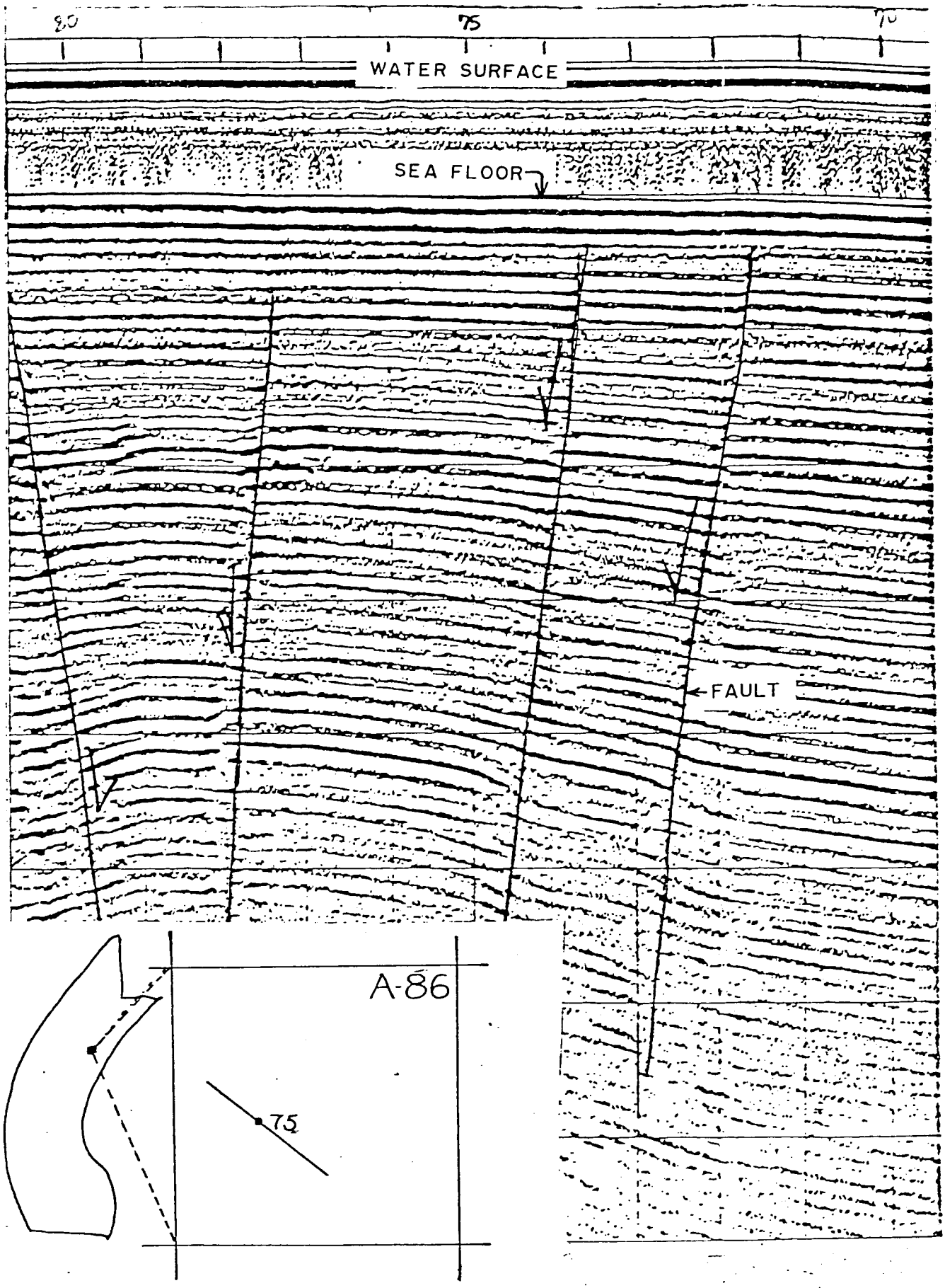

Figure 13. Section of an acoustic profile showing typical faulting above anticlines. Vertical timing line interval is 100 ms (~73m).

REFLECTING SURFACE B

Definition

The older of two prominent reflecting surfaces of regional extent recorded on the acoustic profiles is designated for the purpose of this report as reflecting surface B. The approximate geologic age of the surface can be stated with confidence as late Pleistocene. The precise age in terms of sea level fluctuations during the late Pleistocene is not known. The age designation of late Pleistocene for reflector B is based on the stratigraphic position of the surface relative to strata dated geologically in the Continental Offshore Stratigraphic Text (COST) well No. 1 drilled in South Texas lease block 1076 (Khan and others, 1975). The authors state that "the youngest Pleistocene sediments identified in the COST No. 1 are of Sangamon age. The top of the Sangamonian sediments is placed at 450 feet."

The 137 m (450 ft) depth position in COST No. 1 was plotted on the several acoustic profiles that lie within a few miles of the well and related to the subsurface depth of reflecting surface B on the same profiles. In OCS lease block 1076 the depth from the sea floor to reflector B is approximately 94 m (275 ft). Whether or not the specific horizon in COST No. 1 has been correctly dated as "top of Sangamonian.", reflector B, on the basis of its stratigraphic position, can be safely dated as late Pleistocene.

Regional Configuration and Thickness of Overlying Sediment

Reflector B is an uneven horizon on the acoustic reflection profiles. The areal extent and structural shape of the surface within the continental terrace has been determined by construction of a regional isopach map (fig. 14 and pl. 3).

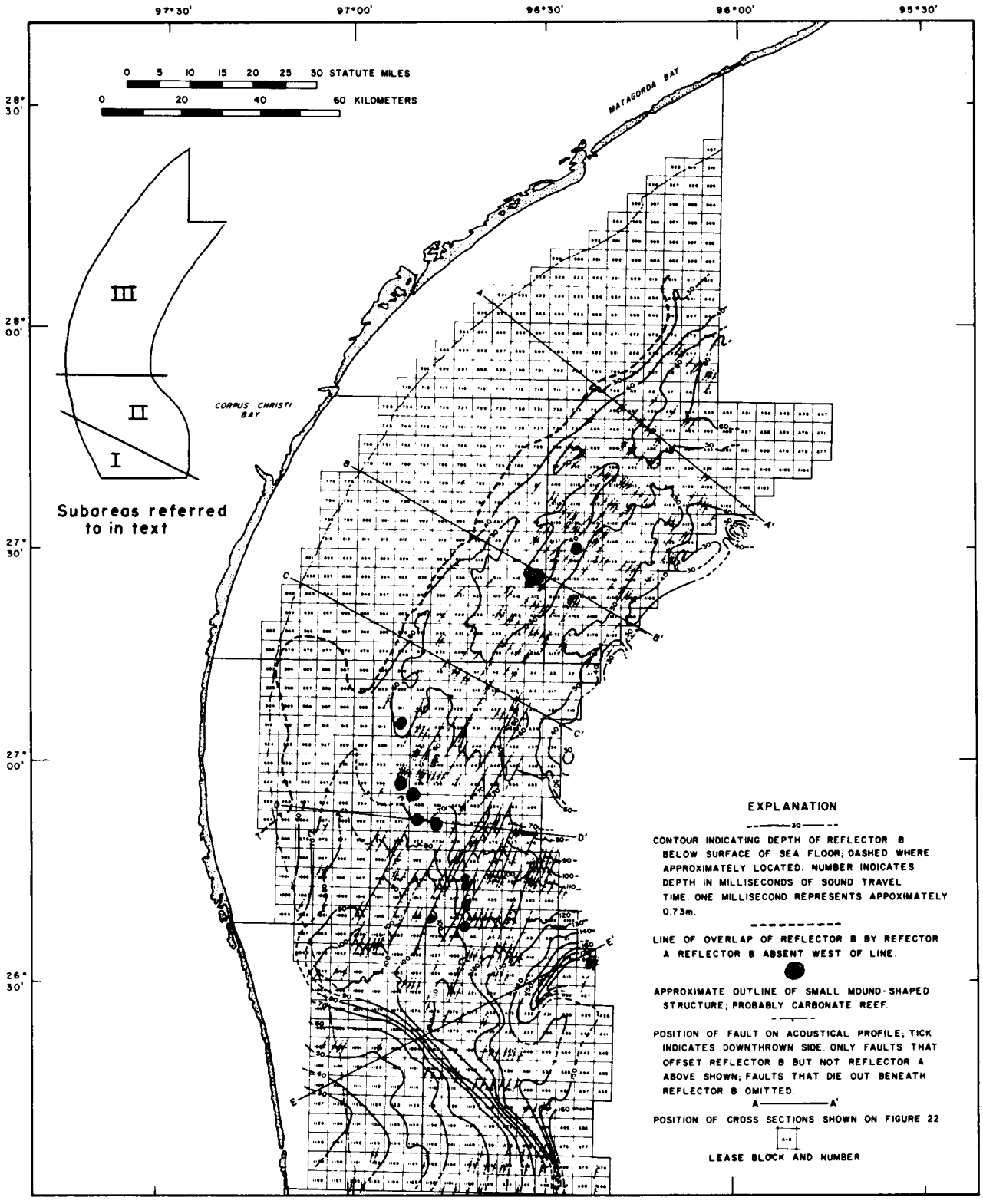

Figure 14. Thickness of sediments above reflector B.

Three subareas (I, II, and III in figure 14) are outlined by the regional variations in sediment thickness. In subarea I, the sediments are relatively thin but thicken at an increased rate toward both the east and northwest. The relatively thick sediments of subarea II form an asymmetric lens that thickens to the east-southeast normal to the regional structural grain of the continental terrace. The maximum thickness of sediment in subarea II is 180 ms (132 m). Over subarea III two northeastward-trending troughs of slightly thicker sediments are separated by an area of thinner sediments. The sediments in subarea III thicken southwestward toward subarea II except at the northeastern edge of subarea III where the sediments thicken to the northeast. Shoreward, the sediments in subarea III above reflector B are overlapped by sediments above reflector A. The line along which reflector B merges with reflector A is shown on figure 14 and plate 3.

The thickness trend of sediments in subarea III follows the structural trend of the deeper-lying folds discussed previously. Crustal downwarping or sag beneath subarea II created a localized depocenter and imposed a slight southwestward tilt on the continental terrace to the north. Timing of at least the incipient stage of crustal sag beneath subarea II as post reflector B is documented by the subsurface position of the reef-like mounds that rest directly on reflector B (see figure 14 and plate 3 for location). The shape of these mounds, their reflecting characteristics, and their pattern of distribution indicate that they are carbonate reefs that grew at or near sea level during a late Pleistocene low stand. The reef-like mounds on reflector B within subarea II are at a depth of 62 to 75 m beneath the surface of the sea floor; those farther north in subarea III are at a shallower subsea floor depth of about 29 m. The acoustic profile section in figure 15

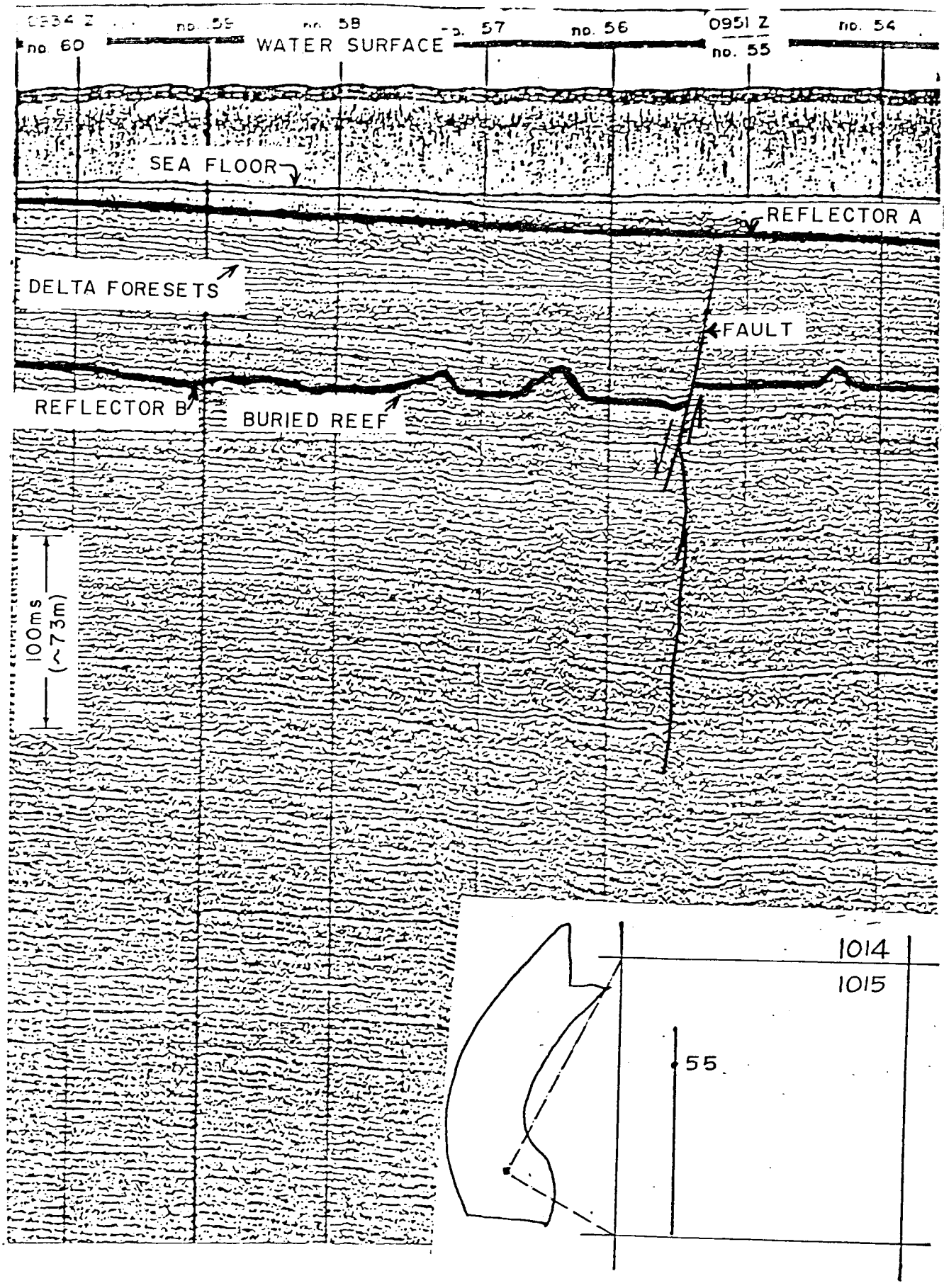

Figure 15. Section of acoustic profile showing buried reef-like structures on Reflector B. Interval between shot points is 610 m.

shows several of the reef-like mounds on reflector B within subarea II as well as the position of reflector B relative to reflector A.

Crustal sagging beneath subarea II in post reflector B time localized a depocenter on the continental shelf and apparently caused changes in the regional drainage patterns on the land adjacent to the continental shelf. The wedge or lens of thicker sediments in subarea II above reflector B is the upper part of the ancestral Rio Grande delta, deposited following diversion of the Rio Grande to a northeastward oriented course.

Displacement by Faulting

Reflector B has been extensively faulted. The location of faults that have displaced reflector B is shown on plate 3. The faults shown are those that have displaced reflector B but not reflector A, except in subarea II where some of the more extensive faults displace reflector A as well as reflector B. The trend of the faults is northeast and follows the trend of the deeper-lying folds.

Some of the faults in subarea III dip to the northwest, others to the southeast, but in subarea II the principal direction of dip is southeast. This situation indicates that the crustal depression or sag beneath subarea II was superimposed as a cross structure on the northeastward trending folds.

REFLECTING SURFACE A

Definition

The younger of the two prominent reflecting surfaces recorded on the acoustic profiles is designated reflecting surface A. It probably represents

the base of the Holocene sequence and does represent the exposed surface of the continental shelf during the most recent low stand of sea level.

Reflector A is coincident with the buried flanks of carbonate reefs of Pleistocene age whose tops have not been covered by sediments of Holocene age. The location of the reefs is shown by figure 16 and plate 4. A piece of carbonate rock dredged from the uncovered upper flank of Southern Reef in leased block A-9 by Texas A & M University has been dated by the radiocarbon (C^{14}) method at 18,990 years BP $\pm$ 370 years. A mass of coral from the Dream Reef in lease block A-41 also obtained by Texas A & M University has been dated at 10,580 years BP $\pm$ 155 years. The water depth at the summit of Southern Reef is 60 m; the water depth at the two summits of Dream Reef is 68 m and 70 m respectively.

Reflector A is defined for the purpose of the report as the surface that represents the last low stand of the sea. The interpretation is based solely on geologic evidence recorded on the acoustic profiles without qualifications as to whether or not the surface itself represents the Holocene/Pleistocene boundary or whether the boundary lies within the basal part of the overlying conformable sequence of sediments.

Regional Configuration, Development and Thickness of Overlying Sediment

Reflector A is an uneven surface and the sediments above it are disconformable to sediments below. The configuration of reflector A is shown by the isopach map for the sequence of sediments between it and the sea floor (fig. 17 and pl. 4). The nature and stratigraphic position of reflector A on the acoustic profiles at selected localities is indicated by figures 18 to 21: figure 18 shows the merger of reflectors A and B on the inner OCS; figure 19 shows the

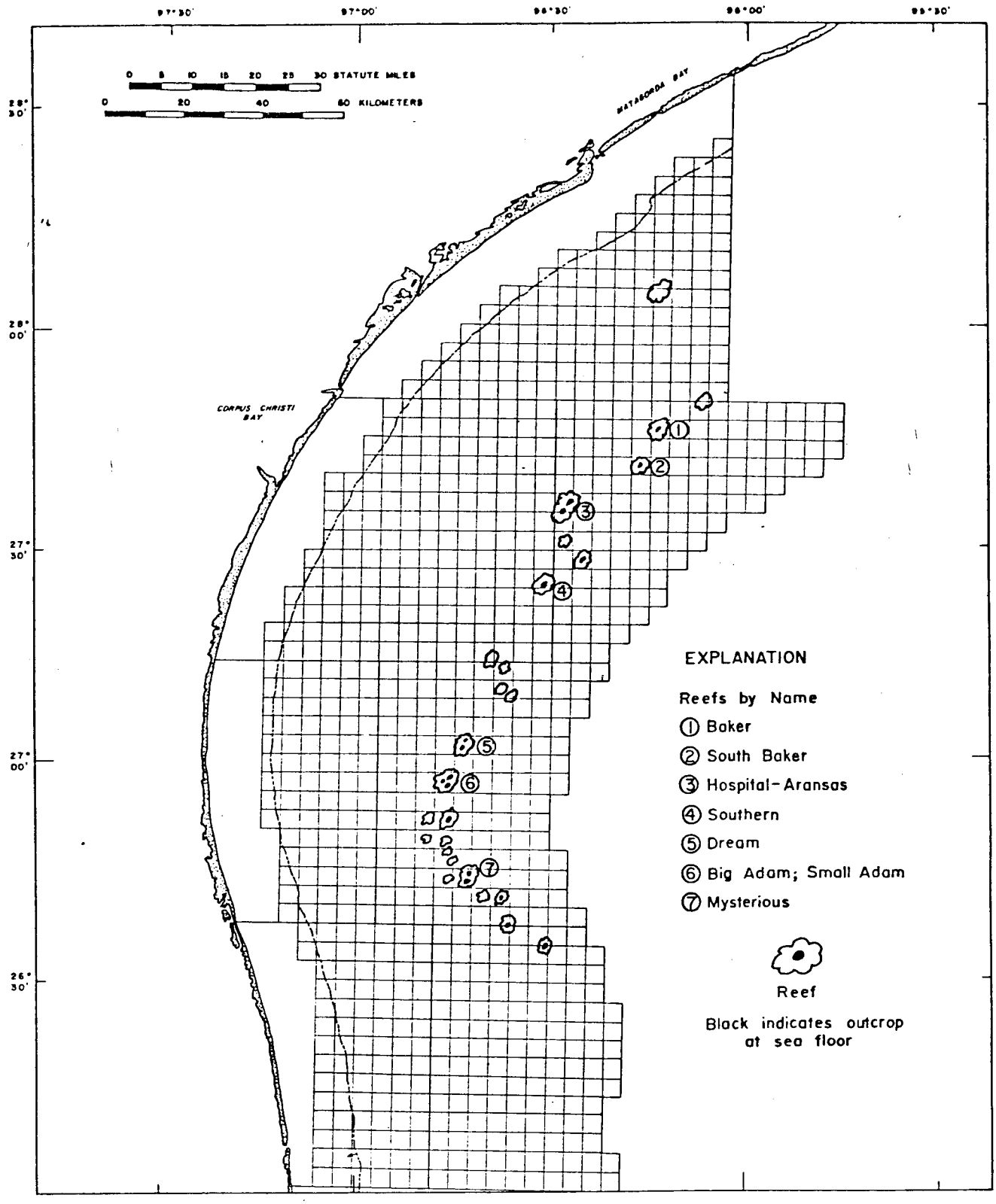

Figure 16. Location of reefs of late Pleistocene age associated with Reflector A.

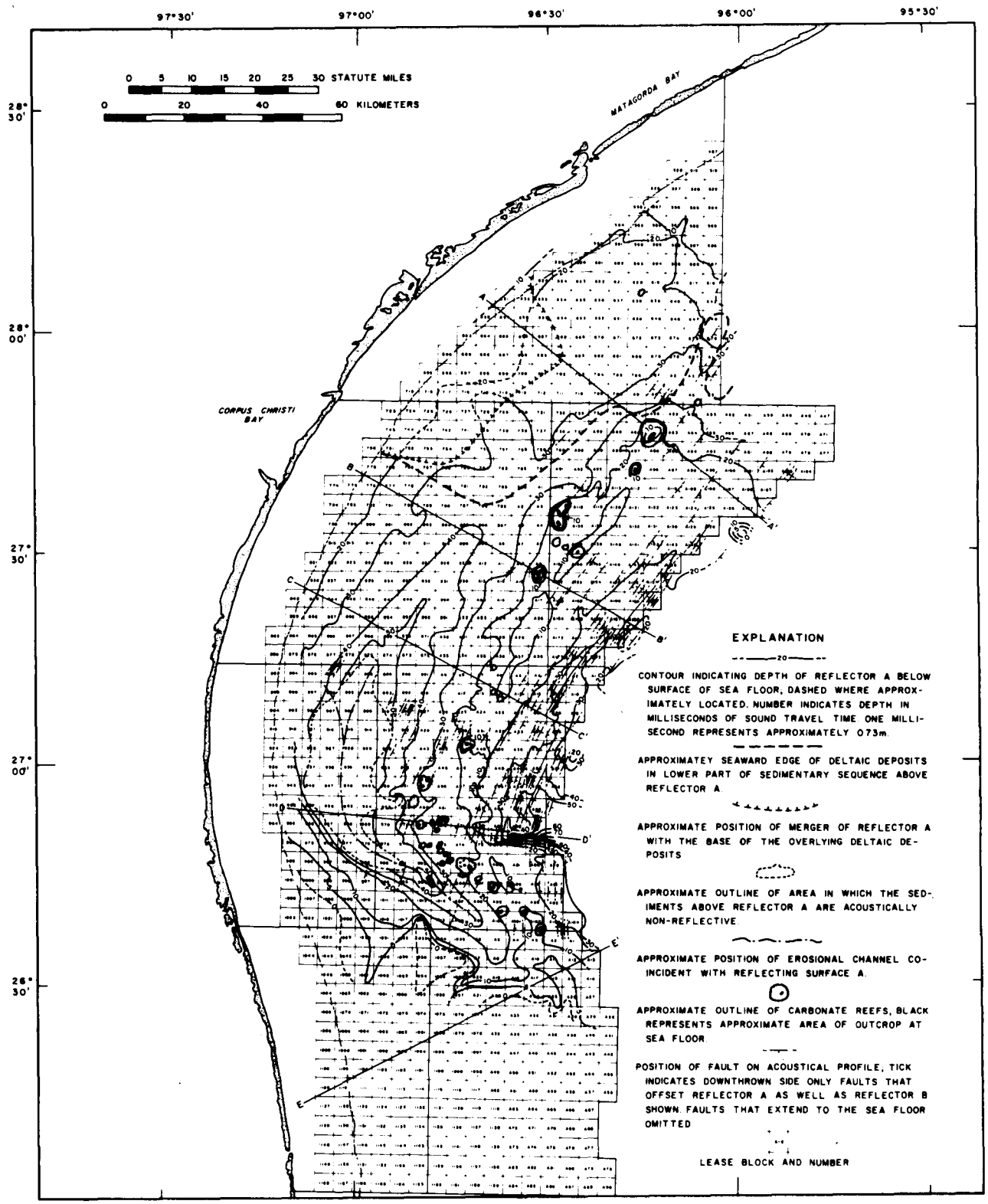

Figure 17. Thickness of sediment above reflector A.

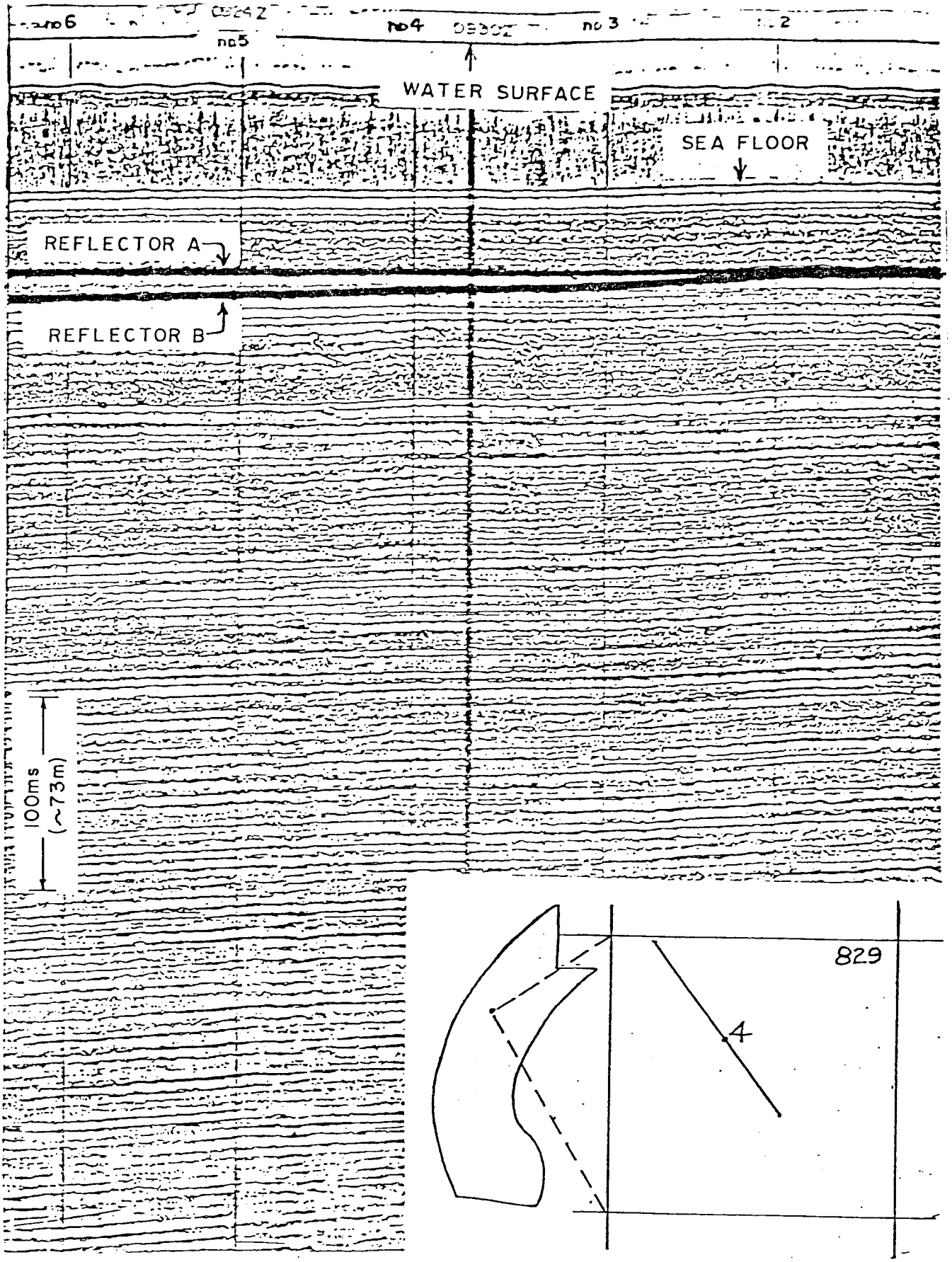

Figure 18. Section of an acoustic profile showing merger of Reflectors A and B on the inner shelf.

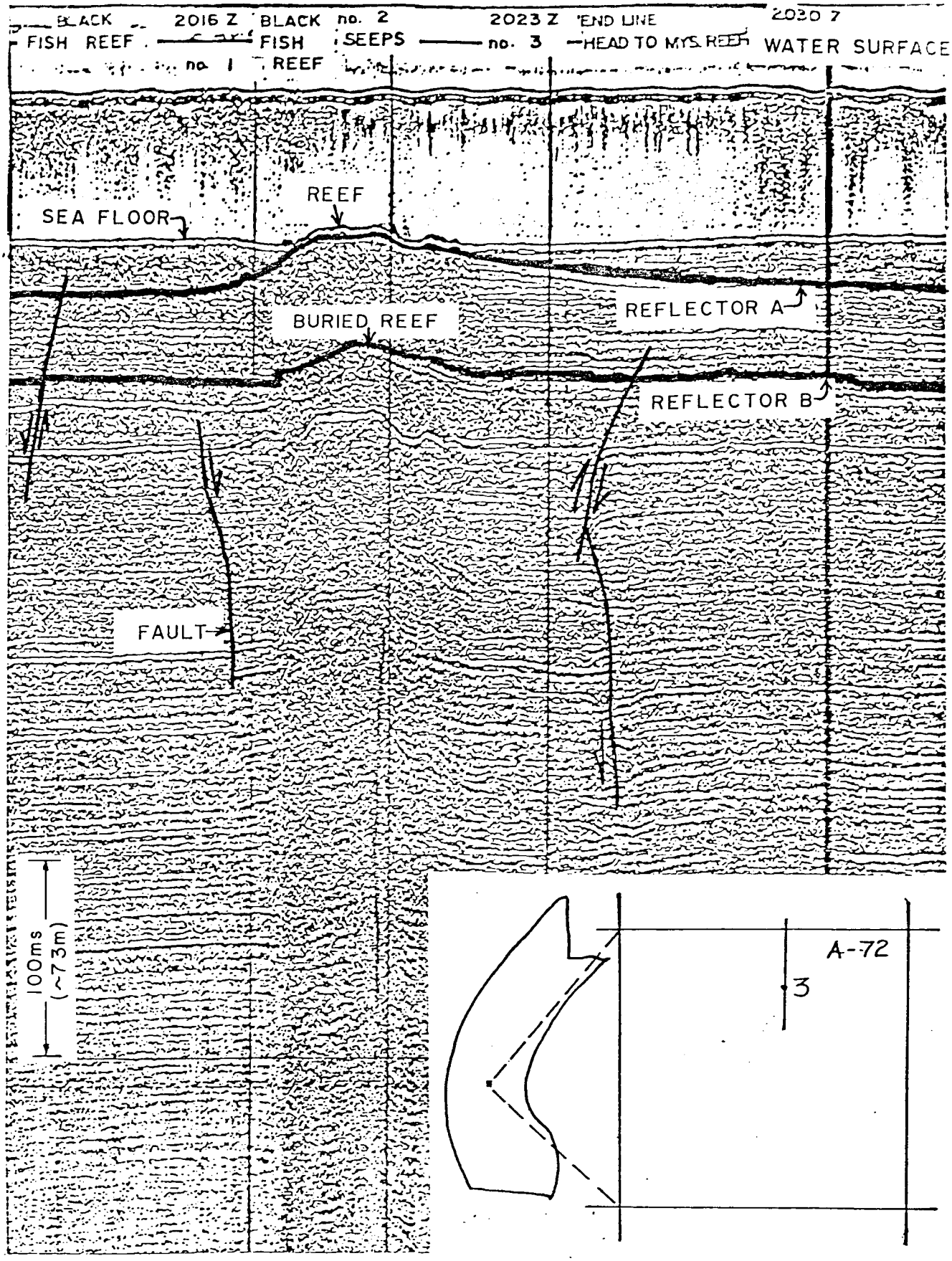

Figure 19. Section of an acoustic profile showing late Pleistocene reef outcrop at sea floor, Reflectors A and B and buried reef on Reflector B.

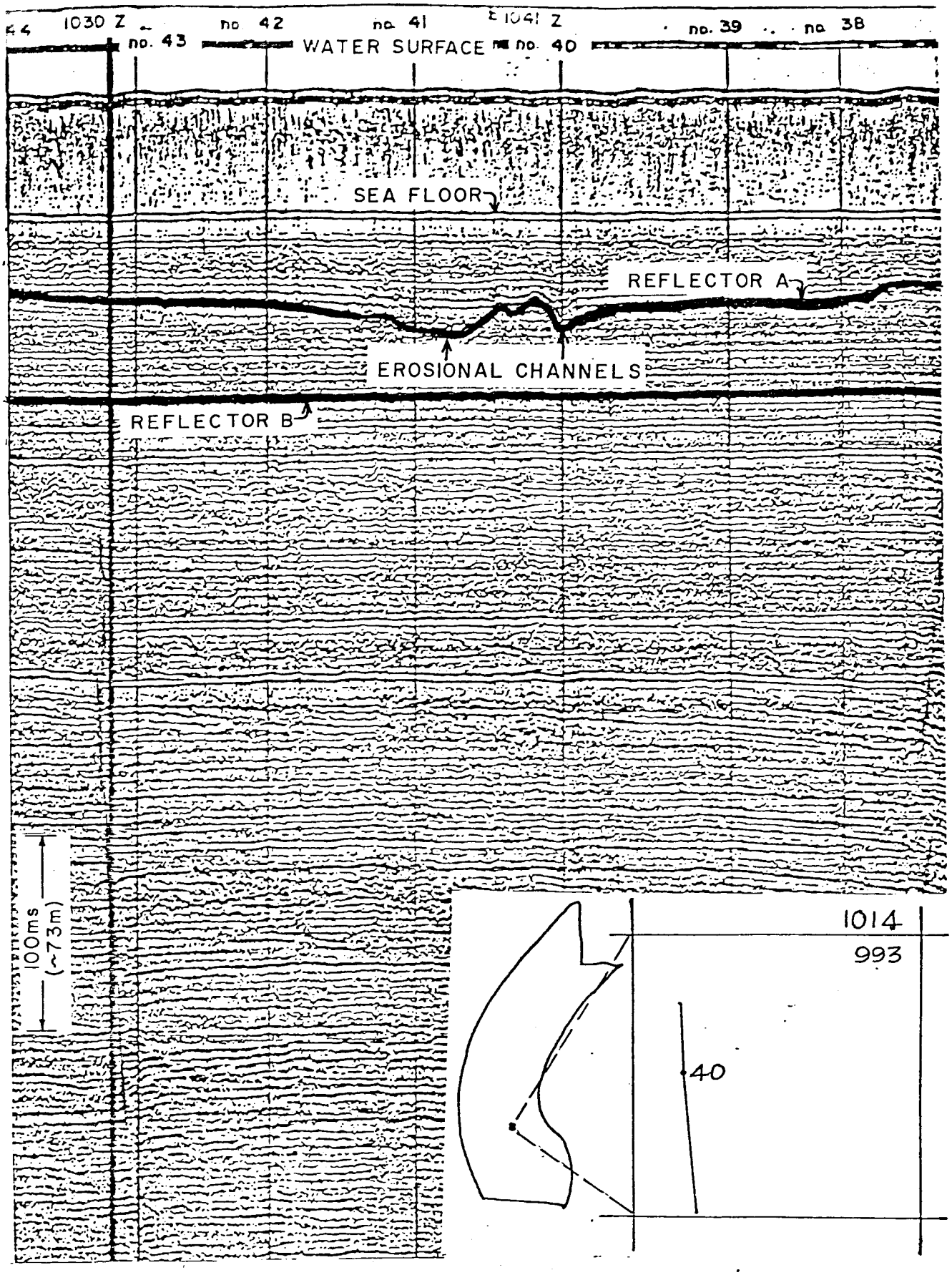

Figure 20. Section of acoustic profile showing erosional surface along Reflector A.

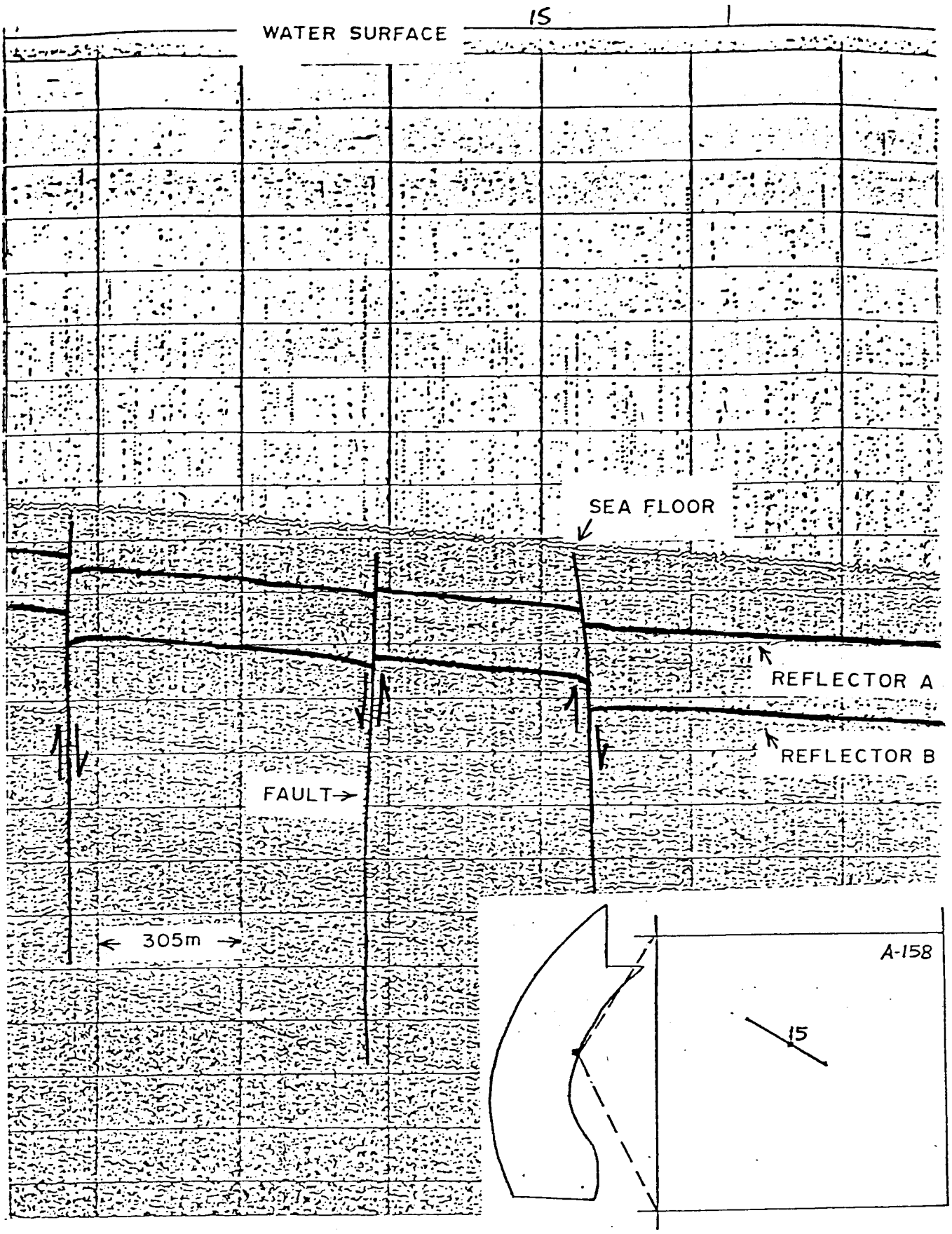

Figure 21. Section of acoustic profile showing Reflectors A and B at the outer edge of the continental terrace.

relationship of reflector A to one of the Pleistocene reefs and to reflector B on the outer shelf; figure 20 shows the erosional surface along reflector A north of the ancestral Rio Grande delta and reflector B below; and figure 21 shows the typical relationship of reflector A to reflector B and to the sea floor near the outer edge on the continental terrace. The regional relationship of reflector A to the sea floor and to reflector B is shown by the series of cross sections on figure 22. The location of the cross sections are shown on plate 4.

The thickness of the post-reflector A sequence over the northern two-thirds of the South Texas OCS ranges from zero to about 70 ms (51 m). There the sequence is thinnest at the northern edge of the study area and along a narrow arcuate belt that is slightly east of mid-shelf. The average thickness of post-reflector A sediments along this belt is 10 ms (7 m). Locally along the arcuate belt the post-reflector A sediments pinch out against carbonate reefs of Pleistocene age that are in the process of being covered by Holocene sedimentation. The reefs are on lenticular Pleistocene barrier strandline deposits that have been covered during the post-reflector A transgression. The thickest sediments are in two depocenters separated by the narrow belt of thinner sediments (fig. 17 and pl. 4).

In the southern third of the South Texas OCS the indicated average thickness of post-reflector A sediments over the ancestral Rio Grande delta is less than 5 ms (3.6 m). The post-reflector A sediments on the delta, as indicated by the acoustic profiles, appear to represent only the latest shelf transgressive phase of Holocene deposition. Three samples of mollusc shells showing no evidence of abrasion and carefully separated on a species-specific basis from bottom station 273 on the outer edge of the delta were dated by the radiocarbon (C^{14}) method at 4,050 years BP $\pm$ 100 years; 4555 years BP $\pm$ 95 years; and 5,520 years BP $\pm$ 105

EXPLANATION

Post reflector A deposits

Reflector A

Strandline deposits beneath Reflector A

Carbonate Reef

Reflector B

Faults

Position of anticlinal crest at depth

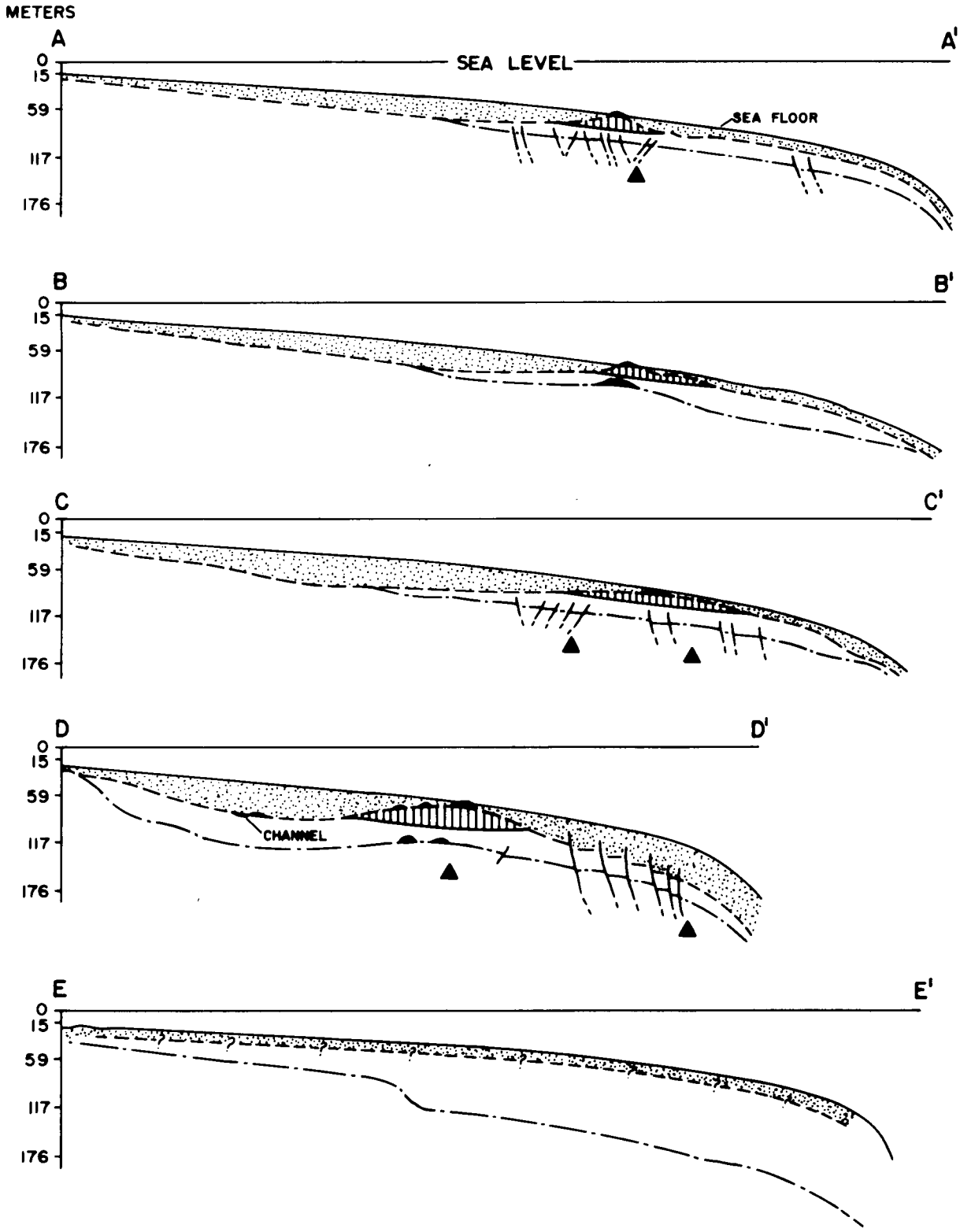

Figure 22. Cross sections showing relations of reflectors A and B across the continental terrace. Locations of the cross sections are on figures 14 and 17.

years respectively. The indicated age of the shells is Holocene. Their position at the outer edge of the delta strongly suggests that deltaic deposition continued well into Holocene time. The stratigraphic position of the Pleistocene/Holocene boundary within the deltaic sequence could not be determined on the acoustic profiles.

The variations in thickness of the sediments above reflector A indicate the topographic relief on the underlying Pleistocene surface. Postulated stages in the development of the surface are shown by three paleogeographic maps, figures 23 to 25. As sea level fell, regional drainage adjusted to the structural depression and to the southwestward tilt of the continental shelf surface toward the depression. The cluster of carbonate reefs in the northern part of the OCS may have formed during a stage of sea level fall (fig. 23). At the lowest stand of sea level, a stream channel was cut along the axis of the structural depression (fig. 24). As sea level rose, the southernmost cluster of carbonate reefs formed (fig. 25). The summit levels of those reefs in the southern cluster still exposed on the sea floor range from 12 to 30 m lower than the exposed summits of the cluster to the north. The difference in reef summit levels between the two areas may reflect influence of the structural depression in the southern area. The depression may have caused an embayment of the sea over that part of the shelf during early stages of the rise in sea level. As noted previously, the indicated age for a part of Southern Reef in the northern cluster is 18,990 years BP and for Dream Reef in the southern cluster is 10,580 years BP. Rejuvenated growth may have occurred as sea level reached the northern cluster during the rise, but no substantiating evidence is available. Furthermore, surface features of the exposed parts of the reefs in the two areas possibly indicate differing degrees of erosion. The reefs in the northern cluster are rounded and relatively smooth and terrace-like pediments are

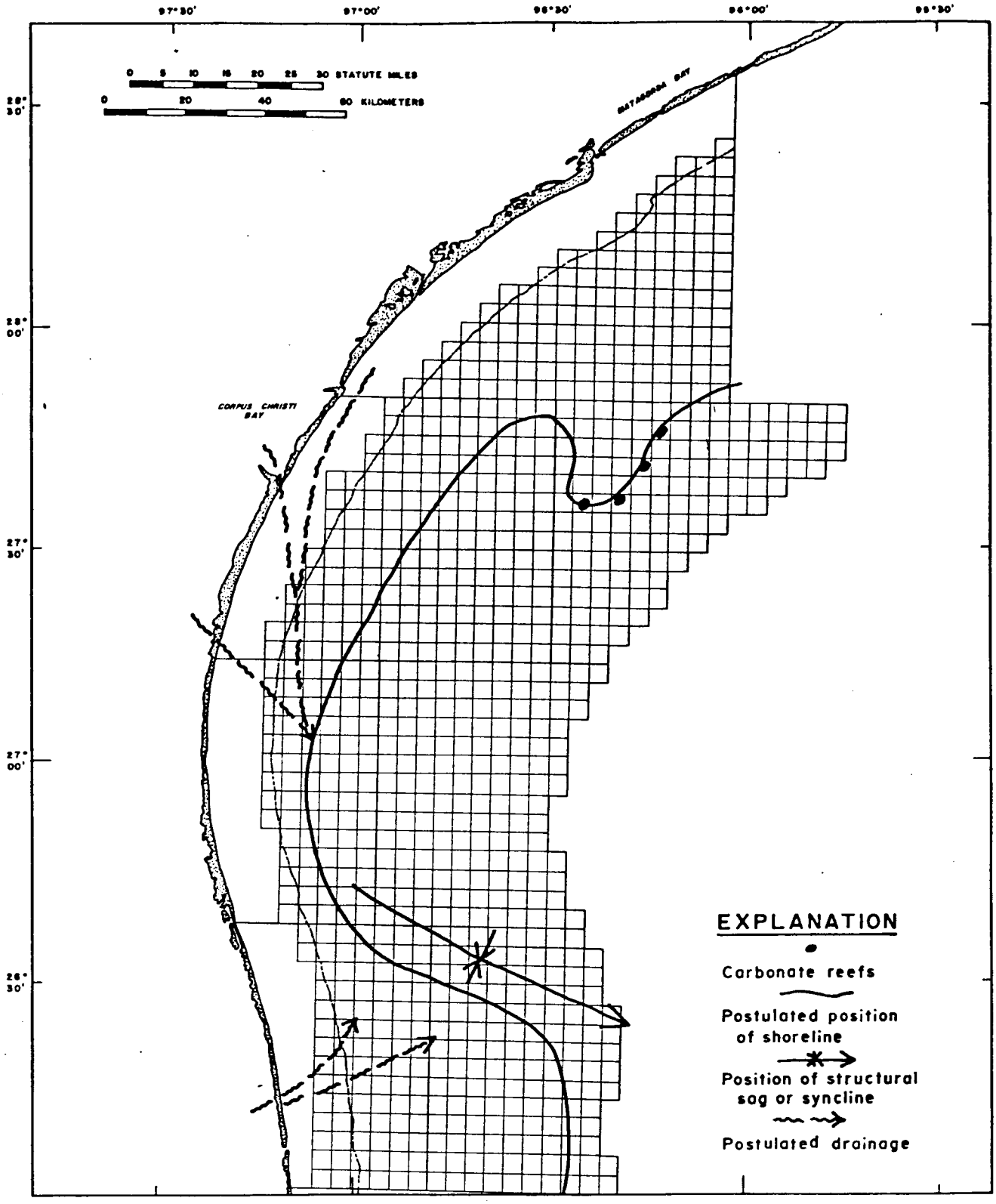

Figure 23. Postulated paleogeography during an early state of the last regression.

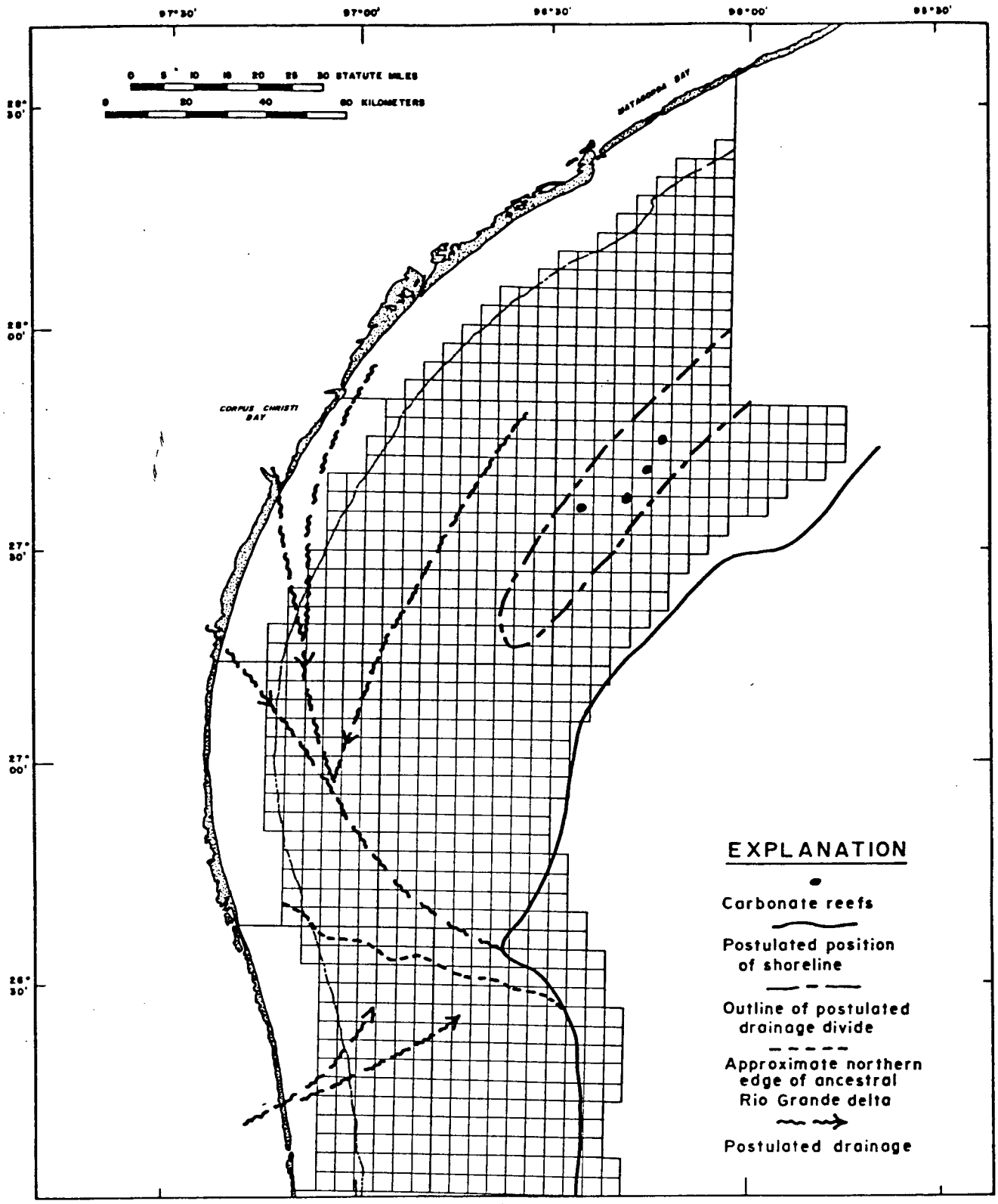

Figure 24. Postulated paleogeography at the last low stand of sea level.

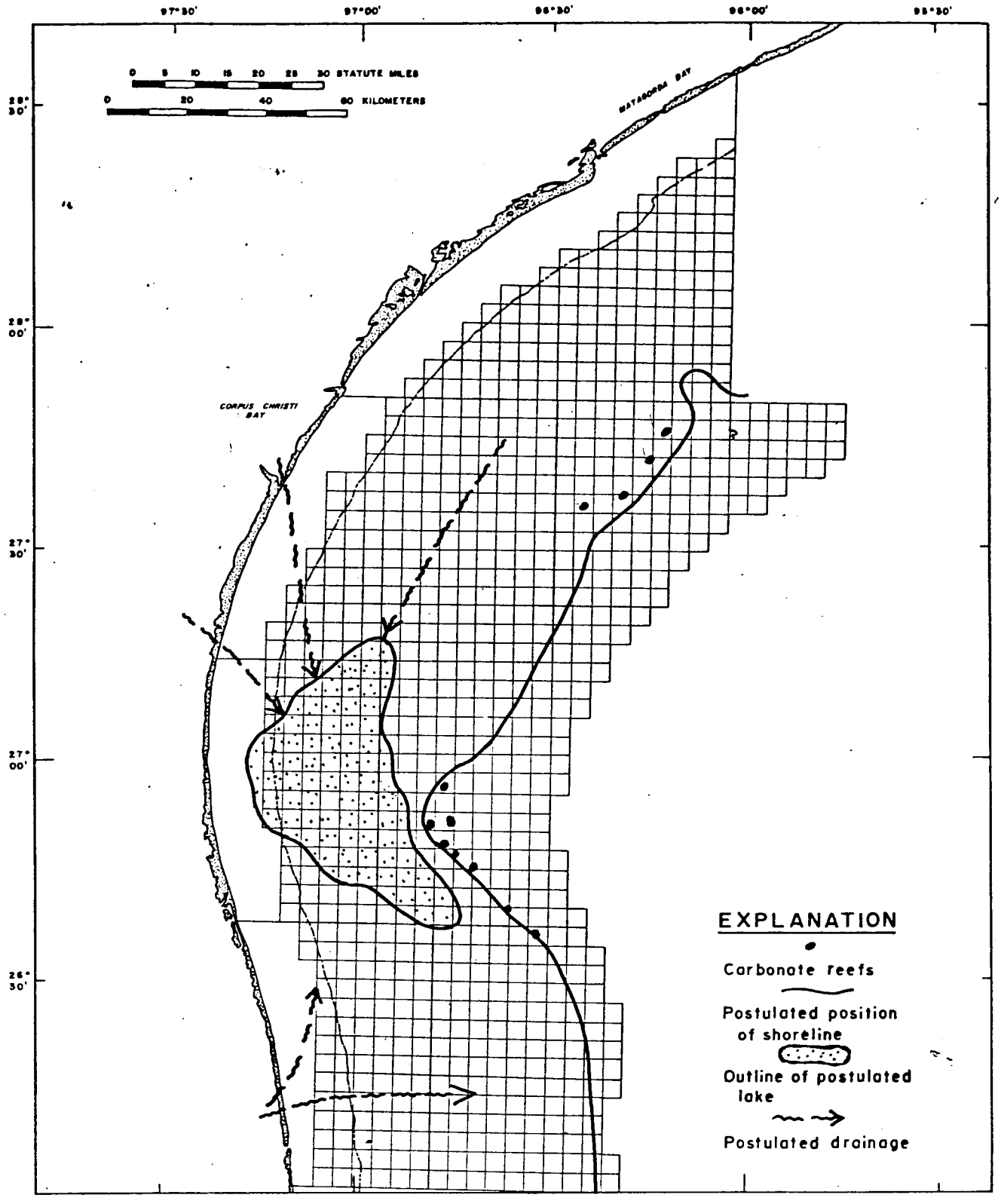

Figure 25. Postulated paleogeography after the rise in sea began in early Holocene time.

locally associated at the base of the flanks; those in the southern cluster have more rugged surfaces marked by numerous pinnacles.

Nature of Post-reflector A Sediments

The nature of sediments above reflector A is known only from cores of a few meters length which have provided samples from the upper part of the sequence. The cores are interlayered mud and sand and characteristics of the sound analogs on the acoustic profiles indicate that over most of the OCS the remainder of the sequence is similar. An exception is the area indicated by pattern on plate 3. This area is nearly coincident with one of the two thicker accumulations of sediment. Within the area the sediments are acoustically non-reflective. On the profiles the boundary between these sediments and those laterally adjacent is extremely sharp and abrupt.

Lacking core data, the non-reflective sediments are interpreted to be lake deposits that are either very highly organic or very highly saline. Reconstruction of the early Holocene paleogeography (fig. 25) suggests that the area in question was eventually cut off from drainage outlet to the sea by the buildup of deltaic and strandline barrier deposits.

In constructing the isopach maps for the post-reflector B and post-reflector A sequences, the relatively narrow belt of lenticular strandline deposits on the outer shelf were considered to be of Pleistocene age and included with the post-reflector B sequence. Whether or not they more properly belong with the post-reflector A sequence is conjectural because the beginning of Holocene time has not been definitely defined. If Holocene time is considered to have begun when sea level started to rise from its last low stand, then the strandline deposits properly belong as a basal unit within

the post-reflector A sequence. If the Holocene is defined as beginning sometime during sea level rise, the strandline deposits probably represent both late Pleistocene and Holocene deposition. The reflecting surface above the strandline deposits is more distinctive on the acoustic profiles than the erosional surface beneath them. Lacking age criteria for precise dating, the deposits were excluded from the post-reflector A sequence solely on the basis of acoustical properties. Continuing study may help to resolve the question.

Faults

The faults that have displaced reflector A and overlying sediments, as well as reflector B, are almost entirely on the outer half of the continental terrace and are concentrated near the outer edge. The location of the faults is shown on figure 17, plate 4.

Most of the faults are above the axial trend of the folds at depth, as indicated by reversed directions of fault plane inclination. Those in the area of thicker post-reflector A sediments at the outer edge of the shelf may be down-to-the-basin faults caused by sediment accumulation. The faulting has been most intensive above the two anticlinal crests that are beneath the outer edge of the shelf and upper slope. The nature of the faulting and the typical magnitude of displacement is exemplified by the section of acoustic profile shown on figure 21. Many if not most of the fault planes dip steeply and show increased throw or displacement with depth, and many extend well up into the post-reflector A sequence. With a few exceptions, correlation of faults between profiles was not attempted because of the large number of closely spaced faults on most profiles and the three-mile or more spacing between profiles. Furthermore, many of the faults of relatively small displacement probably die out over short distances; some no doubt merge or bifurcate laterally and others are

arranged en echelon. More closely spaced acoustic profiles are needed to make a positive correlation of the numerous faults on a regional basis.

NATURAL GAS SEEPS

A number of plume-like traces, some parabolic and others more nearly straight lines, were recorded on both the 3.5 kHz and minisparker acoustic profiles. Although some of the traces, particularly those of pronounced parabolic shape may represent schools of fish, others are believed to represent gas moving upward through the water column from seeps at the sea floor. The plume-like sound-analog traces extend from the sea floor upward to various heights within the water column. Many of the "plumes" are directly above faults that either extend to the sea floor or lie at shallow depth beneath the sea floor. The pattern of the plumes on the sound analogs and the close association of the "plumes" to underlying faults indicates that some probably are natural gas emanations moving to the surface of the sea floor along faults. An example of a possible gas plume is shown by the section of an acoustic profile, figure 26. The parabolic trace to the left of the possible gas emanation probably represents a school of fish as the trace spreads downward from a point in the water column.

A survey specifically directed to the identification of natural petroleum seeps on the sea floor was not an objective of the study. Consequently, no attempt was made to obtain samples. Furthermore, assuming that some of the recorded traces are gas plumes in the water column, it is not known whether the gas is methane coming from shallow depths in relatively recent sediments or gas emanating along faults from petroleum reservoirs at depth.

The "plumes" are most prevalent near the outer edge of the OCS in the northern part of the study area. The locations of the areas on the South Texas OCS where the probable natural gas seeps were recorded are shown on figure 27. Some 200 individual "plumes" were recorded on the acoustic profiles on the areas shown on the figure.

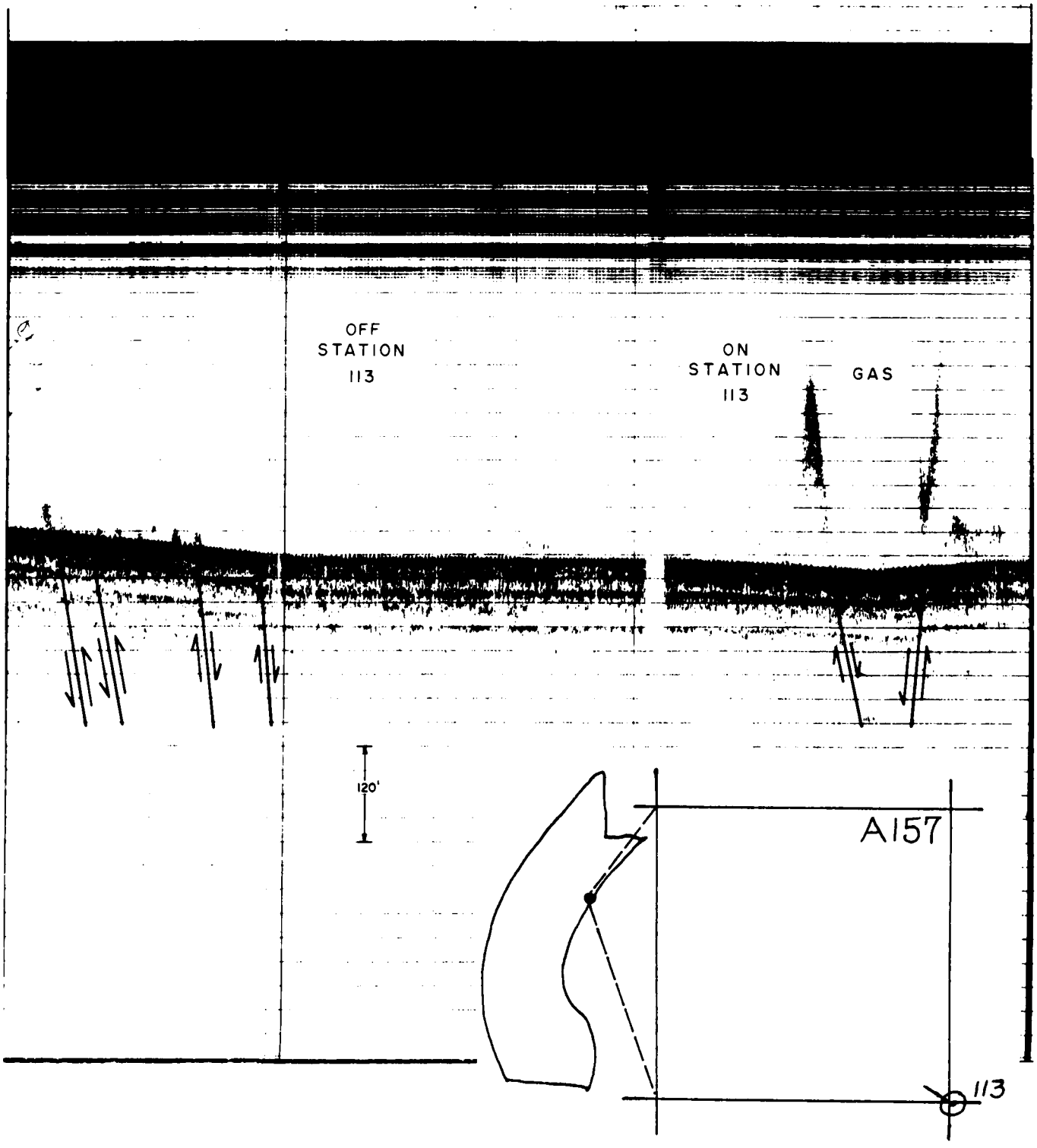

Figure 26. Section of an acoustic profile showing natural gas seep plumes in the water column.

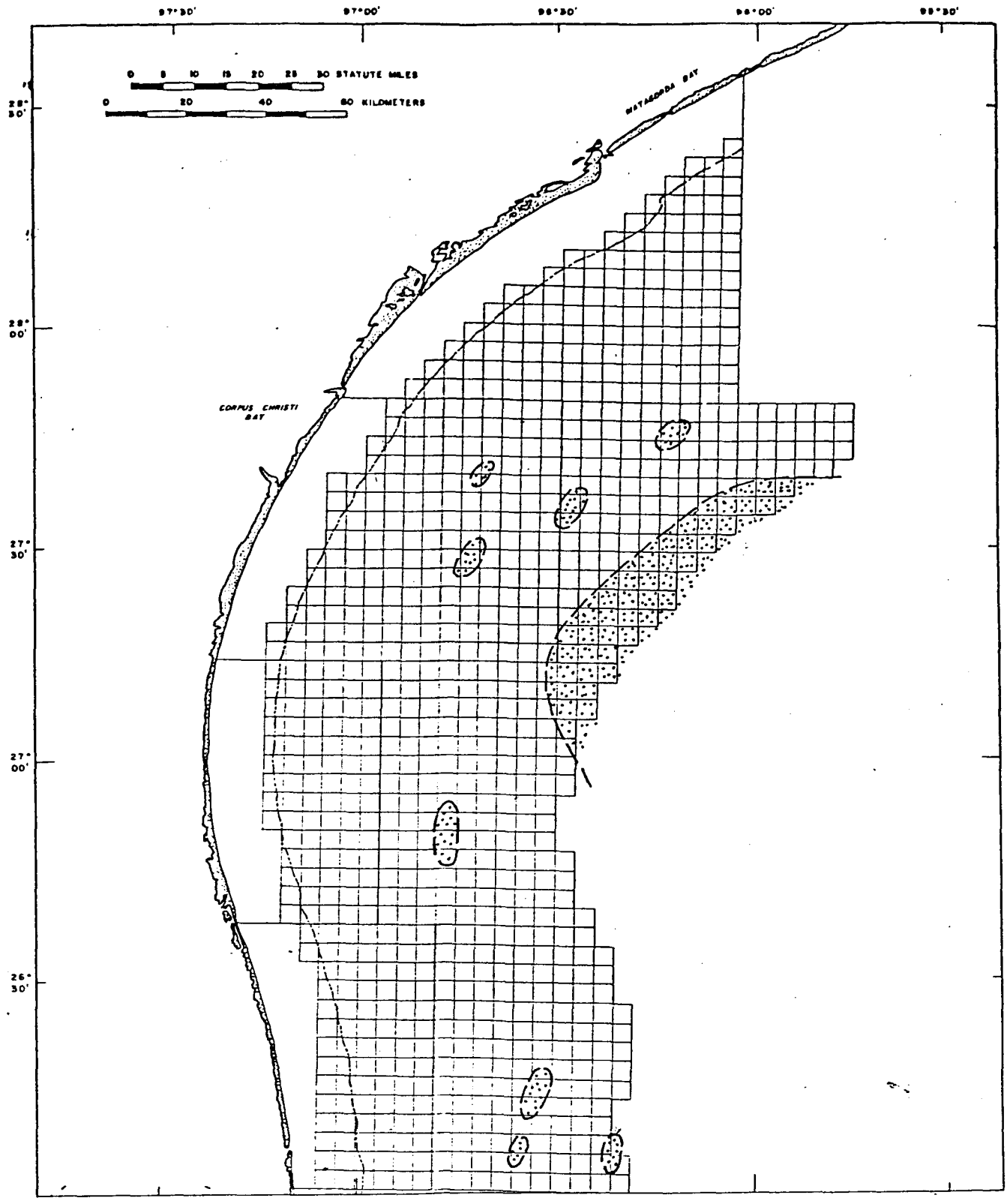

Figure 27. General outline of areas where "plumes" suggesting natural gas seepage were recorded on acoustic profiles.

SEA FLOOR SEDIMENTS

PHYSICAL SEDIMENTOLOGY: SURFICIAL AND NEAR-SURFACE SEDIMENTS

Included under the heading sea floor sediments are both the uppermost or surficial sediments that are along the sea floor/water interface and the underlying sediments to the depth beneath the sea floor penetrated by the box and pipe cores. In the presentation of descriptive and interpretive results that follows, the surficial sediments are discussed first and then the near-surface sediments.

Methods of Study

Grain Size Analysis

A total of 356 samples were analyzed for grain size: 263 bottom grab samples; 28 box core samples employed as replicate samples for evaluating the "within station" grain size variability of sea floor sediments; and 65 water samples for suspended sediments.

The laboratory procedures employed for obtaining grain-size distributions of sea floor sediments follow the sequential format outlined by Chart 1. Individual analytical steps are described briefly as follows:

1. Sample Homogenization and Initial Drying - The original sample was thoroughly mixed and air-dried; a representative work sample split of approximately 75-85 grams was then obtained for analysis.
2. Oxidation of Organic Matter - Carbonaceous organic matter was removed from the sample by oxidation with a 30 percent hydrogen peroxide solution, a step necessary to eliminate potential errors in the Coulter Counter analysis of the mud fraction.

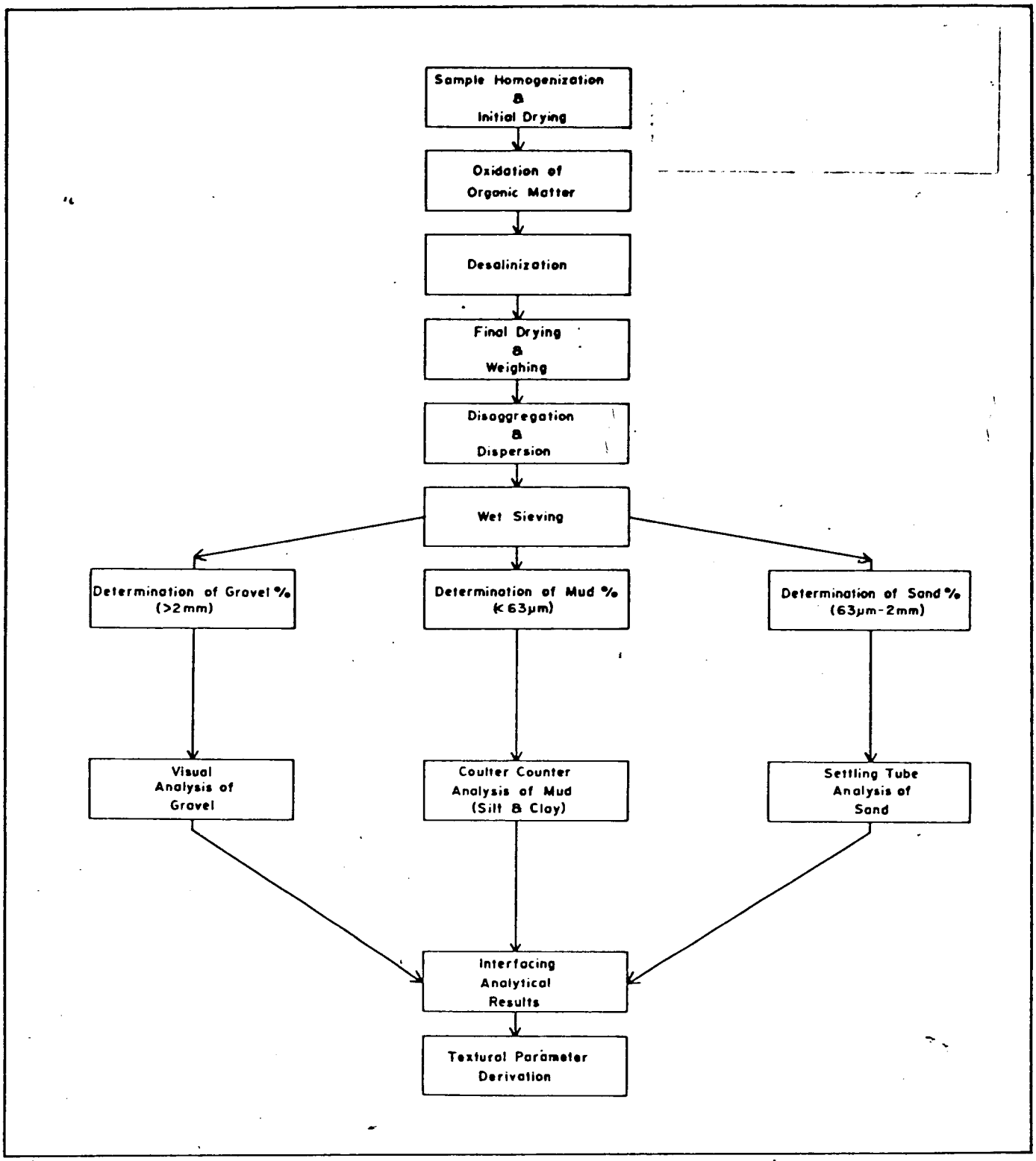

Chart 1. Format for textural analyses of benthic sediment.

3. Desalinization - Soluble salts were removed from the oxidized sample by washing in 800 ml of distilled water. The sample was agitated in a Mason jar, then allowed to settle undisturbed for a minimum of 60 hours. The supernatent wash water was then siphoned off without disturbing the sediment. This step eliminated the weight of salt crystals and allowed sediment dispersion.

4. Final Drying and Weighing - After removal of organic matter and soluble salts, the clean sample was oven-dried at less than 40°C to avoid baking the clay fractions. A final work sample weight was then obtained to within 0.01 g, under the normal ambient temperature and humidity conditions within the USGS Corpus Christi laboratory.

5. Disaggregation and Dispersion - The final work sample was physically disaggregated, then dispersed by soaking in 500 ml of a standard Calgon solution (5 g/l). The suspension was thoroughly mixed and allowed to settle for 24 hours, then checked for flocculation. If dispersion was complete, the sample was then wet-sieved.

6. Wet Sieving - The dispersed sample was washed through a set of 2 mm (#10) and 63 micron (#230) U.S. Standard sieves. The sample was fractionated into gravel (>2mm), sand (2mm - 63 μm), and mud (<63 μm) fractions; the mud fraction was brought to a standard 800 ml volume.

7. Percentage Determinations - The sand and gravel fractions were washed, oven-dried, and weighed; the percentages of sand, gravel, and mud comprising the total sample were then determined.

8. Settling Tube Analysis (Sand) - The grain-size distributions of sand fractions were determined with a Rapid Sediment Analyzer (RSA) at a half-phi interval. The instrument employs a settling tube 1 meter in length,

with an 8 cm internal diameter. The settling tube assembly is a modified version of the basic model described by Schlee (1966). Modifications include incorporation of a different model transducer, and the use of a manual sediment introduction device, rather than a motor-driven device. Accessory equipment include a Hewlett-Packard amplifier (Model 321), and a Heath-Schlumberger strip-chart recorder (Model EU-205-11). Sediment fall times were converted to phi-size cumulative percentages at a 0.5 ∅ interval by employing the fall time-size overlay technique described by Schlee (1966).

In conducting an analysis, a representative sample of the sand fraction was obtained with a microsplitter. Efforts were made to use 3 gm samples; however, if the total sediment had an insufficient sand content, smaller RSA samples were utilized. Sediments with sand fractions comprising less than 0.4 percent of the total sample weight were considered as "pure mud" texturally; the bulk weight of sand in such samples was so minute (<0.5 g) that it was beyond the capability of the RSA instrument to provide reliable size analyses of the sand fractions. Approximately 8 percent of the total samples were in this category. The minimal total sand content for reliable RSA analyses was extended to 2 percent for samples with sand fractions composed almost entirely (>90 percent) of biogenic detritus consisting mainly of planktonic foraminiferal tests; this was necessary because of the aberrant hydraulic behavior of foraminiferal tests within the RSA settling tube. Consequently, when these "ooze sand" fractions comprised less than 2 percent of the total sample, the sample was considered as "pure mud" texturally. However, only 7 samples (#122G, 136G, 155G, 179G, 193G, 197G, 234G) were in this category. All techniques

of sediment introduction, recording, and analog curve interpretation were standardized to minimize operation bias. The recorder sweep speeds employed were 2.5 sec/cm for the first 35 seconds, 5 sec/cm from 35 to 100 seconds, and 10 sec/cm after 100 seconds. All analyses were conducted within a 21-24°C temperature range. On the basis of replicate analyses, the RSA exhibited a precision of $\pm$ 2.3 percent in determining Folk's (1965) graphic mean diameters.

9. Coulter Counter Analysis (Mud) - The grain-size distributions of the silt and clay fractions (< 63 μm) were collectively determined at a half-phi interval electronically, employing a 16-channel model TA Coulter Counter. By conducting duplicate analyses with 200 μm and 30 μm tube apertures, the instrument effectively analyzed the 0.63-63 μm size range. The electrolyte consisted of a 4 percent Calgon solution, pre-filtered through a 0.2 μm filter.

For each sample, a 200 μm tube analysis was conducted first to determine the coarser half of the size frequency distribution. The dispersed mud suspension was homogenized in a 1000 ml beaker by agitation on a Flexa-Mix vibrator equipped with a baffle. A representative sample of the suspension was obtained by sampling with an automatic micro-pipette from the top, middle, and bottom of the beaker. This sampling procedure was repeated until a standard sediment dilution level was achieved which resulted in less than 5 percent coincidence error. The sample was then electronically counted, and the relative percentages of particles in each size class within the operating range of the 200 μm tube (2-40 percent aperture diameter) were determined. During analysis, the sample was agitated and dispersed by a stirring motor operating at a standard speed. Since the state-of-the-art stirring apparatus could not be maintained at a constant rpm, the selected

standard speed was just below the level that produced observable turbulence at the surface of the sample beaker.

After the 200 μm tube analysis, the analyzed suspension was then sieved through a 20 μm micro-mesh sieve, and re-analyzed with the 30 μm tube to obtain the finer half of the size distribution. The 30 μm tube analyses were conducted in an unagitated state, and were completed within 2 hours of their respective 200 μm tube analyses. The size frequency distributions determined by the Coulter Counter are truncated at the lower analytical limit of the 30 μm tube (0.63 μm or 10.62 Ø), which was weighted as 11.0 Ø for the purpose of statistical analysis. The size percentage data from both tubes were arithmetically combined and normalized to provide the full distribution of the mud fraction within the two-tube analytical range. All operational techniques were standardized to minimize operator bias, and to eliminate inconsistent analytical artifacts. The precision of the Coulter analyses is equivalent to that of the pipette technique (Shideler, in prep.). On the basis of triplicate analyses performed on each of three different samples, the minimal precision in determining Folk's (1965) graphic mean diameters is ± 6.4 percent.

10. Gravel Analysis - A visual analysis of the gravel fractions within the sea floor sediments revealed in nearly all instances 100 percent biogenic shell materials; no significant quantity of non-organic gravel detritus was observed. As the South Texas OCS is essentially a sand-mud province, the inclusion of the shell-gravel materials within the composite size analyses was not considered to be of any particular sedimentological benefit. In addition, the shells could produce misleading results by distorting the statistical size parameters derived from the sand and mud fractions. For these reasons, the shell-gravel fractions were not included within the size

analyses, and all size frequency distributions are truncated at the 2 mm (-1.0 Ø) sand-gravel boundary.

11. Interfacing Analytical Results - The individual size frequency distributions determined by RSA (sand) and Coulter Counter (silt and clay) were mathematically combined into a composite size frequency distribution characterizing the entire sample. Cumulative weight percentages of size classes were determined at a 0.5 Ø interval, encompassing a size range from -1.0 Ø (2 mm) to 11.0 Ø (0.49 μm). These data were then utilized in deriving the statistical size parameters.

12. Grain Size Derivation - In deriving textural parameters, data processing was performed by a computer program, employing the computer facilities of the USGS Computer Center Division at the Denver Federal Center. The derived parameters consist of the following:

    1. Single-component sediment percentages: gravel, sand, silt, clay;
    2. Two-component sediment parameters: sand/mud ratios, silt/clay ratios;
    3. Composite sediment parameters: sediment type as determined from Shepard's (1954) classification system based on sand-silt-clay proportions;
    4. Statistical grain-size parameters: moment measures of mean diameter, standard deviation, skewness, and kurtosis; modal diameters.

13. Data Presentation - The derived textural parameters of sea floor sediments at each station are tabulated in Table II, Part II. Baseline maps and diagrams were prepared for each parameter to delineate the areal variability throughout the OCS region.

Colorimetric Analysis

The color characteristics of OCS sea floor sediments were determined from the 263 bottom grab samples in the wet state aboard ship immediately upon

sample recovery. As sediment color at the surface (upper 1 cm) of the grab samples was frequently different from the color at greater depths, both surface and shallow subsurface colors were recorded. Colors were designated in terms of hue-value-chroma combinations, in accordance with the standard GSA rock-color chart based on the Munsell system (Goddard and others, 1970). Surface and subsurface color characteristics of individual stations are tabulated in Table II, Part II and maps were prepared to show regional color variability.

Heavy Mineral Analysis

The bottom sediments were analyzed for total heavy mineral contents, by weight percentage. A total of 276 samples was analyzed; these consisted of representative splits from 260 Smith-MacIntyre grab samples, and 16 replicate grab samples for evaluating "within station" variability.

The laboratory procedures employed for obtaining the heavy mineral percentages of sea floor sediments follow the sequential format outlined by Chart 2. Individual analytical steps are briefly described as follows:

1. Desalinization - The entire sample was washed in 800 ml of distilled water to remove soluble salts and allow dispersion; the wash water was siphoned off after a 24-hour settling period.
2. Disaggregation and Dispersion - Mud lumps in the washed sample were physically disaggregated, and the sample was then dispersed in 250 ml of a standard Calgon solution (5 g/1).
3. Wet Sieving - The dispersed sample was washed through a set of 2 mm (#10) and 63 micron (#230) U.S. Standard sieves. The sample was fractionated into a mud fraction (< 63 μm) that was used for clay mineral analyses by X-ray diffractometer, a gravel fraction (> 2 mm) that was discarded, and a sand fraction (63 μm-2 mm) that was washed and processed for the heavy mineral separations.

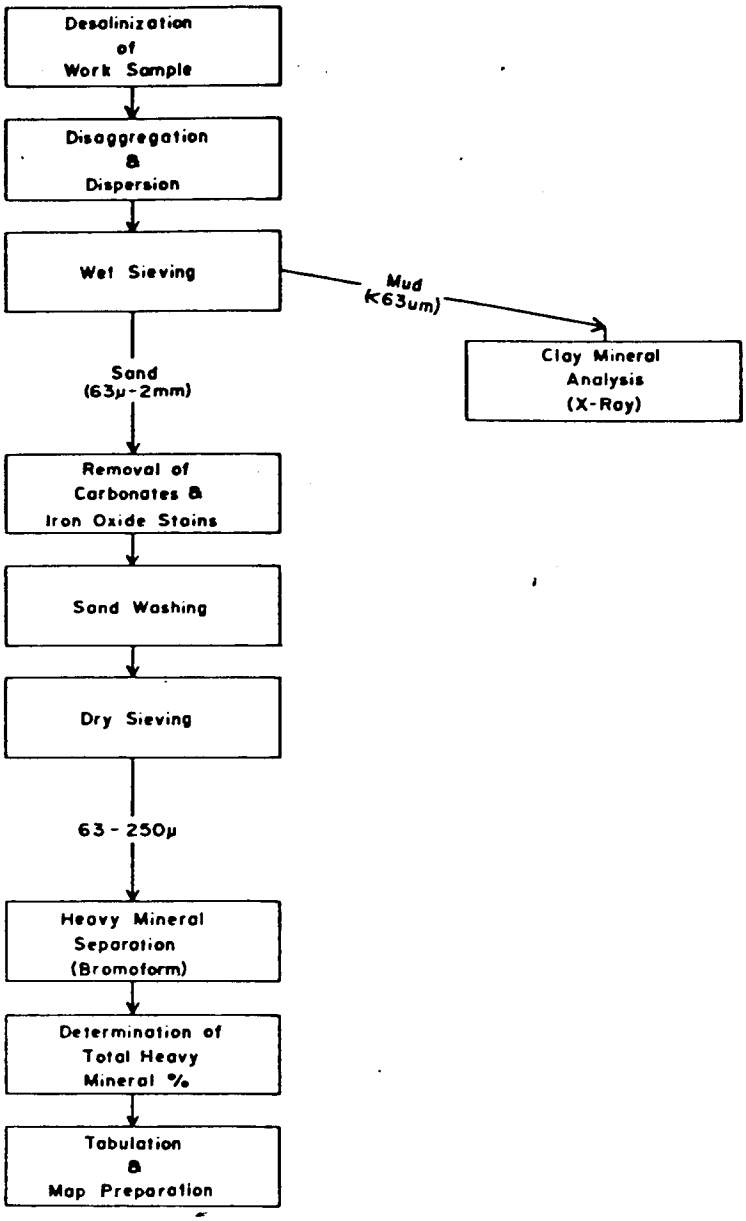

Chart 2. Format for heavy mineral analysis

4. Removal of Carbonates and Iron Oxides - The sand fraction was digested in dilute hydrochloric acid (10 percent) overnight. This step removed extraneous carbonate minerals, and cleaned iron oxide stains off the heavy minerals.

5. Sand Washing - After acidification, the sand fraction was thoroughly washed in a Calgon solution, followed by several rinses with distilled water. The sand was checked for complete removal of HCL by adding a drop of silver nitrate (5 percent) to the wash water and noting the absence of a AgCl precipitate.

6. Dry Sieving - The clean sand was dried, poured through 250 μm (#60) and 63 μm (#230) U.S. Standard sieves, and manually agitated. The 63-250 μm sand fraction was then retained for the heavy mineral separations. This limited size range was utilized, so that variations in heavy mineral contents induced by grain-size differences would be minimal.

7. Heavy Mineral Separations - The heavy mineral fractions were separated in bromoform (CHBr3) which has a specific gravity of 2.89 at 20°C. Separations were performed by centrifuge (International Model BE50), and efforts were made to maintain a constant centrifuging time (20 minutes) and speed (1200 rpm). A standard sample size (< 2 g) and constant bromoform volume (15 ml) were also employed. These procedures were necessary in order to standardize separation efficiency. After centrifuging, the light and heavy mineral fractions were separated by the partial freezing technique (Carver, 1971), using liquid nitrogen.

8. Determination of Heavy Mineral Percentages - After separation, the light and heavy mineral fractions were weighed (.001 g accuracy), and their relative proportions determined for each sample.

9. Data Presentation - The total heavy mineral weight percentage data for each station is tabulated in Part II. A map was prepared to show the areal

variability of total heavy mineral contents throughout the South Texas OCS region.

Texture

The regional textural variability of sea floor sediment is delineated in terms of individual particle-size components, two-component ratios, the total-component composite variability based on all size components, and statistical grain-size parameters.

Single-Component Variability

Textural variability is delineated in terms of gravel, sand, silt, and clay percentages. These individual component percentages can provide insight into sedimentary processes operative within the OCS region.

Gravel

The areal distribution of gravel-size detritus (>2.00 mm) is shown by figure 28 and plate 5, and the percentages of gravel at individual stations are tabulated in Table II, Part II. The gravel essentially is biogenic detritus, consisting predominantly of molluscan shells. The shells are generally highly fragmented; some of the more robust valves are highly etched and generally reflect a substantial degree of weathering. A more diverse assemblage was noted near several of the reefs where coral-algal detritus was mixed with mollusc remains (e.g. stations 80, 191, 196). Inorganic gravel-size material was quantitatively insignificant and consisted of a few polygenetic limestone clasts; the few stations that yielded lithic clasts are noted on Table II, Part II. Regionally, gravel-size detritus comprises less than 0.1 percent of the bottom sediment throughout most of the OCS but locally is as much as 26.65 percent. Gravel concentrations in excess of 1.0 percent are primarily in the

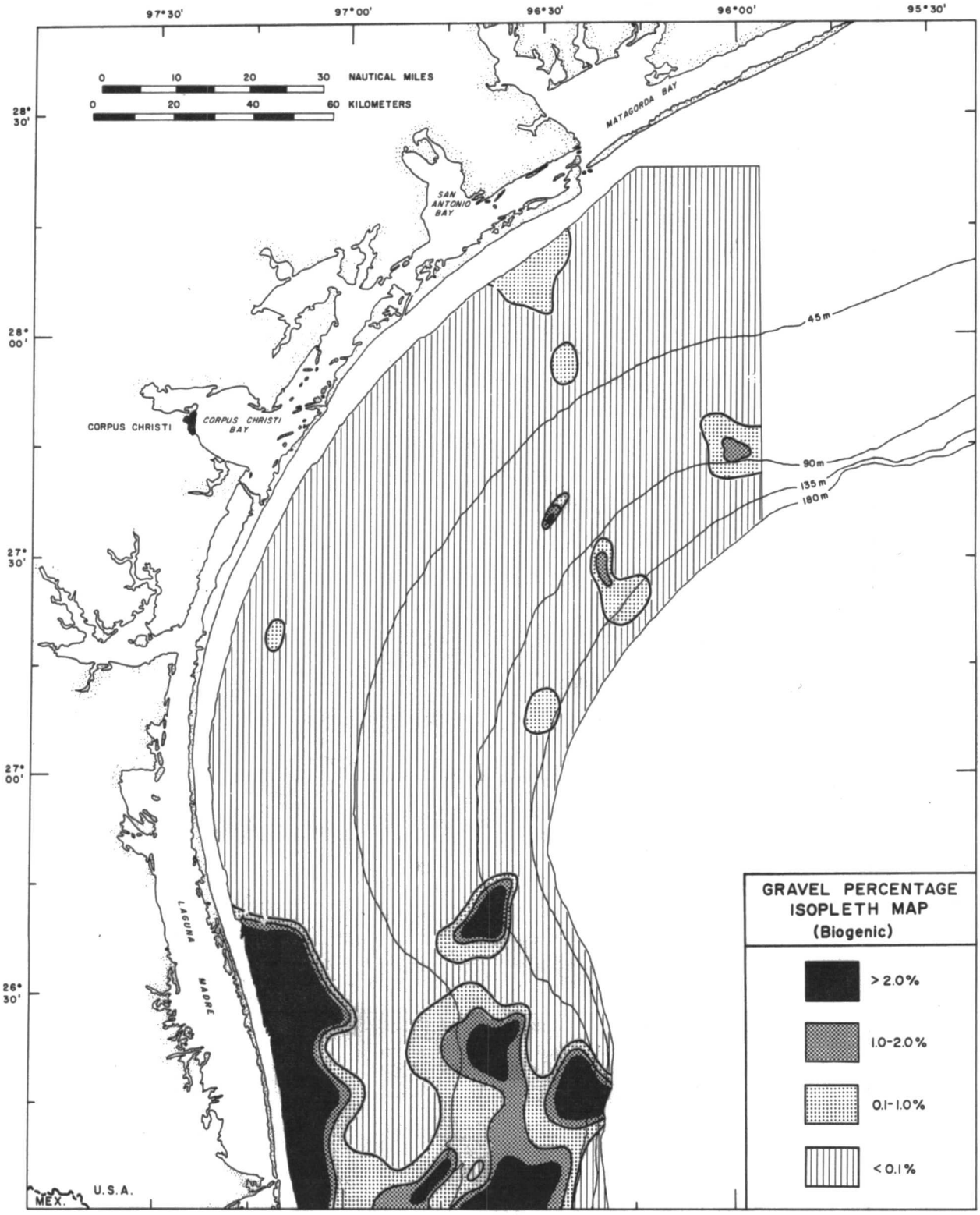

Figure 28. Distribution of gravel.

sector south of 27°N latitude, within the area of the ancestral Rio Grande delta. North of 27°N latitude and seaward of the 45 m isobath, small local concentrations exceed 1.0 percent.

The gravel pattern does not show any systematic relation to the hydraulic regime as presently understood, thus indicating that the shells are largely relict concentrations, rather than modern concentrations established by present ecological conditions. High shell concentrations are most extensive over the ancestral Rio Grande delta, where they extend from the shoreface to the shelf edge. The concentrations probably reflect lag concentrates derived from partially reworked late Pleistocene-early Holocene deposits exposed on the present sea floor. Shell concentrations in the Rio Grande delta area also have been noted by Curray (1960). The conspicuous tongue of low gravel concentrations extending into the delta slightly east of 97°W longitude may relfect a net southward transport of fine-grained modern sediments, resulting in a partial covering of the older shelly deposits.

The local concentration of shelly material along the southern flank of the ancestral Brazos-Colorado delta at 96°W longitude may also reflect a lag concentrate derived from partially reworked late Pleistocene-early Holocene deposits. The local concentrations (>2 percent) at 26°39'N, 96°37'W and 27°34'N, 96°28'W are associated with relict carbonate reefs.

Sand

The areal distribution of sand-size (.063-2.00 mm) detritus in the sediments is shown by the sand percentage isopleth map (fig. 29 and pl. 6). The sand-sized fractions are composed of both terrigenous and biogenic components and sand content of the bottom samples ranges from a trace to a maximum of 90.17 percent. Sand content of less than 5 percent is most common at the stations sampled. The sand isopleth map shows two distinct regional

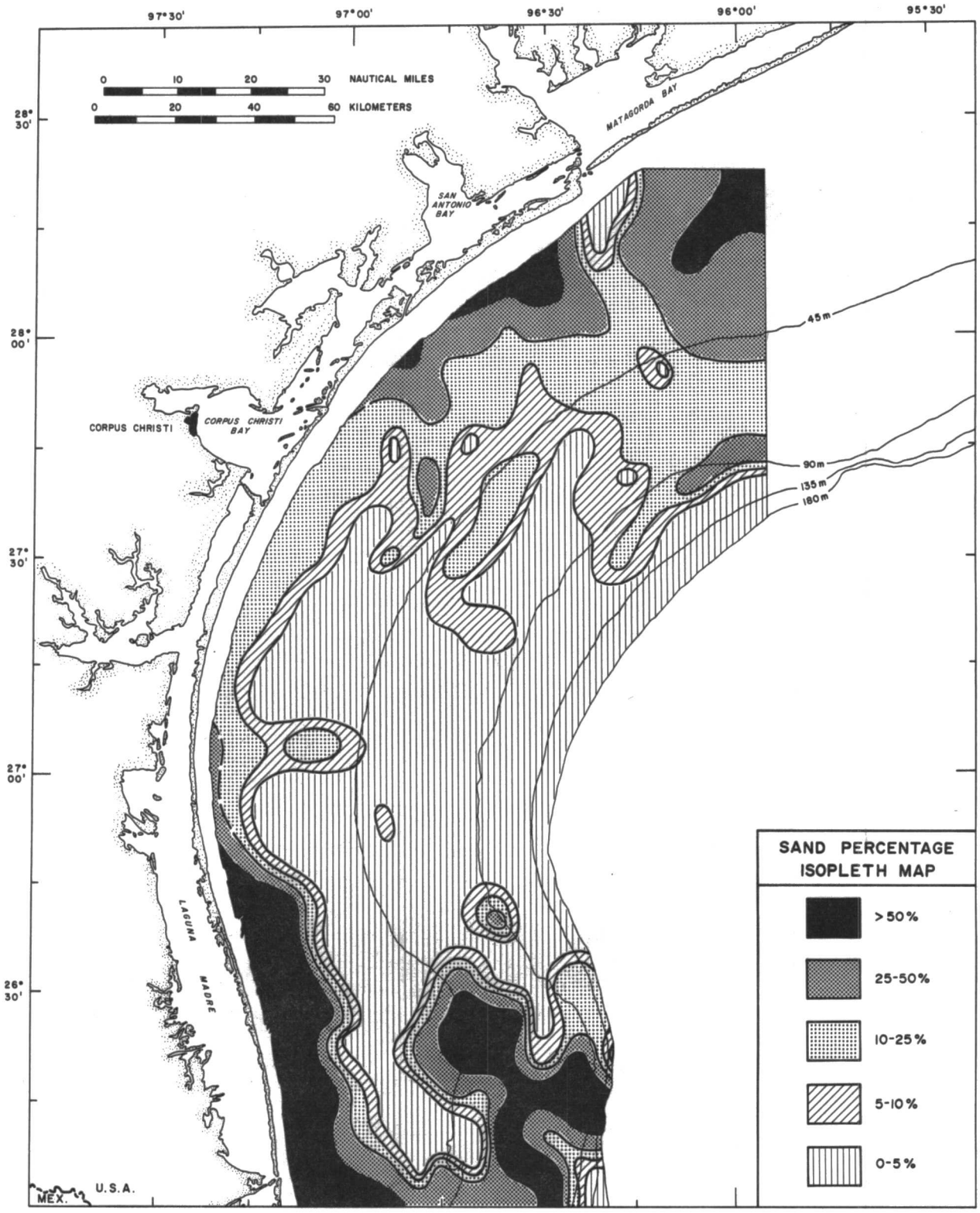

Figure 29. Distribution of sand.

trends: an increase in the sand-sized fraction shoreward; and an increase in the sand-sized fraction both northward and southward from the central sector of the continental shelf. The isopleth spacing indicates that both trends have substantially higher gradients in the southern half of the OCS region. The areas of high sand concentrations (>25 percent) generally are localized along the shoreface and the ancestral Rio Grande and Brazos-Colorado deltas; the central sector of the shelf between the two deltas is a conspicuous sand-deficient mud province. Noteworthy local areas of sand-deficiency include the mud salient extending into the Rio Grande delta east of 97°W longitude, and the salient extending southward from the Matagorda Bay inlet.

The sand distribution pattern probably represents the composite response to various processes, including a combination of tractional and suspension transport systems, both ancient and modern. The regional trend of increasing sand content shoreward appears to reflect both a modern coastal source area for sand detritus and a progressive shoreward increase in significant wave surge energy with decreasing water depth; the trend suggests a net offshore transport component. Regarding the coastwise longitudinal trend along the shelf, the high sand concentrations in the Rio Grande delta area extend to the shelf edge; this absence of depth control suggests that the sands are not in equilibrium with the modern hydraulic regime and thus probably reflects relict deposits of the ancestral delta. These southern sand concentrations are largely coincident with the previously described areas of high shell concentrations, thus supporting a relict origin. The conspicuous mud salient extending into the delta east of 97°W longitude may reflect the southward transport and encroachment of modern muds onto the delta platform; bathymetrically, the salient is located over a relatively low gradient platform area.

This is compatible with the interpretation of Curray (1960), who considered the Rio Grande sands to be relict shallow-water deposits of the basal Holocene transgressive series, with adjacent muds being modern shelf deposits.

The northern sand concentrations associated with the ancestral Brazos-Colorado delta exhibit notable differences compared to the southern sands. The northern sands are not as closely associated with high shell-gravel concentrations, and the percentage isopleths denote much lower gradients. These two factors suggest genetic differences between the northern and southern sand concentrations. The distribution pattern suggests that the northern sands are being derived from an ancestral Brazos-Colorado delta source and are being transported southward by modern coastwise currents, eventually grading into the mud facies of the central sector. The northern sands are interpreted as "palimpsest" deposits which are in partial equilibrium with the modern hydraulic regime. As discussed by Swift and others (1971), the term "palimpsest" refers to Quaternary shelf sediments with petrographic attributes that reflect an earlier depositional evironment, but which have been partially reworked during the Holocene transgression. In the context of hydraulic equilibrium, the term "palimpsest", as used here, refers to a stage of textural adjustment intermediate between "relict" deposits in total disequilibrium, and "modern" deposits in total equilibrium. As a complete adjustment continuum probably exists, the distinction between the three sediment types is essentially a reflection of their relative degrees of adjustment to present hydraulic conditions. The sandy sediments in the northern sector which appear to reflect some net transport southward have evolved to a higher state of hydraulic adjustment than the sand concentrations in the southern sector which appear to be largely autocthonous relict sands of the ancestral Rio Grande delta; the relict sands appear to be only undergoing <u>in situ</u> winnowing, with minimal mass dispersion.

The sand-deficient areas (<25 percent) are interpreted as being largely modern equilibrium mud deposits. These muds cover most of the central region which seems to act as a fine-sediment sink, with mud salients appearing to encroach southward onto the ancestral Rio Grande delta. Southward dispersal of modern mud is supported by the south-trending mud salient extending from the Matagorda Bay inlet (Pass Cavallo). The predominantly southward dispersal of suspended sediment plumes from the Pass Cavallo area has been documented on ERTS imagery (Hunter, personal communication); the plumes may indicate the convergence of the inlet's tidal current regime with south-trending littoral and nearshore currents. Consequently, the mud salient could consist of both Matagorda Bay effluent and south-flowing littoral drift derived from further north. A more sandy effluent appears to be associated with the San Antonio Bay inlet (Cedar Bayou) as suggested by the development of a small south-trending sandy salient. A minor east-trending sandy salient located near 27°N latitide, 97°W longitude is also noteworthy, as it is in the general vicinity of a postulated littoral drift convergence zone (Watson, 1971). In general, the over-all sand distribution pattern suggests a composite fabric of relict, palimpsest, and modern sediments. A regional net advective transport of sediment southward is also suggested.

Silt

The areal variability in the amount of silt-size (3.9-63 μm) detritus is shown by the silt percentage isopleth map (fig. 30 and pl. 7). Silt percentages at individual sample stations range from approximately 6 percent to a maximum of 79 percent. In contrast to the relatively limited distribution of sand-size detritus, silt detritus is a predominant component throughout much of the OCS region. Silt content commonly exceeds 55 percent. The only conspicuous areas

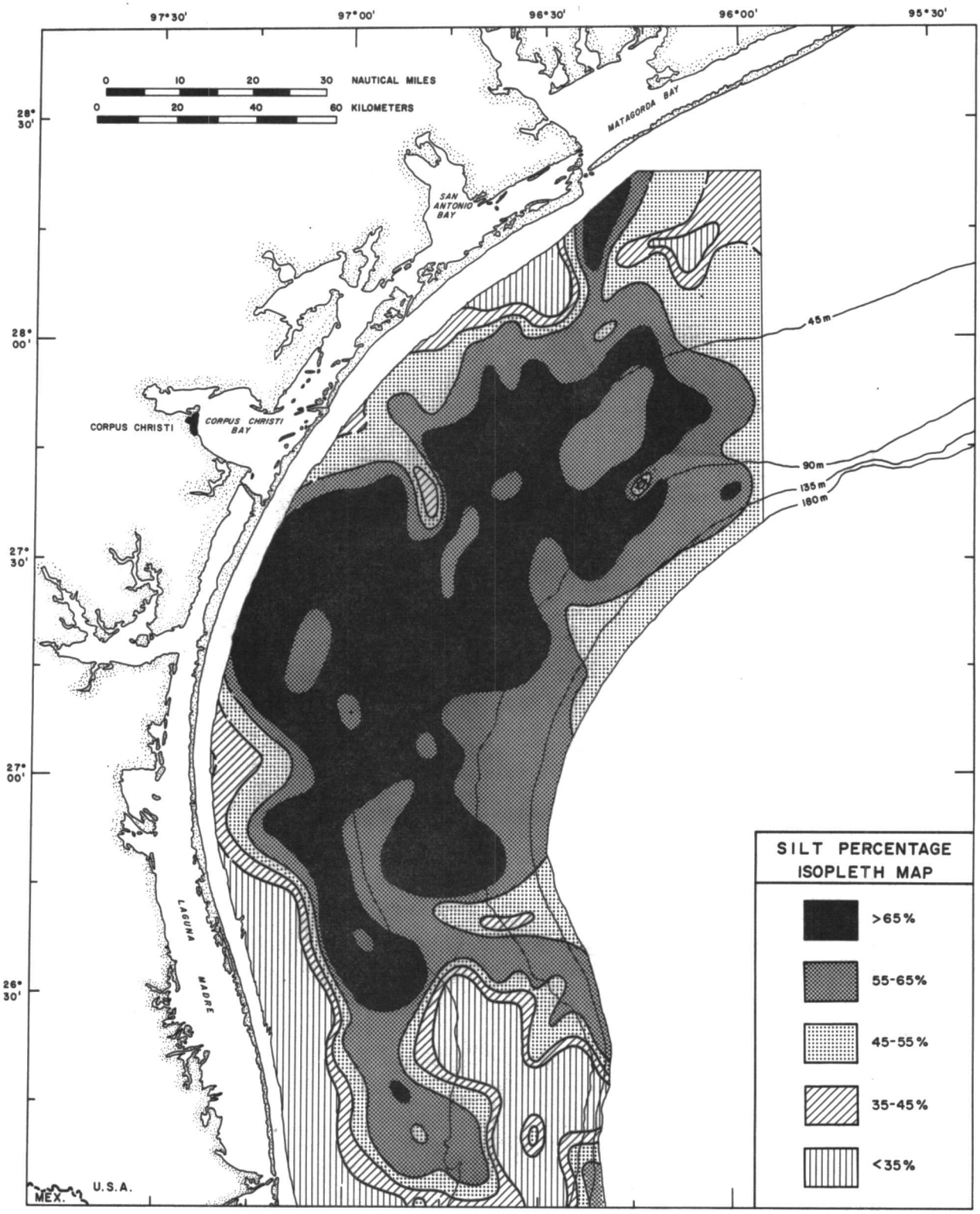

Figure 30. Distribution of silt.

deficient in silt (<45 percent) are the ancestral Rio Grande delta and adjacent shoreface and the ancestral Brazos-Colorado delta. The regional trend indicated by the silt isopleths is a general increase in silt content from peripheral areas toward the central interior of the shelf. The trend is largely the inverse of the regional trend for sand. In addition, the silt trend shows some closure, indicating that the central interior of the OCS region is functioning as a silt depocenter. As delineated by the 55-65 percent isopleth interval, conspicuous local silt salients extend outward from the central interior. The most prominent of these local salients extend southward onto the ancestral Rio Grande delta (east of 97°W longitude), northward to the Matagorda Bay inlet, and westward near 27°30'N south of Corpus Christi Bay.

The distribution pattern for silt appears to reflect largely the modern suspended sediment dispersal system, suggesting that the central interior part of the shelf is hydraulically structured to function as a depocenter for silt-size detritus. The voluminous quantity of silt within the OCS region appears to be derived from a combination of sources; coastal erosion; suspended sediment reflux and adjacent estuaries; southward littoral drift from north of the OCS region; and possibly winnowing of the ancestral Rio Grande and Brazos-Colorado deltas. A significant contribution from the Matagorda Bay inlet area is indicated by the conspicuous silt salient extending southward from this locality. In contrast, the reflux from Corpus Christi Bay appears to be deficient in silt; this is indicated by the conspicuous silt-deficient salient extending southeasterly from the bay's inlet (Aransas Pass). The westward-trending very broad silt salient or bulge near 27°30'N latitude is perplexing. It is in the general vicinity of a postulated semi-permanent current convergence zone, where a

possible seaward return flow may occur (Curray, 1960). If this circulation cell does exist, voluminous quantities of silt may be derived from coastal erosion and transported alongshore by littoral and nearshore currents toward the convergence zone; seaward return flow may then provide an escape route for the advective transport of silt into the central interior where dispersion and deposition could occur both north and south of the convergence node. Strong seaward-flowing currents have been noted by fishermen within the postulated convergence zone (Curray, 1960). In essence, the observed silt distribution pattern is compatible with this postulated convergence circulation cell, since the cell's existence could readily explain the enigmatic westward-trending silt salient near 27°30'N latitude. An answer to the question of the current convergence may come from the physical oceanographic studies being made as a part of the overall South Texas OCS environmental assessment project.

Clay

The areal distribution of clay-size (< 3.9 μm) detritus is shown by figure 31 and plate 8. Clay percentages in bottom sediments at individual stations range from 3.5 percent to a maximum of 53.6 percent. The regional trend indicated by the clay isopleths is a general increase in clay content both seaward as well as toward the central interior. The regional distribution of clay is inversely related to the regional distribution of sand. The major areas deficient in clay are those of high sand concentrations on the two ancestral delta platforms and along the shoreface. The clay isopleths do not denote a seaward closure, as shown by the silt pattern. Similar to the silt pattern, local areas of high clay content (> 25 percent) occur as south-trending salients from Matagorda Bay inlet and east of 97°W longitude on the Rio Grande delta platform. However, a west-trending salient near 27°39'N is notably absent.

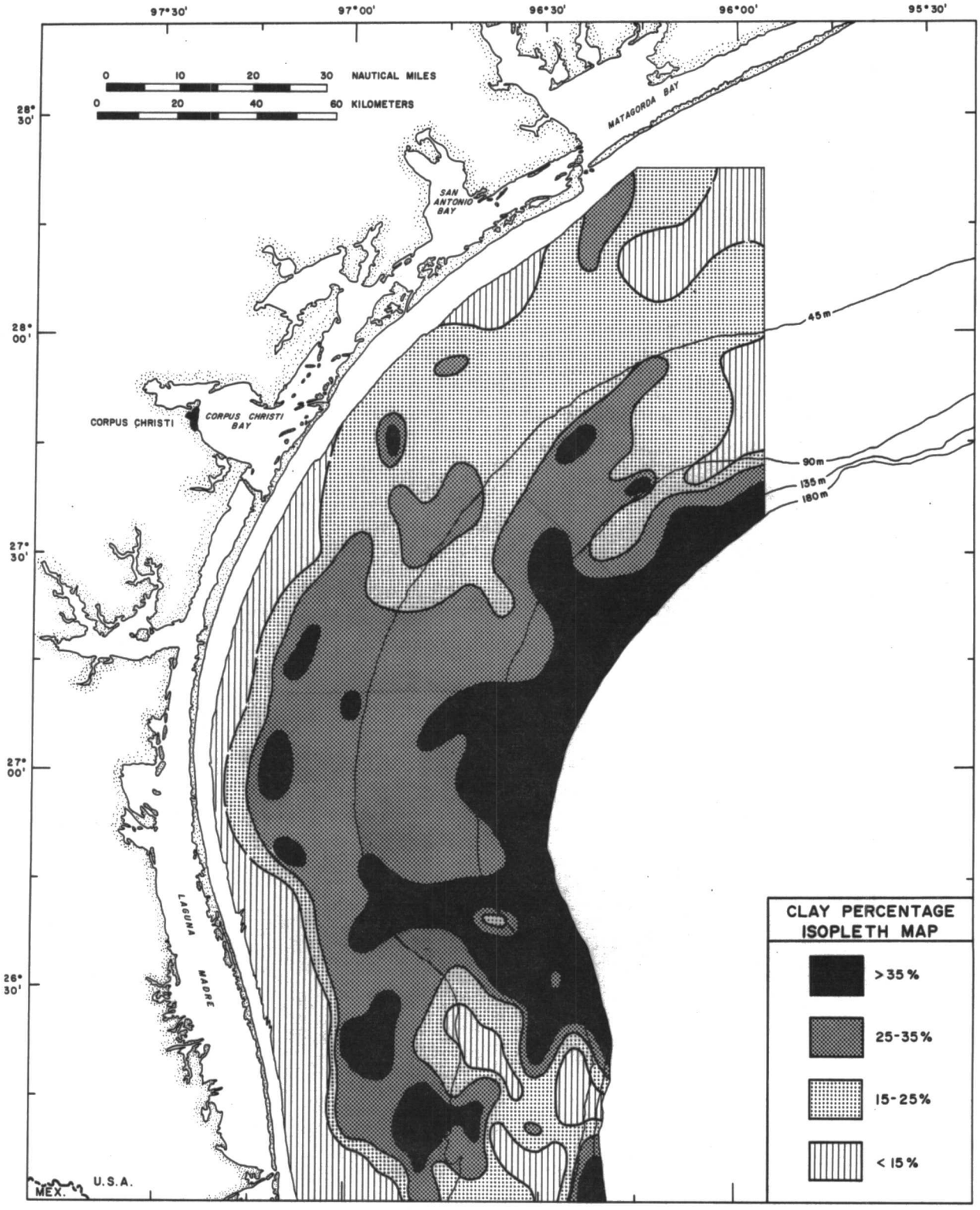

Figure 31. Distribution of clay.

The clay distribution pattern also appears to reflect mainly the modern suspended sediment dispersal system. The general shoreward reduction in clay content is logically attributed to a progressing shoreward increase in significant wave surge energy which would tend to maintain clay particles in suspension. In contrast to silt, the absence of seaward closure on the clay pattern indicates that the clay dispersal system is substantially different. Most silt seems to be hydraulically trapped within the OCS region, thus reflecting a relatively closed dispersal system. In contrast, the clay pattern indicates a more open dispersal system whereby most clay detritus appears to escape from the OCS onto the adjacent continental slope and deep Gulf region. The sources of clay detritus probably are the same as for the silt fraction, namely, coastal erosion, suspended sediment reflux from adjacent estuaries, and possible *in situ* winnowing of relict and palimpsest sediments. Although increasing clay deposition normally occurs in a seaward direction, it is plausible that strong storm waves and tides could redistribute bottom shelf-edge clays *en masse*, possibly resulting in some net shoreward storm displacement. Some of the crenulations exhibited by the clay isopleths in the central sector of the shelf could reflect varying dispersal under alternate fair-weather and storm hydraulic conditions.

Component-Ratio Variability

Sea floor sediment variability also has been delineated in terms of sand/mud and silt/clay ratios. In contrast to single-component percentages, ratios more effectively demonstrate the interrelation of two lithologic components.

Sand/Mud ratios

Sand and mud comprise the two basic textural components of OCS sea floor sediments, and their interrelationships are shown by the ratio isopleth map

(fig. 32 and pl. 9). The sand/mud ratios reach a maximum of 9.1 at individual stations; locally, sand is absent. The ratio isopleth map indicates that mud is by far the more quantitatively significant component. The majority of the OCS region is characterized by ratios less than 0.25; the only areas where sand exceeds mud (>1.0) is on the ancestral Rio Grande and Brazos-Colorado deltas, and along the shoreface. The ratios probably also increase progressively shoreward of the surveyed OCS area. The regional ratio distribution pattern closely reflects the sand percentage pattern, demonstrating a muddy central sector and increasing sand content shoreward as well as both northward and southward.

The ratio distribution map reinforces and more clearly depicts the trends indicated by the individual sand-silt-clay percentage maps. The muddy central sector of the shelf largely reflects the depocenter of modern suspended sediments. The Matagorda Bay inlet area appears to be a major avenue of mud influx. In addition, the convergence and seaward return of muddy nearshore waters may be a prominent source, as suggested by the westward-trending mud salient near 27°N latitude. The regional trend of seaward decreasing ratio values indicates net offshore transport. Regionally, the mud facies also appears to be undergoing net southward transport, resulting in mud migration over the relict sand deposits of the ancestral Rio Grande delta. The southward movement is suggested by the prominent mud salient east of 97°W longitude, and the relatively closely spaced isopleths indicating rapid transition of one sediment type to another. Rapid transitions would be anticipated between genetically dissimilar deposits that are not consanguineous (e.g. modern muds versus relict sands). In contrast, the lower isopleth gradients or more widely spaced isopleths in the northern Brazos-Colorado delta area indicate a more gradual transition between types of sediment, a situation that might be expected in contemporaneous deposits undergoing selective sorting during transport. The gradients suggest that both modern muds and palimpsest sands have a net movement southward.

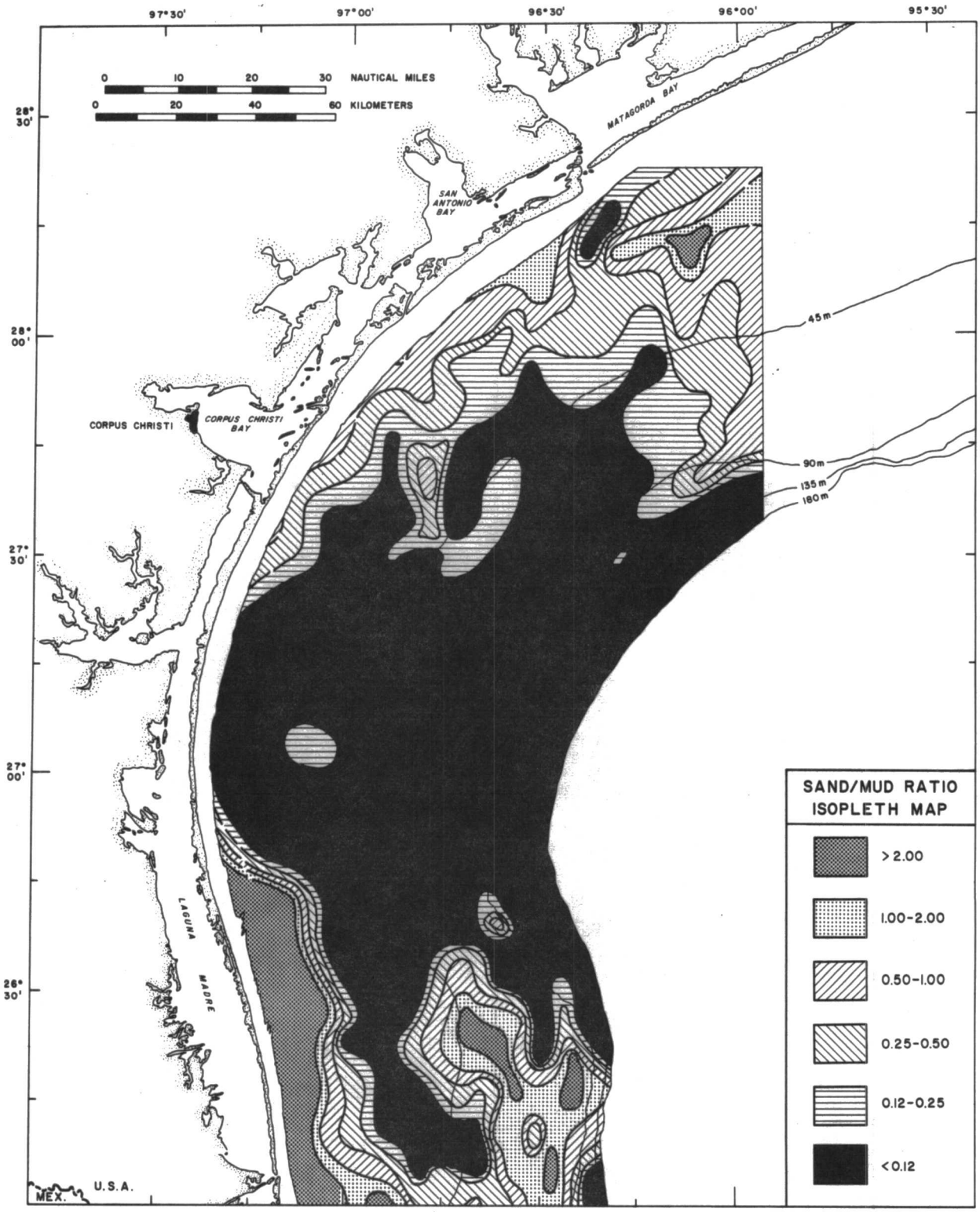

Figure 32. Sand/mud ratios.

Silt/Clay ratios

The regional variability of the dominant mud fraction has been delineated in further detail in terms of the relative proportions of silt and clay. The silt/clay ratios are shown by the ratio isopleth map (fig. 33 and pl. 10). Ratio values range from 0.86 to a maximum of 6.69. Quantitatively, the isopleth map indicates that silt is the highly dominant component. Over most of the OCS, the silt/clay ratios exceed 2.0. The only areas of approximately equal proportions of silt and clay are toward the shelf edge; only rarely is clay the dominant mud component. The ratios indicate a regional trend of increasing silt both shoreward and northward.

As the mud sediments reflect mainly the suspended sediment transport system, the relative proportions of silt and clay can provide some insight into the mechanics of suspended sediment dispersal over the OCS. The regional pattern appears to be the composite response to two separate processes. The increasing proportion of silt shoreward is attributed to increasing wave surge intensity shoreward which maintains progressively larger proportions of clay in suspension in a shoreward direction. The pattern also appears to reflect the influence of semi-permanent coastwise currents. The decreasing proportion of silt southward suggests a net southward transport of mud; this is in agreement with the inference of net southward transport based on the more general sand/mud ratios. It should be noted that the seasonal coastwise currents in the region have a general net southward component during November and December, the period of the OCS survey. The silt/clay ratios are one of the more sensitive indices of sediment dispersal and may be one of the more ephemeral patterns. Although the pattern is valid for the November-December period, substantial modifications could occur during the summer months when coastwise currents have a net northward component.

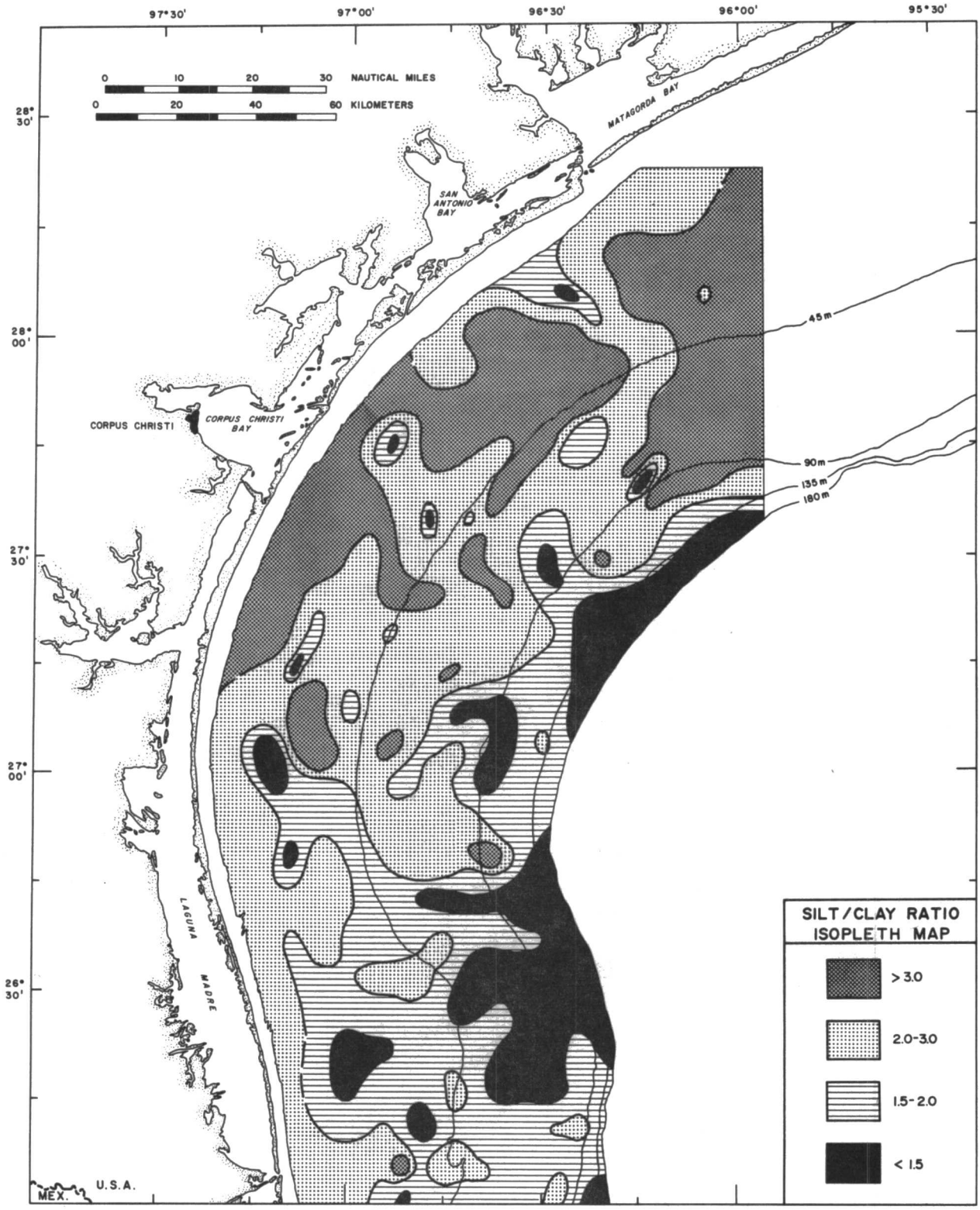

Figure 33. Silt/clay ratios.

Total Component Variability

The total composite variability of sea floor sediments has been evaluated in terms of the combined sand, silt, and clay components. The sediment types have been determined by plotting the relative proportions of the three detrital components on ternary diagrams in accordance with Shepard's (1954) classification system. The composite sediment variability has been related to water depth and geographic location.

Sediment-water depth relationship

For relating total-component sediment variability to depth of water, the OCS was arbitrarily divided into three depth subprovinces: shallow water (<45 m), intermediate water (45-90 m), and deep water (>90 m). Sediment composition within the three depth subprovinces is shown by figure 34 and plate 11. In all three subprovinces, the majority of samples are in the clayey silt category indicating a lack of close depth control on overall sediment type within the OCS region. Both the shallow and intermediate water depths have substantially more variability than the relatively uniform deeper province and contain larger proportions of sandy sediments. These characteristics can be attributed to higher significant wave surge and greater hydraulic variability within the areas of shallow and intermediate water depth. Also, the absence of a well-defined zonation of sediment composition relative to depth of water indicates that hydraulic grading is not regionally developed within the South Texas OCS.

Geographic relationship

As a means of relating total sediment composition to geographic location within the OCS, sample groupings were selected according to three geographic

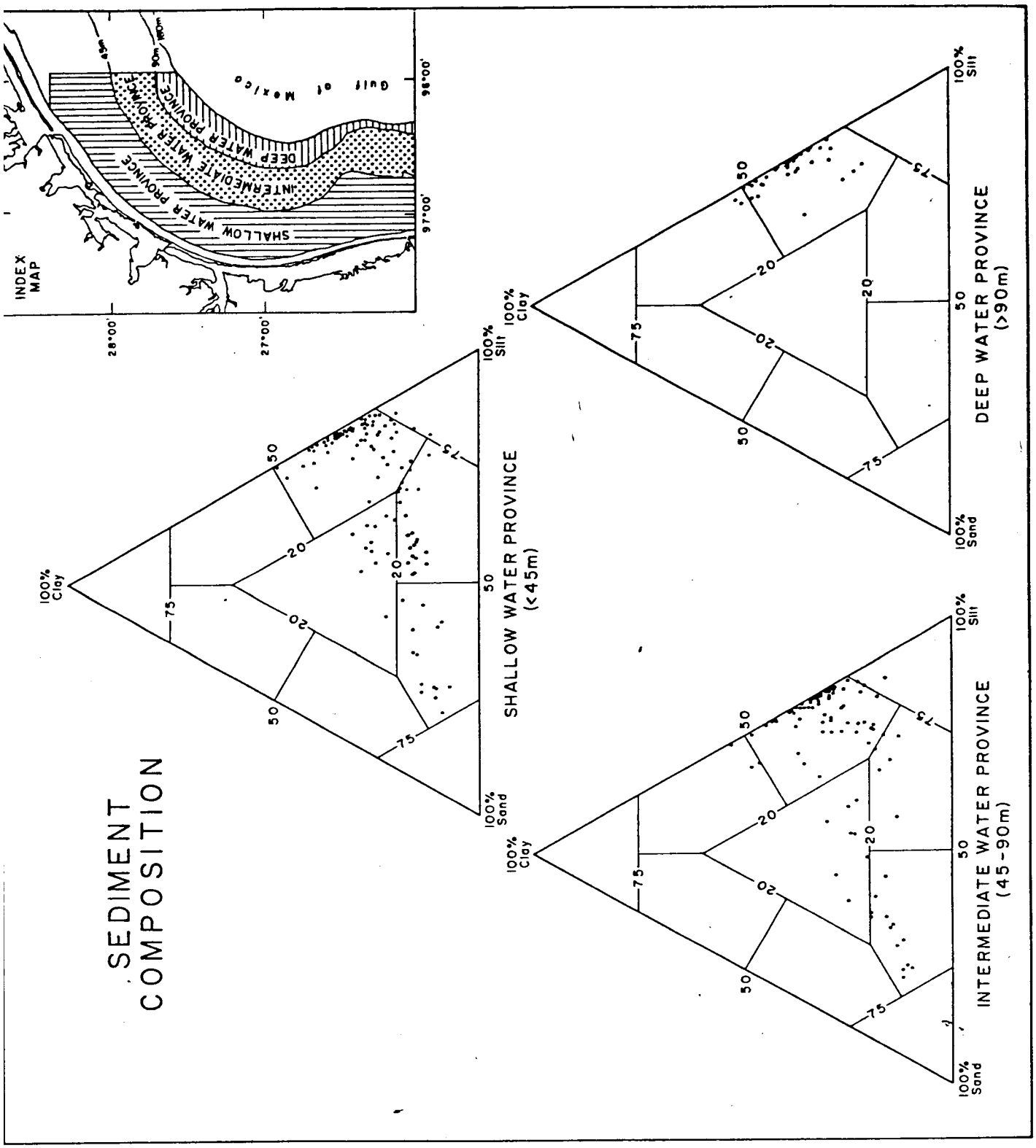

Figure 34. Sediment composition related to water depth.

provinces: northern (sample localities #1-87), central (sample localities #88-185), and southern (sample localities #186-274). These subprovinces were established to compare coastwise compositional variability; province boundaries were established so as to include approximately the same number of samples in each province. Sediment composition within the three provinces is shown by figure 35 and plate 12.

The subprovinces show a definite coastwise variation in general sediment composition. The northern subprovince is characterized by large proportions of both sandy silt and clayey silt, and a relatively high degree of compositional variability. In contrast, the central subprovince is relatively uniform and is made up mainly of clayey silt. The southern province is highly variable and is made up of large proportions of clayey silt, silty sand, and sansicl (sand-silt-clay). The relatively high variability and more sandy nature of the northern and southern subprovinces largely reflects large quantities or coarser relict and palimpsest deposits within those sectors. In contrast, the uniformity of the central subprovince reflects a composition of modern mud deposits in equilibrium with the present hydraulic regime.

General Textural Synthesis

A general synthesis of all the textural variability previously described is shown by the sediment distribution map (fig. 36, pl. 13) which indicates that the sediments over most of the South Texas OCS is clayey silt. The clayey silt covers nearly all of the central subprovince and extends both northward and southward as prominent salients. Clay is the dominant component in a few small local areas concentrated mainly along the shelf edge. The clayey silt grades northward into sandy silt which in turn grades into silty sand in two local areas. The textural gradation in the northern subprovince indicates a

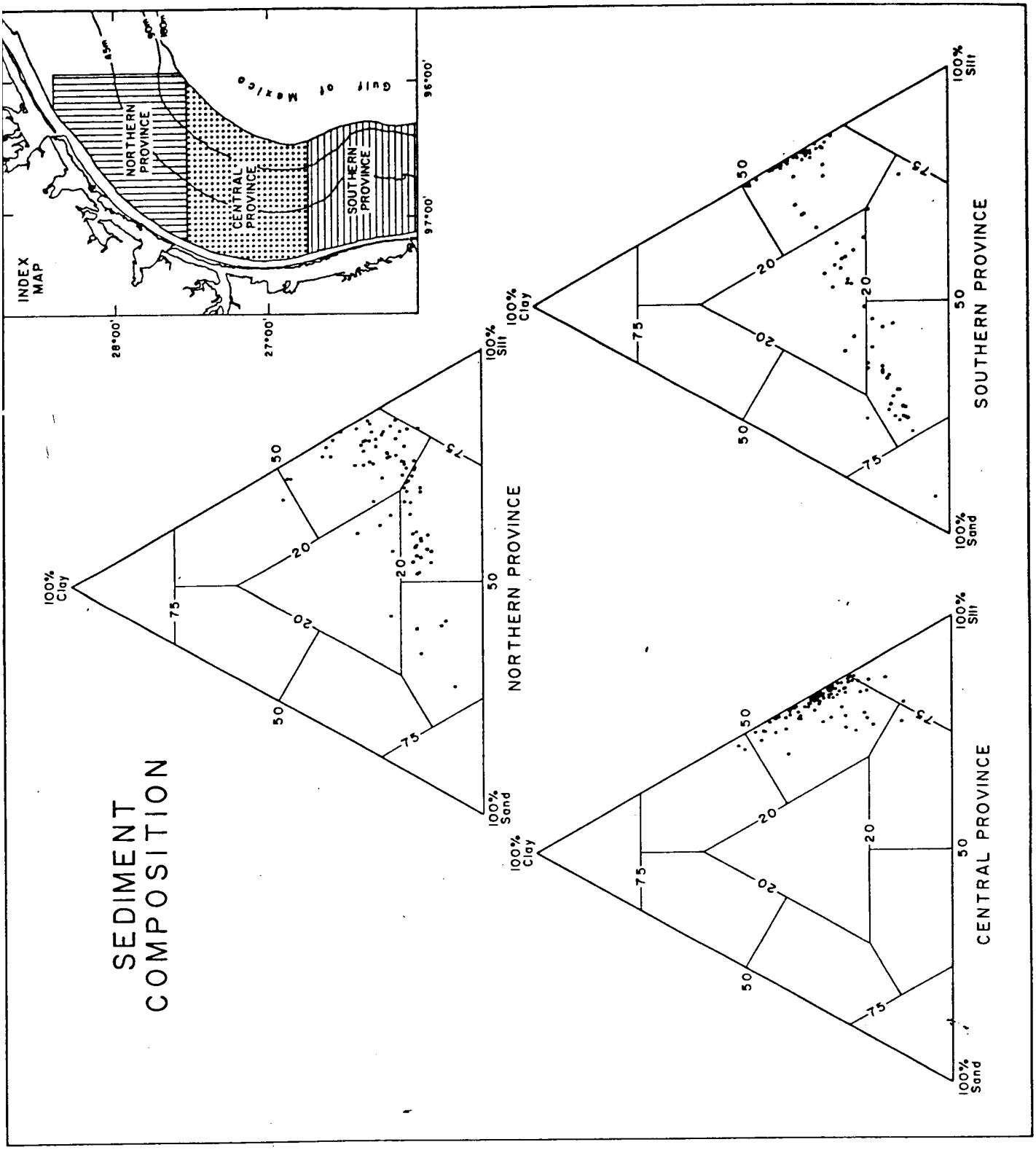

Figure 35. Sediment composition related to geographic subprovinces

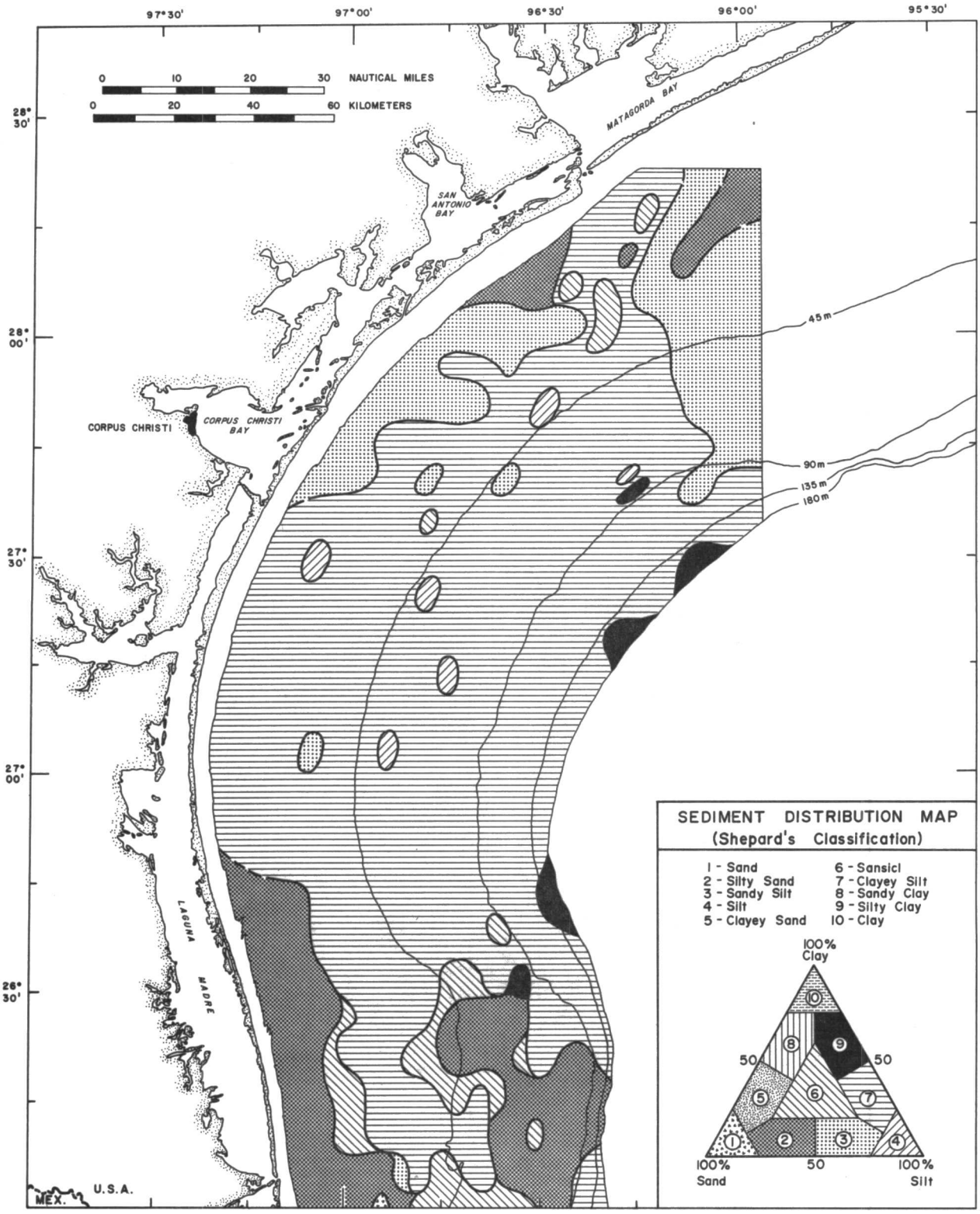

Figure 36. Distribution of sediment by type.

net southward transport of detritus derived from both shoreface erosion and from the reworking of palimpsest deposits comprising the ancestral Brazos-Colorado delta. The clayey silt salient extending southward from the Matagorda Bay inlet area also suggests the southward dispersion of sediment from muddy coastal waters. Perhaps the mixing of bay effluent with southward transported littoral drift from further north may be reflected by the local areas of sansicl (sand-silt-clay) sediments within the clayey silt salient.

In the southern sector the clayey silt blanket appears to be encroaching upon relict silty sands of the ancestral Rio Grande delta. Areas of sansicl (sand-silt-clay) separating the two genetically distinct sedimentary bodies suggest possible mixing zones of relict and modern sediment populations. The prominent westward-trending salient of clayey silt south of Corpus Christi Bay suggests that some of the silt may come from return flow seaward of muddy littoral and nearshore waters localized at a node of current convergence.

In terms of the graded shelf concept (Johnson, 1919), some areas of the OCS do appear to be hydraulically graded. The northern half of the region appears to exhibit a combination of both seaward and southward grading, suggesting partial hydraulic equilibrium; in contrast, relict deposits such as located on the ancestral Rio Grande delta area are largely out of equilibrium. The situation is common along many shelf and coastal areas as a result of the rapid rise in sea level during the Holocene transgression.

Statistical Grain-Size Parameters

The sediments also were evaluated texturally in terms of their statistical grain-size parameters, measures of still greater hydraulic sensitivity for understanding regional sedimentological processes. Parameters determined were

central tendency measures, standard deviations, skewness, and kurtosis. Moment measures were used because of their relatively high sensitivity. However, supplemental graphic measures (Folk and Ward, 1957) were also determined. Both moment measures and graphic measures for each sample station are tabulated in Table IIa and Table IIb, Part II. All size terminology follows the Udden-Wentworth grade scale and is expressed in terms of Krumbein's (1934) phi unit (Ø) transformation.

Central tendency measures

The statistical measures of central tendency provide information regarding energy levels and dispersal gradients. The average grain size of sea floor sediments was determined in terms of mean diameters (first moments) and modal diameters. Supplemental median diameters were also derived, and are in Table II, Part II.

Mean diameters--The average grain-size variability in terms of mean diameters is shown by both a distribution map (fig. 37, pl. 14) and an isopleth map (fig. 38, pl. 15). The mean diameter distribution map shows the actual distribution of average grain size; the isopleth map shows grain-size gradients.

The mean diameter distribution map (fig. 37) indicates that bottom sediments range from clay (8.17 Ø) to fine sand (2.91 Ø). The two sediment types represent the extreme ends of the OCS sediment size spectrum, occurring only in three small isolated localities. Most of the OCS is covered by a combination of fine (6.00-6.99 Ø) and very fine silt (7.00-7.99 Ø). Coarser sediments are more limited in distribution, and are localized along the shoreface as well as in the areas of the ancestral Rio Grande and Brazos-Colorado deltas.

Regional trends are depicted better by the isopleth map (fig. 38) which shows grain-size gradients. The map shows an overall grain-size pattern similar to some of the other patterns, but with a greater degree of hydraulic sensitivity.

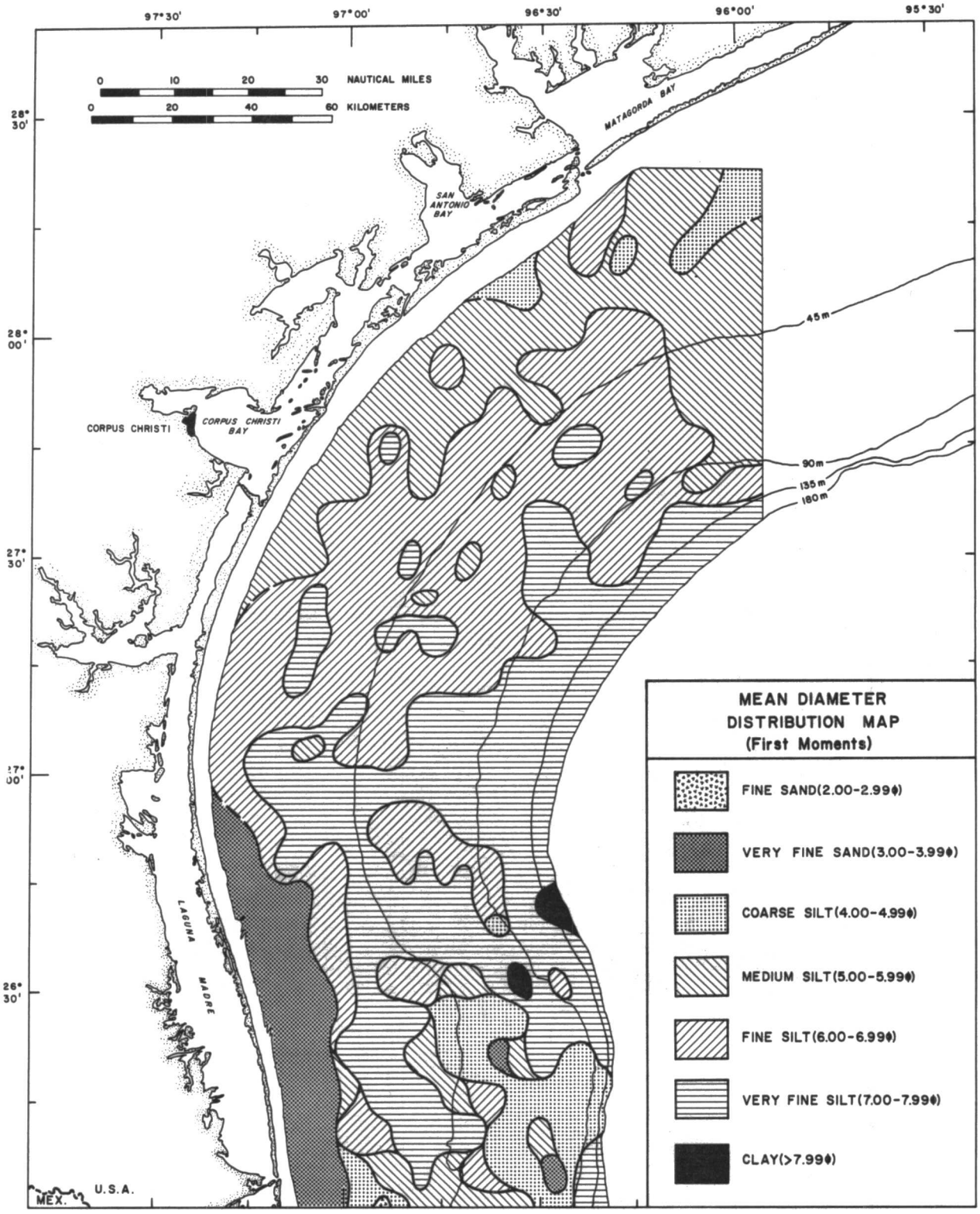

Figure 37. Distribution of sediment by mean diameters.

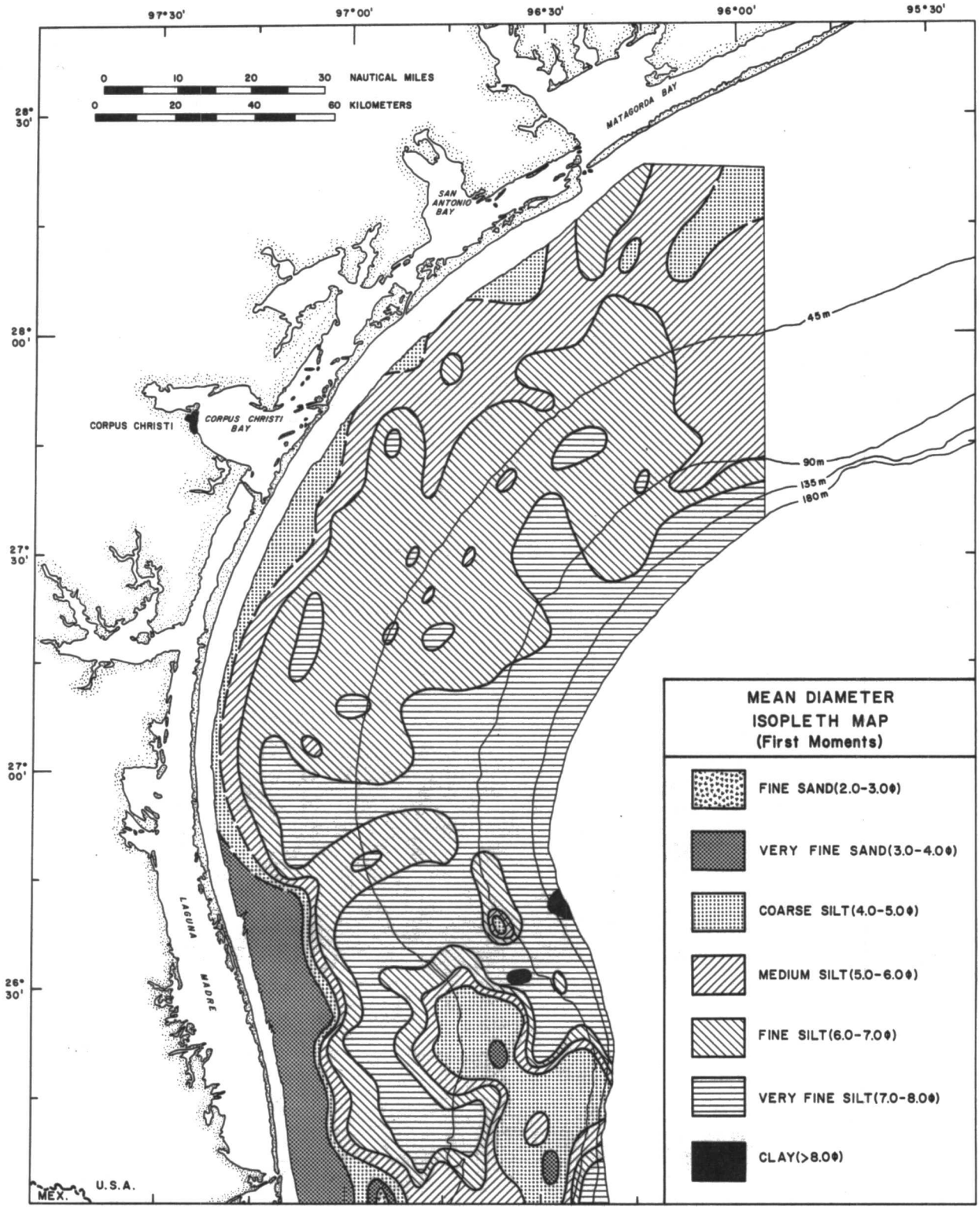

Figure 38. Mean diameter isopleths.

The pattern reflects a composite response indicating size gradients both across and along the shelf. Grain size increases generally shoreward, largely reflecting increasing proximity to coastal source areas and increasing wave energy. Sediments also become coarser both northward and southward from the central sector of the shelf, apparently reflecting both the influence of semi-permanent coastwise currents as well as source area locations. The contrast between the relatively gentle northern gradients and the pronounced southern gradients amplifies their probable genetic distinction. The gentle northward gradients appear to indicate a net southward transport of sediment from the Matagorda Bay inlet area and other northern coastal sources, as well as sediment derived from palimpsest deposits comprising the ancestral Brazos-Colorado delta. The southward transport by coastwise residual currents could produce the observed size reduction in a downcurrent direction. Several previous empirical studies have noted a general size reduction of clastic sediments in the direction of transport (e.g. Pettijohn, 1957, p. 532). In contrast, the abrupt southern gradients suggest that the modern mud blanket is encroaching southward onto coarser relict deposits comprising the ancestral Rio Grande delta; the relict delta sediments appear to be undergoing in situ winnowing and may be supplying some sediment to the mud blanket locally. The prominent mud salient east of 97°W longitude is well-defined and appears to reflect the main avenue of southward mud encroachment.

Modal diameters--The mode is a central tendency measure denoting the most frequently occurring particle size within a grain-size distribution. As noted by Curray (1960), the measure has advantages over other statistical measures in areas containing a large proportion of polymodal sediments because it does not assume a normal size distribution. Curray (1960) has effectively utilized modal diameters in the northwest Gulf of Mexico for tracing discrete sediment masses on the continental shelf. The principal modes of grain size determined

in the present study were differentiated into size classes and are shown by both the modal diameter distribution map (fig. 39, pl. 16) and isopleth map (fig. 40, pl. 17). The modal diameters range from clay (9.61 Ø) to fine sand size (2.14 Ø). Although the regional modal distribution pattern is grossly similar to the mean diameter pattern, some notable differences are apparent. The modal diameter pattern (fig. 39) indicates a higher local variability within the central and northern sectors of the shelf but somewhat less variability than mean diameters within the southern sector. The modal diameter pattern appears to be more effective than the mean diameter pattern in delineating genetically distinct sediment bodies. Most of the areas interpreted as consisting of relict and palimpsest deposits are largely reflected by the fine-sand mode. The most conspicuous example is the ancestral Rio Grande delta and adjacent shoreface which are collectively reflected as a homogenous and texturally distinct entity. The fine-sand modal unit also characterizes some local areas of the ancestral Brazos-Colorado delta which are also interpreted as being largely palimpsest deposits. The sands of the modal unit may be largely immobile and undergoing only in situ winnowing. The fine-sand modal unit (2.00-2.99 Ø) approximates Curray's (1960, p. 238) Type I grain-size modal unit which exhibits the same distribution pattern. Curray noted that this mode is also widely distributed along the Brazos-Colorado northeast of the South Texas OCS. The very fine-sand mode unit (3.00-3.99 Ø) extends from the Brazos-Colorado delta southward to approximately 27°30'N latitude and appears to be derived largely from the ancestral delta itself and transported southward. Some of the sands probably are derived from coastal erosion of the northern shoreface sector as most Gulf coast beach sands have modes within this size class (e.g. Curray, 1960). The very fine-sand modal unit approximates Curray's (1960, p. 238) Type II unit, which exhibits a similar distribution pattern.

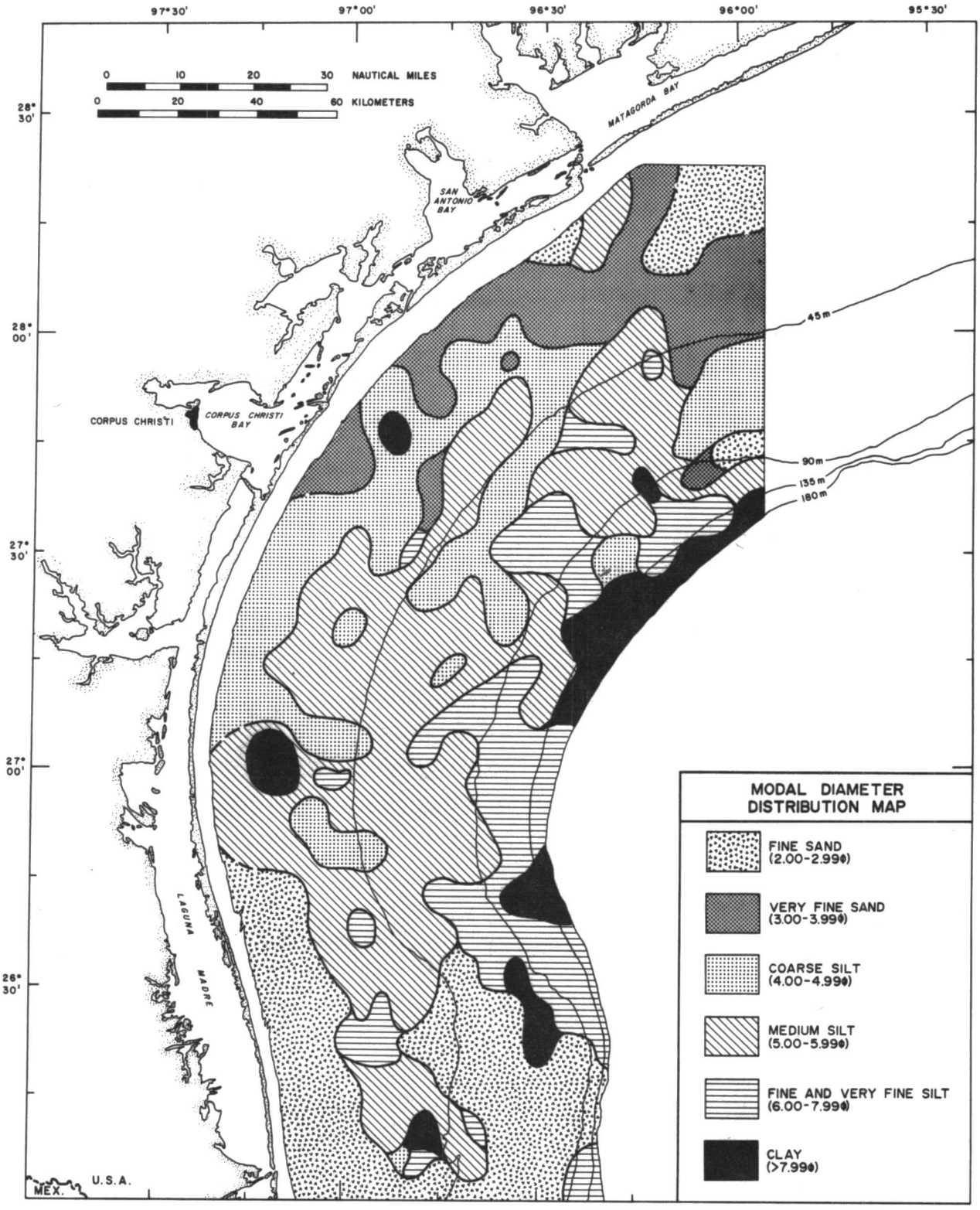

Figure 39. Distribution of sediment by modal diameters.

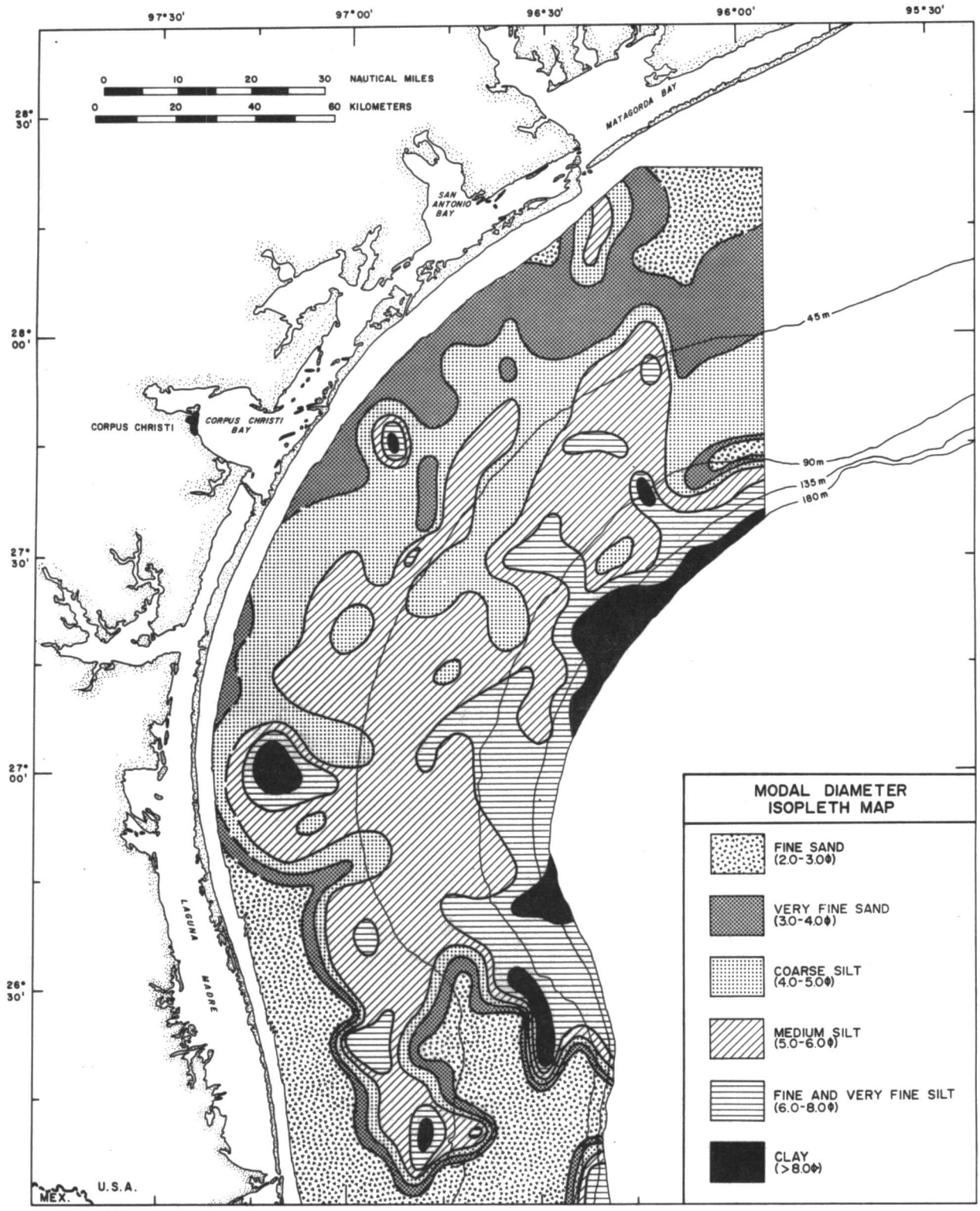

Figure 40. Modal diameter isopleths.

Curray noted that this unit also occurs extensively northeast of the South Texas OCS and he also interpreted the Brazos-Colorado delta as the major source.

The modern mud is comprised of a complex mixture of modal units ranging from coarse silt (4.00-4.99 Ø) to clay (8.0 Ø). The coarse-silt modal unit is localized mainly in the northern sector and generally is in juxtaposition to the very fine-sand unit, suggesting a size gradation associated with southerly transport from sources in the northern sector. The medium-silt modal unit is widely distributed within the interior of the central sector and makes up much of the south-trending salient east of 97°W longitude. Also, it appears to form a west-trending salient at the postulated current convergence zone near 27°N latitude. The fine silt to clay modal units are concentrated toward the shelf edge; this general pattern appears to reflect a seaward decrease in wave energy. A noteworthy feature in the Rio Grande delta area is the juxtaposition of the fine-sand modal unit with sediments ranging from medium silt to clay; except for one small area, coarse silt and very fine sand are conspicuously absent. The absence of a complete size gradation supports the inference that the modern mud blanket is encroaching upon immobile relict sands of the ancestral delta.

The modal diameter isopleth map (fig. 40) shows the same general trends as the mean diameter isopleth map (fig. 38). The major difference is that the areas of fine sands are much more extensive, comprising most of the southern sector of the shelf and much of the northern sector. In addition, a west-trending salient at 27°N latitude is more clearly defined, possibly relating to seaward flow in the postulated convergence zone. Again, the distinction between the gentle northern size gradients and the abrupt southern gradients is clearly demonstrated.

Standard deviations

The sorting characteristics of bottom sediments can provide insight into the energy consistency of the hydraulic regime, and may help reveal genetic difference among sediments within the OCS. Sediment sorting is described in terms of standard deviations (second moments), which are shown by an isopleth map (fig. 41).

Standard deviation values among individual sample stations range from a minimum of 1.51 Ø to a maximum of 3.88 Ø. Employing Folk's (1965) verbal scale, all OCS sediments can be classified as either poorly sorted (1.0-2.0 Ø) or very poorly sorted (2.0-4.0 Ø). The majority of the OCS contains poorly-sorted sediments which comprise most of the central sector, as well as south-trending salients from the Matagorda Bay inlet area and east of 97°N longitude in the Rio Grande delta area. The very poorly-sorted sediments are mainly in the Rio Grande and Brazos-Colorado delta areas and along the shoreface.

A comparison of the standard deviation trends with the average grain-size trends indicated by the mean and modal diameter isopleth maps shows an obvious relationship between the two parameters. Although differences in local variability occur, the regional trends are essentially the same: a general shoreward increase in standard deviation as well as an increase both northward and southward from the central region. Comparison of the trends indicates that sorting characteristics are highly correlated with average grain size. The relatively coarse relict and palimpsest sediments of the shoreface and the two delta areas are generally more poorly sorted than the finer sediments comprising the modern mud blanket. As noted by Moss (1963), several workers have established an empirical relationship between grain size and sorting, with the finer-grained sediments tending to be better sorted.

The standard deviation trends appear to amplify the genetic differences between the relatively poorer-sorted coarser sediments which are interpreted

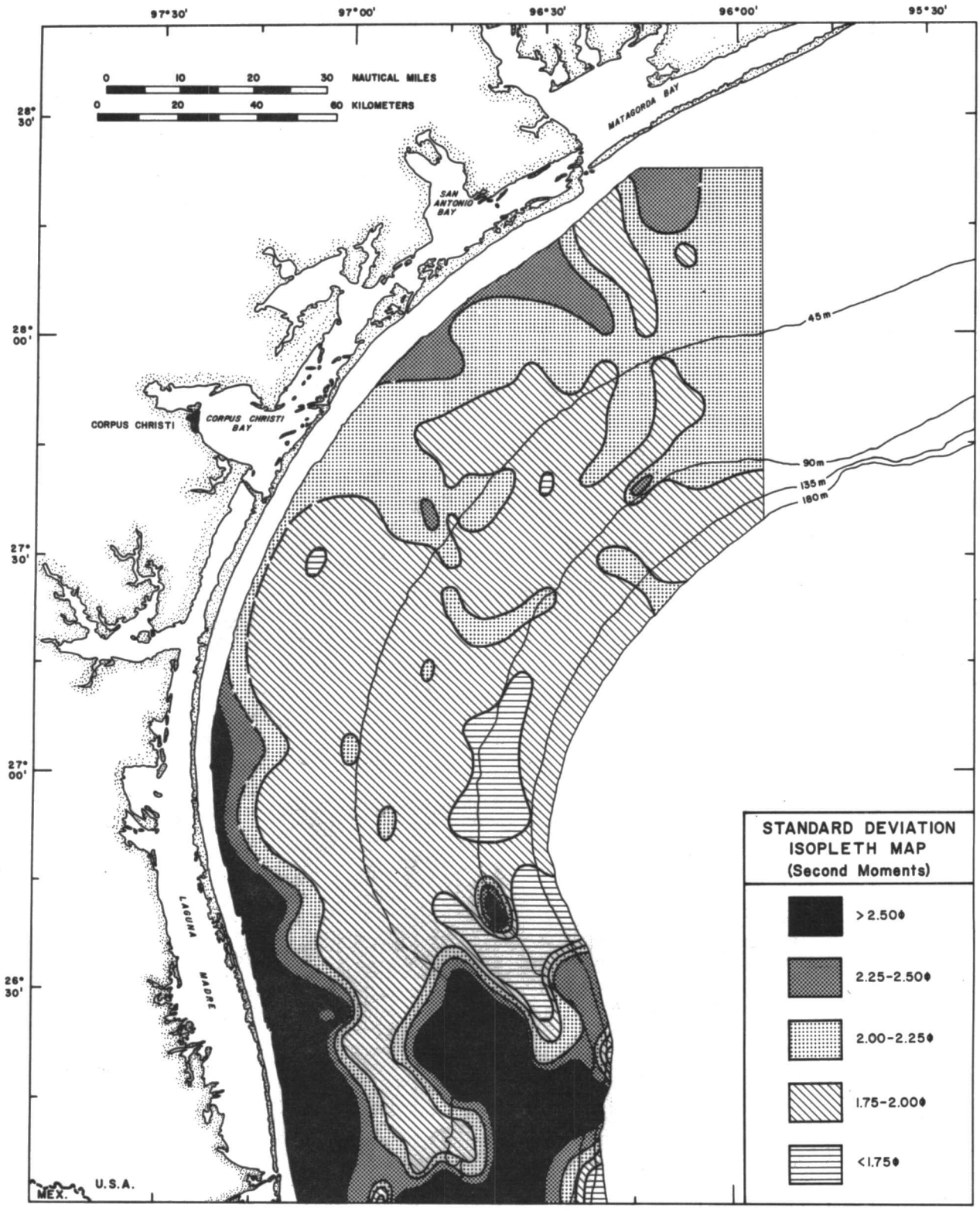

Figure 41. Standard deviation isopleths.

as relict and palimpsest deposits and the better sorted modern mud blanket. The coarser relict and palimpsest sediments are wholly or partially in disequilibrium with the present OCS hydraulic regime; consequently, they may be largely beyond the fair-weather competence range of modern currents and wave surge for effective continuous sorting. The sorting of the coarser sediments may be confined largely to storm-intensified hydraulic conditions. In contrast, the better sorted modern muds are in equilibrium and probably are subjected to nearly continuous hydraulic fractionation during fair-weather suspension transport. Some of the regional standard deviation pattern may also partially reflect progressive sorting gradients established during transport. In employing a Markov process model for simulating one-dimensional shelf sediment transport, Swift and others (1972) noted the progressive evolution of size frequency distributions in the transport direction. They noted that progressive size sorting will occur provided the transport surface will accept grains for permanent deposition. The improved sorting shown by the isopleth map both seaward as well as toward the central sector from the northern and southern deltas could partially reflect sediment transport in those directions.

Skewness measures

Skewness (third moments) is a sensitive measure of the asymmetry of a sediment's size frequency distribution relative to a normal Gaussian distribution; it reflects either particle excesses or deficiencies within the tail portions of a size distribution. As noted by previous workers (e.g. Folk and Ward, 1957; Mason and Folk, 1958; Spencer, 1963; Folk, 1966), both skewness and the associated kurtosis measure can be indicators of sediment sub-population mixing. Skewness has also been related to environmental energy by Duane (1964) for Pamlico Sound sediments. He noted that sediments deposited in relatively high-energy areas where intensive winnowing and truncation of the

fine fractions occurred were coarsely skewed; whereas, sediments deposited in low-energy sheltered environments were associated with fine skewness. However, Friedman (1967) and Cronan (1972) note that polymodal sediments can exhibit variable skewness values, depending on the specific proportions of component sub-populations.

Skewness value for OCS bottom sediments are shown by an isopleth map (fig. 42, pl. 19). Values at individual sample stations range from +0.87 (strongly fine-skewed) to -0.47 (strongly coarse-skewed), employing Folk's (1965) verbal classification scale. The majority of the OCS is composed of strongly fine-skewed sediments. Near-symmetrical sediments are moderately distributed; whereas, coarse-skewed and strongly coarse-skewed sediments are least abundant, being confined largely to the shelf edge area.

Except for the ancestral Rio Grande delta area, the general regional trend is a progressive seaward decrease in fine skewness and a corresponding increase in coarse skewness. The trend appears to reflect largely transport of sediments derived from coastal sources. The skewness pattern exhibits a good correlation with the relative proportions of sand, silt, and clay components, as indicated by the sand/mud and silt/clay ratio maps (figs. 32 and 33). The beach sands comprising adjacent Mustang Island have been texturally characterized by Mason and Folk (1958). They describe the average characteristics of the beach sands as being very well-sorted, fine-grained sand with near-symmetrical mesokurtic distributions. If normal distributions can be considered typical of most of the beach sands comprising the barrier chain marginal to the OCS, then a substantial change must occur within the nearshore zone as the shoreface sector is characterized by strongly fine-skewed sediments. In terms of modal diameters, the shoreface sector is comprised largely of fine to very fine sand and coarse silt; the mixing of these principal modes with finer admixtures is interpreted

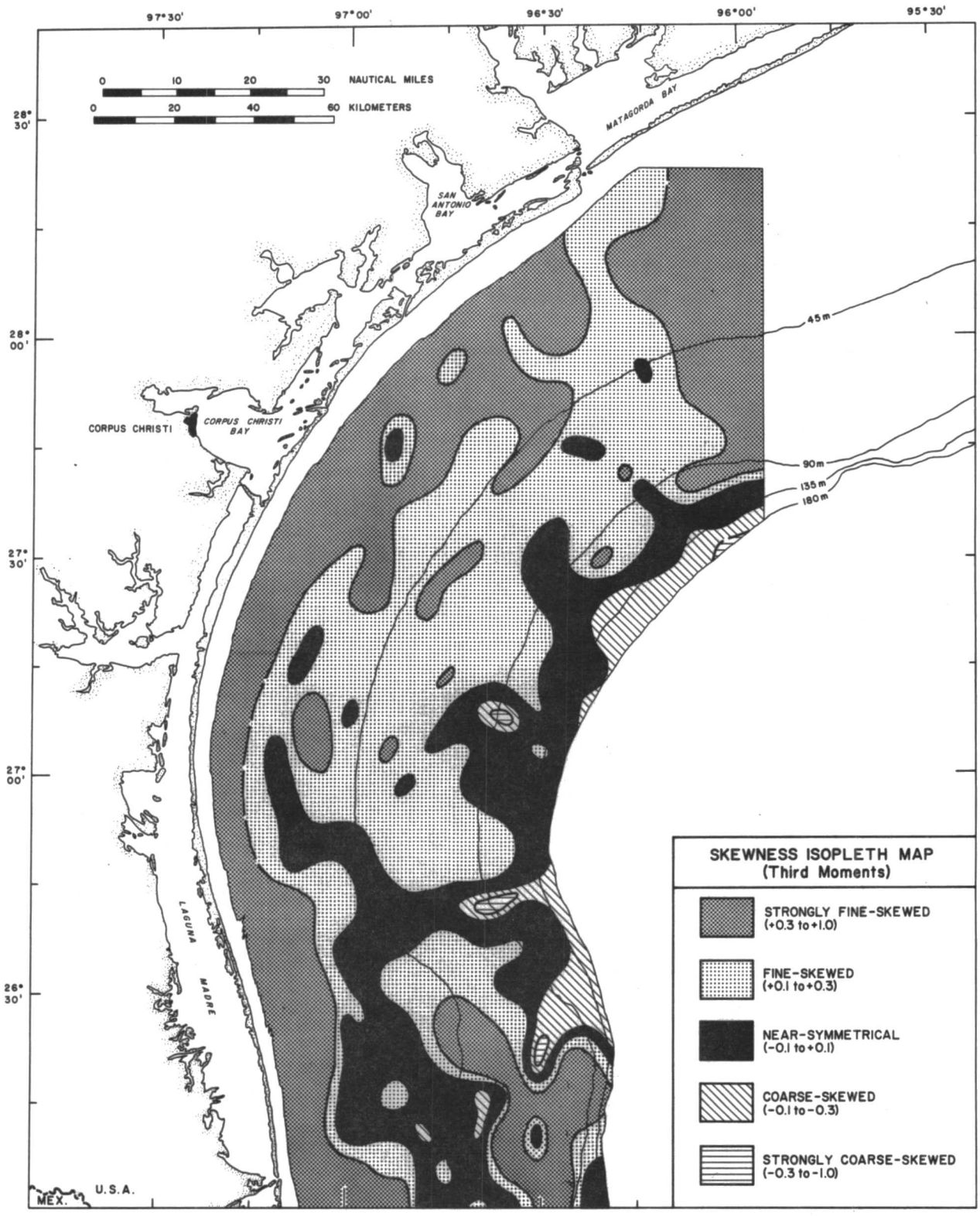

Figure 42.. Sediment skewness.

as the cause of the strongly fine-skewed distribution. The offshore transport of a normally distributed sand-coarse silt population derived from the barrier chain would tend to fractionate the sediments by size along the shoreface in a direction normal to the shoreline. The mixing of these fractionates with finer silt derived from the longshore transport and deposition of suspended sediment may produce the strongly fine-skewed pattern. The mixing process proposed is supported by the standard deviation isopleth map (fig. 41) which indicates generally very poor sorting in the shoreface sector, as contrasted with the very well-sorted beach sands of the adjacent barrier chain. The same relationship occurs in the Rio Grande and Brazos-Colorado areas, which might similarly be explained as a result of mixing a major relict or palimpsest sand-coarse silt population with minor admixtures of finer silt deposited from suspension. As the major sand-coarse silt population quantitatively decreases in a seaward direction, the finer suspended silt component becomes a more prominent population, resulting in a transition from strongly fine-skewed to fine-skewed sediments. Further seaward, as the relative proportion of silt decreases and the clay fraction becomes more prominent, a transition to near-symmetrical distribution occurs. A good correlation exists with the pattern of silt/clay ratios (fig. 33). The near-symmetrical distributions are localized in areas where ratios are less than 2.0. As clay becomes the dominant component near the shelf edge, a transition to coarsely skewed and very coarsely skewed distributions occurs. The coarsely skewed deposits are largely restricted to areas where silt/clay ratios are less than 1.5. The coarse skewness is attributed both to admixtures of detrital silt as well as to the increasing quantitative significance of pelagic foraminiferal admixtures near the shelf edge. In essence, the regional skewness pattern is interpreted as reflecting largely the progressive seaward transport and mixing of sand, silt, and clay populations.

Kurtosis measures

Kurtosis (fourth moments) is a sensitive quantitative measure of the peakedness of a sediment's size distribution relative to a normal Gaussian distribution. In conjunction with skewness, it can also be an indicator of sediment population mixing. As noted by Folk (1966), platykurtic (excessively flat) distributions may reflect the mixing of log-normal populations in nearly equal proportions; whereas, leptokurtic (excessively peaked) distributions may reflect the mixing of a highly dominant population with a highly subordinate population. Mesokurtic (Gaussian) distributions reflect a single log-normal population. In utilizing the fourth moment measures, a value of zero is a mesokurtic distribution; whereas, positive values indicate leptokurtosis and negative values indicate platykurtosis.

Kurtosis values for the OCS region are shown by an isopleth map (fig. 43, pl. 20). Values range from -1.52 to +1.65. Most of the OCS region consists of platykurtic sediments of varying degree; the more strongly platykurtic sediments are concentrated in the southern half of the region. Leptokurtic sediments are relatively scarce and are concentrated mainly along the shoreface sector; some isolated leptokurtic areas are on the ancestral Brazos-Colorado and Rio Grande deltas.

The genetic significance of the kurtosis measure is poorly understood. Consequently, any interpretation of the regional kurtosis distribution pattern is, of necessity, somewhat tenuous. However, there does appear to be some relationship with skewness that supports the seaward sediment population mixing mechanism suggested by the skewness distribution pattern. The leptokurtic sediments are nearly all concentrated in the areas of strongly fine-skewed sediments. This would support the inference that the strong fine-skewness reflects the mixing of a dominant sand-coarse silt population transported offshore

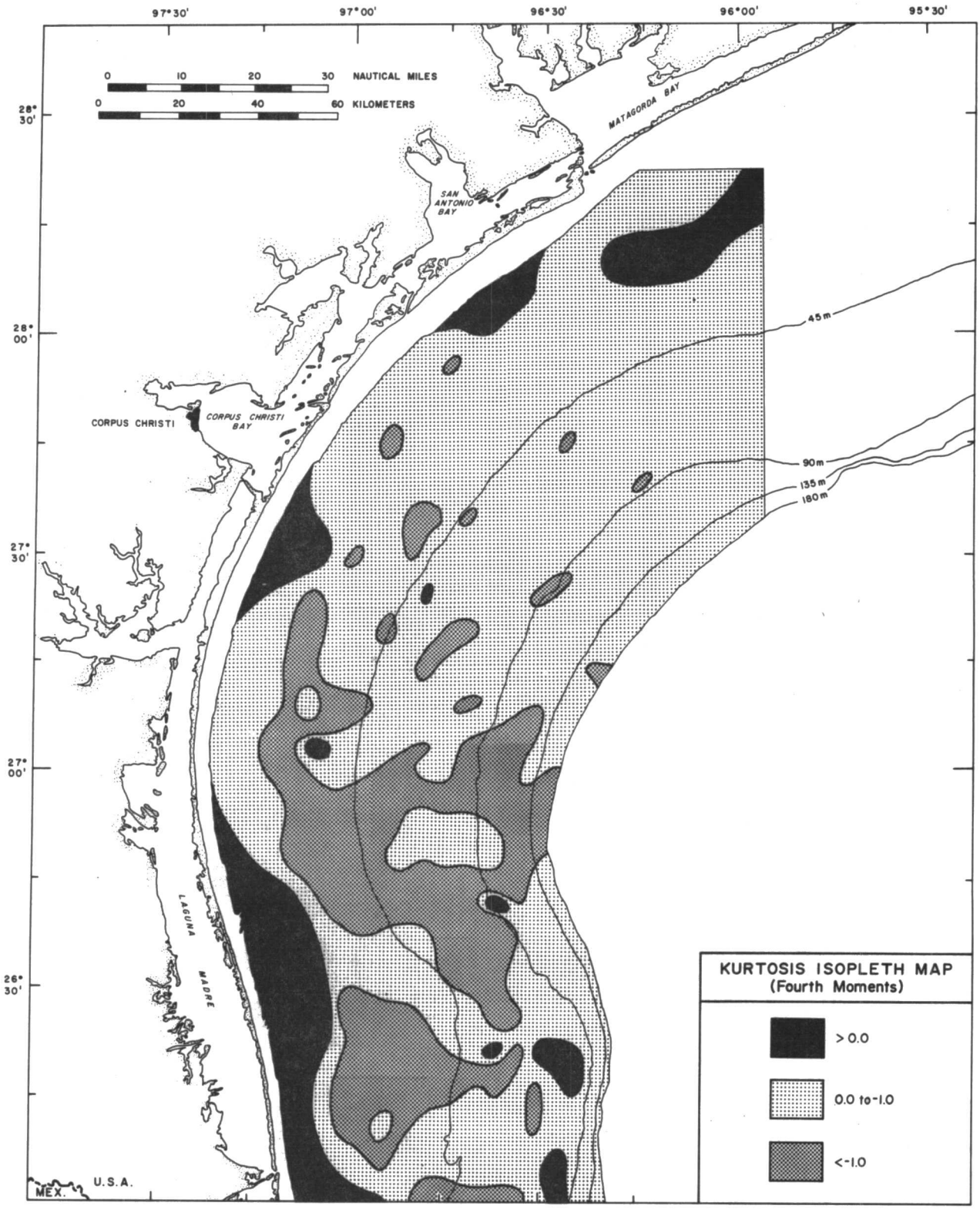

Figure 43. Sediment kurtosis.

with a highly subordinate longshore-transported finer silt population which infiltrated from suspension. The platykurtic sediments throughout most of the OCS apparently reflect the complex mixing of silt and clay fractions of varying sizes derived from multiple sources.

Sediment Color

The variability of color for OCS sea floor sediments was determined at both the surface and shallow subsurface. The specific color characteristics at individual stations are tabulated in Table II, Part II.

Surficial Sediments

Areal variability of the color of surficial sediments within approximately the upper 1 cm is shown by the distribution map (fig. 44, pl. 21). A wide variety of 13 hue-value-chroma combinations was observed; the combinations differentiated into the following five basic color groupings: olive grays (5Y3/2, 5Y4/1, 5Y5/2), olive browns (5Y4/4, 5Y5/6), olives (10Y4/2, 10Y5/4), solid browns (5YR3/4, 5YR4/4, 5YR5/2, 5YR5/6), and yellowish browns (10YR4/2, 10YR5/4). Shades of yellowish brown are the dominant color group; this group is most widely distributed in the shallower parts of the shelf and decreases in area toward the shelf edge. Regionally, color is most variable over the ancestral Brazos-Colorado delta area in the northern sector of the shelf and in the central sector where a conspicuous west-trending multicolored salient is centered along 27°N latitude. The remainder of the region exhibits only minor local variability.

As noted by Stanley (1969), sediment color is a complex function of several environmental and petrologic variables. Color can be sensitive to several environmental factors such as water depth, Eh and pH. The petrologic factors

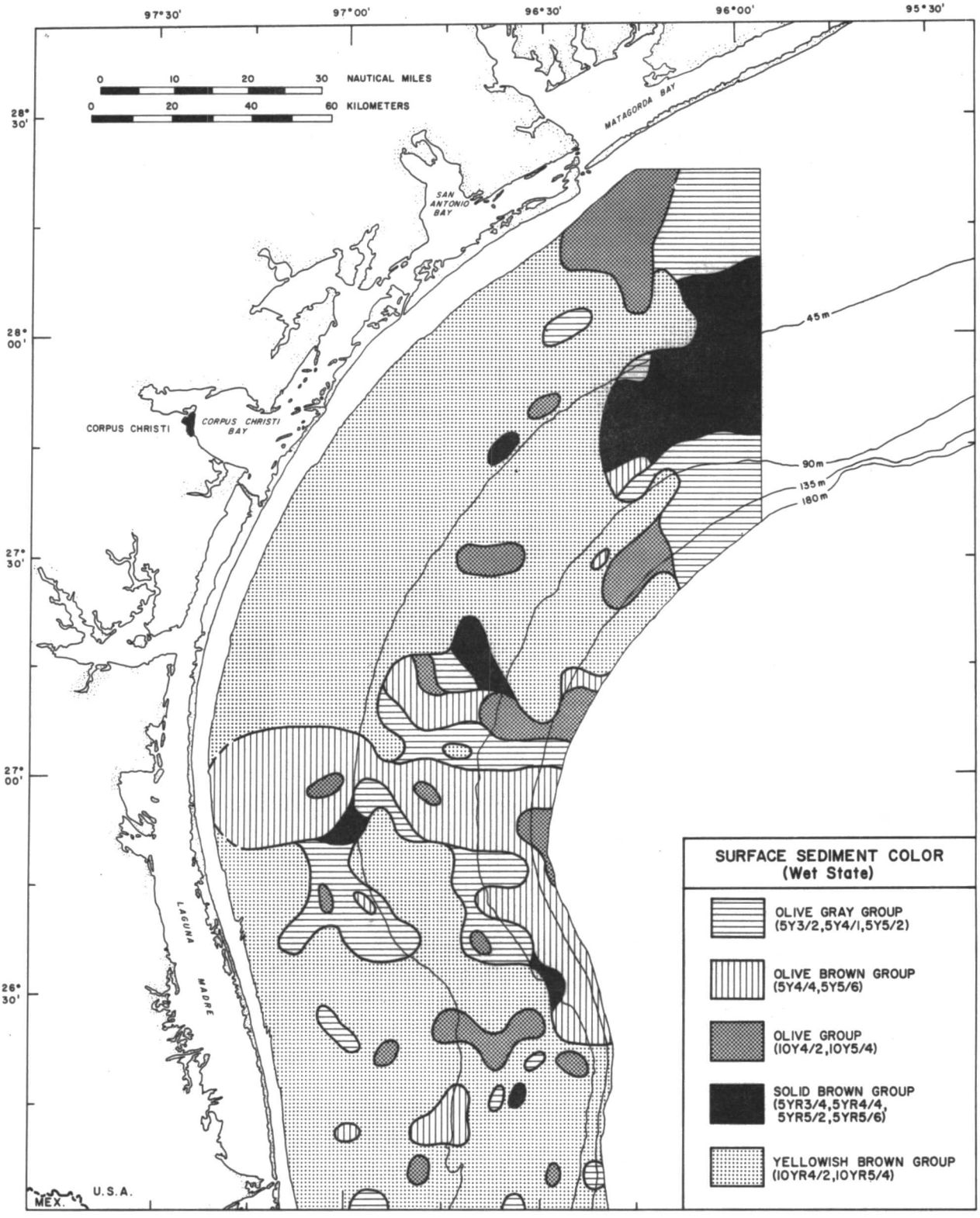

Figure 44. Color of upper 1 cm of bottom sediments.

include texture, mineralogy, and organic content. However, in the present study only textural and heavy mineral parameters were determined; consequently, only the partial influence of these parameters can be evaluated.

The color pattern does not show any apparent relation with sediment texture or total heavy mineral content. In addition, no apparent relation exists with content of $CaCO_3$ or total organic carbon. The color pattern may reflect varying degrees of surface sediment oxidation resulting from variations in sea floor Redox potentials. The extensive yellowish-brown group appears to represent the highest degree of oxidation. The other colors may indicate lower degrees of oxidation. The widespread extent of yellowish-brown sediments suggests that the OCS region can be generally characterized as an oxidizing environment. The cause of multicoloration in northern and central areas is conjectural, but may reflect lower redox potentials associated with higher rates of sedimentation in comparison with the yellowish-brown sectors; the multicolored central salient is localized in the general vicinity of a postulated littoral drift convergence zone (e.g. Watson, 1971).

Near-surface Sediments

The color variability of sediments below the upper 1 cm (fig. 45, pl. 22) is substantially different from the pattern illustrated by surficial sediments. A variety of 20 hue-value-chroma combinations in six basic color groups was observed: solid grays (N5, N4, N3), multicolored grays (5Y2/1, 5Y4/1, 5Y3/2, 5Y5/2, 5GY4/1, 5YR4/1), olive browns (5Y4/4, 5Y5/6), olives (10Y4/2, 10Y5/4), browns (5YR3/2, 5YR3/4, 5YR4/4, 5YR5/2, 5YR5/6), and yellowish browns (10YR4/2, 10YR5/4).

In contrast to surficial sediments, the yellowish brown group is of only minor quantitative significance. The most widely distributed subsurface

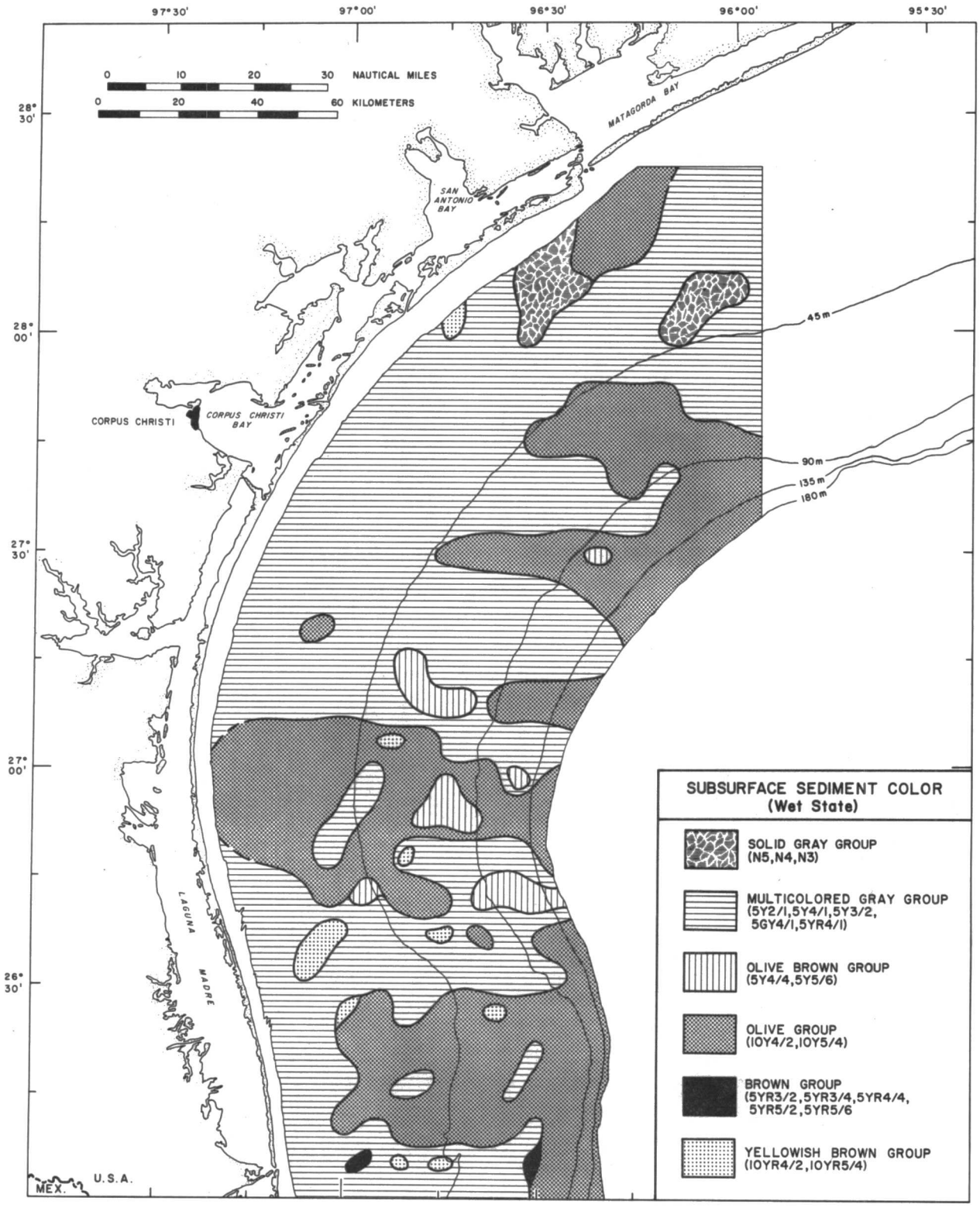

Figure 45. Color of sea floor sediment, 1 to 10 cm depth range.

colors are shades of the multicolored gray group and the olive group. The multicolored gray group is slightly dominant in the northern half of the OCS region, whereas the olive group is slightly dominant in the southern half. The two color groups tend to form east-west trending belts with the olive group becoming relatively more abundant seaward toward the shelf edge. Other groups are of only minor local distribution.

Similar to surficial sediments, the regional subsurface color pattern does not exhibit any apparent systematic relationship with sediment texture, total heavy mineral contents, $CaCO_3$ content, or total organic carbon content. Relative to surficial sediment, the paucity of the yellowish-brown group suggests a generally lower degree of oxidation for the shallow subsurface sediments. In addition, the larger number of hue-value-chroma combinations suggests a greater diversity of subsurface chemical parameters. The cause of the belted pattern made by the multicolored gray and olive groups is conjectural; the belts appear to reflect differing degrees of oxidation, possibly related to variations in the intensity of near-surface sediment aeration by currents or wave surge. The local salient of solid gray and olive sediments in the extreme northern sector appears to reflect suspended sediment influx from Matagorda Bay inlet area.

Heavy Minerals

The general mineralogy of sediments in the South Texas OCS has been previously described by Van Andel and Poole (1960), Van Andel (1960), and Curray (1960) as a part of the American Petroleum Institute Project 51 in the northwest Gulf of Mexico. The authors made a quantitative study of heavy mineral suites and were able to differentiate two distinct regional provinces within the OCS region. A "Rio Grande Province" characterized by a pyroxene-

hornblende association was dispersed northward from the modern and ancestral Rio Grande at the southern extremity of the OCS region. In addition, a "Western Gulf Province" characterized by a hornblende association was dispersed westward, primarily from a Brazos-Colorado river source; the two mineralogical provinces overlap in the general vicinity of 27°N latitude. On the basis of feldspar/quartz ratios in the light mineral fractions, Curray (1960) distinguished a subarkose province in the southern half of the OCS region, and an orthoquartzite province in the northern half. The approximate boundary between the two provinces is near the latitude of Corpus Christi Bay.

In view of the rather detailed previous work, the mineralogy phase of the present study was restricted to a quantitative determination of total heavy mineral contents by weight percentage. It was felt that determination of heavy mineral concentrations might produce valuable environmental baseline data that would provide additional knowledge about the interrelationship of sedimentary processes operative within the South Texas OCS. The regional heavy mineral variability is shown by the isopleth map (fig. 46, pl. 23).

Distribution

The total heavy mineral contents of OCS sea floor sediments range from a trace to a maximum of 32 percent at individual stations. The distribution pattern indicates that over most of the northern and central sectors of the OCS the sediments contain less than one percent heavy minerals. Heavy mineral concentrations exceeding two percent are nearly all within the southern sector of the OCS. The most conspicuous regional trend denoted by the isopleth map is an increase in heavy mineral content southward along the shelf with highest concentrations exceeding four percent localized on the ancestral Rio Grande delta. Of significance is the absence of a well-defined regional gradient

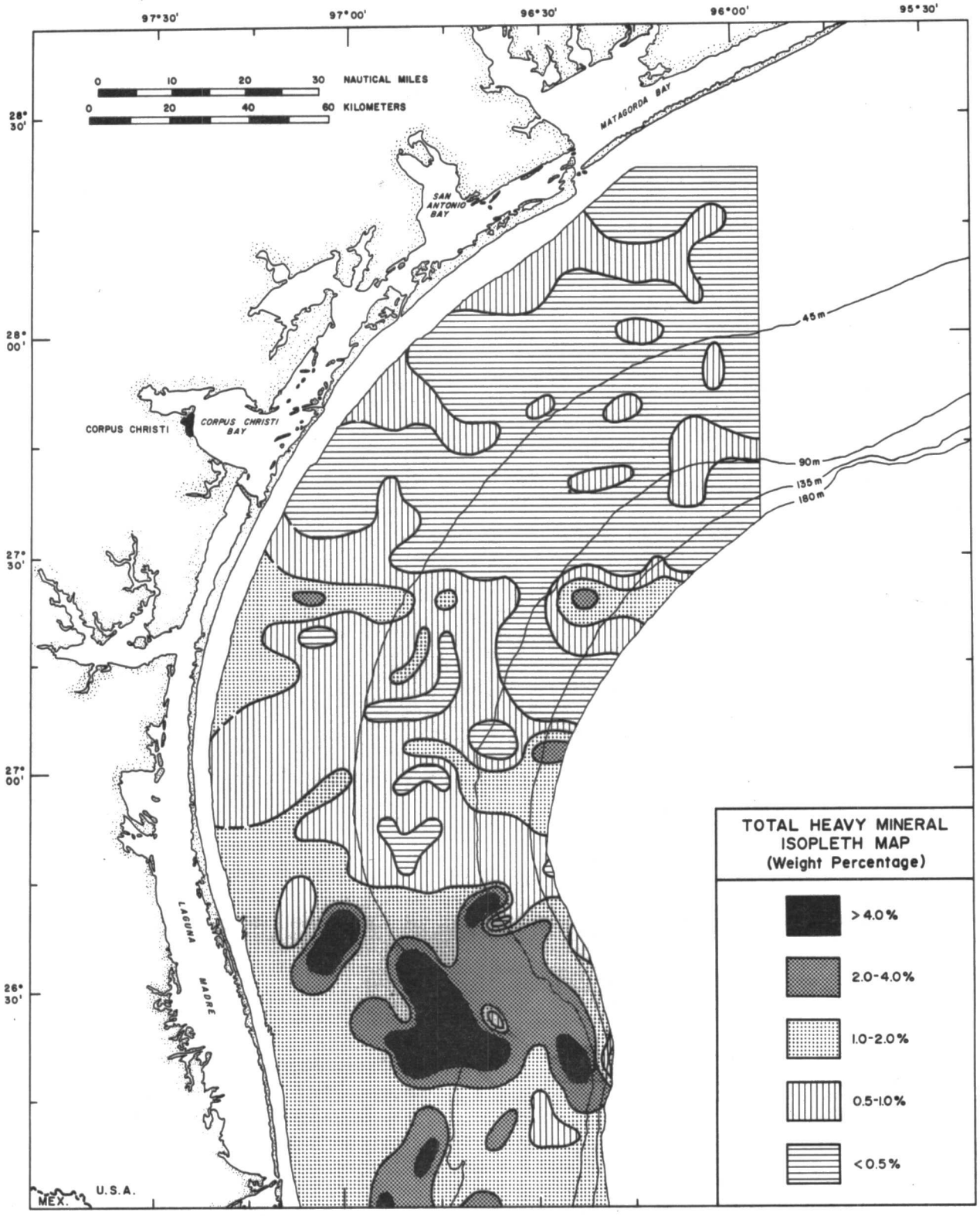

Figure 46. Distribution of heavy minerals.

seaward. Superimposed on the longitudinal gradient is substantial local variability between stations, including three east-trending salients north of 27°N latitude. In addition, replicate analyses of samples derived from 16 stations distributed throughout the OCS region resulted in a mean "within station" variability of 27 percent. This "within station" variability value reflects the total composite variation resulting from sampling techniques, analytical procedures, as well as true in situ differences.

Interpretation

The regional distribution pattern of total heavy mineral percentages does not show either a well-defined or systematic relationship to sediment textural parameters other than a general association with the shelly sands of the ancestral Rio Grande delta area. The absence of a regional seaward trend suggests that regional wave surge intensity is not significantly influential in establishing offshore heavy mineral concentrations. However, the well-defined regional longitudinal trend along the shelf appears to have some hydraulic significance. The trend may partially reflect the net southward transport by coastwide semipermanent currents of heavy mineral-deficient sediments derived from the ancestral Brazos-Colorado delta as compared with heavy mineral-rich sediments of the ancestral Rio Grande delta. In essence, the trend could partially reflect primary differences resulting from sediment provenance. The relict littoral and nearshore sediments of the Rio Grande delta may have intrinsically higher heavy mineral concentrations than the sediments farther north. Additionally, further secondary concentration of heavy minerals also may have occurred within relict deposits of the ancestral Rio Grande delta as the result of in situ winnowing by tidal currents and wave surge during the Holocene transgression. An association has been noted in

Chesapeake Bay between suspected relict or palimpsest sediments and relatively high concentrations of mature heavy minerals (Firek and others, in preparation).

Clay Minerals

Method of Determination

The wet seived fraction from 73 samples analyzed for heavy minerals were used for clay mineral determination. Samples were selected to give a representative distribution for the study area. The sample was homogenized and an aliquot taken. The subsample was passed through a 3-micron filter onto a Salas Flotonic^{R} silver filter with a nominal pore size of 0.45 microns, which served as substrate for X-ray diffraction determination of minerals. The filters were placed directly in a Picker X-ray diffractometer and scanned from 2 degrees 2 theta to 35 degrees 2 theta. Precautions were taken to hold the filter pad in the holder in order to maintain the essential geometry of the instrument. X-ray patterns were made on the air-dried sample using 1000 counts per second full-scale sensitivity, a scanning speed of 2 degrees 2 theta per minute, and a time constant of 5 seconds. Three additional patterns were made from the sample: 1) after treatment with ethylene glycol, 2) after heating to 400°C, and 3) after heating to 550°C.

The quantification of clay minerals was estimated by the following formulas used by J. C. Hathaway (personal communication).

The factors used are as follows:

Montmorillonite - 17A° intensity (ethylene glycol treated)	= 4.0
Chlorite - 14A° @ 400°C	= 1.0
Chlorite - 14A° @ 550°C	= 2.0
Illite - 10A° (ethylene glycol treated)	= 1.0
Mixed layer montmorillonite-mica plus montmorillonite 10A° intensity @ 400°C less 10A° intensity ethylene glycol treated	= 1.0
Kaolinite mean 7A° intensity ethylene glycol treated @ 400°C less 2 x 14A° intensity @ 400°C	= 2.0

Formula used

$$S_1 = \frac{I_{17,EG}}{4} + I_{14,400}° + I_{10,EG}+ \left[\frac{I_{7,EG} + I_{7,400}}{4} - 2 \times I_{14,400}\right]$$

$$\% \text{ Montmorillonite} = \frac{I_{17,EG}}{4} \times \frac{100}{S_1}$$

$$S_2 = I_{14,400} + I_{10,EG} + (I_{10,400} - I_{10,EG}) + \left[\frac{I_{7,EG} + I_{7,400}}{4} - 2 \times I_{14,400}\right]$$

$$\% \text{ Chlorite} = I_{14,400} \times \frac{100}{S_2}$$

$$\% \text{ Mixed layer montmorillonite-illite} = (I_{10,400} - I_{10,EG}) \times \frac{100}{S_2} - \% \text{ M}$$

$$\% \text{ Illite} = I_{10,EG} \times \frac{100}{S_2}$$

$$\% \text{ Kaolinite} = \left[\frac{I_{7,EG} + I_{7,400}}{4} - 2 \times I_{14,400}\right] \times \frac{100}{S_2}$$

The graphic results were examined for peak coherence and for any unexplained peaks by comparison with subjective interpretations of the strip chart recordings. Where no obvious misinterpretations were noted, the calculated values were tabulated. The calculated values by this method may not add up to 100 percent.

Distribution

The results of the X-ray diffraction analyses of the 3.0 to 0.45 um fraction showed that the predominant clay mineral was of the expandable variety, probably Ca-montmorillonite. Illite is the second most common clay mineral, with a chlorite-type mineral occurring in only trace proportions. The expandable clay fraction defined as montmorillonite plus the mixed layered clay ranged from 38.9 to 90.0 percent in the 3.0 to 0.45 micron size range. The distribution of expandable clay is shown by figure 47 (pl. 24). In general the amount of expandable clays

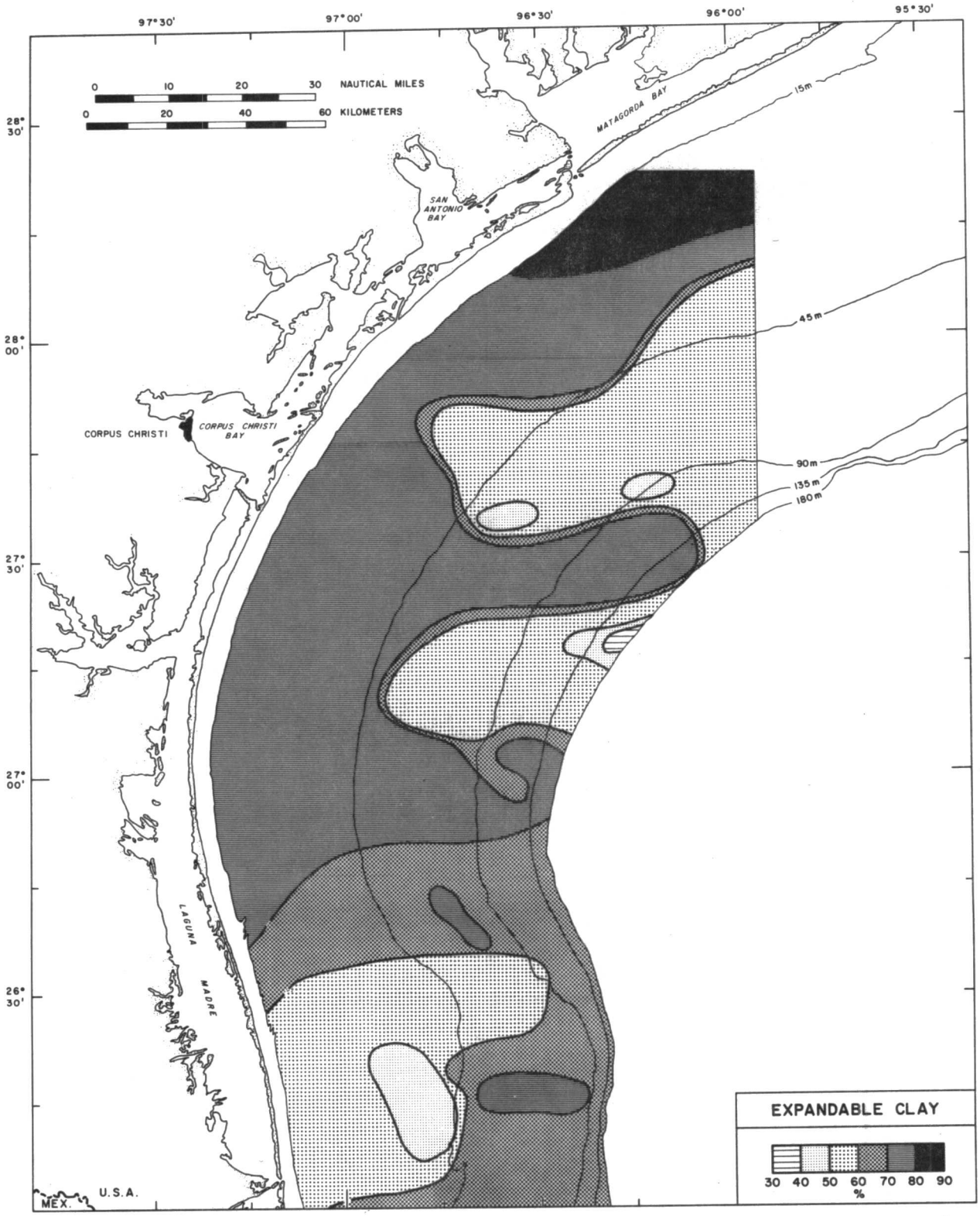

Figure 47. Distribution of expandable clay, surficial bottom sediments.

decreased from north to south with two prominent salients low in expandable clays encroaching onto the shelf from the east. The northernmost of the salients appears to represent clay transported from the Texas-Louisiana shelf to the east. The low expandable clays farther south seem to be related to the gas seep area. The area of low expandable clays on the inner shelf near the mouth of the Rio Grande indicates that the present load of the river is more illitic as compared to the material being delivered to the northern sectors of the study area.

SHALLOW SUBSURFACE SEDIMENTS

The movement and deposition of sea floor sediments are governed by physical oceanographic processes that are operative over varying spans of time and at varying levels of energy. Obviously, the exposition of surficial sediments on the sea floor at a specific time represents the latest response of the sediment particles to the transporting medium. The most recent forces acting on the sediments in terms of magnitude or energy level and extent may have represented either very quiet conditions, very rigorous conditions, or something in the range between the two extremes. The degree to which the surficial sediments are temporal and transitory at a specific time and place is in large part a function of the long-term and composite characteristics of water mass movement over the region. Consequently the characteristics of the shallow subsurface sediments are compared to those of the surficial sediments to: 1) identify the extent of variations in depositional conditions through time, and 2) to identify and determine the extent of those sedimentary units that seem to have been deposited under extreme energy conditions--hurricane passage.

Methods of Study

The nature of the shallow subsurface sediments has been determined from the cores: the box cores that penetrated to a depth of 42 cm (16 in), and the

pipe cores that range in depth of penetration from .1 m (4 in) to 2.5 m (8 ft, 2 in). The average length of pipe core obtained was 1.6 m (5 ft). However, depth of penetration across the ancestral Rio Grande delta in the southern sector of south Texas OCS was generally less than elsewhere. There, hard clays, compact sands and large amounts of shells that lie immediately beneath the thin surficial cover of mud effectively inhibited penetration by the corer in a number of places. The distribution of box core stations is shown by figure 7 and the pipe core stations by figure 6.

In the laboratory, the cores were first X-rayed at 1:1 and then described by megascopic examination and by use of the X-ray film strip. A detailed log, including both diagrammatic and written descriptions, was prepared for each core. The descriptive log for each core was then interpreted and coded as to: 1) number of discrete sand layers, 2) types of sedimentary structures, 3) types and intensity of biogenic structures; 4) degree of sediment modification by bioturbation, 5) types of faunal remains, and 6) estimated total percentage of sand.

During study of the cores, primary attention was given to the depositional aspects of the sediments thought most likely to yield significant and quantitative information on the directions and magnitude of transport over the continental shelf as a function of water mass movement. These aspects are: 1) the number and thickness of discrete sand layers in each core, 2) the areal extent of discrete sand layers that seem to be correlative from core to core, 3) amount of sand relative to finer-textured sediments, 4) presence of ripple laminae or other depositional structures such as cross laminations that indicate extent to which moving water or relatively high energy has been involved in sediment transport, 5) features such as sharp boundaries between sediment types, erosional or scour contact at the base of thick sand layers and geographic

distribution of lithoclasts or rock fragments carried onto the shelf that might indicate the extent of sedimentation over the shelf during hurricanes, and 6) vertical changes in types of sediment that record significant and progressive long-term changes in patterns of sediment movement and deposition during latest Holocene time.

The data from the cores are presented as a series of columnar sections or diagrams on figures 48 through 58. Column one for each station location noted on the figures is a diagram of the box core, column two is a diagram of the pipe core, and column three is a coding for the degree of bioturbation as represented in the core by biogenic structures.

The columnar sections are arranged in approximate sequential order as a series of traverses beginning at the north end of the study area and progressing southward. Some stations have been selectively positioned out of sequence to allow maximum utility in comparing stratigraphic variations geographically across and along the shelf. The number beneath each pipe core indicates the number of discrete sands in the core.

Nature and Stratigraphy of Sediments Cored

Sand/mud ratios and the number of discrete sand sedimentation layers per each 30 cm of core length were determined as a means of establishing the stratigraphic variability of the uppermost Holocene section over the south Texas OCS and to gain some understanding of two sedimentological factors: 1) the temporal variability of sediment dispersal patterns during the late Holocene transgression, and 2) the relative significance of storm versus fair-weather sedimentation. Because the length of the cores varies from station to station the integrated time span reflected by the core maps also is variable, depending upon both core length and local sedimentation rates.

EXPLANATION

Column 1 — Box Core

Column 2 — Pipe Core

Column 3 — Extent of Bioturbation

Number over bracket is bottom station number

Sand

Number at base of core indicates discrete sands

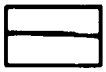

Sand Stringer

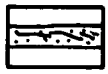

Sand layer having ripple or cross laminae.

Heavy lines at base indicates possible scour during deposition

Lithoclasts and shell remains

Hard Clay

Mud

Predominantly mixtures of silt and clay

Bioturbation Coding

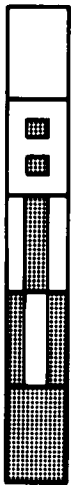

Undetermined

Trace

< 30%

30-60%

> 60%

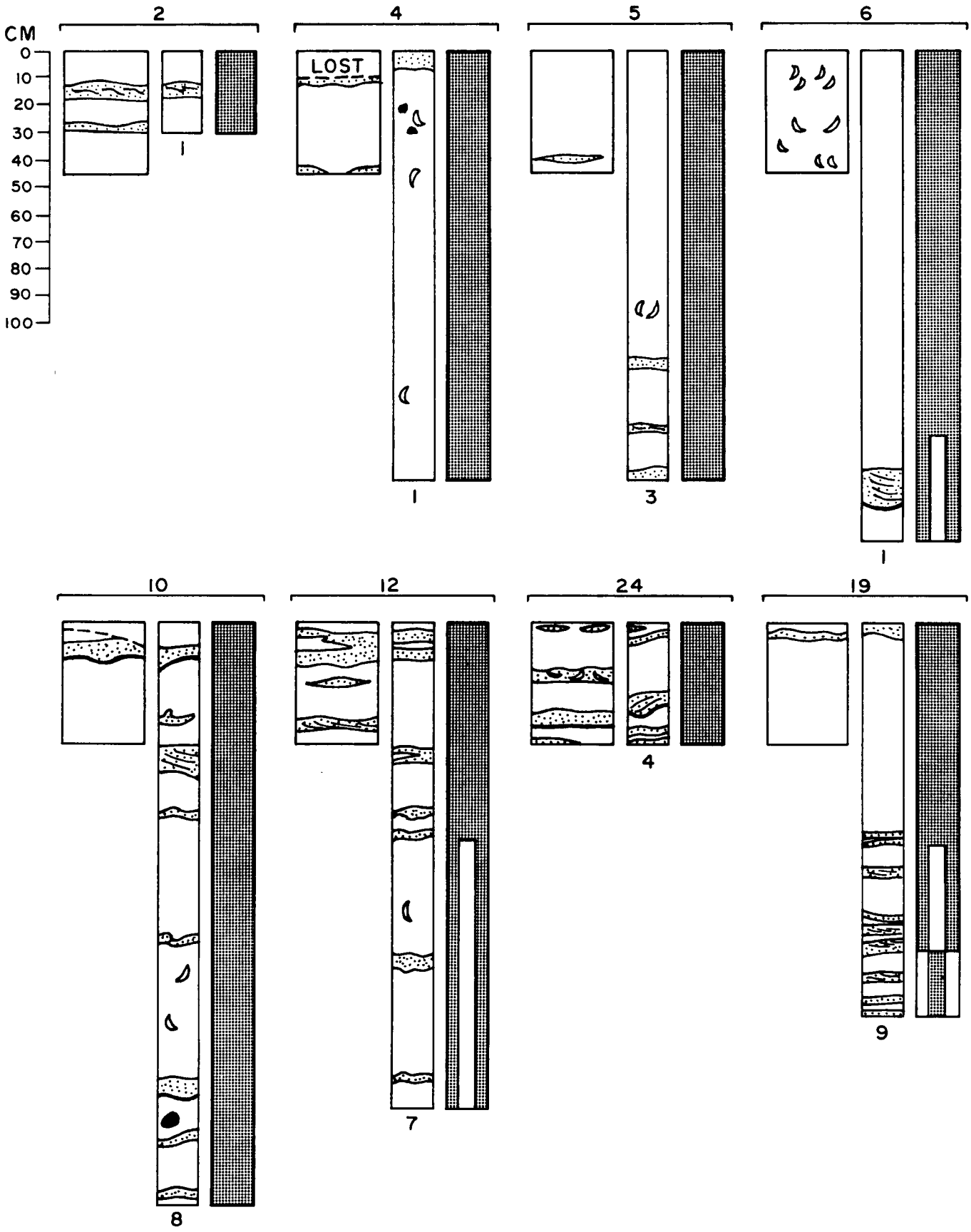

Figure 48. Core diagrams, stations 2 through 24.

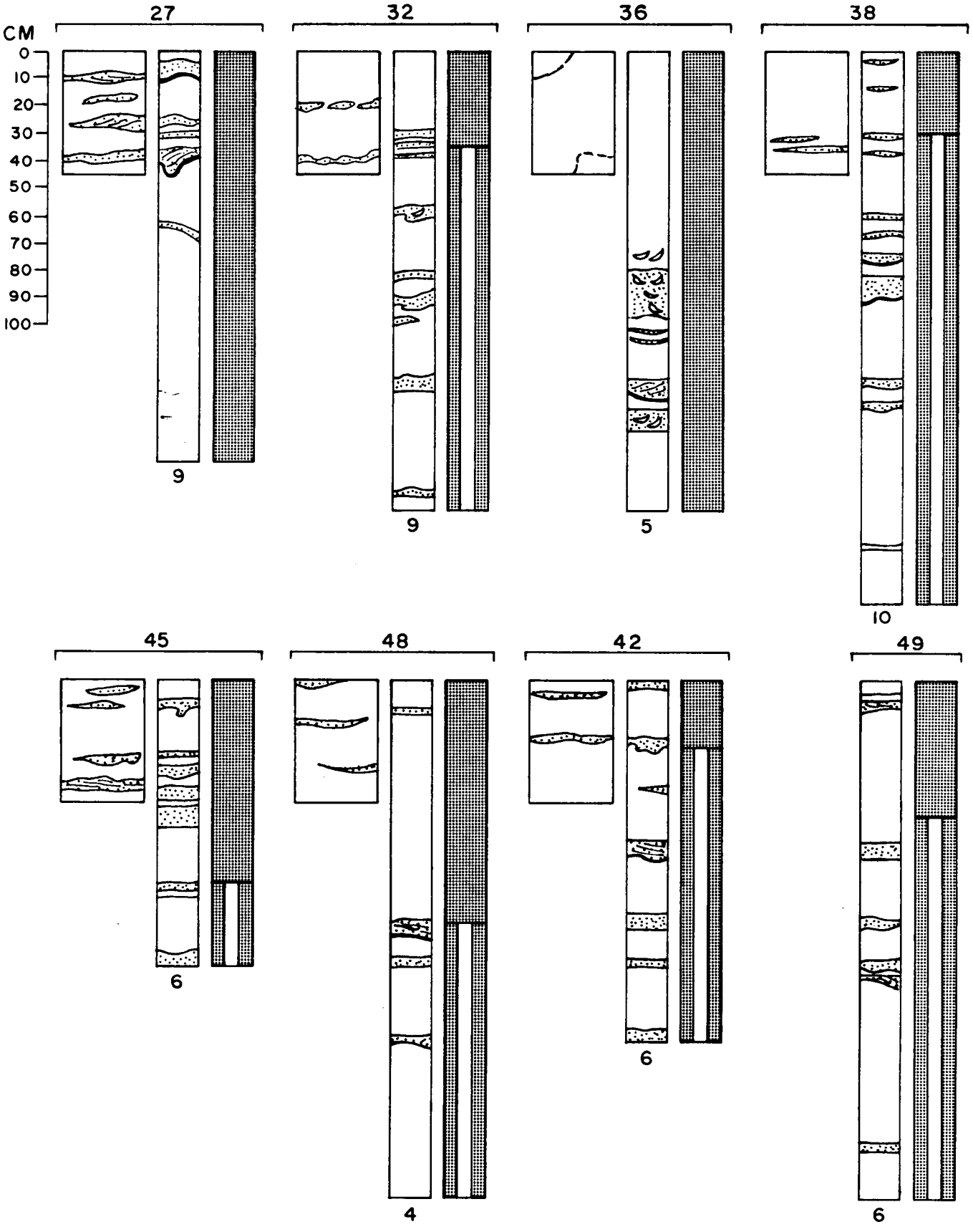

Figure 49. Core diagrams, stations 27 through 49

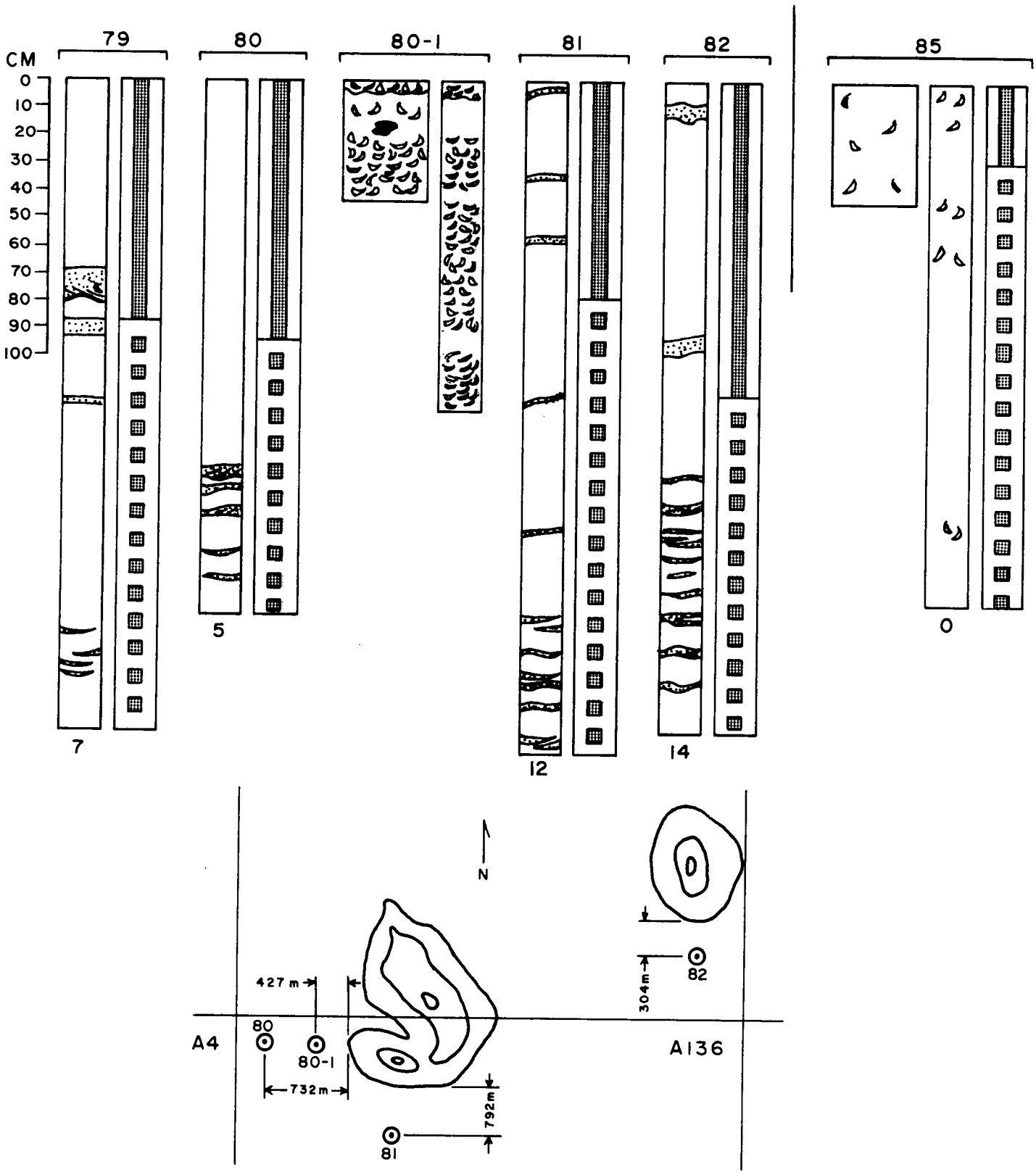

Figure 50. Core diagrams, stations 79 through 85.

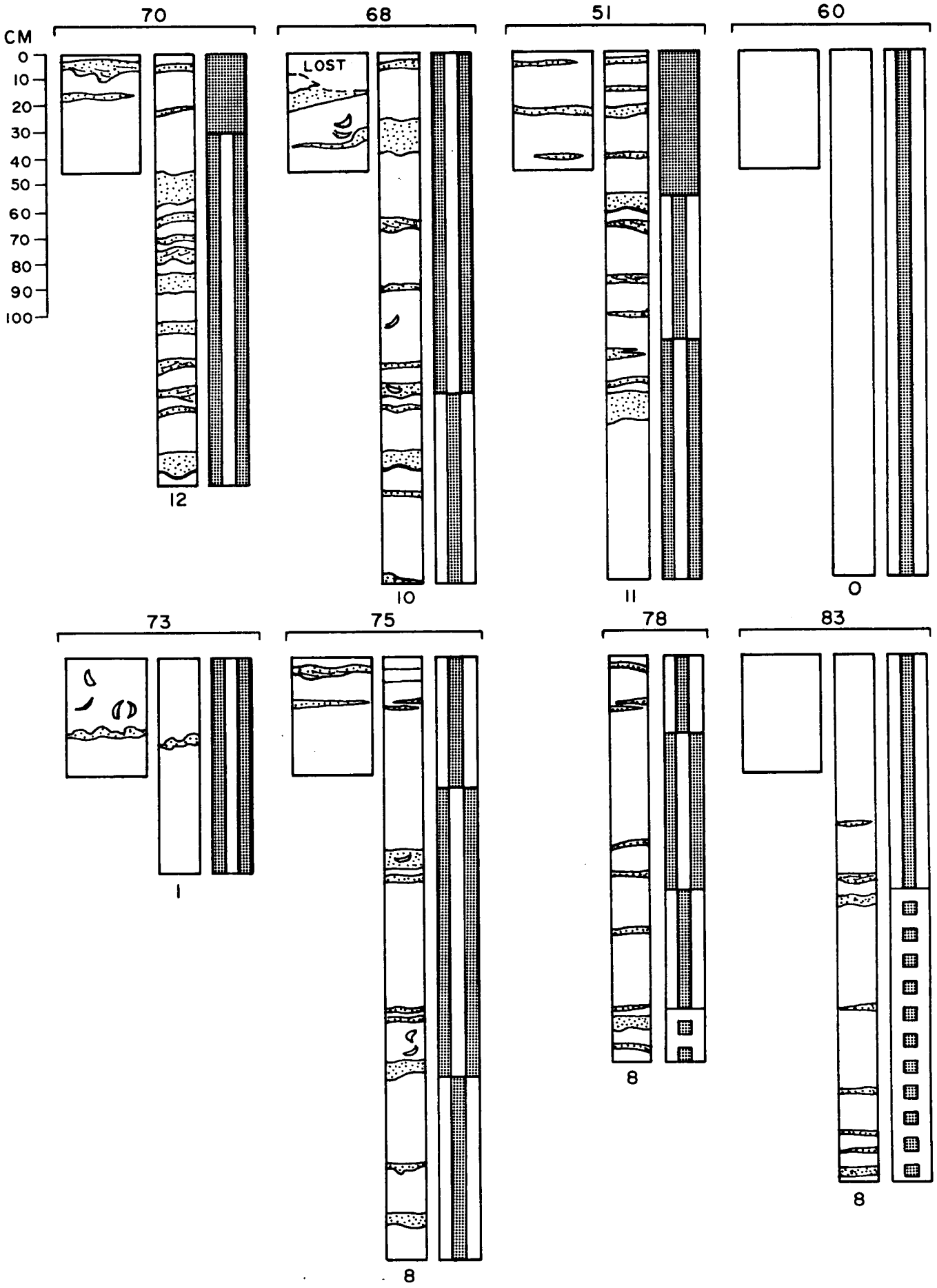

Figure 51. Core diagrams, stations 70 through 83.

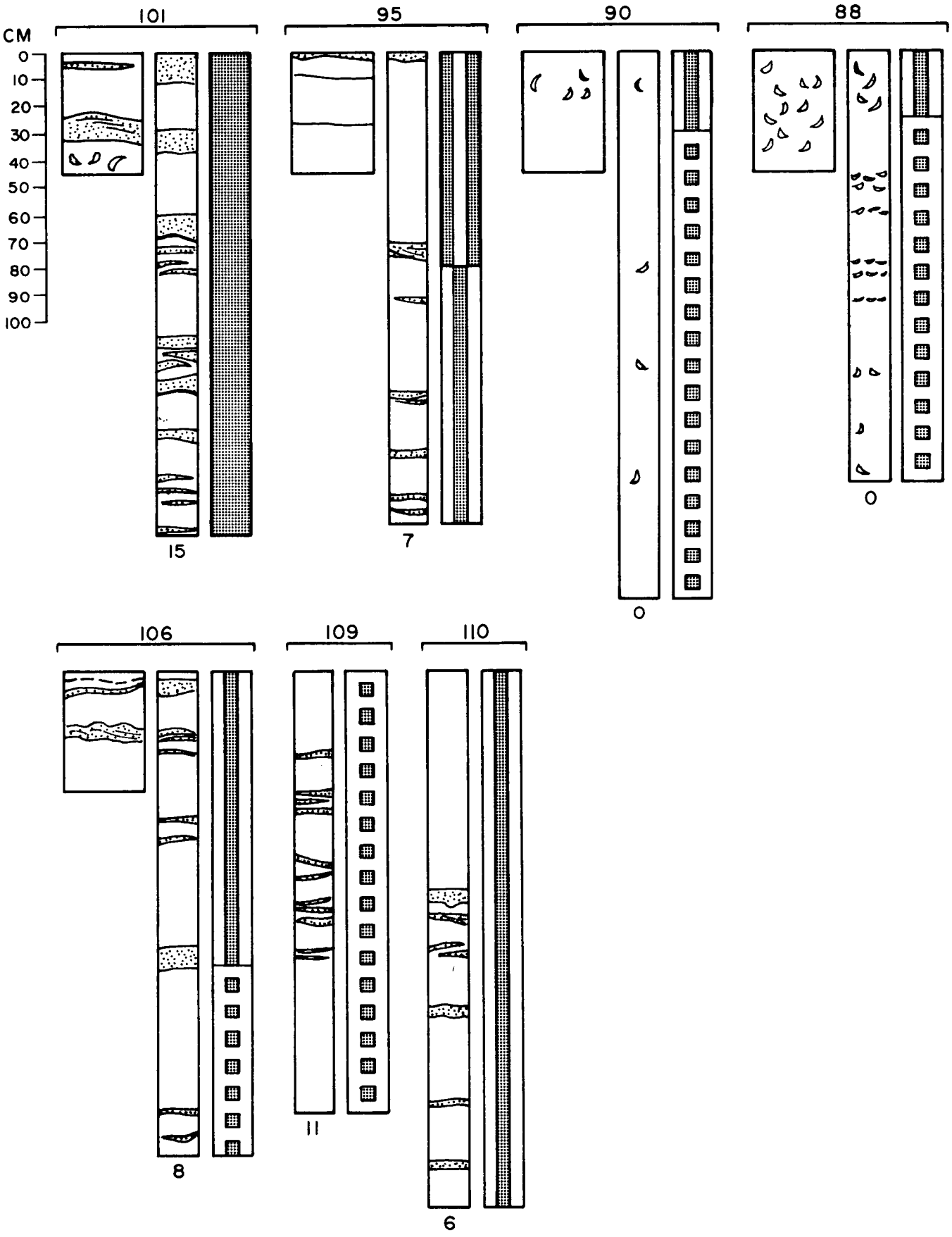

Figure 52. Core diagrams, stations 101 through 110.

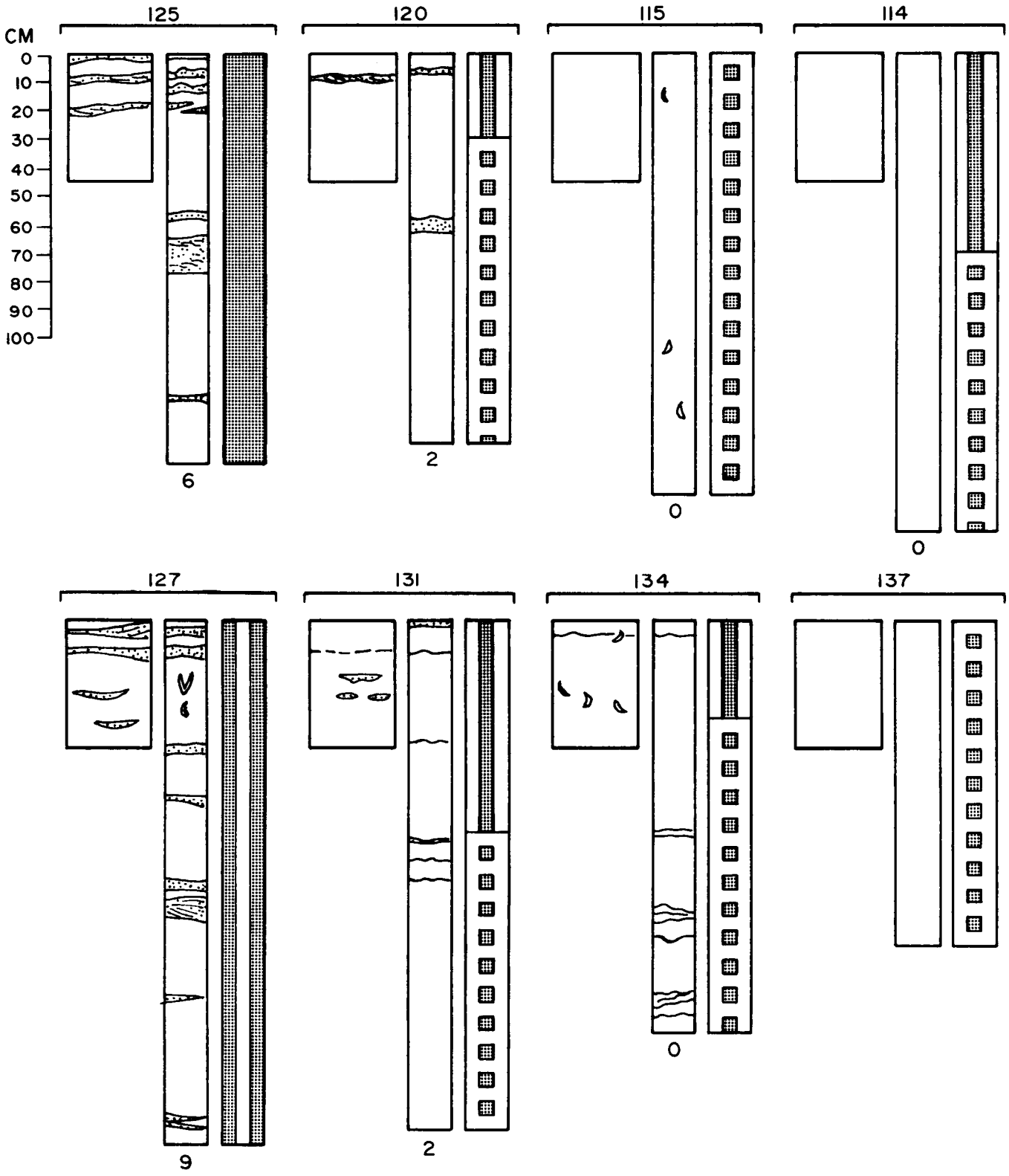

Figure 53. Core diagrams, stations 114 through 137.

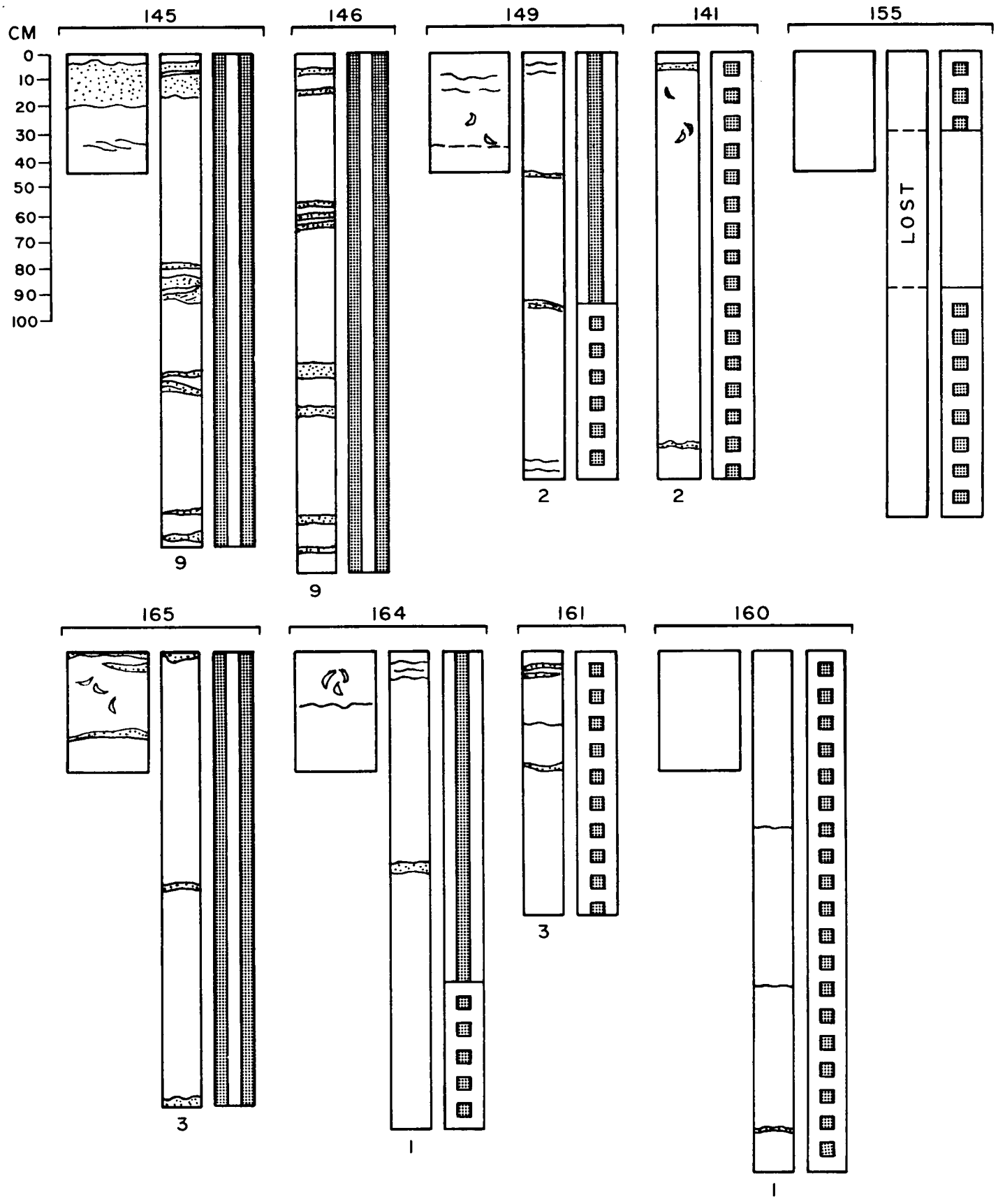

Figure 54. Core diagrams, stations 141 through 160.

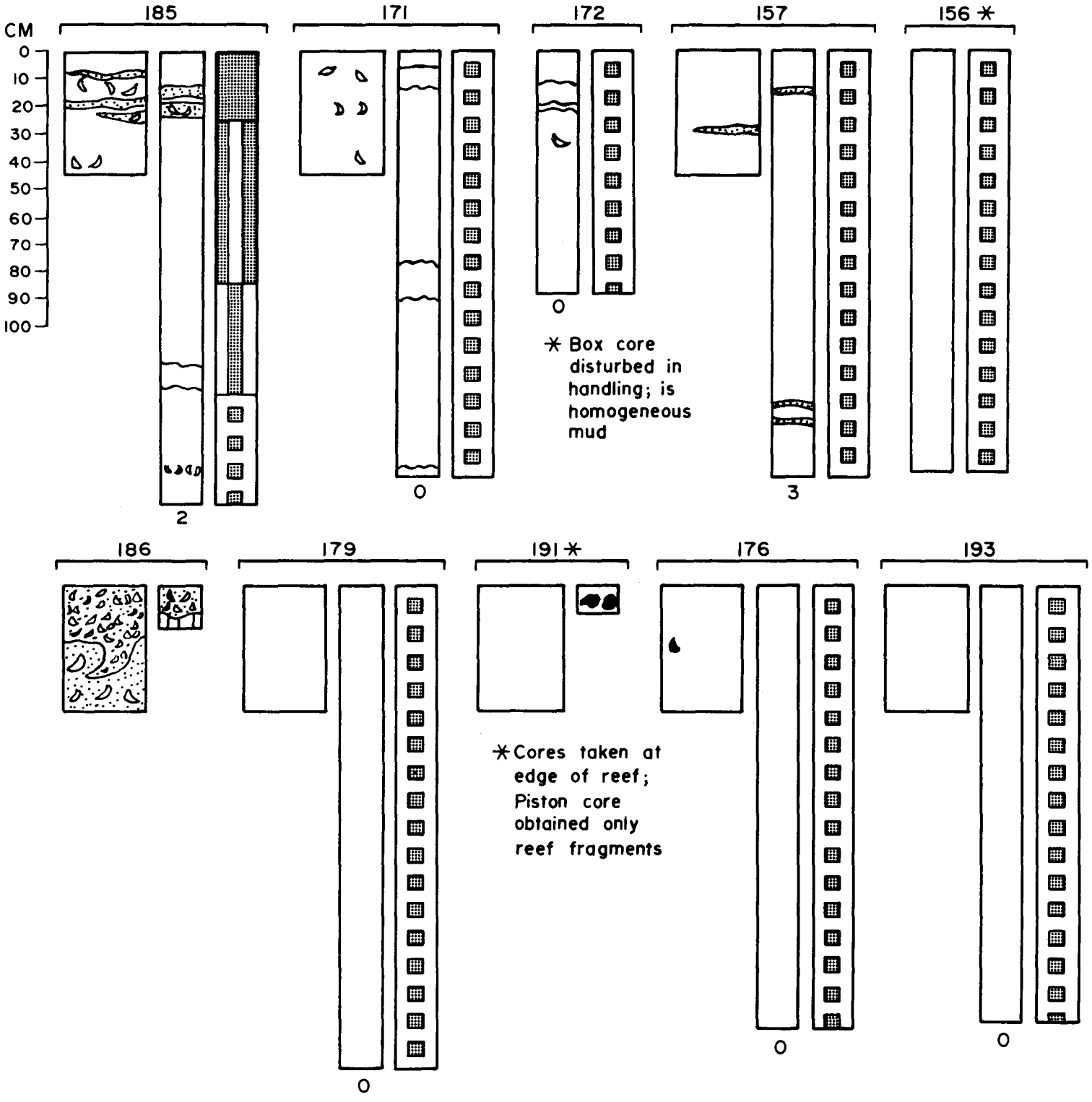

Figure 55. Core diagrams, stations 156 through 193.

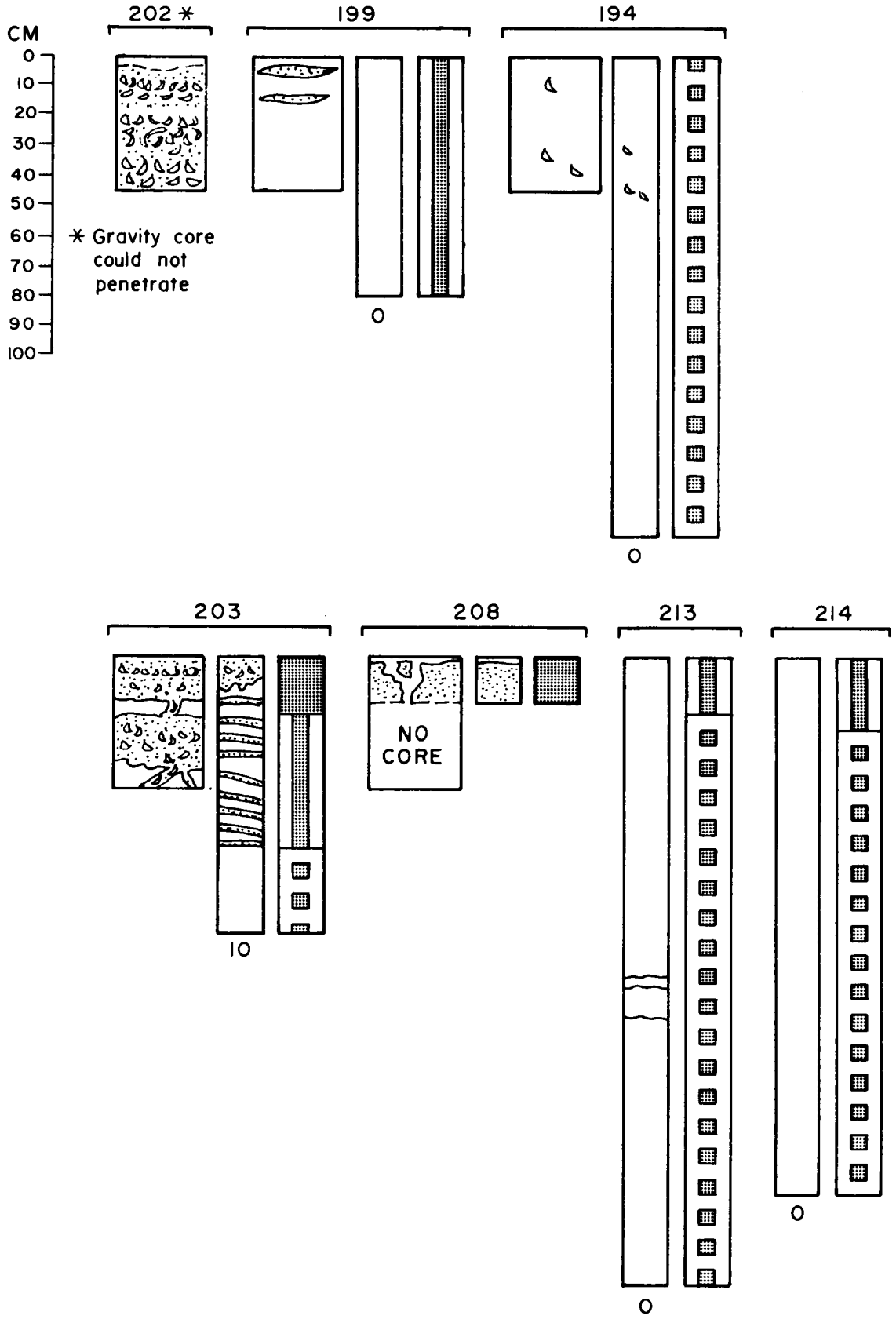

Figure 56. Core diagrams, stations 194 through 214.

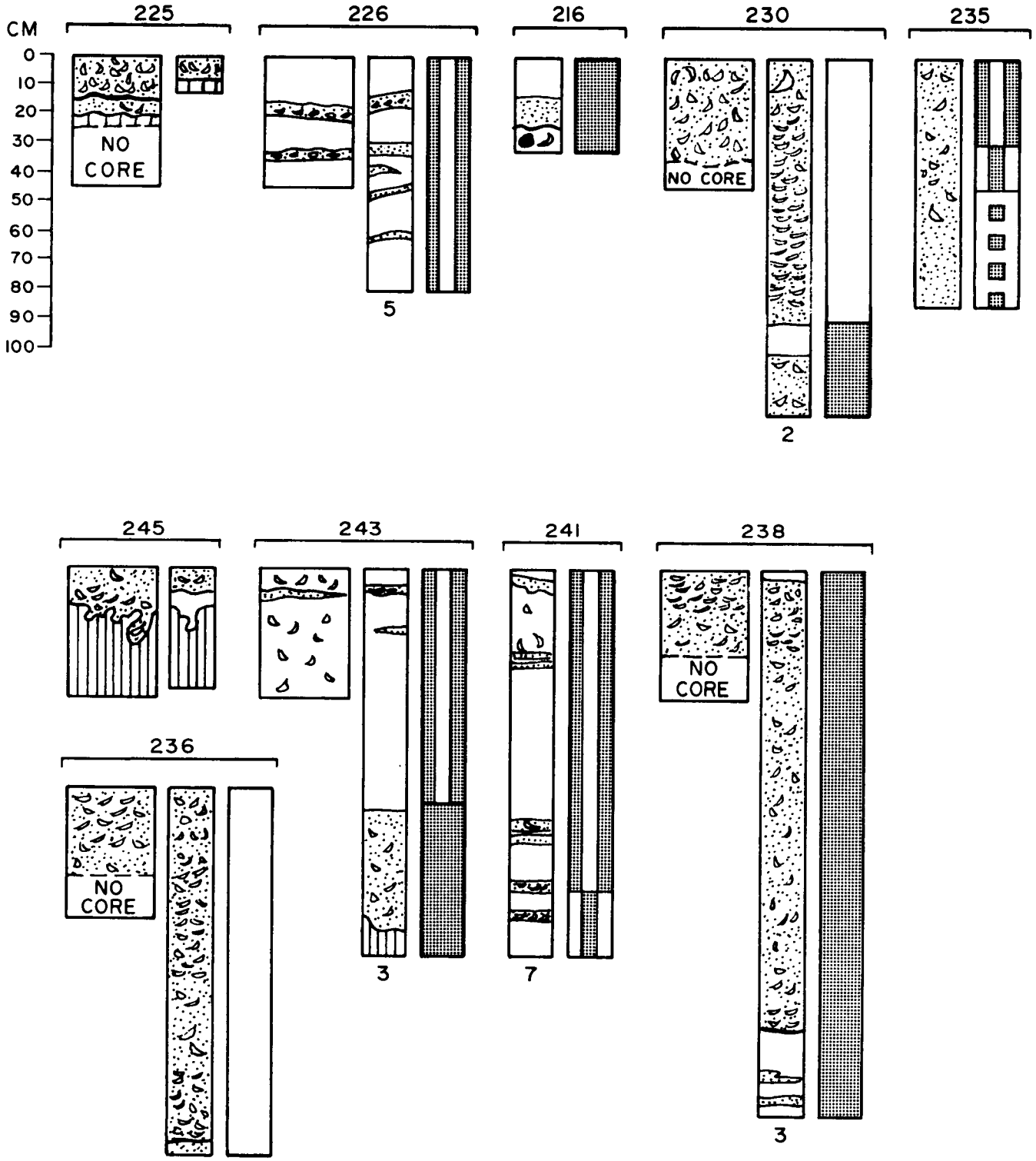

Figure 57. Core diagrams, stations 225 through 245.

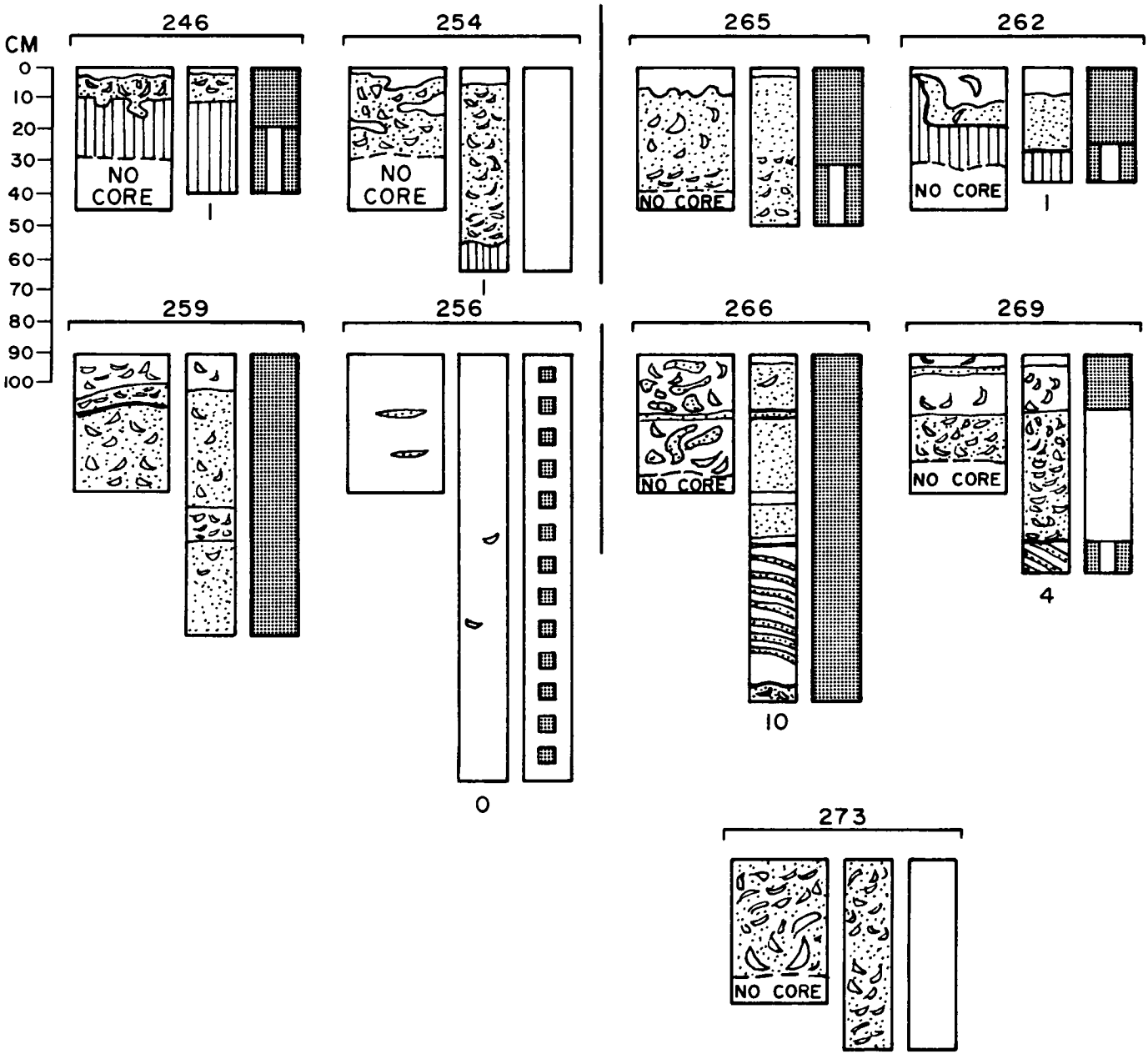

Figure 58. Core diagrams, stations 246 through 273.

Sand/Mud Ratios

The relative proportions of sand and mud in the OCS cores are shown by the ratio isopleth map (fig. 59 and pl. 25). Since relative rather than absolute quantities are of primary interest, all cores are afforded equal significance regardless of core length.

The sand/mud ratios in the cores range from near zero to a maximum of 7.67 at station #208; ratios of less than 0.12 are relatively common. The isopleth map indicates that mud has been the dominant component throughout most of the South Texas OCS during latest Holocene time. The areas where sand is the dominant component (>1.0) are on the ancestral Rio Grande and Brazos-Colorado deltas and along the shoreface.

The regional pattern outlined by the sand/mud ratios indicates a muddy central sector of the shelf and increasing sand contents shoreward as well as both northward and southward away from the central sector. Although the sand/mud ratio map is based on only 88 data points, a comparison of the pattern with the sand/mud ratio pattern of surficial sediments (fig. 32) indicates a high degree of similarity in regional trends, indicating that the basic modern regional pattern of sediment dispersal was established in earlier Holocene time. The central sector of the shelf has persisted as a mud depocenter with sandy sediment influx from peripheral areas. The sand/mud ratio pattern for the cored sediments also indicates net southward transport with sediment encroachment onto older sediments of the ancestral Rio Grande deltaic platform. This is suggested by the relatively low isopleth gradients in the north compared to the high southern gradients adjacent to the delta, and by the prominent mud salient east of 97°W longitude. A seaward transport component is also indicated by the regional seaward gradient of decreasing ratio values.

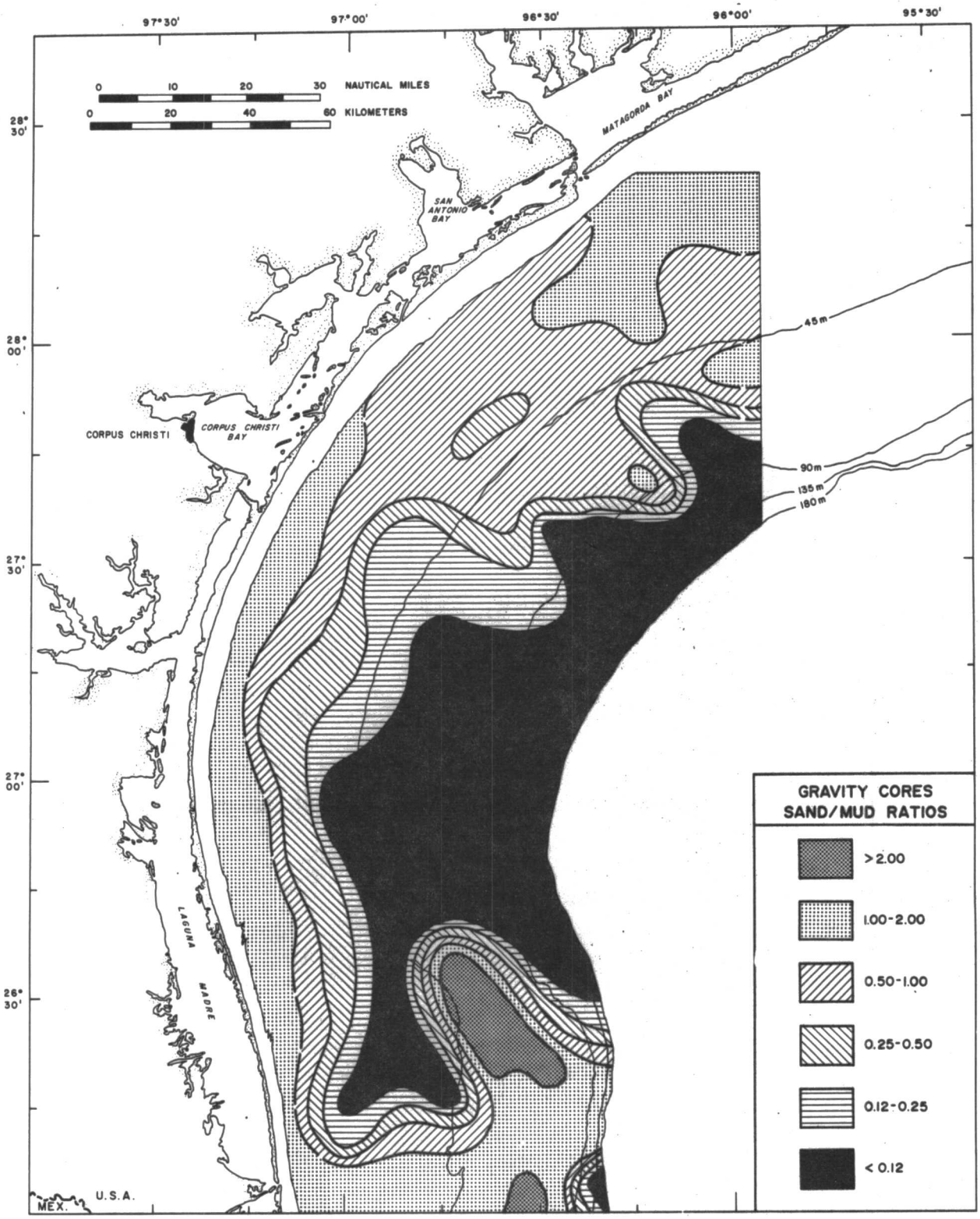

Figure 59. Sand/mud ratios in the pipe cores.

Although the basic regional dispersal patterns of the most recent and the slightly older Holocene sediments appear to have been the same, there are some notable differences. The relative areal distribution of the sand and mud facies in the cores is significantly different from the surficial sediments. Sands are more widely distributed in the cored sediments; whereas, muds are more limited in areal distribution. The more extensive sands in the cores may reflect an earlier period of more rapid sea level rise; under such conditions, the processes of shoreface and coastal erosion might have been accelerated, resulting in larger volumes of sand influx relative to mud influx. During earlier Holocene time, the mud blanket was not as extensively developed and had not encroached as far southward. Another difference between the modern and somewhat earlier Holocene patterns is the general westward displacement of the mud blanket with time, apparently reflecting a normal stratigraphic overlap that developed during the late Holocene transgression. Another significant difference is the contrast in the development of the west-trending mud salient near 27°N latitude at the approximate location of the postulated current convergence node. The core ratio map shows that in earlier Holocene time the salient appears to have been more poorly defined, apparently reflecting an embryonic state of development and suggesting that the enigmatic salient is a very recent feature.

Number and Distribution of Discrete Sands

The total number of discrete sand sedimentation layers greater than 1 cm thick was determined for each core (figs. 48 through 58). As the number of sand layers is partially reliant upon core length, all unit numbers were standardized to a 30 cm core length. An isopleth map of the number of sand layers /30 cm core length (fig. 60 and pl. 26) was constructed to show areal

variations in an effort to gain some insight into the relative efforts of storm versus fair-weather sedimentation. As noted by Hayes (1967), sand layers derived from storm erosion of the Texas coast can be deposited substantial distances seaward (> 18.5 m water depths) over previously muddy sea floor as the result of coastal water reflux following storm surge. The areal variability in the number of sand sedimentation units may provide clues to the relative importance of storm deposition throughout the OCS region.

The number of sand layers in the cores ranges up to a maximum of 5.17 per 30 cm standard core length at station #2 near the Matagorda Bay inlet; in some cores, discrete sand layers are absent. The majority of the OCS region is characterized by less than 1.0 sand unit/30 cm of core. The isopleths indicate a regional trend of increasing sand layers shoreward. Furthermore, in the central sector of the shelf the number of sand layers tends to decrease upward in the cores. The areas having the largest number of sand layers (> 1.00/30 cm) are localized in the vicinity of the ancestral Rio Grande delta and adjacent shoreface; they also are within the shoreward half of the northern and central sectors of the shelf, where they are conspicuous seaward-trending salients.

Correlation of individual sands on a layer-by-layer basis is impossible, considering the rather broad spacing of the cores. However, several of the sand layers seem to extend over significant areas of the shelf. Of special significance is the discrete sand layer that is within the upper 10 cm (4 in) of many of the cores. The possible extent of the sand layer is shown by figure 61. The thickness of the layer ranges from less than one centimeter to eight cm (3.25 in) and it covers almost half of the south Texas OCS. Considering that 10 cm is a relatively short interval, a reasonable argument can be made that the sand represents a single depositional event. In almost all cases, except over the ancestral Rio Grande delta where, as stated previously, the

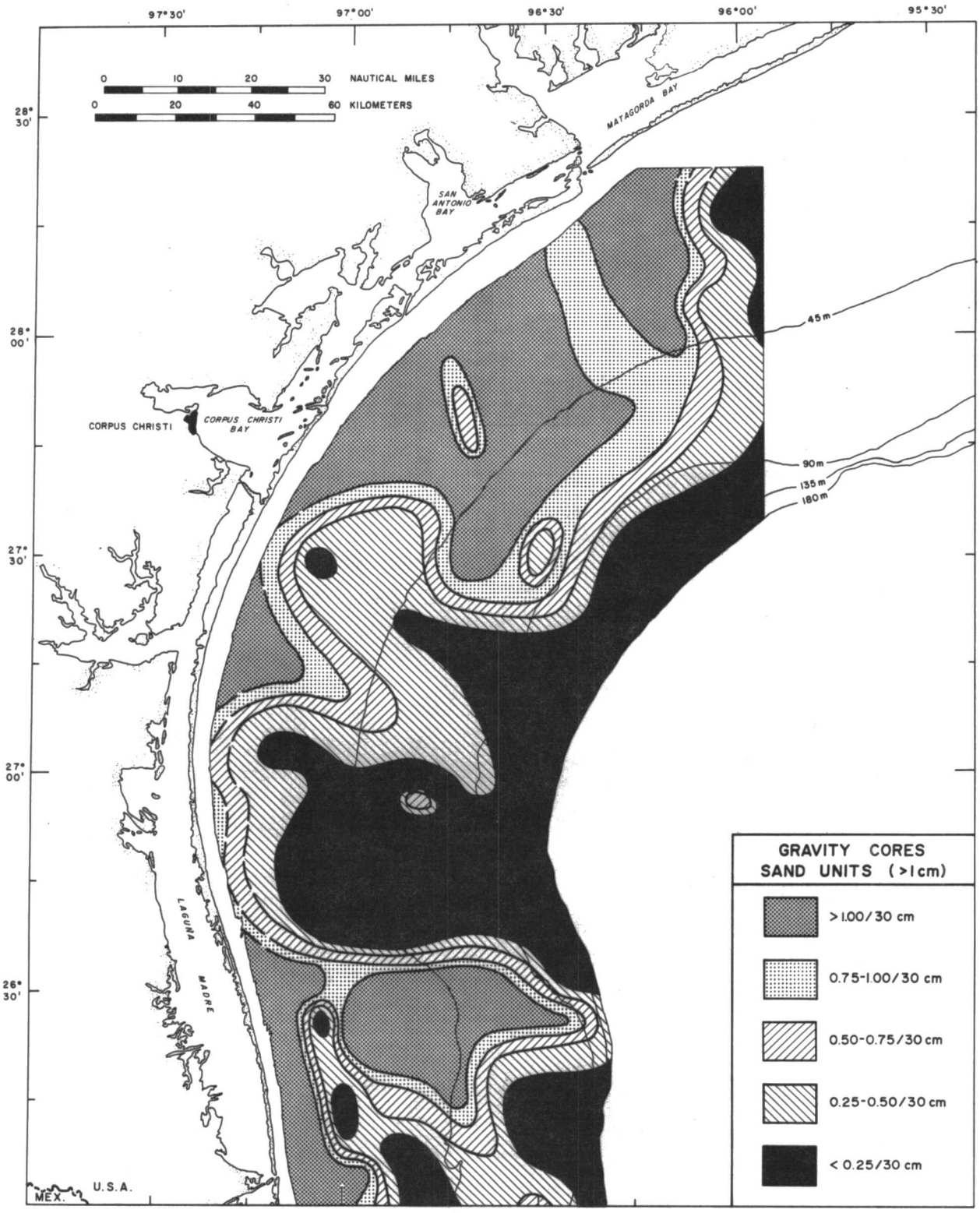

Figure 60. Distribution of discrete sand layers 1 cm thick per 30 cm intervals in the pipe cores.

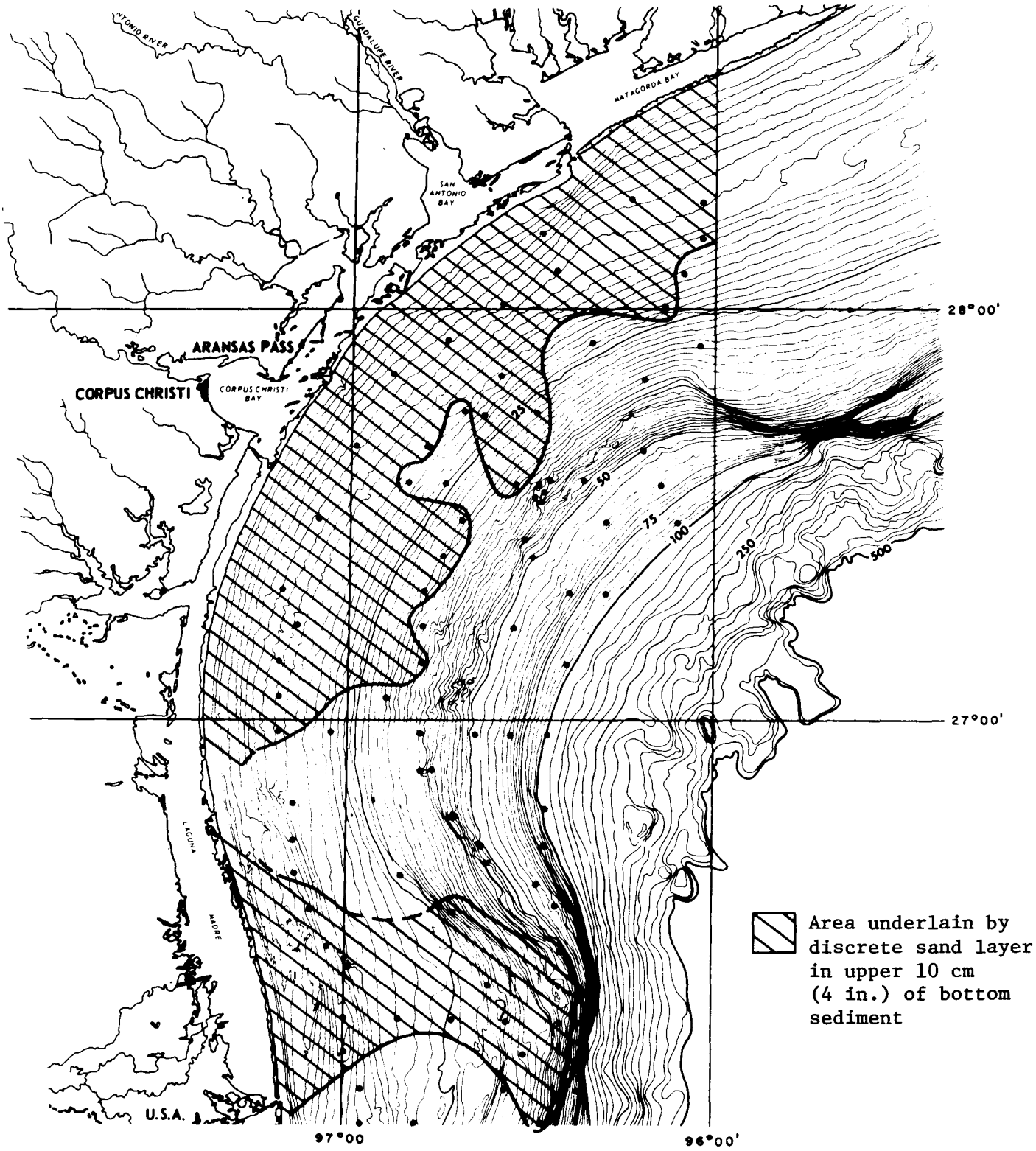

Figure 61. Areal distribution of discrete sand layer in upper 10 cm of sediments.

regime differs, the sand is overlain by a thin layer of mud which forms the surficial and most recent deposit. The mud apparently represents normal depositional conditions or the normal energy level of moving water on the OCS. The sequential arrangement of surficial mud over sand strongly suggests that the sand represents a single depositional event marked by energy sufficient to move sand at least halfway across the shelf, or about 25 miles from shore. The most obvious mechanism for generating the carrying power capable of spreading sand over wide areas of the shelf is hurricane-generated currents. If the sand represents a storm deposit, its presence at such a shallow depth beneath the sea floor indicates that the storm occurred in the recent past. It is interesting to speculate which of several recent storms might have been responsible. Carla in 1962 or Fern in 1971? Both tracked the full extent of the south Texas coast: Carla from south to north, Fern from north to south. Both did considerable erosional damage to the shoreline. Documentation of the energy level reached by water moving along the sea floor during hurricane movement across a shelf, south Texas or otherwise, is an important aspect of environmental assessment. Each of the four cores (42, 49, 51, 78) that outline the southward-oriented salient contains three discrete sand layers that are at very nearly the same depth in each of the other three (figs. 49 and 51). No bottom feature that might have contributed the sand from a nearby source by the process of sea floor erosion has been identified. Thus, it can be concluded with a fair degree of confidence that these sands also represent high energy transport during and following hurricanes.

The regional trend of a shoreward increase in sand layers suggests that the inner parts of the OCS are more intensely affected by episodes of storm deposition. This is the expected pattern for the reflux deposition of sand derived from storm-induced coastal erosion. The prominent seaward-trending

salients outlined by areas containing the maximum number of sand layers (>1.00/30 cm) suggest that storm-reflux deposition is more intensive within the local areas. The conspicuous salient association with the Rio Grande delta probably represents a complex pattern, reflecting not only late Holocene storm activity but also numerous relict deltaic sands. However, the three salients farther north may reflect largely local areas where storm surge reflux has been most prominent since earlier Holocene time. The relatively small salient near 27°15'N may indicate relatively large amounts of storm-reflux deposition associated with the ancestral Baffin Bay. The relatively extensive salient between 27°30' - 28°15'N may reflect the composite reflux from both the ancestral and modern Corpus Christi and San Antonio bays. The northernmost salient appears to be associated with storm-reflux deposition from Matagorda Bay.

In summation, the areal distribution pattern of cored sand layers suggests that the inner OCS is most intensely affected by the storms. Furthermore, prominent seaward-trending salients suggest that storm-reflux deposition has been most prevalent locally along the inner OCS adjacent to the prominent coastal estuaries which appear to have been major sources of sand reflux sediment. During storm flood tides, voluminous quantities of barrier island sand are carried into the back barrier estuarine system as overwash. With passage of the storm's low pressure system, the strong ebb reflux of estuarine waters via tidal inlets probably transports and deposits large volumes of entrained sand seaward of the normal fair-weather zone of sand deposition, thus possibly explaining the presence of the conspicuous seaward-trending salients across the continental shelf.

Depositional Structures

The sediments contain both depositional and biogenic structures. The depositional structures are of primary origin and reflect the mechanics of sediment

transport. The biogenic structures are secondary and indicate the extent of modifications of primary structures by infaunal activity. The depositional structures on the South Texas OCS are typically of small scale.

The most common depositional structures in the cored sands are interlaminations of irregular pattern that range in form from very crude ripple to small-scale foreset and cut and fill; cross laminae, though present, are not common, are of very small scale and where noted are in cores from the inner half of the shelf. Many sand layers have no internal depositional structures; however, the sand in the upper part of the structureless units commonly grades upward into and becomes interlaminated with mud. Graded bedding, though not qualitatively determined by analysis, is apparent. The discrete sands typical have a sharp basal contact with the underlying mud; locally, scour is suggested by the sharp and irregular contact relationship of the base of some of the sand to the underlying mud. The sedimentary structures for all of the cores are illustrated diagrammatically in the columnar sections, figures 48 to 58.

The muds, except where interlaminated with sand, have no megascopic depositional structures. X-ray radiographs reveal, however, that most of the muds consist of microscopically interlaminated silt and clay.

In many of the cores, the depositional structures of the sand layers have been largely destroyed by animal activity which includes both random rearrangement or mixing of original sediment texture as well as segregation of both sand and mud into secondary sedimentary structures. Where modification of the sediment texture and structures has been intense, the cored sediment commonly has a mottled appearance that results from either sand or mud filling numerous biotic burrows.

In summary, the sedimentary structures within the discrete sand layers strongly compliment the broader evidence for extensive spreading of sand across

the shelf as single events associated with storm activity. Irregular to ripple and cross-bedded laminae are in the cores seaward to about 25 miles or more offshore. The extent of the macrodepositional structures over the shelf, as indicated by the cores, are shown by figure 62.

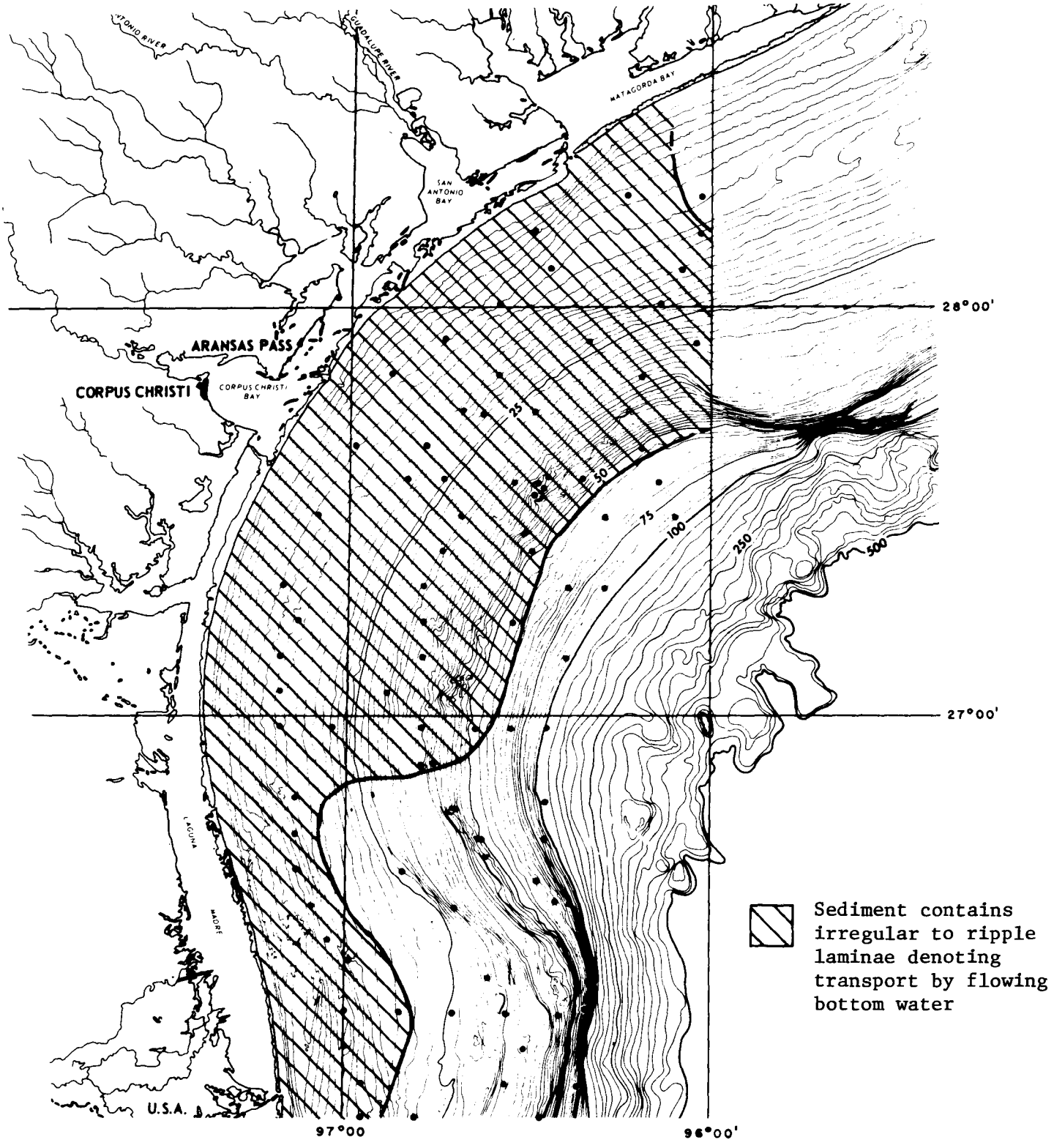

Figure 62. Extent of macrodepositional structures in sand layers, as determined from cores. Dot indicates location of core station.

Animal-Sediment Relationships

Introduction

Recent investigations of various Holocene and ancient sedimentary environments have shown that in many instances biogenic processes affecting the substrate subsequent to deposition are equally as important as the physical processes involved during deposition (Howard and others, 1972). Infaunal activity is an important factor in sediment modification in areas of high biotic populations. An understanding of benthic biological processes contributes significantly to sedimentological, paleoecological, and overall environmental interpretations because bioturbation commonly modifies both grain size relationships and depositional structures to a marked degree in some depositional environments and the modification apparently takes place very soon after sediment deposition.

Organic sediment modification includes the physical destruction of depositional structures, the creation of additional structures in the sediments, and alteration of grain size relationships. Organic sediment transport may be either vertical in the sediment column or lateral. Consequently, biogenic processes are directly involved in geochemical processes and the redistribution of chemical elements in the sediments.

Understanding biologic processes is important to interpretations of depositional environments. Study of the chronology of biogenic sedimentary structures helps to define the depositional history, gives information on rates of sediment deposition or erosion and helps to define key marker beds such as regional storm deposits more precisely. Recognizing certain biological functions makes it easier to interpret other aspects of depositional environments such as aeration of water and sediment, substrate coherence and stability,

and provinciality. Knowledge of the overall extent and intensity of biogenic activity, both laterally and vertically, is a key in predicting the impact of contaminants introduced on and into benthic sediments.

Identification of the benthic community structure and function are necessary for making paleoecological interpretations and for reconstructing ancient depositional environments. Information on bathymetry, temperature, salinity, oxygen, current and wave orientation, and habitat diversity during earlier stages of deposition can be gained from the study of benthic biological processes.

The biogeologic studies have been designed to identify, classify, and interpret significant benthic (macrobenthic infauna) biological processes as they relate to the sedimentological processes operative over the South Texas Outer Continental Shelf. Because data from only 81 of 264 stations were available at the time this report was written, the results must be considered preliminary.

Relatively few studies have been directed toward the interaction of physical and biological processes on the continental shelves. In the United States, investigations of animal-sediment relationships have largely been restricted to the Atlantic coast, especially Georgia (e.g., Howard and Reineck, 1972). Animal-sediment relationships off the Texas coast have received only meager study (e.g., Hunter and others, 1972; Hill, 1974).

Methods of Study

To accomplish the study objectives, samples from 81 stations were examined (fig. 63) and a number of investigative steps were established as outlined in Table I.

Table 1--General outline of investigative steps used in the biogeologic studies of the South Texas OCS

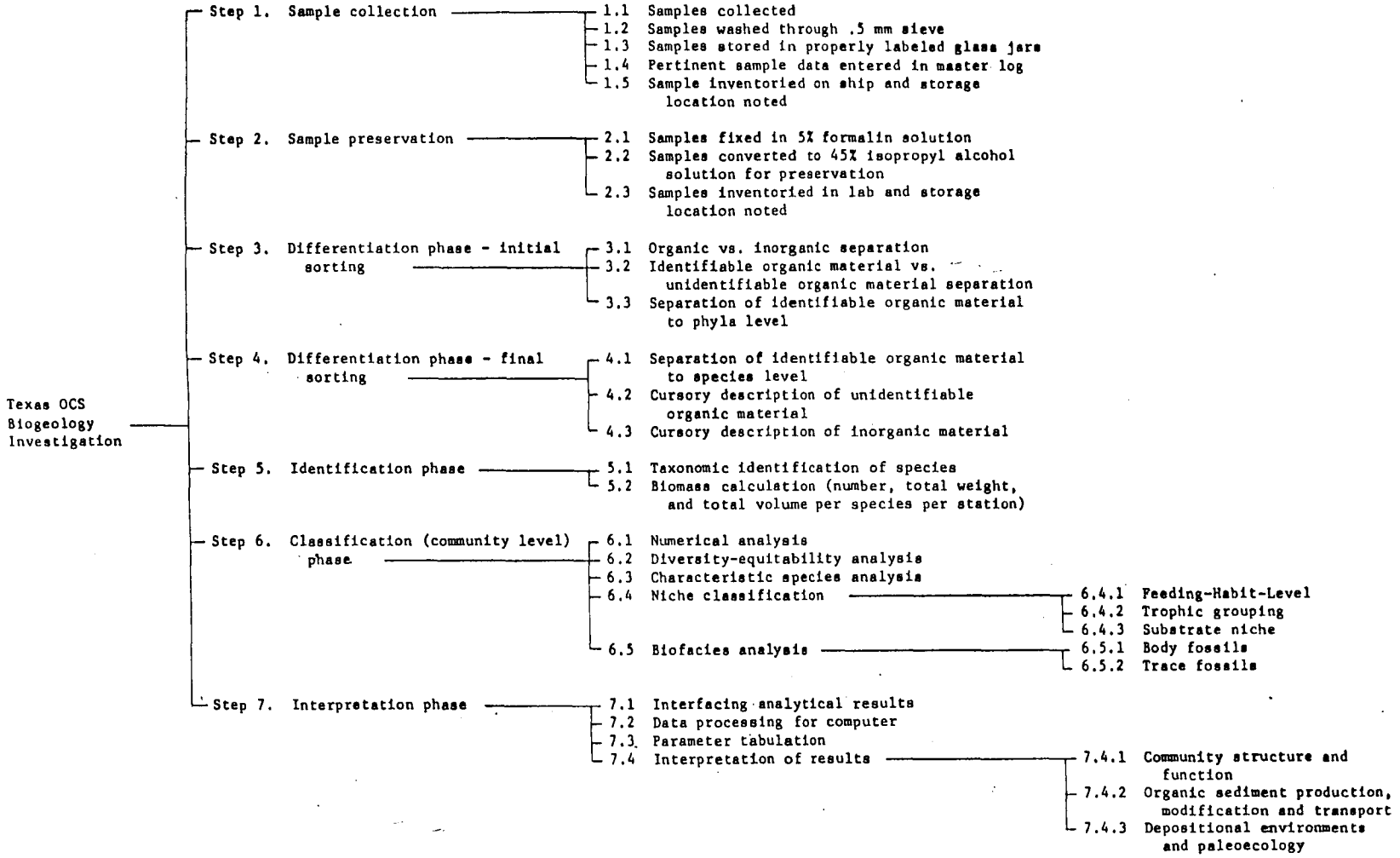

After subsamples for sedimentological and geochemical studies were removed from the bottom samples, the remaining part of the grab sample (0.09 m^3) and the upper 10 cm of the box core were washed aboard ship through a large (46 cm diameter) aluminum funnel having a 0.5 mm mesh "Saran" bag acting as a screen at the terminal end. The sample was gently washed and then stored (sample in bag) in a glass jar in 5 percent buffered formalin. Labels were put inside each bag, in each jar, and the outside of the jar and lid were also labeled. Any significant remarks about the sample were entered into the master station log book kept by the Chief Scientist on each cruise.

The biological samples were removed from the ship to the laboratory after each cruise leg. Each sample was transferred to a 45 percent isopropyl alcohol solution until such a time as it could be sorted, counted, and identified. After all available samples were sorted, a checklist was compiled from the species collected; species were sorted to phyla and then assigned a species identification number (e.g., Polychaete, P-17). All identifications eventually will be submitted for verification to qualified biologists.

The spatial distribution along and normal to shoreline trends were determined by compiling the counts from each traverse. Biomass was determined using a Perkin-Elmer Autobalance AD-2^R, accurate to 1.0×10^{-6} g. For some species, because of their very small size and fragmentation, an average weight per individual was calculated and used in biomass calculations.

A classification type of numerical analysis was utilized to determine macrobenthic infaunal assemblages. The computer program was supplied by Dr. Joseph L. Simon, Department of Biology, University of South Florida. Correlation coefficients were determined using the modified U.S.G.S. RAS-STATPAC program for correlation analysis (D0101) and general regression analysis (D0095).

The Shannon diversity index $H' = -\sum P_i \log_e P_i$ is the proportion of the i^{th} species in the collection (Shannon and Weaver, 1963), was utilized to calculate diversity because it is influenced by two components: the total number of species present (species richness component) and the evenness of distribution of the individuals among the different species (equitability component) (Lloyd and Ghelardi, 1964). To apply Shannon's formula to a sample from a population, it must be estimated by the equation,

$$H'' = -\sum \frac{N_i}{N} \log_e \frac{N_i}{N} \text{ natural bels/individual;}$$

where N_i is the number of individuals in the i^{th} species and

N is the total number of individuals collected.

The species richness component was measured by Margalef's index, $d = (S-1)/\log N$, where s = number of species and N = total number of individuals in the sample (Margalef, 1958). Relative species abundance was measured by Lloyd and Ghelardi's (1964) equitability index, $E = s'/s$, where s' is the number of species predicted for the calculated H' by the "broken-stick" model of MacArthur (1967) and S is the number of species.

Macrobenthic Infaunal Zonation

In order to identify, classify, and interpret significant benthic biological processes as they relate to the sedimentological processes operating in the study area, basic descriptive biological and sedimentological studies were conducted. The study focused on the macrobenthic infauna because they make the most significant biogenic impact on the sediments. Sediment parameters referred to in the discussions are those determined by Gerald L. Shideler in the sedimentology studies.

Before benthic biological processes can be interpreted, macrobenthic infaunal zonation must be described and the factors controlling such zonation defined. Macrobenthic infaunal distribution patterns across the shelf and changes in these distribution patterns through time were determined.

In the western Gulf of Mexico, biological investigations of the continental shelf have been primarily concerned with coastal environments or coral reefs and submerged banks (e.g., Gunter, 1950; Hulings, 1955; Parker and Curray, 1956; Villalobos, 1971; Rezak and Edwards, 1972; Bright and Pequegnat, 1974). Literature concerning the biota of unconsolidated sediments on the continental shelf of the southwestern Gulf of Mexico is relatively rare. However, studies by Pulley (1952a, b), Hildebrand (1954), Kennedy (1959), and Parker (1960) have significantly increased knowledge of the outer shelf soft bottom fauna.

Pulley (1952b) studied the distribution of 238 species and subspecies of bivalves from the Gulf of Mexico, many of which were found off Texas. A major premise of his study was the relationship of species distribution relative to water temperatures. The same year, Pulley (1952a) published an illustrated checklist of the marine molluscs of the Texas coastal waters.

Hildebrand (1954) studied the fauna of the brown shrimp grounds in the western Gulf. Because of his method of collection (commercial shrimp trawls), only the larger mobile molluscs and those smaller ones which live in or attached to other larger organisms were collected.

Kennedy (1959) conducted the first investigation to compare the fauna along a transect extending across the entire width of the continental shelf off the upper Texas coast. He noted changes in the faunal composition across the shelf and listed several species which had not been previously reported from Texas waters. Parker (1960) studied the ecology and distributional patterns of marine macro-invertebrates in the northern Gulf of Mexico. Of the nearly 2,000 samples examined, 300 were collected on the continental shelf and upper continental slope from off Mobile, Alabama to Port Isabel, Texas. Only 100 of the samples, however, were taken for quantitative estimates, and only 25 were from the shelf off south Texas.

No comprehensive studies of the benthic infauna associated with soft-bottoms on the south Texas OCS have been made. Because of the several transgressions and regressions of Gulf waters during the Pleistocene, organisms associated with reefs and banks off south Texas are now locally distributed in soft-bottom areas characterized by a high percent of bioclastic material. Tunnell (1974) reviewed ecological studies and faunal surveys on or around reefs and banks in the Gulf of Mexico and Caribbean.

Studies concerning the establishment and delineation of faunal provinces in the western north Atlantic have generally been led by the work of malacologists. Leading studies in the recognition or discussion of zoogeographic provinces in the Gulf of Mexico include Woodward (1856), Fischer (1880-1887), Tryon (1882-1884), Dall (1889), Johnson (1934), Hedgpeth (1953), Pulley (1952b), Rehder (1954), Moore (1958), Warmke and Abbott (1961), Briggs (1974), and Tunnell (1974).

To determine the significance of variations in the spatial distribution of benthic organisms, the characteristics of macrobenthic infauna are described first relative to the study area in general and then by specific assemblages.

General characteristics of the macrobenthic infauna

Characteristics of macrobenthic infauna to be discussed include number of species and individuals, biomass, diversity, and equitability.

Number of species and individuals.--The 81 samples examined yielded 2965 individuals belonging to 136 species and suspected species representing several taxonomic groups (Table 2). The taxonomic groups having the greatest number of species were Polychaeta (49 percent), followed by Mollusca (29 percent) and Arthropoda (15 percent). The greatest number of individuals collected belong to Polychaeta (40 percent), then Crustacea (31 percent) and Mollusca (23 percent).

Table 2.--Number of species and individuals collected from 81 stations/samples

Taxa	No. of Species	No. of Individuals
Polychaeta	66 (49 percent)	1199 (40 percent)
Crustacea	21 (15 percent)	917 (31 percent)
Mollusca	39 (29 percent)	666 (23 percent)
Others	10 (7 percent)	183 (6 percent)
	136 (100 percent)	2965 (100 percent)

Other taxonomic groups accounted for less than 10 percent of the total number of species and individuals.

The number of species per sample (0.09 m^3) ranged from one to 44 (Table IVa, Part II, and pl. 27) with a mean of 10.6 (Table 3). The regional distribution pattern (fig. 64) shows two general trends. First, the fewest number of species is in the central sector of the study area with increasing numbers radiating to the north, south, and shoreward. Secondly, number of species generally decrease in a seaward direction. The greatest number of species are in the general area of the Brazos-Colorado and Rio Grande ancestral deltas.

The number of individuals per sample (0.09 m^3) ranged from one to 222 (Table IVa, Part II) with a mean of 38.4 (Table 3). Two general trends are evident in the regional distribution pattern (fig. 65, pl. 28). First, numbers of individuals generally decrease across the shelf with increasing water depth. Secondly, the central portion of the study area has fewer individuals than the northern or southern parts. As was the case with species, the greatest number of individuals are in the shallower water and in the general area of the ancestral Brazos-Colorado and Rio Grande delta. The two small offshore areas of relatively high density of individuals are near the reef structures.

In the northwestern Gulf of Mexico, a number of investigators (e.g., Parker, 1956, 1960; Boyer, 1970; Stanton and Evans, 1971, 1972) have reported the close relationship between macro-invertebrate distribution patterns and variations in water depth and type of sediment. Comparison of the regional distribution maps for both numbers of species (fig. 64) and individuals (fig. 65 and pl. 28) suggests a general correlation with water depth. Furthermore, a comparison of these same two maps with the sand-mud isopleth map (fig. 32), a similarity in distribution is evident. A good correlation ($r = .75$) exists between the distribution of species and individuals (Table 4). Greatest number

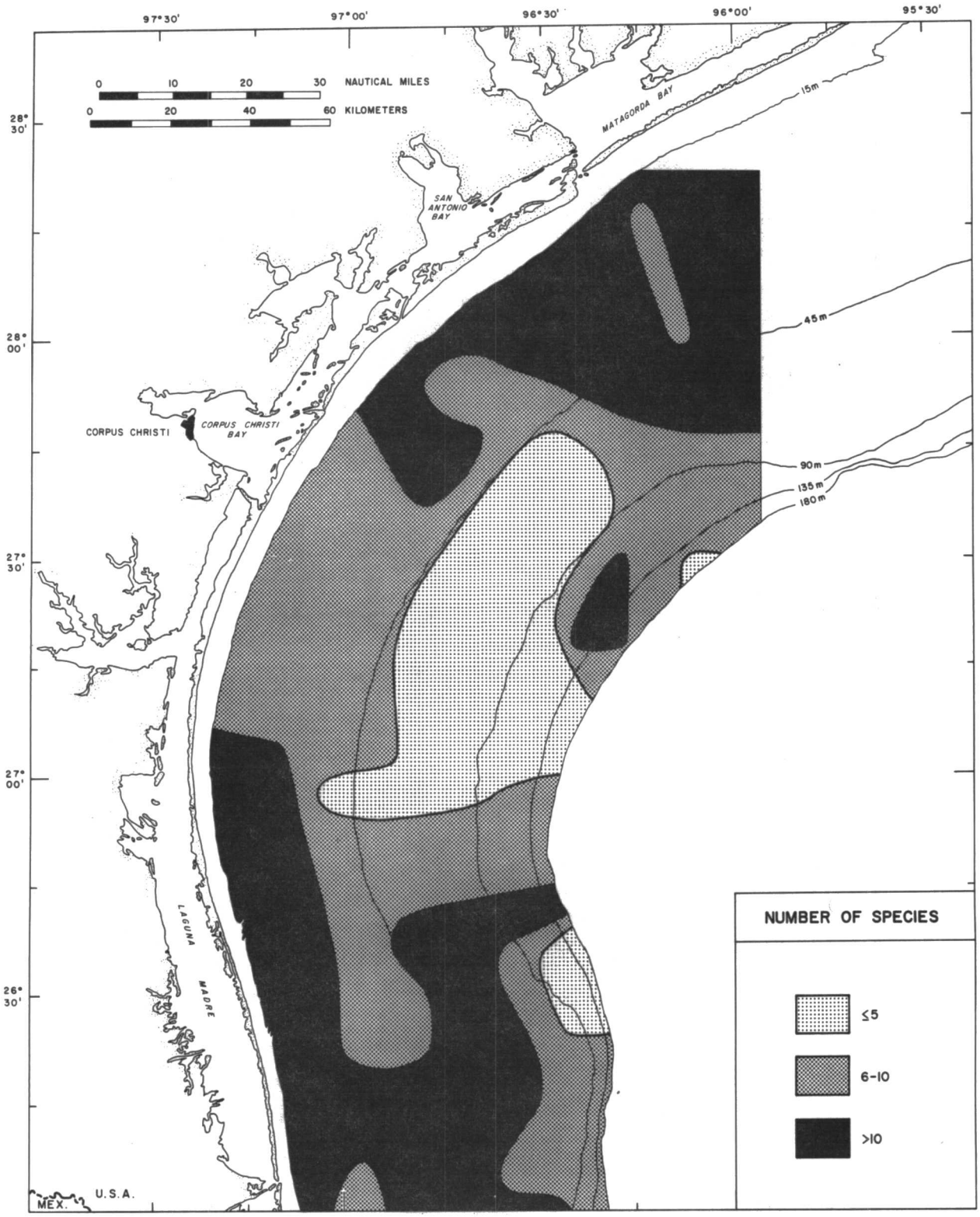

Figure 64. Distribution of total number of species per 0.09 m^3.

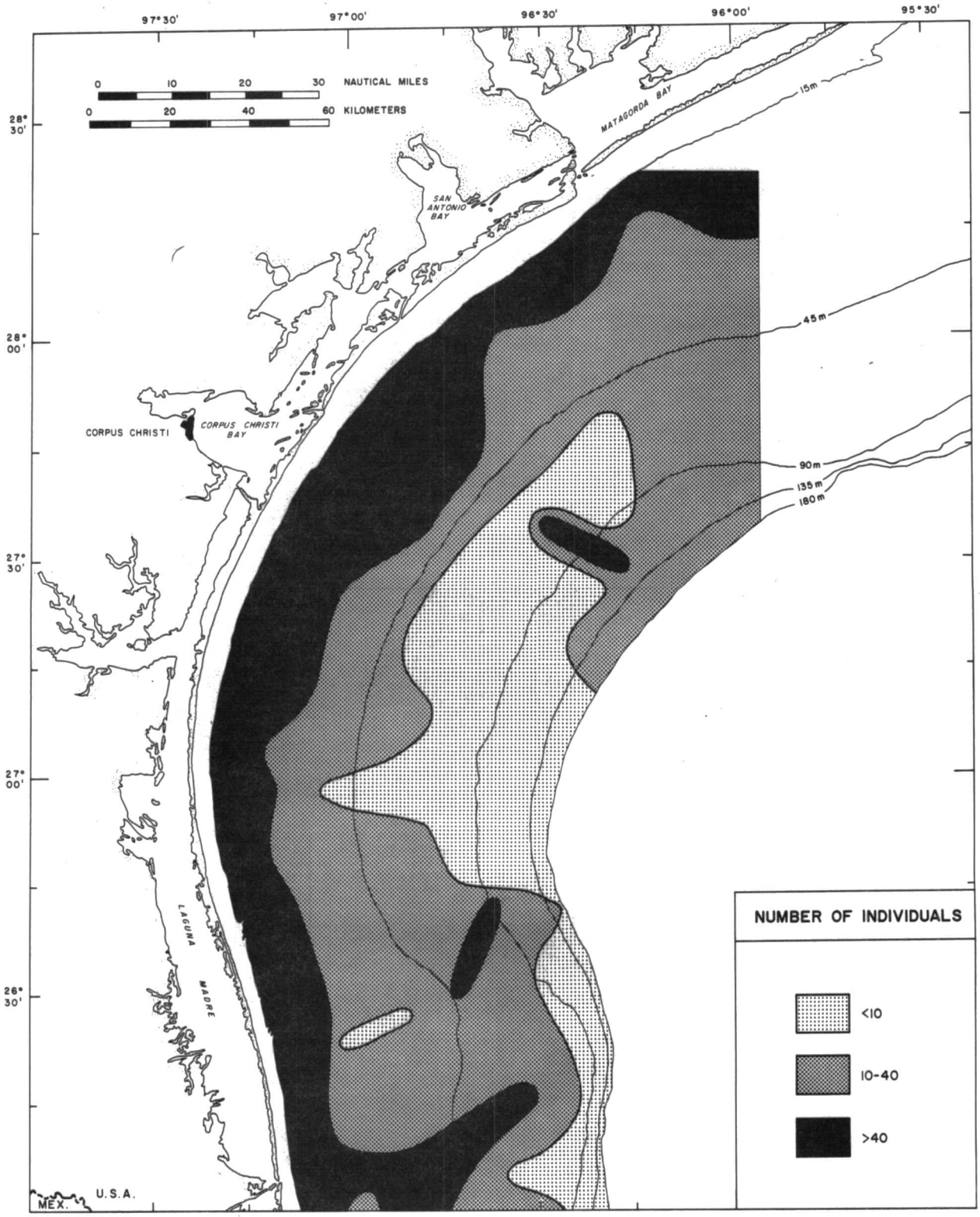

Figure 65. Distribution of total number of individuals per 0.09 m^3.

Table 4--Array of correlation coefficients

	1	2	3	4	5	6	7	8	9
1	1.000								
2	0.7423	1.0000							
3	0.7581	0.8126	1.0000						
4	0.7557	0.2696	0.3624	1.0000					
5	-0.6016	-0.7096	-0.4273	-0.1898	1.0000				
6	0.6914	0.5673	0.5912	0.5128	-0.3154	1.0000			
7	-0.6052	-0.4793	-0.4708	-0.4636	0.3742	-0.8926	1.0000		
8	0.4247	0.3227	0.2433	0.3411	-0.3628	0.5923	-0.6783	1.0000	
9	-0.3194	-0.3307	-0.2952	-0.2089	0.4301	-0.3097	0.5352	-0.3473	1.0000
10	0.4898	0.4385	0.3375	0.2793	-0.6636	0.5207	-0.7333	0.6469	-0.7710

Explanation

1 - No. of species
2 - No. of individuals
3 - Biomass (g)
4 - Diversity (H")
5 - Equitability
6 - Sand-Mud ratio
7 - Mean grain size (Ø)
8 - Standard deviation (Ø)
9 - Water depth (m)
10 - Bioturbation

of species and individuals seem to be in relatively shallow water, and in parts of the shelf having high sand-mud ratios. A more complete discussion concerning factors controlling fauna distribution will be given later.

Overall, the density of species and individuals over the South Texas OCS is low compared to the coastal waters adjacent to the OCS and to parts of the continental shelf further north. For example, Holland et al., (1974) reported 338 benthic taxa from Corpus Christi, Nueces and Copano Bays with maximum standing crops reaching as high as 11,896 individuals/1/2 ft^3. Kritzler and Vittor (1975) reported 190 species of polychaetous annelids alone from the shelf off Mississippi, Alabama, and Florida. The overall low densities are probably the result of such large parts of the South Texas OCS being characterized by fine grain relatively homogenous sediments and rapid sedimentation rates.

Biomass.--Biomass was calculated in grams (wet weight, preserved) and ranged in weight by station (0.09 m^3) from 0.0150 to 3.2089 g (Table IVa, Part II) with a mean of 0.3184 g (Table 3). Gross biomass data in this study were subject to more sources of error than other data for two reasons. First, the biomass per sample was very small and difficult to measure accurately. Secondly, biomass data are greatly influenced by chance recovery of unusually large or heavy organisms. Molluscs are particularly troublesome because of their relatively heavy shell.

The regional distribution pattern for the biomass is shown in figure 66 and plate 29. Areas of larger biomass (>0.15 g) are located in shallower water (generally less than 45 m) and in the extreme northern and southern parts of the study area. Only a few isolated areas of biomass less than 0.04 g exist and these generally are in deep water at the edge of the shelf. The ancestral Rio Grande and Brazos-Colorado deltas have relatively high biomass (>0.15 g) compared to the central sector of the shelf. Isolated areas of higher biomass

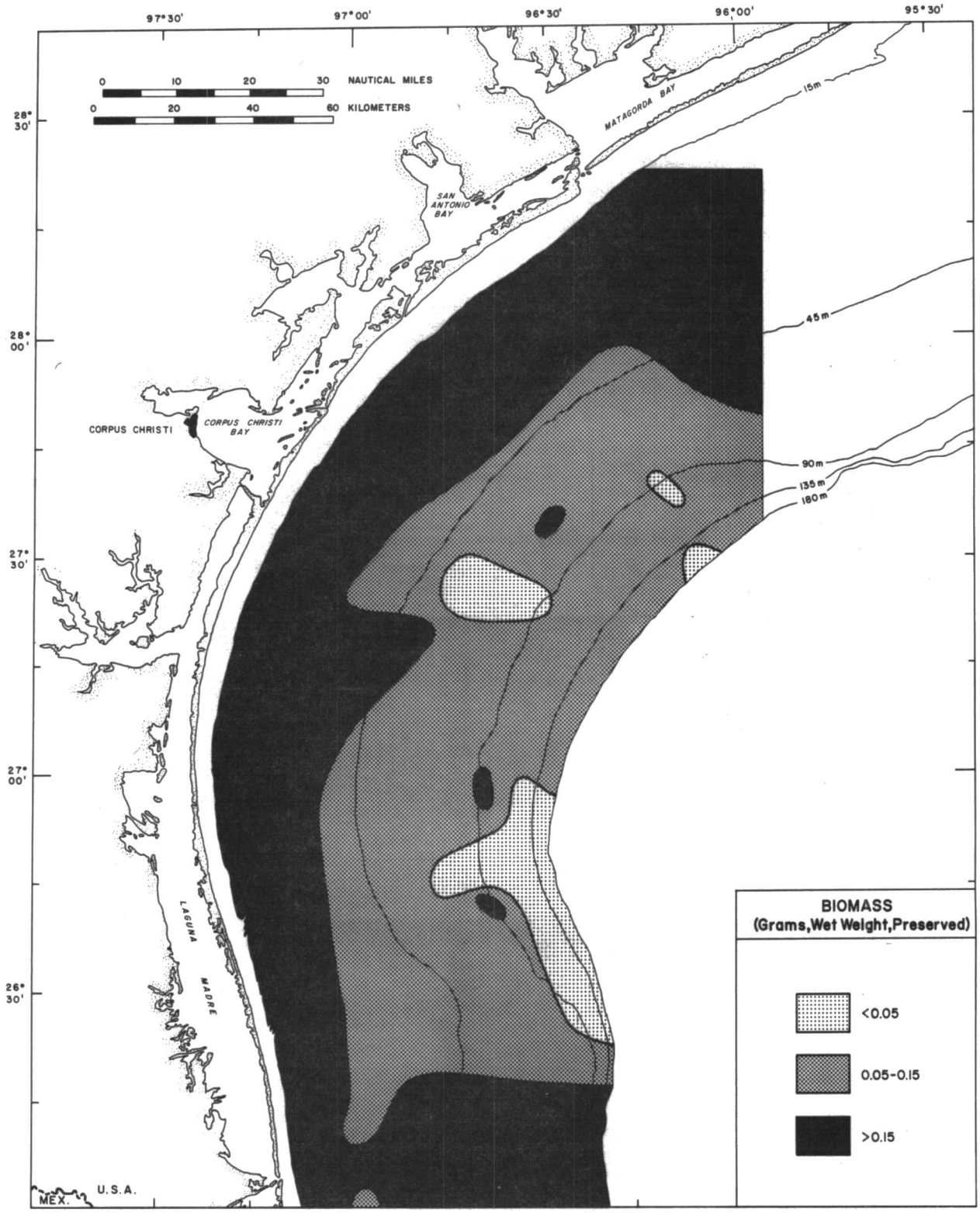

Figure 66. Distribution of total biomass per 0.09 m^3.

in the offshore central sector are in the general vicinity of reef structures.

The general decrease in biomass in a seaward direction agrees with results from a number of studies in other areas: animal densities and biomass decrease with increasing depth and distance from land (e.g., Sanders and Hessler, 1969). The regression coefficients calculated indicate a good correlation (r = .77) between biomass and number of individuals (Table 4).

Reduction in biomass in a seaward direction is normally associated with a decrease in food supply. Based on the distribution pattern of total organic carbon in the sediment (Holmes, this report), however, the available food material seems to be large enough to support a greater biomass. Consequently, grain size sediments seem to be the principal factor controlling the number of species and individuals, as discussed previously, and must be at least partly responsible for the overall small biomass in outer parts of the shelf.

Diversity and equitability.--Calculated diversity (H") values per sample (0.09 m^3) ranged from 0.3046 to 3.1810 (Table IVa, Part II) with an overall mean of 1.8550 bels/individual (Table 3). The regional distribution pattern is very irregular (fig. 67 and pl. 30), but some broad general patterns seem to exist. The lowest diversity values (<1.75) are in the central sector of the study area between the two ancestral deltas to the north and south. Generally, inshore areas have greater diversity values than extreme offshore areas. The highest diversity values (>2.75) are concentrated in the southwest sector of the study area, mostly in shallower water. For the South Texas OCS in general, diversity values are low.

The range of equitability values per sample (0.09 m^3) varied between 0.2180 and 0.0000 (Table IVa, Part II) with a mean value of 0.5449 (Table 3). According to the regional distribution pattern (fig. 68 and pl. 31), most of the South

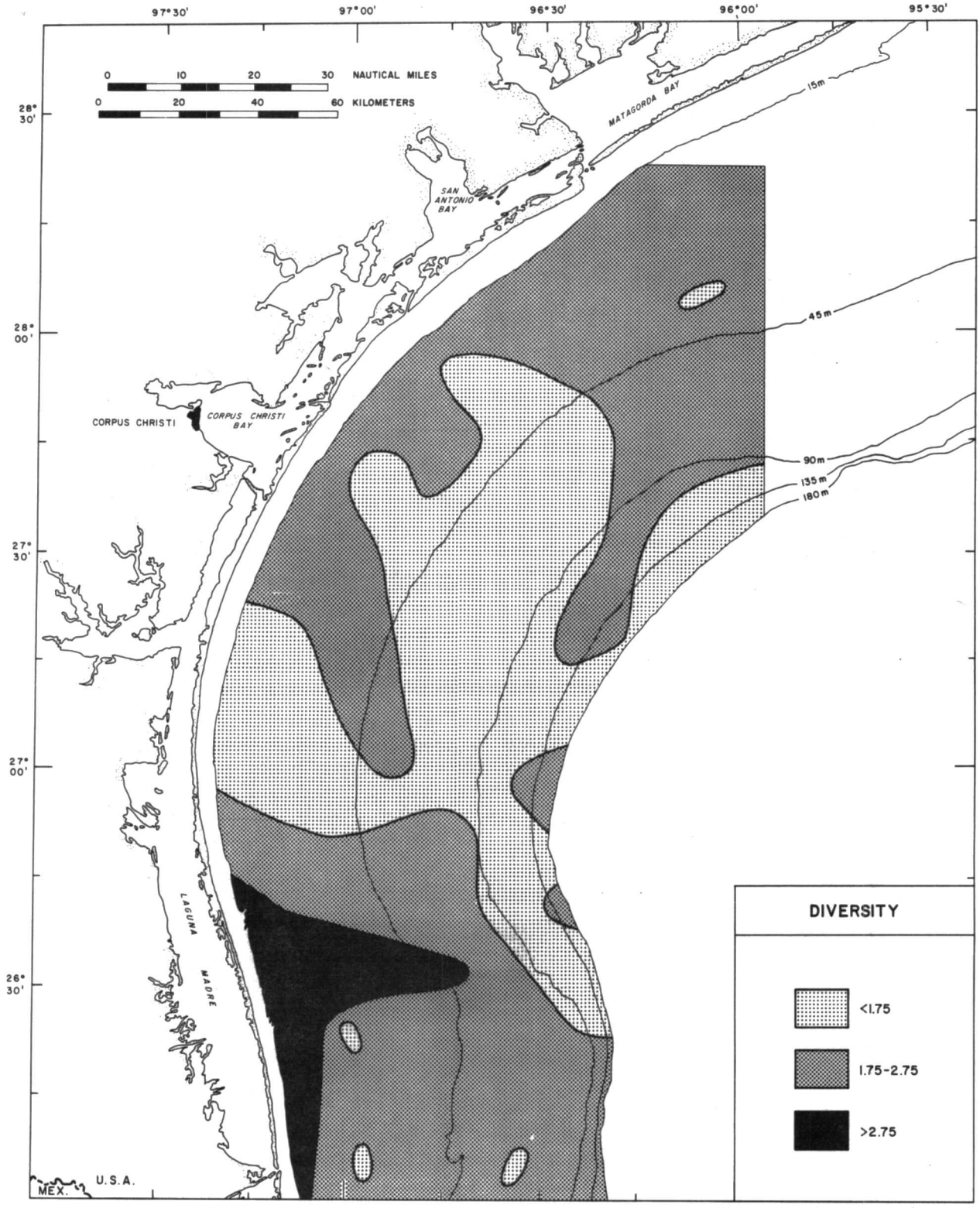

Figure 67. Infaunal diversity (H") per 0.09 m^3.

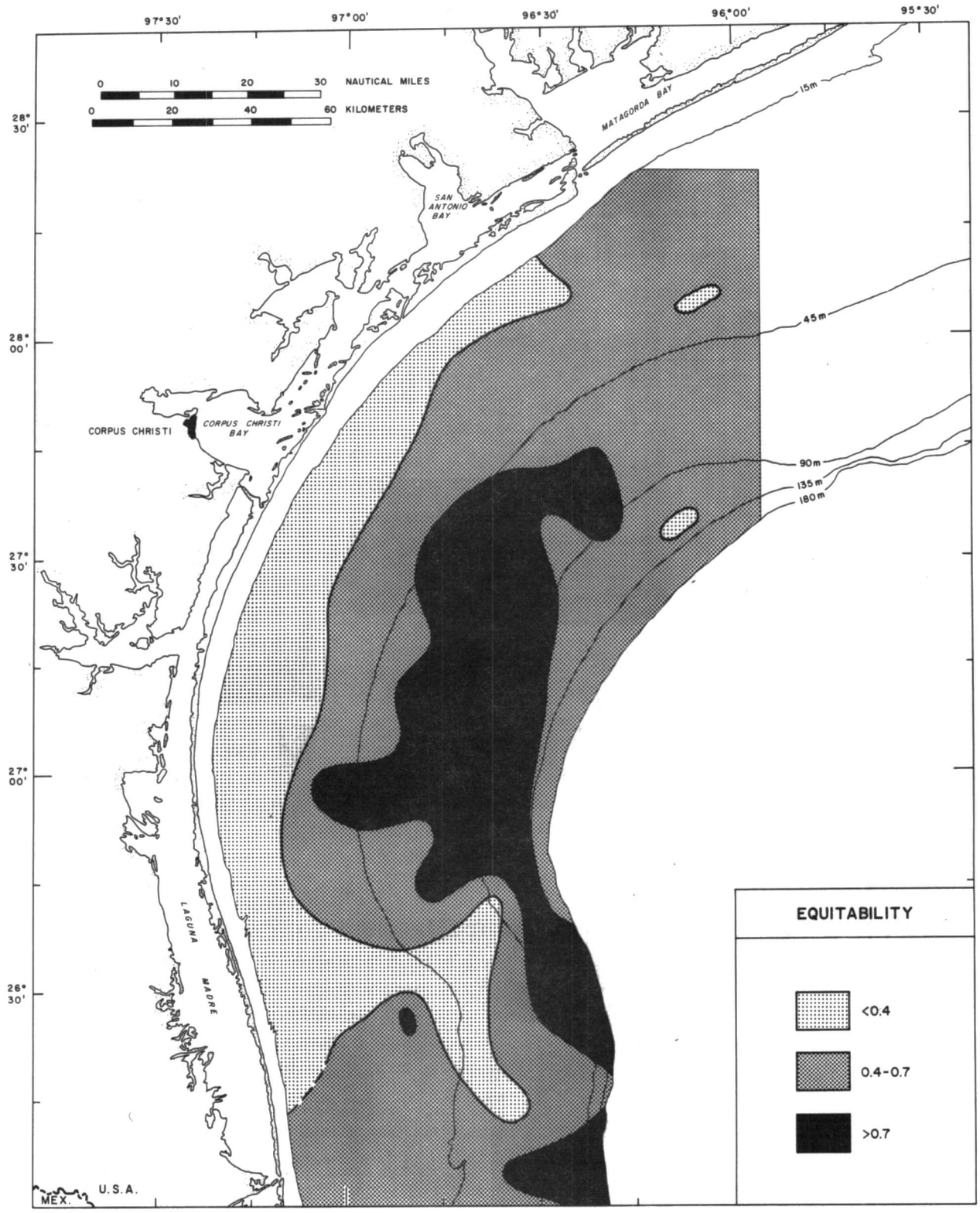

Figure 68. Infaunal equitability per 0.09 m^3.

Texas OCS is characterized by equitability values between 0.4 and 0.7. However, a fairly distinct zonation of equitability values is evident. Lowest values (<0.4) are prevalent in shallower water along the inner OCS and the highest values are concentrated in the outer central sector of the OCS and along the shelf edge in the southern sector. Generally, equitability values increase seaward.

The definition, significance, causes, and uses of various diversity indices have been widely discussed in the literature (e.g., Hulbert, 1971; Hendrickson and Ehrlich, 1971; Margalef, 1957; MacArthur and Wilson, 1967; Sanders, 1968, 1969; Paine, 1966; Klopfer, 1959; Pianka, 1966; Woodwell and Smith, 1969; Johnson, 1970; Fishel, Corbet, and Williams, 1943). The Shannon diversity index was chosen because it is based on both number of species and their relative abundance, is relatively independent of sample size (Sanders, 1968), is normally distributed (Hutcheson, 1970), and is easily calculated. A great deal of literature which attempts to explain observed patterns exists and has been reviewed by Valentine (1971) and others. After reviewing the literature, Stanton (1973) states that "diversity is determined by the interplay of historical factors with the biological and physical factors in the ecosystem of time, stability, and resources". As a measurement of processes operating in an ecologic system, diversity reflects external environmental stresses as well as internal stability and productivity (Beerbower and Jordan, 1969).

The regional distribution patterns of diversity and equitability determined for the South Texas OCS does not agree completely with what has been found elsewhere. In other studies, both diversity and equitability increased in a seaward direction, away from the more variable and rigorous environments of the inner

shelf and coastal waters (e.g., Stanton and Evans, 1971). Over the South Texas OCS, diversity generally decreases and equitability increases with increasing water depth. As number of species depends on the structural diversity of the habitat in contrast to equitability which is more sensitive to the stability of physical conditions (Beerbower and Jordan, 1969), an examination of the physical attributes of the study area helps to explain observed diversity-equitability regional distribution patterns. Areas in shallower water and the ancestral deltas of the Brazos-Colorado and Rio Grande Rivers exhibit the greatest sediment diversity, i.e. habitat diversity, (fig. 41 and pl. 18) and consequently support a more diverse fauna than the relatively homogenous fine grain sediments of the central, deeper water sector of the South Texas OCS. General trends in the areal equitability patterns are similar to those observed in other areas. As water depth decreases, the physical conditions (temperature, salinity, currents) are more variable and the successional sequence leading to high equitability does not have time to develop fully before the ecosystem is returned to a less mature stage because of environmental change (Gibson, 1966).

With the exception of equitability, all the biological characteristics described: number of species and individuals, biomass, and diversity share two common regional trends. First, values for the characteristics described above tend to be highest in shallower water and decrease with increasing water depth. Second, the lowest values of the biological parameters are generally located in the central sector of the study area with values increasing to the north and south. The ancestral deltas of the Brazos-Colorado and Rio Grande generally have higher values than areas of comparable water depth in the central sector. The regional distribution pattern of equitability values reflects an inverse relationship to water depth and geomorphic features relative to the other

biological characteristics. General trends in the biological characteristics seem to be most sensitive to depth of water and grain size of sediment.

Macrobenthic infauna relative to assemblages

The large standard deviations indicated (Table 3) imply that the biological makeup of the South Texas OCS is not homogeneous. It is further implied that the macrobenthic infauna occurs in specific assemblages. As a means of identifying and differentiating macrobenthic infaunal assemblages from the data, a classification by numerical analysis was used. Such analysis has been applied in other studies with good results (e.g., Day and others, 1971; Field, 1970, 1971; Field and McFarlane, 1968; Hughes and others, 1972; Hughes and Thomas, 1971a, b; Stephenson and others, 1970; Santos and Simon, 1974). The computer program for this analysis was supplied by Dr. Joseph L. Simon, Department of Biology, University of South Florida, with permission from Dr. John G. Field of C.S.I.R.O. unit, Capetown, South Africa, who originally developed the program. The description of the program is given by Santos and Simon (1974) and is reviewed briefly. The classification normally consists of four main steps:

1. Similarity (dissimilarity, etc.) matrix computation;
2. application of sorting strategy;
3. application of a test of significance to determine homogeneity; and
4. expressing results by a suitable means.

Czekanowski's coefficient (Bray and Curtis, 1957; Field and McFarlane, 1968) was used to measure the faunal similarity between stations (i.e., interindividual measure). The Czekanowski coefficient as defined is:

$$Cz = \frac{2w}{(a+b)}$$

Table 3--Biological characteristics of the South Texas OCS by sample (macrobenthic infauna per 0.09 m^{-3})

Parameter	Mean	Standard deviation
No. of species	10.6250	7.0484
No. of individuals	38.4000	48.2616
Biomass (g)	0.3184	0.5040
Diversity (H")	1.8550	0.5651
Equitability	0.5449	0.1639

where a = sum of the species scores from sample a

b = sum of the species scores from sample b, and

w = sum of the lesser scores of each common species in the two samples being compared.

Several characteristics of the Czekanowski's coefficient made it suitable for use in this study. For example, large numbers of zeros in the data do not affect the coefficient and it considers the relative abundance of each organism, rather than simply presence or absence. The sorting strategy used was group average sorting for Q or normal analysis, an agglomerative polythetic type system used successfully by Field (1970, 1971). This sorting strategy was selected, as the average level of similarity between stations was investigated not the relations between individuals (Hughes and Thomas, 1971b; Orloci, 1967).

To determine if subsets generated by the similarity analysis differ significantly, the information statistic $2\Delta I$, (Williams and others, 1966; Field, 1969) was used. The results of the analysis are expressed in a hierarchical dendogram. Number of species were log transformed ($\log_e X+1$) to save computer time and species not occurring in at least 5 percent of the samples was eliminated from the analysis.

The results of the numerical analysis using the available data from the South Texas OCS are shown in figure 69. Several major groups (Group I through V) which may be interpreted as macrobenthic infaunal assemblages are evident.

On a scale from 0-100, for similarity to identical faunal lists, the Czekanowski's coefficient varied between 0 and 75.7720; the frequency distribution of the coefficients (percent occurrence) is shown in Table 5. The lower similarity levels at which the major groups become significantly

Table 5--Frequency distribution of Czehanowski's coefficient (percent occurrence)

Coefficient	Percent occurrence
0-10	24.5370
10-20	28.6728
20-30	22.4691
30-40	13.5494
40-50	7.1605
50-60	2.9012
60-70	0.6173
70-80	0.0926
80-90	0.0000
90-100	0.0000

different from each other (generally less than 35 percent) may result from at least two factors. First, the lower levels of sample homogeneity may be indicative of environmental heterogeneity within the study area, or secondly, it may have resulted from the variability inherent in small samples taken from a large and diverse population (Stanton and Evans, 1972). Because organisms commonly have clumped distribution patterns as opposed to being evenly dispersed (Jones, 1961), the second explanation of the relatively lower similarity levels may lie in the physical characteristics of the region.

By mapping the major groups (I-V) shown in figure 69, the approximate regional distribution pattern of each macrobenthic infaunal assemblage as defined by the clustering technique was determined and is shown by figure 70 and plate 32. If these macrobenthic infaunal assemblages are significantly different, the differences should be reflected in a comparison between the characteristics of each assemblage.

Macrobenthic infaunal assemblages are described and compared through a series of characteristics or aspects including number of species and individuals, biomass, diversity, equitability, and faunal composition. For each listed characteristic, except faunal composition, the total and mean values were calculated by assemblage (Table 6). The faunal composition for each assemblage relative to the percent of the total species and individuals represented by each of the major taxa (Polychaeta, Arthropoda, Mollusca) is shown in Table 7.

Assemblage I.--Assemblage I is the largest of the assemblages relative to areal distribution (fig. 70 and pl. 32). It extends along the entire longitudinal axis of the study area and is confined generally to that part of the shelf shoreward of the 45 m isobath, but the seaward boundary is very irregular. Assemblage I covers large portions of the ancestral deltas of the Brazos-Colorado

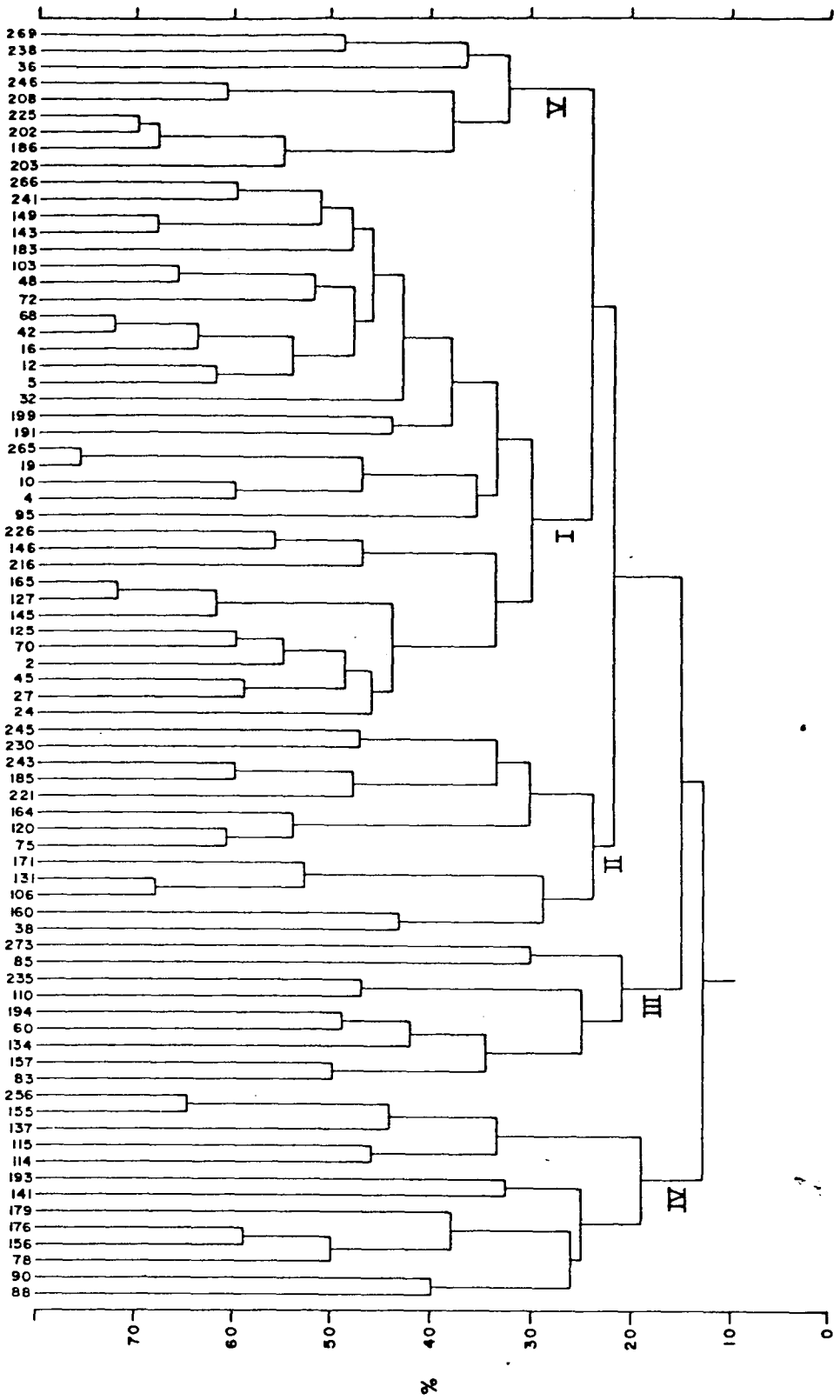

Figure 69. Dendogram showing similarity of stations in terms of the Czekanowski coefficient and group average sorting for Q-mode analysis

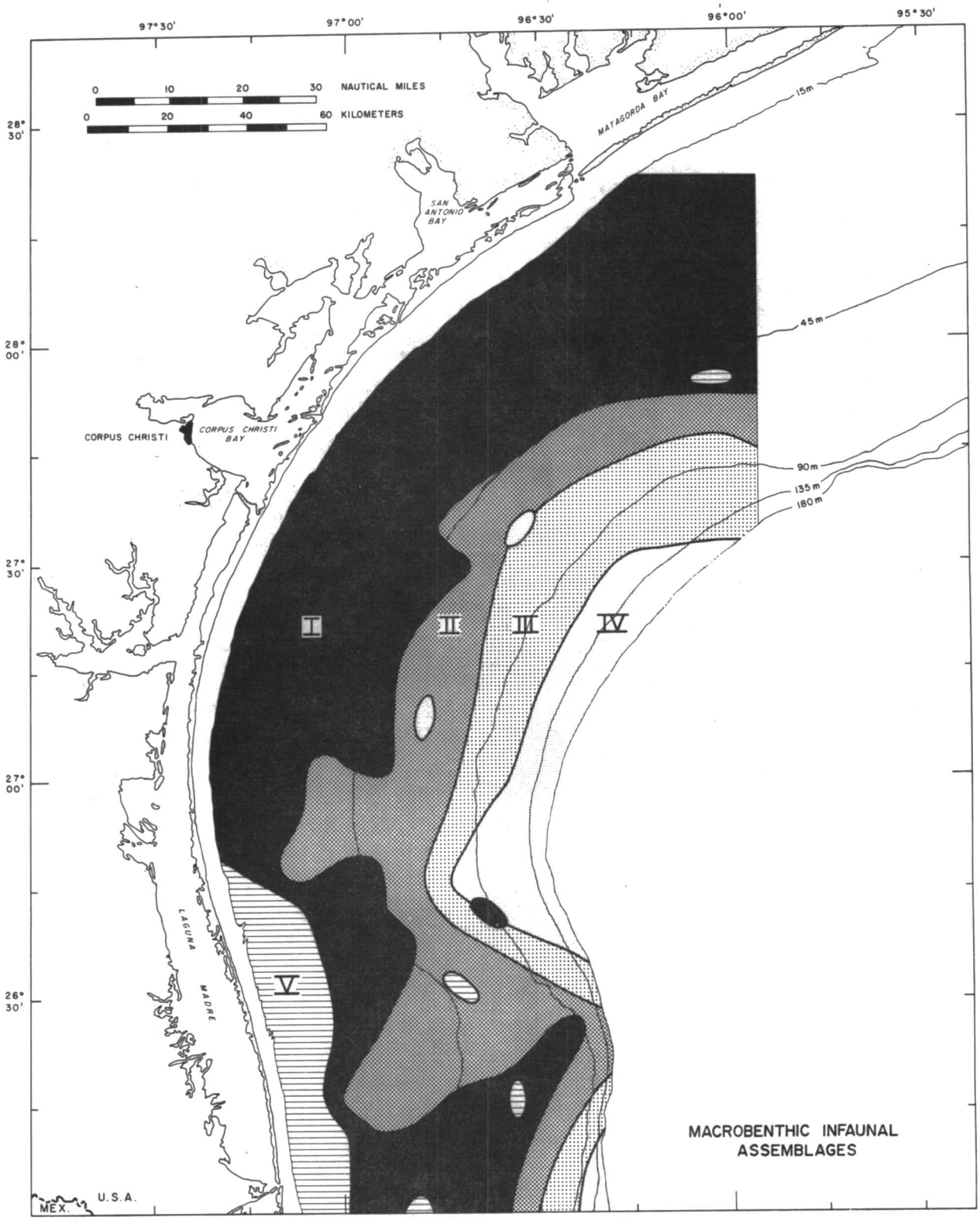

Figure 70. Distribution of macrobenthic infaunal assemblages. Individual assemblages are numbered I - V.

Table 6--Characteristics of macrobenthic infaunal assemblages on the South Texas OCS

Parameters	Assemblages				
	I	II	III	IV	V
No. of stations	34	15	10	13	9
Total no. of species	76	47	37	46	82
Total no. of individuals	1448	182	100	208	1027
Total biomass (g)	9.2680	2.0551	0.6402	1.1573	10.1279
Average no. of species per station	10	8	6	8	25
Average no. of individuals per station	42.5	12.1	10.0	16.0	114.1
Average biomass (g) per station	0.2726	0.1370	0.0640	0.0890	1.1253
Average diversity (H") per station	1.8609	1.7751	1.6126	1.7523	2.6399
Average equitability per station	0.4769	0.6356	0.6968	0.6362	0.3835

Table 7--Distribution of species and individuals among the major taxa relative to specific macrobenthic infaunal assemblages

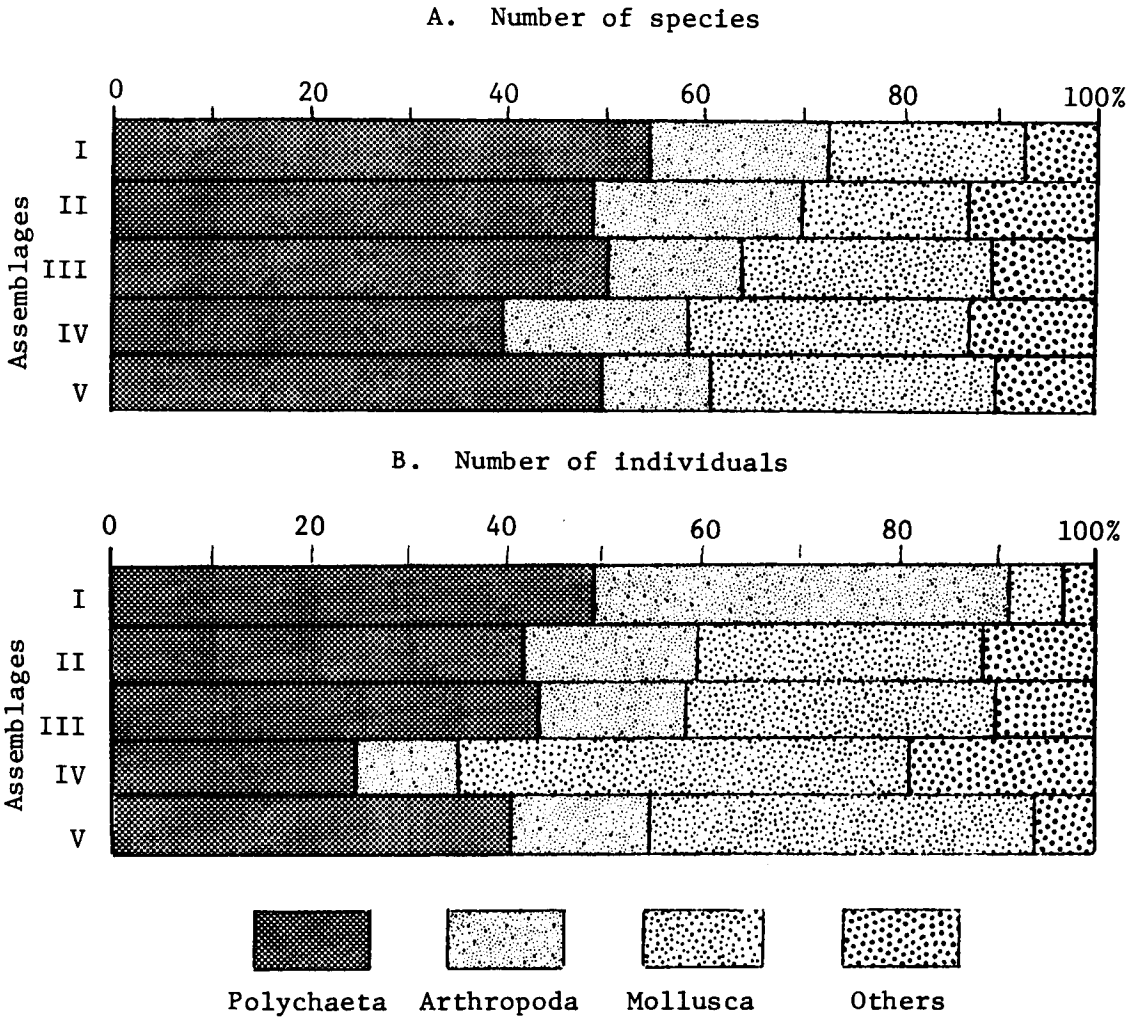

and Rio Grande. In the extreme southern sector assemblage I does extend seaward well beyond the 45 m isobath, reaching depths as great as 90 m.

The assemblage is characterized (Table 6) by the second greatest number of species (10/0.09 m^3), number of individuals (42.5/0.09 m^3), biomass (0.2726 g/0.09 m^3), and diversity (1.8609/0.09 m^3). Only assemblage V had greater values for each aspect. With respect to equitability, assemblage I had the second lowest value (0.4769/0.09 m^3), the lowest value belongs to assemblage V. Of the total number of stations (81), almost 42 percent (34 stations) were clustered in assemblage I (fig. 69).

Assemblage II.--Assemblage II is second in geographic extent (fig. 70 and pl. 32) and is generally bounded shoreward in the northern and central sectors by the 45 m isobath and seaward by the 75 m isobath. In the southern third of the study area, however, the boundaries of assemblage II are extremely irregular, extending from relatively shallow water to the edge of the shelf.

Characteristics of assemblage II (Table 6) are not as uniformly defined as in assemblage I. The characteristics are: (1) third highest number of species, 8/0.09 m^3 (lower than assemblages V, I and the same as IV); (2) fourth highest number of individuals, 12.1/0.09 m^3 (lower than assemblages V, I, IV); (3) third greatest biomass, 0.370 g/0.09 m^3 (lower than assemblages V, I); (4) third greatest diversity, 1.7751/0.09 m^3 (lower than assemblages V, I); and (5) third highest equitability, 0.6356/0.09 m^3 (lower than assemblages III, IV). Approximately 18 percent (15 samples) of the total number of samples (81) are clustered in assemblage II (fig. 69).

The relative percentage of both polychaete species (49 percent) and individuals (42 percent) dominate the faunal composition of assemblage II (Table 7). With respect to number of species/0.09 m^3 arthropods ranked second

(20 percent), molluscs third (18 percent) and other miscellaneous taxa represented less than 10 percent of the total species. Molluscs are the second largest group of individuals/0.09 m^3 (28 percent) followed by arthropods, (18 percent) and miscellaneous taxa (12 percent).

Assemblage III.--Assemblage III (fig. 70 and pl. 32) covers the third largest geographic area among the assemblages (less than assemblages I, II). The general boundaries are the 75 m isobath shoreward and the 120 m isobath seaward. However, the assemblage does not extend to the shelf's edge in the extreme northern sector of the shelf, but both boundaries extend to the edge of the shelf in the southern section.

Assemblage III (Table 6) has the fewest number of species (6/0.09 m^3) and individuals (10/0.09 m^3), smallest biomass (0.0640 g/0.09 m^3), lowest diversity (1.6126/0.09 m^3) and greatest equitability (0.6968/0.09 m^3) relative to the other assemblages. Ten (12 percent) of the 81 samples are clustered in Assemblage III (fig. 69).

Polychaetes are the dominant taxa relative to both numbers of species (50 percent) and individuals (43 percent) in assemblage III (Table 7). Ranked by relative percentage of total species and individuals, molluscs are second in abundance (25 percent and 31 percent respectively) followed by arthropods, (14 percent and 15 percent respectively), and miscellaneous taxa (11 percent and 10 percent respectively).

Assemblage IV.--Assemblage IV is along the edge of the continental shelf in the central sector in water depths generally greater than 120 m (fig. 70 and pl. 32). In areal distribution assemblage IV ranks fourth in area. In overall characteristics assemblage IV generally rank fourth highest (less than assemblages V, I, II) among the assemblages (Table 6); i.e., the number of species (8/0.09 m^3)

and individuals (16/0.09 m^3), biomass (0.0890 g/0.09 m^3) and diversity (1.7523/0.09 m^3). Equitability ranked second highest (0.6326/0.09 m^3) with only assemblage III having a higher average value. Thirteen (16 percent) of the samples are clustered in assemblage IV (fig. 69).

Polychaetes constituted the largest portion (39 percent) of the total number of species in assemblage IV (Table 7). They were followed, in order of decreasing percentages, by molluscs (29 percent), arthropods (19 percent) and other miscellaneous taxa (13 percent). In contrast, molluscs constitute the largest portion (47 percent) of the total individuals and is followed by polychaetes (23 percent), miscellaneous taxa (19 percent) and arthropods (11 percent).

Assemblage V.--Assemblage V has the smallest areal distribution of the five assemblages (fig. 70 and pl. 32). It is located in the southeasternmost part of the South Texas OCS area in water depths generally less than 30 m. The inshore boundary cannot be estimated because of limitation of the study area.

Assemblage V is the most densely populated and the most diverse assemblage. Mean values for the parameters used to characterize the assemblage (Table 6) were relatively very high, including number of species (25/0.09 m^3) and individuals (114.1/0.09 m^3), biomass (1.1253 g/0.09 m^3), and diversity (2.6399/0.09 m^3). The average equitability (0.3835/0.09 m^3) was the lowest in the study area. Of the 81 stations studied, 11 percent (9) were clustered in assemblage V (fig. 69).

Relative to the number of total species and individuals, the largest portion of the fauna in assemblage V was polychaetes (49 percent and 41 percent respectively) followed by mollusca (29 percent and 39 percent respectively), arthropoda (11 percent and 14 percent respectively), and other miscellaneous taxa (11 percent and 6 percent respectively), (Table 7).

Regional trends are evident in the distribution of macrobenthic infaunal species and individuals among the major taxa relative to assemblages (Table 7 and Table IVb, Part II). Polychaetes represent the dominant taxa with regard to both numbers of species and individuals. In a seaward direction, however, polychaete diversity and density decrease. In contrast, the diversity and density of molluscs significantly increase across the shelf with increasing water depth. Arthropod diversity is relatively constant across the shelf, but the density decreases as water depth increases. The individuals are generally spread out among the species within each assemblage (Table 8). An exception is assemblage I where the individuals tend to be concentrated in a few species due to the large numbers of amphipods commonly found in shallower waters. The percentage of species shared between any two assemblages decreases with increasing spatial separation (Table 9). An interesting exception to this regional trend is assemblage IV which shows an increase in the percentage of shared species with other assemblages regardless of the geographic setting.

The reverse in the general trends beyond approximately the 120 m isobath can be explained in the biological concept of the ecotone or "boundary effect" where two habitats overlap; the boundary between the two will be more favorable as a habitat than either type considered alone (Odum, 1959). In the case of assemblage IV, the type of bottom sediment is similar to that for adjacent assemblages but the physical oceanographic regime is different. The faunal composition indicates that water from the deep Gulf circulates over the outer part of the shelf in the central sector causing a change in the environmental conditions. As a result, the mixing of outer shelf and upper slope infauna increases in both the diversity and density of the infauna.

Parker (1960) is the only other study that attempted to recognize assemblages in the study area. Of the several assemblages he describes for the northwestern

Table 8--Percent of individuals found in the most common 5, 10, 15 and 20 species for each macrobenthic infaunal assemblage; e.g. 70% of all individuals in assemblage I belong to the five most common species in that assemblage

	Assemblages				
Most Common:	I	II	III	IV	V
5 species	70	40	48	52	38
10 species	81	63	65	67	54
15 species	87	75	75	76	64
20 species	90	81	82	83	72

Table 9--Similarity of macrobenthic infaunal assemblages relative to percent of shared species

	I	II	III	IV
II	0.8085			
III	0.2958	0.3400		
IV	0.4242	0.4118	0.5641	
V	0.7344	0.5932	0.2933	0.3649

Gulf, three are of particular significance: intermediate shelf assemblage, 22 to 73 m; outer shelf assemblage, 73-119 m; and upper continental slope assemblage, 119-1,098 m. Parker concluded that the distribution of species in the assemblages followed certain ranges of bottom temperatures and then separate according to major sediment types. Similar conclusions have been drawn for other parts of the U.S. continental shelf (e.g., Cerame-Vivas and Gray, 1966). The results of this study generally agree with assemblages observed by Parker but may reflect more detail due to a more dense sampling network. Differences in the two studies will not be discussed in detail because it is impossible to give exact assemblage boundaries, particularly in gradational environments. Differences in sampling technique and analysis also preclude a detail comparison.

Biogenic structures

Biogenic sedimentary structures are useful in determining temporal variations in macrobenthic infaunal zonation. Biogenic sedimentary structures make up a significant part of the "evidence of life" in the sediments and, in most instances, is the only record left by soft-bodied organisms.

As defined by Frey (1973), biogenic sedimentary structures are those "structures produced in the sediments by the activity of organisms upon or within an unconsolidated particulate substrate". In turn, Frey (1973) defines biogenic structures as "tangible evidence of activity by an organism, fossil or recent, other than the production of body parts". Biogenic structures are produced as the animal burrows through the sediment. The burrows vary in type, size, and orientation depending on the animals responsible. Large burrows are commonly indicated by the infilling of sediment; smaller burrows commonly show only on X-ray radiographs. Intense burrowing destroys the original grain size relationship in the sediment as well as depositional layering. Typical examples of biogenic structures in sediments of the South Texas OCS are shown by the sketches of box

EXPLANATION

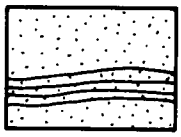

SAND LAYER
Lines indicate mud laminae

MUD

SAND DIFFUSED INTO MUD BY BIOTURBATION

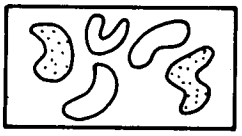

LARGE ANIMAL BURROWS
Stippling indicates those filled by sand

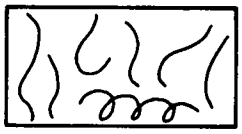

SMALL ANIMAL BURROWS

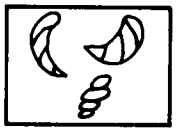

SHELL REMAINS

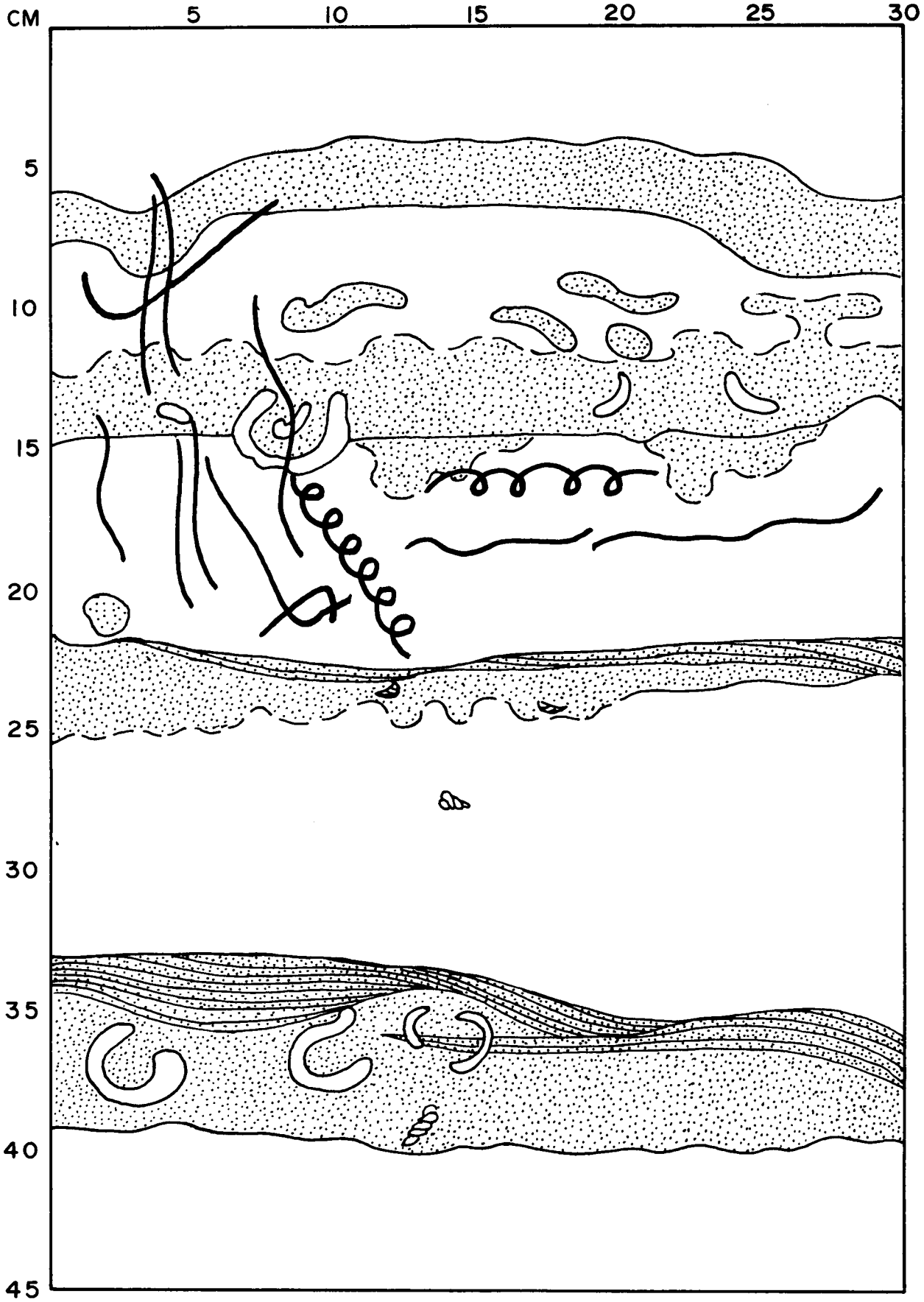

Figure 71. Sketch of box core from station 12 showing biogenic and depositional structures. Top is sea floor surface.

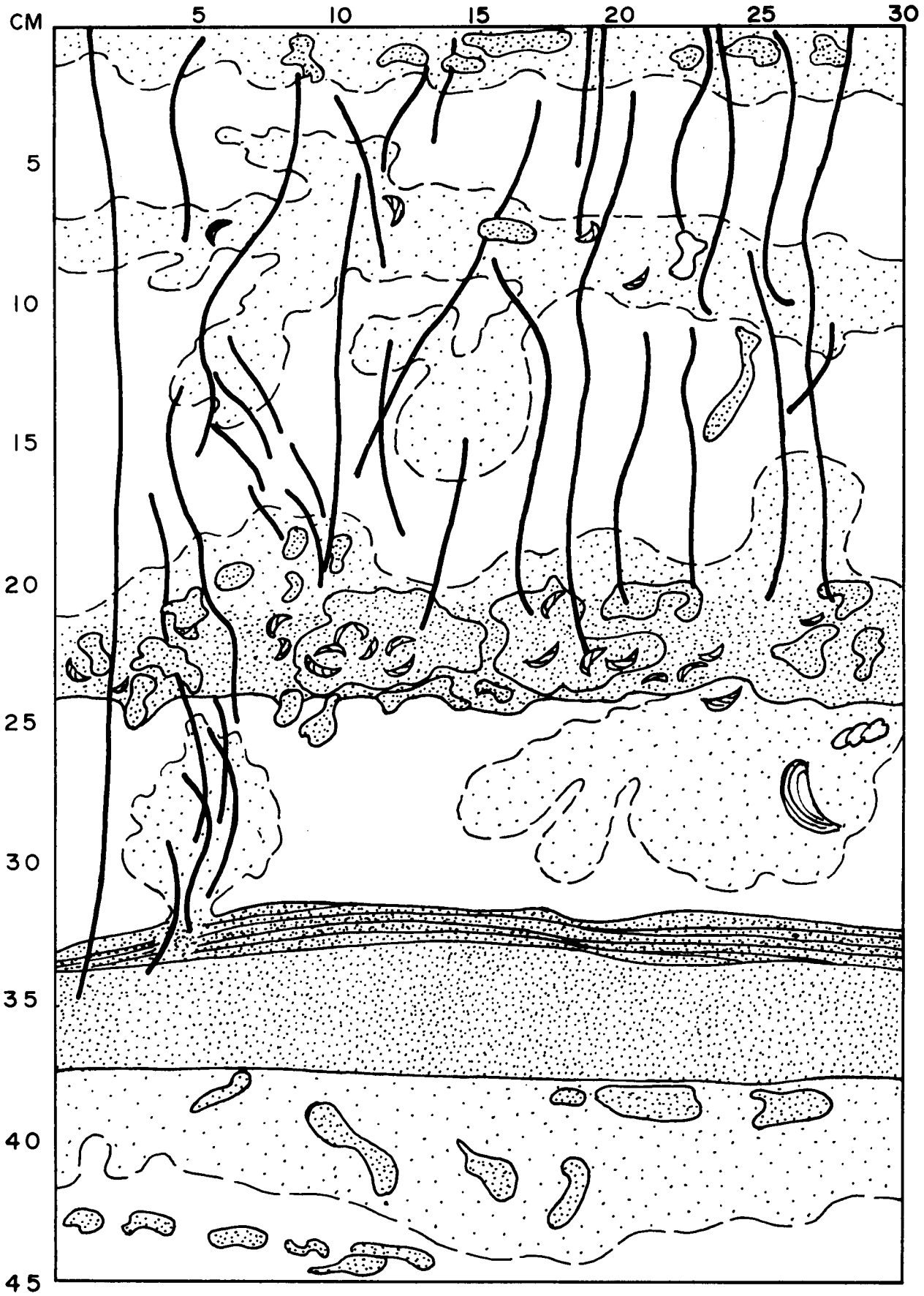

Figure 72. Sketch of box core from station 24 showing biogenic and depositional structures. Top is sea floor surface.

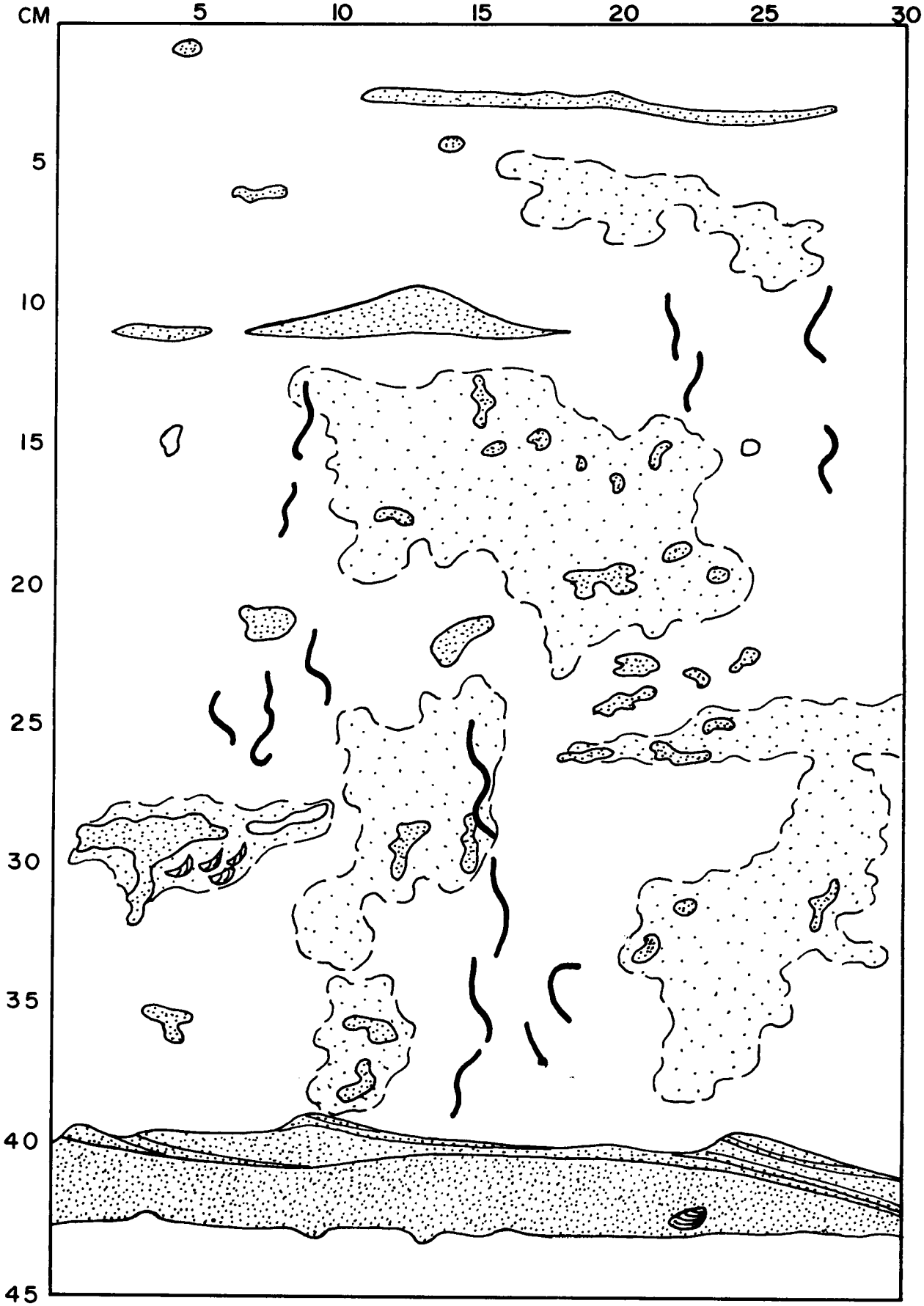

Figure 73. Sketch of box core from station 45 showing biogenic and depositional structures. Top is sea floor surface.

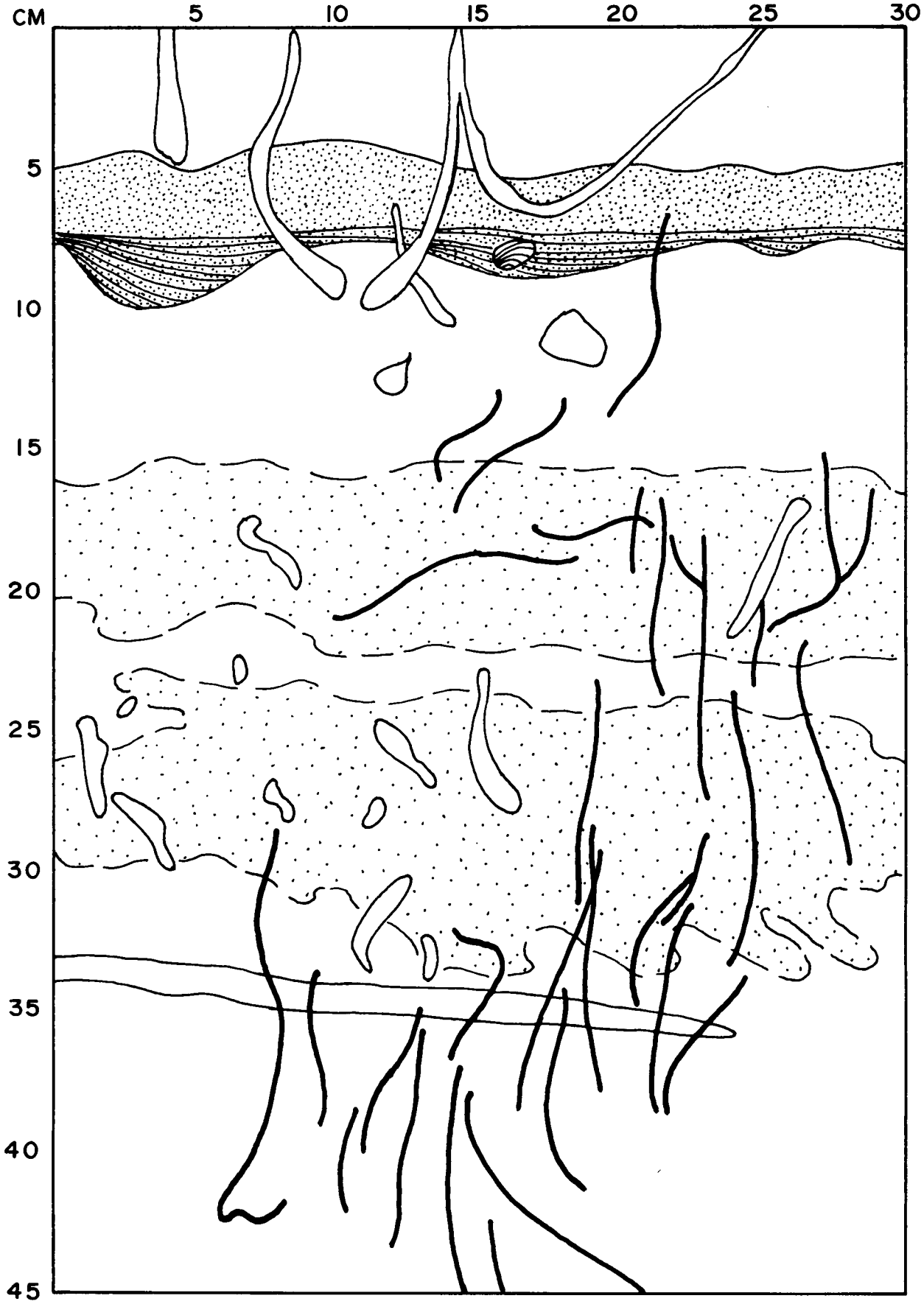

Figure 73a. Sketch of box core from station 75 showing biogenic and depositional structures. Top is sea floor surface.

cores, figures 71 to 73a. Although it is virtually impossible to determine the original diversity and density of fossil assemblages using biogenic sedimentary structures alone, the structures do permit at least an estimation of the assemblages involved (Frey, 1971).

Biogenic sedimentary structures can be used to determine temporal variations in macrobenthic infaunal zonation by two general steps; (a) determine the correlation between present day zonation of biogenic sedimentary structures and macrobenthic infaunal zonation, and (b) determine the correlation between zonation of biogenic sedimentary structures and different time horizons.

Correlation between extent of bioturbation structures and zonation of macrobenthic infauna in upper 25 cm of sediment.--The general term used for discussing biotic activity in sediments is bioturbation. The vertical distribution and variability of bioturbation in a core is determined by estimating the percent bioturbation relative to specific core intervals from X-ray radiographs of the cores. A diagrammatic representation of the degree of bioturbation for each core obtained is shown by column 3 in figures 48 to 58. In the cores, the degree of bioturbation by percent estimate was related to depth intervals: 0-25 cm; 25 to 75 cm; 75-125 cm; and greater than 125 cm.

For comparing the most recent zonation of biogenic sedimentary structures to macrobenthic infaunal zonation, a regional distribution map of bioturbation in the upper 25 cm of all the pipe cores was constructed (fig. 74). The map shows that the degree of bioturbation generally decreases seaward, and that surficial sediments of the ancestral deltas of the Brazos-Colorado and Rio Grande Rivers are characterized by relatively high bioturbation.

Comparison of the regional distribution patterns of macrobenthic infaunal zonation (fig. 70 and pl. 32) and the zonation of bioturbation in the upper 25 cm

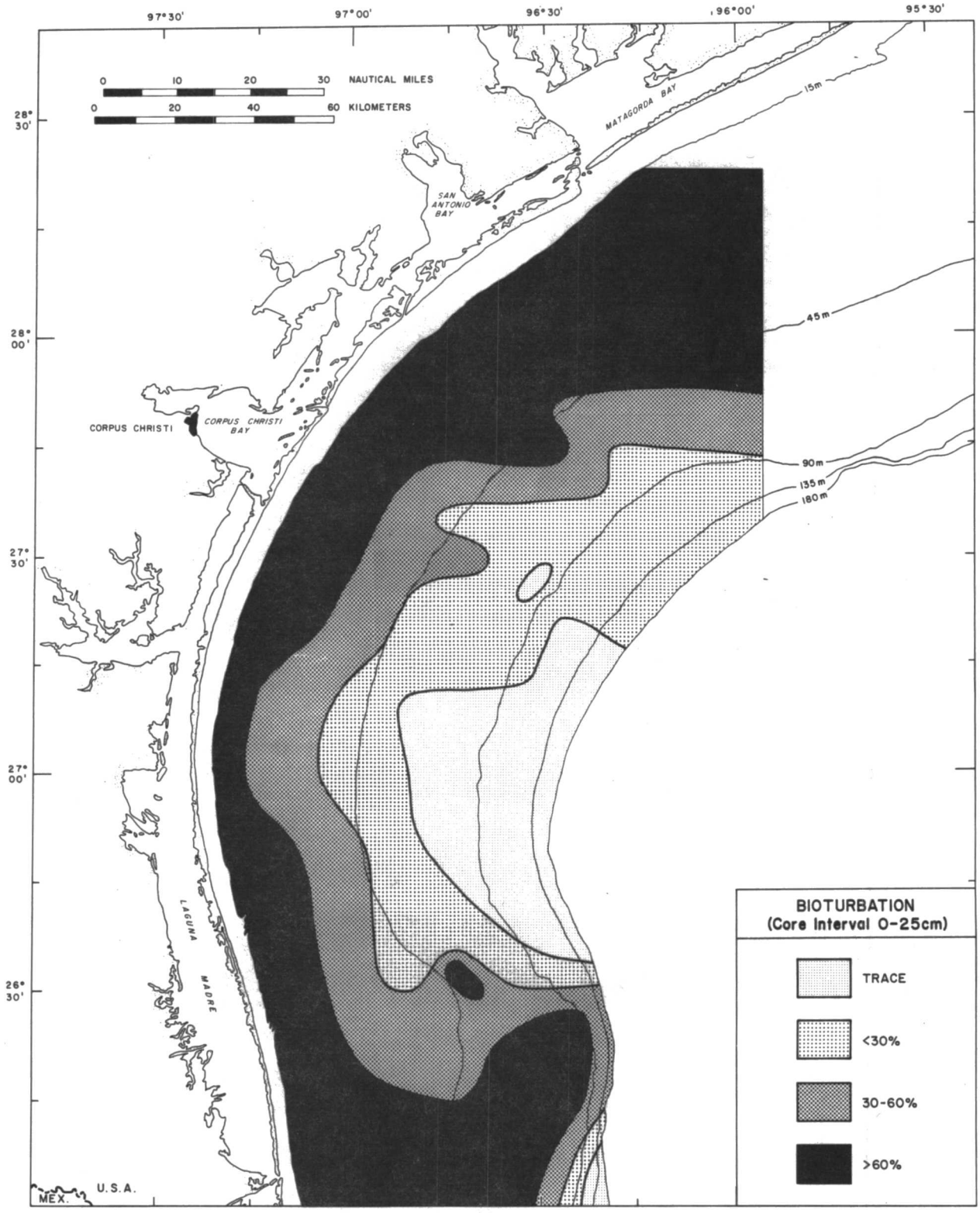

Figure 74. Areal extent and amount of bioturbation in upper 25 cm of pipe cores.

of sediment (fig. 74 and pl. 33) indicates a parallel relationship. Sediments with relatively high diversity and density of biogenic sedimentary structures are associated with the most diverse and dense macrobenthic infaunal assemblages.

Changes in extent of bioturbation with depth in the pipe cores.--The extent of bioturbation was mapped for the deeper core intervals, 25-75 cm, 75-125 cm and greater than 125 cm to determine if changes in the areal distribution of bioturbation have occurred through time (fig. 75 to fig. 77 and plates 34 to 36). The maps show that definite changes in the areal distribution of bioturbation have taken place during the time represented by the cores. Areas of greater than 60 percent bioturbation have increased significantly in size but areas of little evidence of biogenic activity have diminished. Although the extent of the various zones of bioturbation represented by the core intervals have varied, the general regional pattern indicated by the upper 25 cm has remained basically unchanged. Degree of magnitude of bioturbation generally decreases with increasing water depth, and the central sector of the South Texas OCS is characterized by low bioturbation.

Assuming that the parallel relationship between the degree of bioturbation and the most recent macrobenthic infaunal zonation is actual, the density of macrobenthic infauna generally has increased shelfwide during the time interval represented by the length of the pipe cores. It has been estimated that the "sediments obtained in the longer pipe cores would seem to represent an average of approximately 2000 to 2500 years of time" (p. 189, this report). The estimate, however, is tentative and subject to change after further study.

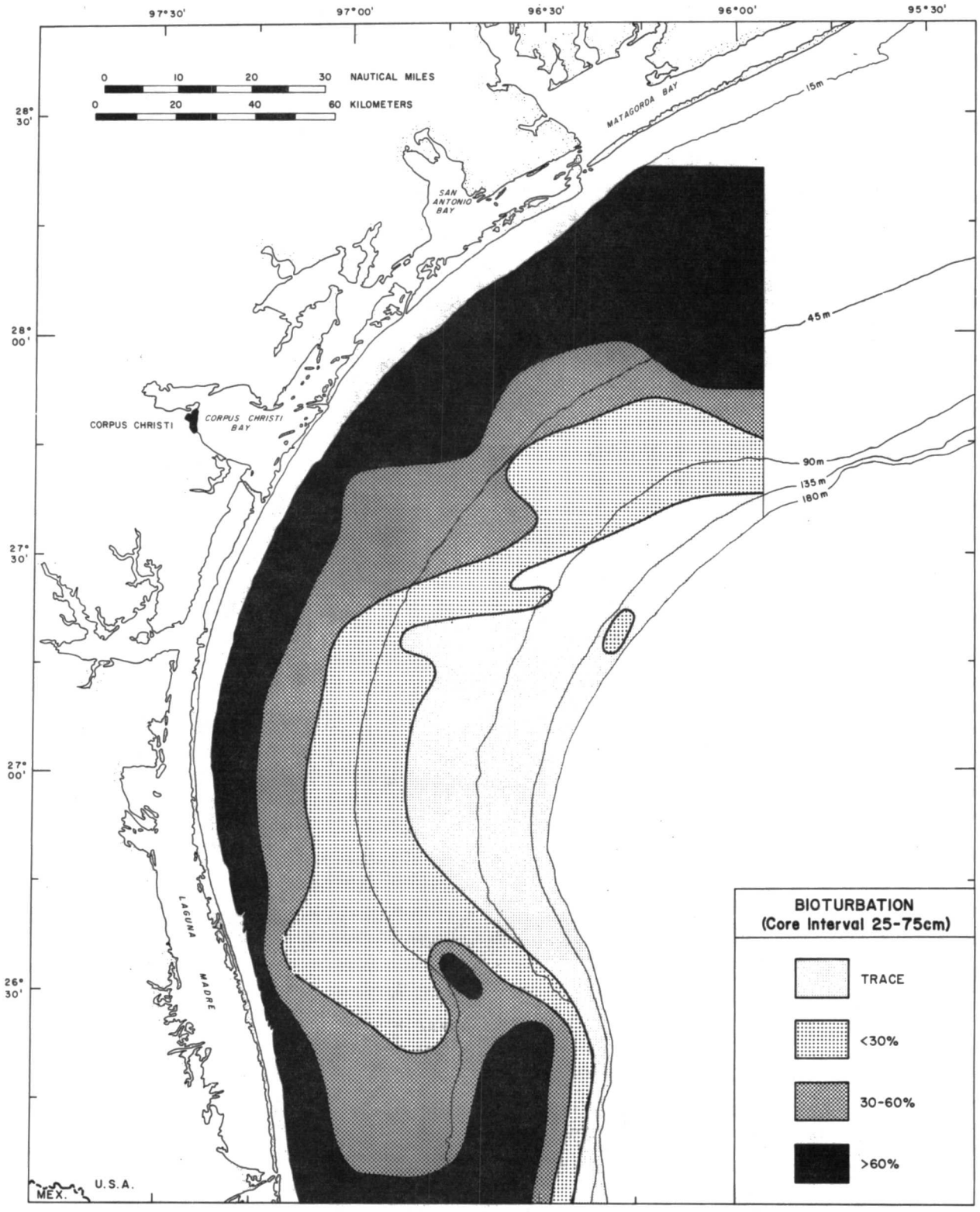

Figure 75. Areal extent and amount of bioturbation, pipe core interval 25 to 75 cm.

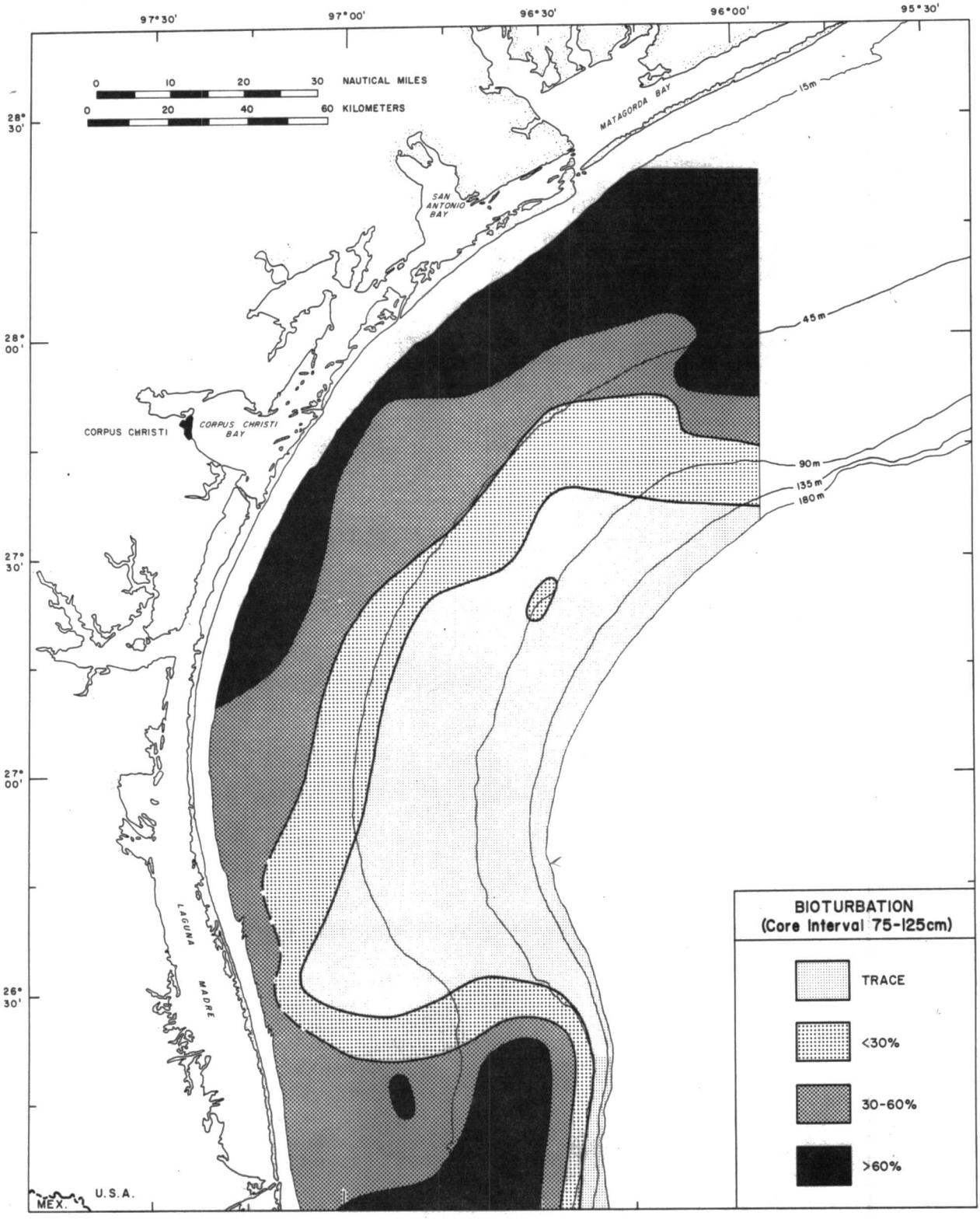

Figure 76. Areal extent and amount of bioturbation, pipe core interval 75 to 125 cm.

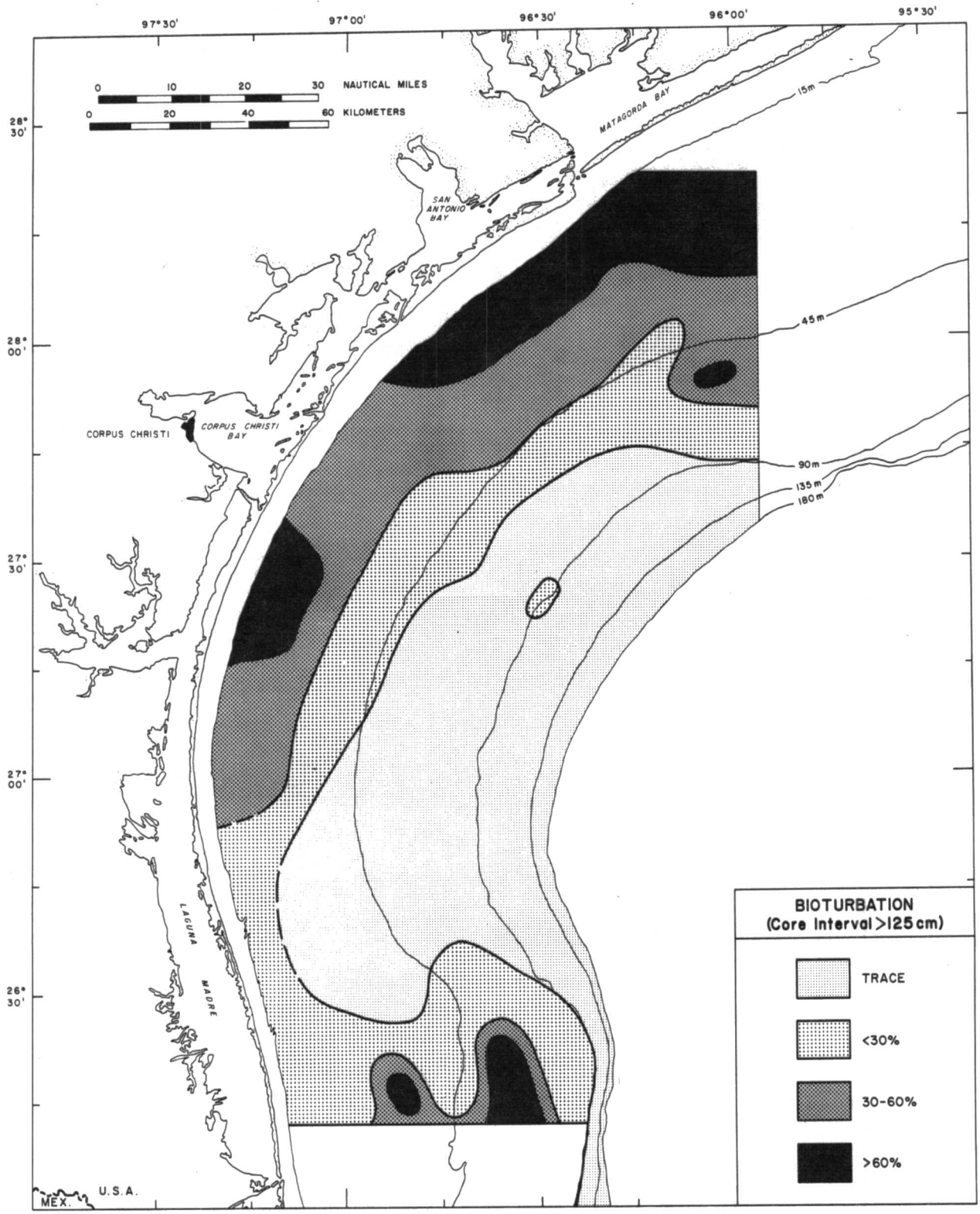

Figure 77. Areal extent and amount of bioturbation, pipe core depth >125 cm.

To more precisely define the correlation between zonation of bioturbation and macrobenthic infaunal zonation, correlation coefficients for bioturbation and various biologic and physical parameters were calculated (Tables 4 and 10). In making these calculations, the several classes of bioturbation based on percentage estimates were given an arbitrary value (trace = 1, < 30 percent = 2, 30-60 percent = 3, > 60 percent = 4). In the broadest perspective, the degree of bioturbation correlates best with water depth; as water depth increases, bioturbation decreases. When the physical and biological aspects determined are introduced into the regression analysis, the factors controlling the areal distribution of bioturbation are in order of relative importance: water depth, equitability, mean grain size, number of individuals, and the standard deviation of grain size. Regression analysis seems to indicate that the distribution of bioturbation is more dependent on physical aspects of the sediment than on biologic aspects. This is somewhat misleading, however, relative to the earlier assumption that trends in the regional distribution of bioturbation generally parallel trends in the distribution patterns of macrobenthic infauna. If the assumption is correct, there should be a correlation between the factors that influence bioturbation distribution and the factors that influence macrobenthic infaunal zonation.

Factors Controlling Macrobenthic Infaunal Zonation

By determining the factors that control macrobenthic infaunal zonation, spatiotemporal variations in biotic regional distribution patterns can be better understood. Although the study was not designed specifically to determine the factors that control macrobenthic infaunal zonation, the variety of environmental aspects measured in the overall investigation (sedimentological, biological, geochemical, etc.) can be assessed as to their impact on observed biotic zonation.

Table 10--Stepbackward regression analysis for bioturbation vs. biological and physical parameters

Dependent Variable	Independent Variable(s)	Multiple Correlation Coefficient
10	1, 2, 3, 4, 5, 6, 7, 8, 9	0.8975
10	1, 2, 4, 5, 6, 7, 8, 9	0.8975
10	1, 2, 5, 6, 7, 8, 9	0.8949
10	2, 5, 6, 7, 8, 9	0.8945
10	2, 5, 7, 8, 9	0.8930
10	2, 5, 7, 9	0.8873
10	5, 7, 9	0.8733
10	5, 9	0.8406
10	9	0.7710

1 - No. of species
2 - No. of individuals
3 - Biomass
4 - Diversity
5 - Equitability
6 - Sand-mud ratio
7 - Mean grain size
8 - Standard deviation
9 - Water depth
10 - Bioturbation

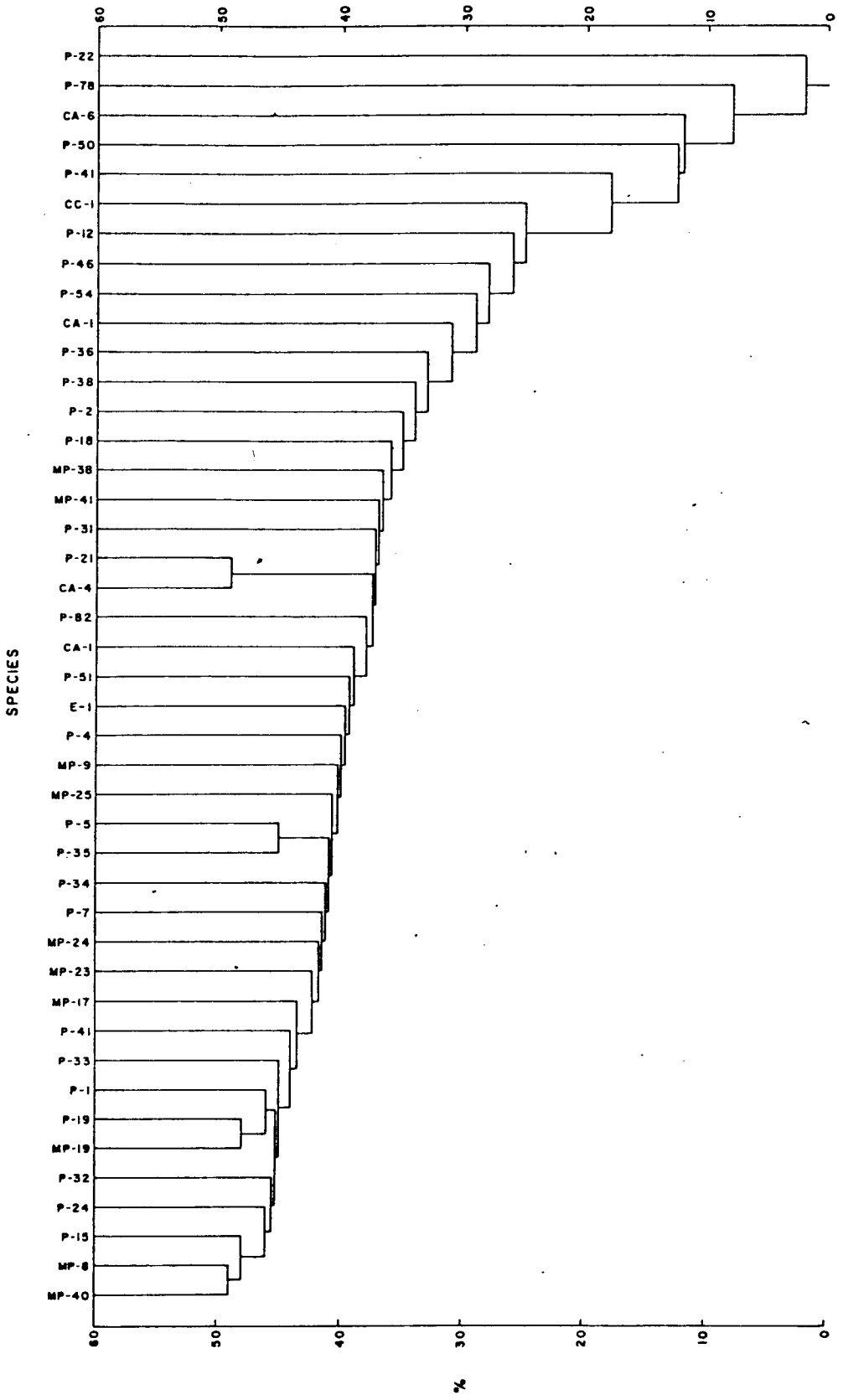

Figure 78. Dendogram showing levels of similarity between distribution patterns of species identified.

Table 11--Frequency distribution of Czekanowski's coefficient (percent occurrence) for R-mode analysis

Coefficient	Percent occurrence
0-10	25.1384
10-20	21,9269
20-30	31.5614
30-40	17.4972
40-50	3.8760
50-60	0.0000
60-70	0.0000
70-80	0.0000
80-90	0.0000
90-100	0.0000

Two general relationships are described with regard to their contributions in controlling macrobenthic infaunal zonation--interspecific relationships and biologic-geologic-hydrologic relationships.

Interspecific relationship

R-mode analysis was used to determine the average level of similarity between individual species relative to their areal distribution patterns. The results of the analyses are expressed in a hierarchial dendrogram (fig. 78). On a scale from 0-100, for similarity to identical areal distribution patterns, the Czekanowski's coefficient varied between 0 and 49.3691; the frequency distribution of the coefficients (percent occurrence) is shown in Table 11. Species not in at least 5 percent of the samples were not included in the analysis; consequently, only 43 macrobenthic infaunal species qualified for analysis.

Relative to controlling macrobenthic infaunal zonation, interspecific relationships seem to be an insignificant factor. No large or distinct grouping of species which could be specifically associated with particular assemblages could be determined from the analysis performed.

Biologic-geologic-hydrologic relationships

To determine if interrelationships existed between biological, geologic, or hydrologic parameters, a series of regression analyses were performed; the results are summarized in Table 4. Stepbackward regression analysis was used to determine multiple correlation coefficients between individual biological characteristics (i.e., dependent variable) and various combinations of physical parameters (i.e., independent variables); the results are listed in Table 12. The dependent variable included number of species, number of individuals, biomass,

diversity, and equitability; independent variables used were sand-mud ratios, mean grain size, standard deviation of grain size, and water depth.

Except for equitability, all biological parameters correlated best with sand-mud ratios. The correlations must be described as only fair, however, because the maximum variation determined was 48 percent. Equitability exhibited a poor correlation with mean grain size with only 18 percent of the variation explained. As additional factors were introduced into the analysis, no significant increase in the percentage of variation explained was evident (Table 12).

Because of the correlation values shown in Tables 4 and 14, the average values for biological parameters were calculated relative to various classes of sand-mud ratios (Table 13). Generally, the number of species and individuals, biomass, and diversity increase with increasing sand-mud ratios. The most significant increase occurred where sand-mud ratios exceed 2.00. In contrast, equitability generally decreased as sand-mud ratios increased with the most significant decrease occurring in sand-mud ratios greater than 2.00.

Visual observation suggests a definite relationship between macrobenthic infaunal zonation and water depth (fig. 70). The observation is supported further when average biological parameters are calculated relative to various classes of water depth (Table 14). As water depth increases to about 120 m, number of species and individuals, biomass, and diversity generally decrease and equitability increases. At about the 120 m isobath, however, a reversal in general trends occurs with the biological parameters increasing, except for biomass which continues to decrease. The reversal in general trends of areal distribution of biological characteristics at about the 120 m isobath is probably the cause for the low correlation coefficients between water depth and the various biological parameters (Table 4).

Table 12--Stepbackward regression analysis for biological parameters vs. physical parameters

Dependent Variable	Independent Variable(s)	Multiple Correlation Coefficient
1	6, 7, 8, 9	0.7111
1	6, 7, 9	0.7099
1	6, 9	0.7002
1	6	0.6914
2	6, 7, 8, 9	0.6233
2	6, 7, 9	0.6229
2	6, 9	0.5903
2	6	0.5673
3	6, 7, 8, 9	0.6563
3	6, 7, 9	0.6518
3	6, 7	0.6046
3	6	0.5912
4	6, 7, 8, 9	0.5182
4	6, 8, 9	0.5167
4	6, 9	0.5155
4	6	0.5128
5	6, 7, 8, 9	0.4976
5	6, 8, 9	0.4933
5	8, 9	0.4866
5	9	0.4301

Variables

1 - No. of species
2 - No. of individuals
3 - Biomass
4 - Diversity
5 - Equitability
6 - Sand-Mud ratio
7 - Mean grain size
8 - Standard deviation
9 - Water depth

Table 13--Some biological parameters of the South Texas OCS relative to sand-mud ratios (macrobenthic infauna per 0.09 m^3)

Parameters	Sand-Mud Ratios					
	0.12	0.13-0.25	0.26-0.50	0.51-1.00	1.01-2.00	2.00
No. of samples	45	8	8	7	6	6
Average no. of species	8	10	13	14	11	28
Average no. of individuals	24	43	36	37	27	156
Average biomass (g)	0.18	0.22	0.30	0.37	0.28	1.48
Average diversity (H")	1.64	1.70	2.22	2.08	2.12	2.69
Average equitability	0.60	0.48	0.49	0.44	0.59	0.37

Table 14--Some biological parameters of the South Texas OCS relative to water depth (macrobenthic infauna per 0.09 m^3)

Parameters	Water Depth (m)				
	0-40	41-80	81-120	121-160	161-220
No. of samples	33	29	10	5	6
Average no. of species	14	8	6	9	8
Average no. of individuals	61	24	14	5	15
Average biomass (g)	0.48	0.22	0.20	0.1	0.1
Average diversity (H")	1.85	1.84	1.68	1.90	1.68
Average equitability	0.43	0.63	0.71	0.59	0.60

Knowing something of the factors controlling zonation is important in classifying the assemblages observed. Depending on the slope of environmental gradients and complexity of the communities involved, communities have been generally classified in other studies as discrete, discontinuous units or continuous gradations of one species assemblage into another (e.g., Gleason, 1939; Mills, 1969). When environmental parameters are gradational, communities tend to be gradational as well (Beals, 1969). On the continental shelf, where parameters such as temperature, salinity, light, etc., tend to vary in a continuous fashion, benthic communities on clastic substrates tend to be continuous and intergrading (Sanders and Hessler, 1969).

Another factor in classifying assemblages is the ecological complexity of the community. Communities characterized by low species diversity and fluctuation in composition under the direct impact of the physical environment are classified as immature or low grade; those characterized by high diversity and a relatively constant composition are mature or high grade communities (Margalef, 1957). Sanders (1968) classifies or grades communities in a similar fashion to Margalef. His concepts are physically controlled (i.e. low grade) and biologically accommodated communities (i.e. high grade). Biologically accommodated communities evolve when physiological stresses are low for long periods of time. As physiological stress increases because of an increase in fluctuating or unfavorable physical conditions, a gradual change in the community takes place from a predominantly biologically accommodated community to a predominantly physically controlled community. In these classifications, assemblages with high interspecific relationships are termed high grade or biologically accommodated while low interspecific relationships imply low grade or physically controlled.

Assemblages on the South Texas OCS are classified as continuous, low grade and physically controlled. This classification agrees with Johnson (1972) who views the nature of shallow water marine benthic communities to be "low-grade communities, largely controlled by the physical environment."

RATE OF DEPOSITION

Rates of sediment deposition for uppermost Holocene sediments on the South Texas OCS have not been documented on a site specific basis for the shelf as a whole. However, two bits of evidence do give some indication of depositional rates in general terms.

A single large articulate specimen of the bivalve mollusc Agriopoma texasiana was obtained in the pipe core at station 127, 21 cm below the water/sediment interface. See figure 53, station #127 for position in the core. The living habitat of the mollusc is in silty mud 4-8 cm below the water/sediment interface in water depths of 8-30 m. The specimen was examined in the core by a biologist and he stated it appeared to have died in the growth position and was not subsequently transported. The radiocarbon date for the specimen is 180 years BP. Assuming that its position below the water/sediment interface while alive was 6 cm, the average rate at which sediment has accumulated over it at site 127 is slightly less than 0.1 cm/yr. Projected over a longer time frame, 0.1 cm/yr would indicate approximately a meter of sediment accumulation per 1000 years at station 127, if the same depositional conditions were maintained.

For the South Texas OCS as a whole the indicated thickness of the total Holocene sequence, as revealed by high resolution seismic reflection profiles, ranges from a few meters to about 48 m locally. The average thickness is about 18 m. The radiocarbon (C^{14}) date of rock from Southern Reef (fig. 16) whose upper part is exposed on the outer part of the shelf is 18,900 years BP $\pm$330 years. (Age determination made by Teledyne Isotopes, Westwood Laboratories). If the average thickness of the Holocene sequence is 18 m, then the indicated average rate of sediment accumulation across the South Texas OCS over the past 18,000-19,000 years has been approximately one meter per 1000 years, or about

the same rate as indicated at site 127. Thus, the sediments obtained in the longer pipe cores would seem to represent an average of approximately 2,000 to 2,500 years. Even, assuming that the reef might be somewhat older than 19,000 years and the rate of deposition somewhat less than one meter per thousand years, the continental shelf off south Texas can be classified as an area of relatively high sediment accumulation during Holocene time.

GEOCHEMISTRY: ORGANIC CARBON, CARBONATE AND TRACE METALS CONTENT OF SURFICIAL SEDIMENTS

Analytical Procedures and Techniques

Organic carbon and carbonate--In the laboratory the 263 subsamples for organic carbon and carbonate analyses were thawed and removed from the plastic tubes. The samples were homogenized, air dried, ground to fine powder and then analyzed for the organic carbon and carbonate content by the method described by Kolpak and Bell (1968). The method for carbonate is as follows: from 0.2 to 1.0 grams of sample material is placed in a digestion tube and 2 ml of 5 percent $FeSO_4$ added. After the system is closed to the atmosphere, 3 ml of 2NHCl are introduced into the digestion tube by gravity feed and O_2 pressurized with a flow rate of 0.5 liters/min. Heat is applied to the digestion tube after effervescence ceases to assure complete digestion. When digestion is complete, the O_2 pressure is increased to 1.0 liter/min to sweep the evolved CO_2 into the buret of a Leco® carbon analyzer.

All gases leaving the digestion assembly are passed through a concentrated H_2SO_4 scrubber to eliminate any water vapor; through a MNO_z trap to remove any SO_2 present; and then through a catalyst furnace to convert CO to CO_2. Only the CO_2, from the digested sample, and excess O_2, used to completely sweep the digestion assembly and purifying train, enter the buret and replace a non-absorbing solution of approximately 0.6N H_2SO_4. Methyl red is added to the solution to facilitate leveling and reading. The gas mixture is passed from the buret by O_2 pressure into the absorption vessel containing 9N KOH where the CO_2 is absorbed in approximately one minute. A release of the pressure allows the remaining O_2 to be returned to the original buret, and the H_2SO_4 solution is then adjusted to atmospheric pressure. Inasmuch as the height of the liquid column above zero is equal to the volume of the absorbed CO_2, the

percentage carbon per gram of sample can be read from the calibrated buret of the Leco® carbon analyzer. The final corrected value is then converted to percent carbonate by the factor of 8.33, which related the carbon value to $CaCO_3$.

Organic carbon was determined by measuring the total carbon minus the carbonate carbon. The procedure for determining the total carbon is as follows: a sample, ranging from 0.2 to 1.0 grams is weighed and placed in a carbon-free ceramic crucible and placed in an induction furnace through which purified O_2 is passed. An iron chip accelerator and a tin-coated copper metal accelerator to start oxidation at a lower temperature are added. The sample is quickly combusted at 1500 C so that all the carbon is converted to CO_2 in approximately one minute. Any sulfur present is converted to SO_2, whereas, iron, copper, silica and associated elements remain as solid oxides. Most solid oxides are retained in the crucible but some particles are carried along by the O_2 stream until trapped by a dust trap. The SO_2 is absorbed in a MNO_2 trap. Beyond this point the CO_2 and O_2 enter the calibrated buret. The remaining procedures are identical to those previously described for the $CaCO_3$ procedure.

The samples were run in triplicate with an average variation of less than 5 percent for both Ca and CO3.

Trace metals--The concentration of trace metals in the sediment samples were determined by atomic absorption techniques. Triplicate subsamples from all 263 samples were run; more than three runs were made on randomly selected subsamples. The procedure of analysis is as follows: in the laboratory, the entire sample was removed from the sampling container, placed in a porcelain dish, mixed and dried at 100°C under infrared lamps. The sample was then removed and ground in a porcelain mortar to pass through a 200 mesh Spex® nylon screen. After homogenization, three subsamples were extracted,

placed in a crucible and heated to 450°C for four hours to ash the organic component of the sample. The sample was then reweighed and transferred to an acid-washed culture tube and leached with concentrated nitric acid at 105°C until oxidation ceased. This method was used for all elements except barium. Barium was brought into solution by a 1:1 mixture of concentrated nitric acid and 30 percent peroxide. The resultant solution was then analyzed by atomic absorption spectrophotometer. Table 15 gives the parameters used in the analysis of the metals.

Table 15--Instrument Parameters and Mode of Analysis

[303PE with an HG2100 Graphite Furnace]

Element	Wave Length	Dilution	Mode	Dry Temp.	Ashing Temp.	Atom. Temp.
Ba	2776	1:20(1:200)	Flameless	100°C	1200°C	2700°C
Cd	2293	1:10	Flameless	100°C	250°C	2100°C
Cu	3262	1:10	Flameless	100°C	900°C	2700°C
Cr	3589	1:100	Flameless	100°C	1200°C	2700°C
Fe	2483	1:1000	Flame	--	--	--
Mn	2801	1:1000	Flame	--	--	--
Ni	2330	1:10	Flameless	100°C	1200°C	2500°C
Pb	2842	1:10	Flameless	100°C	550°C	2000°C
V	3194	1:10	Flameless	100°C	1700°C	2700°C
Zn	2146	1:100	Flame	--	--	--

A measure of analytical precision was obtained by statistical analysis of the results of the triplicate analyses. As these results were obtained from the concurrent "runs", they are a measure of sample homogeneity and reproducibility of the instruments and operator. A further measure of analytical accuracy was obtained by statistical analysis of all "runs" run more than three times. As these were obtained from different "runs", often weeks apart and by different analysts, the approach is a measure of the "accuracy" of the method. The results are summarized in Table 16.

Table 16--Percent deviation from the mean value of trace metal analyses

[Data reported as percent deviation from mean value.]

Element	Analyses in triplicate		Analyses run more than three times	
	Mean	Standard Deviation	Mean	Standard Deviation
Ba	--	--	7.22	5.39
Cd	8.11	6.76	21.63	12.40
Cu	5.64	4.67	11.74	8.18
Cr	7.32	5.10	14.61	6.32
Fe	4.87	4.10	11.91	6.78
Mn	2.08	2.40	9.21	6.08
Ni	4.70	3.87	15.91	7.93
Pb	5.19	4.26	13.36	8.06
V	8.88	5.62	15.80	5.65
Zn	4.03	3.27	10.68	5.19
Average	5.64		13.86	

Amount and Distribution

Organic Carbon

The organic carbon content of the shelf sediments ranges from 0.2 percent to 1.2 percent. The distribution of organic carbon over the shelf is shown by figure 79 and plate 37. The pattern of distribution shows that the values for carbon are highest along the outer part of the shelf and lowest in the extreme northern and southern parts. Relatively high values also extend southward as a salient from Matagorda Bay. The range in values for carbon and its distribution seems to be attributable primarily to a combination of two factors: an area of gas seeps on the outer shelf and the grain size of the bottom sediments. The sediment may trap and retain small amounts of organic carbon during seepage. The fine grained sediments of the outer shelf, high in clay content and less subject to winnowing and aeration by rapidly moving water,

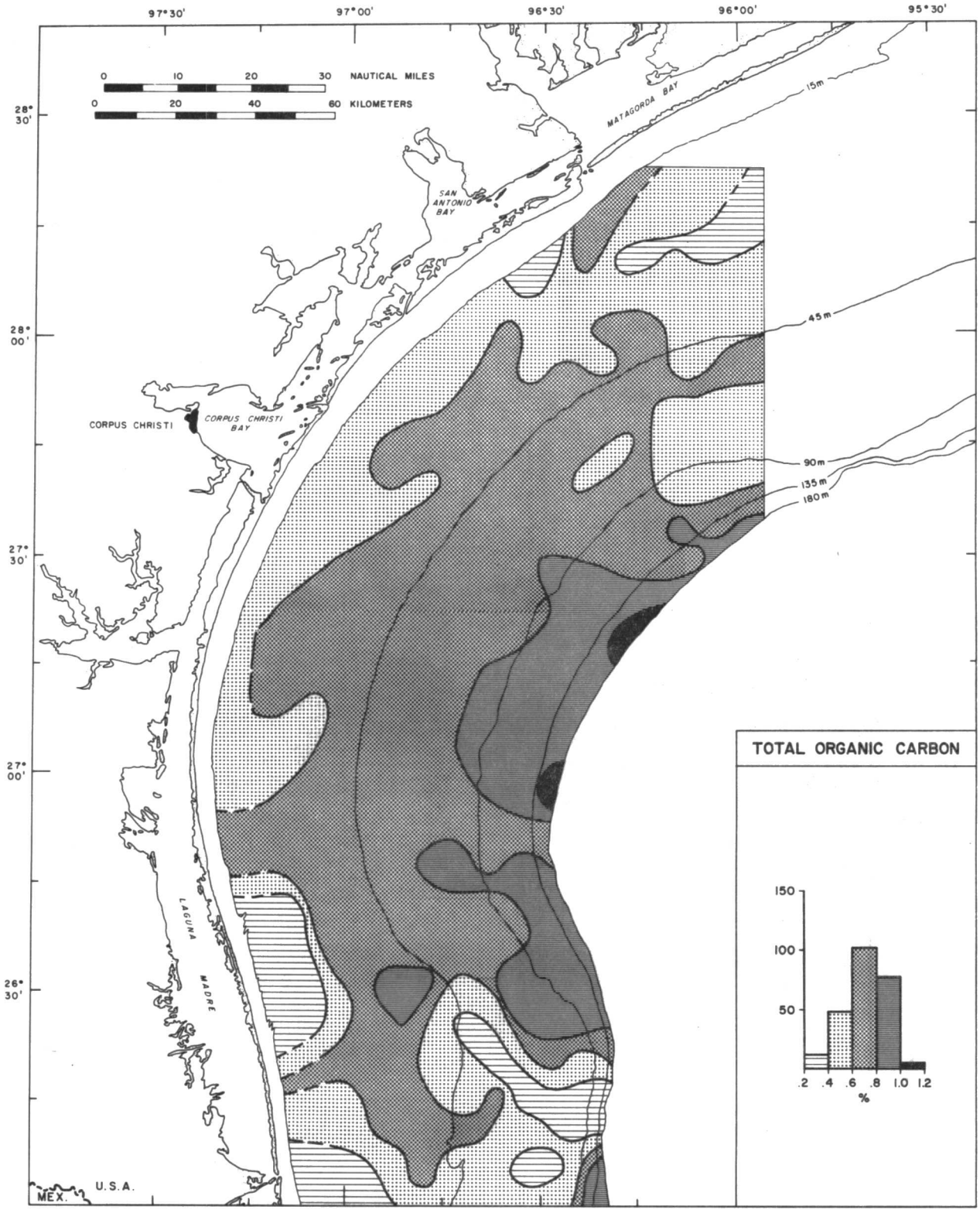

Figure 79. Distribution of organic carbon in percent. Histogram shows number of samples versus concentration.

hold and retain a higher percentage of entrapped organic carbon. Another probable factor explaining the higher amount of organic carbon on the outer shelf is the high concentration of planktonic foraminifera in sediments on the outer part of the shelf. For relating the percentages for organic carbon to the gas seeps, compare figure 79 and figure 27; to relate amount of organic carbon to sediment grain size, compare figure 79 and figures 30 and 31.

Carbonate

The carbonate content of the sediment ranges from less than one percent to 100 percent on the carbonate reefs (fig. 80 and pl. 38). For sediment not in the immediate vicinity of the reefs, the maximum carbonate content was 13.81 percent. Regionally, the carbonate content of the sediment is highest in two widely separated parts of the shelf: one on the northeasternmost outer edge and the other to the southwest on the inner shelf. Percentages are generally lowest in the north-northwest part of the OCS.

The carbonate in the northeastern area is made up almost entirely of planktonic forams which are abundant in the sediment, whereas, the carbonate in the southwestern area is made up of shell debris apparently associated with the ancestral Rio Grande delta.

Trace Metals

The amounts of the 10 trace metals analyzed are tabulated in Table IV, Part II. Amounts and distribution are discussed separately for each element. Maps showing the distribution in μg/g have been prepared for each trace metal and include a histogram of sample frequency versus concentration (figs. 81 to 90, Pls. 39 to 48). A statistical summary of all the trace metals analyses is shown by Table 17.

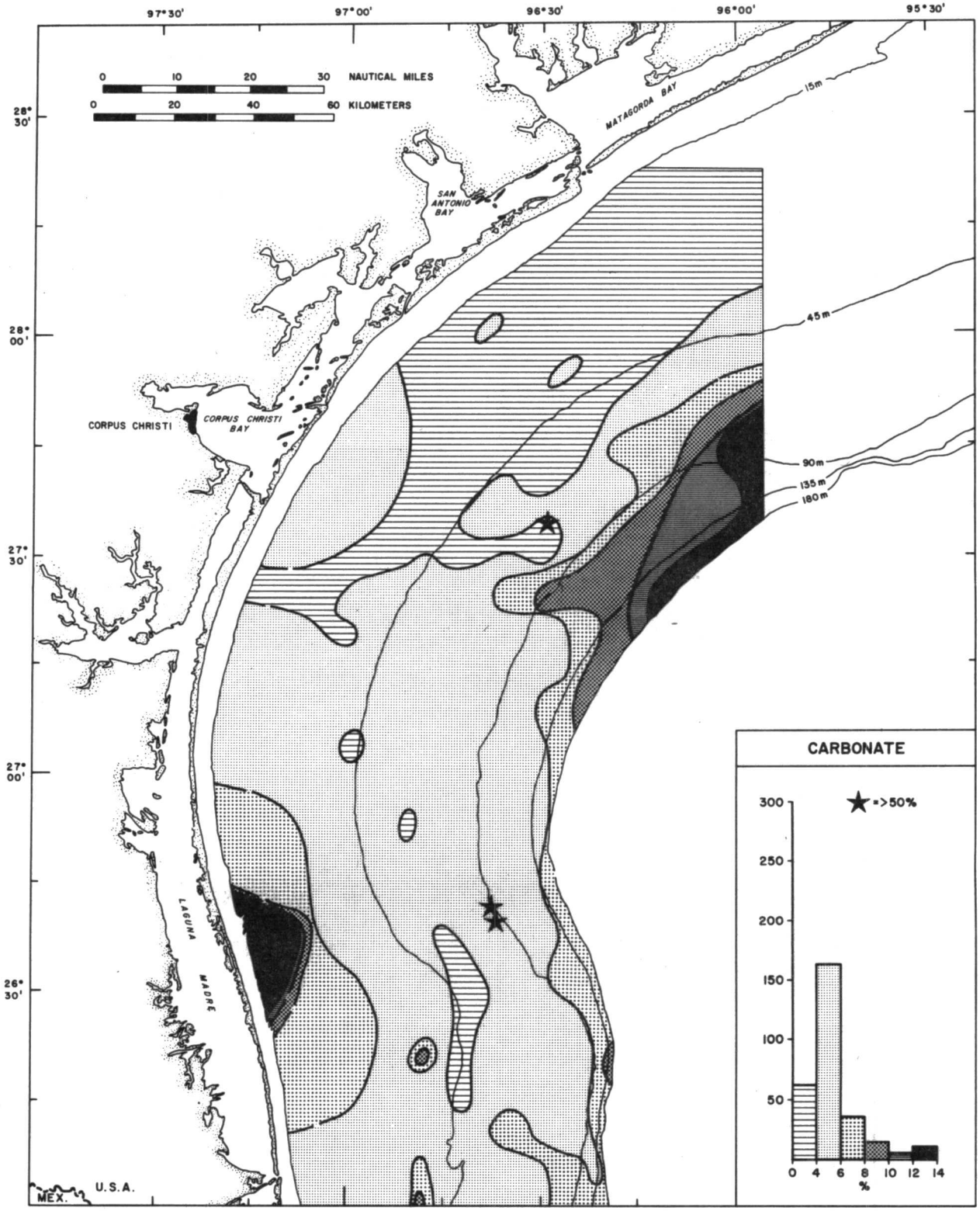

Figure 80. Distribution of carbonate in percent. Histogram shows number of samples versus concentrations.

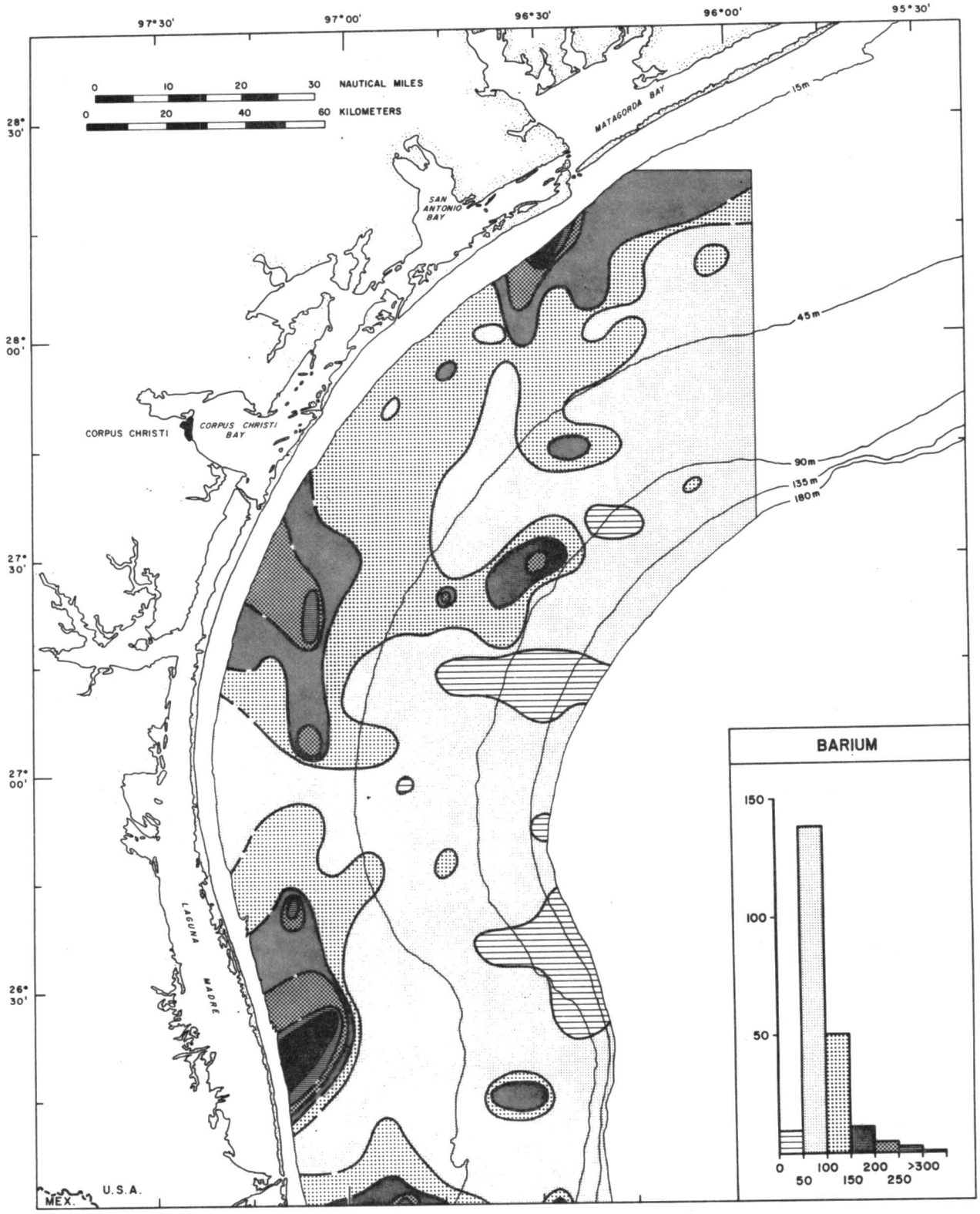

Figure 81. Distribution of barium in ug/g. Histogram shows number of samples versus concentration.

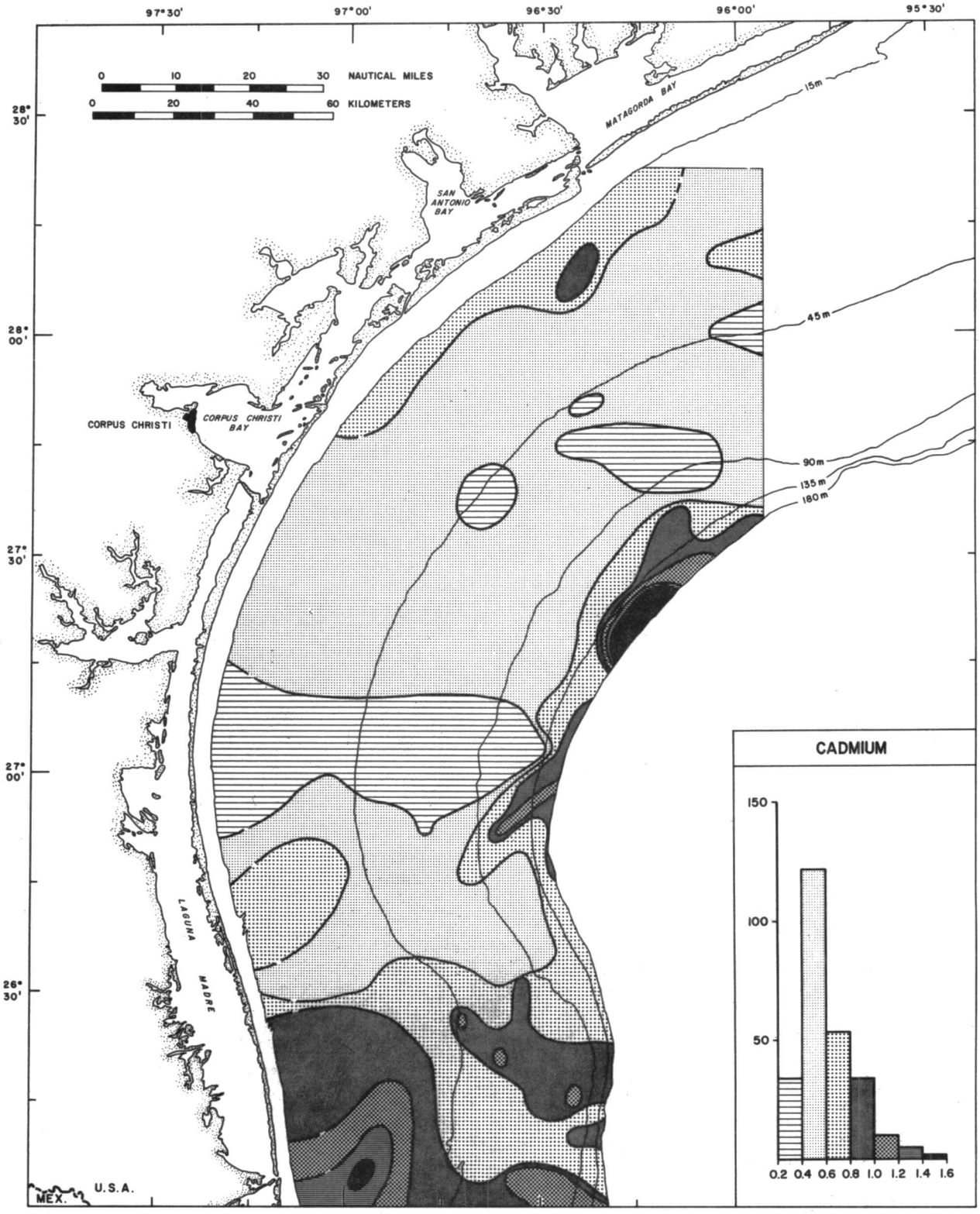

Figure 82. Distribution of cadmium in ug/g. Histogram shows number of samples versus concentration.

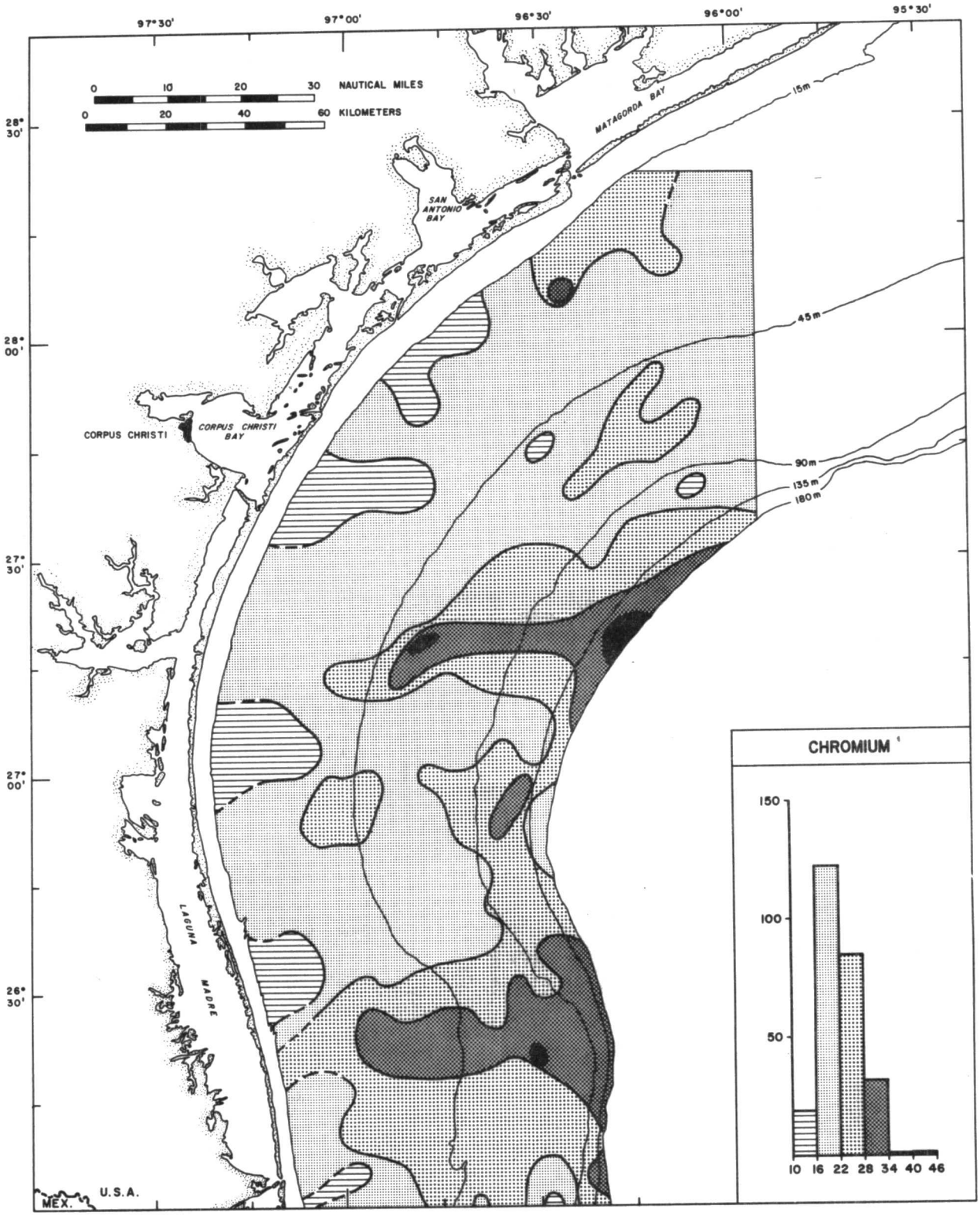

Figure 83. Distribution of chromium in ug/g. Histogram shows number of samples versus concentration.

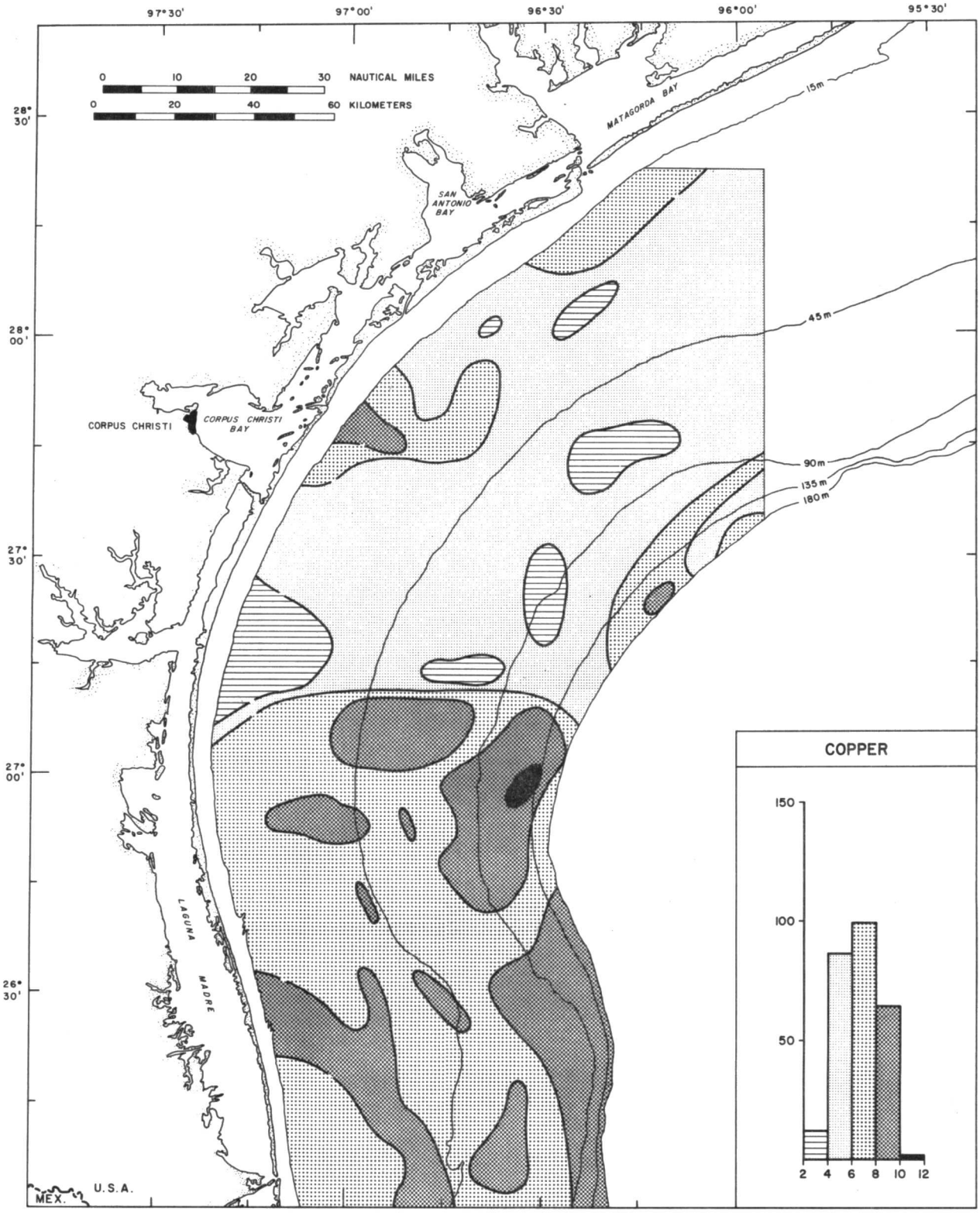

Figure 84. Distribution of copper in ug/g. Histogram shows number of samples versus concentration.

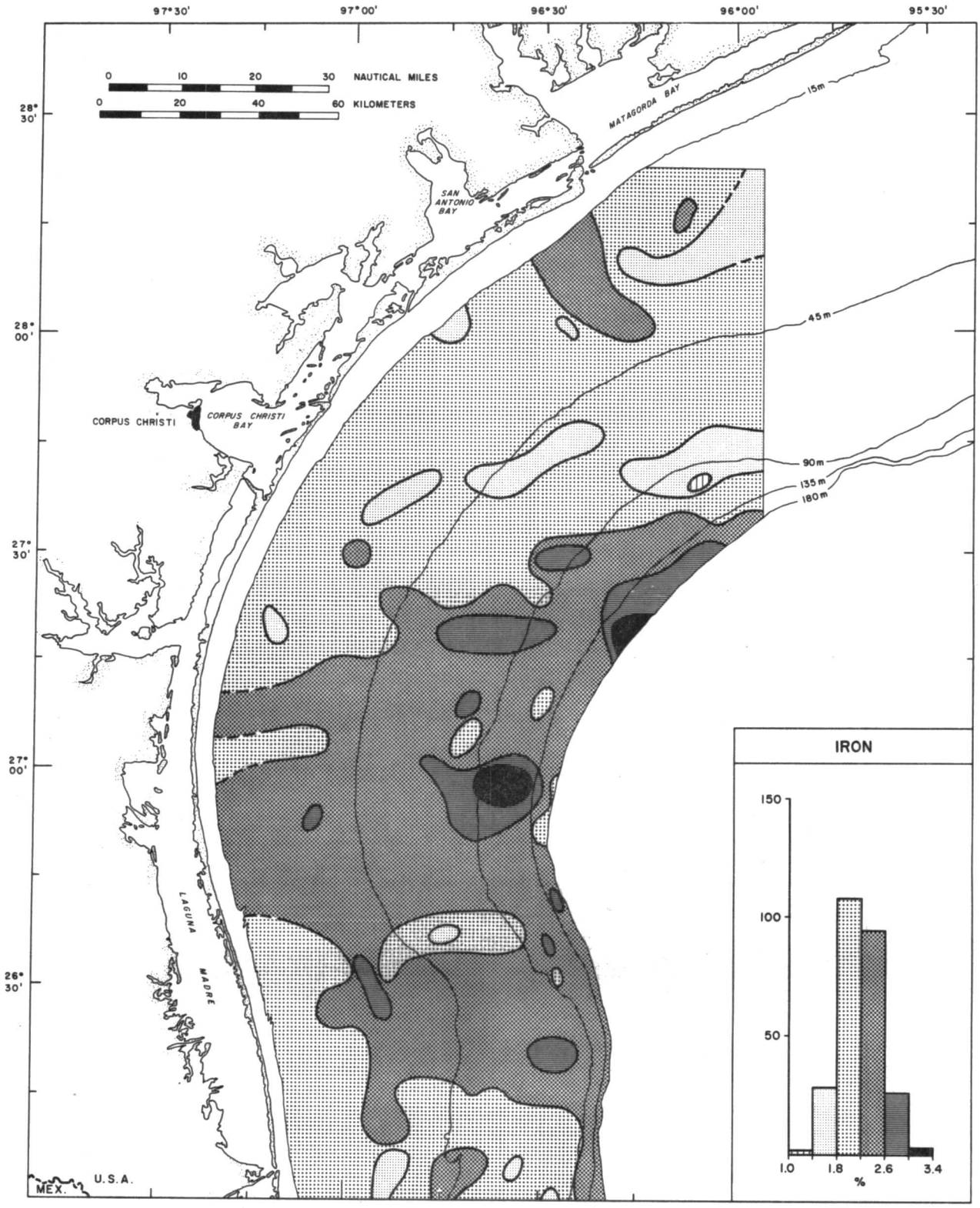

Figure 85. Distribution of iron in percent. Histogram shows number of samples versus concentration.

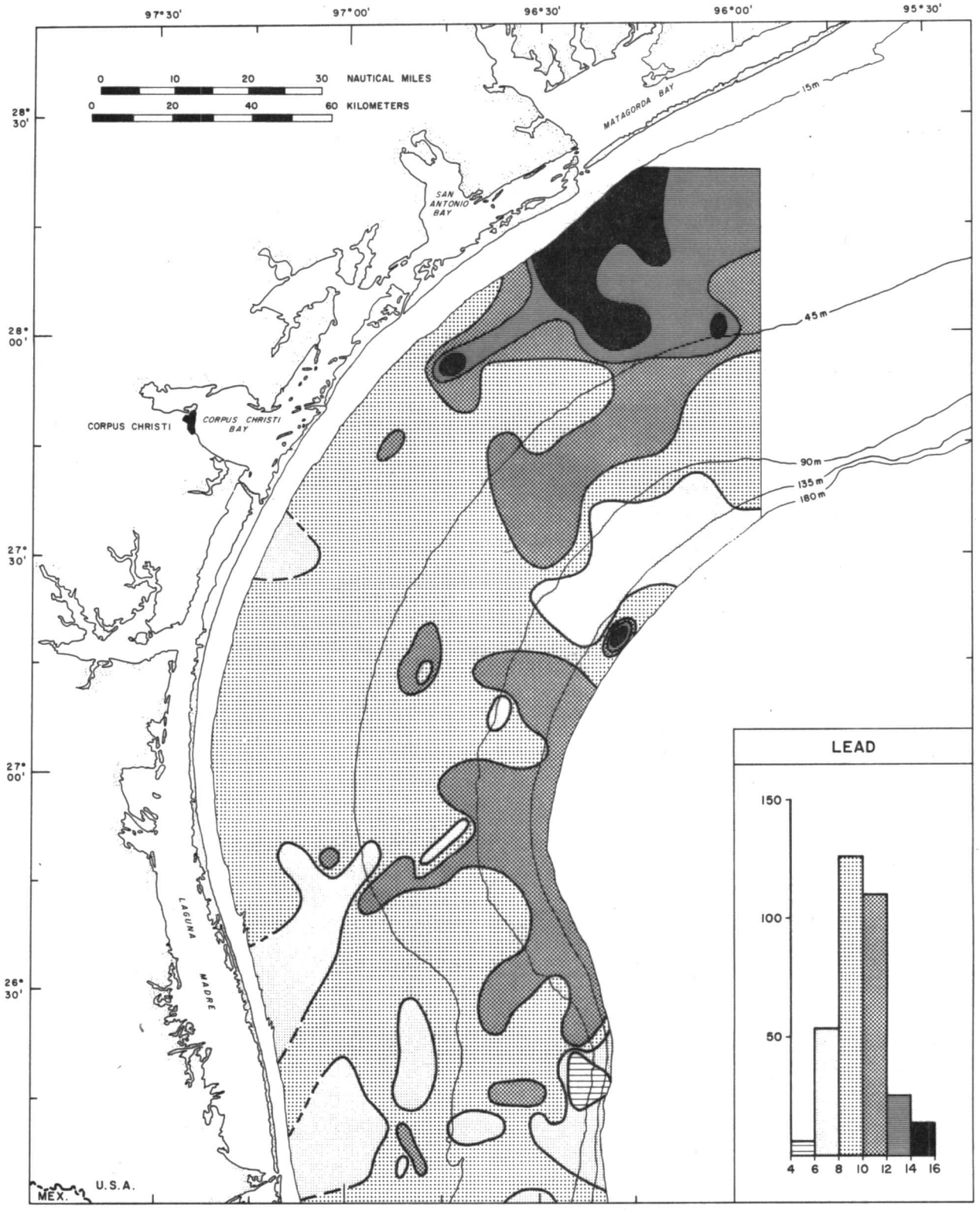

Figure 86. Distribution of lead in ug/g. Histogram shows number of samples versus concentration.

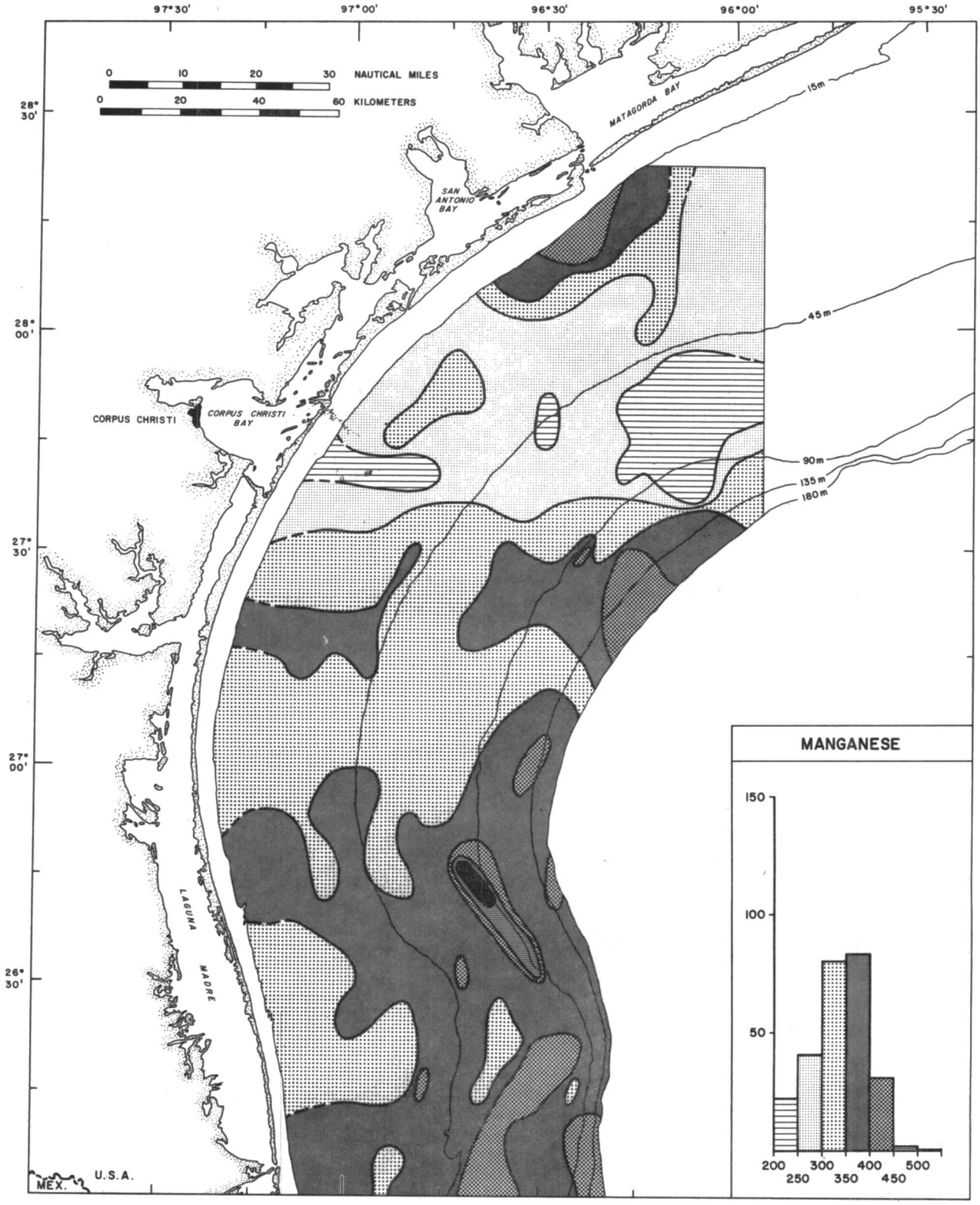

Figure 87. Distribution of manganese in ug/g. Histogram shows number of samples versus concentration.

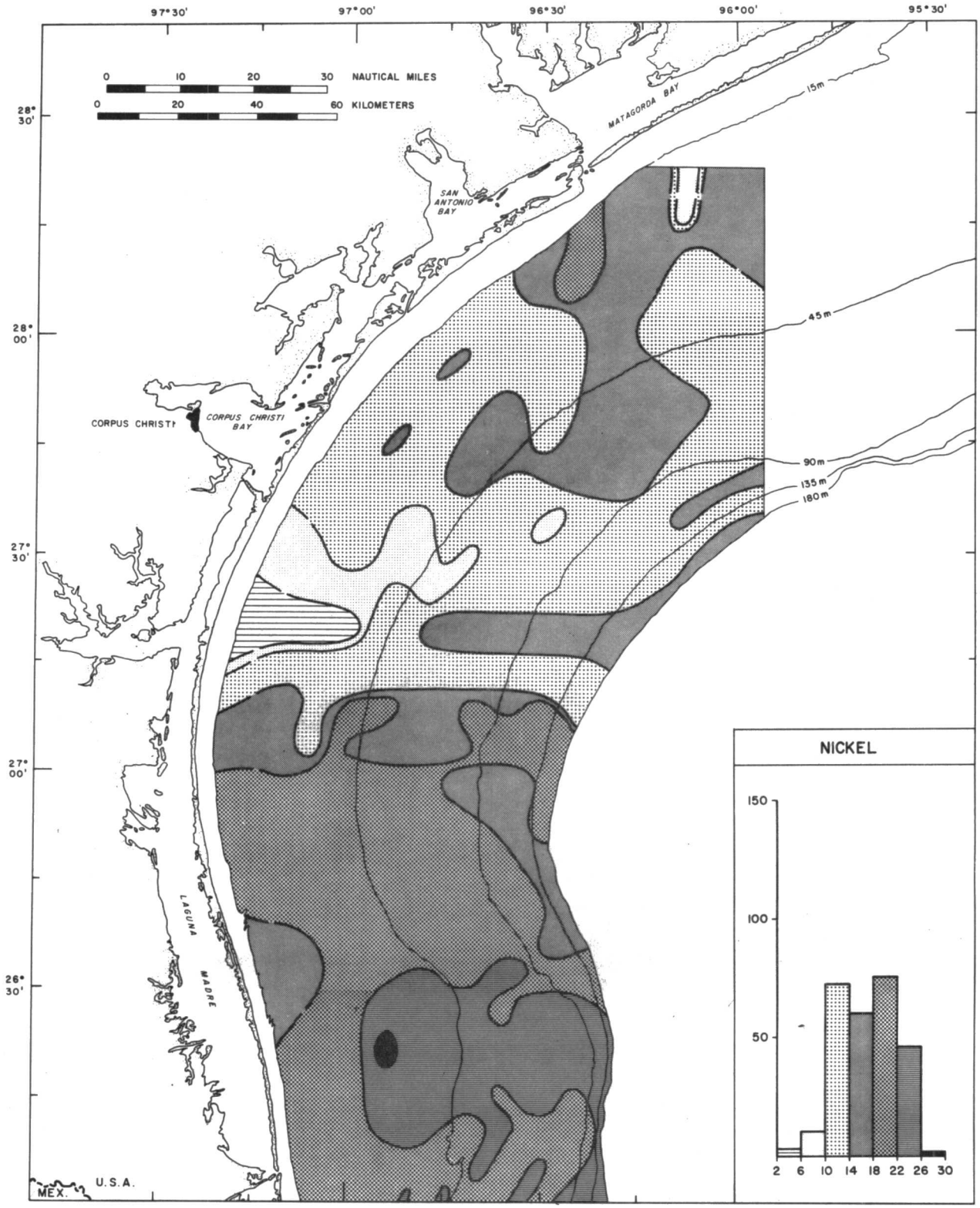

Figure 88. Distribution of nickel in ug/g. Histogram shows number of samples versus concentration.

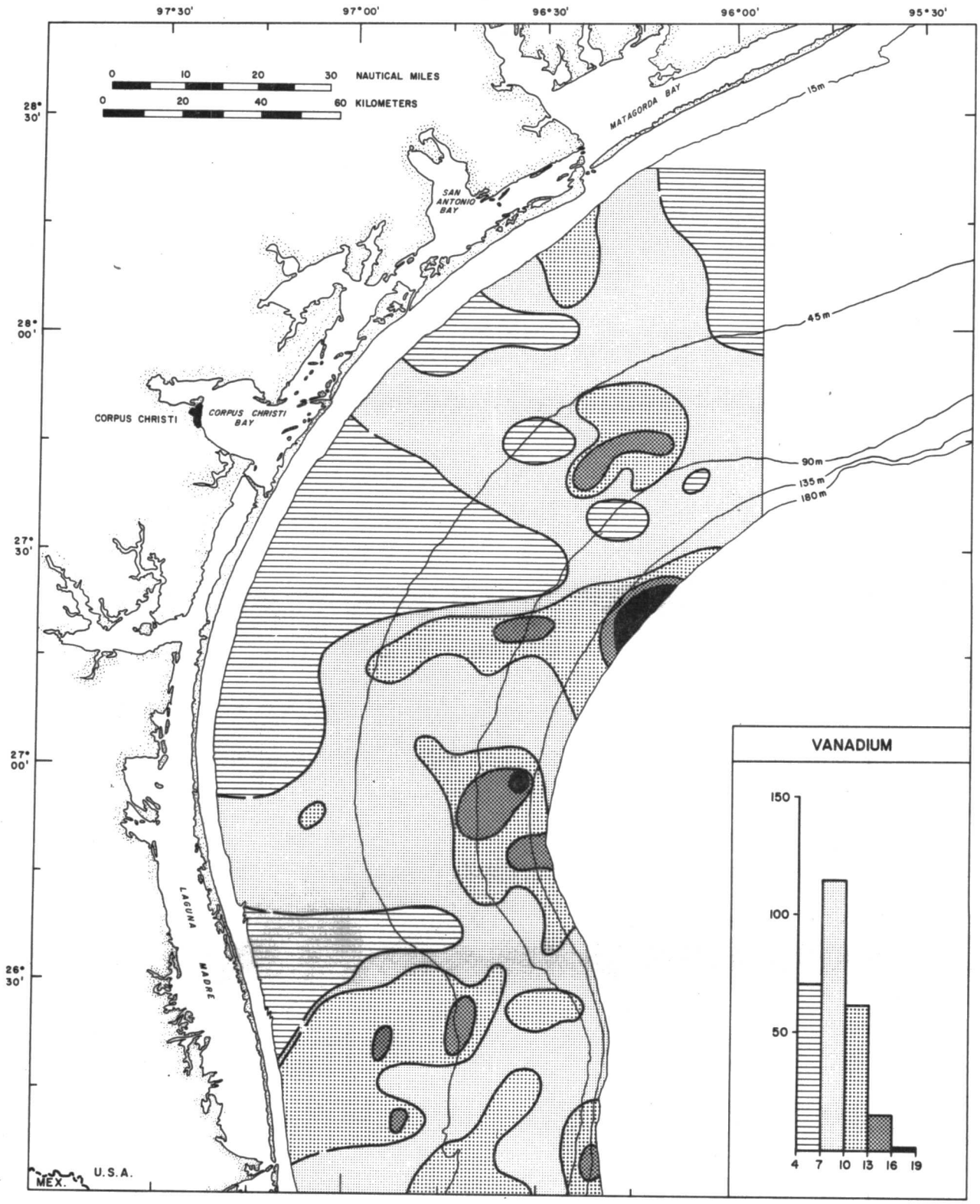

Figure 89. Distribution of vanadium in ug/g. Histogram shows number of samples versus concentration.

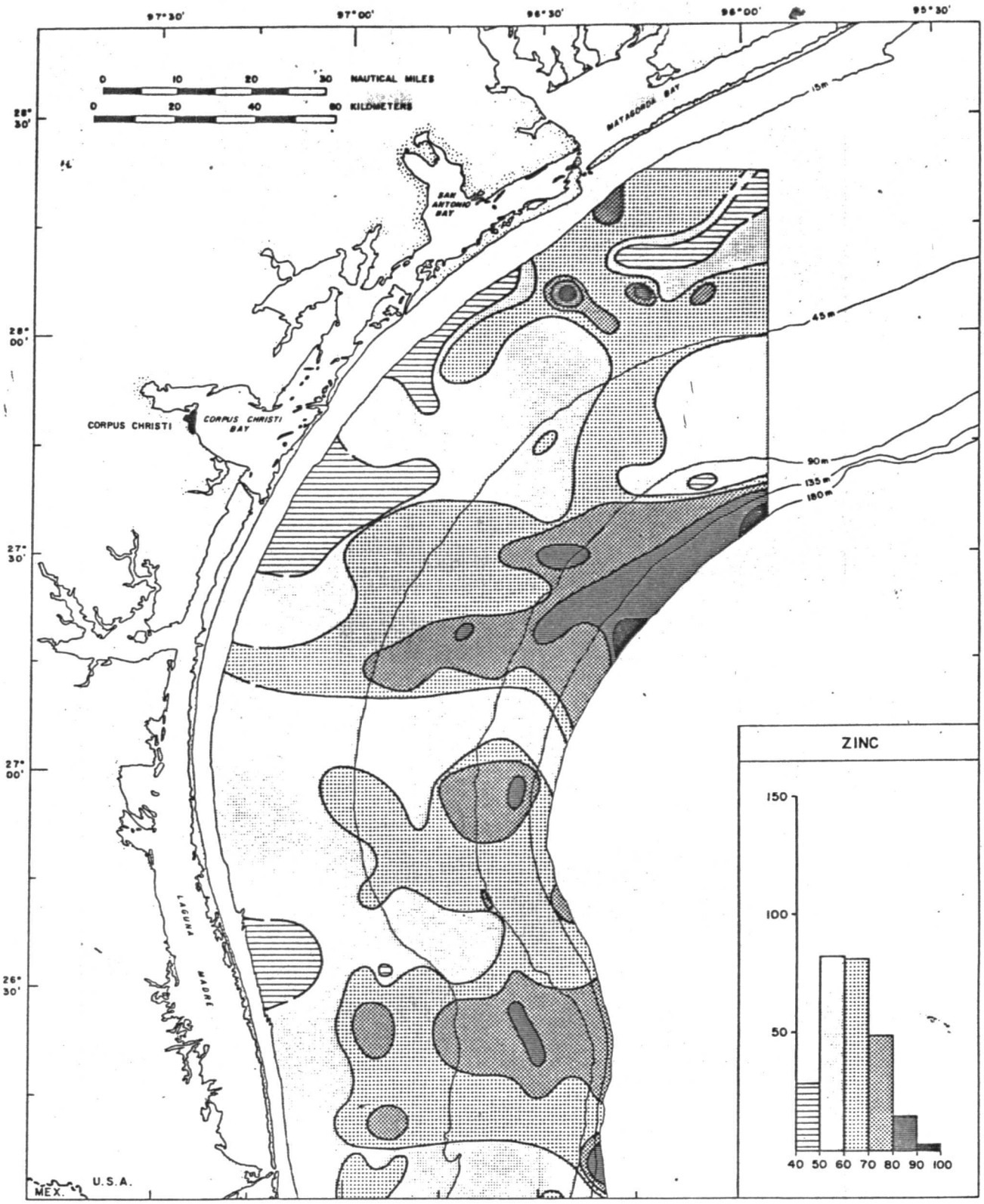

Figure 90. Distribution of zinc in µg/g. Histogram shows number of samples versus concentration.

Table 17--Statistical summary of the ten trace metals analyses

[Data in ug/g(ppm)]

Element	Mean	Standard Deviation
Ba	101.30	52.18
Cd	0.62	0.25
Cu	6.54	1.62
Cr	22.30	5.39
Fe	21869.40	3339.50
Mn	362.60	90.62
Ni	16.93	4.41
Pb	8.94	2.42
V	8.75	2.69
Zn	62.90	11.30

Barium--Concentrations of barium ranged from 31 to 308 µg/g (fig. 81 and pl. 39). The histogram on the figures shows that the distribution of the metal is asymmetrically skewed toward the higher concentration with the dominant mode of 75 µg/g. The distribution pattern for barium indicates three significant areas of highest concentration on the inner part of the OCS. The highest concentrations are associated with oil fields and the barium was most likely introduced onto the sea floor during the drilling of wells. Salients extending seaward across the shelf from the areas of higher concentration may represent seaward migration of barium but sample spacing is not sufficiently dense to fully confirm this assumption.

Cadmium--Concentrations of cadmium range from 0.2 to 1.55 µg/g with an asymmetrical distribution skewed toward the higher values from a strong dominant modal concentration of 0.5 µg/g (fig. 82 and pl. 40). Two areas of high concentration (greater than 1.0 µg/g) occur on the shelf, one at the shelf edge southeast of Corpus Christi, and one on the inner shelf near the mouth of the Rio Grande. The very high concentration on the outer shelf is in the area of suspected gas seeps and possibly can be attributed to emanating gas. The very high concentration

on the inner ancestral Rio Grande delta is not readily explained. However, the concentration gradient indicates a salient oriented seaward from the Rio Grande.

Chromium--Concentrations of chromium range from 4.9 to 42.1 µg/g with a moderately skewed distribution from a modal value of 19 µg/g (fig. 83 and pl. 41). The distribution pattern for chromium shows three areas of concentration: one in the northwestern part of the OCS south of Matagorda Bay; another extending westward from the suspected gas seep area on the outer shelf; and a third extending westward from the outer edge of the ancestral Rio Grande delta. The highest concentrations are in the sediments of the suspected gas seep area.

Copper--Concentrations of copper range from 2.6 to 10.7 µg/g with a symmetrical distribution about a modal value of 7 µg/g (fig. 84 and pl. 42). The most significant features of the distribution pattern for copper are the somewhat elevated concentrations directly east of Corpus Christi Bay and the abrupt increase in concentration south of a line that approximately parallels 27°15'N. The amount of copper also is slightly high within the gas seep area on the outer shelf.

Iron--The amount of iron ranges from 1.13 to 3.34 percent with a symmetrical distribution around a dominant mode of 2.0 percent (fig. 85 and pl. 43). The iron is widely distributed and differences in concentration are not large. Somewhat higher amounts are in the gas seep area of the outer shelf. The distribution of iron seems to be related roughly to the grain size of the host sediment. The higher amounts of iron tend to be in the finer-grained sediments.

Lead--Concentrations of lead in the sediments vary from 2.2 to 16.5 µg/g with a slightly asymmetrical distribution skewed toward the high concentrations (fig. 86 and pl. 44). The area of highest lead content is on the northwest part of the OCS in a two-pronged salient that extends seaward from the outlet

for Matagorda Bay. Lead content also is high in one sample in the gas seep area and is slightly elevated along the outer shelf edge south of the gas seep area.

Manganese--Concentrations of manganese within the sediments range from 206 to 556 µg/g with an asymmetrical distribution skewed toward the lower values from a modal value of 375 µg/g (fig. 87 and pl. 45). The distribution pattern for manganese shows that four separate areas have more manganese than other parts of the shelf: south of the outlet for Matagorda Bay; the area of the gas seeps on the outer shelf; a small area south of Corpus Christi Bay on the inner shelf; and the extensive area in the southern portion of the OCS. Manganese content is highest in the vicinity of the carbonate reef at the northern edge of the ancestral Rio Grande delta.

Nickel--Concentrations of nickel in the sediments range from 3.5 to 26.1 µg/g with a bimodal distribution with modes of 12 and 20 µg/g (fig. 88 and pl. 46). The distribution of nickel appears to be made up of two populations: one characterized by the 12 µg/g mode in the northern half of the OCS, and the other characterized by the 20 µg/g mode in the southern part. The boundary between these two areas is the 27°15'N parallel, which also is the boundary separating the two areas of differing content for copper. In the northern sector, nickel content is highest within the sediments south of Matagorda Bay and in the gas seep area on the outer shelf. The distribution of nickel away from the gas seep region forms a salient that mirrors the pattern for chromium. In the southern sector, only one area of higher nickel content exists, an area of elevated content on the outer edge of the Rio Grande delta that extends landward. The pattern there also seems to mirror the pattern for chromium.

Vanadium--Concentrations of vanadium range from 4.1 to 27.4 µg/g with an asymmetrically skewed distribution toward the higher values from a modal value of 8.5 µg/g (fig. 89 and pl. 47). The content of vanadium is highest in the

gas seep area on the outer shelf where a salient of vanadium-rich sediment extends landward in the same pattern as nickel and chromium. An isolated small area of somewhat higher vanadium content is near the shelf edge south of the gas seep area in the same area where organic C is relatively high. The pattern of distribution for vanadium is random over other parts of the shelf.

Zinc--Concentrations of zinc in the shelf sediment range from 38.9 to 95.4 µg/g with a broad slightly asymmetrical distribution from a dominant mode of 60 µg/g (fig. 90 and pl. 48). Sediment highest in zinc content is within the gas seep area. The salient extending shoreward across the shelf is similar to those for chromium, nickel, and vanadium. Other zinc-enriched sediments are in the area of higher organic C on the outer shelf south of the gas seep region, on the outer edge of the ancestral Rio Grande delta, and in the fine-grained organic-enriched muds south of Matagorda Bay.

SUSPENDED SEDIMENTS

The water column samples for the suspended sediment analyses were obtained from 23 stations spaced along four transects across the shelf. (See figure 8 for location.) Samples were collected from the surface, thermocline depth, and near the bottom during the two-month interval, October 25 to December 22, 1974. When no thermocline was recorded, a water sample was obtained approximately halfway between surface and bottom. As the water samples are not synoptic, only the relative values within a specific station have any reliable scientific significance. A total of 65 samples were analyzed for sediment particle size.

GRAIN SIZE

Method of Analysis

The grain size and approximate concentrations of suspended sediments were determined by Coulter Counter analyses. It should be noted that the water samples were stored under refrigeration for a few months prior to analysis. Consequently, it is possible that some undeterminable changes from the original size distributions or concentration values could have occurred during storage.

Grain-size analyses were conducted according to the following procedures:

1. The water samples were brought to room temperature and aerated in darkness to liberate dissolved gases and minimize organic growth.
2. The entire 250 ml seawater sample was analyzed in its natural untreated state; however, in some instances, only smaller sample volumes were available for analyses.
3. Sample concentrations were maintained at a sufficiently low level to result in less than 5 percent coincidence error; if the original concentration

exceeded this level, the sample was diluted with seawater electrolyte filtered through a 0.2 μm filter until less than 5 percent coincidence was achieved.

4. For each sample, combined 200 μm and 30 μm tube analyses were conducted, providing an analytical range from 0.63 μm (10.62 Ø) to 80.6 μm (3.62 Ø). For the purpose of deriving statistical parameters based on an 0.5 Ø interval, an extrapolated analytical range of 11.0 Ø to 3.5 Ø was utilized.

The approximate concentrations of suspended sediments in the water samples also were determined by Coulter Counter in terms of total particle counts per standard water volume. Employing a 30 μm aperture tube, total particle counts per 0.05 cc were determined for sediments within the 0.63-16 μm size range. A replicate count was made on each sample, and the average of the two values was used as the total particle count; counts were obtained in an unagitated state. Supplemental concentration data were also obtained with the 200 μm tube aperture, which provided total particle counts per 2.0 cc water volume for sediments within the 3.17-101.6 μm size range. Counts were obtained with the 200 μm tube while stirring the sample suspension at a standard speed.

Results and Distribution

The statistical particle-size parameters of the suspended sediments were derived and are tabulated in Table II, Part II. In general, the sediments show a wide range in grain size. In most of the samples, the size of grains has a complex polymodal distribution. The individual modes probably reflect a mixture of organic particulate sub-populations (nanoplankton, microplankton) as well as inorganic sub-populations (silt and clay minerals).

The only individual size parameter evaluated during this study is the mean diameter (first moments) variability within each sample station. The

particular parameter was selected because it provides a good general characterization of the overall particulate system. Figures 91 and 92 are graphs showing the mean grain-size variability of the water column sediments at the 23 sample stations. The station plots are arranged along coast-normal transects; figure 91 shows the two northernmost transects and figure 92 the two southernmost transects. The depth of the thermoclines is indicated by dashed lines on the pertinent graphs.

The overall range of mean grain size for all stations is from a minimum of 9.37 Ø (clay) at station #245 to a maximum of 5.30 Ø (medium silt) at station #155. The stations in the northernmost transect (#10-88) have variable grain size-depth relationships. With the exception of stations 32 and 60, grain-size gradient reversals are associated with well-defined thermoclines; these gradients exhibit increasing grain size from the surface to the thermocline level, followed by decreasing grain size to the sea floor. Although station 32 has a thermocline, grain size decreases with depth. Station 60 has no thermocline and grain size increases slightly as water depth increases.

In the transect including stations 70 to 114, the two shallower stations, 70 and 73, have no thermocline and show a continuous size increase with depth. In contrast, the remaining deeper stations have thermoclines and show prominent gradient reversals. The two intermediate depth stations, 95 and 110, show directions of reversal opposite to that in the two deeper stations,115 and 114.

In the transect including stations 165 to 155, thermoclines are present only in the three deeper stations, 157, 156 and 155. Station 155 shows a prominent gradient reversal, whereas station 156 shows a continuous grain size reduction with depth; a bottom water sample was not available for station 157. Among the three shallower stations, 165, 164 and 160, stations 164 and 160 show gradient reversals of opposite sense; station 165 is lacking a mid-depth water sample but shows a net grain size reduction with depth.

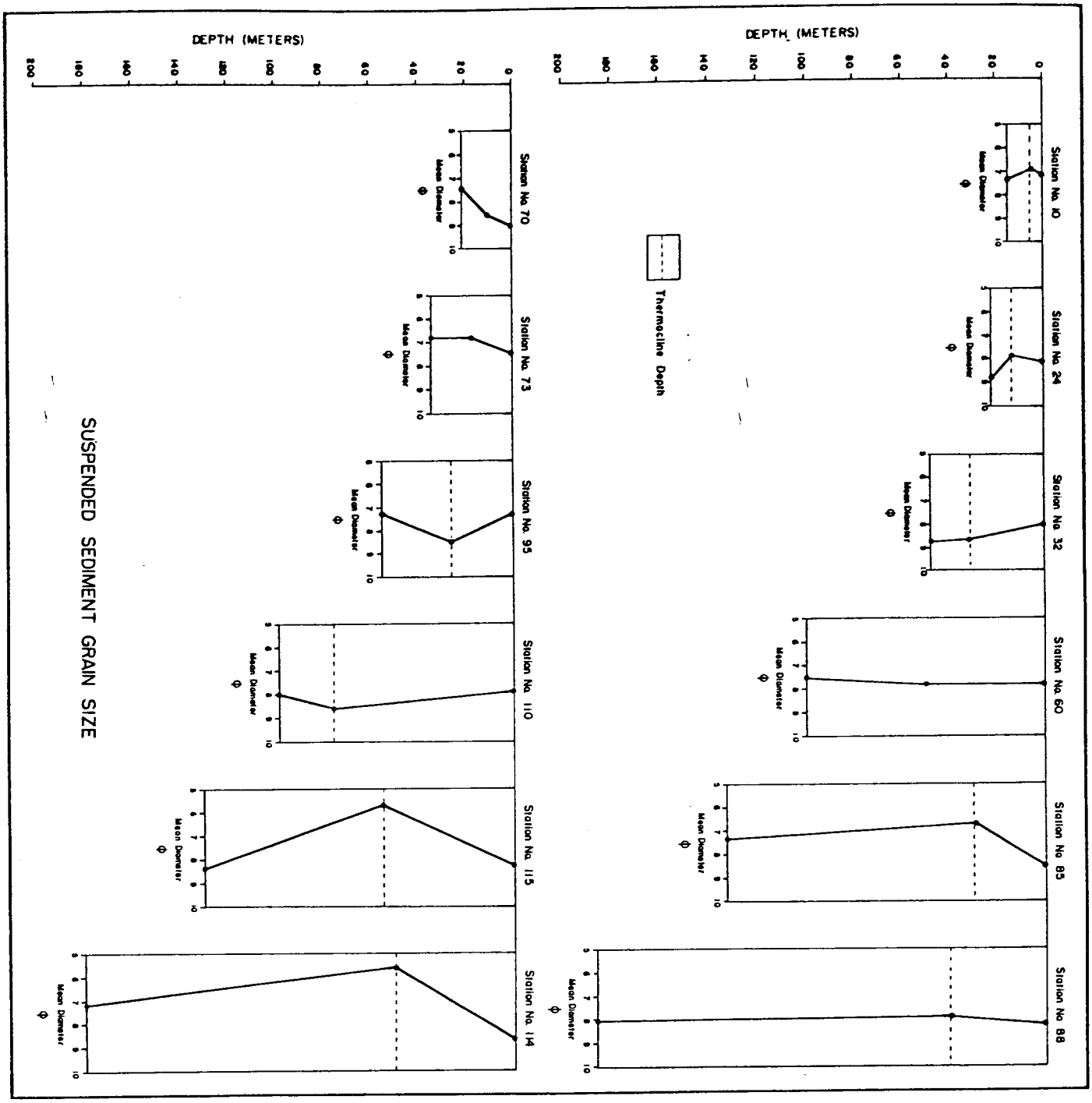

Figure 91. Graphs showing suspended sediment grain size-depth variability: stations 10 to 115.

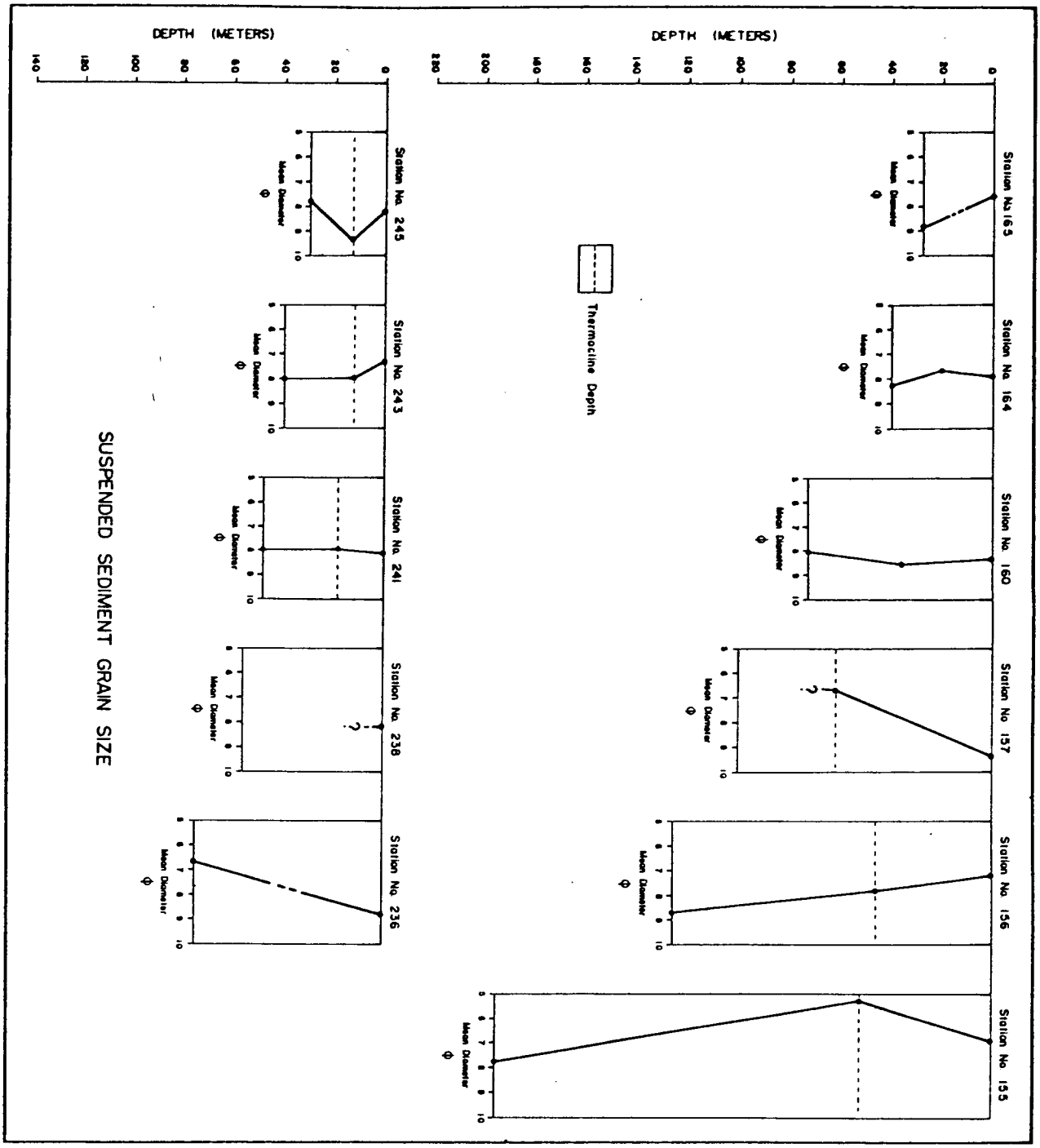

Figure 92. Graphs showing suspended sediment grain size-depth variability: stations 155 to 245.

In the southernmost transect, including stations 245 to 236, thermoclines are developed only in the three shallower stations, 245, 243 and 241. The shallowest station (245) exhibits a prominent gradient reversal; whereas, station 241 shows a very slight reversal. Station 243 shows a slight continuous grain size increase with depth. Complete water column sediment samples are not available for the two deeper stations, 238 and 236; however, station 236 shows a net grain size increase with depth.

In summary, samples of suspended sediments collected at 23 stations show variable relationships of grain size relative to water depth during the survey period. When thermoclines are developed, grain-size gradient reversals generally occur at the thermocline depth, a situation attributable to the density discontinuity of the water column associated with thermoclines. The direction of grain size reversals is variable and dependent upon the direction of the temperature gradients. The cooler, higher density waters generally tend to contain the coarser-grained suspended sediment.

SEDIMENT CONCENTRATIONS

The approximate concentrations of suspended sediments in the OCS water samples were determined by Coulter Counter in terms of total particle counts per unit water volume (table 18). The concentration variability of suspended sediments within the 0.63-16 μm size range is illustrated as a function of depth for each OCS water station (figures 93 and 94). Sediment concentrations among all the water sample stations range from a minimum of 5,746 counts at station 10 to a maximum of 237,297 counts at station 156.

The stations of the northernmost transect (10 to 88) exhibit variable concentration to water depth relationships. The two shallowest stations, 10 and 24, have concentration-gradient reversals associated with thermoclines.

Table 18--Suspended Sediments Concentrations
(particle counts/unit volume)

Station Number	0.63-16 μm size range (30 μm tube analysis/0.05 cc)	3.17-101.6 μm size range (200 μm tube analysis/2 cc)
10WT	5,746	31,057
10WM	15,638	12,958
10WB	12,598	57,014
24WT	97,917	12,148
24WM	177,001	17,255
24WB	46,495	1,946
32WT	39,513	15,362
32WM	46,864	1,238
32WB	95,050	24,936
60WT	10,869	2,001
60WM	16,444	981
60WB	156,651	80,378
70WT	78,704	18,294
70WM	94,344	2,479
70WB	97,620	29,667
73WT	13,763	2,058
73WM	14,395	721
73WB	23,947	10,441
85WT	24,000	1,429
85WM	24,241	383
85WB	127,724	81,381
88WT	19,656	519
88WM	38,123	957
88WB	186,788	22,839
95WT	11,720	2,381
95WM	16,087	2,002
95WB	9,179	2,810
110WT	24,176	529
110WM	29,419	494
110WB	81,807	68,090
114WT	27,441	827
114WM	9,216	116
114WB	116,353	201
115WT	26,611	383
115WM	21,664	218
115WB	99,388	85,588

Table 18--Suspended Sediments Concentrations (particle counts/unit volume)--Cont.

Station Number	0.63-16 μm size range (30 μm tube analysis/0.05 cc)	3.17-101.6 μm size range (200 μm tube analysis/2 cc)
155WT	21,558	677
155WM	11,480	142
155WB	160,252	1,787
156WT	32,817	650
156WM	18,615	154
156WB	237,297	85,173
157WT	28,838	1,027
157WM	18,824	222
157WB	57,946	11,840
160WT	25,493	249
160WM	22,260	1,077
160WB	46,423	343
164WT	27,213	815
164WM	43,612	740
164WB	21,950	1,661
165WT	42,070	435
165WM	19,385	907
165WB	16,669	3,488
238WT	24,560	5,010
235WM	96,485	21,787
236WT	44,643	2,891
236WB	49,482	66,765
241WT	30,344	648
241WM	7,176	344
241WB	16,893	1,338
243WT	29,423	6,857
243WM	21,243	2,992
243WB	35,095	6,883
245WT	67,308	9,102
245WM	141,335	1,878
245WB	68,699	7,879

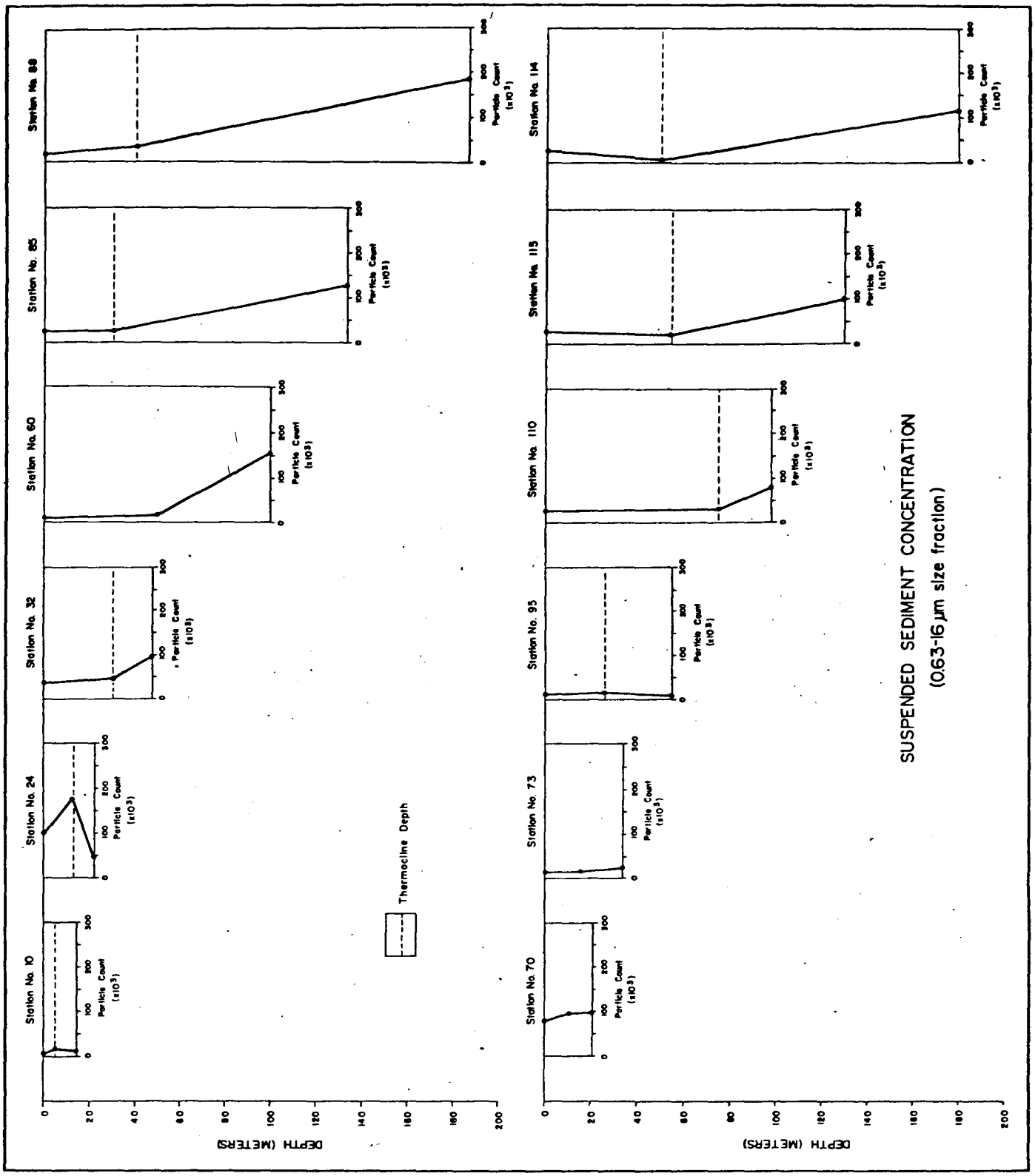

Figure 93. Suspended sediment concentration-depth variability, 0.63 µm size fraction: stations 10 to 115

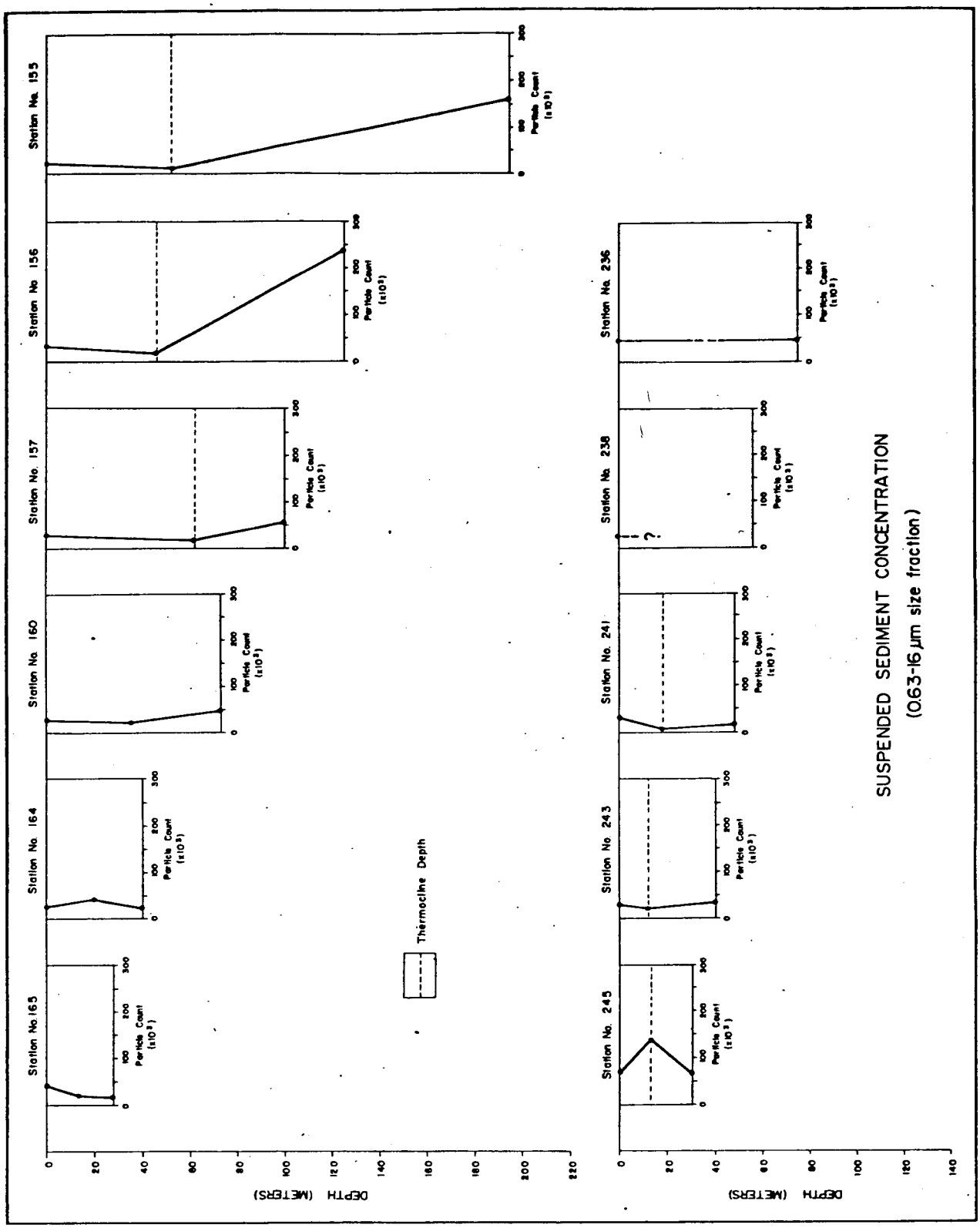

Figure 94. Suspended sediment concentration-depth variability, 0.63 µm size fraction: stations 155 to 245.

Highest concentrations occur at the thermoclines, with station 10 showing a net increase in concentration with depth and station 24 showing a net decrease. All remaining stations show a net increase in sediment concentrations with depth; the highest gradients are below the thermocline level.

In the station transect including stations 70 to 114, the two shallowest stations, 70 and 73, have no thermocline and both have continuous increasing concentrations with depth. All remaining stations have thermoclines and all have gradient reversals except for station 110 which shows a continuous concentration increase with depth; the gradient reversal of the intermediate depth station, 95, results in maximum concentration at the thermocline; whereas the deep stations' reversals(115 and 114) result in minimal concentrations at the thermocline. With the exception of station 95, all other stations show a net increase in sediment concentration with depth.

In the transect including stations 165 to 155, concentration gradient reversals are associated both with thermoclines, stations 157, 156 and 155, and without thermocline development, stations 160 and 164; only the shallowest station, 165, shows a continuous gradient. The intermediate and deep stations, 160, 157, 156 and 155, all show a net increase in sediment concentration with depth; whereas the two shallow stations, 165 and 164, show a net decrease.

In the transect including stations 245 to 236, the three shallower stations, 245, 243 and 241, show concentration gradient reversals associated with thermoclines; concentration minima occur at the thermocline level in stations 243 and 241, whereas a concentration maximum occurs at station 245. Stations 245 and 243 exhibit a net increase in concentration with depth, whereas station 241 shows a net decrease. Insufficient water samples were available for stations 238 and 236; however, a slight net increase in concentration with depth is indicated for station 236.

In summation, variable sediment concentration-depth relationships prevailed over the OCS during the survey period. Concentration gradient reversals occur at the majority of stations; the reversals are most frequently, but not exclusively, associated with thermoclines. The reversals can result in either concentration maxima or minima at the thermocline level. Continuously increasing concentration gradients are also frequently associated with thermoclines but can also occur in unstratified water columns. The majority of stations show a net increase in sediment concentration with depth; however, a net decrease is not uncommon, especially among the shallower stations. In essence, no systematic sediment concentration-depth relationship is readily apparent. This is attributed both to a complex thermo-density structure of the OCS hydraulic regime during the survey period as well as to the non-synoptic nature of the water samples. The water sampling phase extended over a two-month period characterized by highly variable atmospheric and sea state conditions, a factor that would tend to obscure any systematic sediment concentration-depth relationships.

MINERALOGY

Method of Mineral Determination

Aboard ship, a one-to-three liter aliquot, depending on the assessment of the turbidity of the sample by visual inspection, was filtered through a pre-weighed Silas Flotronics silver filter having a 0.45 μm nominal pore diameter. The material was then washed with 100 ml of deionized water in order to remove the salts. The filter pads were frozen and returned to the laboratory.

In the laboratory, the samples were thawed, dried in a desiccator, and placed on a micro balance with desiccant and weighed to a constant weight. The mineralogy was determined by X-ray diffraction. X-ray diffraction patterns

were made using a sensitivity of 100 counts per second full scale, a scanning speed of 2 degrees 2 theta per minute, and a time constant of 2 seconds. Three additional patterns were made on each sample: 1) after treatment with ethylene glycol, 2) after heating to 400°C, and 3) after heating to 550°C. Chlorinity was measured by titration on a separate aliquot taken at the time of the original sampling.

The mineralogy of the suspended sediments was determined by X-ray diffractometer. The X-ray analysis showed that the detrital suspended material is made up primarily of clay minerals with only trace amounts of quartz and other material. Examples of the diffractograms are shown in figure 95. The mineralogical data, although not synoptic, does define two water masses, a montmorillonite-rich water mass over the northwesternmost part of the OCS and an illitic-rich water mass over the remainder of the shelf. The areal distribution of the two water masses has roughly the same distribution as the chlorinity. The physical oceanographic studies may help explain the origin and properties of the two water masses.

A feature of the mineralogy is the low content of montmorillonitic material in the bottom water, indicating that the clay minerals in suspension are not being derived from the surficial bottom sediments which are high in montmorillonitic clay.

Prior to the preparation of the material for mineralogical analysis, the concentration of suspended material and chlorinity was determined. The results are listed in Table VI, Part II.

TRACE METALS CONTENT

Procedures and Analytical Techniques

Samples of suspended sediments analyzed for trace metals content were taken from surface waters, mid-waters and bottom waters by means of 30 liter

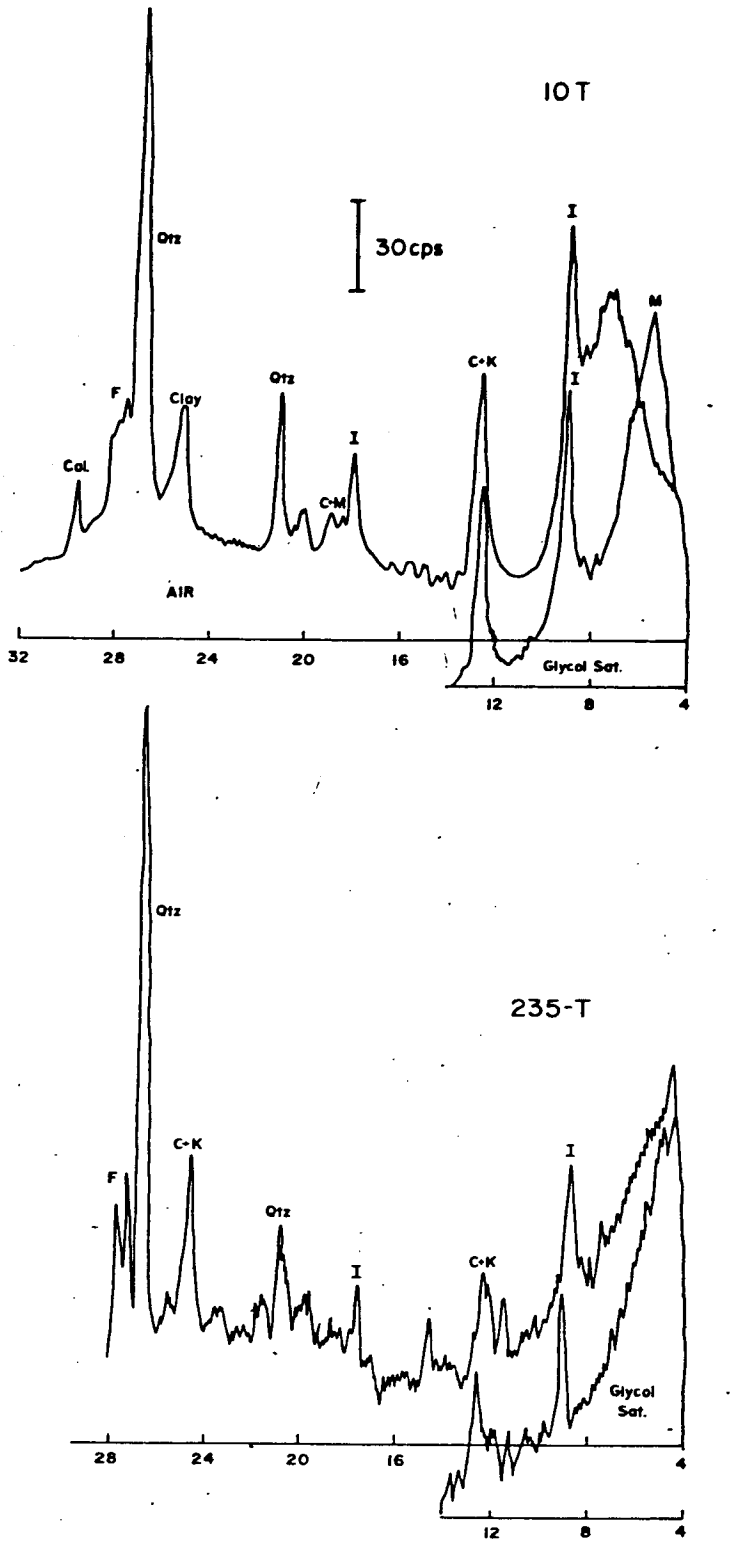

Figure 95. Diffractograms of minerals identified in suspended sediments. Sample 10T is from surface water in the northern part of the OCS; sample 235T is from surface water in the southern part. Both samples were air dried and ethylene glycol treated. M-montmorillonite; I-illite; C+K - chlorite plus kaolinite; Qtz - quartz; F - feldspar; Cal - calcite.

Niskin bottles. The Niskin bottles are constructed of PVC and latex and contain no interior metal parts. They were washed with concentrated nitric acid prior to the initial cruise and washed with water between each station. Once the samples were on deck, they were racked and the water samples transferred to acid-washed, one-gallon, polyethylene bottles. Four such bottles from each 30 l. Niskin were transferred to an onboard laboratory. One of these sub-samples was reserved for other analyses and the other three filtered for trace metals analysis. See figure 96 for location of sample stations.

Filtration was accomplished by an adaptation of the in situ filters of Davey and Soper (1975) to a laboratory procedure. Filters were made by heat-sealing 0.4 μm Nuclepore® filter material to make bags 3.5 cm in diameter by 7 cm length. The filter bags were encapsulated in polyethylene vials to which entrance and exit tubes had been sealed at each end. The inline filter capsules were washed with 1:1 nitric acid and deionized water before use. On board ship, the filters were attached to polyethylene bottles containing the water to be filtered by means of polyethylene fittings sealed to the bottle cap. Approximately 10 liters of seawater were then allowed to flow through the filter. Once the filtration was complete, the encapsulated filters were sealed in polyethylene bags and frozen for transport to the analytical laboratory on shore.

Analytical preparation was performed in an Envirco® clean bench which utilizes a filtered air flow to isolate the interior of the bench from the remainder of the laboratory. All weighings were made on a Perkin Elmer AD-2 Autobalance readable to 0.1 μg placed in the clean bench. Only deionized water and redistilled nitric acid (G. Fredrick Smith Chemical Co.) were used in the analytical procedure. All labware was washed with 1:1 nitric acid and deionized water before use.

In the analytical laboratory, samples were thawed, the filter capsules opened and the filter bags carefully inverted. A jet of deionized water was

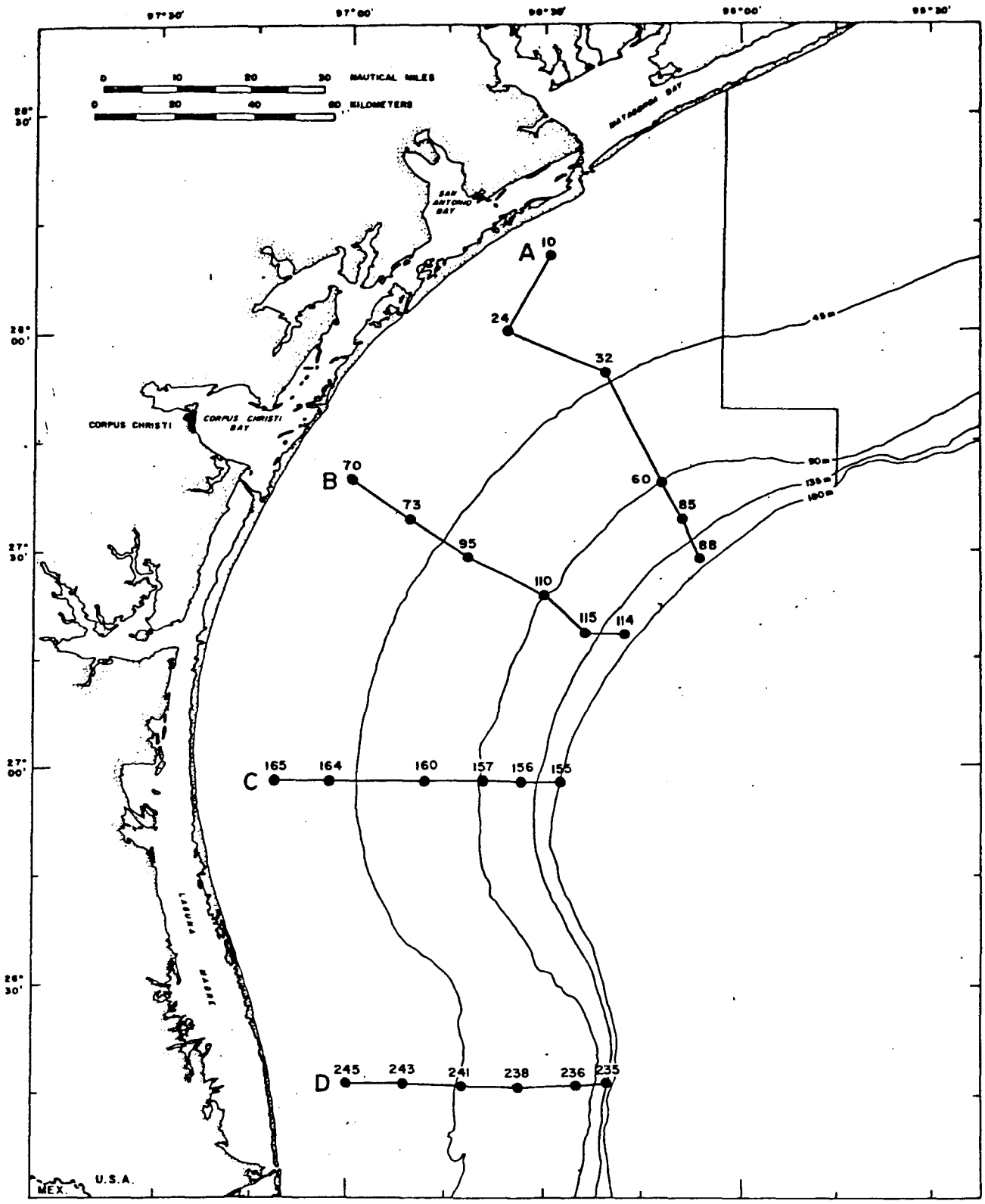

Figure 96. Location of samples analyzed for trace metals in suspended sediments.

then directed onto the exposed filtering surface. The water and dislodged particulate material was collected in a 100 ml polyethylene beaker; 70 to 100 ml of deionized water was used in this step. The procedure serves the double purpose of transferring the particulate material and removing any residual salt. This suspension was then filtered under vacuum on a 25 mm diameter, 0.4 μm pore size Nuclepore filter which had been acid washed, dried over anhydrous magnesium perchlorate and weighed. The filters with sample material were then placed in a desiccator over anhydrous magnesium perchlorate for 24 hours and then reweighed.

The filter and sample were then placed in a 50 ml teflon beaker. Two ml of concentrated nitric acid were added and the samples taken to dryness under infrared lamps at a temperature of 80°C. One ml of concentrated nitric acid was then pipetted onto the dry sample. The sample and acid were allowed to equilibrate for one-half hour and were then transferred to an acid-washed lucite sample cup. This solution was then used for analysis by atomic absorption spectroscopy.

All analyses were performed on a Perkin Elmer model 303 atomic absorption spectrophotometer using a model 2100 HGA graphite furnace. Dilutions were made when necessary with concentrated nitric acid.

Blank values were determined for all metals analyzed on the deionized water and redistilled nitric acid. A procedural blank was determined by taking one of the original acid washed filter capsules through the entire procedure as if it were a sample. This was the blank value used in all calculations.

The sample size, 0.1 to 15 mg total weight, made contamination a critical problem in the analysis. Contamination can be divided into three types: contamination associated with the ship, i.e. paint chips, stack cinders, or rust which might have fallen into the water and been included in the sample;

contamination associated with the filtering and analytical procedure, i.e. atmospheric dust in the laboratories or metals used in the manufacture of the filters, beakers, pipette tips, etc. and not removed, and finally impure reagents.

Contamination associated with the ship was monitored in two ways. First, careful visual scrutiny of the filters coupled with microscopic observation of any samples with suspicious particles. This did not indicate any obvious contamination. Second, samples of various paints used on the ship were taken and analyzed (Table 19). Comparison of the pattern of metal concentrations in the paints with that of samples suspected of being contaminated showed no correlation. It is believed that ship contamination was kept to a minimum during sampling.

Table 19--Ship Paint Analysis

	%					ppm			
Sample	Fe	Cr	Cu	Zn	Pb	Ni	Mn	Cd	V
Laboratory, blue	0.4	9.6	2.4	9.6	3.8	1200	--	182	55
Deck, red	3.0	0.8	0.2	3.2	0.3	440	1500	53	266
Hull, green	1.2	35	0.5	18	9.4	270	--	207	375
Superstructure, white	1.0	12	58	15	2.1	420	--	246	133

Atmospheric contamination was kept to a minimum by performing sample preparation in a clean bench which utilizes filtered forced air flow to eliminate atmospheric dust. Metal contamination from the laboratory ware was not so easily controlled. Sommerfeld and others (1975) have shown that both zinc and iron are contaminates of disposable pipette tips of the type commonly used to introduce a sample into the graphite furnace. Robertson (1968) has shown that a number of plastics and glasses commonly used for the manufacture of laboratory ware contain traces of metals. For this reason all laboratory

ware was washed in 1:1 nitric acid before use. However, it was determined that the disposable pipette tips and lucite sample cups had to be washed in concentrated nitric acid before an acceptable blank could be obtained.

The two reagents used in processing the samples were deionized water and redistilled nitric acid from G. Fredrick Smith Co. The deionized water showed concentration levels of all metals too low to quantitatively determine. In the acid, only iron, zinc, and cadmium showed determinable levels (Table 20). These values are probably due to pipette tip contamination since the procedural blank was lower in zinc and iron than the acid blank.

Table 20--Blank Values

	Cd	Fe	Zn	Pb	Cu	Cr
Redistilled nitric acid	0.8 ppb	0.3 ppm	12 ppb	-	-	-
Procedural blank	0.8 ppb	0.24 ppm	8 ppb	0.014 ppm	60 ppb	40 ppb

	Ni	V	Mn
Redistilled nitric acid	-	-	-
Procedural blank	.04 ppm	11 ppb	10 ppb

In view of the several sources of contamination, a procedural blank was run. This was done by taking an acid washed encapsulated filter, sealing it in a polyethylene bag, freezing it, and then placing it in the normal processing stream with the samples (Table 20). These are the blank values used in calculating dry weight concentrations.

It is extremely difficult to put error limits on the analysis. Duplicate analyses were run for samples of sufficient amount. These analyses are given in Table 21.

Table 21 shows a precision of between 30 and 50 percent, except for iron and zinc, where the precision is considerably worse. This might be expected from the blank values and from the fact that, of the metals analyzed, iron and zinc are most commonly used both on board ship and in the laboratory.

Table 21--Replicate Analyses

Sample #	Sample Wt., mg	Cd	Fe%	Zn ppm	Pb	Cu	Cr	Ni	V	Mn
10M a	5.041	1.3	1.1	500	50	85	20	32	9.4	380
b	1.272	1.7	3.0	1500	55	140	35	16	5.5	480
10B a	7.586	1.5	1.4	270	26	44	15	57	7.9	880
b	1.720	ND	2.1	5800	17	130	9	29	5.8	820
24B a	3.073	2.5	2.5	7500	58	84	490	218	19.3	1300
b	5.170	1.7	1.2	3800	31	88	16	25	9.6	1200
60B a	12.14	0.9	3.3	233	28	35	80	89	51.6	1400
b	14.69	0.7	4.1	110	14	21	55	48	23.2	840
c	15.95	0.5	3.8	399	15	22	43	38	22.6	1300
d	15.36	0.9	4.6	17600	23	39	75	77	29.8	840
85B a	5.220	0.0	1.5	190	21	26	21	67	7.1	620
b	6.424	0.3	1.4	350	20	4	18	36	6.5	880
70B a	3.576	0.8	2.4	110	20	19	19	25	9.1	530
b	3.757	0.3	0.8	430	21	55	18	32	7.7	350
245T a	2.633	4.2	2.8	4000	410	260	97	72	24.3	410
b	3.136	3.4	2.2	2900	488	170	98	26	29.0	300
241B a	3.280	2.4	1.7	1100	55	52	16	40	9.1	1800
b	2.787	2.2	0.6	2100	61	29	13	36	5.7	1200
238B a	2.819	175.	2.0	2900	46	290	18	28	6.7	970
b	1.794	123.	2.0	500	45	140	16	22	10.7	590
157B a	3.330	0.2	1.4	520	21	31	16	24	10.4	820
b	5.829	0.1	1.9	1600	26	11	15	29	6.5	830

Amount and Distribution

Because of the difficulties involved in analyzing the very small amounts of sample material the results can be discussed only as general trends or averages. Two types of analyses were used to gain information from the data. Histograms were made for each metal with all stations divided into top, mid and bottom samples as a means of relating the distribution of metal concentrations to water depth. Maps showing areal distribution of metals in both surface and bottom waters were compiled to show geographic variations.

The histograms (figs. 97, 98 and 99) show that the metals can be divided into two groups. Group one includes cadmium, chromium, copper, nickel and lead and all show a similar pattern: a spread of values in the top and mid-water samples; and a possible bimodal character to the histograms and minimal values for the bottom water samples. Group two (fig. 99) includes manganese and vanadium which

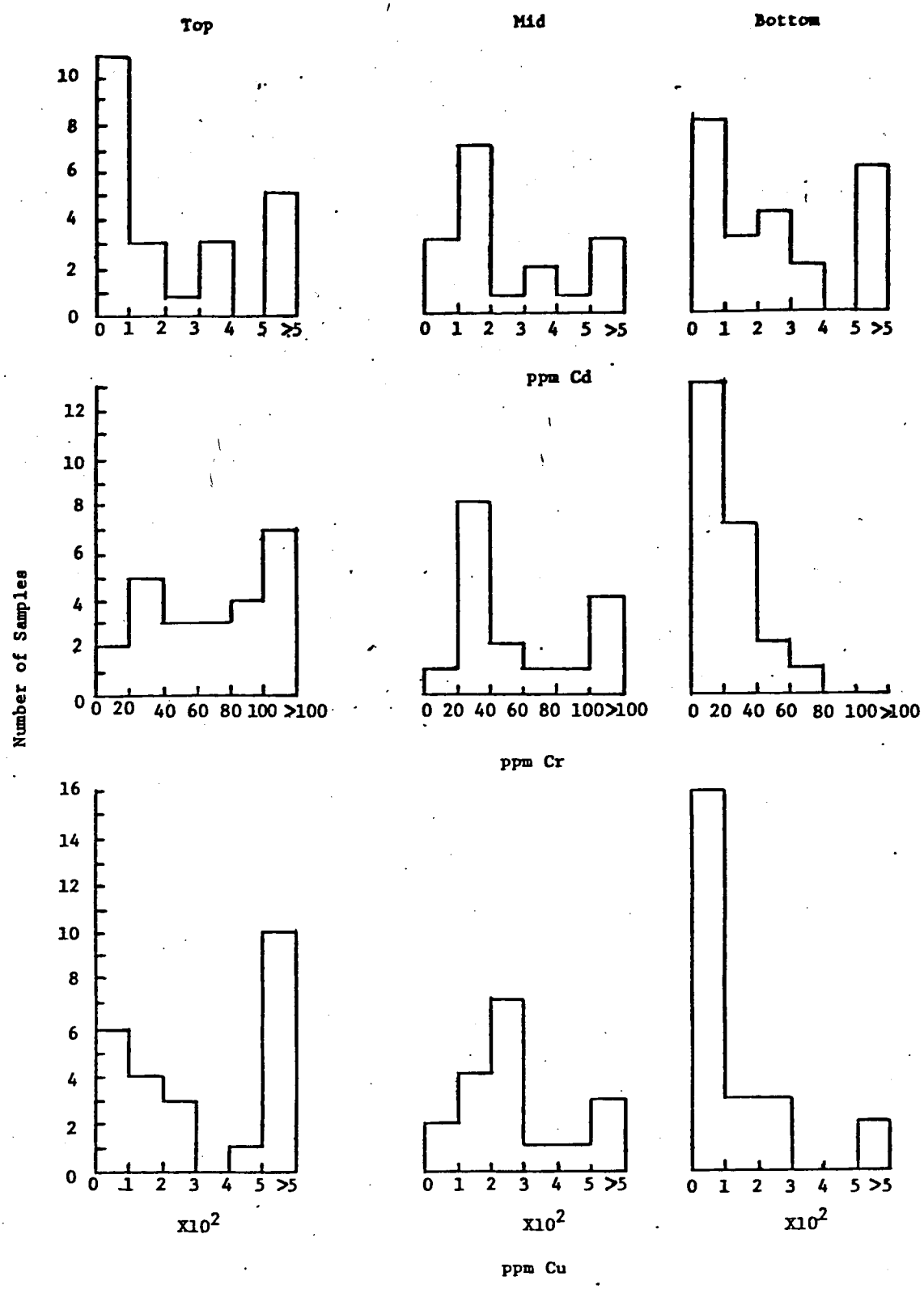

Figure 97. Histograms showing amounts of cadmium, chromium and copper in suspended sediments at three levels in the water column.

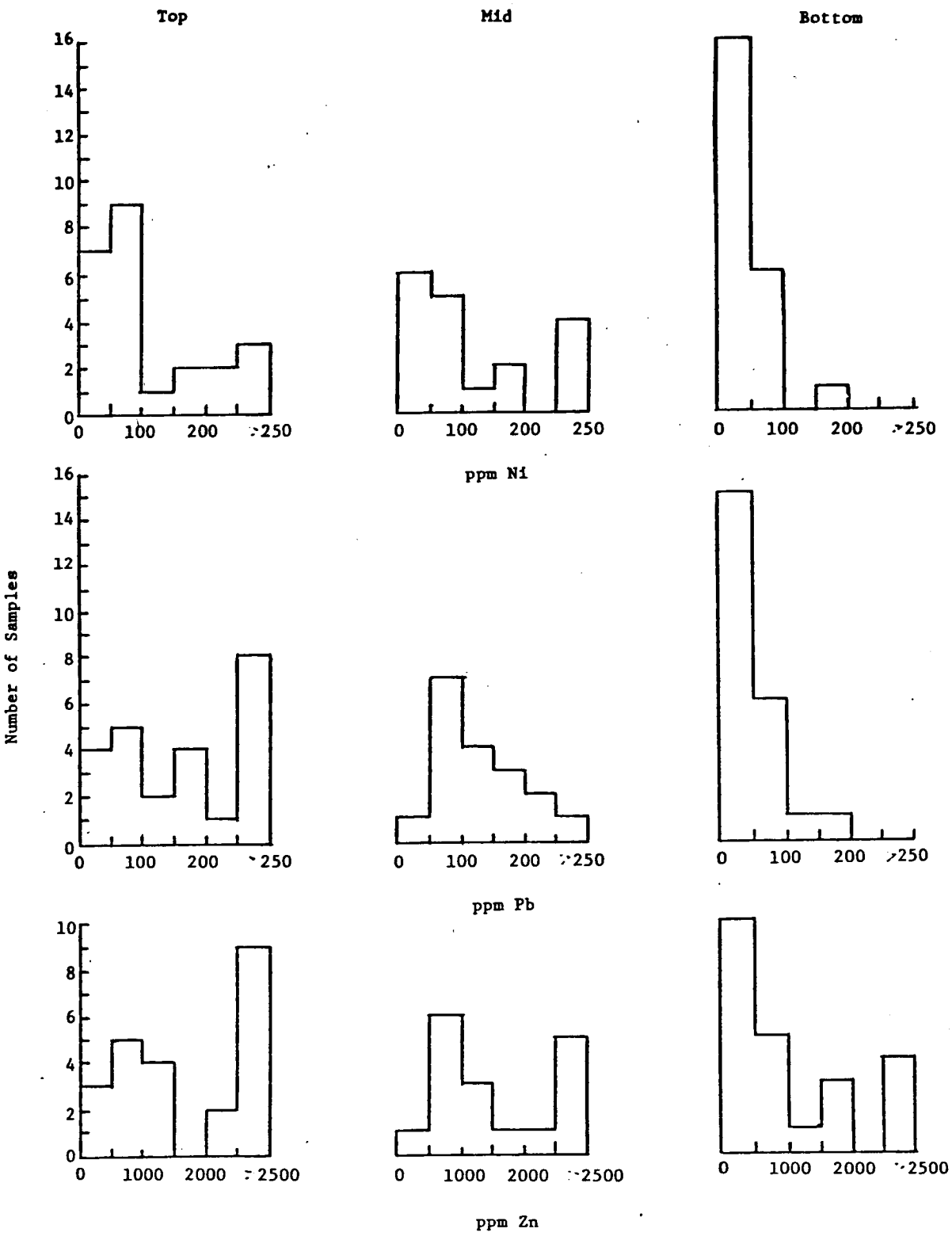

Figure 98. Histograms showing amounts of nickel, lead and zinc in suspended sediments at three levels in the water column.

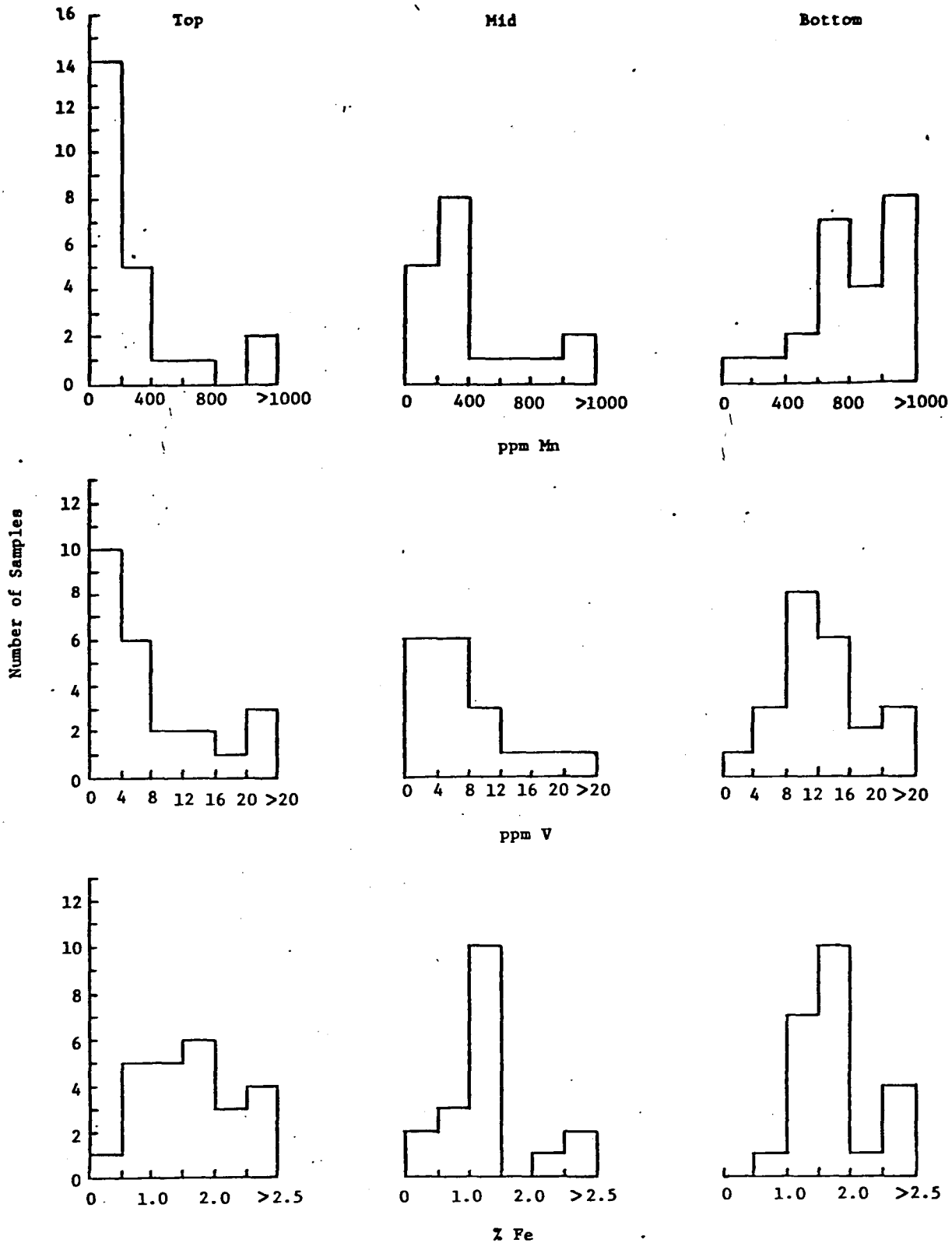

Figure 99. Histograms showing amounts of manganese, vanadium and iron in suspended sediments at three levels in the water column.

have a distinctly different pattern: high values in the bottom samples; and lower values in mid and top samples. The patterns for iron and zinc are not so distinct, probably as a result of the contamination problems encountered with the two elements during analysis. However, iron does show some similarity to manganese and vanadium, but zinc would appear to belong to the first group. In essence, the bottom samples are distinctly different in metal concentrations from the majority of the top and mid water samples, suggesting at least two sources for the trace metals in the suspended materials. Betzer (1974) suggests that the two most likely sources could be organic and inorganic particulate material. Bostrom and others (1974) have shown that the metals Cr, Cu, Cd, Ni, Pb and Zn are enriched in planktonic organisms relative to shale but that Fe, Mn and V are in the same proportions as in shale. If this relationship is generally applicable, it suggests that the bottom suspended sediment samples analyzed for the South Texas OCS are inorganic in nature and the top and mid-depth particulate matter is more organic.

The samples were taken on four transects oriented normal to the longitudinal trend of the shelf. The six sample stations were evenly spaced along each line (fig. 96). The shoreline has a north to northeast orientation in the sample area. Therefore, the four sampling lines run east to southeast. Consequently, lines drawn through the first sample station of each line, the second sample of each line, etc. would be more or less parallel to shore and have a north to northeast orientation. For discussion, the four transects have been designated from north to south A, B, C and D (fig. 96). As the study area is roughly rectangular, it has been drawn as a rectangle for the preparation of maps showing distribution of the trace metals. The maps show the sampling stations as being equidistant from one another (figs. 100 to 107). They are in fact not equidistant (fig. 96), but a rectangular representation does allow for a

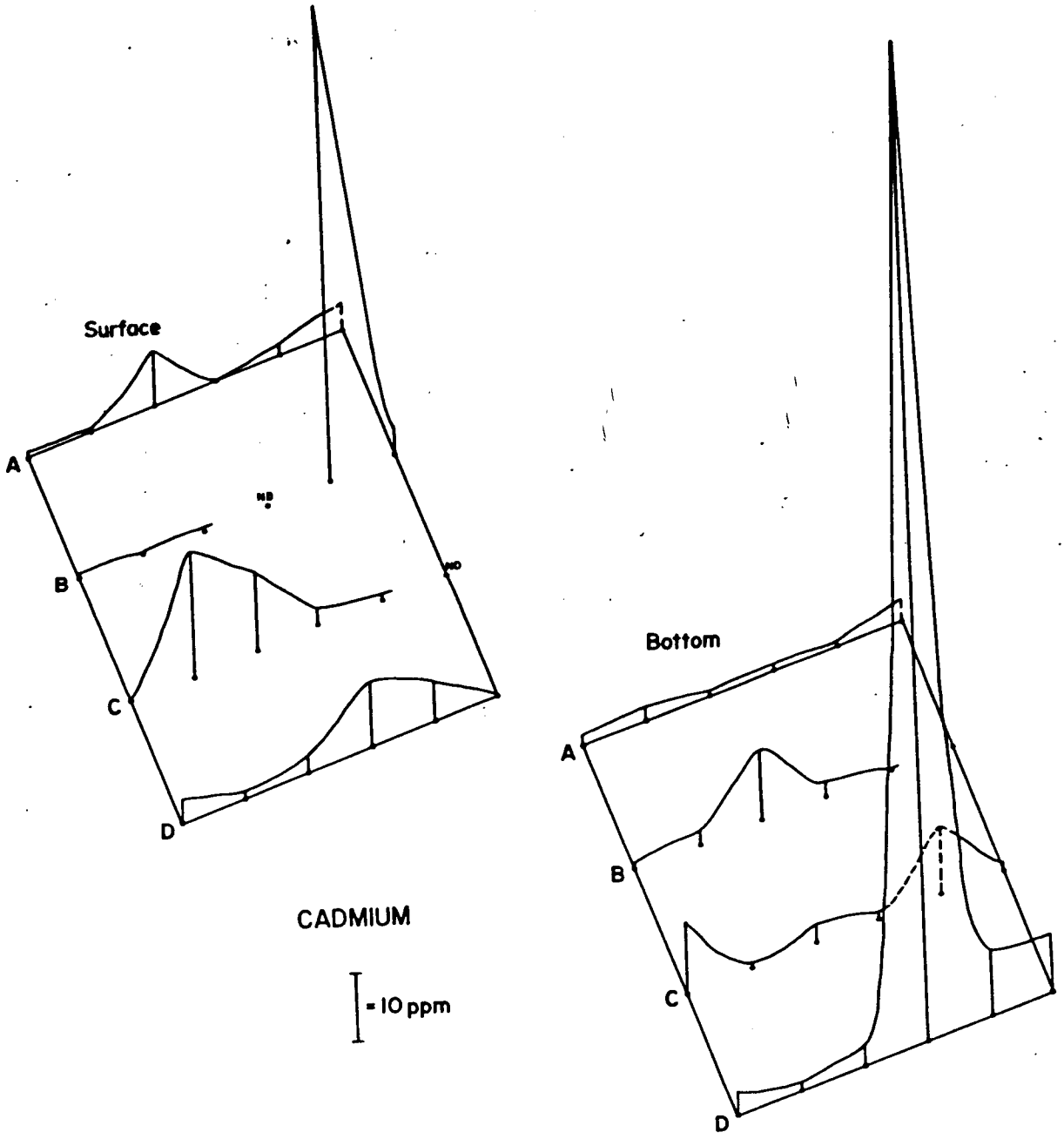

Figure 100. Areal distribution of cadmium at surface and bottom levels. Letters A, B, C, and D indicate the four sample transects from north to south.

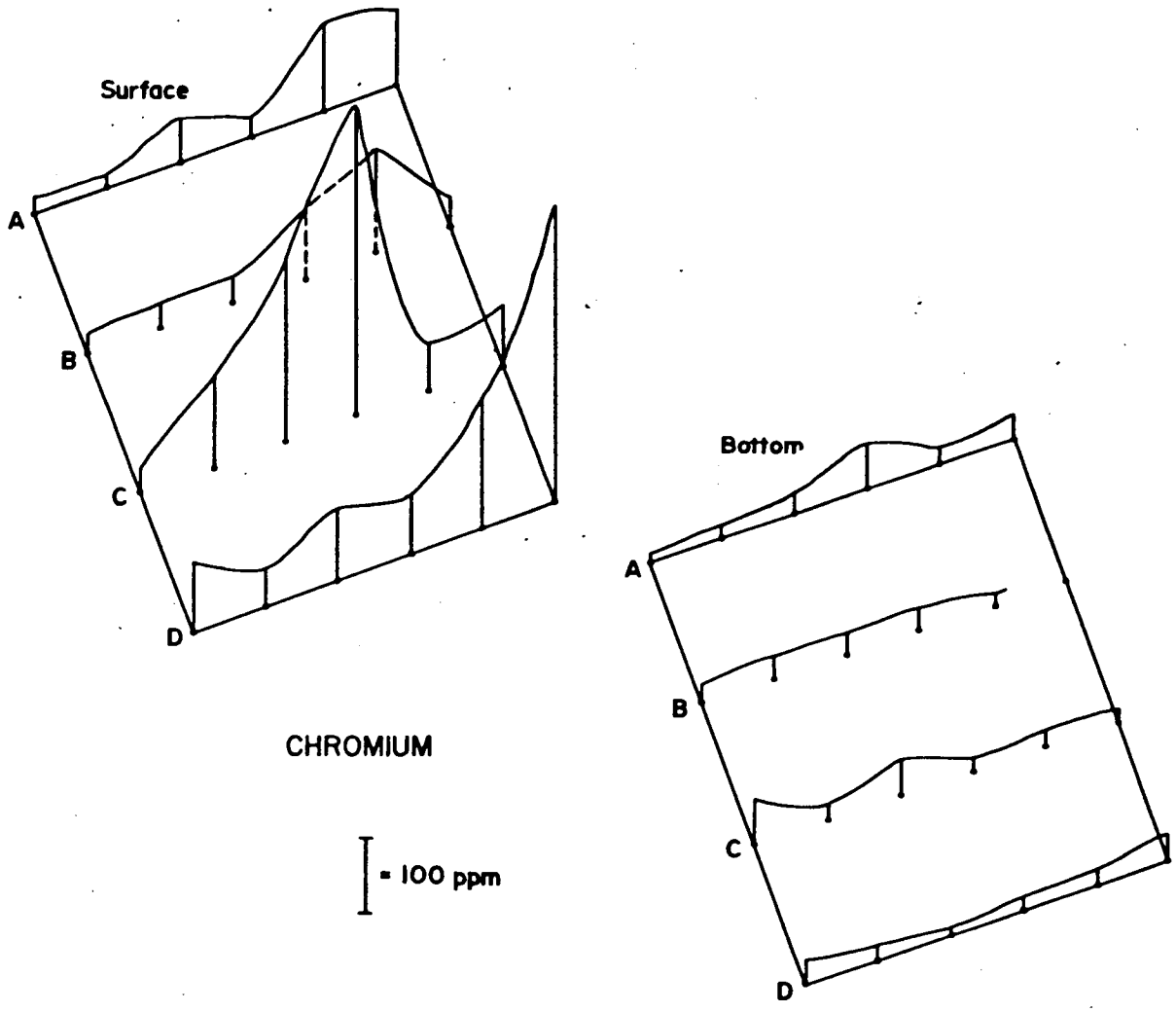

Figure 101. Areal distribution of chromium at surface and bottom levels. A, B, C, and D indicate the four sample transects from north to south.

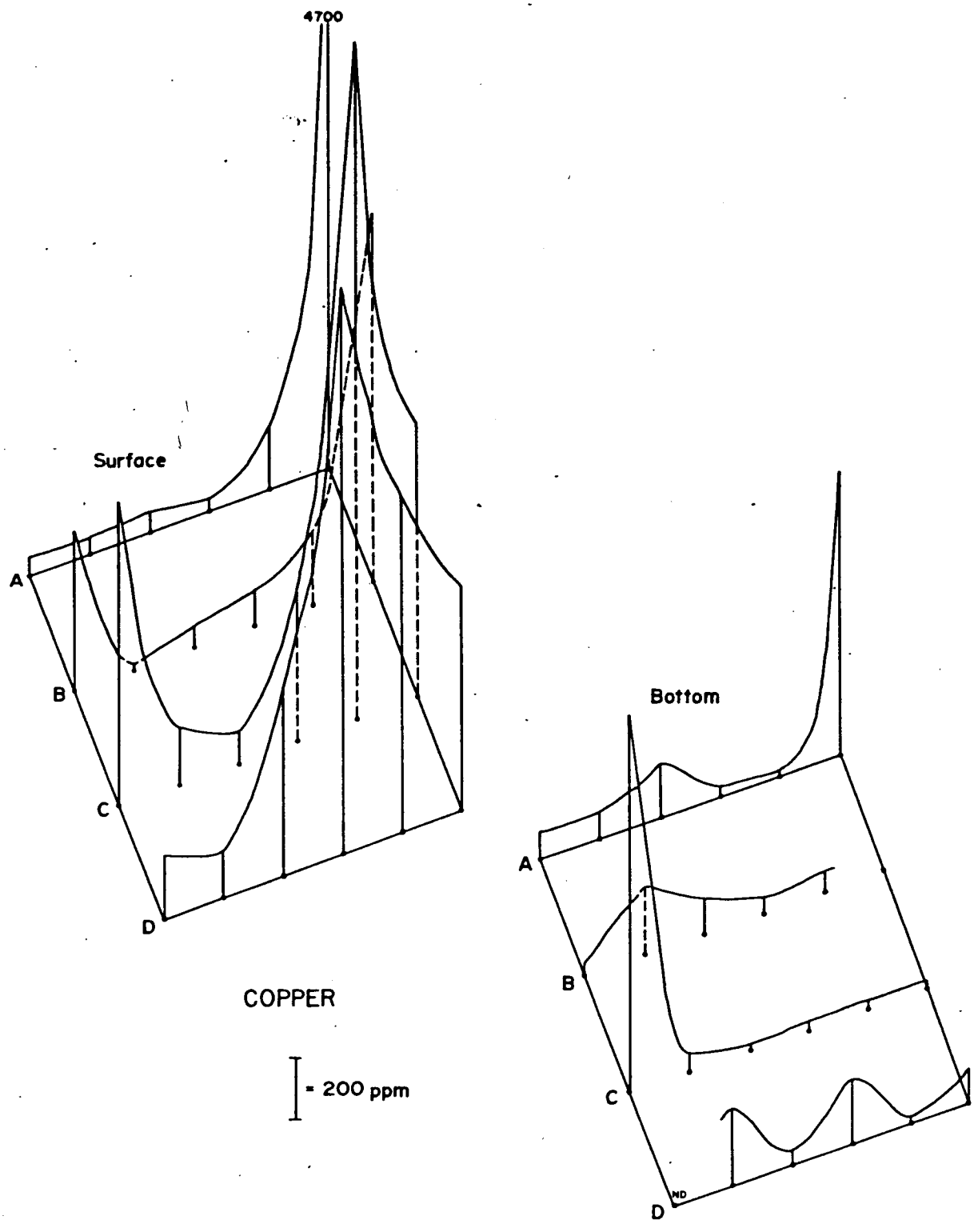

Figure 102. Areal distribution of copper at surface and bottom levels. A, B, C, and D indicate the four sample transects from north to south.

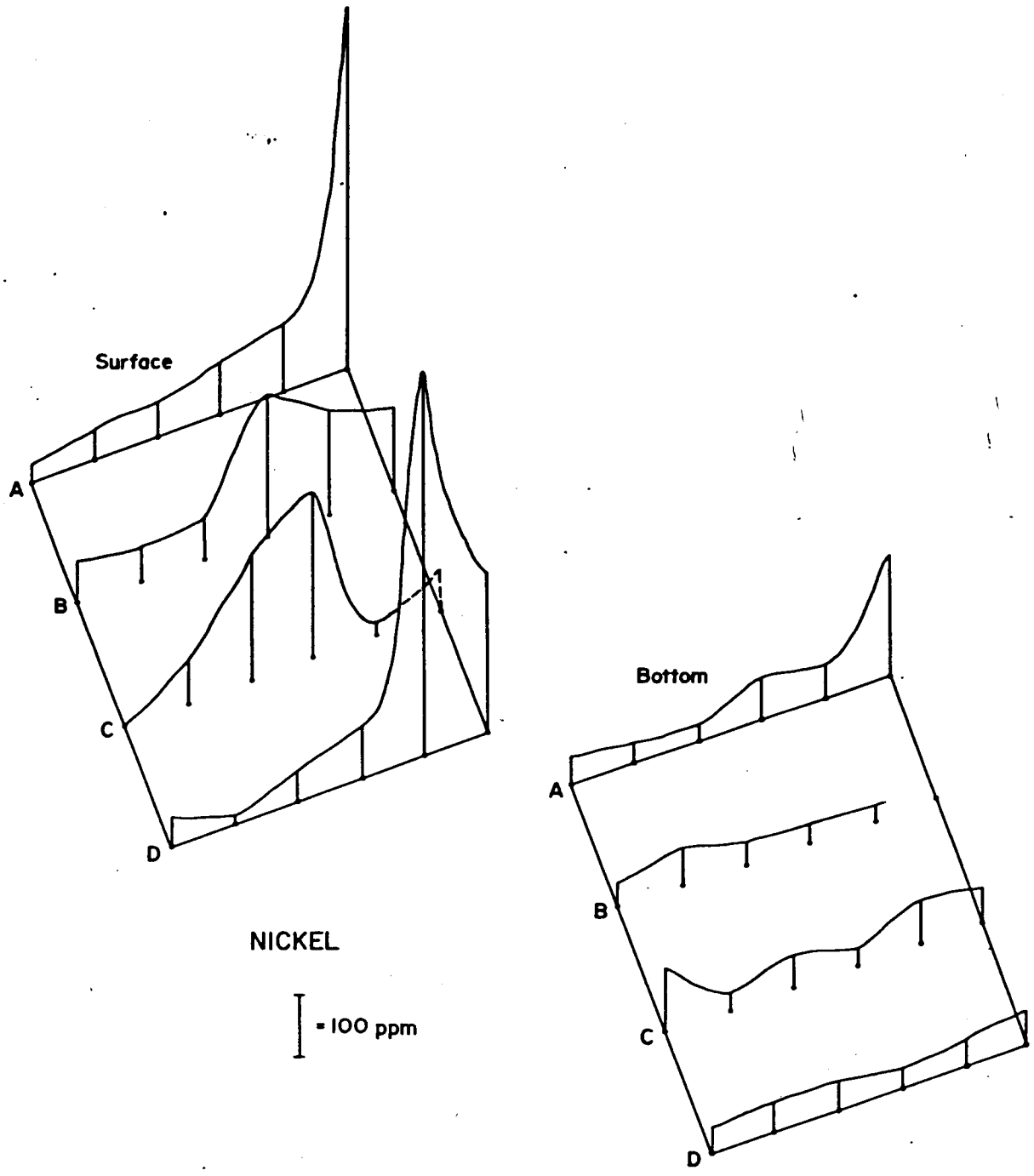

Figure 103. Areal distribution of nickel at surface and bottom levels. A, B, C, and D indicate the four sample transects from north to south.

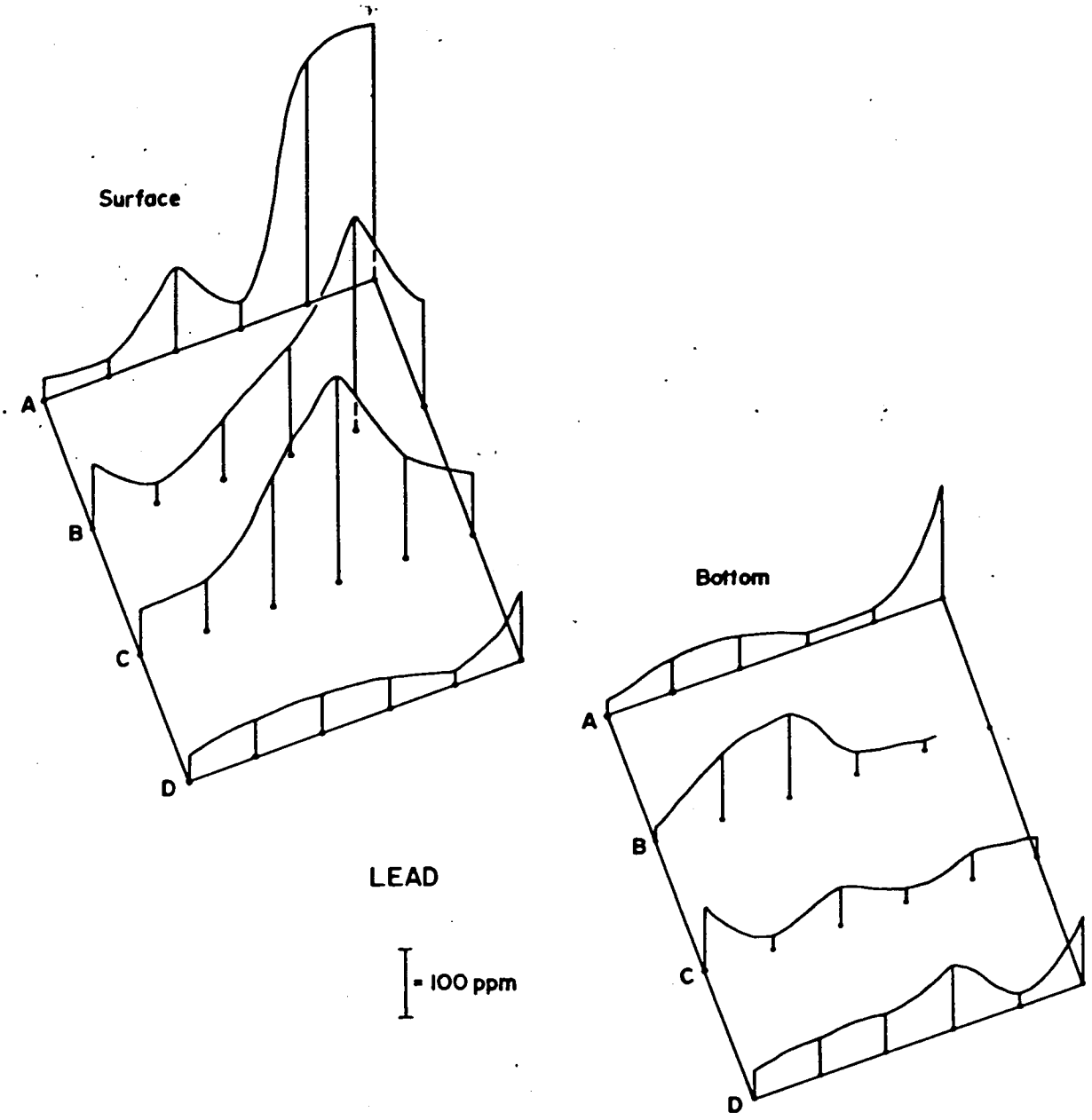

Figure 104. Areal distribution of lead at surface and bottom levels. A, B, C, and D indicate the four sample transects from north to south.

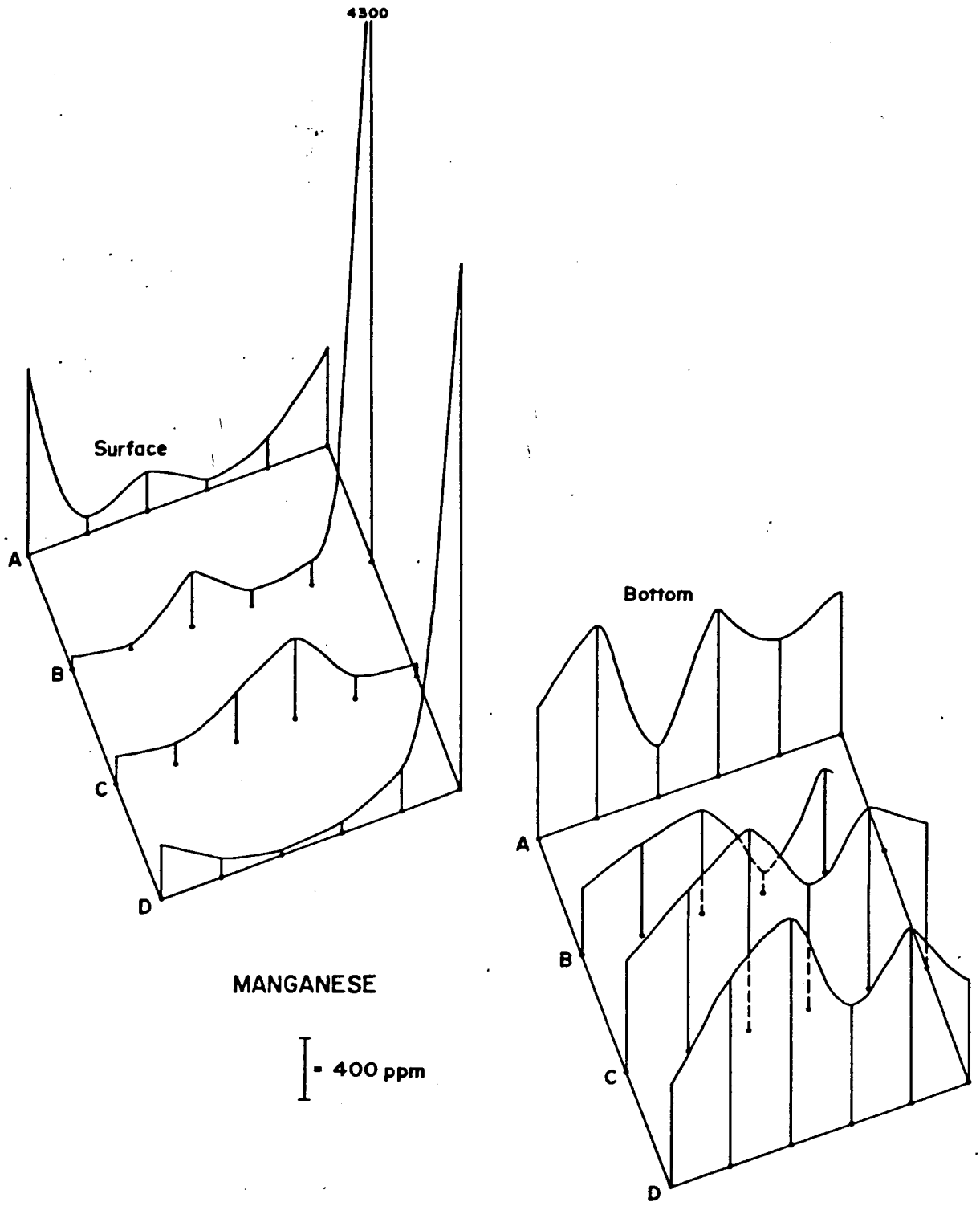

Figure 105. Areal distribution of manganese at surface and bottom levels. A, B, C, and D indicate the four sample transects from north to south.

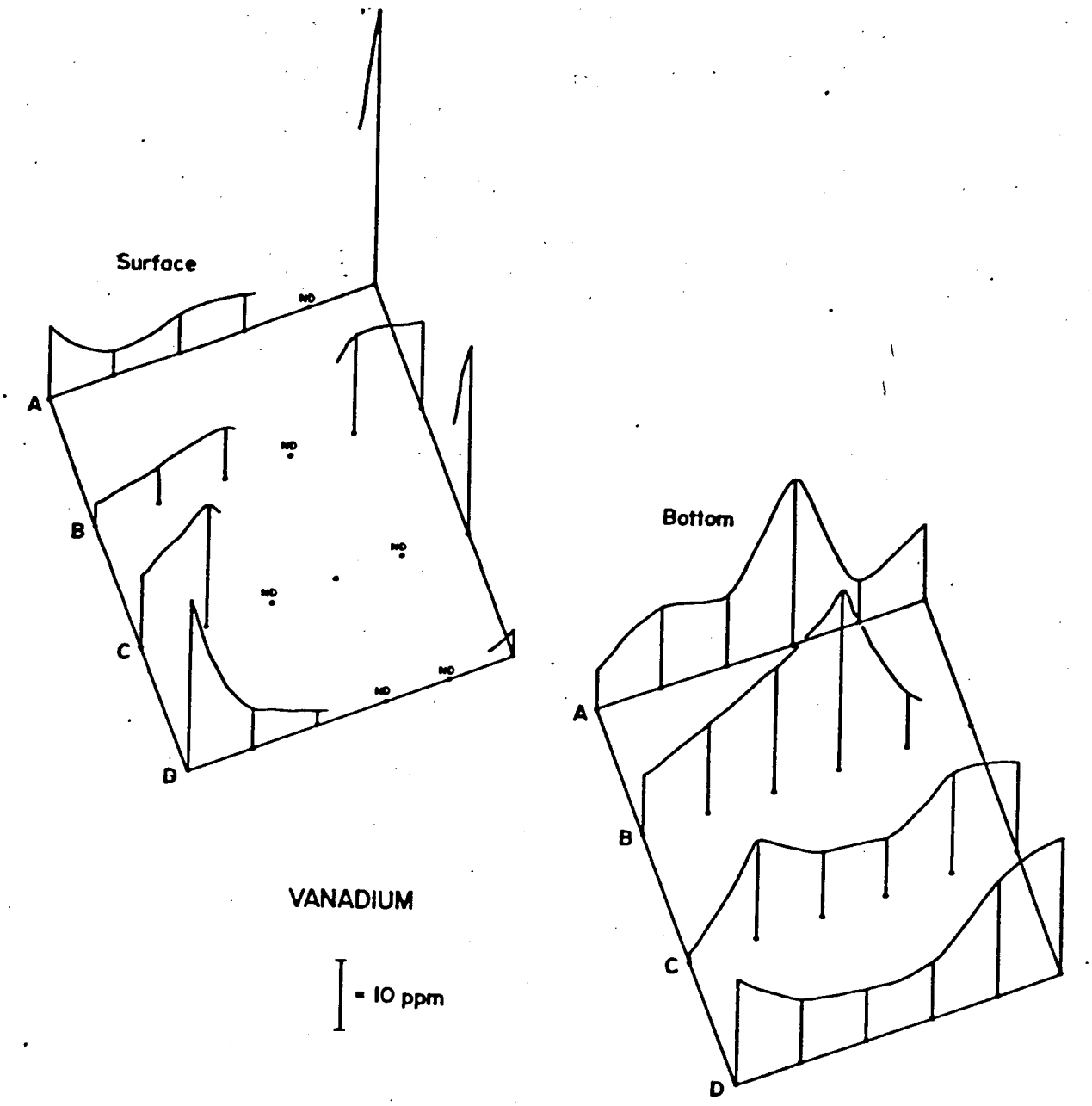

Figure 106. Areal distribution of vanadium at surface and bottom levels. A, B, C, and D indicate the four sample transects from north to south.

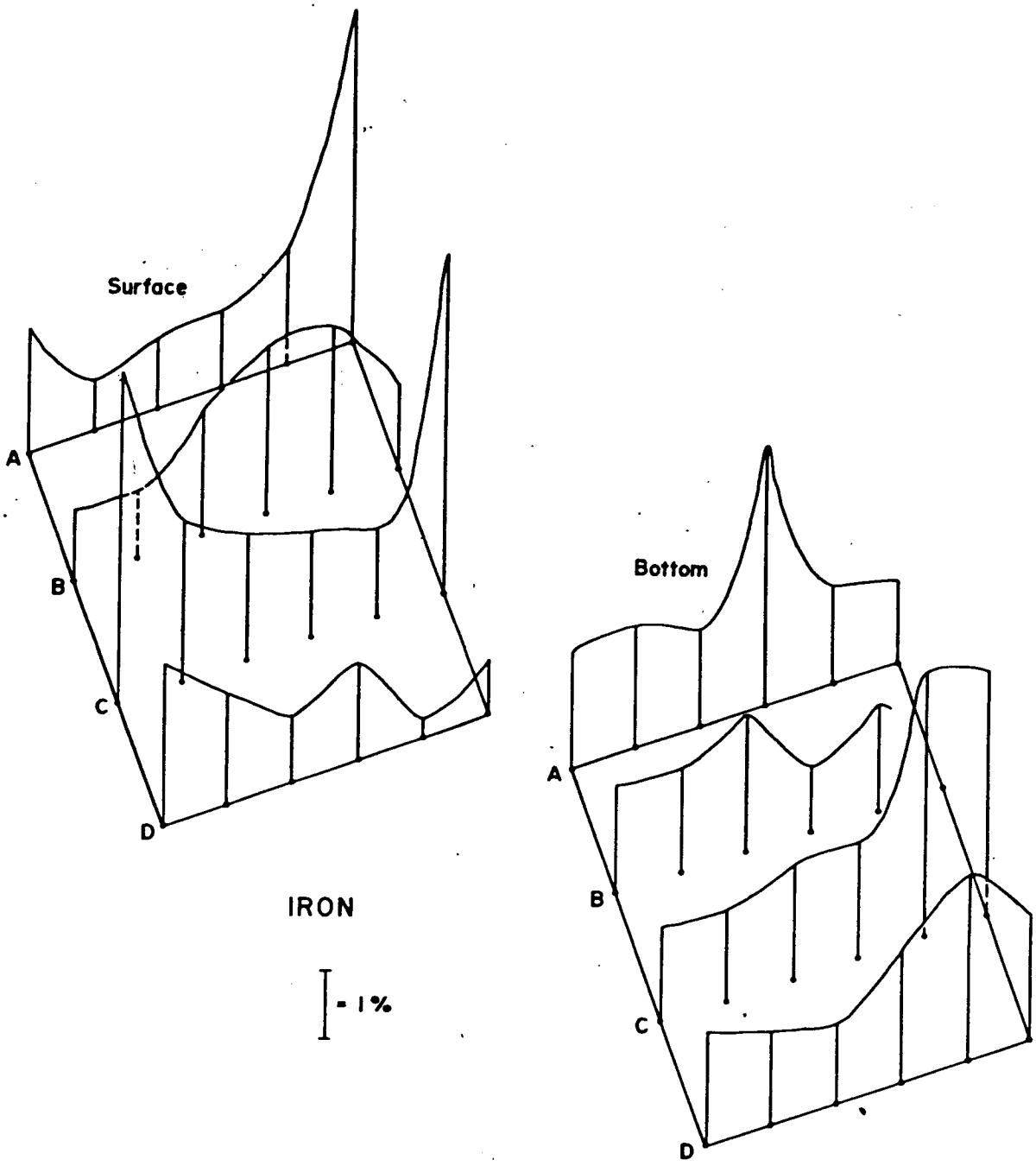

Figure 107. Areal distribution of iron at surface and bottom levels. A, B, C, and D indicate the four sample transects from north to south.

graphical representation of concentrations from station to station. The graphs indicate that the trace metal concentrations in bottom water suspended sediments is much more invariant than those of surface waters. The surface waters show an apparent higher ridge of metal concentrations offshore. Care should be used in drawing conclusions from this, however, because of the time span represented by the samples. Zinc concentrations were not graphed because the individual data points were not considered reliable.

In summary, trace metal concentrations in suspended sediments from the waters of the south Texas Continental Shelf show decidedly different patterns when the surface and bottom waters are compared. The bottom samples appear to be predominantly inorganic in nature, probably resuspended sediments, a situation found by Feely (1975) for the near-bottom nepheloid layer in areas of the Gulf of Mexico off the continental shelf. The surface samples show a greater variability probably because of the influence of biogenic material on the trace metal concentrations. The concentration maps can be used to establish background levels of trace metals in suspended metals from the South Texas Outer Continental Shelf if non-systematic concentration spikes are disregarded until further investigation shows them to be real and not contamination.

SEA FLOOR STABILITY

Sediment Strength

Surficial and shallow subsurface sediments of the South Texas OCS are typically fine grained, as indicated by the textural analyses: silt is the predominant grain size and coarse sand is absent. The discrete sand layers are thinner than the mud layers separating them, except over parts of the ancestral Rio Grande delta where pavements of relict sand are indicated. Characteristically, the sediments are soft rather than firm and compact. Although no tests were made to determine mass physical properties such as bearing and shear strength, the stability and strength of the near surface sediments can be deduced in general terms from the grain size variability within the sediments. The general range in grain size for the near surface sediments is shown by the sand/mud ratio map, figure 32. Bearing strength of the sediments can be assumed to be greatest in areas where the sand/mud ratio is higher than 1.00 and least in areas where the ratio is less than 0.12. The more unstable areas in terms of near-surface bearing strength are those where the textural gradients are steepest.

The nature of sediments below the depths cored to reflecting surface A (fig. 17 and pl. 4), as suggested by the acoustic profiles, probably is similar to the near-surface sediments over most of the South Texas OCS. Possible exceptions are: 1) the area of acoustically silent sediments indicated on figure 17 and plate 4; and 2) the basal deltaic deposits in the Holocene sequence over the northern part of the South Texas OCS where sand content may be higher (see fig. 17 and pl. 4 for location). As discussed previously, the prominence of reflector A on the acoustic profiles suggests that it represents a relatively firm subsurface. The depth of reflector A beneath the sea floor is shown on figure 17 and plate 4.

The only occurrences of lithified strata or rocks within the sequence above reflectors A and B seem to be the series of mound-shaped masses recorded on the acoustic profiles and mapped on figures 14 and 17 and on plates 3 and 4 as reefs. Those that project above reflector A and are exposed at the sea floor have been identified as carbonate reefs. Similar masses are at shallow subsea floor depth along reflector A and others more deeply buried are along reflector B. The reefs are thought to be associated with underlying barrier strandline deposits of probable high sand content and relatively competent bearing strength.

At somewhat greater depth is reflector B. Its strength as a sound reflector also suggests a relatively firm surface. Furthermore, if reflector A represents in part a surface of subaerial erosion, the sediments between reflector B and reflector A probably are more compact than those above reflector A.

Noted previously was the fact that reflector A cannot be identified in the acoustic profiles over the ancestral Rio Grande delta. Sediments there from reflector B upward are a series of fluvial-deltaic deposits. The relative portions of sand and mud with depth within the delta are not known, but the acoustic profiles indicate extensive channeling and development of foreset bedding. Consequently, the individual deposits of sand and mud likely are more discontinuous, lenticular and pod-shaped than elsewhere.

Slumping

Displacement of sediments by gravity sliding or slumping along the sea floor is restricted to the outer edge of the ancestral Rio Grande delta. The location of the area of unstable sediments is shown on figure 108. Within the area outlined, slumps of relatively large scale displacement are

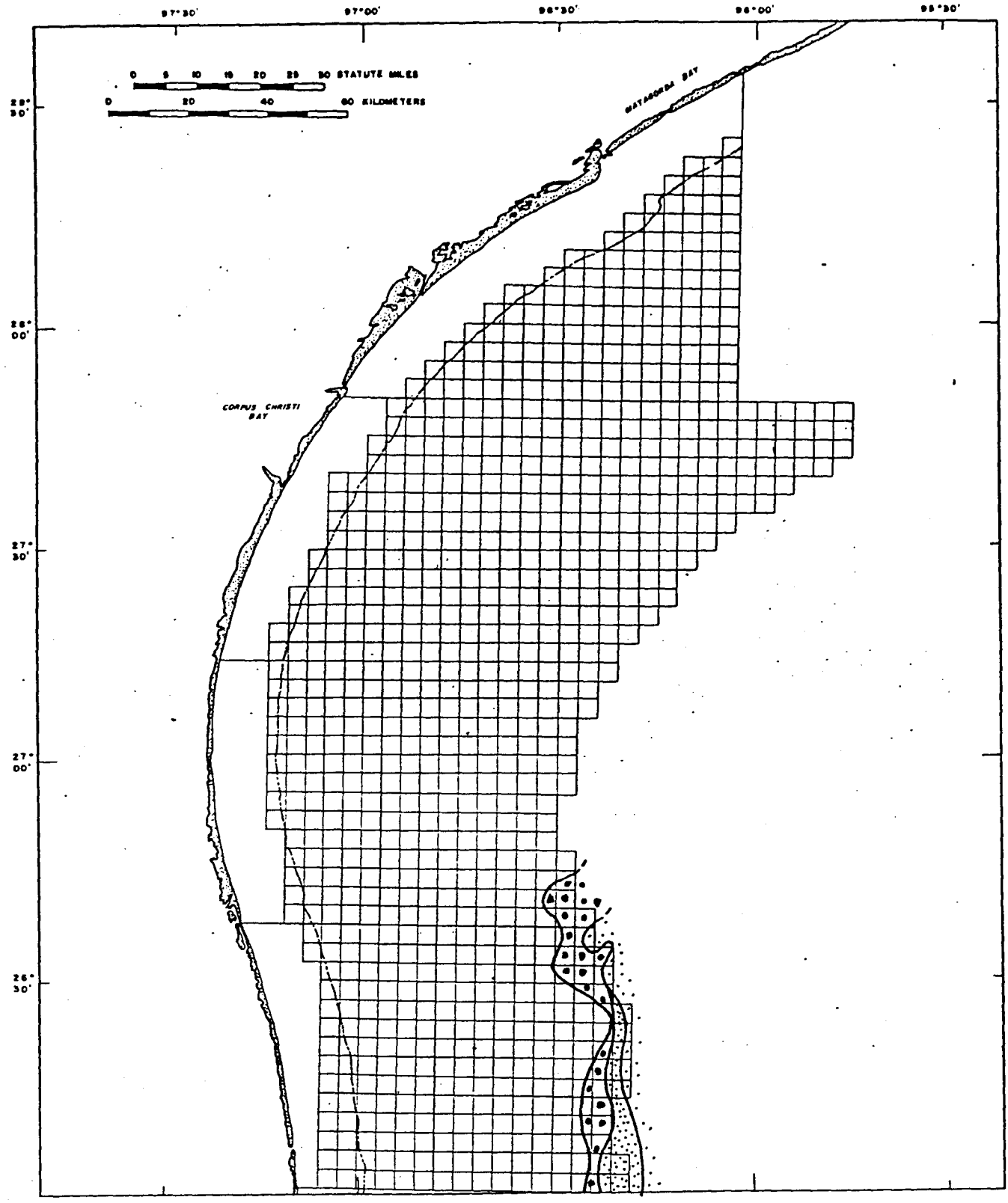

Figure 108. Areas of slumped sea floor sediments: widely spaced small stippling indicates area of large slumps on upper continental slope; closely spaced stippling indicates area of small slumps on the outer edge of the continental shelf; large dots indicate older slumped sediments underlying undisturbed younger deltaic deposits.

characteristic of the seaward part where the outer edge of the delta is coincident with the upper continental slope. Slumping typical of the upper slope is shown by figure 109. Incipient slumping of smaller scale is more typical of the brow of the delta at the outer edge of the continental shelf (fig. 110).

Landward and adjacent to the area of active slumping is a belt of older slumped sediments now covered by undeformed strata (fig. 108). These sediments were contorted by slumping when they occupied the peripheral margin of the ancestral delta. As the delta prograded seaward, the older slumped sediments were progressively covered by flat-lying delta plain sediments. An example of the relationship of the buried slumped sediments to the overlying undisturbed sediments is shown by figure 111. In places, the overlying undisturbed sediments are thinner than shown on the figure.

Within the area of buried slumped sediments are subsurface muds that have been rendered unstable by the progressive accumulation of overlying sediments. The weight of increasing overburden has caused the muds to flow under pressure. The muds are highly deformed and commonly extend upward as diapiric masses into overlying beds. An example of the mud diapirism is shown by figure 112.

Chronology of Faulting

Fault movement relative to the key reflecting surfaces A and B has progressed upward and outward across the continental terrace with time. The youngest faults are near the outer edge of the terrace with some exceptions. The geographic position of late Pleistocene/Holocene faulting relative to the stratigraphic position or geologic age of the strata affected is shown on figure 113 and plate 5.

Approximately the inner third of the shelf, except beneath the ancestral Rio Grande delta, has not been faulted during late Pleistocene time. The

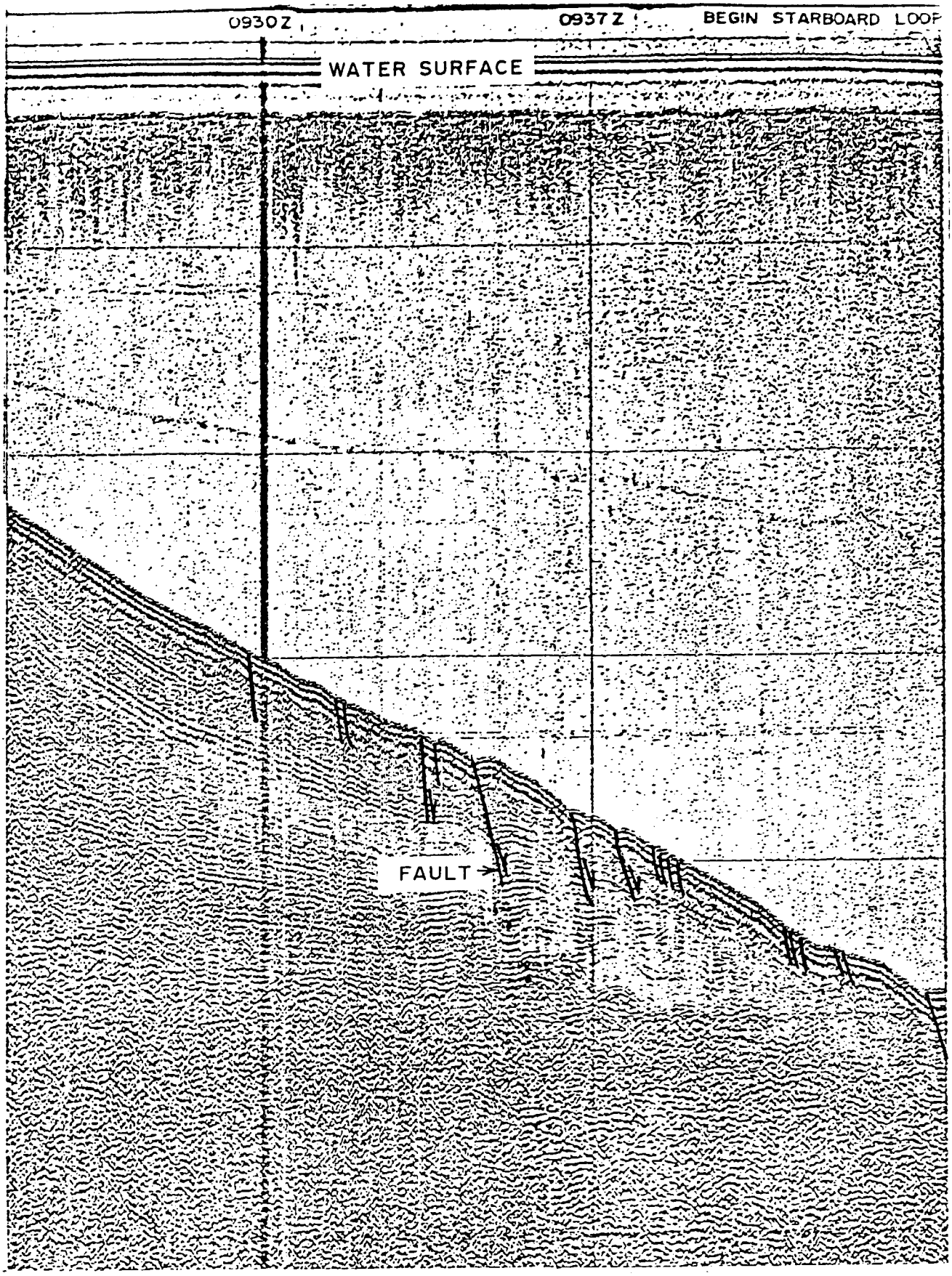

Figure 109. Section of acoustic profile showing large slumps on the upper continental slope. Horizontal scale between time marks in 610 m. Timing line interval (vertical) is 100 ms (~73m).

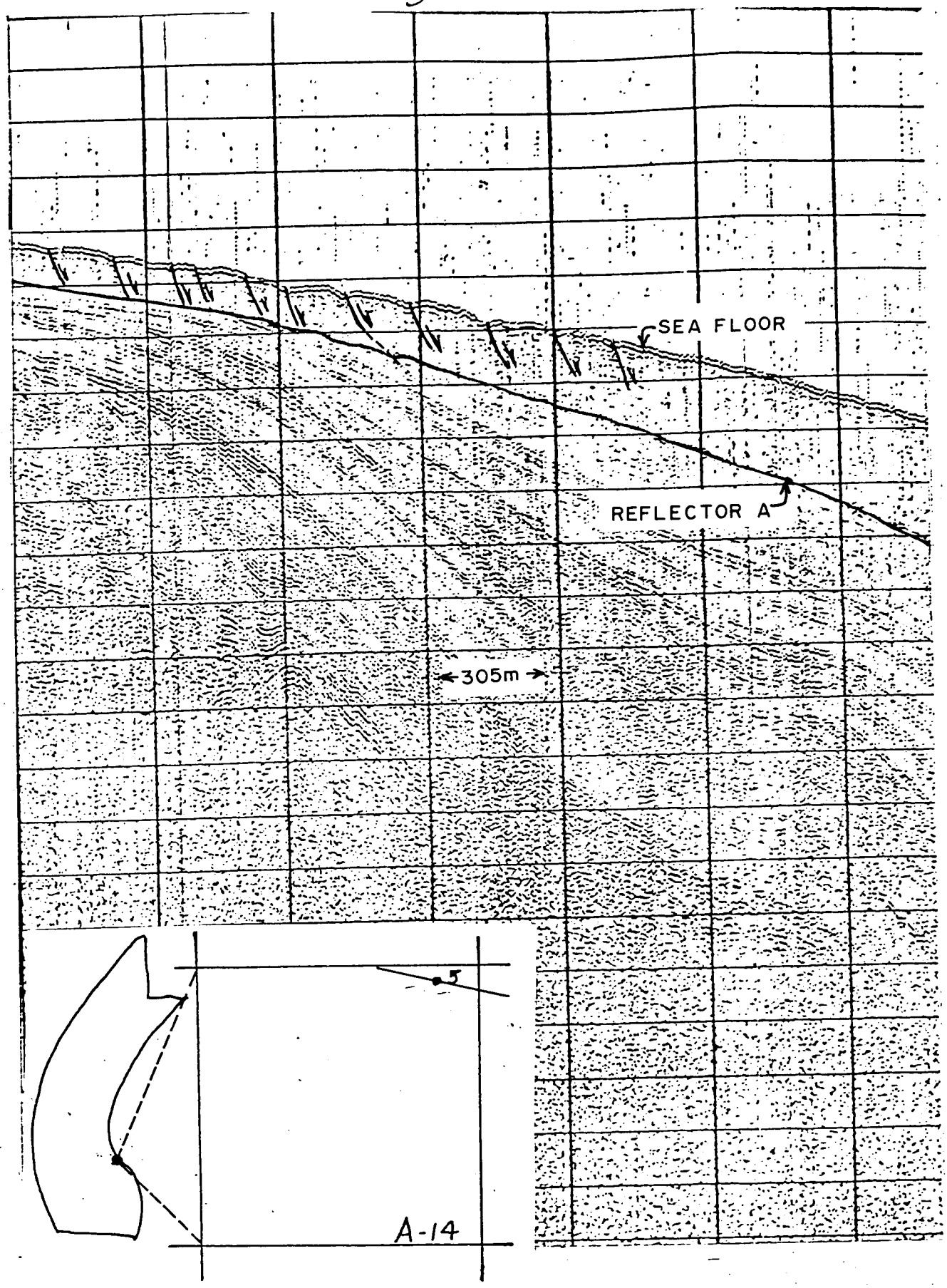

Figure 110. Section of acoustic profile showing small slump at edge of the continental shelf. Timing line interval (vertical) is 10 ms (~7.3 m).

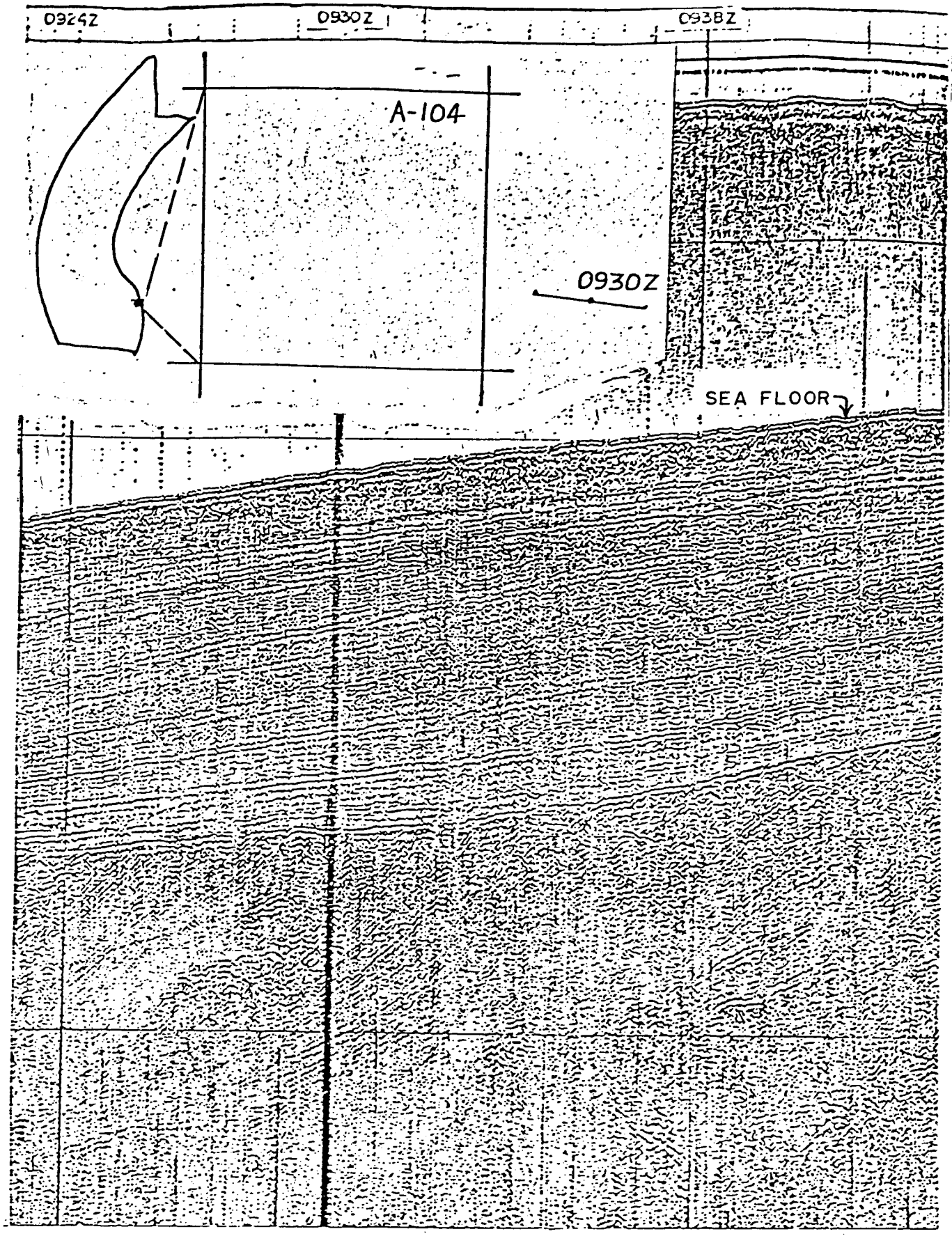

Figure 111. Older slumped sediments overlain by younger undisturbed sediments. Horizontal scale between time marks is 610 m. Timing line interval (vertical) is 100 ms (~73 m).

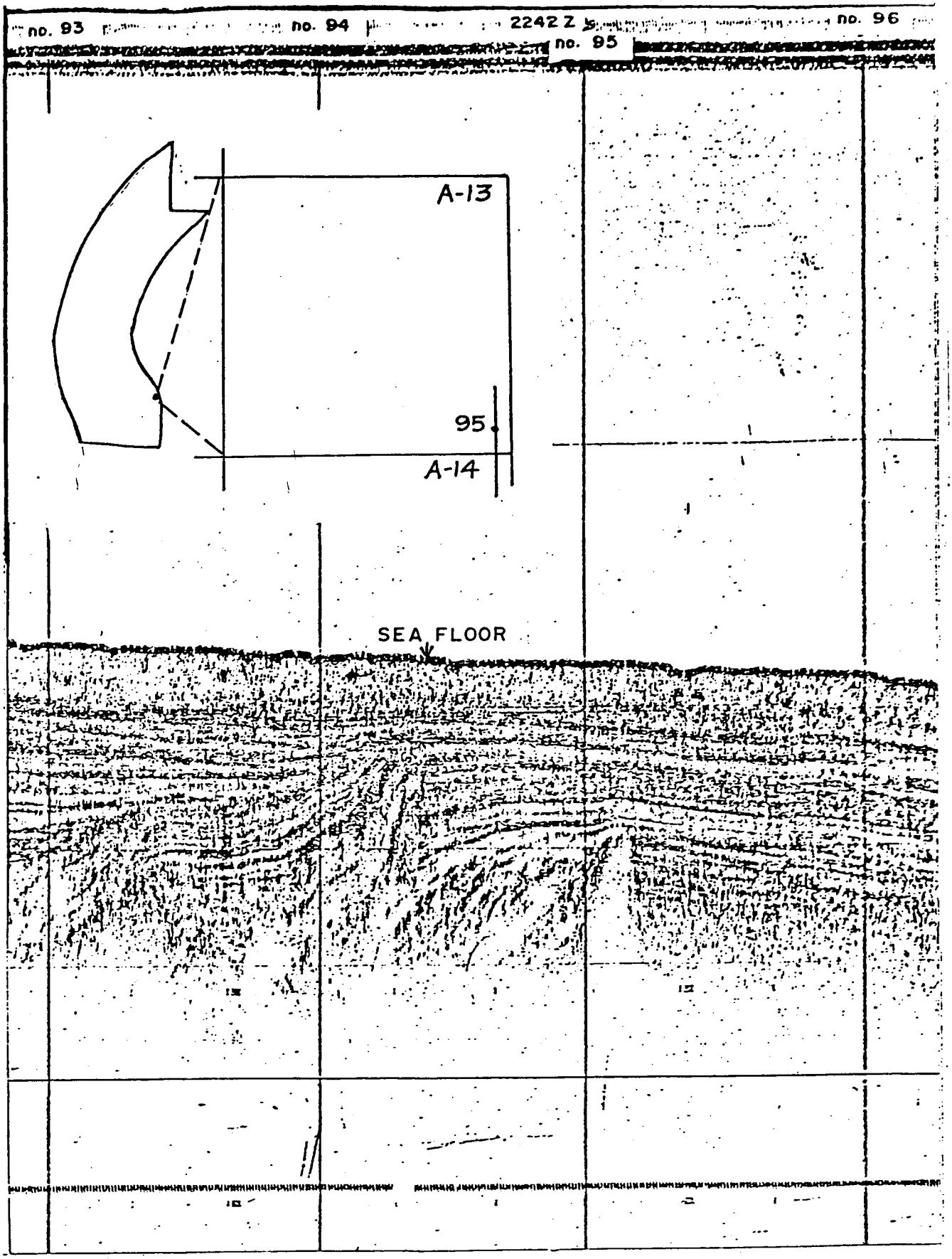

Figure 112. Section of an acoustic profile showing mud diapirs in deltaic sediments. Horizontal scale between shot points is 610 m. Timing line interval (vertical) is 100 ms (~73 m).

mid-shelf was extensively faulted in post reflector B time and the outer shelf to a lesser extent. The outer one-quarter to one-third of the shelf has been extensively faulted during Holocene time. The few faults that extend to the sea floor, excluding those associated with slumping, are at mid-shelf and near the outer edge of the shelf. See figure 113 and plate 5 for location of faults that extend to the sea floor.

The seaward migration of fault movement probably reflects response within the continental terrace to a combination of factors: the increasing load of accumulating sediments with time; progressive outbuilding of the continental terrace by the process of sedimentation; and a seaward shift in the movement along the folds within the terrace from mid to outer shelf. The folding probably reflects adjustments within the continental terrace to deeply buried mobile material: shale, salt or both.

Whether the movements indicated by the faults have progressed rather uniformly through time or whether they have been episodic is not known. Evidence for fairly extensive faulting over a relatively short period of time is suggested by the development of the crustal sag associated with reflector B. Perhaps the faulting represents a mix of both short and long term adjustments within the continental terrace. The history of faulting during late Pleistocene and Holocene times suggests that movements of a similar nature and pattern might occur in the future. The part of the shelf probably most susceptible to future movements is the outer third (fig. 114); however, the most recent faulting, though not intensive, has been scattered rather widely, indicating that the structural adjustments within the continental terrace, probably related to diapirism at depth, are not confined to the outer edge of the continental terrace.

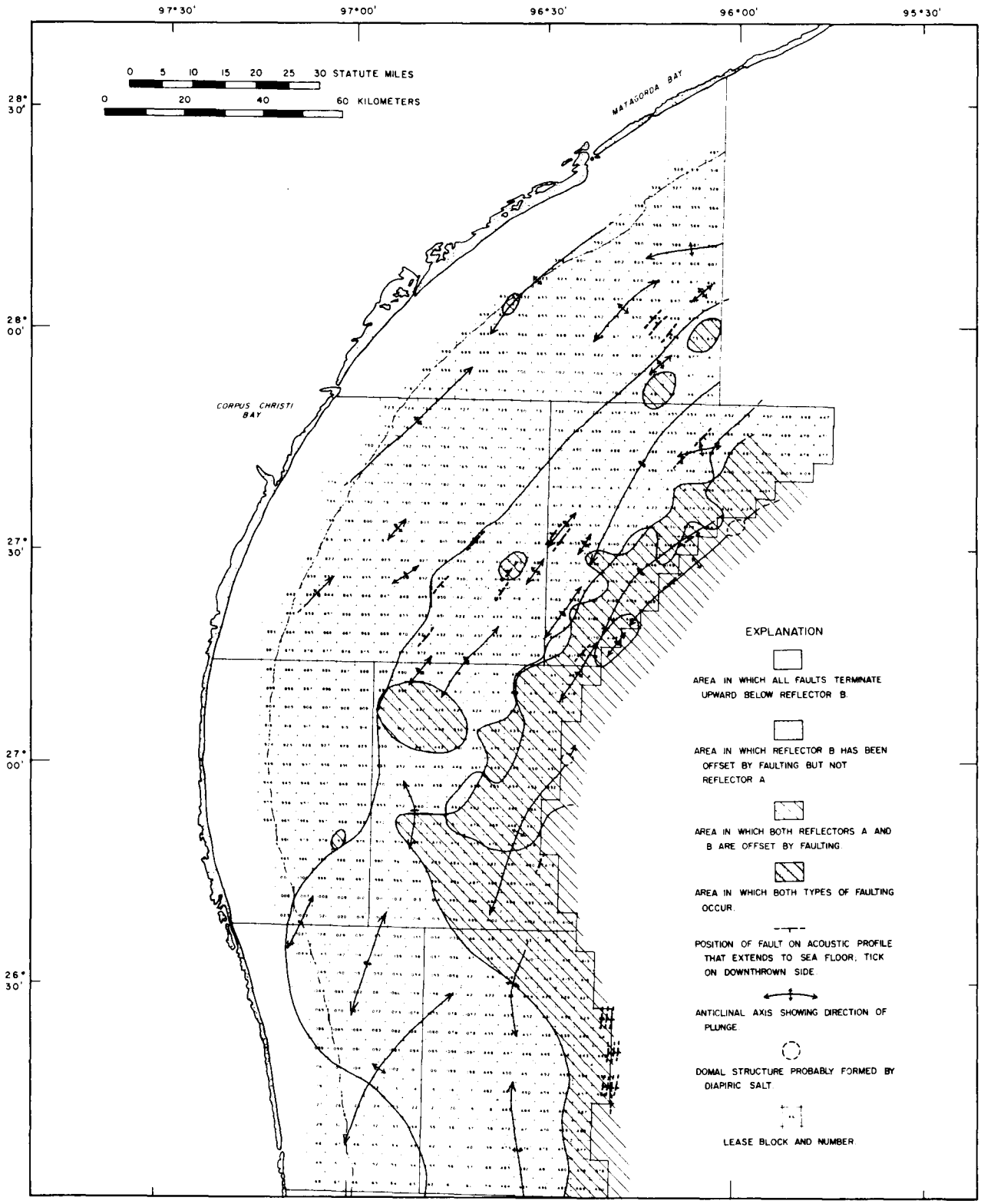

Figure 113. Chronology of faulting during late Pleistocene and Holocene times.

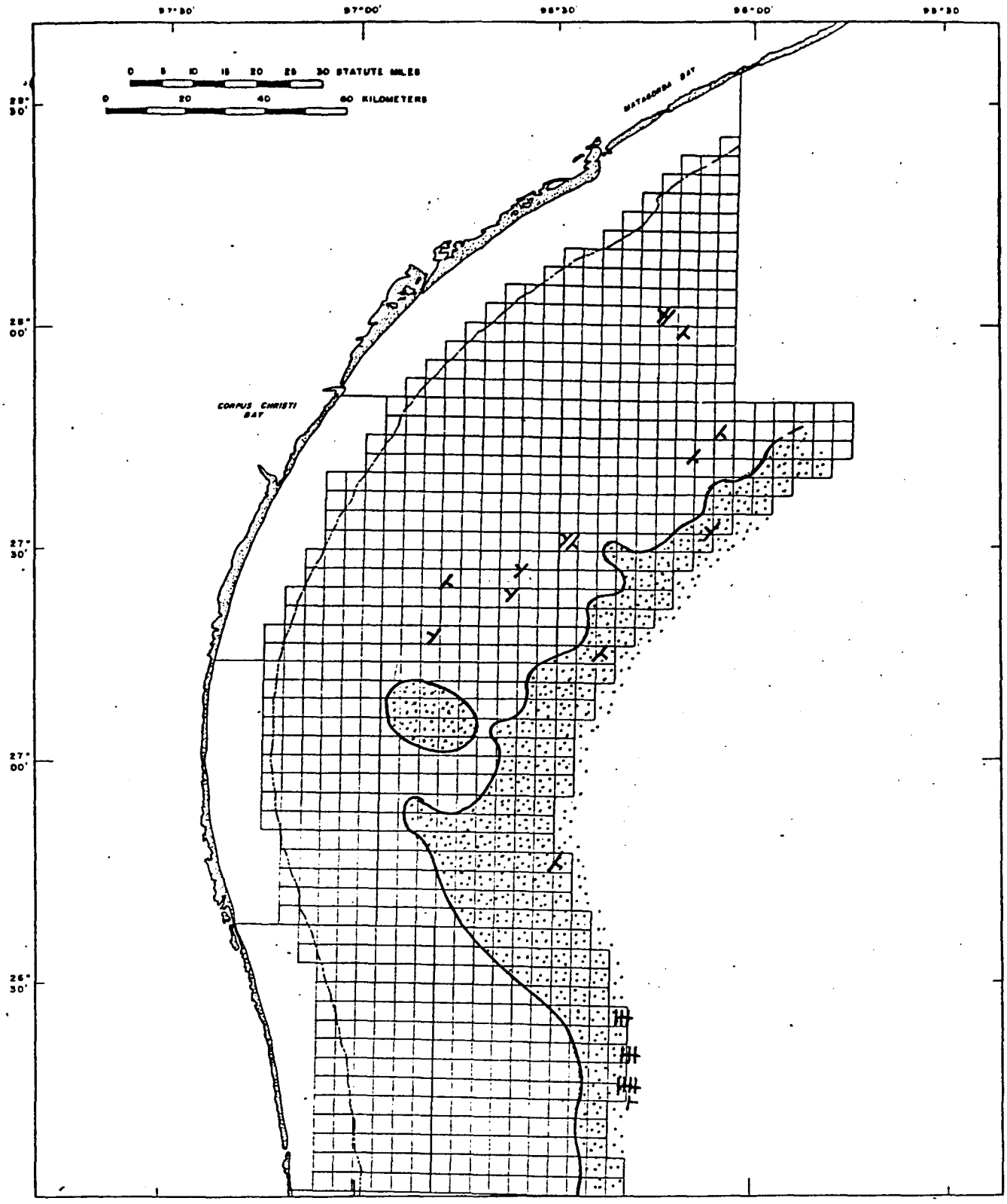

Figure 114. Areas of most recent faulting on the south Texas OCS. Stippled areas have been extensively faulted in Holocene time. Symbols indicate faults that extend upward to the sea floor. Ticks on bar indicate direction of downthrow.

SALIENT GEOLOGIC CHARACTERISTICS OF THE SOUTH TEXAS OUTER CONTINENTAL SHELF

GEOLOGIC FRAMEWORK

Summary

1. The primary geologic structures at depth within the continental terrace are a series of folds that trend generally northeastward. Extensive secondary geologic structures associated with the folds are numerous faults that tend to converge downward from above the anticlinal crests. Increased throw with depth along many of the fault planes indicates progressive movement through time. Consequently the faults terminate upward at varying depths beneath the surface of the sea floor. Faults offset sediments of latest Pleistocene and Holocene sediments extensively and a few extend to the surface of the sea floor.

2. A localized syncline of broad closure that trends southeastward across the southern third of the OCS is a cross structure imposed on the northeastward trend of the older and deeper lying folds. The origin of the fold is not known but the sag possibly was formed by basinward migration or flowage of deep-lying salt from beneath the continental shelf.

Implications

The geologic structures within the continental terrace have influenced sediment transport and depositional patterns during late Pleistocene and Holocene times. Formation of the southeastward-trending syncline in the southern part of the OCS diverted drainage of both the Rio Grande and rivers to the north along the coast and imposed a slight southward tilt on the

northern two-thirds of the South Texas OCS. The synclinal sag became a depocenter for the rivers along the coast and for sediments delivered to the shelf from farther north that migrated southward in response to the southward structural tilt of the shelf.

The influence of the structural sag on the depositional patterns on the shelf continued throughout the Holocene and almost to the present. Whether or not a minor influence is still being exerted is questionable. The acoustic profiles show a tongue or salient of mud that extends southward across the central part of the ancestral Rio Grande delta. The salient of transgressive mud represents the latest deposition over the delta and indicates net southward movement of sediment.

The folds within the continental terrace also have influenced the pattern of sediment movement in the past. During the last low stand of the sea when most of the shelf surface was land, tributary streams were established parallel to and between anticlinal folds. The configuration of the shoreline during the last low stand and the growth portion of the reefs may have been controlled in part by the location of the folds.

Throughout the span of geologic time represented by the sound analogs recorded on the acoustic profiles faulting has occurred along the crests of the anticlinal folds within the continental terrace.

SEA FLOOR SEDIMENTS

Summary

Surficial sediments--Texturally, the OCS sea floor is composed predominantly of mud. Quantitatively, the highly dominant mud component is the silt fraction, which appears to be effectively trapped hydraulically within the OCS environment. In contrast, the subordinate clay fraction appears to reflect a more

open dispersal system, with substantial clay detritus escaping into deeper Gulf environments. The majority of the OCS region can be classified as a clayey silt province. Sand detritus is quantitatively dominant only along the shoreface sector, and within portions of the ancestral Brazos-Colorado and Rio Grande deltas of the northern and southern sectors. Gravel detritus is quantitatively minor, and is concentrated mainly in the southern sector within the ancestral Rio Grande delta, as well as in the vicinity of isolated carbonate banks. The gravel fraction is composed almost entirely of biogenic materials; it consists mainly of molluscan shells, and occasional coral-algal reef debris in the vicinity of carbonate banks.

Textural variability is most pronounced in the ancestral delta regions of the northern and southern sectors, with transitions being most abrupt within the southern sector. Genetically, the textural variability indicates a composite fabric of modern, palimpsest, and relict sea floor deposits. The southern delta sector appears to be composed largely of relict Pleistocene-early Holocene deposits, which are characterized by relatively coarse textures, as well as high shell and heavy mineral concentrations; these sea floor sediments appear to be relatively immobile lag deposits which are in disequilibrium with modern hydraulic conditions. The variable deposits of the northern delta sector are also relatively coarse-textured; they appear to be composed largely of palimpsest or partially reworked sediments which are presently experiencing some net southward mass transport, thus reflecting a condition of partial hydraulic equilibrium. The central OCS sector constitutes a fine-sediment depocenter, and is relatively uniform lithologically. The sector contains an extensive blanket of modern mud sediment that appears to be experiencing some net southward mass transport, thereby encroaching upon relict deposits of the southern ancestral delta. The influx of modern mud into the OCS region appears

to reflect sediment contributions from multiple sources; the sources include coastal and shoreface erosion along the Padre Island barrier chain, suspended sediment effluent from adjacent estuaries, and possible in situ winnowing of relict and palimpsest deposits comprising the ancestral Rio Grande and Brazos-Colorado deltas.

Textural parameters exhibit consistent regional trends of increasing sediment coarseness shoreward, as well as both northward and southward from the central sector. The trends reflect a composite response to both ancient and modern processes. Ancient processes are reflected by the presence of the relict and palimpsest deposits comprising the ancestral deltas. The trends further suggest that regional energy and residual southward-flowing coastwise currents are among the dominant hydraulic factors controlling the modern sediment dispersal system. Net seaward diffusive transport, in conjuction with net southward advective transport, appear to be prominent mechanisms of sedimentation within the OCS region. The color variability of sea floor deposits suggests varying degrees of oxidation, possibly attributable to varying rates of sedimentation within the OCS region.

Shallow subsurface sediments--The stratigraphic variability of the shallow upper Holocene deposits exposed in the gravity cores indicates that the basic regional dispersal pattern exhibited by present sea floor sediments was initiated during earlier Holocene time. However, the relative proportions of sand and mud were different, with the sand facies being more widely distributed during the earlier Holocene. The cores illustrate a general westward displacement of the lithofacies pattern, thus indicating a stratigraphic overlap relationship developed during the late Holocene transgression.

The cores further suggest that the shallower, inner portion of the OCS region is the sector most intensely affected by the storm hydraulic regime.

Many discrete sand sedimentation units appear to reflect storm-generated deposits resulting from the seaward reflux of coastal waters following storm surges. Sand sedimentation units are most abundant in local areas adjacent to prominent coastal estuaries which appear to have been major sources of storm-reflux sediment.

Implications

1. The OCS sea floor is predominantly a mud province which might have a greater tendency for retention of industrial pollutants, as compared to a more permeable and aerated sandy province.
2. Areas of pronounced textural variability, such as the northern and southern delta sectors, would be more prone to differential compaction and subsidence. This could produce instability hazards associated with platform and pipeline construction. The probability of this particular hazard would tend to be greatest in areas of rapid textural transitions, such as within the southern Rio Grande delta sector.
3. The central OCS sector functions as a mud depocenter, a dispersal pattern that appears to have long persisted since earlier Holocene time. Therefore, this sector could also conceivably function as a receptacle for the long-term retention of any pollutants introduced into the sediment dispersal system.
4. The basic regional sediment transport patterns inferred from the sediment trends indicate a net offshore component, as well as a net southward component. If these inferred transport patterns are real and can be verified by physical oceanographic data, they could produce a net long-term concentration of pollutants toward the southern sector of the OCS region.

5. The seaward reflux of coastal waters following storm surges could be highly influential in the dispersal of pollutants along the shallower, inner portions of the OCS region, especially in proximity to prominent estuaries.

RATE OF SEDIMENTATION

The rate of sediment deposition during all of Holocene time appears to have been relatively high, exceeding a meter per thousand years locally. Previous reports on the surficial geology of the South Texas OCS have indicated either a relatively thin cover of Holocene sediments or have designated the surficial sediments as relict Pleistocene deposits.

The average thickness of the Holocene sequence, as interpreted from the geophysical data, is about 18 m. One aspect of the second year of study on the South Texas OCS has been designed to acquire data for determining rates of deposition during latest Holocene time, or for the uppermost several meters of sediment.

ANIMAL-SEDIMENT RELATIONSHIPS

Summary

1. The South Texas OCS is not homogeneous relative to distribution patterns of biological components. Generally, number of species and individuals, biomass, and diversity decrease with increasing water depth. Equitability increases across the shelf as water depth increases. The central sector has less dense and diverse infaunal populations than the general areas of the ancestral Rio Grande and Brazos-Colorado deltas to the south and north.
2. Five macrobenthic infaunal assemblages in the study area can be defined relative to species distribution and density, diversity-equitability and

biogenic sedimentary structures. The most dense and diverse assemblage (V) is located in the southwestern corner of the study area, while assemblages near the shelf's edge in the central sector show relatively low density and diversity.

3. Polychaeta, Arthropoda, and Mollusca are the dominant infaunal taxa. As water depth increases, the relative percentage of polychaete species and individuals decreases. In contrast, the number of molluscs species and individuals increase seaward. The number of arthropod species shows minor fluctuations across the shelf; the number of arthropod individuals significantly decreases with increasing water depth, primarily because of a large reduction in the number of amphipods.
4. Bioturbation, or modification of original depositional textures and structures in the sediments ranges in a systematic pattern from very high to very low. Diversity and density of biogenic structures decrease as mean grain size decreases.
5. Zonation of biogenic sedimentary structures generally parallel macrobenthic infaunal zonation and can be defined in terms of diversity, density, and distribution. Substrates with relatively high diversity and density of biogenic sedimentary structures are associated with macrobenthic infaunal assemblages characterized by higher numbers of species and individuals, larger biomass, and increased diversity. Distribution patterns of bioturbation are useful in identifying spatiotemporal variations in macrobenthic infaunal zonation.
6. Temporal variations in macrobenthic infaunal zonation have occurred over the last several thousand years. In general, density and diversity of macrobenthic infauna have increased over the study area.

7. Biologic-geologic-hydrologic relationships are important factors controlling macrobenthic infaunal zonations; in contrast interspecific relationships seem to be insignificant.
8. Overall, macrobenthic infaunal zonation in the South Texas OCS is best described as continuous, low grade and physically controlled. Sand-mud ratios and rates of deposition seem to be particularly important in controlling the diversity and density of macrobenthic infauna.
9. Macrobenthic infaunal zonation is helpful in determining regional distribution patterns of sediment facies, rates of sediment deposition and major changes in current patterns. A more detailed description of the significant benthic biological processes as they relate to the sedimentological processes operative over the South Texas OCS will be possible after all samples collected during the first year of study have been analyzed.

Implications

Relative to offshore petroleum development on the South Texas OCS, several environmental implications relative to the results of this study may be noted:

1. Because the most dense and diverse macrobenthic infaunal assemblages occur in shallower water and in the general area of the ancestral deltas of the Brazos-Colorado and Rio Grande rivers to the north and south respectively, the impact on infaunal populations resulting from man's activities would be greatest in those areas.
2. In the same sectors of the OCS noted above, where infaunal activity is greatest, the mixing of the sediment vertically occurs relatively rapidly as a result of the biologic activity. Any pollutants

introduced into these areas will be more readily worked downward into the muddy sediments. Consequently the probability of long-term retention and higher concentration of pollutants increases.

TRACE METALS CONTENT, SURFICIAL SEDIMENTS

1. As a regional pattern, the trace metals content of sediments in estuaries adjacent to the continental shelf are relatively higher than in the sediments of the OCS.
2. Compared to the average trace metals content for the South Texas OCS as a whole, only cadmium and manganese are significantly high. For several trace metals, including cadmium, the highest concentrations are in the area of suspected gas seeps along the outer edge of the shelf in the northeastern part of the OCS.
3. The suspected gas seeps appear to be emanating upward along fault planes and may be depositing trace metals in the sea floor sediments, thus explaining the higher concentrations of some trace metals there.
4. In the South Texas OCS, the average levels for all trace metals determined are lower than the average levels for the segment of the northwestern Gulf shelf immediately to the north. For the overall northern Gulf of Mexico continental shelf, the average levels within the South Texas OCS are comparable.

Knowledge of trace metals concentrations in sediments of other continental shelves of the United States is too scant to permit comparison with the shelf off south Texas.

SEA FLOOR STABILITY

1. The South Texas OCS is not a seismically active area. However, the folds and associated faults within the continental terrace indicate relatively

low-level, long-term and progressive movements, probably related to sediment accumulation and diapirism.

2. Fault movement, although more prevalent on the outer part of the shelf during Holocene time has not been restricted to that part of the shelf in more recent times.
3. Disturbance of sea floor sediments by slumping is restricted to the outer periphery of the ancestral Rio Grande delta.

REFERENCES

Beals, C. W., 1969, Vegetational change along altitudinal gradients: Science, v. 165, p. 981-985.

Beerbower, J. R., and Jordan, D., 1969, Application of information theory to paleontologic problems: Taxonomic diversity: J. Paleon, v. 43, no. 5, p. 1184-1198.

Betzer, P., 1975, Baseline Environmental Survey of the Mississippi, Alabama, Florida (MAFLA) Lease Areas. F. T. Manheim, (ed.) State University System of Florida Institute of Oceanography, St. Petersburg, Fla., p. 114 (unpublished).

Bostrom, K., Toensun, O., and Brohm, I., 1974, Plankton: its chemical composition and its significance as a source of pelagic sediments: Chemical Geology, v. 14, p. 255-272.

Boyer, P. S., 1970, Actuopaleontology of the larger invertebrates of the coast of Louisiana: Ph.D. Thesis, Rice University, 97 p.

Bray, J. R., and Curtis, J. T., 1957, An ordination of the upland forest communities of southern Wisconsin: Ecol. Monogr., v. 27, p. 325-349.

Briggs, J. C., 1974, Marine zoogeography: McGraw-Hill, New York. 475 p.

Bright, T. J., and Pequegnat, L. H., 1974, Biota of the West Florida Garden Bank: Univ. Tex. Biomed. Inst., Galveston and Gulf Publ. Co., Houston, Texas, 435 p.

Carver, R. E., 1971, Heavy mineral separation, in Carver, R. E. (Editor): Procedures in Sedimentary Petrology, John Wiley and Sons, Inc., N.Y., 653 p.

Cerame-Vivas, M. J., and Gray, I. E., 1966, The distributional patterns of benthic invertebrates of the continental shelf off North Carolina: Ecology, v. 47, no. 2, p. 260-270.

Cronan, D. S., 1972, Skewness and kurtosis in polymodal sediments from the Irish Sea: Jour. Sed. Petrology, v. 42, p. 102-106.

Curray, J. R., 1960, Sediments and history of Holocene transgression, continental shelf, Northwest Gulf of Mexico, in Shepard, et al. (Editors), Recent Sediments, Northwest Gulf of Mexico, AAPG, Tulsa, 394 p.

Dall, W. H., 1889, A preliminary catalogue of the shell-bearing marine mollusks and brachiopods of the southeastern coast of the United States, with illustrations of many of the species: Bull. U.S. Nat. Mus., v. 37, 229 p.

Day, J. H., Field, J. G., and Montgomery, M., 1971, The use of numerical methods to determine the distribution of the benthic fauna across the continental shelf of North Carolina: J. Anim. Ecol. v. 40, p. 93-126.

Duane, D. B., 1964, Significance of skewness in recent sediments, Western Pamlico Sound, North Carolina: Jour. Sed. Petrology, v. 34, p. 864-874.

Feely, R. A., 1975, Major-element composition of the particulate matter in the near bottom nepheloid layer of the Gulf of Mexico. Marine Chemistry, v. 3, p. 121-156.

Field, J. G., and McFarlane, 1968, Numerical methods in marine ecology. I. A. quantitative 'similarity' analysis of Rocky Shore samples in False Bay, South Africa: Zool. Afr. v. 3, p. 9-138.

Field, J. G., 1969, The use of the information statistic in the numerical classification of heterogeneous systems: J. Ecol. v. 57, p. 564-569.

_____, 1970, The use of numerical methods to determine benthic distribution patterns from dredgings in False Bay: Trans. R. Soc. Afr. v. 39, p. 183-200.

_____, 1971, A numerical analysis of changes in the soft-bottom fauna along a transect across False Bay, South Africa: J. Exp. Mar. Biol. Ecol. v. 7, no. 3, p. 214-244.

Firek, F. Shideler, G. L., and Fleischer, P., in prep., Heavy Mineral Variability in Bottom Sediments of the Lower Chesapeake Bay, Virginia.

Fisher, P. 1880-1887, Manuel de conchylioligie et de paleotologie conchyliologique ou histoire naturelle de mollusques vivants et fossils, 1367 p.

Fisher, R. A., Corbet, A. S., and Williams, C. B., 1943. The relation between the number of species and the number of individuals in a random sample of an animal population: J. Anim. Ecol. v. 12, p. 42-58.

Folk, R. L., and Ward, W. C., 1957, Brazos River bar, a study in the significance of grain size parameters: Jour. Sed. Petrology, v. 27, p. 3-26.

Folk, R. L., 1965, Petrology of Sedimentary Rocks, Hemphill's, Austin, 159 p.

_____, 1966, A review of grain-size parameters: Sedimentology, v. 6, p. 73-93.

Frey, R. W., 1971, Ichnology - the study of fossil and recent lebbensspuren, in Perkins, B. F. (ed.). Trace Fossils Soc. Eco. Paleo. and Mineralogists Field Guide. School of Geoscience, Louisiana State Univ. Misc. Pub., v. 71-1, p. 91-125.

_____, 1973, Concepts in the study of biogenic sedimentary structures, J. Sed. Pet. v. 43, no. 1, p. 6-19.

Friedman, G. M., 1967, Dynamic processes and statistical parameters compared for size frequency distribution of beach and river sands: Jour. Sedimentary Petrology, v. 37, p. 327-354.

Gibson, L. B., 1966, Some unifying characteristics of species diversity: Contrib. Cushman Found. Foram. Res. v. 17, p. 117-124.

Gleason, H. A., 1939, The individualistic concept of the plant association: Am. Midland Nat. v. 21, p. 92-110.

Goddard, E. N., Trask, P. D., DeFord, R. K., Rove, O. N., Singewald, J. T., and Overbeck, R. M., 1970, Rock-color chart: Geol. Soc. America.

Gunter, G., 1950, Seasonal population changes of certain invertebrates of the Texas coast, including the commercial shrimp: Publ. Inst. Mar. Sci. v. 1, no. 2, p. 7-52.

Hayes, M. O., 1967, Hurricanes as geologic agents: Case studies of hurricanes Carla, 1961, and Cindy, 1963: Texas Bureau of Economic Geology, Rept. Invest. no. 61, 54 p.

Hedgpeth, J. W., 1953, An introduction to the zoogeography of the Gulf of Mexico with reference to the invertebrate fauna: Publ. Inst. Mar. Sci. v. 3, no. 1, p. 101-224.

Hendrickson, J. A., Jr., and Ehrlich, P. R., 1971, An expanded concept of "species diversity". Notulae Naturae, no. 439, 6 p.

Hildebrand, H. H., 1954, A study of the brown shrimp (Penaeus aztecus Ives) grounds in the western Gulf of Mexico: Publ. Inst. Mar. Sci., v. 3, no. 2, p. 233-366.

Hill, G. W., 1974, Macrobenthos zonation in relation to sediment facies on the Gulf of Mexico inner shelf, northern Padre Island, Texas: Am. Assoc. Pet. Geol., Ann. Mtg. Abstracts, v. 1, p. 45.

Holland, J. S., Maciolik, N. J., Kalke, R. D., Oppenheimer, C. H., 1974, A benthos and plankton study of Corpus Christi, Copano and Aransas Bay System: Second Annual Report to the Texas Water Development Board. 121 p.

Howard, J. D., Frey, R. W., and Reineck, H. E., 1972. Georgia coastal region, Sapelo Island, U.S.A.: Sedimentology and biology, Senckenbergiana maritima, v. 4, 223 p.

Howard, J. D. and Reineck, H. E., 1972, Georgia coastal region, Sapelo Island, U.S.A. : Sedimentology and biology, IV. Physical and biogenic sedimentary structures of the nearshore shelf. Senckenbergiana maritima, v. 4, p. 81-124.

Hughes, R. N. Peer, D. L., and Mann, K. H., 1972. Use of multivariate analysis to identify functional components of the benthos in St. Margaret Bay, Nova Scotia: Limnol. Oceanogr. v. 17, no. 1, p. 111-121.

Hughes, R. N., and Thomas, M. L. H., 1971a, Classification and ordination of benthic samples from Bedeque Bay, an estuary in Prince Edward Island, Canada: Mar. Biol. v. 10, no. 3, p. 227-235.

_____, 1971b, The classification and ordination of shallow-water benthic samples from Prince Edward Island, Canada: J. Exp. Mar. Biol. Ecol. v. 7, p. 1-39.

Hulbert, S. H., 1971, The nonconcept of species diversity: A critique and alternative parameters. Ecology, v. 52, p. 577-586.

Hulings, N. C., 1955, An investigation of the benthic invertebrate fauna from the shallow waters of the Texas coast. Masters Thesis, Texas Christian University, 88 p.

Hunter, R. E., Watson, R. L., Hill, G. W., and Dickinson, K. A., 1972. Modern depositional environments and processes, northern and central Padre Island, Texas, in Tench, R. N., and W. D. Hodgen (eds.). Padre Island National Seashore Field Guide. Gulf Coast Assoc. Geol. Soc. Ann. Mtg., v. 1, 27 p.

Hutchenson, K., 1970, A test for comparing diversities based on the Shannon Formula: J. Theor. Biol. v. 29, p. 151-154.

Johnson, C. W., 1934, List of marine Mollusca of the Atlantic coast from Laborador to Texas: Proc. Bost. Soc. Nat. Hist. v. 40, no. 1, p. 1-204.

Johnson, D. W., 1919, Shore Processes and Shoreline Development: John Wiley, N. Y., 584 p.

Johnson, R. G., 1970, Variations in diversity within benthic communities: Am. Naturalist, v. 104, p. 285-300.

_____, 1971, Conceptual models of benthic marine communities: in Schopf, T. J. M. (ed.), Models in Paleobiology, Freeman, Cooper and Co., San Francisco, p. 148-159.

Jones, M. L., 1961, A quantitative evaluation of the benthic fauna off Point Richmond, California: Univ. Calif. Publs. Zool. v. 67, no. 3, p. 219-320.

Kennedy, E. A., 1959, A comparison of the molluscan fauna along a transect extending from the shoreline to a point near the edge of the Texas continental shelf. Masters Thesis, Tex. Christian Univ., 136 p.

Klopfer, P. H., 1959, Environmental determinants of faunal diversity: Am. Naturalist, v. 93, p. 337-342.

Kolpak, R. L. and Bell, S. A., 1968, Gasometric determination of carbon in sediments by hydroxide absorption: Jour. Sed. Petrology, v. 38, p. 617-620.

Kritzler, H., and Vittor, B., 1975, Baseline environmental survey of the Mississippi, Alabama, Florida (MAFLA) lease areas: Manheim, F. T., (ed.), State University System of Florida, Institute of Oceanography, St. Petersburg, Fla., 127 p. (unpublished).

Krumbein, W. C., 1934, Size frequency distributions of sediments: Jour. Sed. Petrology, v. 4, p. 65-77.

Lloyd, M., and Ghelardi, R. J., 1964, A table for calculating the "Equitability" component of species diversity: J. Anim. Ecol. v. 33, p. 217-227.

MacArthur, R. H., 1957, On the relative abundance of species: Proc. Nat. Acad. Sci., v. 43, p. 293-295.

MacArthur, R. H., and Wilson, E. O., 1967, The theory of island biography: Princeton Univ. Press, 203 p.

Margalef, R., 1957, La teoria de la informacion en ecologia Memorias de la real academia de ciencias y artes (Barcelona) v. 33, p. 373-449.

_____, 1958, Information theory in ecology: Gen. Sys. v. 3, p. 36-71.

Mason, C. C., and Folk, R. L., 1958, Differentiation of beach, dune, and aeoloan flat environments by size analysis: Mustang Island, Texas: Jour. Sed. Petrology, v. 28, p. 211-226.

Mills, E. L., 1969, The community concept in marine zoology with comments on contunua and instability in some marine communities: A review: J. Fish Res. Board Can. v. 26, p. 1415-1428.

Moore, D. R., 1958, Notes on Blanquilla Reef, the most northerly coral formation in the western Gulf of Mexico: Publ. Inst. Mar. Sci. v. 5, p. 151-155.

Moss, A. J., 1963, The physical nature of common sandy and pebbly deposits. Part II: Amer. Jour. Sci., v. 261, p. 297-343.

Odum, E. P., 1959, Fundamentals of Ecology. W. B. Saunders Col., Philadelphia, 546 p.

Orloci, L., 1967, Data centering: A review and evaluation with reference to component analysis: Syst. Zool. v. 16, p. 208-212.

Paine, R. T., 1966, Food web complexity and species diversity. Am. Naturalist, v. 100, p. 65-75.

Parker, R. H., and Curray, J. R., 1956, Fauna and bathymetry of banks on continental shelf, northwest Gulf of Mexico: Am. Assoc. Pet. Geol. Bull. v. 40, no. 10, p. 2428-2439.

Parker, R. H., 1956. Macro-invertebrate assemblages as indicators of sedimentary environments in east Mississippi Delta Region: Am. Assoc. Petroleum Geologists Bull. v. 40, no. 2, p. 295-376.

_____, 1960, Ecology and distributional patterns of marine macroinvertebrates, northern Gulf of Mexico, p. 307-337 in Shepard, F. P., F. B. Phleger, and T.H. van Andel (eds.). Recent sediment, northern Gulf of Mexico: Am. Assoc. Pet. Geol., Spec. Publ., Tulsa, Okla., 394 p.

Pettijohn, F. J., 1957, Sedimentary Rocks: Harper & Brothers, n. Y., 718 p.

Pianka, E. R., 1966, Latitudinal gradients in species diversity: A review of concepts. Am. Naturalist, v. 100, p. 33-46.

Pulley, T. E., 1952a, An illustrated checklist of the marine mollusks of Texas: Tex. J. Sci. v. 2, p. 167-199.

_____, 1952b, A zoogeographic study based on the bivalves of the Gulf of Mexico: Ph.D. Dissertation, Harvard Univ. 215 p.

Rehder, H. A., 1954, Mollusks, p. 469-474 in Galtsoff, P. (ed.). The Gulf of Mexico, its origin, waters and marine life. U.S. Fish Bull. v. 55, no. 89, 604 p.

Rezak, R., and Edwards, G. S., 1972, Carbonate sediments of the Gulf of Mexico, p. 263-280 in Rezak, R. and V. J. Henry (eds.). Contributions on the geological and geophysical oceanography of the Gulf of Mexico: Texas A&M Univ. Ocn. Stud. v. 3, 303 p.

Robertson, D. E., 1968, Role of contamination in trace element analysis of sea water: Analytical Chemistry, v. 40, p. 1067-1072.

Sanders, H. L., 1968, Marine benthic diversity, A comparative study: Am. Naturalist, v. 102, no. 925, p. 243-282.

_____, 1969, Benthic marine diversity and stability-time hypothesis. Brookhaven Symposium in Biology No. 22, Diversity and Stability in Ecological Systems, p. 71-81.

Sanders, H. L., and Hessler, 1969, Ecology of the deep-sea benthos: Science, v. 163, p. 1419-1424.

Santos, S. L., and Simon, J. L., 1974. Distribution and abundance of the polychaetous annelids in a south Florida estuary: Bull. Mar. Sci., v. 24, no. 3, p. 669-689.

Schlee, J., 1966, A modified Woods Hole rapid sediment analyzer: Jour. Sed. Petrology, v. 36, p. 403-413.

Shannon, C. E., and Weaver, W., 1963, The mathematical theory of communication: Univ. Illinois Press, Urbana, 117 p.

Shepard, F. P., 1954, Nomenclature based on salt-silt-clay ratios: Jour. Sed. Petrology, v. 24, p. 151-158.

Shepard, F. P., Phleger, F. B., and van Andel, Tj. H. (Editors), 1960, Recent Sediments, Northwest Gulf of Mexico, AAPG, Tulsa, 394 p.

Shideler, G. L., in press, A comparative appraisal of electronic and pipette techniques in routine mud analysis. Sedimentology.

Sommerfeld, M. R., Love, T. D., and Olsen, R. D., 1975, Trace metal contamination of disposable pipette tips. Atomic Absorption Newsletter, v. 14, p. 31.

Spencer, D. W., 1963, The interpretation of grain-size distribution curve of clastic sediments: Jour. Sed. Petrology, v. 33, p. 180-190.

Stanley, D. J., 1969, Atlantic continental shelf and slope of the United States - color of marine sediments: U.S. Geol. Survey Prof. Paper 529-D, 15 p.

Stanton, R. J., and Evans, I., 1971, Environmental controls of benthic macrofaunal patterns in the Gulf of Mexico adjacent to the Mississippi Delta. Gulf Coast Assoc. Geol. Socs. Trans., v. 21, p. 371-378.

_____, 1972. Recognition and interpretation of modern molluscan biofacies, in Contributions on the geological and geophysical oceanography of the Gulf of Mexico. Texas A&M Oceanogr. Stud. v. 3, p. 203-222.

Stanton, R. J., 1973, Diversity: Texas A&M Univ. unpublished report, 19 p.

Stephenson, W., Williams, W. T., and Lance, F. N., 1970, The macrobenthos of Moreton Bay: Ecol. Monogr. v. 40, no. 4, p. 459-494.

Swift, D. J. P., Stanley, D. J., and Curray, J. R., 1971, Relict sediments on continental shelves: a reconsideration: Jour Geology, v. 79, p. 322-346.

Swift, D. J. P., Ludwick, J. R., and Boehmer, W. R., 1972, Shelf sediment transport: a probability theory, in Swift et al (editors) Shelf Sediment Transport: Process and Pattern, Dowden, Hutchinson & Ross, Stroudsburg, Pa., 656 p.

Tryon, G. W., 1882-1884, Structural and systematic conchology. Tryon, Philadelphia, 3 vols., 312, 430, and 453.

Tunnell, J. W., 1974, Ecological and geographical distribution of Mollusca of Lobos and Enmedio coral reefs, southwestern Gulf of Mexico. Ph.D. Dissertation, Texas A&M Univ., 158 p.

Valentine, J. W., 1971, Resource supply and species diversity patterns. Lethaia v. 4, p. 51-61.

Van andel, Tj. H., 1960, Sources and dispersion of Holocene sediments, northern Gulf of Mexico, in Shepard et al (Editors), Recent Sediments, Northwest Gulf of Mexico, AAPG, Tulsa, 394 p.

Van andel, Tj. H., and Poole, D. H., 1960, Sources and dispersion of Holocene sediments, northern Gulf of Mexico: Jour. Sed. Petrology, v. 30, p. 91-122.

Villalobos, A., 1971, Estudios ecologicos en un arrecife coralino en Veracruz, Mexico. p. 532-545 in Symposium on investigations and resources of the Caribbean Sea and adjacent regions, preparatory to CICAR, organized jointly by UNESCO and FAO.

Warmke, G. L., and Abbott, R. T., 1961, Caribbean seashells: Livingston Publishing Co., Pennsylvania, 349 p.

Watson, R. L., 1971, Origin of shell beaches, Padre Island, Texas: Jour. Sed. Petrology, v. 41, p. 1105-1111.

Williams, W. T., Lambert, J. M., and Lance, G. N., 1966, Multivariate methods in plant ecology. V. Similarity analyses and information-analysis. J. Ecology, v. 54, p. 427-445.

Woodward, S. P., 1851-1856. A manual of the Mollusca. John Weale, London, 486 p.

Woodwell, G. M., and Smith H. H. (eds.), 1969. Diversity and stability in ecological systems. Brookhaven Symposium in Biology No. 22, Upton, N. Y., 264 p.

ENVIRONMENTAL ASSESSMENT OF THE SOUTH TEXAS OUTER CONTINENTAL SHELF

GEOLOGIC INVESTIGATIONS

PART II--Inventory of Data Archived and Analysed

TABLE OF CONTENTS

INVENTORY OF DATA ARCHIVED AND DATA ANALYSES

DATA ARCHIVED

The listings that follow include inventories of all samples specified for archiving by the contract plus all raw data sheets generated during the field investigations and during analysis of the sample material and study in the laboratory. All samples and hard copy of raw data listed are held by the USGS office, Corpus Christi, Texas. All sample material and raw data acquired during the geologic field investigations but transferred to other elements of the South Texas OCS Assessment Project for analysis and reporting are so indicated on the lists.

Samples

Sample material is listed by type of sample, quantity of material retained, condition of storage, and number of samples archived.

- Surficial bottom grab for texture and mineralogy. 200 cm^3 wet in capped plastic tubes at room temperature ---------- 263

- Surficial bottom grab for trace metals, organic C and carbonate. 200 cm^3 wet in capped plastic tubes frozen ---------- 263

- Pipe cores. One half of each core in original plastic liner stored in D-tubing in formalin atmosphere at room temperature ---------- 88

- Box cores: slabs approximately 30 x 45 x 2.54 cm stored in metal trays wrapped in plastic at room temperature ---------- 74

- Washings from box cores (infauna) stored in glass jars in 45 percent isopropyl alcohol at room temperature ---------- 74

Hard copy data

Included under this heading are all work sheets and documentation of various types generated during the acquisition of the original field material and during the subsequent stages of analysis and processing. The listing indicates type and number of items. Items transferred to other elements of the project for analysis and reporting are indicated by an asterisk.

- Chief scientists' log book ---------- 1
- Shipboard station logs ---------- 274
- Analogs for seismic reflection profiles ---------- 28 rolls
- Log books for geophysical data ---------- 2
- Atomic Absorption Spectrophotometer recordings for analysis of trace metals in bottom sediments in replicate for each station and for 10 elements ---------- 8,712
- Laboratory log book recordings for organic C in triplicate for each of 263 stations ---------- 792
- Laboratory log book recording for carbonates in triplicate for each of 263 stations ---------- 792
- Atomic Absorption Spectrophotometer (using graphite furnace) records for 9 trace elements at each of 24 suspended sediment stations at three levels in water column ---------- 72
- Coulter Counter grain size two-tube analyses for suspended sediment samples (seven bottles broke aboard ship) ---------- 65
- Coulter Counter grain size two-tube analyses for size ranges 63 μm - 0.63 μm for each grab sample plus 28 box core samples ---------- 291
- Rapid Sediment Analyzer analog recordings plus computation sheet for each recording for sediments of size range 63 μm to 2 mm ---------- 520
- X-ray tracings for clay mineralogy of suspended sediments ---------- 72
- X-ray tracings for clay mineralogy of surficial bottom sediments at each of 74 stations ---------- 74

- Handdrawn sketch of sediment type, depositional structures and biogenic structures of each box core ---------- 74

- X-ray radiograph of each box core at 1:1 ---------- 74

- Strip log diagram showing sediment stratigraphy and description for each pipe core ---------- 88

- X-ray radiogram in single strip for each pipe core at 1:1 ---------- 88

*[1] - XBT bar graph recordings of depth and temperature for station casts ---------- 128

*[2] - Sediment samples from box core to be held as backup for hydrocarbon analysis if needed (transferred frozen) ---------- 74

- Original analog tapes for all Hi-Fix navigation positioning ---------- 35 rolls

- Hi-Fix map plots at 1:96,000 for all stations and for geophysical shot points for those tracks obtained by Hi-Fix ---------- 4

- Hi-Fix geographic and Lambert X-Y coordinate plots for stations and shot points ---------- 27 sheets

- Work copy maps at 1:480,000 for all data compiled in map form ---------- 58

- Side scan sonar imagery for traverses other than reef runs ---------- 4 rolls

*[3] - Side scan sonar imagery for traverses over reefs ---------- 4 rolls

- 36 mm color slides of box core slabs taken aboard ship (one roll of exposures too underexposed to print) ---------- 36

- 36 mm color slides of box core slabs taken in laboratory ---------- 74

- 36 mm color slides of various operations aboard ship ---- 24

- Black and white 7.6 x 10.2 cm photo prints of box core slabs ---------- 74

- Black and white 11.4 x 16.5 cm photo prints of pipe cores (2 to 3 cores on a print) ---------- 30

*[1] - transferred to Texas A&M (subcontract from NOAA for historical summary of physical oceanographic data)
*[2] - transferred to University of Texas, Marine Science Institute at Port Aransas
*[3] - transferred to Texas A&M for use on BLM-funded reef study project

ANALYTICAL DATA

All basic analyses for trace metals chemistry, organic C, carbonates, clay mineralogy, and sediment physical properties have been formated for computer storage and retrieval and are presented as computer printouts in the tables that follow. The data formating follows a modification of the USGS RASS key punch system which allows for a statistical package to be generated, and provides for storage and retrieval of data. The software package generated provides for direct transfer of basic analytical data to the Environmental Data System (NODC, NOAA) and also for further inhouse statistical manipulation by the scientific investigators.

The steps involved in generating the software are: 1) hand copying of basic data onto computer coding forms (USGS Form 9-1634); 2) transfer of data from coding forms to cards by key punch; and 3) retrieval of data as computer read-out tables. The tables were programmed to provide space between data categories or columns to facilitate use.

All analytical data listed in the tables are keyed to the station index (Table 1). Included in Table 1 are: 1) the station index numbers coded as to the types of samples collected at the station; 2) navigation fix numbers (Hi-Fix or Loran); 3) geographic coordinates as computed from the navigation fixes; 4) lambert coordinates as computed from the navigation fix numbers; 5) water depth; 6) megascopic characteristics of the sample at time of collection; 7) length of pipe cores; 7) month; 8) date; and 9) Greenwich Mean Time. The analytical data listed in all tables that follow Table 1 are keyed to the station index number listed in Table 1. A legend explaining the columnar arrangement of data accompanies each table.

Table I - Sample Station Index

Explanation for Table

Column 1 - Sample number and type

G = Grab	X = XBT
C = Core (Pipe)	D = Drift bottle
B = Box core	W = Suspended sediment sample

Column 2 - Approximate position (LORAN, HI-FIX)

Column 3 - Latitude

Column 4 - Longitude

Column 5 - Lambert coordinate, X position

Column 6 - Lambert coordinate, Y position

Column 7 - Water depth (meters)

Column 8 - Distribution of sample

111111 = All of the following apply:
- Textural analysis
- Mineralogical analysis
- Trace element analysis
- Carbon analysis
- Archive sample available

1111111 = In addition, a quality control sample was taken (for trace metals)

Column 9 - Core length (centimeters)

Column 10 - Month

0 = October
1 = November
2 = December

Column 11 - Date

Column 12 - Greenwich Mean Time

Table I - Sample Station Index

1	2	3	4	5	6	7	8	9	10	11	12
001G		28154472	96200997	28575452	1657891	020	111111		0	27	1350
002G		28153794	96141617	28891923	1658375	020	111111		0	27	0915
002C		28154246	96141283	28894807	1663016	020		33	0	27	0915
002B	1	28153794	96141617	28891923	1658375	020			0	27	0915
002X	1	28153794	96141617	28891923	1658375	020			0	27	0915
002D	1	28153794	96141617	28891923	1658375	020			0	27	0915
003G		28153446	96082073	29209790	1662505	024	111111		0	27	0900
004G		28152810	96022889	29524510	1663908	020			0	27	0650
004C		28153121	96024134	29513299	1666770	020		178	0	27	0650
004B	1	28152810	96022889	29524510	1663908	020			0	27	0650
004X	1	28152810	96022889	29524510	1663908	020			0	27	0650
004D	1	28152810	96022889	29524510	1663908	020			0	27	0650
005G		28101855	96023710	29525069	1351182	031			0	27	1730
005C		28102045	96023599	27915703	9185205	031		163	0	27	1730
005B		28102073	96023920	29523140	1353339	031			0	27	1730
005X	1	28101855	96023710	29525069	1351182	031			0	27	1730
005D	1	28101855	96023710	29525069	1351182	031			0	27	1730
006G		28102528	96083631	29203486	1349988	027	111111		0	27	1945
007G		28103366	96112612	29051343	1354765	026	111111		0	27	2020
007X	1	28103366	96112612	29051343	1354765	026			0	27	2020
008G		28103338	96172341	28731653	1346945	023	111111		0	27	2055
008X	1	28103338	96172341	28731653	1346945	023			0	27	2055
009G		28104108	96231388	28417880	1347574	022	111111		0	29	0030
010G		28104144	96290537	28103355	1341044	015	1111111		0	29	0200
010C	1	28104144	96290537	28103355	1341044	015		249	0	29	0200
010B		28104485	96291786	28092111	1344247	015			0	29	0200
010X	1	28104144	96290537	28103355	1341044	015			0	29	0200
010D	1	28104144	96290537	28103355	1341044	015			0	29	0200
010W		28102766	96303234	28025834	1325465	015			0	29	0200
011G		28053228	96321080	27944016	1025332	020	111111		0	27	0500

Continued

Table I - Sample Station Index

1	2	3	4	5	6	7	8	9	10	11	12
012G		28053045	96261537	28262355	1030320	027	1111111		0	28	0615
012C		28053044	96261465	28263000	1030328	027		193	0	28	0615
012B		28053089	96261602	28261763	1030759	027			0	28	0615
012D	1	28053045	96261537	28262355	1030320	027			0	28	0615
013G		28052720	96202296	28578026	1034089	027	111111		0	28	1700
014G		28051896	96142593	28897947	1033181	030	111111		0	27	0820
014X	1	28051896	96142593	28897947	1033181	030			0	27	0820
015G		28051238	96113057	29055153	1030268	032	111111		0	30	0900
016G		28050690	96053489	29373807	1032526	033	111111		0	30	1000
016C		28050299	96053876	29370443	1028486	033		188	0	30	1000
016X	1	28050690	96053489	29373807	1032526	033			0	30	1000
016D	1	28050690	96053489	29373807	1032526	033			0	30	1000
016B		28045871	96054023	29369230	1024132	033			1	12	
017G		28050094	96024239	29528440	1030375	035	111111		0	30	1115
018G		27594605	96024694	29532396	712329	054	111111		0	30	1205
019G		27595696	96084593	29210360	715356	019	111111		0	30	1500
019C		27595321	96083971	29216032	711786	019		152	0	30	1500
019X	1	27595696	96084593	29210360	715356	019			0	30	1500
019D	1	27595696	96084593	29210360	715356	019			0	30	1500
019B		27595121	96084203	29214001	709635	019			1	12	
020G		28000574	96143680	28895675	716679	037	111111		0	30	1610
021G		28000997	96202961	28579351	713630	028	111111		0	30	1720
021X		28000997	96202961	28579351	713630	028			0	30	1720
022G		28001607	96262186	28263494	712744	027	111111		0	30	1610
023G		28002204	96321659	27945427	711943	024	111111		0	30	1855
024G		28002338	96351218	27788012	710012	022	111111		0	30	1940
024C		28002469	96350915	27790704	711387	022			0	30	1940
024X	1	28002338	96351218	27788012	710012	022			0	30	1940
024D	1	28002338	96351218	27788012	710012	022			0	30	1940
024B		28002036	96351041	27789665	706999	023			1	12	0252

Continued

Table I - Sample Station Index

1	2	3	4	5	6	7	8	9	10	11	12
024W	1	28002338	96351218	27788012	710012	022			0	30	1940
025G		28002930	96380983	27628664	712734	021	111111		0	30	2114
026G		28003381	96440640	27308978	710967	015	111111		0	30	2150
027G		27552052	96440969	27312155	394531	021	111111		0	30	2233
027C		27552017	96440775	27313905	394209	021		016	0	30	2233
027X	1	27552052	96440969	27312155	394531	021			0	30	2233
027D	1	27552052	96440969	27312155	394531	021			0	30	2233
027B		27552002	96440840	27313326	394047	021			1	12	0130
028G		27551488	96381795	27627795	395079	025	111111		0	31	0007
029G		27551490	96352139	27786178	398331	027	111111		0	31	0043
029X	1	27551490	96352139	27786178	398331	027			0	31	0043
030G		27550925	96322535	27944215	395906	031	111111		0	30	2220
031G		27550283	96262921	28263760	396280	036	111111		0	31	0225
032G		27550331	96204229	28575020	403708	048	1111111		0	31	0355
032C		27545960	96203877	28578261	400028	048		173	0	31	0355
032X	1	27550331	96204229	28575020	403608	048			0	31	0355
032D	1	27550331	96204229	28575020	403708	048			0	31	0355
032B		27545946	96204058	28576643	399857	044			1	12	2101
032W	1	27550331	96204229	28575020	403708	048			0	31	0355
033G		27545047	96144690	28894115	398109	052	111111		0	31	0645
034G		27531288	96121968	29028537	302702	052	111111		0	31	0745
035G		27544845	96085672	29208293	403603	054	111111		0	31	0830
036G		27543408	96025936	29529218	397040	056	111111		0	31	0940
036C		27544329	96030462	29524257	406627	056		178	0	31	0940
036X	1	27543408	96025936	29529218	397040	056			0	31	0940
036D	1	27543408	96025936	29529218	397040	056			0	31	0940
036B		27542885	96025890	29529758	391771	059			1	12	1605
037G		27492429	96060386	29371467	80086	060	111111		0	31	1115
038G		27493455	26120170	29049945	82622	064	111111		0	31	1215
038C		27492819	96115843	29053035	76264	064		206	0	31	1215

Continued

Table I - Sample Station Index

1	2	3	4	5	6	7	8	9	10	11	12
038X	1	27493455	26120170	29049945	82622	064			0	31	1215
038D	1	27493455	26120170	29049945	82622	064			0	31	1215
038B		27493209	96115270	29058087	80326	065			1	12	1837
039G		27494601	96174593	28740626	86916	066	111111		0	31	1325
040G		27495146	96234329	28419669	85140	047	111111		0	31	1427
040X	1	27495146	96234329	28419669	85140	047			0	31	1427
041G		27495610	96293593	28102967	83013	040	111111		0	31	1734
042G		27500016	96352865	27786211	80349	033	111111		0	31	1820
042C		27495989	96352691	27787781	80111	033		127	0	31	1820
042X	1	27500016	96352865	27786211	80349	033			0	31	1820
042D	1	27500016	96352865	27786211	80349	033			0	31	1820
042B		27500514	96352992	27784969	85351	035			1	12	2259
043G		27502346	96410705	27481931	97746	027	111111		0	31	1932
044G		27500341	96471694	27150243	71071	022	111111		0	31	2019
045G		27501513	96530422	26838227	77134	019	111111		0	31	1850
045C		27501847	96530937	26833543	80428	019		104	0	31	1850
045X	1	27501513	96530422	26838227	77134	019			0	31	1850
045D	1	27501513	96530422	26838227	77134	019			0	31	1850
045B		27495848	96530132	25223922	7907478	019			1	11	
046G		27450613	96530981	25220071	7612171	023	111111		1	01	0320
047G		27450396	96471746	25536650	7614149	022	111111		1	01	0400
048G		27445796	96412459	25853742	7612516	031	111111		1	01	0445
048C		27445848	96411605	25861407	7613151	031		234	1	01	0445
048X	1	27445796	96412459	25853742	7612516	031			1	01	0445
048D	1	27445796	96412459	25853742	7612516	031			1	01	0445
048B		27445841	96412478	25853568	7612968	035			1	12	0038
049C		27442886	96381610	26023510	7585594	036		231	1	01	1500
050G		27445246	96353120	26171305	7611638	042	111111		1	01	1530
051G		27444982	96293654	26489969	7613909	054	111111		1	01	1615
051C		27444804	96293916	26487644	7612079	054			1	01	1615

Continued

Table I - Sample Station Index

1	2	3	4	5	6	7	8	9	10	11	12
051X	1	27444982	96293654	26489969	7613909	054			1	01	1615
051D	1	27444982	96293654	26489969	7613909	054			1	01	1615
051B		27445529	96293891	26487754	7619404	053			1	12	0144
052G		27444853	96264527	26643854	7615083	058	111111		1	01	1715
053G		27444515	96235060	26800836	7614255	061	111111		1	01	1750
053X	1	27444515	96235060	26800836	7614255	061			1	01	1750
054G		27444022	96175113	27123855	7614785	063	111111		1	01	1828
055G		27443538	96120257	27437085	7615484	082	111111		1	01	1929
055X		27443538	96120257	27437085	7615484	082			1	01	1929
056G		27442960	96060826	27755500	7615574	091	111111		1	01	2008
057G		27442489	96002111	28067459	7616865	092	111111		1	01	2050
057X		27442489	96002111	28067459	7616865	092			1	01	2050
058G		27390443	96002818	28067500	7293196	125	111111		1	01	2211
059G		27391198	96061311	27756958	7294805	115	111111		1	02	1605
060G		27391915	96120581	27439987	7296146	100	1111111		1	02	1330
060C		27392261	96115724	27447631	7299784	100		211	1	02	1330
060X	1	27391915	96120581	27439987	7296146	100			1	02	1330
060D	1	27391915	96120581	27439987	7296146	100			1	02	1330
060B		27391823	96120755	27438442	7295190	100			1	12	0405
060W	1	27391915	96120581	27439987	7296146	100			1	02	1330
061G		27392252	96150184	27281663	7296700	093	111111		1	02	1215
062G		27411241	96172756	27148703	7405436	082	111111		1	02	1125
062X	1	27411241	96172756	27148703	7405436	082			1	02	1125
063G		27393551	96234936	26807156	7301630	072	111111		1	02	1030
064G		27394083	96293846	26493205	7301897	062	111111		1	02	0935
064X	1	27394083	96293846	26493205	7301897	062			1	02	0935
065G		27393717	96353758	26170380	7293197	052	111111		1	02	0850
066G		27394977	96412695	25856086	7301293	041	111111		1	02	0805
066X	1	27394977	96412695	25856086	7301293	041			1	02	0805
067G		27394861	96441679	25703400	7298024	037	111111		1	02	0725

Continued

Table I - Sample Station Index

1	2	3	4	5	6	7	8	9	10	11	12
068G		27395033	96471685	25541492	7297473	032	111111		1	02	0650
068C		27395607	96471984	25538729	7303224	032		193	1	02	0650
068X	1	27395033	96471685	25541492	7297473	032			1	02	0650
068D	1	27395033	96471685	25541492	7297473	032			1	02	0650
068B		27394647	96471825	25540289	7293551	031			1	13	1505
069G		27394935	96531261	25221649	7292263	026	111111		1	02	0610
070G		27395584	96590386	24905757	7294906	021	1111111		1	02	0510
070C		27395847	96590768	24902296	7297522	021		175	1	02	0510
070X	1	27395584	96590386	24905757	7294906	021			1	02	0510
070D	1	27395584	96590386	24905757	7294906	021			1	02	0510
070B		27395846	96591078	24899504	7297473	020			1	13	1356
070W	1	27395584	96590386	24905757	7294906	021			1	02	0510
071G		27344446	97021221	24740060	6978491	022	111111		1	03	0540
072G		27344279	96583693	24933791	6979098	026	111111		1	03	0630
073G		27344152	96502047	25380506	6983449	034	1111111		1	03	0725
073C		27343727	96502375	25377613	6979127	034		99	1	03	0725
073X	1	27344152	96502047	25380506	6983449	034			1	03	0725
073D	1	27344152	96502047	25380506	6983449	034			1	03	0725
073B		27343756	96502615	25375446	6979384	035			1	13	1633
073W	1	27344152	96502047	25380506	6983449	034			1	03	0725
074G		27343717	96472159	25541520	6981212	036	111111		1	03	0840
075G		27343875	96442693	25698651	6984964	044	111111		1	03	0840
075C		27343131	96442904	25696858	6977431	044		284	1	03	0840
075X	1	27343875	96442693	25698651	6984964	044			1	03	0840
075D	1	27343875	96442693	25698651	6984964	044			1	03	0910
075B		27343481	96441978	25705134	6981077	045			1	13	1552
076G		27343504	96413310	25855110	6983433	048	111111		1	03	1015
077G		27342660	96390782	25985954	6976800	053	111111		1	03	1100
078G		27342764	96334730	26274329	6982177	064	111111		1	03	1348
078C	1	27342764	96334730	26274329	6982177	064		178	1	03	1348

Continued

Table I - Sample Station Index

1	2	3	4	5	6	7	8	9	10	11	12
D78X	1	27342764	96334730	26274329	6982177	064			1	03	1348
D78D	1	27342764	96334730	26274329	6982177	064			1	03	1348
D79C		27325122	96294252	26496126	6886754	078		257	1	03	1451
D80X	1	27342095	96285517	26537286	6979538	075			1	02	2220
D80D	1	27342095	96285517	26537286	6979538	075			1	02	2220
D80B		27342438	96285669	26535868	6982985	075			1	14	1008
D80G		27342095	96285517	26537286	6979538	072	111111		1	02	1534
D80C		27341702	96290689	26526805	6975409	072		130	1	02	1534
D81C		27333757	96285584	26537388	6935733	076		267	1	02	2354
D82C		27350384	96265892	26641185	7024536	078		246	1	02	2310
D83G		27344320	96220967	26901764	7008006	102	111111		1	02	2205
D83C		27344140	96222014	26892377	7006030	102		224	1	02	2205
D83X	1	27344320	96220967	26901764	7008006	102			1	02	2205
D83D	1	27344320	96220967	26901764	7008006	102			1	02	2205
D83B		27344788	96222349	26889251	7012517	090			1	14	0852
D84G		27341113	96150926	27280589	6982185		111111		1	02	2118
D85G		27335990	96093164	27584582	6976375	133	1111111		1	02	1954
D85C		27340179	96092136	27593796	6978454	133		205	1	02	1954
D85X	1	27335990	96093164	27584582	6976375	133			1	02	1954
D85D	1	27335990	96093164	27584582	6976375	133			1	02	1954
D85B		27340027	96091252	27601775	6977065	130			1	12	0458
D85W	1	27335990	96093164	27584582	6976375	133			1	02	1954
D86G		27335848	96033883	27902057	6980952	154	111111		1	02	1915
D87G		27334692	95573107	28233191	6975808	202	111111		1	02	1805
D88G		27284228	96063458	27749970	6658657	186	1111111		1	03	1900
D88C		27284489	96063487	27749663	6661325	186		168	1	03	1900
D88X	1	27284228	96063458	27749970	6658657	186			1	03	1900
D88D	1	27284228	96063458	27749970	6658657	186			1	03	1900
D88B		27283660	96063378	27750795	6652976	186			1	12	0608
D88W	1	27284228	96063458	27749970	6658657	186			1	03	1900

Continued

Table I - Sample Station Index

1	2	3	4	5	6	7	8	9	10	11	12
089G		27285646	96122385	27435199	6667170		111111		1	02	2021
090G		27290373	96181512	27118761	6668890	122	111111		1	03	2100
090C		27290001	96182385	27110960	6664998	122		211	1	03	2100
090X	1	27290373	96181512	27118761	6668890	122			1	03	2100
090D	1	27290373	96181512	27118761	6668890	122			1	03	2100
090B		27285701	96183056	27104978	6661861	118			1	14	0741
091G		27290447	96205762	26972419	6667115	110	111111		1	03	2200
092G		27285313	96240021	26808195	6652894	103	111111		1	03	2244
092X	1	27285313	96240021	26808195	6652894	103			1	03	2244
093G		27291024	96295848	26485295	6664925	084	111111		1	03	0010
094G		27291283	96354799	26170530	6662672	080	111111		1	03	0123
094X		27291283	96354799	26170530	6662672	080			1	03	0123
095G		27291345	96414246	25851332	6658612	055	1111111		1	03	0245
095C		27291319	96413801	25855339	6658408	055		183	1	03	0245
095X	1	27291345	96414246	25851332	6658612	055			1	03	0245
095D	1	27291345	96414246	25851332	6658612	055			1	03	0245
095B		27291026	96413159	25861167	6655529						
095W	1	27291345	96414246	25851332	6658612	055			1	13	2008
096G		27292198	96443823	25692931	6664992	051	111111		1	04	0326
097G		27292288	96473691	25532025	6663694	044	111111		1	04	0355
097X	1	27292288	96473691	25532025	6663694	044			1	04	0355
098G		27292507	96502967	25376426	6663824	041	111111		1	04	0315
099G		27292670	96532216	25221082	6663460	026	111111		1	04	0440
099X	1	27292670	96532216	25221082	6663460	036			1	04	0440
100G		27292954	96591901	24899716	6662356	028	111111		1	04	0520
101G		27293650	97051218	24581611	6665700	022	111111		1	04	0600
101C		27293720	97051313	24580752	6666390	022		193	1	04	0600
101X	1	27293650	97051218	24581611	6665700	022			1	04	0600
101D	1	27293650	97051218	24581611	6665700	022			1	04	0600
101B		27293810	97050474	24588296	6667296	023			1	13	1759

Continued

Table I - Sample Station Index

1	2	3	4	5	6	7	8	9	10	11	12
102G		27241750	97050770	24589257	6343658	026	111111		1	04	0700
103G		27241189	96591934	24903256	6341631	032	111111		1	04	0745
103X	1	27241189	96591934	24903256	6341631	032			1	04	0745
104G		27241141	96532556	25222079	6345084	042	111111		1	04	0820
105G		27240981	96473040	25542163	6347679	052	111111		1	04	0905
106G		27240458	96444330	25692824	6344465	058	111111		1	04	0950
106C		27240706	96443526	25700034	6347069	058		193	1	04	0950
106X	1	27240458	96444330	25692824	6344465	058			1	04	0950
106D	1	27240458	96444330	25692824	6344465	058			1	04	0950
106B		27240626	96443721	25698288	6346235	060			1	13	2139
107G		27240723	96414290	25855355	6349429	065	111111		1	04	1030
108G		27240641	96360108	26163406	6353122	078	111111		1	04	1105
108X	1	27240641	96360108	26163406	6353122	078			1	04	1105
109C		27263521	96305503	26436835	6507598	092		175	1	04	1145
110G		27235786	96295758	26491109	6349553	095	1111111		1	04	1327
110C		27235094	96295547	26493117	6342603	095		230	1	04	1327
110X	1	27235786	96295758	26491109	6349553	095			1	04	1327
110D	1	27235786	96295758	26491109	6349553	095			1	04	1327
110B		27240139	96295361	26494630	6353178	098			1	13	2308
110W	1	27235786	96295758	26491109	6349553	098			1	13	2308
111G		27234791	96240122	26812415	6344725	110	111111		1	04	1447
112G		27235163	96182722	27113340	6353604	143	111111		1	05	1754
112X	1	27235163	96182722	27113340	6353604	145			1	04	1545
113G		27233690	96122294	27441880	6344565	182	111111		1	05	1711
114G		27183049	96182489	27121075	6029428	180	1111111		1	05	1525
114C		27182867	96181666	27128523	6027719	180		188	1	05	1525
114X	1	27183049	96182489	27121075	6029428	180			1	05	1525
114D	1	27183049	96182489	27121075	6029428	180			1	05	1525
114W	1	27183049	96182489	27121075	6029428	180			1	13	0258
114B		27182604	96183285	27113973	6024807	175			1	14	1347

Continued

Table I - Sample Station Index

1	2	3	4	5	6	7	8	9	10	11	12
115G		27183507	96241747	26803012	6028647	133	1111111		1	04	1417
115C		27183451	96241337	26806722	6028138	133		175	1	04	1417
115X	1	27183507	96241747	26803012	6028138	133			1	04	1417
115D	1	27183507	96241747	26803012	6028138	133			1	04	1417
115B		27182945	96240431	26814973	6023167						
115W	1	27183507	96241747	26803012	6028138	130			1	14	1229
116G		27184065	96300920	26485702	6029136	105	111111		1	05	1200
117G		27184061	96360583	26164069	6024133	090	111111		1	05	1045
117X	1	27184061	96360583	26164069	6024133	090			1	05	1045
118G		27184600	96415401	25849975	6024968	072	111111		1	05	0910
119G		27184921	96444626	25694580	6026023	067	111111		1	05	0830
120G		27185314	96473993	25537896	6027839	060	111111		1	05	0745
120C		27185646	96474233	25535685	6031163	060		142	1	05	0745
120X	1	27185314	96473993	25537896	6027839	060			1	05	0745
120D	1	27185314	96473993	25537896	6027839	060			1	05	0745
120B		27184919	96474432	25534000	6023800	061			2	13	2010
121G		27185216	96503544	25379621	6024747	052	111111		1	05	0710
122G		27185521	96533245	25219938	6025755	046	111111		1	05	0635
122X	1	27185521	96533245	25219938	6025755	046			1	05	0635
123G		27185769	96592724	24899932	6024314	035	111111		1	04	0540
124G		27190138	97051512	24586145	6024408		111111		1	04	
125G		27190558	97110746	24268327	6025210	022	111111		1	05	0350
125C		27190900	97110472	24270761	6028694	022		152	1	05	0350
125X	1	27190558	97110746	24268327	6025210	022			1	05	0350
125D	1	27190558	97110746	24268327	6025210	022			1	05	0350
125B		27180401	97111439	24262730	5962980	023			2	11	
126G		27135114	97110275	24275882	5707782	025	111111		1	05	0800
127G		27135216	97081167	24430292	5710453	028		198	1	05	0830
127C	1	27135216	97081167	24430292	5710453	028			1	05	0830
127X	1	27135216	97081167	24430292	5710453	028			1	05	0830

Continued

Table I - Sample Station Index

1	2	3	4	5	6	7	8	9	10	11	12
127D	1	27135216	97081167	24430292	5710453	028			1	05	0830
127B		27134673	97073069	24467330	5705380	028			2	11	
128G		27134771	97002184	24854396	5710760	038	111111		1	06	0930
129G		27134624	96562937	25064233	5711813	044	111111		1	06	1000
129X	1	27134624	96562937	25064233	5711813	044			1	06	1000
130G		27133999	96503934	25380240	5709530	072	111111		1	05	2350
131G		27133371	96474656	25536272	5705264	072	111111		1	05	2221
131C		27133793	96474194	25540381	5709580	072		190	1	05	2221
131X	1	27133371	96474656	25536272	5705264	072			1	05	2221
131D	1	27133371	96474656	25536272	5705264	072			1	05	2221
131B		27133264	96475555	25528171	5704070	063			1	14	1657
132G		27133411	96445276	25693137	5707812	072	111111		1	05	2155
133G		27133125	96385790	26013460	5709493	082	111111		1	05	2119
134G		27132560	96330476	26332280	5708595	103	111111		1	05	2018
134C		27132849	96330330	26333558	5711531	103			1	05	2018
134X	1	27132560	96330476	26332280	5708595	103			1	05	2018
134D	1	27132560	96330476	26332280	5708595	103			1	05	2018
134B		27132760	96331364	26324248	5709942	101			1	14	1524
135G		27132324	96271599	26647117	5711196	131	111111		1	05	1940
136G		27131480	96212370	26965220	5707951	184	111111		1	05	1901
137G		27081055	96243046	26801745	5397965	185	1111111		1	21	1739
137C		27080376	96243128	26801118	5391094	185		130	1	21	1739
137X	1	27081055	96243046	26801745	5397965	185			1	21	1739
137D	1	27081055	96243046	26801745	5397965	185			1	21	1739
137B		27080893	96241804	26812990	5396520	158			2	13	
138G		27080730	96302354	26482873	5389525	125	111111		1	21	1834
139G		27081842	96361180	26168129	5395900	102	111111		1	21	1910
139X	1	27081842	96361180	26168129	5395900	102			1	21	1910
140G		27084405	96404956	25916866	5418085	088	111111		1	14	2259
141G		27082220	96475830	25529909	5390617	068	111111		1	14	2133

Continued

Table I - Sample Station Index

1	2	3	4	5	6	7	8	9	10	11	12
141C		27082517	96474687	25540199	5393756	068			1	14	2133
141X	1	27082220	96475830	25529909	5390617	068			1	14	2133
141D	1	27082220	96475830	25529909	5390617	068			1	14	2133
142G		27081923	96534754	25214489	5383489	055	111111		1	14	2019
142X	1	27081923	96534754	25214489	5383489	055			1	14	2019
143G		27083475	96593044	24904561	5395346	043	111111		1	06	1430
144G		27084057	97051719	24591289	5397593	032	111111		1	06	1330
145G		27082553	97111324	24269843	5378933	025	111111		1	06	1125
145C		27084110	97111341	24269522	5394659	025		200	1	06	1125
145X	1	27082553	97111324	24269843	5378933	025			1	06	1125
145D	1	27082553	97111324	24269843	5378933	0,5			1	06	1125
145B		27083035	97103986	24299940	5384120	027			2	11	
146G		27032980	97111747	24269125	5080327	028	1111111		1	21	2224
146C		27032308	97111370	24272602	5073580	028		201	1	21	2224
146X	1	27032980	97111747	24269125	5080327	028			1	21	2224
146D	1	27032980	97111747	24269125	5080327	028			1	21	2224
147G		27032257	97053174	24581729	5076390	034	111111		1	21	2152
147X	1	27032257	97053174	24581729	5076390	034			1	21	2152
148G		27032081	96592983	24908898	5078398	044	111111		1	21	2117
149G		27032047	96534490	25220712	5081903	057	1111111		1	21	1416
149C		27031330	96534321	25222330	5074406	057		198	1	21	1416
149D	1	27032047	96534490	25220712	5081903	057			1	21	1416
149X	1	27032047	96534490	25220712	5081903	057			1	21	1416
149B		27032047	96534490	25220712	5081903	057			2	10	
150G		27031134	96475291	25539020	5076840	072	111111		1	21	1503
151G		27030832	96430080	25803110	5077443	086	111111		1	21	1533
151X	1	27030832	96430080	25803110	5077443	086			1	21	1533
152G		27053284	96412779	25885101	5224548	090	111111		1	14	2328
153G		27030405	96360540	26178680	5078611	096	111111		1	21	1614
153X	1	27030405	96360540	26178680	5078611	096			1	21	1614

Continued

Table I - Sample Station Index

1	2	3	4	5	6	7	8	9	10	11	12
154G		27024645	96305623	26458435	5065144	135	111111		1	21	1647
155G		26574545	96274234	26638620	4764070	195	1111111		1	19	1905
155C		26574710	96274115	26639670	4765752	195		185	1	19	1905
155W	1	26574545	96274234	26638620	4764070	195			1	19	1905
155X	1	26574545	96274234	26638620	4764070	195			1	19	1905
155D		26574545	96274234	26638620	4764070	195			1	19	1905
155B		26574844	96273144	26648434	4767251	195			2	12	
156G		26574848	96332672	26327024	4762218	125	1111111		1	19	2059
156C		26575439	96332672	26326939	4768184	125		160	1	19	2059
156W	1	26574848	96332672	26327024	4762218	125			1	19	2059
156D	1	26574848	96332670	26327024	4762218	125			1	19	2059
156X	1	26574848	96332670	26327024	4762218	125			1	19	2059
156B		26575446	96332693	26326748	4768255	125			2	12	
157G		26575138	96390804	26018208	4760506	100	1111111		1	19	2241
157C		26575157	96391187	26014736	4760646	100		152	1	19	2241
157W	1	26575138	96390804	26018208	4760506	100			1	19	2241
157X	1	26575138	96390804	26018208	4760506	100			1	19	2241
157D	1	26575138	96390804	26018208	4760506	100			1	19	2241
157B		26575397	96391822	26008960	4762991	102			2	12	
158G		26580019	96450333	25696665	4764821	082	111111		1	19	0353
159G		27004045	96475548	25538749	4924481	074	111111		1	19	0427
160G		26580448	96475754	25539000	4767003	073	1111111		1	19	0510
160C		26580009	96475733	25539251	4762565	073			1	19	0510
160X	1	26580448	96475754	25539000	4767003	073			1	19	0510
160D	1	26580448	96475754	25539000	4767003	073			1	19	0510
160W	1	26580448	96475754	25539000	4767003	073			1	19	0510
160B		26582464	96485390	25487690	4786660	073			2	12	
161C		26572853	96485102	25491111	4730054	072		102	1	20	0635
162G		26580503	96505066	25382381	4765474	065	111111		1	20	1546
162X	1	26580503	96505066	25382381	4765474	065			1	20	1546

Continued

Table I - Sample Station Index

1	2	3	4	5	6	7	8	9	10	11	12
163G		26580448	96563718	25068914	4760932	052	111111		1	21	1326
164G		26580421	97023391	24746194	4756802	040	1111111		1	21	1201
164C		26580785	97023270	24747244	4760494	040		183	1	21	1201
164X	1	26580421	97023391	24746194	4756802	040			1	21	1201
164D	1	26580421	97023391	24746194	4756802	040			1	21	1201
164W	1	26580421	97023391	24746194	4756802	040			1	21	1201
164B						040			2	10	
165G		26581214	97111912	24270970	4759600	028	1111111		1	21	2310
165C		26581201	97112293	24267516	4759438	028		150	1	21	2310
165X	1	26581214	97111912	24270970	4759600	028			1	21	2310
165D	1	26581214	97111912	24270970	4759600	028			1	21	2310
165W	1	26581214	97111912	24270970	4759600	028			1	21	2310
165B		26573475	97094548	24356070	4722740	028			2	12	
166G		26525307	97115713	24239897	4437116	026	111111		1	21	0056
167G		26525334	97053863	24582575	4441060		111111		2	10	
168G		26525062	96594611	24901768	4441992	044	111111		1	21	1115
169G		26524313	96535931	25215838	4438300	057	111111		1	20	1500
169X	1	26524313	96535931	25215838	4438300	057			1	20	1500
170G		26524211	96505667	25381212	4439396	063	111111		1	20	1435
171G		26525425	96480426	25537141	4453723	072	111111		1	19	0237
171C		26524724	96480281	25538548	4446668	072		153	1	19	0237
171X	1	26525425	96480426	25537141	4453723	072			1	19	0237
171D	1	26525425	96480426	25537141	4453723	072			1	19	0237
171B		26524266	96480880	25533186	4441969	072			2	12	
172C		26523998	96463137	25621439	4440462	080		099	1	19	0216
172X	1	26523998	96463137	25621439	4440462	080			1	19	0216
173G		26524208	96422212	25847071	4445726	093	111111		1	19	0129
174G		26524282	96363038	26165500	4451120	101	111111		1	19	0038
174X	1	26524282	96363038	26165500	4451120	101			1	19	0038
175G		26523476	96335242	26308634	4445157	123	111111		1	19	1758

Continued

Table I - Sample Station Index

1	2	3	4	5	6	7	8	9	10	11	12
176G		26471400	96274007	26650972	4126656	212	111111		1	18	0217
176C		26472068	96273684	26653794	4133445	212		196	1	18	0217
176D	1	26471400	96274007	26650972	4126656	212			1	18	0217
176B		26470999	96274567	26645966	4122528	212			2	13	
176X	1	26471400	96274007	26650972	4126656	212			1	18	0217
177G		26471810	96332296	26340235	4125891	102	111111		1	19	1552
177X	1	26471810	96332296	26340235	4125891	102			1	19	1552
178G		26472406	96391753	26018876	4127084	095	111111		1	19	1507
179G		26460921	96415996	25872789	4049397	095	111111		1	19	1421
179C		26461710	96415947	25873118	4057387	095			1	19	1421
179X	1	26460921	96415996	25872789	4049397	095			1	19	1421
179D	1	26460921	96415996	25872789	4049397	095			1	19	1421
179B		26461347	96420723	25866138	4053605	092			2	12	
180G		26473091	96450832	25700949	4129472	078	111111		1	19	1250
181G		26472908	96480403	25541771	4125450	064	111111		1	19	1216
181X	1	26472908	96480403	25541771	4125450	064			1	19	1216
182G		26473203	96510390	25378756	4126273	056	111111		1	19	1138
183G		26473315	96565712	25058704	4123340	047	111111		1	19	1102
183X	1	26473315	96565712	25058704	4123340	047			1	19	1102
184G		26473698	97022928	24757694	4123625	034	111111		1	19	1025
185G		26474453	97083617	24425191	4127541	032	1111111		1	19	0940
185C		26474536	97083461	24426591	4128393	032		175	1	19	0940
185X	1	26474453	97083617	24425191	4127541	032			1	19	0940
185D	1	26474453	97083617	24425191	4127541	032			1	19	0940
185B		26474548	97083301	24428045	4128527	032			2	10	
186G		26423136	97083388	24430666	3811392	030	111111		1	17	1944
186C		26423026	97083477	24429867	3810276	030			1	17	1944
186B		26423120	97083616	24428594	3811211	030			1	17	1944
186X	1	26423136	97083388	24430666	3811392	030			1	17	1944
186D	1	26423136	97083388	24430666	3811392	030			1	17	1944

Continued

Table I - Sample Station Index

1	2	3	4	5	6	7	8	9	10	11	12
187G		26422857	97024542	24746659	3812093	033	111111		1	17	2018
188G		26421969	96565656	25063100	3806299	045	111111		1	17	2217
188X	1	26421969	96565656	25063100	3806299	045			1	17	2217
189G		26421877	96510557	25381373	3800000	057	111111		1	17	2302
190G		26421536	96452627	25689081	3810695	068	111111		1	17	0018
191G		26421973	96381737	26077924	3820662	098	1111111		1	18	2156
191C		26422257	96381167	26083045	3823602	098			1	18	2156
191X	1	26421973	96381737	26077924	3820662	098			1	18	2156
191D	1	26421973	96381737	26077924	3820662	098			1	18	2156
191W	1	26421973	96381737	26077924	3820662	098			1	18	2156
191B		26421776	96372455	26115842	3819376	100			2	12	
192G		26420255	96334187	26327990	3807079	112	111111		1	18	2321
193G		26415875	96275012	26647008	3808268	170	111111		1	18	0053
193C		26420197	96275487	26642640	3811443	170		150	1	18	0053
193X	1	26420197	96275487	26642640	3811443	170			1	18	0053
193D	1	26420197	96275487	26642640	3811443	170			1	18	0053
193B		26415510	96275574	26641966	3804510	170			2	13	
194G		26364799	96275103	26651243	3494541	123	111111		1	23	1952
194C		26364869	96275531	26647343	3495186	123		168	1	23	1952
194X	1	26364799	96275103	26651243	3494541	123			1	23	1952
194D	1	26364799	96275103	26651243	3494541	123			1	23	1952
194B		26364735	96275202	26650351	3493886	125			2	12	
195G		26364699	96333573	26338452	3488601	098	111111		1	08	0327
196G		26393296	96374445	26110268	3652747	085	111111		1	08	0122
196X		26393296	96374445	26110268	3652747	085			1	08	0122
197G		26370258	96394440	26012742	3499467		111111		1	07	2425
198G		26364351	96451391	25704923	3478835		111111		1	07	2337
199G		26370691	96510905	25382333	3495126	052	111111		1	07	1700
199C		26370231	96510887	25382558	3409486	052		091	1	07	1700
199X	1	26370691	96510905	25382333	3495126	052			1	07	1700

Continued

Table I - Sample Station Index

1	2	3	4	5	6	7	8	9	10	11	12
199D	1	26370691	96510905	25382333	3495126	052			1	07	1700
199B		26370501	96510830	25383039	2493218	050			1	18	2040
200G		26370716	96565716	25066436	3491377	040	111111		1	07	2111
201G		26370516	97024843	24747696	3485560	035	111111		1	07	2018
202G		26370614	97083904	24429515	3483017	025	111111		1	07	1859
202C		26371373	97083603	24432160	3490701	025			1	07	1859
202X	1	26370614	97083904	24429518	3490701	025			1	07	1859
202D	1	26370614	97083904	24429515	3490701	025			1	07	1859
202B		26371698	97083969	24428804	3493946	025			1	17	1902
203G		26320266	97053975	24595628	3178409	025	111111		1	07	0620
203C		26315340	97054091	24597674	3169053	025		130	1	07	0620
203X	1	26320266	97053975	24595628	3178409	025			1	07	0620
203D	1	26320266	97053975	24595628	3178409	025			1	07	0620
203B		26320919	97054060	24594778	3184993	025			1	16	2059
204G		26315124	96595729	24906762	3170463	035	111111		1	07	0700
205G		26315393	96270156	25065319	3175108	040	111111		1	07	0735
206G		26315437	96540689	25224945	3177529	042	111111		1	07	0835
207G		26315007	96482682	25533836	3177220	046	111111		1	07	0930
208G		26313645	96421951	25867603	3168083	056	111111		1	07	1005
208C		26314405	96422841	25859407	3175636	056		016	1	07	1005
208X	1	26313645	96421951	25867603	3168083	056			1	07	1005
208D	1	26313645	96421951	25867603	3168083	056			1	07	1005
208B		26314400	96423099	25857069	3175553	055			2	12	
209G		26314167	96364229	26173773	3177919	075	111111		1	07	1120
210G		26313456	96334273	26336947	3173109	088	111111		1	07	1145
211G		26313403	96305019	26493646	3175012	095	111111		1	07	1215
212G		26312602	96280131	26647145	3169372	100	111111		1	08	0417
212X	1	26312602	96280131	26647145	3169372	100			1	08	0417
213C		26341378	96270977	26691208	3339473	117		220	1	08	0500
214C		26313857	96251027	26802275	3184570	118		183	1	23	1912

Continued

Table I - Sample Station Index

1	2	3	4	5	6	7	8	9	10	11	12
214X	1	26313857	96251027	26802275	3184570	118			1	23	1912
216G		26262565	96251431	26803812	2868619	092	1111111		1	23	1808
216C		26261868	96251388	26804314	2861594	092		041	1	23	1808
216X	1	26262565	96251431	26803812	2868619	092			1	23	1808
216D	1	26262565	96251431	26803812	2868619	092			1	23	1808
216W		26262565	96251431	26803812	2868619	092			1	23	1808
217G		26262918	96310483	26485187	2867056	078	111111		1	23	1425
218G		26262405	96335620	26329519	2859463	065	111111		1	23	1329
218X	1	26262405	96335620	26329519	2859463	065			1	23	1329
219G		26263028	96364984	26171618	2863360	058	111111		1	23	1300
220G		26263667	96423742	25855629	2865213	046	111111		1	23	1222
220X	1	26263667	96423742	25855629	2865213	046			1	23	1222
221G		26264136	96511889	25381629	2863500	043	111111		1	23	0939
222G		26264115	96541352	25222922	2861249	038	111111		1	17	1536
222X	1	26264115	96541352	25222922	2861249	038			1	17	1536
223G		26264508	96570692	25065278	2863251	038	111111		1	16	0514
223X	1	26264508	96570692	25065278	2863251	038			1	16	0514
224G		26264424	97000977	24899104	2860397	035	111111		1	16	0407
225G		26264083	97031462	24731145	2954992	026	111111		1	17	0004
225C		26264631	97031197	24733492	2860552	026		025	1	17	0004
225B		26263469	97032553	24721300	2846681	026			1	17	0004
225X	1	26264083	97031462	24731145	2954992	026			1	17	0004
225D	1	26264083	97031462	24731145	2954992	026			1	17	0004
226G		26241589	96590672	24958208	2711320	036	1111111		1	18	1120
226C		26241988	96590121	24963167	2715404	036			1	18	1120
226B		26242053	96590465	24960033	2716020	036			1	18	1120
226X	1	26241589	96590672	24958208	2711320	036			1	18	1120
226D	1	26241589	96590672	24958208	2711320	036			1	18	1120
227G		26212737	96542278	25218510	2544367	039	111111		1	23	1023
228G		26211694	96483605	25533987	2539861	043	111111		1	23	1105

Continued

Table I - Sample Station Index

1	2	3	4	5	6	7	8	9	10	11	12
228X	1	26211894	96483605	25533987	2539861	043			1	23	1105
229G		26211839	96423787	25859772	2543885	076	111111		1	23	1148
230G		26211393	96365528	26171439	2543933	052	1111111		1	23	1525
230C		26212302	96365928	26167662	2553048	052		125	1	23	1525
230X	1	26211393	96365528	26171439	2543933	052			1	23	1525
230D	1	26211393	96365528	26171439	2543933	052			1	23	1525
230B		26211443	96365305	26173460	2544964	051			2	12	
231G		26211226	96340076	26330200	2544649	060	111111		1	23	1600
232G		26211372	96310567	26489425	2548589	068	111111		1	23	1641
232X	1	26211372	96310567	26489425	2548589	068			1	23	1641
233G		26210793	96251839	26805381	2547823	083	111111		1	23	1723
233X	1	26210793	96251839	26805381	2547823	083			1	23	1723
234G		26210092	96191940	27132015	2546258	142	111111		2	03	2200
235G		26163147	96210568	27039982	2772599	108	1111111		2	04	2229
235C		26162813	96210579	27039941	2269220	108		089	2	04	2209
235X	1	26163147	96210568	27039982	2772599	108			2	04	2209
235D	1	26163147	96210568	27039982	2772599	108			2	04	2209
235W	1	26163147	96210568	27039982	2772599	108			2	04	2209
236G		26154380	96251922	26810018	2220606	075	1111111		2	03	2106
236C		26153999	96245442	26832655	2219131	075		150	2	03	2106
236B		26153291	96245702	26830402	2209952	075			2	03	2106
236X	1	26154380	96251922	26810018	2220606	075			2	03	2106
236D	1	26154380	96251922	26810018	2220606	075			2	03	2106
236W	1	26154380	96251922	26810018	2220606	075			2	03	2106
237G		26155646	96310813	26492216	2228284	063	111111		2	03	2023
238G		26155323	96340145	26334500	2222577	056	1111111		2	03	1856
238B		26155864	96341050	26326178	2227910	056			2	03	1856
238C		26154997	96340366	26332538	2219254	056		196	2	03	1856
238X	1	26155323	96340145	26334500	2222577	056			2	03	1856
238D	1	26155323	96340145	26334500	2222577	056			2	03	1856

Continued

Table I - Sample Station Index

1	2	3	4	5	6	7	8	9	10	11	12
238W	1	26155323	96340145	26334500	2222577	056			2	03	1856
239G		26155344	96365051	26180614	2220458	053	111111		2	03	1824
239X	1	26155344	96365051	26180614	2220458	053			2	03	1824
240G		26160411	96395133	26015861	2228802	051	111111		1	22	0050
241G		26160675	96424972	25853449	2229139	048	1111111		1	22	2215
241C		26160553	96424999	25853216	2227901	048		137	1	22	2215
241W	1	26160675	96424972	25853449	2229139	048			1	22	2215
241X	1	26160675	96424972	25853449	2229139	048			1	22	2215
241D	1	26160675	96424972	25853449	2229139	048			1	22	2215
242G		26161113	96483894	25535517	2229182	043	111111		2	03	1655
243G		26160644	96512558	25383898	2222445	042	1111111		2	03	1515
243C		26161057	96513165	25378313	2226536	042		140	2	03	1515
243B		26160594	96514000	25370774	2221762	042			2	03	1515
243X	1	26160644	96512558	25383898	2222445	040			1	15	1911
243D	1	26160644	96512558	25383898	2222445	040			1	15	1911
243W	1	26160644	96512558	25383898	2222445	040			1	15	1911
244G		26161181	96542734	25218380	2225748	037	111111		2	03	1448
245G		26163066	97000948	24906723	2240965	050	1111111		1	18	1447
245C		26162285	97001016	24906197	2233065	050		043	1	18	1447
245B		26162739	97001120	24905193	2237639	050			1	18	1447
245X	1	26163066	97000948	24906723	2240965	030			1	18	1704
245D	1	26163066	97000948	24906723	2240965	030			1	18	1704
245W	1	26163066	97000948	24906723	2240965	030			1	18	1704
246G		26106304	97000836	24911791	1900123	028	111111		2	04	1434
246C		26110856	97002318	24898103	1915636	028		046	2	04	1434
246B		26110608	97001758	24093232	1913187	028			2	04	1434
246X	1	26105304	97000836	24911791	1900123	028			2	04	1435
246D	1	26105304	97000836	24911791	1900123	028			2	04	1434
247G		26110194	96543220	25217900	1912862	037	111111		2	04	1536
248G		26105291	96512964	25384314	1905673	040	111111		2	04	1610

Continued

Table I - Sample Station Index

1	2	3	4	5	6	7	8	9	10	11	12
248X	1	26105291	96512964	25384314	1905873	040			2	04	1610
249G		26105599	96484042	25538608	1911016	043	111111		2	04	1632
250G		26105384	96425285	25855068	1913200	048	111111		2	04	1712
250X	1	26105384	96425285	25855068	1913200	048			2	04	1712
251G		26105125	96395926	26013234	1912858	050	111111		2	04	1820
252G		26104841	96370803	26169259	1912288	050	111111		2	04	1855
252X	1	26104841	96370803	26169259	1912188	050			2	04	1855
253G		26110371	96342437	26318106	1929979	054	111111		2	04	2005
254G		26104940	96312254	26483953	1918095	065	111111		2	04	2042
254C		26104292	96311813	26488077	1911612	065		069	2	04	2042
254B		26104935	96312591	26480887	1917999	065			2	04	2042
254X	1	26104935	96312591	26480887	1917999	065			2	04	2042
254D	1	26104935	96312591	26480887	1917999	065			2	04	2042
255G		26101860	96241800	LORAN H1	FIX	088	111111		2	07	0505
256G		26051740	96229000	LORAN H1	FIX	112	111111		2	07	0541
256C		26051740	96229000	LORAN H1	FIX	112		132	2	07	0541
256B		26051740	96229000	LORAN H1	FIX	112			2	07	0541
256X	1	26051740	96229000	LORAN H1	FIX	112			2	07	0541
256D	1	26051740	96229000	LORAN H1	FIX	112			2	07	0541
257G		26051200	96286000	LORAN H1	FIX	065	111111		2	07	0428
258G		26051740	96311200	LORAN H1	FIX	063	111111		2	07	0410
259G		26051800	96341200	LORAN H1	FIX	056	1111111		2	06	0324
259C		26051800	96341200	LORAN H1	FIX	056		102	2	06	0324
259B		26051800	96341200	LORAN H1	FIX	056			2	06	0324
259X	1	26051800	96341200	LORAN H1	FIX	056			2	06	0324
259D	1	26051800	96341200	LORAN H1	FIX	056			2	06	0324
260G		26062400	96401200	LORAN H1	FIX	048	111111		2	07	0249
261G		26051500	96454500	LORAN H1	FIX	045	111111		2	07	0210
262G		26053822	96464845	25540871	1590185	043	111111		2	07	0155
262C		26053561	96484193	25541378	1587559	043		046	2	07	0155

Continued

Table I - Sample Station Index

1	2	3	4	5	6	7	8	9	10	11	12
262B		26053569	96484366	25539802	1587612	043			2	07	0155
262X	1	26053822	96464845	25540871	1590185	043			2	07	0155
262D	1	26053822	96464845	25540871	1590185	043			2	07	0155
263G		26054401	96513968	25379223	1593905	040	111111		2	07	0040
264G		26054420	96542879	22255054	1992119		111111		2	07	0015
265G		26055058	96572619	25063251	1996550	032	1111111		2	06	2340
265C		26055298	96572744	25062082	1598960	032		056	2	06	2340
265B		26055173	96572609	25063327	1597708	032			2	06	2340
265D	1	26055058	96572619	25063251	1996550	032			2	06	2340
266G		26002435	96572323	25069979	1267233	032	111111		2	07	1401
266C		26001984	96572224	25070940	1262686	032		137	2	07	1401
266B		26001957	96572863	25065109	1262342	032			2	07	1401
266D	1	26002435	96572323	25069979	1267233	032			2	07	1401
267G		26003414	96543755	25219187	1276969	032	111111		2	07	1505
268G		26002679	96514189	25381368	1273618	040	111111		2	07	1528
268X	1	26002679	96514189	25381368	1273618	040			2	07	1528
269G		26002503	96484988	25538318	1273911	045	1111111		2	07	1549
269C		26002022	96485113	25537249	1269033	045		086	2	07	1549
269B		26002780	96490223	25527013	1276557	045			2	07	1549
269X	1	26002503	96484988	25538318	1273911	045			2	07	1549
269D	1	26002503	96484988	25538318	1273911	045			2	07	1549
270G		26000869	96455031	25702376	1259632	047	111111		2	07	1636
271G		26000000	96393000	LORAN H1	FIX	048	111111		2	07	1024
271X		26000000	96393000	LORAN H1	FIX	048			2	07	1024
272G		26004500	96343500	LORAN H1	FIX	057	111111		2	07	0930
273G		26001500	96282500	LORAN H1	FIX	073	1111111		2	07	0824
273C		26001500	96282500	LORAN H1	FIX	073		061	2	07	0824
273B		26001500	96282500	LORAN H1	FIX	073			2	07	0824
273X		26001500	96282500	LORAN H1	FIX	073			2	07	0824
273D		26001500	96282500	LORAN H1	FIX	073			2	07	0824
274G		25593500	96221000	LORAN H1	FIX	134	111111		2	07	0705

Table IIA - Physical Properties, Surficial Bottom Sediments and Suspended Sediments

Explanation for Table

Column 1 - Sample station number (first 3 digits), and sample type (alpha character): G = Smith-MacIntyre grab sample, GR = replicate Smith-MacIntyre grab sample (heavy mineral analysis only), B = box core, W = suspended sediment water sample (T = top water, M = mid-depth water, B = bottom water).

Column 2 - Gravel percentages: asterisks indicate stations where occasional inorganic lithic clasts were observed.

Column 3 - Sand percentage

Column 4 - Silt percentage

Column 5 - Clay percentage

Column 6 - Sediment type using Shepard's (1954) ternary classification system

Column 7 - Sand/Mud ratio

Column 8 - Silt/Clay ratio

Column 9 - First moment measure (mean diameter)

Column 10 - Second moment measure (standard deviation)

Column 11 - Third moment measure (skewness)

Column 12 - Fourth moment measure (kurtosis)

Column 13 - Data card designation number (S1 = sediment property card #1)

Table IIB - Physical Properties, Surficial Bottom Sediments and Suspended Sediments

Explanation for Table

Column 14 - Reiteration of sample station number and sample type (see Column 1)

Column 15 - Median diameter

Column 16 - Modal diameter

Column 17 - Coarsest one-percentile diameter (from cumulative probability curve)

Column 18 - Folk's graphic mean diameter (M_Z)

Column 19 - Folk's inclusive graphic standard deviation ($_I$)

Column 20 - Folk's inclusive graphic skewness (Sk_I)

Column 21 - Folk's graphic kurtosis (K_G)

Column 22 - Total heavy mineral content (weight percentage)

Column 23 - Wet-state color of surficial sediments (upper 1 cm), using GSA rock color chart designations based on the Munsell system: GD = questionalble color designation

Column 24 - Wet-state color of shallow subsurface sediments (below 1 cm), using GSA rock color chart designations based on the Munsell system: ND = no difference from surficial sediment color, QD = questionable color designation

Column 25 - Data card designation number (S2 = sediment property card #2)

Note: For both ~~appendices~~ Tables, a dashed line in any columnar space indicates that the respective property was not determined for that specific sample.

Table IIA - Textural Properties, Surficial Bottom and Suspended sediments

1	2	3	4	5	6	7	8	9	10	11	12	13
001G	0.0	1.42	68.24	30.34	7	0.01	2.25	6.91	1.90	0.16	-0.98	S1
002G	0.0	32.28	45.77	21.95	6	0.48	2.08	5.86	2.27	0.28	-0.93	S1
003G	0.0	37.15	46.15	16.70	3	0.59	2.76	5.35	2.31	0.36	-0.52	S1
004G	0.0	54.41	35.53	10.06	2	1.19	3.53	4.57	2.10	0.61	0.62	S1
005G	0.0	36.16	48.04	15.80	3	0.57	3.04	5.42	2.15	0.42	-0.33	S1
006G	0.0	68.95	24.14	6.91	2	2.22	3.49	4.15	1.89	0.87	2.33	S1
007G	0.0	39.57	48.01	12.42	3	0.65	3.86	5.07	2.09	0.47	0.02	S1
008G	0.0	53.87	37.27	8.86	2	1.17	4.21	4.58	1.94	0.68	1.16	S1
009G	0.0	7.50	66.47	26.03	7	0.08	2.55	6.56	1.98	0.18	-0.86	S1
010G	0.52	52.07	31.92	16.01	2	1.09	1.99	5.02	2.39	0.41	-0.60	S1
011G	0.44*	58.20	26.83	14.97	2	1.39	1.79	4.67	2.31	0.58	0.09	S1
012G	0.0	46.08	31.41	22.51	6	0.85	1.40	5.52	2.48	0.36	-0.88	S1
013G	0.0	23.87	53.57	22.57	6	0.31	2.37	5.99	2.23	0.29	-0.85	S1
014G	0.0	22.31	62.93	14.76	3	0.29	4.26	5.70	1.94	0.39	-0.16	S1
015G	0.0	33.40	51.78	14.82	3	0.50	3.50	5.45	2.06	0.41	-0.29	S1
016G	0.0	33.93	49.51	16.56	3	0.51	2.99	5.49	2.19	0.37	-0.45	S1
017G	0.0	31.11	52.72	16.17	3	0.45	3.26	5.49	2.14	0.35	-0.45	S1
018G	0.06	30.72	52.21	17.07	3	0.44	3.06	5.56	2.17	0.32	-0.58	S1
019G	0.0	36.88	47.80	15.32	3	0.58	3.12	5.43	2.15	0.40	-0.36	S1
020G	0.0	11.61	65.29	23.10	7	0.13	2.83	6.45	1.94	0.17	-0.66	S1
021G	0.0	25.23	50.07	24.69	6	0.34	2.03	6.10	2.29	0.23	-0.97	S1
022G	0.09	26.26	56.03	17.71	3	0.36	3.16	5.73	2.08	0.35	-0.54	S1
023G	0.05	33.96	50.25	15.78	3	0.51	3.18	5.46	2.12	0.39	-0.42	S1
024G	0.0	19.95	61.19	18.85	3	0.25	3.25	5.90	2.12	0.22	-0.64	S1
025G	0.0	37.14	50.42	12.44	3	0.59	4.05	5.16	2.02	0.49	0.13	S1
026G	0.03	39.86	44.53	15.61	3	0.66	2.85	5.22	2.22	0.52	-0.00	S1
027G	0.0	19.18	54.25	26.57	7	0.24	2.04	6.25	2.33	0.18	-1.05	S1
028G	0.0	16.05	65.63	18.32	7	0.19	3.58	5.83	2.03	0.35	-0.48	S1
029G	0.0	23.21	57.75	19.04	3	0.30	3.03	5.85	2.09	0.33	-0.61	S1
030G	0.0	8.72	70.50	20.78	7	0.10	3.39	6.25	1.94	0.28	-0.62	S1

Continued

Table IIA - Textural Properties, Surficial Bottom and Suspended sediments

1	2	3	4	5	6	7	8	9	10	11	12	13
031G	0.11	14.96	60.67	24.37	7	0.18	2.49	6.25	2.17	0.27	-0.90	S1
032G	0.0	15.54	67.80	16.66	7	0.18	4.07	6.10	1.89	0.29	-0.27	S1
033G	0.0	9.96	62.74	27.36	7	0.11	2.29	6.71	2.00	0.07	-0.78	S1
034G	0.0	4.89	66.60	28.51	7	0.05	2.34	6.83	1.91	0.13	-0.84	S1
035G	0.0	23.91	58.68	17.41	3	0.31	3.37	5.81	2.05	0.34	-0.53	S1
036G	0.03	23.19	61.78	15.03	3	0.30	4.11	5.64	2.00	0.34	-0.29	S1
037G	0.07	16.85	66.43	16.72	3	0.20	3.97	5.86	1.98	0.30	-0.35	S1
038G	0.03	14.28	66.37	19.36	7	0.17	3.43	6.08	1.99	0.26	-0.56	S1
039G	0.0	11.03	62.56	26.41	7	0.12	2.37	6.54	2.07	0.18	-0.93	S1
040G	0.0	11.88	66.97	21.15	7	0.13	3.17	6.24	1.95	0.26	-0.63	S1
041G	0.0	9.00	75.29	15.71	4	0.10	4.79	5.94	1.80	0.45	-0.01	S1
042G	0.0	10.98	69.86	19.16	7	0.12	3.65	6.17	1.88	0.32	-0.45	S1
043G	0.0	18.32	64.79	16.89	3	0.22	3.84	5.76	1.98	0.43	-0.26	S1
044G	0.03	32.81	51.83	15.36	3	0.49	3.38	5.36	2.11	0.44	-0.29	S1
045G	0.0	21.26	60.40	18.34	3	0.27	3.29	5.83	2.09	0.31	-0.62	S1
046G	0.0	4.01	49.37	46.62	7	0.04	1.06	7.43	2.19	-0.08	-1.30	S1
047G	0.0	17.33	66.15	16.52	7	0.21	4.00	5.79	1.94	0.42	-0.26	S1
048G	0.0	4.77	72.50	22.72	7	0.05	3.19	6.44	1.89	0.27	-0.67	S1
050G	0.01	5.54	70.65	23.81	7	0.06	2.97	6.49	1.92	0.26	-0.71	S1
051G	0.0	8.08	73.98	17.94	7	0.09	4.12	6.11	1.86	0.37	-0.31	S1
052G	0.0	1.57	60.62	37.82	7	0.02	1.60	7.32	1.89	0.07	-1.09	S1
053G	0.0	0.77	62.56	36.67	7	0.01	1.71	7.36	1.79	0.05	-0.86	S1
054G	0.0	10.03	60.98	28.99	7	0.11	2.10	6.78	2.04	0.11	-0.92	S1
055G	0.0	14.36	66.61	19.03	7	0.17	3.50	6.09	1.99	0.26	-0.55	S1
056G	0.04	17.19	63.12	19.68	7	0.21	3.21	6.06	2.07	0.24	-0.64	S1
057G	1.13	35.99	50.47	13.54	3	0.56	3.73	5.25	2.21	0.31	-0.49	S1
058G	0.03	4.81	66.21	28.98	7	0.05	2.28	6.85	1.93	0.10	-0.77	S1
059G	0.01	33.10	53.36	13.54	3	0.49	3.94	5.44	2.05	0.40	-0.17	S1
060G	0.0	15.27	65.92	18.81	7	0.18	3.50	6.08	1.98	0.29	-0.51	S1
061G	0.0	7.72	44.07	48.21	9	0.08	0.91	7.42	2.32	-0.09	-1.33	S1

Continued

Table IIA - Textural Properties, Surficial Bottom and Suspended sediments

1	2	3	4	5	6	7	8	9	10	11	12	13
062G	0.0	3.72	75.05	21.23	4	0.04	3.54	6.36	1.87	0.36	-0.46	S1
063G	0.0	6.91	63.83	29.26	7	0.07	2.18	6.75	2.02	0.11	-0.97	S1
064G	0.05	1.27	70.81	27.92	7	0.01	2.54	6.98	1.73	0.21	-0.70	S1
065G	0.0	18.97	62.72	18.32	3	0.23	3.42	5.88	2.03	0.34	-0.55	S1
066G	0.0	5.32	67.06	27.61	7	0.06	2.43	6.62	2.02	0.21	-0.96	S1
067G	0.0	4.29	68.77	26.94	7	0.04	2.55	6.62	1.97	0.22	-0.91	S1
068G	0.02	40.10	44.14	15.76	3	0.67	2.80	5.44	2.13	0.41	-0.44	S1
069G	0.03	5.91	69.33	24.75	7	0.06	2.80	6.41	2.02	0.28	-0.85	S1
070G	0.0	19.22	62.37	18.41	3	0.24	3.39	5.87	2.03	0.37	-0.50	S1
071G	0.0	7.62	72.49	19.88	7	0.08	3.65	6.08	1.96	0.39	-0.45	S1
072G	0.0	4.39	74.50	21.11	7	0.05	3.53	6.20	1.97	0.38	-0.57	S1
073G	0.0	5.52	64.91	29.57	7	0.06	2.19	6.65	2.10	0.18	-1.11	S1
074G	0.0	23.77	45.63	30.60	6	0.31	1.49	6.47	2.33	0.13	-1.25	S1
075G	0.0	2.21	70.29	27.50	7	0.02	2.56	6.65	1.98	0.25	-0.95	S1
076G	0.0	9.13	60.20	30.67	7	0.10	1.96	6.71	2.11	0.13	-1.10	S1
077G	0.0	11.48	66.19	22.32	7	0.13	2.97	6.23	2.01	0.28	-0.73	S1
080G	26.65*	0.00	65.32	34.68	7	0.00	1.88	7.15	1.90	0.10	-1.08	S1
083G	0.0	5.81	67.81	26.38	7	0.06	2.57	6.61	1.98	0.21	-0.84	S1
084G	0.0	10.77	66.44	22.79	7	0.12	2.92	6.36	1.99	0.21	-0.67	S1
085G	0.02	3.66	59.21	37.13	7	0.04	1.59	7.27	1.94	0.00	-0.87	S1
086G	0.03	3.26	57.90	38.84	7	0.03	1.49	7.37	1.91	-0.04	-0.75	S1
087G	0.0	3.40	48.96	47.64	7	0.04	1.03	7.66	1.97	-0.29	0.23	S1
088G	0.0	3.45	46.50	50.05	9	0.04	0.93	7.80	1.91	-0.22	-0.49	S1
089G	0.0	3.15	60.57	36.28	7	0.03	1.67	7.23	1.90	0.01	-0.86	S1
090G	0.0	11.10	63.31	25.59	7	0.12	2.47	6.42	2.09	0.18	-0.91	S1
091G	1.67	9.76	69.26	20.98	7	0.11	3.30	6.11	2.02	0.38	-0.53	S1
092G	0.0	1.63	67.27	31.10	7	0.02	2.16	7.05	1.88	0.16	-0.95	S1
093G	0.0	0.00	57.24	42.76	7	0.00	1.34	7.76	1.59	0.03	-0.86	S1
094G	0.0	1.85	68.51	29.64	7	0.02	2.31	6.96	1.86	0.15	-0.89	S1
095G	0.0	13.68	67.53	18.80	7	0.16	3.59	5.99	1.98	0.38	-0.46	S1

Continued

Table IIA - Textural Properties, Surficial Bottom and Suspended sediments

1	2	3	4	5	6	7	8	9	10	11	12	13
096G	0.0	13.24	63.73	23.03	7	0.15	2.77	6.25	2.07	0.28	-0.79	S1
097G	0.0	3.44	71.13	25.42	7	0.04	2.80	6.61	1.91	0.24	-0.82	S1
098G	0.0	2.53	65.24	32.23	7	0.03	2.02	7.02	1.93	0.11	-1.01	S1
099G	0.0	11.45	67.96	20.59	7	0.13	3.30	6.17	1.97	0.34	-0.56	S1
100G	0.0	0.83	68.32	30.85	7	0.01	2.21	6.93	1.90	0.19	-1.03	S1
101G	0.0	12.67	75.98	11.35	4	0.15	6.69	5.56	1.70	0.59	0.85	S1
102G	0.0	0.82	66.48	32.70	7	0.01	2.03	7.04	1.89	0.15	-1.06	S1
103G	0.0	1.50	73.26	25.24	7	0.02	2.90	6.55	1.91	0.31	-0.79	S1
104G	0.0	1.87	74.00	24.13	7	0.02	3.07	6.62	1.81	0.30	-0.64	S1
105G	0.0	5.24	78.84	15.92	4	0.06	4.95	5.98	1.79	0.48	0.03	S1
106G	0.0	9.75	65.34	24.91	7	0.11	2.62	6.44	2.04	0.25	-0.86	S1
107G	0.0	2.52	68.20	29.27	7	0.03	2.33	6.85	1.91	0.20	-0.93	S1
108G	0.0	4.95	72.94	22.11	7	0.05	3.30	6.43	1.89	0.28	-0.64	S1
110G	0.0	3.29	60.09	36.62	7	0.03	1.64	7.10	2.06	0.08	-1.22	S1
111G	0.0	1.32	59.43	39.25	7	0.01	1.51	7.45	1.81	0.03	-0.98	S1
112G	0.56	1.99	53.10	44.90	7	0.02	1.18	7.62	1.90	-0.17	-0.26	S1
113G	0.07	3.63	50.22	46.15	7	0.04	1.09	7.59	2.03	-0.17	-0.77	S1
114G	0.04	1.96	46.37	51.67	9	0.02	0.90	7.88	1.84	-0.23	-0.40	S1
115G	0.0	1.19	51.35	47.47	7	0.01	1.08	7.75	1.86	-0.08	-1.00	S1
116G	0.01	2.88	68.67	28.46	7	0.03	2.41	6.84	1.90	0.18	-0.88	S1
117G	0.0	6.09	67.57	26.34	7	0.06	2.57	6.60	2.02	0.20	-0.92	S1
118G	0.0	7.04	62.01	30.95	7	0.08	2.00	6.80	2.07	0.12	-1.07	S1
119G	0.0	1.17	66.28	32.55	7	0.01	2.04	7.05	1.91	0.13	-1.05	S1
120G	0.0	0.00	69.50	30.50	7	0.00	2.28	7.06	1.80	0.20	-0.92	S1
121G	0.03	2.43	71.69	25.88	7	0.02	2.77	6.65	1.91	0.23	-0.79	S1
122G	0.0	0.00	66.05	33.95	7	0.00	1.95	7.06	1.95	0.15	-1.14	S1
123G	0.0	2.75	70.39	26.85	7	0.03	2.62	6.57	1.99	0.25	-0.95	S1
124G	0.0	3.53	59.84	36.63	7	0.04	1.63	7.17	1.96	0.04	-1.08	S1
125G	0.15	5.58	73.99	20.42	7	0.06	3.62	6.18	1.95	0.34	-0.50	S1
126G	0.0	1.00	72.65	26.35	7	0.01	2.76	6.66	1.91	0.29	-0.84	S1

Continued

Table IIA - Textural Properties, Surficial Bottom and Suspended sediments

1	2	3	4	5	6	7	8	9	10	11	12	13
127G	0.0	3.96	56.24	39.79	7	0.04	1.41	7.26	2.03	0.00	-1.15	S1
128G	0.0	3.09	69.59	27.31	7	0.03	2.55	6.71	1.90	0.22	-0.86	S1
129G	0.0	0.73	71.70	27.57	7	0.01	2.60	6.86	1.81	0.22	-0.81	S1
130G	0.0	0.89	69.74	29.37	7	0.01	2.37	6.89	1.90	0.19	-0.96	S1
131G	0.0	1.73	66.16	32.11	7	0.02	2.06	6.92	2.01	0.17	-1.13	S1
132G	0.0	2.44	75.08	22.48	4	0.03	3.34	6.42	1.90	0.33	-0.65	S1
133G	0.0	1.90	69.31	28.78	7	0.02	2.41	6.86	1.89	0.17	-0.91	S1
134G	0.0	0.66	65.54	33.80	7	0.01	1.94	7.25	1.75	0.12	-0.90	S1
135G	0.0	0.74	61.56	37.71	7	0.01	1.63	7.36	1.81	0.07	-0.99	S1
136G	0.0	0.00	52.79	47.21	7	0.00	1.12	7.75	1.83	-0.08	-1.02	S1
137G	0.0	1.98	53.11	44.91	7	0.02	1.18	7.61	1.92	-0.10	-0.85	S1
138G	0.23	3.56	63.58	32.85	7	0.04	1.94	7.02	1.96	0.10	-1.00	S1
139G	0.0	0.68	55.21	44.10	7	0.01	1.25	7.69	1.74	-0.03	-0.92	S1
140G	0.0	0.48	57.22	42.30	7	0.00	1.35	7.59	1.82	-0.00	-1.05	S1
141G	0.0	1.00	67.20	31.80	7	0.01	2.11	7.10	1.81	0.15	-0.90	S1
142G	0.0	0.94	69.64	29.41	7	0.01	2.37	6.95	1.85	0.21	-0.91	S1
143G	0.03	1.85	60.94	37.22	7	0.02	1.64	7.18	1.97	0.08	-1.19	S1
144G	0.0	3.61	76.67	19.72	7	0.04	3.89	6.29	1.83	0.37	-0.38	S1
145G	0.0	2.38	72.04	25.58	7	0.02	2.82	6.59	1.93	0.27	-0.82	S1
146G	0.0	9.26	51.24	39.50	7	0.10	1.30	7.12	2.17	-0.02	-1.20	S1
147G	0.0	16.37	71.38	12.25	3	0.20	5.83	5.48	1.81	0.60	0.66	S1
148G	0.0	8.45	65.96	25.59	7	0.09	2.58	6.48	2.02	0.21	-0.92	S1
149G	0.0	0.88	75.69	23.43	4	0.01	3.23	6.52	1.86	0.33	-0.65	S1
150G	0.0	0.00	63.54	36.46	7	0.00	1.74	7.36	1.76	0.10	-1.01	S1
151G	0.0	0.87	67.23	31.90	7	0.01	2.11	7.05	1.85	0.15	-0.99	S1
152G	0.0	0.47	62.22	37.31	7	0.00	1.67	7.47	1.70	0.06	-0.87	S1
153G	0.0	0.00	57.86	42.14	7	0.00	1.37	7.66	1.71	0.07	-1.14	S1
154G	0.0	0.00	66.77	33.23	7	0.00	2.01	7.21	1.76	0.17	-0.96	S1
155G	0.0	0.00	60.44	39.54	7	0.00	1.53	7.47	1.78	0.06	-1.09	S1
156G	0.0	0.00	62.67	37.33	7	0.00	1.68	7.41	1.75	0.09	-1.00	S1

Continued

Table IIA - Textural Properties, Surficial Bottom and Suspended sediments

1	2	3	4	5	6	7	8	9	10	11	12	13
157G	0.0	0.00	58.20	41.80	7	0.00	1.39	7.67	1.68	0.05	-1.04	S1
158G	0.0	0.64	66.46	32.89	7	0.01	2.02	7.12	1.84	0.14	-1.00	S1
159G	0.0	1.15	67.45	31.40	7	0.01	2.15	7.11	1.80	0.15	-0.88	S1
160G	0.0	1.15	67.08	31.77	7	0.01	2.11	7.01	1.89	0.15	-1.01	S1
162G	0.0	1.89	63.56	34.55	7	0.02	1.84	7.16	1.89	0.09	-1.03	S1
163G	0.0	2.37	65.78	31.85	7	0.02	2.06	7.01	1.91	0.12	-1.02	S1
164G	0.0	1.35	65.35	33.30	7	0.01	1.96	7.12	1.86	0.11	-0.98	S1
165G	0.0	3.49	53.76	42.74	7	0.04	1.26	7.46	1.94	-0.06	-1.00	S1
166G	0.0	1.72	70.16	28.11	7	0.02	2.50	6.82	1.87	0.20	-0.89	S1
167G	0.0	1.76	64.33	33.91	7	0.02	1.90	7.01	1.98	0.10	-1.14	S1
168G	0.06	1.28	64.18	34.54	7	0.01	1.86	7.11	1.92	0.09	-1.09	S1
169G	0.0	7.23	63.74	29.03	7	0.08	2.20	6.66	2.04	0.17	-1.04	S1
170G	0.0	0.76	69.88	29.37	7	0.01	2.38	6.84	1.91	0.21	-0.99	S1
171G	0.0	0.89	70.54	28.58	7	0.01	2.47	6.85	1.86	0.23	-0.92	S1
173G	0.0	0.00	71.12	28.88	7	0.00	2.46	7.06	1.68	0.27	-0.75	S1
174G	0.0	0.00	62.99	37.01	7	0.00	1.70	7.43	1.71	0.11	-1.01	S1
175G	0.0	0.00	61.18	38.82	7	0.00	1.58	7.46	1.76	0.07	-1.06	S1
176G	0.0	0.67	49.89	49.44	9	0.01	1.01	7.80	1.82	-0.13	-0.84	S1
177G	0.04	0.00	60.59	39.31	7	0.00	1.54	7.51	1.76	0.08	-1.10	S1
178G	0.0	0.47	74.91	24.62	7	0.00	3.04	6.71	1.77	0.30	-0.65	S1
179G	0.0	0.00	66.43	33.57	7	0.00	1.98	7.16	1.81	0.15	-1.03	S1
180G	0.0	0.00	70.18	29.82	7	0.00	2.35	6.94	1.81	0.23	-0.95	S1
181G	0.0	0.40	67.84	31.76	7	0.00	2.14	7.04	1.84	0.17	-1.00	S1
182G	0.0	0.97	74.22	24.81	7	0.01	2.99	6.66	1.83	0.29	-0.70	S1
183G	0.0	1.39	63.12	35.50	7	0.01	1.78	7.10	1.95	0.07	-1.14	S1
184G	0.03	1.40	67.66	30.94	7	0.01	2.19	6.87	1.97	0.14	-1.05	S1
185G	0.22	1.63	58.65	39.72	7	0.02	1.48	7.33	1.93	-0.00	-1.06	S1
186G	11.47	67.31	22.28	10.41	2	2.06	2.14	3.89	2.43	0.64	0.45	S1
187G	0.0	1.05	68.74	30.22	7	0.01	2.27	6.84	1.94	0.17	-1.04	S1
188G	0.01	1.15	64.56	34.28	7	0.01	1.88	7.08	1.92	0.08	-1.01	S1

Continued

Table IIA - Textural Properties, Surficial Bottom and Suspended sediments

1	2	3	4	5	6	7	8	9	10	11	12	13
189G	0.02	0.00	61.17	38.83	7	0.00	1.58	7.30	1.88	0.07	-1.20	S1
190G	0.0	0.00	54.87	45.13	7	0.00	1.22	7.72	1.70	0.00	-1.11	S1
191G	9.03	13.63	50.70	35.67	7	0.16	1.42	6.62	2.92	-0.47	0.30	S1
192G	0.0	0.00	51.67	48.33	7	0.00	1.07	7.84	1.68	-0.04	-1.01	S1
193G	0.0	0.00	46.90	53.10	9	0.00	0.88	8.04	1.64	-0.11	-0.91	S1
194G	0.0	0.00	58.14	41.86	7	0.00	1.39	7.69	1.65	0.05	-0.99	S1
195G	0.0	0.00	63.76	36.24	7	0.00	1.76	7.43	1.70	0.13	-1.00	S1
196G	26.03	41.05	38.39	20.56	6	0.70	1.87	4.32	3.88	-0.03	-1.52	S1
197G	0.42	0.00	60.35	39.65	7	0.00	1.52	7.52	1.71	0.09	-1.08	S1
198G	0.11	0.00	67.56	32.44	7	0.00	2.08	7.12	1.82	0.17	-1.03	S1
199G	0.03	0.89	65.28	33.83	7	0.01	1.93	7.18	1.86	0.08	-0.88	S1
200G	0.0	0.00	60.49	39.51	7	0.00	1.53	7.49	1.79	0.02	-1.00	S1
201G	0.0	1.74	67.51	30.76	7	0.02	2.19	6.97	1.89	0.14	-0.92	S1
202G	8.23	73.73	17.47	8.80	2	2.81	1.98	3.70	2.22	0.84	1.65	S1
203G	10.02	69.57	20.05	10.38	2	2.29	1.93	3.86	2.37	0.68	0.81	S1
204G	0.0	1.61	65.07	33.32	7	0.02	1.95	6.97	1.98	0.09	-0.96	S1
205G	0.0	1.70	66.35	31.94	7	0.02	2.08	7.04	1.90	0.06	-0.86	S1
206G	0.0	0.68	71.10	28.22	7	0.01	2.52	6.85	1.86	0.20	-0.85	S1
207G	0.03	1.88	67.36	30.76	7	0.02	2.19	6.98	1.88	0.11	-0.70	S1
208G	0.10	46.25	30.89	22.86	6	0.86	1.35	5.27	2.86	0.18	-1.30	S1
209G	0.0	0.00	56.67	43.33	7	0.00	1.31	7.69	1.70	0.01	-1.02	S1
210G	0.0	0.00	46.35	53.65	9	0.00	0.86	8.17	1.51	-0.05	-0.92	S1
211G	0.0	0.57	57.13	42.30	7	0.01	1.35	7.67	1.70	0.01	-0.90	S1
212G	0.0	13.68	51.41	34.91	7	0.16	1.47	6.43	2.30	-0.18	-0.62	S1
216G	0.0	10.46	52.34	37.19	7	0.12	1.41	7.11	2.20	-0.18	-0.54	S1
217G	0.0	1.08	51.09	47.83	7	0.01	1.07	7.82	1.74	-0.13	-0.55	S1
218G	2.00	53.54	27.22	19.24	2	1.15	1.41	4.86	2.83	0.29	-1.16	S1
219G	0.99	50.45	30.81	18.74	2	1.02	1.64	4.96	2.75	0.28	-1.12	S1
220G	0.97	66.73	19.50	13.77	2	2.01	1.42	4.19	2.61	0.56	-0.24	S1
221G	0.06	1.51	63.89	34.60	7	0.02	1.85	7.08	1.97	0.08	-1.07	S1

Continued

Table IIA - Textural Properties, Surficial Bottom and Suspended sediments

1	2	3	4	5	6	7	8	9	10	11	12	13
222G	0.0	0.00	62.77	37.23	7	0.00	1.69	7.30	1.85	0.06	-1.10	S1
223G	0.0	1.10	64.48	34.41	7	0.01	1.87	7.09	1.94	0.10	-1.07	S1
224G	1.74	23.93	48.96	27.11	6	0.31	1.81	6.01	2.64	0.01	-1.15	S1
225G	7.23	66.94	21.86	11.20	2	2.02	1.95	3.98	2.48	0.62	0.21	S1
226G	0.0	0.59	58.87	40.54	7	0.01	1.45	7.45	1.83	-0.00	-1.00	S1
227G	0.0	1.09	58.23	40.68	7	0.01	1.43	7.41	1.89	-0.00	-1.08	S1
228G	0.66*	32.95	42.33	24.72	6	0.49	1.71	5.65	2.74	0.08	-1.25	S1
229G	1.38	57.23	26.79	15.98	2	1.34	1.68	4.55	2.72	0.39	-0.82	S1
230G	2.90	71.19	17.17	11.64	2	2.47	1.47	3.94	2.50	0.65	0.30	S1
231G	1.15	47.82	27.20	24.98	6	0.92	1.09	5.20	3.03	0.17	-1.40	S1
232G	0.0	8.10	46.22	45.68	7	0.09	1.01	7.49	2.17	-0.36	0.05	S1
233G	2.07	68.85	19.85	11.29	2	2.21	1.76	4.00	2.48	0.62	0.21	S1
234G	0.0	0.00	58.51	41.49	7	0.00	1.41	7.63	1.68	0.05	-1.00	S1
235G	2.13	57.11	26.91	15.98	2	1.33	1.68	4.67	2.66	0.39	-0.79	S1
236G	3.68	69.64	18.31	12.05	2	2.29	1.52	4.06	2.52	0.60	0.03	S1
237G	0.75	54.33	26.27	19.41	2	1.19	1.35	4.79	2.86	0.31	-1.12	S1
238G	1.16	67.80	19.14	13.06	2	2.11	1.47	4.11	2.57	0.58	-0.11	S1
239G	0.49	28.75	41.44	29.82	6	0.40	1.39	6.15	2.75	-0.07	-1.26	S1
240G	0.66	18.04	50.21	31.75	7	0.22	1.58	6.55	2.50	-0.14	-0.85	S1
241G	0.21	27.36	49.36	23.27	6	0.38	2.12	5.78	2.62	0.04	-1.09	S1
242G	0.0	1.08	62.29	36.63	7	0.01	1.70	7.20	1.93	0.05	-1.04	S1
243G	0.0	1.14	65.33	33.52	7	0.01	1.95	7.12	1.87	0.11	-1.00	S1
244G	0.0	0.68	64.70	34.62	7	0.01	1.87	7.04	1.96	0.12	-1.17	S1
245G	1.62	33.15	38.61	28.25	6	0.50	1.37	5.90	2.84	-0.00	-1.30	S1
246G	0.10	28.47	44.09	27.44	6	0.40	1.61	6.00	2.70	-0.01	-1.18	S1
247G	0.07	7.79	61.67	30.55	7	0.08	2.02	6.78	2.15	-0.06	-0.58	S1
248G	0.0	0.70	61.70	37.60	7	0.01	1.64	7.26	1.91	0.07	-1.14	S1
249G	0.0	0.56	50.32	49.12	7	0.01	0.02	7.86	1.77	-0.11	-0.84	S1
250G	0.13	2.61	64.01	33.37	7	0.03	1.92	7.10	1.95	0.03	-0.74	S1
251G	0.20	4.70	57.89	37.40	7	0.05	1.55	7.27	2.03	-0.15	-0.16	S1

Continued

Table IIA - Textural Properties, Surficial Bottom and Suspended sediments

1	2	3	4	5	6	7	8	9	10	11	12	13
252G	1.72	58.38	27.18	14.44	2	1.40	1.88	4.47	2.65	0.40	-0.64	S1
253G	---	55.83	27.96	16.22	2	1.26	1.72	4.57	2.77	0.34	-0.74	S1
254G	0.31	28.07	46.80	25.13	6	0.39	1.86	5.94	2.60	0.03	-1.15	S1
255G	0.44	47.48	36.62	15.90	2	0.90	2.30	4.96	2.57	0.30	-0.86	S1
256G	0.0	1.26	59.90	38.84	7	0.01	1.54	7.52	1.74	0.02	-0.75	S1
257G	2.60	69.71	20.16	10.14	2	2.30	1.99	3.89	2.40	0.68	0.57	S1
258G	2.98	63.54	23.15	13.31	2	1.74	1.74	4.12	2.76	0.37	-0.35	S1
259G	10.47	58.93	26.25	14.83	2	1.43	1.77	4.50	2.61	0.44	-0.60	S1
260G	0.0	5.49	64.13	30.38	7	0.06	2.11	6.85	2.04	0.03	-0.68	S1
261G	7.00	26.14	53.26	20.60	6	0.35	2.59	5.60	2.48	0.13	-0.91	S1
262G	0.71	1.86	62.36	35.78	7	0.02	1.74	7.24	1.90	0.01	-0.84	S1
263G	0.10	20.65	60.11	19.24	3	0.26	3.13	5.59	2.32	0.25	-0.66	S1
264G	0.20	44.78	36.80	18.41	2	0.81	2.00	5.02	2.71	0.24	-1.09	S1
265G	0.46*	47.99	38.71	13.30	2	0.92	2.91	4.65	2.46	0.40	-0.52	S1
266G	0.20	63.06	25.24	11.70	2	1.71	2.16	4.10	2.45	0.60	0.14	S1
267G	1.91	90.17	6.24	3.59	1	9.18	1.74	2.91	1.55	---	---	S1
268G	4.67*	64.13	21.10	14.17	2	1.79	1.43	4.27	2.66	0.50	-0.45	S1
269G	1.96*	27.84	45.87	26.30	6	0.39	1.74	5.91	2.69	0.03	-1.20	S1
270G	0.88	29.93	44.27	25.81	6	0.43	1.72	5.83	2.67	0.06	-1.22	S1
271G	3.72	34.66	41.76	23.58	6	0.53	1.77	5.61	2.71	0.12	-1.21	S1
272G	4.68	33.93	41.71	24.36	6	0.51	1.71	5.68	2.75	0.06	-1.28	S1
273G	1.59	63.15	25.07	11.77	2	1.71	2.13	4.21	2.46	0.56	0.00	S1
274G	0.0	0.42	53.21	46.37	7	0.00	1.15	7.82	1.68	-0.03	-0.91	S1

continued

Table IIA - Textural Properties, Surficial Bottom and Suspended sediments

1	2	3	4	5	6	7	8	9	10	11	12	13
004GR	---	---	---	---	---	---	---	---	---	---	---	S1
010GR	---	---	---	---	---	---	---	---	---	---	---	S1
019GR	---	---	---	---	---	---	---	---	---	---	---	S1
022GR	---	---	---	---	---	---	---	---	---	---	---	S1
026GR	---	---	---	---	---	---	---	---	---	---	---	S1
091GR	---	---	---	---	---	---	---	---	---	---	---	S1
095GR	---	---	---	---	---	---	---	---	---	---	---	S1
101GR	---	---	---	---	---	---	---	---	---	---	---	S1
147GR	---	---	---	---	---	---	---	---	---	---	---	S1
186GR	---	---	---	---	---	---	---	---	---	---	---	S1
203GR	---	---	---	---	---	---	---	---	---	---	---	S1
220GR	---	---	---	---	---	---	---	---	---	---	---	S1
233GR	---	---	---	---	---	---	---	---	---	---	---	S1
252GR	---	---	---	---	---	---	---	---	---	---	---	S1
266GR	---	---	---	---	---	---	---	---	---	---	---	S1
273GR	---	---	---	---	---	---	---	---	---	---	---	S1
016B	0.0	33.76	46.91	19.33	3	0.51	2.43	5.68	2.27	0.28	-0.82	S1
019B	0.0	34.77	45.19	20.04	3	0.53	2.25	5.74	2.36	0.35	-0.69	S1
024B	0.0	27.03	56.18	16.79	3	0.37	3.35	5.56	2.21	0.28	-0.58	S1
027B	0.0	20.90	57.79	21.30	6	0.26	2.71	6.01	2.24	0.15	-0.83	S1
032B	0.03	24.34	53.58	22.07	6	0.32	2.43	6.08	2.17	0.23	-0.90	S1
036B	0.03	30.05	53.34	16.61	3	0.43	3.21	5.59	2.19	0.29	-0.62	S1
051B	0.01	6.79	67.02	26.20	7	0.07	2.56	6.61	1.98	0.17	0.86	S1
070B	0.0	4.36	70.02	25.02	7	0.05	2.82	6.54	1.96	0.22	-0.81	S1
075B	0.0	12.14	67.58	20.28	7	0.14	3.33	6.09	2.01	0.34	-0.61	S1
085B	0.0	6.98	54.74	38.28	7	0.08	1.43	7.22	2.05	-0.07	-0.86	S1
106B	0.0	0.87	73.87	25.26	7	0.01	2.92	6.71	1.83	0.25	-0.77	S1
110B	0.0	2.39	66.92	30.69	7	0.02	2.18	7.06	1.82	0.12	-0.81	S1
120B	0.0	1.85	66.42	31.73	7	0.02	2.09	6.96	1.95	0.16	-1.07	S1
125B	0.0	3.84	71.26	24.89	7	0.04	2.86	6.58	1.92	0.24	-0.77	S1

continued

Table IIA - Textural Properties, Surficial Bottom and Suspended sediments

1	2	3	4	5	6	7	8	9	10	11	12	13
145B	0.0	5.74	60.61	33.65	7	0.06	1.80	6.96	2.04	0.05	-1.07	S1
160B	0.0	1.99	75.88	22.13	4	0.02	3.43	6.37	1.90	0.33	-0.65	S1
165B	0.0	2.94	75.86	21.19	7	0.03	3.58	6.28	1.89	0.35	-0.59	S1
179B	0.0	0.56	64.42	35.03	7	0.01	1.84	7.28	1.79	0.10	-0.95	S1
185B	0.12	2.55	73.23	24.21	7	0.03	3.02	6.42	1.96	0.30	-0.79	S1
194B	71.53	0.00	55.33	44.67	7	0.00	1.24	7.78	1.63	0.03	-1.02	S1
199B	0.0	1.47	71.50	27.03	7	0.01	2.65	6.72	1.91	0.22	-0.79	S1
202B	12.26	72.30	19.16	8.54	2	2.61	2.24	3.74	2.25	0.71	1.30	S1
225B	4.73	64.40	21.31	14.29	2	1.81	1.49	4.09	2.67	0.54	-0.15	S1
245B	0.94	44.20	38.98	16.82	2	0.79	2.32	4.87	2.68	0.26	-1.03	S1
254B	1.90	35.85	38.91	25.23	6	0.56	1.54	5.75	2.78	0.05	-1.32	S1
259B	0.96	45.17	34.10	20.74	6	0.82	1.64	5.14	2.84	0.16	-1.23	S1
266B	0.45	44.84	38.43	16.73	2	0.81	2.30	4.98	2.65	0.26	-1.04	S1
273B	3.15	60.14	22.46	17.40	2	1.51	1.29	4.58	2.74	0.42	-0.81	S1
010WT	0.0	1.51	78.14	20.35	4	0.02	3.84	7.16	1.21	0.11	0.97	S1
010WM	0.0	0.85	78.71	20.44	4	0.01	3.85	6.89	1.46	0.32	-0.08	S1
010WB	0.0	0.07	73.05	26.88	7	0.00	2.72	7.28	1.30	0.20	-0.03	S1
024WT	0.0	1.33	45.07	53.60	9	0.01	0.84	8.13	1.82	-0.18	-0.63	S1
024WM	0.0	1.72	49.68	48.60	7	0.02	1.02	7.85	1.83	-0.13	-0.77	S1
024WB	0.0	0.75	33.92	65.33	9	0.01	0.52	8.84	1.97	-0.36	-0.77	S1
032WT	0.0	1.38	40.68	57.94	9	0.01	0.70	7.99	1.78	-0.21	-0.63	S1
032WM	0.0	1.44	35.60	62.96	9	0.01	0.57	8.58	2.21	-0.32	-1.08	S1
032WB	0.0	0.04	31.44	68.52	9	0.00	0.46	8.68	1.39	-0.27	0.21	S1
060WT	0.0	3.03	44.64	52.33	9	0.03	0.85	7.81	2.19	-0.15	-1.23	S1
060WM	0.0	4.67	43.87	51.46	9	0.05	0.85	7.82	2.24	-0.12	-1.32	S1
060WB	0.0	0.00	65.68	34.32	7	0.00	1.91	7.48	1.34	0.09	-0.44	S1
070WT	0.0	1.04	16.66	82.30	10	0.01	0.20	9.01	1.70	-0.68	1.40	S1
070WM	0.0	3.74	26.29	69.97	9	0.04	0.38	8.58	2.32	-0.45	-0.79	S1
070WB	0.0	3.18	61.24	35.57	7	0.03	1.72	7.42	1.94	0.03	-0.89	S1
073WT	0.0	1.77	58.39	39.84	7	0.02	1.47	7.46	2.02	0.07	-1.24	S1

continued

Table IIA - Textural Properties, Surficial Bottom and Suspended sediments

1	2	3	4	5	6	7	8	9	10	11	12	13
073WM	0.0	6.50	56.82	36.69	7	0.07	1.55	6.84	2.50	0.17	-1.51	S1
073WB	0.0	0.66	88.40	10.94	4	0.01	8.08	6.76	1.21	0.53	2.11	S1
085WT	0.0	1.29	26.79	71.92	9	0.01	0.37	8.63	1.68	-0.48	0.10	S1
085WM	0.0	5.92	62.44	31.64	7	0.06	1.97	6.74	2.49	0.29	-1.30	S1
085WB	0.0	0.00	71.93	28.07	7	0.00	2.56	7.29	1.21	0.15	0.04	S1
088WT	0.0	0.62	32.43	66.95	9	0.01	0.48	8.33	1.61	-0.34	-0.24	S1
088WM	0.0	2.07	50.48	47.46	7	0.02	1.06	7.85	2.36	-0.01	-1.60	S1
088WB	0.0	0.52	55.43	44.05	7	0.01	1.26	8.00	1.66	0.06	-0.80	S1
095WT	0.0	2.99	65.82	31.19	7	0.03	2.11	7.27	1.84	0.12	-0.65	S1
095WM	0.0	0.72	39.49	59.79	9	0.01	0.66	8.53	1.83	-0.24	-0.83	S1
095WB	0.0	3.26	64.91	31.83	7	0.03	2.04	7.28	1.90	0.10	-0.80	S1
110WT	0.0	1.70	48.86	49.45	9	0.02	0.99	7.92	2.33	-0.09	-1.49	S1
110WM	0.0	2.98	31.79	65.23	9	0.03	0.49	8.57	2.35	-0.38	-0.97	S1
110WB	0.0	1.27	48.08	50.65	9	0.01	0.95	8.02	1.41	-0.25	0.81	S1
114WT	0.0	1.84	27.17	70.99	9	0.02	0.38	8.72	2.10	-0.50	-0.33	S1
114WM	0.0	20.49	60.67	18.84	3	0.26	3.22	5.56	2.26	0.67	0.25	S1
114WB	0.0	11.53	41.86	46.61	9	0.13	0.90	7.21	2.98	0.04	-1.87	S1
115WT	0.0	6.87	30.92	62.22	9	0.07	0.50	8.26	2.50	-0.33	-1.19	S1
115WM	0.0	8.93	74.67	16.39	7	0.10	4.56	5.70	1.89	0.61	0.40	S1
115WB	0.0	1.00	24.65	74.35	9	0.01	0.33	8.44	1.45	-0.56	1.58	S1
155WT	0.0	12.21	53.72	34.07	7	0.14	1.58	6.91	2.46	0.17	-1.36	S1
155WM	0.0	24.58	60.08	15.34	3	0.33	3.92	5.30	2.09	0.81	1.21	S1
155WB	0.0	3.67	46.51	49.82	9	0.04	0.93	7.83	2.55	-0.05	-1.73	S1
156WT	0.0	8.39	45.52	46.09	9	0.09	0.99	7.18	2.60	0.01	-1.69	S1
156WM	0.0	3.45	44.26	52.29	9	0.04	0.85	7.79	2.44	-0.10	-1.54	S1
156WB	0.0	0.63	36.63	62.74	9	0.01	0.58	8.72	1.58	-0.19	-0.70	S1
157WT	0.0	1.12	11.20	87.68	10	0.01	0.13	9.32	1.50	-0.99	3.80	S1
157WM	0.0	4.79	65.17	30.04	7	0.05	2.17	6.72	2.35	0.33	-1.15	S1
157WB	0.0	---	---	---	---	---	---	---	---	---	---	S1
160WT	0.0	7.59	21.24	71.17	9	0.08	0.30	8.40	2.25	-0.51	-0.52	S1

continued

Table IIA - Textural Properties, Surficial Bottom and Suspended sediments

1	2	3	4	5	6	7	8	9	10	11	12	13
160WM	0.0	1.31	28.41	70.27	9	0.01	0.40	8.63	2.00	-0.43	-0.57	S1
160WB	0.0	11.24	27.58	61.17	9	0.13	0.45	8.05	2.69	-0.26	-1.47	S1
164WT	0.0	8.09	38.58	53.34	9	0.09	0.72	7.86	2.53	-0.17	-1.45	S1
164WM	0.0	0.82	53.63	45.55	7	0.01	1.18	7.69	2.31	0.02	-1.60	S1
164WB	0.0	0.86	39.51	59.63	9	0.01	0.66	8.33	1.94	-0.26	-0.93	S1
165WT	0.0	8.81	38.21	52.98	9	0.10	0.72	7.60	2.68	-0.11	-1.68	S1
165WM	0.0	2.34	26.34	71.33	9	0.02	0.37	8.57	2.08	-0.48	-0.36	S1
165WB	0.0	0.08	22.89	77.03	10	0.00	0.30	8.94	1.50	-0.41	0.31	S1
236WT	0.0	1.86	29.25	68.89	9	0.02	0.42	8.81	2.03	-0.46	-0.38	S1
236WM	---	---	---	---	---	---	---	---	---	---	---	S1
236WB	0.0	4.89	76.24	18.88	4	0.05	4.04	6.74	1.58	0.13	-0.02	S1
238WT	0.0	0.59	38.37	61.04	9	0.01	0.63	8.21	1.80	-0.21	-0.87	S1
238WM	---	---	---	---	---	---	---	---	---	---	---	S1
238WB	---	---	---	---	---	---	---	---	---	---	---	S1
241WT	0.0	1.05	41.46	57.49	9	0.01	0.72	8.10	2.32	-0.21	-1.40	S1
241WM	0.0	0.33	44.43	55.24	9	0.00	0.80	7.95	2.28	-0.14	-1.41	S1
241WB	0.0	1.90	48.58	49.52	9	0.02	0.98	8.00	2.03	-0.10	-1.22	S1
243WT	0.0	0.07	71.25	28.68	7	0.00	2.48	7.31	1.69	0.32	-0.67	S1
243WM	0.0	0.04	50.93	49.03	7	0.00	1.04	7.97	1.90	-0.02	-1.36	S1
243WB	0.0	1.54	55.60	42.86	7	0.02	1.30	7.98	1.73	-0.00	-0.63	S1
245WT	0.0	0.06	48.27	51.67	9	0.00	0.93	8.25	1.88	-0.08	-1.35	S1
245WM	0.0	0.68	17.76	81.55	10	0.01	0.22	9.37	1.84	-0.80	1.21	S1
245WB	0.0	2.44	59.10	38.46	7	0.02	1.54	7.81	1.87	0.03	-0.80	S1

Table IIA - Physical Properties, Surficial Bottom Sediments and Suspended Sediments

Explanation for Table

Column 1 - Sample station number (first 3 digits), and sample type (alpha character): G = Smith-MacIntyre grab sample, GR = replicate Smith-MacIntyre grab sample (heavy mineral analysis only), B = box core, W = suspended sediment water sample (T = top water, M = mid-depth water, B = bottom water).

Column 2 - Gravel percentages: asterisks indicate stations where occasional inorganic lithic clasts were observed.

Column 3 - Sand percentage

Column 4 - Silt percentage

Column 5 - Clay percentage

Column 6 - Sediment type using Shepard's (1954) ternary classification system

Column 7 - Sand/Mud ratio

Column 8 - Silt/Clay ratio

Column 9 - First moment measure (mean diameter)

Column 10 - Second moment measure (standard deviation)

Column 11 - Third moment measure (skewness)

Column 12 - Fourth moment measure (kurtosis)

Column 13 - Data card designation number (S1 = sediment property card #1)

Table IIB - Physical Properties, Surficial Bottom Sediments and Suspended Sediments

Explanation for Table

Column 14 - Reiteration of sample station number and sample type (see Column 1)

Column 15 - Median diameter

Column 16 - Modal diameter

Column 17 - Coarsest one-percentile diameter (from cumulative probability curve)

Column 18 - Folk's graphic mean diameter (M_Z)

Column 19 - Folk's inclusive graphic standard deviation (σ_I)

Column 20 - Folk's inclusive graphic skewness (Sk_I)

Column 21 - Folk's graphic kurtosis (K_G)

Column 22 - Total heavy mineral content (weight percentage)

Column 23 - Wet-state color of surficial sediments (upper 1 cm), using GSA rock color chart designations based on the Munsell system: GD = questionalble color designation

Column 24 - Wet-state color of shallow subsurface sediments (below 1 cm), using GSA rock color chart designations based on the Munsell system: ND = no difference from surficial sediment color, QD = questionable color designation

Column 25 - Data card designation number (S2 = sediment property card #2)

Note: For both ~~appendices~~ Tables, a dashed line in any columnar space indicates that the respective property was not determined for that specific sample.

Table IIB - Textural Properties, Surficial Bottom and Suspended Sediments

14	15	16	17	18	19	20	21	22	23	24	25
001G	6.64	5.09	3.94	6.91	1.99	0.19	0.78	---	QD	ND	S2
002G	5.36	3.57	3.24	5.89	2.34	0.33	0.73	0.319	QD	ND	S2
003G	4.89	2.66	2.46	5.32	2.41	0.31	0.89	0.436	QD	ND	S2
004G	3.79	2.66	2.43	4.41	2.02	0.55	1.06	0.714	QD	ND	S2
005G	4.84	3.23	2.87	5.39	2.18	0.41	0.91	0.065	5Y5/2	5Y3/2	S2
006G	3.35	2.73	2.72	3.99	1.72	0.68	1.37	0.600	5Y5/2	5Y3/2	S2
007G	4.62	2.71	2.77	5.00	2.12	0.34	1.01	0.691	QD	ND	S2
008G	3.88	3.06	2.74	4.40	1.85	0.53	1.22	0.552	10Y4/2	ND	S2
009G	6.22	5.09	3.32	6.58	2.08	0.22	0.84	0.532	10Y4/2	ND	S2
010G	3.91	2.68	2.54	4.90	2.38	0.60	0.77	0.687	QD	N5	S2
011G	3.83	3.56	2.63	4.85	2.30	0.65	1.07	0.788	10YR4/2	N4	S2
012G	4.57	3.52	2.82	5.61	2.54	0.53	0.74	0.420	10YR5/4	N4	S2
013G	5.45	3.52	3.14	6.02	2.37	0.33	0.79	0.468	10YR5/4	5Y4/1	S2
014G	5.32	3.61	3.22	5.63	2.00	0.29	1.00	0.483	10Y5/4	5Y4/1	S2
015G	4.94	3.22	2.91	5.39	2.10	0.37	0.90	0.306	10YR4/2	5Y2/1	S2
016G	5.05	3.14	2.85	5.47	2.24	0.33	0.85	0.575	5YR4/4	N3	S2
017G	5.04	3.23	2.80	5.47	2.22	0.31	0.92	0.418	5YR5/6	N3	S2
018G	5.14	3.15	2.82	5.53	2.25	0.29	0.85	0.483	5YR4/4	5Y4/1	S2
019G	4.96	3.19	2.87	5.39	2.17	0.36	0.89	0.271	10YR5/4	N4	S2
020G	6.16	5.24	3.22	6.48	2.03	0.19	0.98	0.781	---	---	S2
021G	5.70	3.23	2.97	6.14	2.44	0.25	0.73	0.397	10YR4/2	5Y4/1	S2
022G	5.25	3.55	3.15	5.70	2.15	0.33	0.86	0.448	5Y4/1	ND	S2
023G	4.91	3.19	2.88	5.41	2.16	0.38	0.86	0.295	QD	N4	S2
024G	5.58	4.73	2.79	5.87	2.24	0.20	0.95	0.319	QD	5YR4/1	S2
025G	4.62	3.57	2.82	5.09	2.03	0.40	1.04	0.089	10YR4/2	5Y3/2	S2
026G	4.44	3.55	2.80	5.21	2.24	0.52	1.06	0.351	10YR4/2	ND	S2
027G	5.79	4.60	2.73	6.27	2.46	0.25	0.77	0.387	10YR4/2	5Y3/2	S2
028G	5.26	4.21	2.93	5.85	2.08	0.39	0.94	0.484	10YR4/2	5Y3/2	S2
029G	5.34	3.61	3.12	5.81	2.17	0.33	0.85	0.477	10YR4/2	5Y3/2	S2
030G	5.84	4.59	3.34	6.24	2.01	0.28	0.90	0.413	10YR4/2	5Y3/2	S2

Continued

Table IIB - Textural Properties, Surficial Bottom and Suspended Sediments

14	15	16	17	18	19	20	21	22	23	24	25
031G	5.71	4.15	3.34	6.28	2.28	0.34	0.79	0.116	10YR4/2	5Y3/2	S2
032G	5.81	5.24	3.23	5.99	2.00	0.19	1.14	0.482	10YR4/2	5Y4/1	S2
033G	6.54	6.08	3.06	6.74	2.13	0.11	0.94	0.290	5Y3/2	ND	S2
034G	6.57	6.00	3.74	6.84	2.00	0.17	0.85	0.233	5YR4/4	5Y3/2	S2
035G	5.35	3.62	3.30	5.75	2.11	0.32	0.86	0.375	5YR4/4	5Y3/2	S2
036G	5.26	4.74	2.82	5.58	2.08	0.26	1.00	0.570	5YR4/4	5Y3/2	S2
037G	5.49	4.68	2.85	5.84	2.06	0.26	1.05	0.446	5YR4/4	5Y3/2	S2
038G	5.72	5.07	2.97	6.07	2.08	0.24	0.95	0.459	5Y5/6	10Y4/2	S2
039G	6.09	5.09	3.37	6.57	2.21	0.20	0.82	0.647	5Y5/6	10Y4/2	S2
040G	5.90	5.20	3.35	6.22	2.04	0.24	0.91	0.268	10YR4/2	10Y4/2	S2
041G	5.42	4.65	3.69	5.89	1.82	0.40	1.05	0.545	10Y4/2	5Y3/2	S2
042G	5.79	5.10	3.39	6.15	1.96	0.29	0.96	0.447	10YR4/2	QD	S2
043G	5.10	4.61	3.23	5.71	2.02	0.45	0.95	0.378	10YR4/2	QD	S2
044G	4.63	3.19	2.85	5.30	2.14	0.48	0.91	0.563	10YR4/2	5Y3/2	S2
045G	5.34	4.11	2.87	5.79	2.15	0.32	0.87	0.690	---	---	S2
046G	7.63	9.57	3.42	7.42	2.26	-0.11	0.65	0.405	10YR4/2	QD	S2
047G	5.22	4.14	3.34	5.75	1.98	0.41	0.94	0.430	10YR5/4	QD	S2
048G	6.03	5.12	3.42	6.42	1.95	0.30	0.85	0.632	10YR4/2	QD	S2
050G	6.05	5.14	3.41	6.50	2.00	0.31	0.88	0.464	5YR3/4	5Y4/1	S2
051G	5.68	4.23	3.43	6.07	1.91	0.33	0.96	0.194	QD	10Y4/2	S2
052G	7.09	6.05	3.90	7.32	1.97	0.14	0.75	0.498	QD	10Y4/2	S2
053G	7.18	6.16	4.06	7.39	1.87	0.13	0.82	0.310	QD	10Y4/2	S2
054G	6.53	6.08	3.37	6.82	2.17	0.16	0.85	0.170	QD	10Y4/2	S2
055G	5.72	5.07	2.96	6.06	2.08	0.24	0.96	0.157	QD	10Y4/2	S2
056G	5.73	4.74	2.92	6.03	2.17	0.21	0.95	0.924	QD	10Y4/2	S2
057G	5.02	2.66	2.23	5.18	2.26	0.20	0.84	0.753	5Y5/2	10Y4/2	S2
058G	6.58	5.56	2.96	6.89	1.99	0.19	0.86	0.166	---	---	S2
059G	5.08	3.20	2.84	5.36	2.07	0.28	0.94	0.573	5Y5/2	10Y4/2	S2
060G	5.72	5.08	3.31	6.04	2.07	0.25	0.96	0.455	10YR4/2	5GY4/1	S2
061G	7.78	9.61	3.36	7.50	2.37	-0.17	0.67	0.402	5Y5/2	10Y4/2	S2

Continued

Table IIB - Textural Properties, Surficial Bottom and Suspended Sediments

14	15	16	17	18	19	20	21	22	23	24	25
062G	5.83	5.04	3.43	6.38	1.92	0.41	0.93	0.536	5Y4/4	10Y4/2	S2
063G	6.53	5.11	3.37	6.75	2.13	0.14	0.81	0.531	10YR4/2	5GY4/1	S2
064G	6.64	5.74	3.93	6.99	1.81	0.26	0.89	0.410	10YR4/2	5GY4/1	S2
065G	5.39	4.08	3.31	5.85	2.09	0.34	0.87	0.320	10YR4/2	5GY4/1	S2
066G	6.18	5.06	3.52	6.63	2.11	0.29	0.77	0.322	10YR4/2	5GY4/1	S2
067G	6.21	5.07	3.48	6.62	2.06	0.28	0.79	0.433	10YR4/2	5GY4/1	S2
068G	4.83	3.54	3.67	5.41	2.14	0.43	0.85	0.273	10YR4/2	5GY4/1	S2
069G	5.84	4.63	3.26	6.44	2.09	0.38	0.79	0.523	10YR4/2	5Y4/1	S2
070G	5.27	3.71	3.25	5.82	2.07	0.41	0.86	0.356	10YR4/2	5Y4/1	S2
071G	5.44	4.57	3.37	6.08	2.01	0.44	0.91	0.453	10YR4/2	5Y3/2	S2
072G	5.52	4.54	3.43	6.19	2.00	0.48	0.85	0.493	10YR4/2	5Y3/2	S2
073G	6.25	4.21	3.44	6.66	2.18	0.25	0.71	0.623	10YR4/2	5Y3/2	S2
074G	6.14	3.62	3.34	6.44	2.43	0.19	0.63	0.436	10YR4/2	5Y3/2	S2
075G	6.13	5.09	3.81	6.65	2.07	0.34	0.77	0.481	10YR4/2	5Y3/2	S2
076G	6.37	5.05	3.38	6.73	2.22	0.20	0.75	0.418	10YR4/2	5Y4/1	S2
077G	5.76	4.65	3.27	6.23	2.09	0.31	0.85	0.459	10YR4/2	5Y4/1	S2
080G	6.93	6.09	4.29	7.14	2.01	0.13	0.78	0.388	---	---	S2
083G	6.22	5.16	3.38	6.65	2.08	0.27	0.84	0.389	10YR4/2	5Y3/2	S2
084G	6.02	5.19	2.97	6.38	2.09	0.22	0.93	0.343	10YR4/2	5Y3/2	S2
085G	7.15	6.07	3.15	7.31	2.00	0.09	0.78	0.479	5Y3/2	10Y4/2	S2
086G	7.27	6.15	3.06	7.42	1.96	0.07	0.81	0.455	5Y5/2	10Y4/2	S2
087G	7.85	9.23	2.58	7.74	1.95	-0.11	0.84	0.464	5Y5/2	10Y4/2	S2
088G	8.00	9.53	2.97	7.87	1.94	-0.13	0.83	0.331	5Y5/2	10Y4/2	S2
089G	7.10	6.07	3.25	7.26	1.97	0.09	0.80	0.521	10Y4/2	ND	S2
090G	6.06	4.67	3.00	6.44	2.19	0.23	0.81	0.251	10Y4/2	ND	S2
091G	5.46	4.58	3.40	6.14	2.10	0.14	0.91	0.453	5Y4/4	ND	S2
092G	6.74	6.00	3.86	7.08	1.98	0.21	0.81	0.422	ND	ND	S2
093G	7.63	6.59	3.49	7.79	1.66	0.11	0.82	0.395	10YR4/2	10Y4/2	S2
094G	6.69	6.04	3.86	6.98	1.97	0.19	0.85	0.358	10Y4/2	ND	S2
095G	5.41	4.21	3.42	5.95	2.03	0.41	0.89	0.457	10Y4/2	ND	S2

Continued

Table IIB - Textural Properties, Surficial Bottom and Suspended Sediments

14	15	16	17	18	19	20	21	22	23	24	25
096G	5.75	4.68	3.37	6.25	2.17	0.32	0.83	0.406	10YR4/2	QD	S2
097G	6.22	5.08	3.69	6.62	2.00	0.28	0.83	0.391	10YR4/2	QD	S2
098G	6.79	6.01	3.75	7.02	2.05	0.15	0.80	0.360	10YR4/2	QD	S2
099G	5.66	4.66	3.53	6.16	2.04	0.36	0.91	0.506	10YR4/2	QD	S2
100G	6.57	5.11	4.04	6.94	1.97	0.25	0.75	0.679	10YR4/2	5Y4/1	S2
101G	5.07	4.62	3.27	5.48	1.67	0.43	1.31	0.538	10YR4/2	5Y4/1	S2
102G	6.74	5.13	4.05	7.05	1.97	0.21	0.75	2.011	10YR4/2	5Y4/1	S2
103G	5.95	5.03	3.89	6.55	1.98	0.41	0.80	1.119	10YR4/2	5Y4/1	S2
104G	6.15	5.19	3.93	6.64	1.88	0.35	0.89	1.319	10YR4/2	5Y4/1	S2
105G	5.43	4.55	3.65	5.92	1.79	0.44	1.02	0.822	10YR4/2	5Y4/1	S2
106G	6.03	4.66	3.53	6.46	2.16	0.28	0.82	1.072	10YR4/2	5Y4/1	S2
107G	6.45	5.50	3.79	6.87	2.00	0.27	0.81	0.583	10YR4/2	5Y4/1	S2
108G	6.05	4.70	3.48	6.43	1.95	0.29	0.88	0.857	10YR4/2	5Y4/1	S2
110G	6.81	5.08	3.62	7.10	2.14	0.16	0.69	0.481	10YR4/2	QD	S2
111G	7.32	6.12	3.88	7.47	1.88	0.09	0.78	2.452	10Y4/2	QD	S2
112G	7.69	9.51	3.10	7.67	1.92	-0.03	0.79	1.120	10Y4/2	ND	S2
113G	7.75	9.55	2.86	7.60	2.10	-0.11	0.80	1.709	10YR4/2	10Y4/2	S2
114G	8.09	8.60	3.05	7.94	1.88	-0.14	0.86	0.608	---	---	S2
115G	7.83	9.57	3.90	7.78	1.93	-0.05	0.75	0.898	10YR4/2	5Y4/1	S2
116G	6.48	5.20	3.52	6.86	2.00	0.25	0.82	0.291	10YR4/2	5Y4/1	S2
117G	6.26	4.23	3.44	6.62	2.13	0.24	0.80	0.468	10YR4/2	5Y4/1	S2
118G	6.51	5.62	3.66	6.79	2.19	0.17	0.76	0.792	5YR3/4	5Y4/1	S2
119G	6.78	5.22	3.96	7.07	2.01	0.18	0.77	0.456	10YR4/2	5Y4/1	S2
120G	6.71	5.64	4.35	7.08	1.89	0.26	0.81	1.228	10YR4/2	5Y4/1	S2
121G	6.23	5.11	3.62	6.66	2.00	0.29	0.82	0.730	10YR4/2	5Y4/1	S2
122G	6.69	5.20	4.30	7.05	2.04	0.23	0.73	0.927	10YR4/2	5Y4/1	S2
123G	6.07	4.62	3.53	6.57	2.06	0.34	0.75	0.571	10YR4/2	5Y4/1	S2
124G	7.03	5.17	3.82	7.20	2.05	0.09	0.75	0.303	10YR4/2	10Y4/2	S2
125G	5.59	4.57	3.00	6.17	1.97	0.43	0.87	0.895	QD	ND	S2
126G	6.13	5.03	4.01	6.67	1.98	0.37	0.79	1.356	10YR4/2	5Y4/1	S2

Continued

Table IIB - Textural Properties, Surficial Bottom and Suspended Sediments

14	15	16	17	18	19	20	21	22	23	24	25
127G	7.18	5.16	3.46	7.28	2.10	0.04	0.72	1.090	10YR4/2	QD	S2
128G	6.29	5.15	3.59	6.72	1.98	0.29	0.81	0.505	10YR4/2	5Y4/1	S2
129G	6.48	5.57	4.06	6.87	1.90	0.27	0.85	0.785	10YR4/2	5Y4/1	S2
130G	6.52	5.61	4.02	6.90	2.01	0.25	0.80	1.286	5Y4/4	ND	S2
131G	6.52	5.06	3.92	6.93	2.11	0.25	0.72	0.736	10Y4/2	QD	S2
132G	5.93	4.64	3.66	6.42	0.97	0.36	0.85	0.321	5Y4/1	ND	S2
133G	6.60	5.73	3.83	6.86	2.00	0.19	0.82	0.724	QD	5Y3/2	S2
134G	7.03	6.11	4.12	7.27	1.84	0.17	0.82	0.333	QD	ND	S2
135G	7.17	5.70	4.10	7.38	1.88	0.14	0.76	0.109	5Y4/4	QD	S2
136G	7.82	9.53	4.35	7.77	0.92	-0.06	0.79	0.240	5Y4/4	QD	S2
137G	7.69	9.53	3.79	7.64	1.98	-0.05	0.77	0.137	10Y4/2	ND	S2
138G	6.76	5.20	3.46	7.05	2.05	0.17	0.78	0.355	10YR4/2	10Y4/2	S2
139G	7.66	6.55	4.15	7.71	1.81	0.01	0.80	0.618	QD	10Y4/2	S2
140G	7.52	6.19	4.26	7.61	0.91	0.03	0.77	0.887	5Y4/4	ND	S2
141G	6.80	5.64	3.99	7.12	1.89	0.22	0.81	0.240	5Y5/6	5Y4/4	S2
142G	6.56	5.56	4.04	6.97	1.95	0.27	0.81	0.465	5Y5/2	ND	S2
143G	6.98	5.17	3.92	7.18	2.05	0.13	0.71	0.530	10YR4/2	5Y4/1	S2
144G	5.78	5.08	3.49	6.26	1.86	0.39	0.93	0.808	10YR4/2	5Y4/1	S2
145G	6.10	4.72	3.55	6.61	2.00	0.35	0.81	0.766	10YR4/2	5Y4/1	S2
146G	7.14	9.15	3.40	7.12	2.26	-0.02	0.72	0.781	5Y4/4	10Y4/2	S2
147G	4.88	4.12	3.27	5.39	1.75	0.51	1.18	0.749	5Y4/4	10Y4/2	S2
148G	6.12	4.15	3.49	6.47	2.13	0.24	0.79	0.832	5Y4/4	10Y4/2	S2
149G	6.02	5.08	3.93	6.52	1.94	0.37	0.86	0.729	10YR4/2	ND	S2
150G	7.14	6.10	4.45	7.37	1.85	0.16	0.79	1.761	5Y5/2	10Y4/2	S2
151G	6.80	5.20	4.03	7.06	1.95	0.18	0.79	1.000	10YR4/2	5Y3/2	S2
152G	7.31	6.20	4.20	7.50	1.78	0.12	0.84	0.503	5Y3/2	ND	S2
153G	7.43	6.16	4.68	7.65	1.78	0.14	0.73	0.000	5Y5/2	ND	S2
154G	6.90	6.03	4.39	7.21	1.85	0.22	0.80	2.158	5Y5/2	ND	S2
155G	7.31	6.11	4.41	7.48	1.87	0.10	0.76	0.785	5Y4/4	10Y4/2	S2
156G	7.22	6.12	4.46	7.43	1.83	0.14	0.80	1.210	5Y4/4	ND	S2

Continued

Table IIB - Textural Properties, Surficial Bottom and Suspended Sediments

14	15	16	17	18	19	20	21	22	23	24	25
157G	7.50	6.20	4.54	7.68	1.76	0.11	0.77	1.604	5Y4/4	10Y4/2	S2
158G	6.85	5.62	4.27	7.13	1.94	0.19	0.79	0.488	5Y4/4	ND	S2
159G	6.83	6.09	3.96	7.13	1.89	0.20	0.84	0.122	5Y4/4	10Y4/2	S2
160G	6.72	5.21	3.95	7.02	1.99	0.20	0.78	0.530	10Y4/2	ND	S2
162G	6.98	5.70	3.82	7.17	1.99	0.13	0.77	0.484	5Y4/4	10Y4/2	S2
163G	6.80	5.20	3.87	7.02	2.01	0.14	0.79	0.792	5Y5/2	ND	S2
164G	6.90	6.07	3.93	7.12	1.96	0.15	0.80	1.162	10Y4/2	ND	S2
165G	7.51	9.23	3.48	7.48	2.02	-0.03	0.77	0.610	5Y5/6	10Y4/2	S2
166G	6.48	5.11	3.78	6.84	1.96	0.25	0.80	1.033	5Y5/6	10Y4/2	S2
167G	6.81	4.69	3.75	7.01	2.08	0.13	0.73	0.860	---	---	S2
168G	6.91	5.22	3.93	7.11	2.02	0.13	0.76	0.822	5YR5/2	5Y5/2	S2
169G	6.30	5.04	3.52	6.66	2.14	0.22	0.76	0.383	10YR4/2	10Y4/2	S2
170G	6.44	4.66	4.08	6.83	1.99	0.28	0.73	0.754	5Y5/2	10Y4/2	S2
171G	6.44	5.11	4.03	6.85	1.94	0.29	0.78	0.332	5Y4/4	ND	S2
173G	6.63	5.70	4.44	7.07	1.74	0.34	0.84	0.528	5Y4/4	ND	S2
174G	7.21	6.12	4.47	7.43	1.78	0.16	0.78	0.828	5Y5/6	10Y4/2	S2
175G	7.29	6.12	4.42	7.47	1.84	0.12	0.77	1.088	10Y4/2	ND	S2
176G	7.96	9.22	4.13	7.82	1.89	-0.11	0.79	0.418	10Y4/2	ND	S2
177G	7.31	6.08	4.46	7.52	1.84	0.14	0.74	0.678	5Y5/2	ND	S2
178G	6.25	5.52	4.14	6.73	1.84	0.35	0.89	0.507	5Y5/2	ND	S2
179G	6.90	5.21	4.37	7.16	1.90	0.19	0.77	0.705	5Y5/2	ND	S2
180G	6.53	5.17	4.61	6.94	1.88	0.30	0.77	0.719	10YR4/2	5Y5/2	S2
181G	6.73	5.20	4.16	7.05	1.92	0.23	0.77	0.592	10YR4/2	5Y5/2	S2
182G	6.20	5.21	4.02	6.66	1.91	0.34	0.86	0.389	10YR4/2	ND	S2
183G	6.95	4.68	3.89	7.09	2.05	0.09	0.73	0.830	10YR4/2	10Y4/2	S2
184G	6.62	4.23	3.85	6.86	2.07	0.17	0.74	1.159	5Y5/2	ND	S2
185G	7.30	5.13	3.76	7.33	2.01	0.02	0.74	1.114	10YR4/2	10Y4/2	S2
186G	2.66	2.16	0.78	3.86	2.27	0.80	1.03	0.716	10YR4/2	5Y3/2	S2
187G	6.51	5.05	3.99	6.83	2.03	0.22	0.75	1.092	10Y4/2	ND	S2
188G	6.87	5.13	3.30	7.09	1.99	0.15	0.73	1.244	5Y4/4	ND	S2

Continued

Table IIB - Textural Properties, Surficial Bottom and Suspended Sediments

14	15	16	17	18	19	20	21	22	23	24	25
189G	7.18	5.16	4.35	7.30	1.96	0.09	0.70	1.410	10YR4/2	10Y4/2	S2
190G	7.70	6.13	4.61	7.73	1.78	0.02	0.75	1.401	10YR4/2	10Y4/2	S2
191G	6.98	6.11	-0.62	7.04	2.74	-0.14	1.24	6.218	5Y4/4	ND	S2
192G	7.90	9.18	4.49	7.85	1.75	-0.04	0.78	0.792	5Y4/4	ND	S2
193G	8.15	9.20	4.55	8.05	1.70	-0.09	0.80	1.173	5Y5/6	5Y4/4	S2
194G	7.57	6.50	4.52	7.71	1.72	0.10	0.78	1.592	5Y4/4	10Y4/2	S2
195G	7.18	6.10	4.47	7.45	1.78	0.20	0.77	3.516	5Y5/2	ND	S2
196G	5.47	---	-0.74	4.51	3.90	-0.24	0.59	0.325	5Y5/2	ND	S2
197G	7.33	6.05	4.56	7.52	1.79	0.14	0.75	2.655	10Y4/2	ND	S2
198G	6.80	5.20	4.37	7.13	1.91	0.23	0.76	1.105	10YR4/2	ND	S2
199G	6.97	5.20	4.03	7.20	1.94	0.15	0.77	2.137	5Y5/2	ND	S2
200G	7.42	6.68	4.35	7.50	1.90	0.04	0.81	1.186	5Y5/2	ND	S2
201G	6.72	5.17	3.64	7.00	1.97	0.19	0.79	32.026	10YR4/2	ND	S2
202G	2.71	2.21	2.00	3.64	2.02	0.77	0.56	0.638	5Y5/2	ND	S2
203G	2.77	2.54	-0.01	3.88	2.21	0.77	0.26	3.553	10YR4/2	ND	S2
204G	6.69	5.07	2.96	6.98	2.04	0.19	0.72	1.515	10YR4/2	5Y4/1	S2
205G	6.96	5.11	2.95	7.09	1.98	0.09	0.78	1.580	10YR4/2	5Y4/1	S2
206G	6.48	5.14	4.07	6.87	1.94	0.27	0.80	1.780	10YR4/2	5Y4/1	S2
207G	6.66	5.20	2.73	7.03	1.91	0.26	0.78	14.509	10YR4/2	5Y4/1	S2
208G	5.08	2.56	1.57	5.44	2.81	0.21	0.63	2.277	10YR4/2	5Y4/1	S2
209G	7.64	7.18	4.52	7.70	1.79	0.04	0.78	3.499	10YR4/2	5Y4/1	S2
210G	8.18	9.52	5.05	8.18	1.57	-0.01	0.80	---	10YR4/2	5Y4/1	S2
211G	7.56	6.20	4.35	7.68	1.76	0.08	0.77	---	10YR4/2	5Y4/1	S2
212G	7.04	6.15	2.24	7.07	2.36	-0.06	1.00	2.086	5YR5/2	5Y5/2	S2
216G	7.19	6.14	2.42	7.27	2.27	-0.05	0.98	2.215	5Y4/4	10Y4/2	S2
217G	7.87	9.50	3.35	7.86	1.76	-0.02	0.79	2.404	10Y4/2	ND	S2
218G	2.94	2.18	2.11	4.54	2.74	0.77	0.66	3.739	10Y4/2	ND	S2
219G	3.37	2.53	2.07	4.70	2.69	0.66	0.68	0.537	10YR4/2	ND	S2
220G	2.74	2.20	2.22	4.19	2.50	0.81	0.82	9.151	10Y4/2	ND	S2
221G	6.85	5.14	2.53	7.10	2.05	0.15	0.73	1.780	10YR4/2	5Y5/2	S2

Continued

Table IIB - Textural Properties, Surficial Bottom and Suspended Sediments

14	15	16	17	18	19	20	21	22	23	24	25
222G	7.18	6.04	4.34	7.30	1.96	0.08	0.76	2.600	10YR4/2	10Y4/2	S2
223G	6.88	5.09	3.94	7.09	2.02	0.14	0.74	2.623	10YR4/2	10Y4/2	S2
224G	5.96	2.15	2.03	5.85	2.88	0.00	0.81	1.865	10YR4/2	ND	S2
225G	2.67	2.17	1.56	3.97	2.35	0.81	0.95	1.230	5Y3/2	ND	S2
226G	7.41	7.06	4.14	7.45	1.92	0.03	0.77	1.945	5Y5/2	10Y4/2	S2
227G	7.40	6.13	3.95	7.42	1.98	0.01	0.75	1.885	10Y4/2	ND	S2
228G	5.59	2.20	2.00	5.66	2.84	0.08	0.622	4.523	10YR4/2	10Y4/2	S2
229G	2.85	2.18	2.02	4.35	2.62	0.79	0.72	4.430	10YR4/2	10Y4/2	S2
230G	2.70	2.24	1.43	4.02	2.37	0.81	0.96	5.012	10Y4/2	ND	S2
231G	4.81	2.15	0.90	5.34	2.93	0.27	0.59	2.138	10YR4/2	10Y4/2	S2
232G	7.74	9.21	2.24	7.67	2.22	-0.17	1.07	1.688	5Y5/2	ND	S2
233G	2.75	2.23	1.27	4.01	2.34	0.79	0.93	4.918	10Y4/2	ND	S2
234G	7.49	6.18	4.45	7.64	1.75	0.10	0.78	0.249	10YR4/2	10Y4/2	S2
235G	3.06	2.56	1.93	4.46	2.58	0.74	0.74	2.481	10YR4/2	10Y4/2	S2
236G	2.75	2.51	1.64	4.09	2.41	0.79	0.86	2.857	10YR4/2	10Y4/2	S2
237G	2.91	2.15	1.95	4.52	2.76	0.77	0.65	0.868	10YR4/2	10Y4/2	S2
238G	2.72	2.20	2.00	4.13	2.46	0.81	0.84	1.747	5YR4/2	5Y3/2	S2
239G	6.49	2.17	2.07	6.06	2.92	-0.13	0.60	1.181	5Y5/2	10Y4/2	S2
240G	6.70	2.18	2.15	6.29	2.82	-0.15	0.96	1.648	10YR4/2	10Y4/2	S2
241G	5.79	2.14	2.00	5.67	2.82	0.01	0.66	1.510	5Y5/6	10Y4/2	S2
242G	7.04	5.18	3.86	7.20	2.01	0.10	0.73	1.249	10YR4/2	5Y5/2	S2
243G	6.90	5.17	3.95	7.13	1.96	0.15	0.77	1.618	10YR4/2	5Y5/2	S2
244G	6.77	5.10	4.07	7.03	2.05	0.17	0.72	1.353	10YR4/2	10Y4/2	S2
245G	6.15	2.19	1.62	5.93	2.93	-0.04	0.60	0.780	10YR4/2	5Y5/2	S2
246G	6.18	2.20	2.05	5.96	2.86	-0.05	0.62	0.504	5Y4/4	10Y4/2	S2
247G	6.71	5.18	2.26	6.89	2.29	0.02	0.98	---	10YR5/4	5Y5/2	S2
248G	7.14	5.17	4.07	7.27	2.00	0.08	0.73	1.599	10YR4/2	10Y4/2	S2
249G	7.95	9.52	4.29	7.88	1.83	-0.06	0.79	3.405	5Y4/4	10Y4/2	S2
250G	6.91	5.22	2.81	7.14	1.99	0.14	0.79	1.337	5Y4/4	10Y4/2	S2
251G	7.20	6.11	2.25	7.37	2.01	0.06	0.84	1.175	10YR4/2	10Y4/2	S2

Continued

Table IIB - Textural Properties, Surficial Bottom and Suspended Sediments

14	15	16	17	18	19	20	21	22	23	24	25
252G	2.88	2.22	0.43	4.30	2.53	0.77	0.76	2.825	10YR4/2	10Y4/2	S2
253G	2.92	2.23	0.52	4.40	2.63	0.76	0.74	1.803	10YR4/2	10Y4/2	S2
254G	6.01	2.59	2.09	5.90	2.77	-0.00	0.64	0.571	10YR4/2	5Y5/2	S2
255G	4.51	2.60	1.64	5.01	2.52	0.33	0.76	0.775	10YR4/2	10Y4/2	S2
256G	7.36	6.21	3.65	7.55	1.79	0.12	0.80	1.496	5Y5/2	10Y4/2	S2
257G	2.72	2.23	1.42	3.88	2.25	0.78	1.02	1.212	10Y4/2	ND	S2
258G	2.81	2.52	-0.64	4.17	2.65	0.66	0.92	1.511	10YR4/2	5YR5/2	S2
259G	2.90	2.57	1.68	4.35	2.53	0.78	0.79	1.028	10YR4/2	5Y3/2	S2
260G	6.62	5.23	2.55	6.94	2.15	0.14	0.90	1.043	10YR4/2	5Y5/2	S2
261G	5.35	2.20	2.00	5.48	2.68	0.12	0.71	1.802	10YR4/2	ND	S2
262G	7.15	6.12	2.93	7.27	1.97	0.08	0.78	4.057	10Y4/2	5Y5/2	S2
263G	4.95	4.51	2.13	5.45	2.52	0.29	1.00	2.910	QD	10YR4/2	S2
264G	4.73	2.17	1.95	5.11	2.70	0.25	0.67	2.396	10YR4/2	5Y5/2	S2
265G	4.14	2.52	2.24	4.69	2.44	0.38	0.82	0.610	10YR4/2	5YR3/2	S2
266G	2.77	2.20	2.01	4.04	2.35	0.79	0.97	1.165	5Y4/1	ND	S2
267G	2.46	2.18	1.90	2.51	0.96	0.49	3.49	4.483	5Y4/1	ND	S2
268G	2.76	2.18	1.51	4.25	2.56	0.80	0.78	3.037	10YR4/2	5Y4/1	S2
269G	5.90	2.17	2.03	5.82	2.88	0.01	0.63	3.113	10YR4/2	5Y4/1	S2
270G	5.79	2.52	2.07	5.80	2.82	0.04	0.63	1.735	10YR5/4	5Y5/2	S2
271G	5.49	2.57	1.65	5.67	2.80	0.12	0.65	2.772	10YR4/2	5Y5/2	S2
272G	5.82	2.15	2.24	5.69	2.86	0.00	0.61	1.479	5Y5/2	ND	S2
273G	2.85	2.58	1.48	4.10	2.33	0.78	0.94	1.605	10YR4/2	10Y4/2	S2
274G	7.80	6.21	4.31	7.84	1.73	0.02	0.77	1.837	10YR4/2	10Y4/2	S2

Continued

Table IIB - Textural Properties, Surficial Bottom and Suspended Sediments

14	15	16	17	18	19	20	21	22	23	24	25
004GR	---	---	---	---	---	---	---	1.345	---	---	S2
010GR	---	---	---	---	---	---	---	0.766	---	---	S2
019GR	---	---	---	---	---	---	---	2.123	---	---	S2
022GR	---	---	---	---	---	---	---	0.202	---	---	S2
026GR	---	---	---	---	---	---	---	0.440	---	---	S2
091GR	---	---	---	---	---	---	---	0.515	---	---	S2
095GR	---	---	---	---	---	---	---	0.351	---	---	S2
101GR	---	---	---	---	---	---	---	0.364	---	---	S2
147GR	---	---	---	---	---	---	---	0.174	---	---	S2
186GR	---	---	---	---	---	---	---	0.826	---	---	S2
203GR	---	---	---	---	---	---	---	3.427	---	---	S2
220GR	---	---	---	---	---	---	---	8.840	---	---	S2
233GR	---	---	---	---	---	---	---	4.271	---	---	S2
252GR	---	---	---	---	---	---	---	2.612	---	---	S2
266GR	---	---	---	---	---	---	---	1.141	---	---	S2
273GR	---	---	---	---	---	---	---	1.442	---	---	S2
016B	5.28	3.17	2.84	5.67	2.33	0.28	0.76	---	---	---	S2
019B	5.16	3.18	2.98	5.72	2.44	0.38	0.81	---	---	---	S2
024B	5.20	2.65	2.56	5.45	2.36	0.21	0.93	---	---	---	S2
027B	5.78	2.65	2.59	5.94	2.40	0.12	0.90	---	---	---	S2
032B	5.76	3.58	3.27	6.06	2.28	0.22	0.76	---	---	---	S2
036B	5.25	3.09	2.77	5.52	2.28	0.23	0.86	---	---	---	S2
051B	6.33	5.53	3.13	6.61	2.10	0.19	0.84	---	---	---	S2
070B	6.20	4.59	3.29	6.56	2.03	0.26	0.80	---	---	---	S2
075B	5.53	4.16	3.39	6.07	2.07	0.38	0.85	---	---	---	S2
085B	7.23	6.15	2.98	7.28	2.15	-0.01	0.85	---	---	---	S2
106B	6.34	5.15	4.24	6.70	1.42	0.27	0.85	---	---	---	S2
110B	6.81	6.03	3.53	7.09	1.91	0.18	0.86	---	---	---	S2
120B	6.59	5.15	3.92	6.96	2.05	0.23	0.75	---	---	---	S2
125B	6.19	5.08	3.10	6.60	1.99	0.29	0.84	---	---	---	S2

Continued

Table IIB - Textural Properties, Surficial Bottom and Suspended Sediments

14	15	16	17	18	19	20	21	22	23	24	25
145B	6.84	5.12	3.34	6.97	2.14	0.08	0.76	---	---	---	S2
160B	5.87	4.23	3.75	6.35	1.96	-0.36	0.83	---	---	---	S2
165B	5.77	4.23	3.72	6.25	1.94	0.38	0.84	---	---	---	S2
179B	7.05	5.72	4.17	7.30	1.87	0.17	0.78	---	---	---	S2
185B	5.85	4.61	3.59	6.42	2.00	0.40	0.78	---	---	---	S2
194B	7.68	6.24	4.66	7.80	1.70	0.08	0.77	---	---	---	S2
199B	6.30	5.09	3.18	6.74	1.97	0.31	0.80	---	---	---	S2
202B	2.84	2.58	-0.06	3.72	2.07	0.68	1.55	---	---	---	S2
225B	2.70	2.17	0.52	4.16	2.56	0.79	0.93	---	---	---	S2
245B	4.52	2.12	1.96	4.94	2.65	0.28	0.67	---	---	---	S2
254B	5.98	2.56	1.71	5.85	2.85	-0.00	0.63	---	---	---	S2
259B	5.06	2.17	-0.05	5.29	2.77	0.17	0.63	---	---	---	S2
266B	4.56	2.20	2.02	4.99	2.62	0.29	0.67	---	---	---	S2
273B	2.89	2.51	1.98	4.46	2.66	0.79	0.72	---	---	---	S2
010WT	7.08	6.67	3.96	7.15	1.14	0.11	1.17	---	---	---	S2
010WM	6.60	6.15	4.09	6.87	1.47	0.29	1.10	---	---	---	S2
010WB	7.11	6.52	4.45	7.27	1.28	0.20	1.00	---	---	---	S2
024WT	8.14	8.01	3.97	8.22	1.91	-0.04	0.85	---	---	---	S2
024WM	7.93	7.69	3.94	7.89	1.95	-0.07	0.86	---	---	---	S2
024WB	9.83	10.52	4.13	9.00	1.92	-0.61	0.68	---	---	---	S2
032WT	8.21	8.11	3.97	7.99	1.91	-0.16	0.91	---	---	---	S2
032WM	9.74	10.22	3.95	8.69	2.18	-0.64	0.65	---	---	---	S2
032WB	8.64	8.00	4.89	8.78	1.36	0.03	0.88	---	---	---	S2
060WT	8.15	10.10	3.87	7.79	2.30	-0.21	0.67	---	---	---	S2
060WM	8.12	10.18	3.84	7.89	2.30	-0.17	0.65	---	---	---	S2
060WB	7.42	7.15	4.76	7.47	1.38	0.06	0.99	---	---	---	S2
070WT	9.56	10.09	3.99	9.30	1.58	-0.43	1.21	---	---	---	S2
070WM	9.81	10.10	3.86	8.49	2.31	-0.73	0.68	---	---	---	S2
070WB	7.25	6.55	3.87	7.54	2.09	0.12	0.90	---	---	---	S2
073WT	7.18	5.62	3.94	7.52	2.09	0.17	0.68	---	---	---	S2

Continued

Table IIB - Textural Properties, Surficial Bottom and Suspended Sediments

14	15	16	17	18	19	20	21	22	23	24	25
073WM	5.89	4.14	3.83	6.76	2.49	0.42	0.53	---	---	---	S2
073WB	6.57	6.20	4.17	6.67	1.12	0.24	1.52	---	---	---	S2
085WT	9.16	9.57	3.97	8.63	1.71	-0.44	1.02	---	---	---	S2
085WM	5.69	4.60	3.83	6.80	2.53	0.52	0.54	---	---	---	S2
085WB	7.22	6.66	4.73	7.26	1.19	0.07	0.96	---	---	---	S2
088WT	8.65	9.03	3.92	8.31	1.68	-0.29	1.01	---	---	---	S2
088WM	7.50	10.53	3.93	7.79	2.30	0.10	0.57	---	---	---	S2
088WB	7.74	7.08	4.37	8.09	1.73	0.22	0.81	---	---	---	S2
095WT	6.98	6.19	3.84	7.39	1.97	0.21	1.07	---	---	---	S2
095WM	8.90	10.20	4.30	8.62	1.83	-0.25	0.71	---	---	---	S2
095WB	6.96	6.21	3.87	7.42	2.02	0.21	0.96	---	---	---	S2
110WT	7.94	10.22	3.93	7.87	2.33	-0.07	0.59	---	---	---	S2
110WM	9.87	10.20	3.89	8.57	2.36	-0.70	0.68	---	---	---	S2
110WB	8.02	7.68	3.87	8.10	1.39	0.01	1.24	---	---	---	S2
114WT	9.65	10.13	3.92	8.64	2.16	-0.63	0.94	---	---	---	S2
114WM	4.56	4.11	3.73	5.82	2.33	0.73	1.63	---	---	---	S2
114WB	5.75	4.12	3.77	6.82	2.71	0.46	0.48	---	---	---	S2
115WT	9.67	10.11	3.81	8.25	2.51	-0.69	0.66	---	---	---	S2
115WM	4.93	4.23	3.80	5.71	1.92	0.61	1.21	---	---	---	S2
115WB	8.55	8.18	4.00	8.63	1.40	-0.10	1.62	---	---	---	S2
155WT	6.22	3.69	3.77	6.90	2.57	0.31	0.59	---	---	---	S2
155WM	4.43	4.06	3.73	5.28	1.97	0.71	2.00	---	---	---	S2
155WB	7.78	10.24	3.86	7.79	2.41	-0.03	0.56	---	---	---	S2
156WT	6.95	4.17	3.79	7.14	2.54	0.09	0.53	---	---	---	S2
156WM	8.29	10.50	3.87	7.83	2.45	-0.24	0.56	---	---	---	S2
156WB	8.75	10.20	4.94	8.76	1.56	-0.05	0.68	---	---	---	S2
157WT	9.76	9.68	3.98	9.50	1.33	-0.49	1.82	---	---	---	S2
157WM	5.75	5.52	3.84	6.84	2.41	0.53	0.59	---	---	---	S2
157WM	---	---	---	---	---	---	---	---	---	---	S2
160WT	9.57	9.70	3.83	8.29	2.28	-0.74	0.80	---	---	---	S2

Continued

Table IIB - Textural Properties, Surficial Bottom and Suspended Sediments

14	15	16	17	18	19	20	21	22	23	24	25
160WM	9.42	10.10	3.97	8.61	2.04	-0.54	0.78	---	---	---	S2
160WB	9.66	10.13	3.76	8.16	2.61	-0.70	0.54	---	---	---	S2
164WT	8.50	10.20	3.79	7.82	2.56	-0.33	0.59	---	---	---	S2
164WM	7.15	10.51	4.05	7.60	2.28	0.20	0.57	---	---	---	S2
164WB	8.83	10.03	4.07	8.41	1.97	-0.32	0.74	---	---	---	S2
165WT	8.72	10.11	3.81	7.79	2.59	-0.43	0.52	---	---	---	S2
165WM	9.36	10.05	3.91	8.46	2.18	-0.55	0.99	---	---	---	S2
165WB	9.13	8.11	4.48	9.07	1.45	-0.18	0.90	---	---	---	S2
236WT	9.75	10.20	3.93	8.89	2.02	-0.62	0.83	---	---	---	S2
236WM	---	---	---	---	---	---	---	---	---	---	S2
236WB	6.69	6.50	3.85	6.69	1.63	0.03	1.21	---	---	---	S2
238WT	8.57	8.63	4.25	8.26	1.88	-0.23	0.76	---	---	---	S2
238WM	---	---	---	---	---	---	---	---	---	---	S2
238WB	---	---	---	---	---	---	---	---	---	---	S2
241WT	8.95	10.12	3.98	8.14	2.31	-0.44	0.59	---	---	---	S2
241WM	8.42	10.19	4.16	7.93	2.35	-0.26	0.61	---	---	---	S2
241WB	7.95	10.12	3.92	8.03	2.04	-0.02	0.66	---	---	---	S2
243WT	6.88	6.05	4.81	7.40	1.80	0.37	0.94	---	---	---	S2
243WM	7.91	10.12	4.59	7.97	1.95	0.02	0.65	---	---	---	S2
243WB	7.72	7.17	3.95	8.10	1.79	0.19	0.81	---	---	---	S2
245WT	8.20	10.14	4.69	8.20	1.90	-0.02	0.62	---	---	---	S2
245WM	10.13	10.16	4.16	9.29	1.78	-0.71	2.25	---	---	---	S2
245WB	7.47	6.68	3.90	7.96	1.97	0.21	0.80	---	---	---	S2

Table III - Clay Mineralogy, Surficial Bottom Sediments

Explanation for Table

Column 1 - Sample number

Column 2 - % Montmorillonite

Column 3 - % Mixed layer clay

Column 4 - % Illite

Column 5 - % Chlorite

Table III - Clay Mineralogy, Surficial Bottom Sediments

1	2	3	4	5
001G	84.2	7.6	5.2	2.9
004G	82.1	0.0	8.0	9.8
007G	75.6	0.0	17.0	7.2
010G	81.9	7.7	7.2	3.0
014G	74.7	12.3	9.2	3.7
017G	69.4	0.0	24.9	5.6
021G	73.6	0.0	18.9	7.4
024G	75.1	0.0	17.0	8.0
027G	75.7	0.0	17.3	6.9
032G	71.7	0.0	16.5	11.9
035G	55.5	0.0	34.4	10.6
039G	63.2	0.0	30.2	6.3
042G	57.3	0.0	31.1	6.4
046G	62.9	0.0	13.7	23.4
050G	50.6	0.0	36.8	10.5
053G	59.6	0.0	29.6	10.8
056G	52.3	11.0	29.2	7.3
060G	47.2	12.3	34.0	6.3
063G	57.6	1.6	34.5	6.1
067G	82.7	0.0	9.5	7.6
070G	88.0	0.0	8.7	2.6
076G	47.6	28.9	17.0	6.3
080G	72.0	0.0	25.4	5.7
085G	81.0	0.0	14.4	4.4
088G	74.3	0.0	18.5	7.0
091G	70.0	2.7	18.1	9.0
095G	70.0	9.1	17.1	3.7
098G	72.4	1.5	21.7	4.3
102G	76.4	0.0	15.4	7.9
105G	54.7	5.3	33.3	6.6

Continued

Table III - Clay Mineralogy, Surficial Bottom Sediments

1	2	3	4	5
110G	67.7	0.0	20.7	11.5
114G	39.5	0.0	46.1	14.2
115G	42.5	34.0	17.3	6.0
118G	67.9	0.0	24.8	7.1
122G	79.7	0.0	14.3	5.8
125G	47.0	10.1	38.0	4.7
129G	47.9	0.0	38.0	14.2
132G	55.0	1.9	31.1	11.2
136G	59.0	3.7	26.7	10.5
139G	53.6	4.5	33.9	7.8
142G	71.9	0.0	15.2	12.8
146G	70.1	0.0	23.2	6.6
147G	73.7	0.0	16.4	9.8
153G	77.9	4.6	12.5	5.0
155G	79.4	0.0	13.6	6.9
156G	61.3	0.0	26.2	12.5
157G	71.1	0.0	17.6	11.1
160G	78.8	0.0	14.6	6.4
164G	75.0	3.9	15.7	5.2
165G	73.0	0.0	13.4	13.5
171G	73.8	0.0	20.7	5.4
180G	62.8	4.3	26.8	6.0
183G	67.5	13.7	12.5	6.2
186G	79.3	0.0	13.7	6.9
190G	74.5	0.0	19.5	5.8
193G	74.4	5.1	15.4	4.9
196G	11.1	38.9	37.9	12.5
197G	76.3	3.0	12.2	8.3
200G	0.0	79.0	16.2	4.6
203G	55.6	16.2	21.0	7.3

Continued

Table III - Clay Mineralogy, Surficial Bottom Sediments

1	2	3	4	5
210G	51.4	18.4	24.0	6.0
216G	63.8	2.8	25.6	7.6
223G	53.5	7.1	30.6	9.0
227G	42.2	0.0	49.9	15.7
230G	67.2	19.3	8.9	4.4
235G	74.3	0.0	16.9	8.7
236G	73.2	0.0	18.5	8.1
238G	73.6	0.6	16.4	9.2
241G	80.0	0.0	9.5	10.4
243G	48.7	0.0	35.4	15.7
245G	57.1	11.8	22.0	8.9
246G	54.6	0.0	37.2	8.1
250G	42.0	13.3	33.8	10.7
255G	59.0	11.5	20.9	8.4
260G	67.1	0.0	25.9	6.9
267G	61.6	8.4	26.0	4.3

Table IVA

Biological Properties of Samples Collected on the South Texas OCS - Card #1

Legend for Columnar Data in the Table

Column 1 - Sample station number and sample type. The first three digits enumerate the sample station; the alpha character, the type of sample with G representing the Smith-MacIntyre bottom grab sample, and B representing the box core. For example, 012G ==Station 12, grab sample.

Column 2 - Total number of species

Column 3 - Percent of total species represented by Polychaeta

Column 4 - Percent of total species represented by Arthropoda

Column 5 - Percent of total species represented by Mollusca

Column 6 - Percent of total species represented by miscellaneous taxa

Column 7 - Total number of individuals

Column 8 - Percent of total individuals represented by Polychaeta

Column 9 - Percent of total individuals represented by Arthropoda

Column 10 - Percent of total individuals represented by Mollusca

Column 11 - Percent of total individuals represented by miscellaneous taxa

Column 12 - Total biomass (g)

Column 13 - Percent of total biomass represented by Polychaeta

Column 14 - Percent of total biomass represented by Arthropoda

Column 15 - Percent of total biomass represented by Mollusca

Column 16 - Percent of total biomass represented by miscellaneous taxa

Column 17 - Diversity (H")

Column 18 - Equitability

Column 19 - Data card designation number (B1 = biological property card #1)

Table IVA - Biological Properties of Samples Collected on the South Texas OCS

1	2	3	4	5	6	7	8	9	10	11	12	13	14	15	16	17	18	19
106G	004	75	00	00	25	0005	80	00	00	20	00.0150	95	00	00	05	01.3322	.7728	B1
110G	003	99	00	00	00	0003	99	00	00	00	00.0395	99	00	00	00	01.0986	.8628	B1
114G	013	46	00	39	15	0039	18	00	51	31	00.0995	59	00	24	17	02.1498	.4545	B1
115G	011	37	18	27	18	0013	31	23	31	15	00.1031	42	05	44	09	02.3517	.6274	B1
120G	003	33	00	33	33	0007	14	00	72	14	00.1995	00	00	93	07	00.7963	.6605	B1
125G	009	56	11	22	11	0076	38	58	03	01	00.3471	28	60	08	04	01.3008	.3337	B1
127G	008	51	12	12	25	0126	05	88	02	05	00.7353	03	71	10	16	01.6034	.2180	B1
131G	005	80	00	20	00	0007	71	00	29	00	00.0842	12	00	88	00	01.5498	.7406	B1
134G	004	75	25	00	00	0005	80	20	00	00	00.0783	94	06	00	00	01.3322	.7728	B1
137G	003	33	00	00	67	0009	11	00	00	89	00.0520	18	00	00	82	00.6837	.6142	B1
141G	005	60	00	40	00	0012	75	00	25	00	00.1037	97	00	03	00	01.5454	.7381	B1
143G	010	60	20	10	10	0018	67	11	17	05	00.1734	27	01	64	08	02.1391	.5863	B1
145G	006	33	33	17	17	0051	06	86	02	06	00.2802	09	72	05	14	00.7348	.3176	B1
146G	013	55	15	15	15	0033	21	67	06	06	00.2638	43	38	00	19	01.5591	.2868	B1
149G	008	61	13	13	13	0014	79	07	07	07	00.0843	40	00	44	16	01.9702	.6425	B1
155G	010	10	10	60	20	0020	05	10	65	20	00.0712	08	04	32	56	02.1378	.5857	B1
156G	008	51	12	25	12	0008	51	12	25	12	00.0250	42	02	04	52	02.0794	.7009	B1
157G	005	60	00	00	40	0005	60	00	00	40	00.6374	06	00	00	94	01.6094	.7740	B1
160G	005	40	00	40	20	0006	50	00	33	17	00.0834	10	00	45	45	01.5607	.7467	B1
164G	005	40	00	20	40	0006	33	00	33	33	00.0988	11	00	75	14	01.5607	.7467	B1
165G	012	42	33	17	08	0097	13	81	04	02	00.4864	08	70	17	05	01.2231	.2369	B1
171G	009	67	11	11	11	0012	58	08	17	17	00.0628	99	00	00	00	02.1383	.6510	B1
176G	006	33	17	17	33	0009	22	12	33	33	00.0269	28	18	01	53	01.6770	.0793	B1
179G	008	75	25	00	00	0008	75	25	00	00	00.0252	98	02	00	00	02.0794	.7009	B1
183G	010	50	30	10	10	0016	69	19	06	06	00.0948	53	07	00	40	02.0636	.5540	B1
185G	011	55	09	18	18	0025	52	24	12	12	00.2056	28	04	51	17	02.1925	.5551	B1
186G	027	63	04	22	11	0220	45	20	29	06	01.2323	64	06	27	03	02.5486	.2968	B1
191G	011	55	27	09	09	0102	11	86	02	01	00.2362	45	18	31	06	01.4967	.3230	B1
193G	014	44	21	21	14	0022	32	32	27	09	00.0311	28	24	06	42	02.5001	.5525	B1
194G	005	60	00	40	00	0005	60	00	40	00	00.0390	99	00	01	00	01.6094	.7740	B1

continued

Table IVA - Biological Properties of Samples Collected on the South Texas OCS

1	2	3	4	5	6	7	8	9	10	11	12	13	14	15	16	17	18	19
002G	009	67	22	00	11	0021	48	43	00	09	00.1568	26	57	00	17	01.8974	.5398	R1
004G	016	81	13	00	06	0052	88	10	00	02	00.4670	54	43	00	03	02.3298	.4245	R1
005G	014	64	22	07	07	0024	79	13	04	04	00.2912	43	52	01	04	02.3576	.4762	R1
010G	015	53	20	20	07	0055	67	20	11	02	00.3502	74	05	17	04	02.3279	.4522	R1
012G	018	61	22	11	06	0055	78	15	05	02	00.3998	79	18	00	03	02.1942	.3397	R1
016G	011	73	09	00	18	0029	90	03	00	07	00.2715	46	35	00	19	01.6761	.3703	R1
019G	009	56	11	11	22	0032	72	13	06	09	00.5942	87	02	00	11	01.9955	.8320	R1
024G	012	67	17	08	08	0039	51	43	03	03	00.1901	53	32	08	07	01.9790	.4315	R1
027G	009	78	22	00	00	0077	49	51	00	00	00.7198	49	51	00	00	01.5254	.4038	R1
032G	012	49	33	08	08	0019	47	37	05	11	00.0841	44	24	01	31	02.3786	.5868	R1
036G	019	37	26	26	11	0028	32	25	36	07	00.2141	29	40	07	24	02.7599	.4953	R1
038G	012	33	25	33	09	0021	19	19	57	05	00.1229	11	01	57	31	02.1729	.5007	R1
042G	009	67	22	00	11	0030	90	07	00	03	00.1685	72	20	00	08	01.6991	.4616	R1
045G	016	69	19	12	00	0112	48	50	02	00	00.6445	42	55	03	00	01.8310	.2889	R1
048G	015	40	40	07	13	0043	63	30	02	05	00.3923	53	26	08	13	02.1819	.4036	R1
051G	004	25	25	25	25	0012	08	76	08	08	00.0870	07	07	43	43	00.8370	.5131	R1
060G	008	38	25	25	12	0010	40	30	20	10	00.0402	36	25	06	33	02.0253	.6720	R1
068G	011	73	18	00	09	0048	83	15	00	02	00.2138	89	05	00	06	02.0010	.4394	R1
070G	008	61	13	13	13	0071	14	84	01	01	00.3307	11	84	01	04	00.7498	.2405	R1
073G	007	58	14	14	14	0047	81	02	02	15	00.2413	49	00	13	38	01.2212	.4056	R1
075G	006	49	17	17	17	0008	51	12	25	12	00.1112	20	01	67	12	01.7329	.7124	R1
078G	005	40	00	40	20	0008	50	00	38	12	00.0656	34	00	46	20	01.4942	.7093	R1
080G	003	33	33	33	00	0004	50	25	25	00	01.4454	01	97	02	00	00.7714	.6503	R1
083G	005	80	00	00	20	0006	83	00	00	17	00.0933	86	00	00	14	01.5607	.7467	R1
085G	010	50	20	10	20	0031	16	74	03	07	00.0956	22	54	01	23	01.4961	.3552	R1
088G	002	50	00	50	00	0011	09	00	91	00	00.0303	97	00	03	00	00.3046	.6877	R1
090G	011	18	18	46	18	0043	07	16	72	05	00.1377	04	03	82	11	01.9846	.4728	R1
095G	004	75	00	00	25	0006	83	00	00	17	00.0488	73	00	00	27	01.2424	.7207	R1
103G	008	50	38	00	12	0018	55	28	00	17	00.0850	49	05	00	46	01.9231	.6186	R1

continued

Table IVA - Biological Properties of Samples Collected on the South Texas OCS

1	2	3	4	5	6	7	8	9	10	11	12	13	14	15	16	17	18	19
199G	011	46	09	36	09	0019	48	10	32	10	00.1392	23	02	56	19	02.3057	.6065	B1
202G	044	55	09	20	16	0222	51	13	29	07	03.2089	51	16	12	21	03.1810	.2924	B1
203G	027	60	07	26	07	0097	37	10	50	03	01.3055	50	12	36	02	02.9197	.3928	B1
208G	026	46	08	31	15	0053	30	04	55	11	00.5930	67	01	22	10	02.8182	.3780	B1
216G	005	20	20	00	60	0005	20	20	00	60	00.0444	02	11	00	87	01.6094	.7740	B1
221G	006	50	00	17	33	0007	57	00	14	29	00.0801	35	00	02	63	01.7479	.7212	B1
225G	036	50	08	31	11	0208	36	08	52	04	02.6360	37	15	46	02	03.0383	.3217	B1
226G	006	17	50	00	33	0009	11	67	00	22	00.0727	01	29	00	70	01.5811	.6318	B1
230G	012	66	00	17	17	0012	66	00	17	17	00.1267	45	00	15	40	02.4849	.6374	B1
235G	009	45	11	33	11	0009	45	11	33	11	00.3794	12	85	01	02	02.1972	.6811	B1
238G	020	45	15	35	05	0176	07	31	61	01	00.3379	22	17	50	11	01.9741	.2578	B1
241G	014	58	14	21	07	0018	61	17	17	05	00.1278	88	02	00	10	02.5532	.5745	B1
243G	012	49	17	17	17	0016	55	13	13	19	00.1627	18	22	20	40	02.3394	.5700	B1
245G	014	51	21	14	14	0022	36	14	36	14	00.2516	35	21	18	26	02.3459	.4909	B1
246G	011	55	18	18	09	0023	52	13	26	09	00.1456	30	06	46	18	02.2689	.5898	B1
254G	009	33	33	22	12	0016	19	25	50	06	00.3636	08	10	72	10	01.8346	.5150	B1
256G	006	33	17	17	33	0006	33	17	17	33	00.3860	02	84	04	10	01.7918	.7472	B1
259G	005	60	00	20	20	0005	60	00	20	20	00.1682	60	00	18	22	01.6094	.7740	B1
265G	007	57	14	00	29	0020	80	05	00	15	00.2142	46	24	00	30	01.5353	.5231	B1
266G	009	78	11	00	11	0024	63	33	00	04	00.1125	77	11	00	12	01.8059	.5037	B1
269G	015	60	07	20	13	0052	35	13	48	04	00.4546	20	49	28	03	02.2508	.4265	B1
273G	012	51	08	33	08	0016	50	13	31	06	00.1940	40	02	53	05	02.4260	.6793	B1

Table IVB

Biological Properties of Samples Collected on the South Texas OCS (Cont.)
Card #2

Legend for Columnar Data in the Table

Column 20 - Sample station number and sample type. The first three digits enumerate the sample station, the alpha character, the type of sample with G representing the Smith-MacIntyre bottom grab sample, and B representing the box core. For example ORG = station 12 grab sample.

Column 21 - Number of species (Polychaeta)

Column 22 - Number of individuals (Polychaeta)

Column 23 - Biomass (Polychaeta)

Column 24 - Number of species (Crustacea)

Column 25 - Number of individuals (Crustacea)

Column 26 - Biomass (Crustacea)

Column 27 - Number of species (Mollusca)

Column 28 - Number of individuals (Mollusca)

Column 29 - Biomass (Mollusca)

Column 30 - Number of phyla (Others)

Column 31 - Number of species (Others)

Column 32 - Number of individuals (Others)

Column 33 - Biomass (Others)

Column 34 - Data card designation number (B2 = biological property card #2)

Table IVB - Biological Properties of Samples Collected on the South Texas OCS

20	21	22	23	24	25	26	27	28	29	30	31	32	33	34
002G	006	010	0.0411	002	009	0.0894	000	000	0.0000	001	001	002	0.0262	B2
004G	013	046	0.2539	002	005	0.1999	000	000	0.0000	001	001	001	0.0131	B2
005G	009	019	0.1244	003	003	0.1507	001	001	0.0030	001	001	001	0.0131	B2
010G	008	037	0.2597	003	011	0.0189	003	006	0.0585	001	001	001	0.0131	B2
012G	011	043	0.3152	004	008	0.0708	002	003	0.0006	001	001	001	0.0131	B2
016G	008	026	0.1245	001	001	0.0960	000	000	0.0000	002	002	002	0.0510	B2
019G	005	023	0.5192	001	004	0.0156	001	002	0.0005	002	002	003	0.0641	B2
024G	008	020	0.1001	002	017	0.0618	001	001	0.0151	001	001	001	0.0131	B2
027G	007	038	0.3498	002	039	0.3700	000	000	0.0000	000	000	000	0.0000	B2
032G	006	009	0.0373	004	007	0.0200	001	001	0.0006	001	001	002	0.0262	B2
036G	007	009	0.0624	005	007	0.0857	005	010	0.0150	002	002	002	0.0510	B2
038G	004	004	0.0138	003	004	0.0015	004	012	0.0697	001	001	001	0.0379	B2
042G	006	027	0.1218	002	002	0.0336	000	000	0.0000	001	001	001	0.0131	B2
045G	011	054	0.2724	003	056	0.3540	002	002	0.0181	000	000	000	0.0000	B2
048G	006	027	0.2080	006	013	0.1032	001	001	0.0302	002	002	002	0.0510	B2
051G	001	001	0.0060	001	009	0.0060	001	001	0.0371	001	001	001	0.0379	B2
060G	003	004	0.0146	002	003	0.0099	002	002	0.0026	001	001	001	0.0131	B2
068G	008	040	0.1900	002	007	0.0102	000	000	0.0000	001	001	001	0.0131	B2
070G	005	010	0.0356	001	059	0.2790	001	001	0.0030	001	001	001	0.0131	B2
073G	004	038	0.1191	001	001	0.0002	001	001	0.0302	001	001	007	0.0919	B2
075G	003	004	0.0224	001	001	0.0015	001	002	0.0742	001	001	001	0.0131	B2
078G	002	004	0.0221	000	000	0.0000	002	003	0.0304	001	001	001	0.0131	B2
080G	001	002	0.0171	001	001	0.0259	001	001	0.0005	000	000	000	0.0000	B2
083G	004	005	0.0802	000	000	0.0000	000	000	0.0000	001	001	001	0.0131	B2
085G	005	005	0.0213	002	023	0.0510	001	001	0.0009	001	002	002	0.0223	B2
088G	001	001	0.0293	000	000	0.0000	001	010	0.0010	000	000	000	0.0000	B2
090G	002	003	0.0062	002	007	0.0039	005	031	0.1130	001	002	002	0.0146	B2
095G	003	005	0.0357	000	000	0.0000	000	000	0.0000	001	001	001	0.0131	B2
103G	004	010	0.0415	003	005	0.0041	000	000	0.0000	001	001	003	0.0393	B2

continued

Table IVB - Biological Properties of Samples Collected on the South Texas OCS

20	21	22	23	24	25	26	27	28	29	30	31	32	33	34
106G	003	004	0.0143	000	000	0.0000	000	000	0.0000	001	001	001	0.0007	B2
110G	003	003	0.0395	000	000	0.0000	000	000	0.0000	000	000	000	0.0000	B2
114G	006	007	0.0592	000	000	0.0000	005	020	0.0239	002	002	012	0.0166	B2
115G	004	004	0.0436	002	003	0.0048	003	004	0.0456	002	002	002	0.0092	B2
120G	001	001	0.0010	000	000	0.0000	001	005	0.1854	001	001	001	0.0131	B2
125G	005	029	0.0981	001	044	0.2081	002	002	0.0278	001	001	001	0.0131	B2
127G	004	007	0.0243	001	110	0.5202	001	002	0.0742	002	002	007	0.1167	B2
131G	004	005	0.0100	000	000	0.0000	001	002	0.0742	000	000	000	0.0000	B2
134G	003	004	0.0736	001	001	0.0047	000	000	0.0000	000	000	000	0.0000	B2
137G	001	001	0.0094	000	000	0.0000	000	000	0.0000	002	002	008	0.0426	B2
141G	003	008	0.1002	000	000	0.0000	002	004	0.0035	000	000	000	0.0000	B2
143G	006	012	0.0474	002	002	0.0016	001	003	0.1112	001	001	001	0.0131	B2
145G	002	003	0.0238	002	044	0.2019	001	001	0.0151	001	001	003	0.0393	B2
146G	007	007	0.1128	002	022	0.0994	002	002	0.0006	002	002	002	0.0510	B2
149G	005	011	0.0339	001	001	0.0002	001	001	0.0371	001	001	001	0.0131	B2
155G	001	001	0.0054	001	002	0.0031	006	013	0.0228	002	002	004	0.0399	B2
156G	004	004	0.0104	001	001	0.0004	002	002	0.0011	001	001	001	0.0131	B2
157G	003	003	0.0384	000	000	0.0000	000	000	0.0000	001	002	002	0.5990	B2
160G	002	003	0.0081	000	000	0.0000	002	002	0.0373	001	001	001	0.0379	B2
164G	002	002	0.0108	000	000	0.0000	001	002	0.0742	002	002	002	0.0138	B2
165G	005	013	0.0405	004	078	0.3395	002	004	0.0802	001	001	002	0.0262	B2
171G	006	007	0.0623	001	001	0.0002	001	002	0.0002	001	001	002	0.0001	B2
176G	002	002	0.0074	001	001	0.0047	001	003	0.0003	002	002	003	0.0145	B2
179G	006	006	0.0246	002	002	0.0006	000	000	0.0000	000	000	000	0.0000	B2
183G	005	011	0.0504	003	003	0.0064	001	001	0.0001	001	001	001	0.0379	B2
185G	006	013	0.0568	001	006	0.0090	002	003	0.1043	001	002	003	0.0354	B2
186G	017	099	0.7920	001	045	0.0734	006	064	0.3371	003	003	012	0.0298	B2
191G	006	011	0.1069	003	088	0.0420	001	002	0.0742	001	001	001	0.0131	B2
193G	006	007	0.0086	003	007	0.0074	003	006	0.0019	002	002	002	0.0138	B2
194G	003	003	0.0387	000	000	0.0000	002	002	0.0003	000	000	000	0.0000	B2

continued

Table IVB - Biological Properties of Samples Collected on the South Texas OCS

20	21	22	23	24	25	26	27	28	29	30	31	32	33	34
199G	005	009	0.0316	001	002	0.0030	004	006	0.0784	001	001	002	0.0262	B2
202G	024	113	1.6456	004	028	0.5190	009	065	0.3807	003	007	016	0.6636	B2
203G	016	036	0.6465	002	010	0.1619	007	048	0.4734	002	002	003	0.0238	B2
208G	012	016	0.3948	002	002	0.0062	008	029	0.1298	002	004	006	0.0622	B2
216G	001	001	0.0010	001	001	0.0047	000	000	0.0000	001	003	003	0.0387	B2
221G	003	004	0.0277	000	000	0.0000	001	001	0.0014	002	002	002	0.0510	B2
225G	018	075	0.9688	003	016	0.4037	011	109	1.2036	003	004	008	0.0598	B2
226G	001	001	0.0010	003	006	0.0207	000	000	0.0000	002	002	002	0.0510	B2
230G	008	008	0.0564	000	000	0.0000	002	002	0.0192	002	002	002	0.0510	B2
235G	004	004	0.0467	001	001	0.3214	003	003	0.0021	001	001	001	0.0092	B2
238G	009	012	0.0748	003	054	0.0588	007	109	0.1664	001	001	001	0.0379	B2
241G	008	011	0.1127	002	003	0.0019	003	003	0.0001	001	001	001	0.0131	B2
243G	006	009	0.0295	002	002	0.0359	002	002	0.0332	002	002	003	0.0641	B2
245G	007	008	0.0878	003	003	0.0534	002	008	0.0463	002	002	003	0.0641	B2
246G	006	012	0.0441	002	003	0.0080	002	006	0.0672	001	001	002	0.0262	B2
254G	003	003	0.0285	003	004	0.0370	002	008	0.2602	001	001	001	0.0379	B2
256G	002	002	0.0093	001	001	0.3214	001	001	0.0167	002	002	002	0.0386	B2
259G	003	003	0.1002	000	000	0.0000	001	001	0.0302	001	001	001	0.0379	B2
265G	004	016	0.0985	001	001	0.0516	000	000	0.0000	002	002	003	0.0641	B2
266G	007	015	0.0863	001	008	0.0130	000	000	0.0000	001	001	001	0.0131	B2
269G	009	018	0.0930	001	007	0.2240	003	025	0.1268	002	002	002	0.0138	B2
273G	006	008	0.0774	001	002	0.0033	004	005	0.1042	001	001	001	0.0092	B2

Table V - Trace Metals Content, Surficial Sediments

Explanation for Table

Column 1 - Sample number

Column 2 - Cadmium in µg/g

Column 3 - Chromium in µg/g

Column 4 - Copper in µg/g

Column 5 - Iron in percent

Column 6 - Manganese in µg/g

Column 7 - Nickel in µg/g

Column 8 - Lead in µg/g

Column 9 - Vanadium in µg/g

Column 10 - Zinc in µg/g

Column 11 - Barium in µg/g

Column 12 - Carbonate percent

Column 13 - Organic carbon percent

Table V - Trace Metal, Surficial Sediments

	1	2	3	4	5	6	7	8	9	10	11	12	13
G	001	.071	24.3	6.6	19700	404	16.6	15.7	8.5	59.7	1761	.286	.455
G	002	.072	25.3	6.2	21200	360	17.8	15.6	9.3	61.4	180	.890	.409
G	003	.055	17.7	4.1	24000	259	9.9	13.5	6.3	63.2	250	.823	.274
G	004	.056	18.8	4.4	16800	292	17.8	12.8	6.1	47.8	141	.726	.352
G	005	.060	19.2	4.4	16400	291	14.2	12.4	6.4	52.6	106	.766	.322
G	006	.053	22.2	4.5	17600	299	13.3	12.4	7.8	45.6	81	.428	.114
G	007	.047	22.4	5.0	18400	322	17.5	14.1	7.8	48.6	97	.717	.251
G	008	.057	20.7	4.6	17500	308	15.3	12.9	7.0	45.4	126	.646	.262
G	009	.088	26.1	7.6	23600	413	22.4	16.5	10.9	63.7	162	1.173	.439
G	010	.079	26.5	7.3	23400	410	17.9	16.1	12.9	61.7	308	.647	.448
G	011	.062	18.1	4.9	19600	318	15.3	11.9	9.6	44.5	203	.616	.304
G	012	.081	30.5	5.8	22100	347	20.4	18.2	11.5	98.0	131	.785	.357
G	013	.050	20.3	3.8	19400	289	16.9	13.2	8.0	69.8	243	.803	.344
G	014	.045	21.1	4.1	19600	283	14.5	13.2	9.2	82.3	107	.930	.473
G	015	.047	18.6	3.6	19600	313	12.9	12.6	7.8	55.0	80	.767	.287
G	016	.046	19.8	4.1	20800	273	13.2	12.6	8.4	71.8	81	.816	.343
G	017	.042	17.3	4.0	19400	253	12.9	11.5	6.4	62.8	73	.810	.376
G	018	.038	18.0	4.2	19300	267	12.9	14.1	6.9	71.5	96	1.054	.585
G	019	.050	20.2	3.5	19200	264	11.5	13.8	8.4	62.6	73	.773	.351
G	020	.049	18.7	5.1	22600	348	13.8	15.9	6.8	68.3	118	1.067	.382
G	021	.047	21.2	4.6	25200	290	16.5	14.2	8.7	72.7	72	.939	.316
G	022	.055	15.7	3.4	17600	237	12.7	11.3	5.5	59.5	119		
G	023	.048	17.7	4.9	19200	244	12.6	12.1	6.9	56.4	166	.843	.362
G	024	.054	16.9	4.0	18900	268	11.5	12.6	6.0	64.0	78	1.004	.371
G	025	.044	13.8	3.8	18100	248	12.3	10.8	5.7	58.5	85	1.106	.650
G	026	.067	14.4	5.2	17000	263	10.8	9.1	6.7	47.2	116	.882	.472
G	027	.048	17.8	4.2	21100	302	14.0	14.6	6.9	60.8	166	1.028	.439
G	028	.053	18.0	6.1	21200	251	13.6	9.5	9.0	63.3	102	1.028	.374
G	029	.053	17.3	5.9	21500	283	13.2	9.4	7.3	50.0	91	1.040	.360
G	030	.047	16.7	5.6	19900	256	13.7	8.2	7.2	50.0	119	.961	.417

continued

Table V - Trace Metal, Surficial Sediments

1	2	3	4	5	6	7	8	9	10	11	12	13
G 031	.044	19.9	5.5	20300	312	13.3	9.8	9.7	58.1	104	1.245	.621
G 032	.045	17.8	5.6	19000	277	14.4	9.1	8.6	53.4	110	.991	.434
G 033	.050	20.2	6.7	18000	252	15.3	11.0	9.8	65.2	94	1.155	.426
G 034	.047	23.4	5.8	21900	239	14.4	10.2	9.8	62.5	90	1.239	.492
G 035	.044	19.4	5.0	19100	210	12.7	9.7	8.7	51.2	64	1.184	.601
G 036	.049	20.8	5.5	20300	218	12.8	9.7	8.9	54.7	98	1.273	.673
G 037	.046	23.2	5.3	19600	224	14.8	9.1	9.1	53.6	57	1.375	.849
G 038	.053	19.8	5.8	20600	232	16.2	10.2	10.1	57.0	64	1.217	.704
G 039	.052	25.8	5.6	22300	249	15.3	10.4	11.0	62.2	52	1.246	.517
G 040	.064	22.5	5.9	22200	257	14.1	9.8	10.9	56.5	74	1.067	.455
G 041	.043	18.2	5.5	19800	240	13.6	9.2	9.1	52.5	100	1.091	.473
G 042	.049	20.0	5.5	20400	279	16.9	9.4	7.6	54.3	98	1.029	.365
G 043	.059	17.9	6.3	18000	323	13.8	10.4	7.4	51.0	116	1.198	.400
G 044	.054	15.2	5.7	17600	300	12.6	9.4	7.3	46.4	110	.911	.446
G 045	.063	18.4	6.1	19100	292	13.1	9.5	7.9	51.2	96	1.022	.520
G 046	.054	20.7	8.1	21900	345	17.3	11.2	8.0	58.3	136	1.387	.567
G 047	.054	17.3	6.2	17900	265	12.6	8.3	7.6	50.6	116	.890	.369
G 048	.054	21.4	6.7	21100	250	17.1	9.8	8.5	58.4	108	1.093	.406
G 050	.050	16.5	5.4	18000	260	15.8	10.0	6.6	53.5	93	1.155	.445
G 051	.041	15.7	5.0	14600	243	12.7	9.9	6.4	49.4	100	1.210	.449
G 052	.036	17.1	5.6	16000	250	14.4	10.3	6.8	52.9	159	1.234	.510
G 053	.039	17.4	6.0	17100	271	15.4	11.4	7.3	60.1	162	1.297	.461
G 054	.038	27.7	7.1	20700	276	15.8	11.4	14.7	68.3	110	1.428	.764
G 055	.036	25.7	6.7	19900	238	14.8	10.2	13.9	61.3	64	1.377	.801
G 056	.030	16.8	4.9	14700	206	12.3	9.3	8.1	50.3	64	1.538	1.027
G 057	.044	17.3	5.0	15800	257	12.9	9.3	7.4	50.2	70	2.001	1.530
G 058	.047	20.9	6.6	19600	324	14.8	9.4	8.8	56.6	62	1.950	1.320
G 059	.036	14.0	4.3	12400	227	11.3	7.2	6.2	43.3	41	1.795	1.233
G 060	.033	20.7	6.4	17300	242	13.6	9.6	12.8	55.3	74	1.547	.948
G 061	.035	20.7	5.5	18800	276	14.7	9.8	11.9	59.4	72	1.571	.802

continued

Table V - Trace Metal, Surficial Sediments

1	2	3	4	5	6	7	8	9	10	11	12	13
G 062	.035	20.4	5.5	17900	236	15.1	8.5	8.9	54.9	72	1.297	.685
G 063	.050	23.1	6.8	21100	257	16.3	11.0	10.1	65.7	76	1.146	.528
G 064	.040	21.7	5.7	19700	262	16.2	10.8	7.4	57.0	86	1.278	.439
G 065	.037	18.0	5.3	17600	251	12.6	10.3	7.3	50.4	72	.946	.510
G 066	.038	18.9	5.3	17300	236	13.1	9.8	6.6	51.0	79	1.101	.419
G 067	.044	19.8	5.9	18500	280	14.6	9.8	7.4	55.0	98	1.042	.391
G 068	.034	12.9	4.5	15000	207	10.7	7.9	5.6	41.0	104	.654	.296
G 069	.046	15.4	5.6	18500	229	11.7	8.1	5.2	46.0	128	1.164	.497
G 070	.054	15.6	5.6	18200	246	12.8	8.1	5.3	45.2	124	1.126	.532
G 071	.052	15.7	6.0	18800	292	13.3	9.3	5.9	45.0	140	1.053	.560
G 072	.046	17.4	6.1	17400	251	13.0	8.8	5.9	48.4	128	1.006	.535
G 073	.050	17.0	4.6	18600	321	9.0	8.2	4.1	61.6	106	1.111	.469
G 074	.041	18.3	5.5	20800	347	9.6	9.4	4.4	64.4	136	1.092	.453
G 075	.043	20.0	5.6	20700	325	12.2	9.3	5.0	71.7	88	1.105	.460
G 076	.039	20.0	5.3	19300	352	10.8	7.8	5.1	73.1	70	1.079	.515
G 077	.038	20.5	5.1	20800	314	12.5	7.9	5.7	70.4	68	1.133	.526
G 080	.109	16.6	3.6	11400	418	6.9	4.5	7.4	47.8	90	9.514	9.178
G 083	.044	20.9	4.2	20000	323	12.1	7.5	5.7	72.9	39	1.432	.696
G 084	.045	23.1	5.0	21700	349	12.6	7.0	6.5	74.7	49	1.707	1.001
G 085	.083	25.0	5.3	23500	357	14.1	7.5	9.3	77.0	82	2.117	1.201
G 086	.073	24.6	4.8	22400	372	13.4	6.4	7.4	80.7	70	2.055	1.281
G 087	.096	27.4	6.8	23700	348	14.7	6.8	8.5	91.0	78	2.430	1.529
G 088	.129	28.0	5.4	28800	367	15.6	6.3	10.2	87.1	71	2.347	1.598
G 089	.086	27.7	6.9	24500	368	10.7	6.4	9.4	88.8	58	1.867	1.258
G 090	.067	23.7	4.5	23200	404	10.8	6.1	7.0	75.4	82	1.640	.985
G 091	.048	20.8	4.2	20600	317	9.2	6.7	6.4	69.4	50	1.592	.991
G 092	.059	27.2	5.4	26400	420	10.7	8.1	7.1	81.4	154	1.469	.670
G 093	.058	26.7	6.4	27800	346	13.5	10.7	6.9	87.4	208	1.241	.394
G 094	.048	22.1	5.3	23600	372	11.3	9.5	6.2	78.7	196	1.254	.548
G 095	.045	20.2	4.6	20600	305	9.5	7.5	5.8	65.5	70	1.081	.469

continued

Table V - Trace Metal, Surficial Sediments

1	2	3	4	5	6	7	8	9	10	11	12	13
G 096	.063	20.1	4.6	20500	335	10.0	8.6	5.8	65.5	80	.996	.447
G 097	.051	19.9	5.3	20300	325	9.4	9.1	5.1	73.7	102	1.114	.488
G 098	.047	20.7	5.3	19600	363	9.4	8.9	5.1	69.6	178	1.088	.461
G 099	.050	21.0	5.5	21500	310	13.3	8.9	5.9	69.3	136	1.044	.447
G 100	.057	22.8	6.2	24000	343	13.7	9.7	6.2	72.9	160	1.201	.473
G 101	.043	16.5	4.0	17500	305	8.7	7.0	4.7	49.4	190	1.056	.572
G 102	.064	19.7	4.8	20100	336	10.0	8.6	4.0	54.3	266	1.308	.637
G 103	.055	20.0	5.7	20300	310	9.2	8.8	5.7	59.4	142	1.111	.479
G 104	.055	21.4	5.6	23200	352	10.6	8.7	6.0	61.2	150	1.197	.468
G 105	.049	19.5	5.2	20700	333	9.8	8.5	5.4	58.6	124	1.094	.443
G 106	.054	20.4	4.9	21200	342	11.7	8.0	5.8	62.5	216	1.172	.481
G 107	.046	22.8	5.3	21900	340	11.5	8.1	6.4	64.0	116	1.187	.533
G 108	.058	24.6	5.6	22600	351	11.4	8.4	6.6	68.0	178	1.219	.604
G 110	.059	21.7	5.0	20900	358	11.5	7.2	6.1	67.0	60	1.416	.640
G 111	.060	24.6	5.0	22300	393	12.5	7.3	10.4	71.2	74	1.635	.810
G 112	.104	32.4	6.1	27500	407	13.7	7.6	12.6	82.9	71	1.999	1.068
G 113	.145	31.7	7.8	28200	413	19.1	11.6	18.8	80.0	60	2.353	1.513
G 114	.155	42.2	7.3	32100	413	17.4	14.6	27.4	95.4	58	2.204	1.143
G 115	.063	30.7	5.0	25400	374	14.3	7.6	12.4	79.4	145	1.755	.865
G 116	.050	32.6	6.2	29700	378	17.8	8.8	13.3	83.2	90	1.517	.703
G 117	.047	28.8	4.7	26000	328	14.6	7.8	13.1	71.5	150	1.357	.649
G 118	.051	33.3	6.7	27100	355	17.5	13.9	12.5	83.3	94	1.118	.494
G 119	.040	30.4	5.1	26100	342	14.9	9.0	12.6	77.4	88	1.277	.478
G 120	.055	35.0	5.6	27000	343	16.0	10.5	12.4	78.4	97	1.253	.491
G 121	.044	25.7	5.2	23800	237	10.9	8.9	9.8	68.0	108	1.019	.453
G 122	.040	19.5	4.0	19800	341	10.7	8.8	9.3	60.3	88	1.320	.538
G 123	.044	19.1	4.2	19400	351	4.2	8.7	5.9	60.4	120	1.138	.416
G 124	.062	20.6	3.9	18900	402	3.9	9.8	5.5	57.7	256	1.376	.614
G 125	.059	17.5	3.5	17500	363	3.5	8.0	5.5	52.7	188	1.308	.638
G 126	.058	21.4	3.6	21000	329	12.0	8.2	6.1	62.1	160	1.382	.585

continued

Table V -- Trace Metal, Surficial Sediments

	1	2	3	4	5	6	7	8	9	10	11	12	13
G	127	.056	20.5	3.9	21600	354	13.3	10.0	6.9	62.0	124	1.164	.496
G	128	.044	23.4	4.4	22000	334	10.4	8.6	7.3	66.6	108	1.236	.501
G	129	.060	26.8	4.8	24400	360	13.8	8.8	10.0	76.9	82	1.350	.559
G	130	.052	31.8	4.7	24100	385	12.0	10.1	10.1	76.4	60	1.249	.489
G	131	.044	27.0	3.0	24800	341	11.0	7.7	9.4	71.2	62	1.136	.463
G	132	.041	21.2	2.6	19500	307	11.1	8.8	8.4	63.7	46	1.205	.564
G	133	.043	25.6	2.9	22900	337	13.7	10.5	12.9	79.5	37	1.379	.512
G	134	.043	25.6	3.9	21500	319	14.9	10.4	9.5	68.0	41	1.362	.526
G	135	.058	24.5	5.0	22400	290	10.9	10.5	12.5	73.3	41	1.692	.800
G	136	.068	28.0	4.5	24000	370	12.2	10.7	10.5	79.7	48	2.169	1.193
G	137	.087	29.4	4.1	24700	306	13.1	7.7	10.2	79.9	54	1.943	1.175
G	138	.072	18.6	8.5	26100	364	19.4	10.1	8.6	56.8	38	1.770	.925
G	139	.022	16.8	7.5	24500	311	17.3	7.1	7.2	51.0	56	1.374	.711
G	140	.029	19.7	8.7	27800	359	19.2	9.3	9.4	59.2	76	1.367	.567
G	141	.021	20.1	8.6	25000	348	17.8	9.7	9.3	58.0	77	1.293	.561
G	142	.023	19.4	8.0	26000	325	20.4	9.8	8.4	59.1	78	1.343	.582
G	143	.023	18.5	8.0	25600	309	18.3	10.6	8.2	56.1	85	1.264	.493
G	144	.022	16.9	7.6	24000	323	17.0	9.2	6.9	49.7	226	1.041	.543
G	145	.022	15.5	7.6	22400	284	16.2	9.1	6.9	45.3	118	1.201	.598
G	146	.021	14.1	6.8	20100	296	15.3	8.4	6.4	43.5	87	1.010	.575
G	147	.020	11.2	6.2	17600	268	13.7	7.3	5.1	38.4	236	1.065	.493
G	148	.021	16.9	7.9	22900	334	17.7	9.9	7.8	50.5	110	1.184	.472
G	149	.021	17.9	8.0	24300	345	17.9	9.1	7.7	53.7	100	1.255	.525
G	150	.036	15.1	7.3	21000	319	16.5	8.9	6.6	51.3	88	1.303	.536
G	151	.035	17.2	7.5	21800	321	16.7	8.8	6.2	53.1	68	1.445	.549
G	152	.047	16.4	8.0	22200	337	17.2	9.5	6.7	53.0	73	1.437	.496
G	153	.037	24.4	9.9	24400	367	19.4	8.4	8.9	65.7	66	1.438	.535
G	154	.033	17.2	8.0	22700	444	19.2	8.0	6.5	56.0	80	1.571	.614
G	155	.102	17.0	8.3	20000	353	19.3	11.6	7.6	56.8	74	1.939	.924
G	156	.095	32.5	10.7	33400	420	23.8	11.7	17.2	80.4	77	1.488	.591

continued

Table V - Trace Metal, Surficial Sediments

1	2	3	4	5	6	7	8	9	10	11	12	13
G 157	.046	26.7	9.4	31700	391	22.6	10.6	15.0	73.8	80	1.412	.599
G 158	.057	27.4	8.9	29800	342	22.4	10.5	12.9	71.1	90	1.328	.542
G 159	.049	25.0	9.0	28600	349	22.0	9.5	14.1	67.3	66	1.179	.489
G 160	.038	18.7	7.4	23100	307	18.7	8.4	7.9	58.3	53	1.078	.517
G 162	.037	20.1	7.9	24900	305	20.2	8.9	8.1	59.7	42	1.212	.489
G 163	.040	22.5	7.9	26600	370	19.7	8.8	8.1	63.0	81	1.179	.533
G 164	.054	22.5	8.6	25800	383	20.6	9.5	8.7	68.2	87	1.279	.511
G 165	.039	17.2	7.4	22400	335	21.0	7.3	6.6	52.5	86	1.029	.583
G 166	.040	21.1	8.1	23500	356	18.7	8.2	8.7	58.1	135	1.420	.657
G 167	.045	24.9	9.4	27900	361	21.0	8.9	10.1	68.2	124	1.286	.542
G 168	.043	23.7	8.9	24200	383	20.5	8.0	8.9	65.4	76	1.328	.524
G 169	.041	18.6	7.8	22600	315	19.0	8.8	9.7	61.7	55	1.182	.537
G 170	.048	26.3	8.7	24000	356	21.1	9.4	11.9	68.8	60	1.183	.471
G 171	.037	21.3	7.8	20600	310	19.2	8.8	9.9	58.0	75	1.244	.532
G 173	.055	26.8	9.2	26200	383	21.9	7.7	13.3	71.1	75	1.372	.611
G 174	.105	28.6	9.2	27200	399	22.5	11.2	12.8	72.7	91	1.313	.623
G 175	.070	19.6	7.1	21100	379	20.4	8.3	11.8	65.8	49	1.480	.701
G 176	.083	18.4	7.9	24300	401	22.3	9.6	12.5	63.6	66	1.547	.803
G 177	.057	22.6	8.3	23400	375	22.5	11.9	7.4	66.2	54	1.499	.638
G 178	.070	19.0	8.1	23300	407	20.0	11.4	6.3	69.4	69	1.285	.533
G 179	.079	21.8	7.9	23900	687	20.4	8.2	11.0	67.9	68	1.400	.564
G 180	.059	19.9	8.2	24200	381	20.4	10.1	8.2	62.6	100	1.404	.528
G 181	.059	18.9	7.1	23600	369	19.4	7.5	9.4	65.2	67	1.351	.510
G 182	.053	20.1	7.2	21800	333	18.9	10.1	7.0	62.1	84	1.258	.504
G 183	.057	18.0	6.8	21600	519	18.7	7.5	7.6	54.0	115	1.312	.523
G 184	.083	19.0	7.7	23000	335	18.0	10.3	6.1	54.5	87	1.355	.585
G 185	.068	20.8	8.2	25100	367	18.8	6.3	8.1	54.6	142	1.433	.649
G 186	.059	18.9	7.7	23300	355	18.4	8.9	8.5	50.4	260	1.628	1.399
G 187	.062	18.7	7.0	22700	341	18.5	7.2	9.5	50.2	144	1.316	.543
G 188	.051	21.6	8.1	25500	365	19.5	11.2	8.6	61.6	94	1.344	.569

continued

Table V - Trace Metal, Surficial Sediments

	1	2	3	4	5	6	7	8	9	10	11	12	13
G	189	.045	23.1	7.1	24600	347	19.8	9.4	7.8	55.9	71	1.234	.524
G	190	.045	21.2	7.4	25700	362	20.7	9.3	7.2	61.5	58	1.175	.484
G	191	.056	22.2	8.0	26000	936	21.2	9.6	11.3	75.9	92	4.857	4.113
G	192	.046	24.1	7.8	25200	380	20.8	9.6	9.1	63.0	81	1.437	.625
G	193	.068	26.4	8.7	27800	400	23.2	10.0	10.5	70.9	45	1.612	.766
G	194	.052	28.7	8.9	27200	379	22.4	10.1	10.9	68.7	44	1.463	.608
G	195	.055	24.4	7.8	25900	445	21.4	9.0	8.9	64.4	46	1.238	.550
G	196	.075	18.9	6.5	19200	490	18.7	7.0	8.0	47.2	68	7.973	7.276
G	197	.055	19.8	7.5	21700	380	18.0	9.1	7.5	52.0	36	1.268	.492
G	198	.042	19.1	6.8	15900	360	19.2	9.0	6.4	54.3	50	1.134	.454
G	199	.043	18.0	6.4	20500	368	19.1	9.7	6.2	52.4	78	1.296	.529
G	200	.044	20.1	6.9	23400	369	19.0	9.9	6.9	54.1	76	1.359	.575
G	201	.044	19.2	7.1	23300	353	19.1	9.4	6.9	51.7	116	1.303	.574
G	202	.070	14.1	6.7	18700	315	16.8	7.9	5.4	43.7	150	1.270	1.029
G	203	.059	15.6	6.2	18600	323	16.8	7.5	5.9	44.8	224	1.217	.869
G	204	.044	17.5	6.6	21700	347	18.8	8.3	5.7	55.8	75	1.378	.597
G	205	.053	22.4	8.2	26300	377	21.5	9.1	7.5	68.4	78	1.399	.553
G	206	.069	17.6	7.1	17900	362	18.4	10.5	8.0	48.9	62	1.276	.482
G	207	.073	25.2	9.1	23500	382	23.8	11.2	12.3	61.7	60	1.422	.584
G	208	.069	22.1	7.0	22300	415	21.4	9.5	9.1	57.0	62	.939	.377
G	209	.056	23.9	8.3	22800	376	22.1	10.6	10.4	60.5	65	1.381	.514
G	210	.094	29.5	8.6	21700	357	22.8	11.5	9.3	75.5	70	1.488	.521
G	211	.060	23.8	8.1	22700	497	20.0	10.3	9.6	66.0	54	1.463	.512
G	212	.065	23.1	8.0	20200	351	20.3	9.2	9.5	65.1	44	1.278	.750
G	216	.070	33.4	9.2	24400	383	23.7	10.9	12.0	77.5	37	1.404	.669
G	217	.077	29.2	8.5	23800	356	24.4	9.9	11.3	76.9	53	1.436	.570
G	218	.091	33.3	8.6	24200	317	23.2	9.9	12.8	85.5	39	1.184	.613
G	219	.075	25.8	7.1	19400	329	21.6	7.6	9.8	72.9	46	.936	.447
G	220	.115	33.6	9.1	24800	390	25.4	9.4	14.3	81.5	84	.868	.577
G	221	.073	26.5	7.4	22100	322	20.3	7.8	10.8	65.8	81	1.337	.583

continued

Table V - Trace Metal, Surficial Sediments

1	2	3	4	5	6	7	8	9	10	11	12	13
G 222	.096	33.4	9.0	26400	378	22.6	9.8	12.8	79.3	85	1.474	.571
G 223	.124	31.4	8.8	25000	343	24.0	9.0	12.9	71.8	86	1.391	.634
G 224	.087	26.6	7.5	22500	378	19.7	7.8	10.5	68.3	112	1.270	.745
G 225	.090	23.4	8.7	23300	339	21.2	8.0	13.1	58.0	300	1.005	.828
G 226	.080	26.1	7.6	21900	381	23.2	8.3	9.1	64.4	137	1.411	.650
G 227	.089	32.2	8.5	25600	303	26.1	10.0	13.5	72.3	75	1.344	.586
G 228	.090	28.6	7.3	23800	398	22.5	7.4	11.2	67.6	74	1.596	1.062
G 229	.069	30.8	7.8	23600	397	22.0	8.4	13.3	76.4	118	.831	.414
G 230	.100	31.4	7.9	25300	322	25.9	8.0	14.2	77.8	56	.832	.635
G 231	.076	28.5	7.0	21500	327	21.7	6.9	10.2	71.5	61	1.000	.451
G 232	.098	41.5	8.7	26900	404	25.3	8.5	12.6	80.2	65	1.214	.505
G 233	.092	30.3	8.4	26800	400	23.0	5.4	13.8	70.4	64	1.004	.787
G 234	.068	30.3	8.5	24400	398	24.1	6.0	12.2	76.7	56	1.338	.691
G 235	.087	29.4	8.3	23700	388	22.5	5.5	12.8	72.4	68	1.224	1.003
G 236	.101	26.0	7.6	22500	336	21.1	5.7	11.6	65.1	72	1.044	.873
G 237	.085	24.9	7.7	23900	351	24.3	11.3	9.7	71.4	192	.952	.625
G 238	.066	25.3	7.9	24400	424	22.3	11.3	9.7	69.5	156	.736	.381
G 239	.076	21.4	7.3	21700	408	19.1	10.6	8.8	62.0	161	1.147	.488
G 240	.074	24.7	7.2	22100	348	22.1	8.7	8.6	67.9	97	1.058	.488
G 241	.073	23.5	6.9	19200	355	23.8	8.2	7.9	63.6	76	.962	.462
G 242	.089	23.4	7.2	19300	405	25.2	7.9	8.5	65.4	77	1.264	.571
G 243	.067	25.0	7.5	19100	335	21.4	7.0	8.6	64.4	87	1.260	.567
G 244	.070	27.7	8.3	22700	346	23.2	8.7	10.2	69.8	82	1.333	.584
G 245	.091	21.6	7.0	18900	309	18.9	6.9	10.1	54.2	89	1.311	.812
G 246	.066	26.0	7.6	20800	384	20.0	7.4	10.4	62.1	85	1.096	.539
G 247	.095	26.9	8.0	22500	377	22.2	7.7	10.4	77.8	101	1.242	.560
G 248	.070	32.5	9.4	23500	359	24.0	10.4	14.0	77.0	76	1.333	.542
G 249	.082	25.8	7.9	20500	393	23.1	8.3	10.4	67.9	60	1.353	.519
G 250	.079	25.3	7.2	21100	373	21.0	7.2	9.1	66.8	62	1.278	.566
G 251	.064	25.0	7.2	20100	381	21.6	7.8	8.4	67.5	81	1.317	.559

continued

Table V - Trace Metal, Surficial Sediments

1	2	3	4	5	6	7	8	9	10	11	12	13
G 252	.063	27.9	8.1	21600	425	22.7	6.1	11.7	70.0	72	1.030	.699
G 253	.065	22.3	7.2	20200	368	20.0	9.4	10.7	61.0	71	1.443	.978
G 254	.073	24.4	7.0	19000	374	20.8	5.7	9.3	65.9	80	1.187	.601
G 255	.058	23.2	7.6	18500	441	21.6	6.9	11.1	65.4	76	1.272	.879
G 256	.074	32.4	8.8	24200	407	24.3	7.3	13.8	81.0	82	1.525	.612
G 257	.110	18.9	7.0	19500	382	21.6	11.1	9.9	50.7	31	1.273	.981
G 258	.121	20.9	7.3	19600	395	25.1	9.2	9.3	54.2	56	1.022	.683
G 259	.116	24.6	7.7	22500	383	21.6	9.2	9.7	54.9	74	.995	.644
G 260	.081	24.8	8.1	23000	418	23.0	8.9	10.9	56.8	81	1.149	.566
G 261	.078	22.7	7.9	22500	361	20.6	8.7	10.1	53.8	86	1.120	.555
G 262	.095	22.5	8.7	20300	393	21.7	10.5	8.7	53.9	140	1.453	.646
G 263	.072	15.5	6.1	17200	329	19.4	6.7	7.2	41.7	125	1.349	.888
G 264	.087	19.7	8.0	21300	335	19.5	9.5	8.4	50.9	116	.950	.482
G 265	.119	15.2	6.6	16500	382	20.0	7.6	7.3	43.6	238	.909	.530
G 266	.091	18.4	7.6	19000	422	19.0	8.5	8.2	48.6	176	.880	.609
G 267	.079	16.4	7.1	17600	324	15.1	9.8	9.6	45.9	224	.514	.348
G 268		19.3	8.1	20500	403	22.0	8.1	9.5	50.7	288	1.036	.656
G 269	.137	18.5	7.0	20200	366	20.0	8.6	10.4	51.1	176	1.639	1.060
G 270	.081	23.4	8.3	24700	384	24.0	9.0	10.8	57.3	238	1.303	.655
G 271	.085	18.2	7.9	19700	440	21.5	8.2	8.1	50.1	116	1.143	.699
G 272	.084	22.0	6.7	20300	405	24.7	7.5	10.5	58.6	69	1.148	.676
G 273	.116	14.8	7.0	17900	357	24.3	7.3	8.3	49.2	191	1.389	.865
G 274	.128	25.7	9.8	24200	431	25.2	8.9	10.7	66.0	46	1.528	.667

TABLE VI - TRACE METALS CONTENT OF SUSPENDED SEDIMENTS

Explanation for Table

Column 1 - Sample number, T = Top, M = Middle, B = Bottom

Column 2 - Date

Column 3 - Time, GMT

Column 4 - Chlorinity in parts per thousand

Column 5 - Mass in milligrams per liter

Column 6 - Cadmium in parts per million

Column 7 - Copper in parts per million

Column 8 - Chromium in parts per million

Column 9 - Nickel in parts per million

Column 10 - Lead in parts per million

Column 11 - Manganese in parts per million

Column 12 - Vanadium in parts per million

Column 13 - Zinc in parts per million

Column 14 - Iron in parts per million

Table VI - Trace Metal content of Suspend Sediments

1	2	3	4	5	6	7	8	9	10	11	12	13	14
010WT	029	0200	15.3	2.30	1.1	57	20	25	32	1240	11.4	963	1.9
010WM	029	0200	15.6	2.52	1.5	112	28	24	52	433	7.5	1010	2.1
010WB	029	0200	17.4	21.01	1.5	86	12	43	22	849	6.9	266	1.8
024WT	030	1940	15.3	3.62	0.4	59	14	41	25	112	4.1	51	0.8
024WM	030	1940	15.3	----	1.9	101	17	38	68	143	3.4	759	1.0
024WB	030	1940	18.3	----	2.1	86	16	25	45	1260	14.5	5650	1.9
032WT	031	0355	18.7	0.13	8.1	67	58	53	126	271	6.4	203	1.1
032WM	031	0355	18.2	0.47	0.1	256	22	98	61	309	1.2	1730	0.1
032WB	031	0355	19.0	0.88	0.3	178	24	20	49	344	10.6	5040	1.4
060WT	113	0455	20.1	1.39	0.3	37	28	74	37	65	5.9	1200	1.2
060WM	113	0455	20.1	----	4.3	140	231	179	123	266	18.2	3610	1.4
060WB	113	0455	19.9	140.10	0.8	29	63	63	20	1090	25.2	247	4.0
070WT	102	0510	15.2	1.27	0.9	530	27	64	96	82	2.7	1060	1.0
070WM	102	0510	15.9	----	1.8	1480	34	19	---	31	1.9	12100	0.7
070WB	102	0510	17.9	52.25	0.5	37	18	29	20	439	8.4	272	1.6
073WT	103	0725	15.1	0.55	0.8	13	36	53	30	24	4.9	2320	1.0
073WM	103	0725	18.1	2.75	1.4	299	111	50	111	288	11.8	880	1.5
073WB	103	0725	18.9	12.75	2.3	225	35	52	96	580	13.7	378	1.6
085WT	112	0458	20.2	----	1.9	202	115	99	364	192	---	637	1.7
085WM	112	0458	20.2	0.67	1.9	205	26	81	146	371	7.7	2090	1.0
085WB	112	0458	20.2	112.55	0.1	15	21	51	21	750	6.8	539	1.5
088WT	113	1900	15.3	2.31	3.7	1690	93	556	370	662	41.7	1400	5.1
088WM	113	1900	15.6	2.52	100.0	50	31	80	80	253	5.9	1020	1.3
088WB	113	1900	17.4	21.01	3.4	938	32	186	166	871	12.1	888	1.3
095WT	103	0245	19.1	7.69	0.7	70	34	63	90	360	7.6	769	1.9
095WM	103	0245	19.6	3.09	---	---	---	---	---	----	---	----	---
095WB	103	0245	19.3	15.67	11.0	118	22	31	124	682	18.3	3500	2.1
110WT	104	1327	19.6	2.40	---	111	96	221	166	103	---	1060	2.6
110WM	104	1327	19.7	2.50	---	---	---	---	---	---	---	----	---
110WB	104	1327	20.1	6.75	1.6	50	33	26	32	145	27.1	104	1.0

Continued

Table VI - Trace Metal content of Suspend Sediments

1	2	3	4	5	6	7	8	9	10	11	12	13	14
114wT	113	0258	20.1	4.28	3.5	1210	48	129	165	4270	12.9	6500	1.3
114wM	113	0258	20.1	3.05	---	88	57	263	132	154	57.0	3100	3.6
114wB	113	0258	20.1	0.90	2.6	71	8800	4470	---11	100	45.4	----	6.8
115wT	114	1229	20.0	9.87	78.0	242	133	167	321	134	14.8	246	2.5
115wM	114	1229	19.4	11.12	9.2	184	98	103	195	122	14.7	577	1.4
115wB	114	1229	19.8	33.50	0.2	65	15	20	15	681	8.5	234	1.6
155wT	119	1905	19.1	2.09	---	905	79	68	91	66	28.3	3890	5.2
155wM	119	1905	19.5	2.95	19.0	222	149	--	93	1080	6.7	1080	1.4
155wB	119	1905	19.6	6.36	0.8	21	15	52	29	946	13.3	136	3.7
156wT	119	2059	19.7	1.91	0.6	2240	67	15	153	121	----	2600	1.3
156wM	119	2059	19.8	4.32	21.0	194	125	347	326	17	----	2140	3.6
156wB	119	2059	20.0	2.18	9.7	25	19	64	39	1180	14.9	80	4.0
157wT	119	2241	18.9	2.32	2.6	423	423	254	303	513	0.2	2320	1.6
157wM	119	2241	19.8	0.19	2.7	----	----	----	83	----	----	----	----
157wB	119	2241	20.1	10.90	0.2	15	15	27	23	826	8.5	1060	1.7
160wT	119	0510	----	0.51	13.0	102	241	195	195	331	---	27500	1.9
160wM	119	0510	19.6	2.39	0.2	645	181	167	62	820	---	7530	1.2
160wB	119	0510	18.4	3.22	3.0	20	45	44	53	1310	9.8	834	1.7
164wT	121	1201	18.3	4.03	19.0	188	122	65	70	141	18.5	8020	2.5
164wM	121	1201	18.5	2.28	3.2	258	48	653	213	755	11.0	298	1.1
164wB	121	1201	18.8	4.00	0.7	56	17	20	18	1040	14.7	1800	1.3
165wT	121	2301	16.9	0.80	0.4	992	32	---	64	170	11.1	7270	5.1
165wM	121	2301	17.3	1.07	8.4	207	10	415	26	150	15.5	-----	0.5
165wB	121	2301	17.6	2.11	11.0	1230	58	95	95	796	1.5	892	1.3
235wT	204	2229	21.4	2.09	6.1	1120	175	598	120	287	3.3	3860	0.3
235wM	204	2229	19.7	1.01	0.2	1050	174	1420	71	271	3.9	2060	----
235wB	204	2229	----	2.78	9.4	16	19	35	23	1140	20.7	80	2.8
236wT	203	2106	19.0	----	0.5	736	409	245	300	3440	----	8530	0.8
236wM	203	2106	----	----	1.4	425	3260	1450	285	6910	----	1330	2.8
236wB	203	2106	20.1	13.80	8.3	109	32	49	97	670	17.4	569	1.9

Continued

Table VI - Trace Metal content of Suspend Sediments

1	2	3	4	5	6	7	8	9	10	11	12	13	14
238wT	203	1945	19.5	4.03	9.4	1850	79	79	343	87	----	2090	1.5
238wM	203	1945	21.1	2.97	9.9	1520	36	--	168	219	5.4	2710	1.3
238wB	203	1945	19.8	12.79	---	213	17	25	45	778	8.6	1700	2.0
241wT	122	2245	----	2.21	1.7	632	99	281	260	34	2.2	639	1.0
241wM	122	2245	18.8	1.31	1.1	225	79	38	222	142	1.1	772	0.3
241wB	122	2245	19.8	4.08	2.3	41	14	79	58	1490	7.4	1640	1.2
243wT	115	1910	18.3	6.92	0.8	153	54	13	203	127	5.8	675	1.7
243wM	115	1910	17.4	22.17	2.6	302	28	68	85	262	11.0	944	1.1
243wB	115	1910	19.2	23.25	1.2	256	19	46	55	1220	9.5	866	1.4
245wT	115	1704	----	11.75	3.8	215	97	49	449	356	27.7	3460	2.5
245wB	115	1704	----	4.25	4.3	209	27	79	152	323	4.2	63400	1.2
245wB	115	1704	16.9	30.14	3.8	----	32	38	38	861	15.6	360	1.7

The Department of the Interior Mission

As the Nation's principal conservation agency, the Department of the Interior has responsibility for most of our nationally owned public lands and natural resources. This includes fostering sound use of our land and water resources; protecting our fish, wildlife, and biological diversity; preserving the environmental and cultural values of our national parks and historical places; and providing for the enjoyment of life through outdoor recreation. The Department assesses our energy and mineral resources and works to ensure that their development is in the best interests of all our people by encouraging stewardship and citizen participation in their care. The Department also has a major responsibility for American Indian reservation communities and for people who live in island territories under U.S. administration.

The Minerals Management Service Mission

As a bureau of the Department of the Interior, the Minerals Management Service's (MMS) primary responsibilities are to manage the mineral resources located on the Nation's Outer Continental Shelf (OCS), collect revenue from the Federal OCS and onshore Federal and Indian lands, and distribute those revenues.

Moreover, in working to meet its responsibilities, the **Offshore Minerals Management Program** administers the OCS competitive leasing program and oversees the safe and environmentally sound exploration and production of our Nation's offshore natural gas, oil and other mineral resources. The MMS **Minerals Revenue Management** meets its responsibilities by ensuring the efficient, timely and accurate collection and disbursement of revenue from mineral leasing and production due to Indian tribes and allottees, States and the U.S. Treasury.

The MMS strives to fulfill its responsibilities through the general guiding principles of: (1) being responsive to the public's concerns and interests by maintaining a dialogue with all potentially affected parties and (2) carrying out its programs with an emphasis on working to enhance the quality of life for all Americans by lending MMS assistance and expertise to economic development and environmental protection.